Conference Proceedings

Power Plant Chemical Technology 1996

International Conference
Kolding, Denmark, 4-6 September 1996

OSTI

N   C   H

S

Analysis

Trace Element Mass Balance for Cadmium at MKS3

FLUE GAS
1.1%

COAL
94.2%   BOILER   95.6%   ESP   1.4%   SDA PLANT   0.0% ← PROCESS WATER
1.8% ← BURNED LIME

2.5%   94.2%   2.1%

BOTTOM ASH   FLY ASH   RESIDUAL PRODUCT
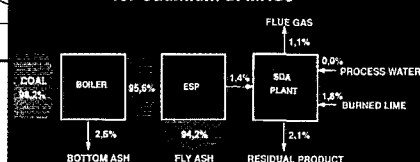
Materials

Process Technology   **Water Treatment**

DISCLAIMER

Portions of this document may be illegible in electronic image products. Images are produced from the best available original document.

Contents
Conference Proceedings
Power Plant Chemical Technology 1996

<div style="border:1px solid">

Session 1
Combustion and Flue Gas Cleaning

</div>

Contents
Conference Proceedings
Power Plant Chemical Technology 1996

Session 4
Chemical Monitoring and Control

Conclusion of the Conference

Contents
Conference Proceedings
Power Plant Chemical Technology 1996

Session 1
Combustion and Flue Gas Cleaning

Contents
Conference Proceedings
Power Plant Chemical Technology 1996

Session 2
Materials and Corrosion

Contents
Conference Proceedings
Power Plant Chemical Technology 1996

Session 3
Water/Steam Cycle Chemistry

Contents
Conference Proceedings
Power Plant Chemical Technology 1996

Session 4
Chemical Monitoring and Control

Conclusion of the Conference

Dr. Heinz Gutberlet

VEBA Kraftwerke Ruhr AG

P.O. Box 10 01 25

45801 Gelsenkirchen

Germany

Flue Gas Cleaning Chemistry

1. Introduction

The introduction of modern flue gas cleaning technology into fossil-fuelled power stations has repeatedly confronted the power station chemists with new and interesting problems over the last 15 - 20 years. Both flue gas desulphurization by lime washing and catalytic removal of nitrogen oxides are based on simple basic chemical reactions (Figure 1):

♦ the reaction of limestone, water and atmospheric oxygen with the pollutant sulphur dioxide to form calcium sulphate, and

♦ the reduction of nitrogen oxides by means of ammonia to give nitrogen and water.

Owing to their simple basic principles, i.e. the use of readily available starting materials, the production of safe, useful end products and, last but not least, the possibility of implementing all this on an industrial scale by means of efficient process engineering, limestone desulphurization and catalytic removal of nitrogen oxides dominate the world market and, little by little, are becoming still more widespread.

It could be asked what, given this increasingly mature technology, is still to be done by power station chemists and what expert groups still have to consider today.

2) $\cdot SO_5^- + HSO_3^- \;\rightarrow\; SO_4^{2-} + \cdot SO_4^- + H^+$

        $\cdot SO_4^- + HSO_3^- \;\rightarrow\; SO_4^{2-} + \cdot SO_3^- + H^+$
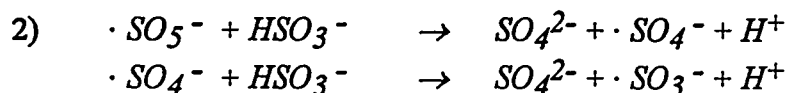
In both reaction mechanisms, both sulphate and sulphite free radicals are formed, in accordance with the following overall equation:

$$\cdot SO_5^- + 2HSO_3^- \;\rightarrow\; 2SO_4^{2-} + \cdot SO_3^- + 2H^+$$
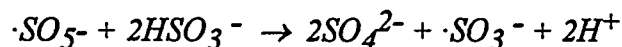
If, owing to a complete reaction, sulphite or hydrogensulphite ions are no longer available to maintain the chain reaction, the peroxomonosulphate free radicals react with other oxidizable substances, for example heavy-metal ions, such as Mn^{2+} or Fe^{2+}, and consequently regenerate the M^{3+} ions necessary for chain initiation. The peroxomonosulphate also acts as oxidant.

$$\cdot SO_5^- + M^{2+} + H^+ \;\rightarrow\; HSO_5^- + M^{3+}$$
$$HSO_5^- + M^{2+} + H^+ \;\rightarrow\; SO_4^- + M^{3+} + H_2O$$
$$\cdot SO_4^- + M^{2+} \;\;\;\;\rightarrow\; SO_4^{2-} + M^{3+}$$
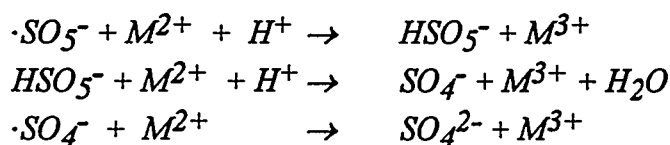
Since a peroxosulphate free radical causes the formation of three M^{3+} ions in this reaction chain, this is referred to as sulphite-induced autoxidation of the metal ions. In desulphurization systems, this is evident from precipitation of manganese dioxide (MnO_2) and a darkening of the calcium sulphate, since Mn^{3+} ions tend towards disproportionation.

$$2Mn^{3+} + 2H_2O \;\rightarrow\; MnO_2 \downarrow + Mn^{2+} + 4H^+$$

The peroxosulphate (free radical) is such a strong oxidant that, once the readily oxidizable species have been consumed, even substances which are normally difficult to oxidize are attacked. Sulphite-induced oxidation can consequently also result in the formation of free halogens.

However, the prerequisite is that the steady-state concentration of sulphite moves towards zero. However, the oxidant is constantly re-formed from the absorbed SO_2. When excess sulphite is no longer available as reducing agent, the strongly oxidizing species remain in solution. In practice, this can be measured, for example, through a high redox potential of the absorber suspension of from -400 to -500 mV. In addition, chain

termination reactions between the free radicals cause the formation of the by-products dithionate and peroxodisulphate, which can be found in the absorber suspension.

$$\cdot SO_3^- + \cdot SO_3^- \rightarrow S_2O_6^{2-}$$
$$\cdot SO_3^- + \cdot SO_5^- \rightarrow S_2O_8^{2-}$$
$$\cdot SO_4^- + \cdot SO_4^- \rightarrow S_2O_8^{2-}$$
$$\cdot SO_5^- + \cdot SO_5^- \rightarrow S_2O_8^{2-} + O_2$$
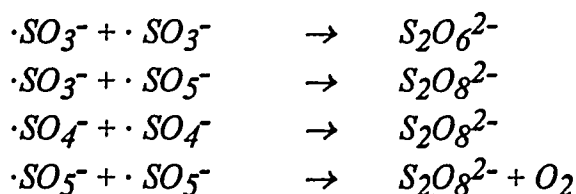
Chemical analysis of the absorber suspension for dithionate and peroxodisulphate gives - even in unfamiliar systems - a clear indication of the operating conditions of desulphurization systems (Fig. 3). The occurrence of peroxodisulphate (the concentration can rise to a few hundred milligrams per litre) always excludes the presence of free sulphite. For this reason, the desulphurization efficiency is usually very good, since the transfer of SO_2 into the washing liquid is only gas phase limited, but not liquid phase limited. This is then also the case in a process at reduced pH (for example 4.0), which guarantees, amongst other things, a high degree of utilization of the limestone. In addition to peroxodisulphate, a moderate concentration of dithionate also arises (up to 1000 mg/l).

Significantly higher concentrations of dithionate in the absence of peroxodisulphate are also an indication of good oxidation kinetics, but indicate a relative deficiency of oxygen molecules in the liquid phase. The sulphite free radicals dimerize instead of reacting with O_2. This may be associated, for example, with the performance of the oxidation air system or may occur at very high specific SO_2 conversions.

If sulphite or hydrogensulphite can be detected in higher concentrations, dithionate is frequently found only in low concentrations, if at all. This is the case if, for example, the free-radical chain reaction is suppressed by interfering substances. In Germany we collected initial experience of this when our slag tap fired boilers were retrofitted with flue gas desulphurization systems. In spite of the same desulphurization system engineering and the same SO_2 content in the flue gas, a number of desulphurization systems fitted to slag tap fired boilers exhibited a significantly worse oxidation behaviour than the same systems fitted to dry furnaces. At first, we thought this was due to problems in the oxidation air system. It later became apparent that the cause was of a chemical nature. The much higher nitrogen oxide levels in the flue gases from slag tap fired furnaces result in the formation of sulphur/nitrogen compounds in the desulphurization system. In simplified form, the following reactions occur, amongst

others:

$$2\,NO_2 + H_2O \quad\rightarrow\quad NO_2^- + NO_3^- + 2\,H^+$$
$$NO_2^- + 2\,HSO_3^- + H^+ \quad\rightarrow\quad HON(SO_3)_2^{2-} + H_2O$$
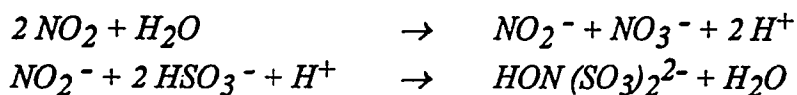
In the aqueous phase, nitrogen oxides form nitrite, which reacts further with hydrogensulphite to form hydroxylamine disulphonate (HADS). Like other species, HADS can kinetically retard the free-radical sulphite oxidation chain reaction by reacting, as reducing agent, with the trivalent metal ions necessary for chain initiation, i.e. the formation of sulphite free radicals. If only a few sulphite free radicals are formed, i.e. if the steady-state concentration of sulphite free radicals is low, no dithionate is formed either.

We have carried out a detailed investigation of the formation of sulphur/nitrogen compounds (SN compounds) as derivatives of the hydroxylamine and ammonia; the effect on the reaction kinetics of sulphite oxidation has also been demonstrated in laboratory experiments. The chemical mode of operation of a flue gas desulphurization system is also characterized by the type and amount of SN compounds formed. However, we will report this in detail elsewhere (1).

2.2 Inhibition of limestone dissolution

In addition to gaseous flue-gas components, such as nitrogen oxides or halogen compounds, dust-like materials entering the desulphurization system in the form of clean gas dust can adversely affect the chemistry in the system or even cause the process to fail. The following are some results from our own investigations on the deactivation of limestone by aluminium which is observed in many desulphurization systems around the world (2,3). The fly ash from the burning of hard coal represents a source of aluminium ions; in the weakly acidic medium in the absorber circuit of flue gas desulphurization systems, aluminium can be dissolved out of the cleaned gas dust entering the system and can thus enter the aqueous phase as Al^{3+} ions. Water molecules add coordinatively to aluminium ions, forming an hexaqua complex, which can function as a cation acid and release H^+ ions.

$$Al^{3+} + 6H_2O \Leftrightarrow [Al(H_2O)_6]^{3+}$$

$$[Al(H_2O)_6]^{3+} \Leftrightarrow [Al(H_2O)_5OH]^{2+} + H^+ \Leftrightarrow [Al(H_2O)_4(OH)_2]^+ + 2H^+$$

$$\Leftrightarrow \underset{\text{aluminium hydroxide}}{[Al(H_2O)_3(OH)_3]} + 3H^+ \Leftrightarrow \underset{\text{aluminate}}{[Al(H_2O)_2(OH)_4]} + 4H^+$$
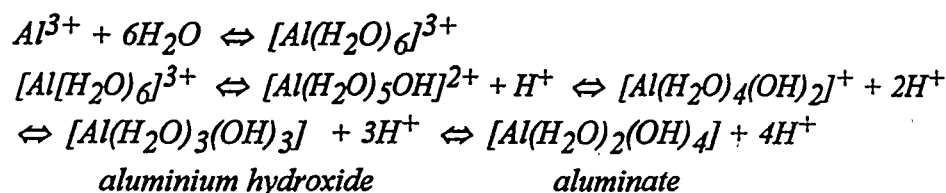
It is known that aluminium precipitates as insoluble hydroxide from aqueous solution in a pH range from 4 to 6, i.e. the preferred operating range of flue gas desulphurization systems. Aluminium ions alone therefore do not have an adverse effect on limestone reactivity in FGD plants.

However, the introduction of hydrogen fluoride (HF) with the flue gas also increases the concentration of fluoride ions in the absorber circuit, which can form fluoro complexes with aluminium. These are generally referred to as AlF_x (x = 1 - 6). These complexes have good water solubility in the pH range around 5, in contrast to aluminium hydroxide. We have studied absorber suspensions and artificial salt solutions using ^{19}F-NMR spectroscopy in order to determine which species are present and cause the known reduction in reactivity of the limestone (Fig. 4, 5, 6).

It is evident from the spectra that, depending on the availability of fluoride and aluminium ions, complexes containing from one to four fluoride ions are formed. Free fluoride F^- is virtually absent at equilibrium, so that aluminium can dissolve even fluoride which has already precipitated as calcium fluoride, for example in accordance with the following equation:

$$CaF_2 + Al^{3+} \rightarrow Ca^{2+} + AlF_2^+$$
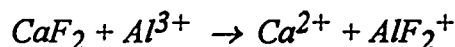
At a pH > 5.5, the solubility of aluminium and fluoride drops, i.e. the complex is precipitated. It is obvious that this precipitation takes place at the phase interface of the limestone particles present in the absorber suspension, preventing diffusion of H^+ ions and calcium ions or hydrogencarbonate ions:

$$CaCO_3 + H^+ \rightarrow Ca^{2+} + HCO_3^-$$
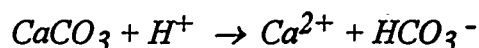
Figure 7 shows an example for inhibited limestone dissolution in a laboratory experiment.

In practice, the occurrence of aluminium blinding is evident from a drop in the pH of the absorber circuit to 3.5 - 4.0, although the limestone metering control is generally reset to

a pH of 5.0 -5.5. If the limestone metering is not switched from automatic to manual or if the target pH is not changed to a value of 3.5 - 4.0, overmetering of limestone occurs, resulting in a high limestone content (> 10%) in the calcium sulphate.

Laboratory studies of absorber suspensions have shown that the aluminium fluoro complexes form a strong buffering system (Fig. 8), so that increasing the pH from 3.5 - 4.0 to the normal value of 5.0 - 5.5 is only possible by means of a considerable amount of strongly alkaline chemicals (NaOH, Ca(OH)$_2$), in contrast to the generally unbuffered systems in unaffected desulphurization units. This surprised us initially since the buffer effect of AlF_x is not immediately evident from this formula.

On closer investigation, however, it can be seen that the aluminium fluoro complexes are also hexacoordinated with water and hydroxyl ions, giving rise to a multispecies system of cation acids, for example:

a) $[Al(H_2O)_5OH]^{2+} + F^- \leftrightarrow [Al(H_2O)_5F]^{2+} + OH^-$ *(increase of pH)*

b) $[Al(H_2O)_5F]^{2+} + OH^- \leftrightarrow [Al(H_2O)_4(OH)F]^+ + H_2O$

(buffering system)

$[Al(H_2O)_4F_2]^+ + OH^- \leftrightarrow [Al(H_2O)_3(OH)F_2] + H_2O$
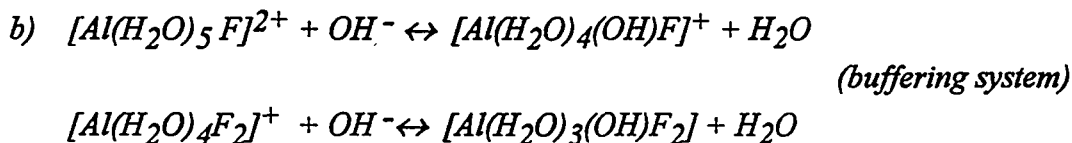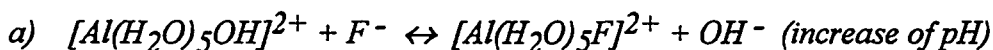
The formation of the buffering system makes it clear that aluminium blinding not only involves inhibition of limestone dissolution, but also the dissolved complex ions stabilize the pH at a low level.

In our experience, the following are possible remedial measures:

◆ Avoidanc of aluminium sources, in most cases fly ash, through improved electroprecipitator efficiency or the use of a prescrubber.

◆ Operation of the flue gas desulphurization system at a low pH. This requires that the system is operated at very good oxidation efficiency, so that free sulphite only arises at low concentration, if at all.

◆ Precipitation of the complexes by increasing the pH to above 6.0 using strong bases, which have to be added to the absorber circuit. These must be metered in in such an amount that the buffering system is overcome. This measure provides long-term

1.8

assistance only if the sources of aluminium ions are only temporary, i.e. there is no long-term introduction at increased loading levels.

2.3 Adverse effect of antifoam

As a final example from the area of flue gas desulphurization, I will describe an effect in which a small cause again has a large effect. Some time ago, we had considerable problems in one of our flue gas desulphurization systems with foaming of the absorber suspension together with overflow of the suspension into the raw gas duct. The cause of the foaming was identified as organic impurities, which could not easily be removed from the system. The obvious countermeasure was to use an antifoam.

However, before we used the agent in the large system in the amounts recommended by the manufacturer, we decided to carry out a trial on a smaller flue gas desulphurization line in order to determine any adverse effects in advance.

Figure 9 shows the result. At an addition rate of only 2 ppm of antifoam as a single dose, i.e. 350 g per 170 m^3 of suspension, the desulphurization efficiency dropped dramatically. The SO$_2$ concentration in the cleaned gas rose spontaneously after addition from 160 mg/m^3 to a value outside the measurement range, i.e. above 400 mg/m^3, and remained there for several hours. The effect only subsided after about 6 hours. The polyglycol-based antifoam is usually used in ten times the concentration. Like the foam formers, antifoams are surface-active substances. They accumulate strongly at the surface of the liquid and consequently change not only the surface tension, but also the phase interface for material transfer.

This example is intended to show how much the performance of a desulphurization system can be impaired by traces of substances. It illustrates that only starting materials of defined quality (this applies to the limestone, process water and oxidation air) can ensure fault-free operation.

3. Flue gas denitrification

The tasks of power plant chemistry can be subdivided into three major fields:

- in-service monitoring (routine),
- problem analysis,

♦ chemical process improvements.

This shall additionally be demonstrated by an example of flue gas denitrification at a coal-fired power plant by the SCR method. Frankly speaking SCR systems need no expensive permanent chemical in-service monitoring.

The key parameter which informs about the operating behaviour of the DENOX system is the ammonia slip, that is the NH_3 quantity not converted at the catalysts. The NH_3 slip should be mininum to avoid fouling of the air heater and pollution of fly ash by NH_3. Under certain conditions NH_3 can also proceed to the waste water of the desulphurization system.

For in-service monitoring it is normally sufficient to determine the NH_3 contained in fly ash at daily intervals and follow up its development in time (Figure 10).

In most cases the NH_3 content in ash increases steadily and one can derive from its pattern when measures are to be taken to counter negative effects of the NH_3-slip. The figure shows, for example, a graph for a unit as is used by VKR for mointoring a DENOX system.

When the NH_3 content in ash rises, it is usually checked which of the three causes given below are the responsible ones.

The main causes for NH_3-slip are:

♦ notable fouling of catalysts,
♦ desactivation of catalysts,
♦ uneven NH_3 distribution.

Fouling means a loss of catalytic surface due to coverage of the ducts or lanes by fly ash. The cause is mostly not of chemical nature, but often results from the flow conditions inside the reactor, especially when there are dust deposits of large extension.

To check the fouling rate of the reactor it is generally necessary to perform an inspection.

The assessment is, however, not always easily done. In honeycomb-type catalysts fouled

1.10

ducts are in most cases easily detected, but in plated type catalysts the plugging may be invisible. The dust is accumulated between the piled catalyst cages and is detected only when the modules are removed (Figure 11).

Desactivation of catalysts, by contrast, calls for an extensive chemical assessment of the catalysts and a performance test at specimen elements under realistic test conditions. The procedure applied by us is as follows:

In the various catalyst layers specimen catalysts are installed which, in case of honeycomb-type catalysts, are removed as complete elements whenever necessary. As regards plate-type catalysts, separate plates are removed from a multitude of cages. When withdrawing samples attention is to be paid to removing catalysts through which flue gas had flown, that means not only from sections in which large areas are fouled.

The first is to determine the activity constant of the intact and uncleaned catalyst element in the socalled bench reactor. We have operated since 1990 such a reactor (4) into which the whole honeycomb body (150 mm x 150 mm edge length) or square plate assembled elements are placed (Figure 12).

The composition and temperature of the gauging gas are adjusted to the working conditions or to the design conditions of the reactor, depending on the requirements. This also includes the adjustment of the water vapour concentration in flue gas which is necessary for the determination of service-relevant K values. Only the dust content is not considered.

One obtains activity constants depending on the layers which normally permit to calculate, if several samples are analyzed, an average activity constant close to the actual value for the respective catalyst layer. As the conditions of the layers are differing after an extended operating period, both with regard to catalyst type and time of use, the activity inventory of the reactor can only be assessed after an appropriate differentiated analysis.

As an example we would like to present the DENOX system of the Buer District Heat Power Plant which has been in operation since December 1985 and belonged to the first industrial-scale DENOX systems in Germany. The power plant is firing bituminous coal with a very high ash content: the raw gas dust content is about 50 g/m^3. It was necessary to optimize the flue gas flow in order to achieve a more uniform ash concentration.

Originally the plant was equipped with three catalyst layers. In the course of time the layers were replaced; in that process makes of differing flow types underwent a performance test under difficult flue gas conditions. That is why today four catalyst layers from different manufacturers are being used. The analysis of the activity constant permits to calculate in conjunction with the specific surfaces of the catalyst types, the activity potential for each separate layer (Figure 13). In this way, if necessary, the next layer to be replaced, namely that with the lowest potential, can be found out. In addition, it is possible to forecast how much time is left until the next layer is to be replaced. For that purpose we additionally determine the ageing function which has a decisive influence on the expected time of exchange. The knowledge of the ageing function follows from regular determinations of the potential in the course of the operating time of the DENOX reactor.

Knowledge of the probable reloading time yields the economic benefit of regular catalyst inspections.

The assessment of the potential accessible through determining the activity constants and the comparison with the operating behaviour of the plant make it possible to detect causes of NH_3-slip other than fouling and desactivation.

Quite often the reason for ammonia slip is uneven NH_3 distribution.

An NH_3 unbalance occurs, for example, if the NH_3 injection is incorrectly adjusted or there is a malfunction e.g. as a result of plugged nozzles. It is particularly relevant in case of high efficiencies. At points of high NH_3 concentrations the stoichiometric ratio of NH_3 and NO is shifted towards high values. When the ratio comes close to 1 or exceeds the figure, an NH_3 slip occurs at these points and cannot be prevented either by sufficient catalyst potential (Figure 14). At the same points the NO value is extremely low. In this case it is necessary to adjust the NH_3 injection. We use with preference an automatic measuring equipment (MARA) which makes a rapid traverse of the NO_x pattern downstream of the last catalyst layer possible so that an NH_3 adjustment can be accomplished within a single measuring day Figure 15 shows as an example the NO_x-profile before and after adjustment of the NH_3-injection. A variation coefficient of around 15 % is quite good and in most cases meets the target for even NH_3 distribution.

These examples of the chemistry in flue gas cleaning systems illustrate that many interesting and demanding subjects still remain for the chemist to deal with. Although it is certainly correct that power plants will not and should not become chemical plants, it is becoming increasingly obvious that smooth operation of environmental protection systems also involves chemical activities the extent of which should not be underrated. The particular attraction is the large number of processes, covering the entire path of the fuel from coaling to the chimney and requires interdisciplinary thinking. Chemists are not only needed as analysts, but must also work out their analytical results and interpret them for the plants. This is only possible if engineering and chemistry are in-house together. It is our experience that complex questions can be dealt with particularly well in expert teams.

References

1) H. Gutberlet, S. Finkler, B. Pätsch, R. van Eldik, R. Prinsloo, Bildung von Schwefel- und Schwefel-Stickstoff-Verbindungen in Rauchgasentschwefelungsanlagen und ihr Einfluß auf die Oxidationskinetik von Sulfit, VGB-Kraftwerkstechnik 76(2), 193 (1996).

2) R. W. Farmer, J. B. Jarvis, R. Moser, Effects of aluminium / fluoride chemistry on wet limestone flue gas desulfurization, Spring National AlCh E meeting, Houston, Texas, 78 (1987)

3) N. Ukawa, S. Okino, T. Iwaki, M. Oshima, Y. Watanabe, The effects of fluoride complexes in wet limestone flue gas desulfurization, Journal of chemical engineering of Japan 25(2), 146 (1992)

4) H. Gutberlet, Power Plant Chemistry in Flue Gas Cleaning Systems, VGB-Kraftwerkstechnik 74(1), 54 (1994)

basic chemical reactions

flue gas desulfurization by limestone srubbing

$$2\ CaCO_3 + 2\ SO_2 + O_2 + 4\ H_2O \longrightarrow 2\ CaSO_4 * 2\ H_2O + 2\ CO_2$$
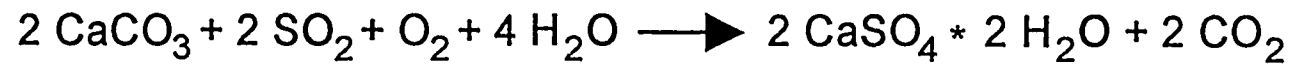
flue gas denitrification by selective catalytic reduction

$$4\ NO + 4\ NH_3 + O_2 \longrightarrow 4\ N_2 + 6\ H_2O$$

Fig. 1
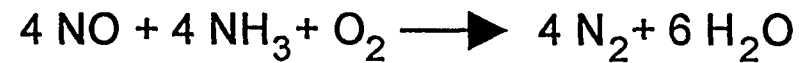
part steps of flue gas desulfurization

$$2\,CaCO_3 \quad + \quad 2\,SO_2 \quad + \quad O_2 \quad + \quad 4\,H_2O \longrightarrow 2\,CaSO_4 * 2\,H_2O \quad + \quad 2\,CO_2$$

dissolution   absorption   dissolution   precipitation   desorption

mass transfer types

solid→liquid   gas→liquid   gas→liquid   liquid→solid   liquid→gas

free radical reaction
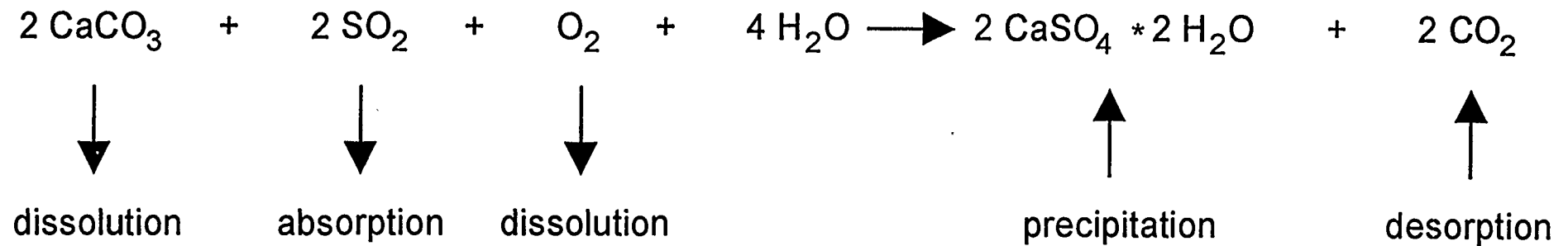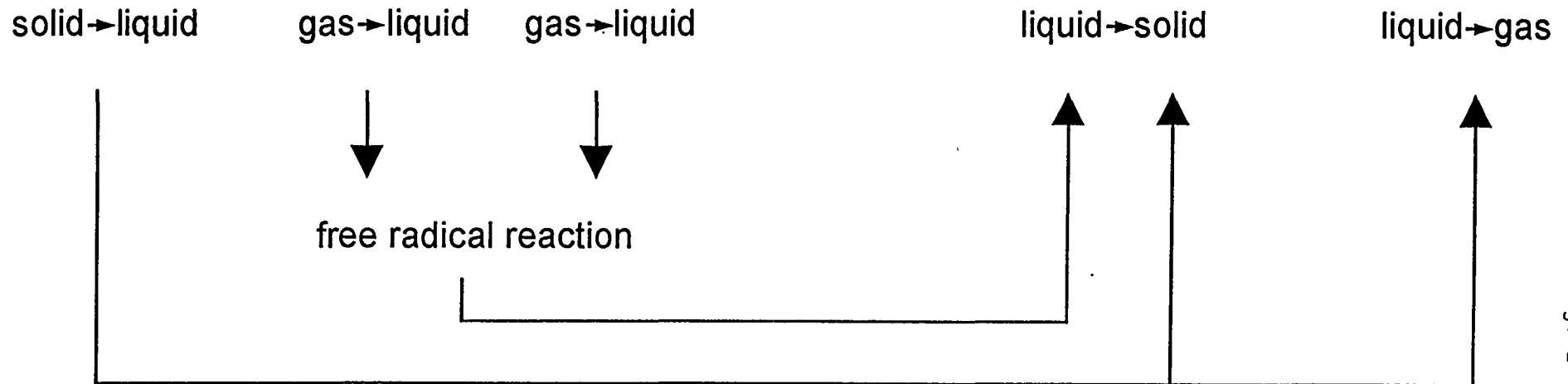
Fig. 2

sulphur compounds in FGD - scrubber liquids

mg/l	high - dust DENOX			no DENOX upstream FGD wet bottom boilers		
	Knepper[1]	Scholven B	Scholven F	Shamrock	Datteln	Rauxel
$S_2O_6^{2-}$	750	300	200	<10	n.d.	25
$S_2O_8^{2-}$	n.d.	20	25	n.d.	n.d.	n.d.
SO_3^-	n.d.	n.d.	n.d.	510	60	160

1) only one oxidation air compressor in operation

Fig. 3

Fig. 4

^{19}F-NMR-spectra of FGD-scrubbing liquids

Top spectrum: S hamrock, KZV$^?$= 28,3; peaks labeled −128.6, KF; −Si$_x$H$_y$F$_z^{4x+y-z}$; −145.0; −150.0; −155,1; AlF$_3$. X-axis: −125, −130, −135, −140, −145, −150, −155.

Middle spectrum: Rauxel, KZV$^?$= 1,2; peaks −155.8, −156.5.

Bottom spectrum: Scholven, KZV$^?$= 1,1; peaks −156.5, AlF^{2+}; AlF$_2^+$, −156.0. X-axis: −151, −152, −153, −154, −155, −156, −157, −158, −159, chemische Verschiebung (ppm).

$^?$ KZV: Konzentrationsverhältnis F/Al

AlF^{2+} = − 156,5 ± 0,5 ppm   AlF$_2^+$ = − 156,0 ± 0,5 ppm   AlF$_3$ = − 155,0 ± 0,5 ppm

AlF$_4^-$ = − 154,5 ± 0,5 ppm   Si$_x$H$_y$F$_z^{4x+y-z}$ = 147,5 ± 5,0 ppm   KF = 128,5 ± 0,5 ppm

Fig. 5

-155.3

-156.3

KZV=5

-155.3

-156.3

KZV=4

-155.3

-156.2

KZV=3

AIF₃

-156.2

-155.2

-156.8

KZV=2

-156.2

-156.7

AIF₂⁺

AIF²⁺

KZV°=1

-151 -152 -153 -154 -155 -156 -157 -158 -159

chemische Verschiebung (ppm)

$^{\circ}$ Konzentrationsverhältnis F / Al

$AlF^{2+} = -156{,}5 \pm 0{,}5$ ppm $AlF_2^{\cdot} = -156{,}0 \pm 0{,}5$ ppm $AlF_3 = -155{,}0 \pm 0{,}5$ ppm

$AlF_4^{\cdot} = -154{,}5 \pm 0{,}5$ ppm

^{19}F-NMR-spectra of AlF_x-Complexes
at different F/Al-Ratios, pH = 4.0

Fig. 6

19F-NMR-spectra of AlFₓ at
different pH-values, F/Al = 3.0
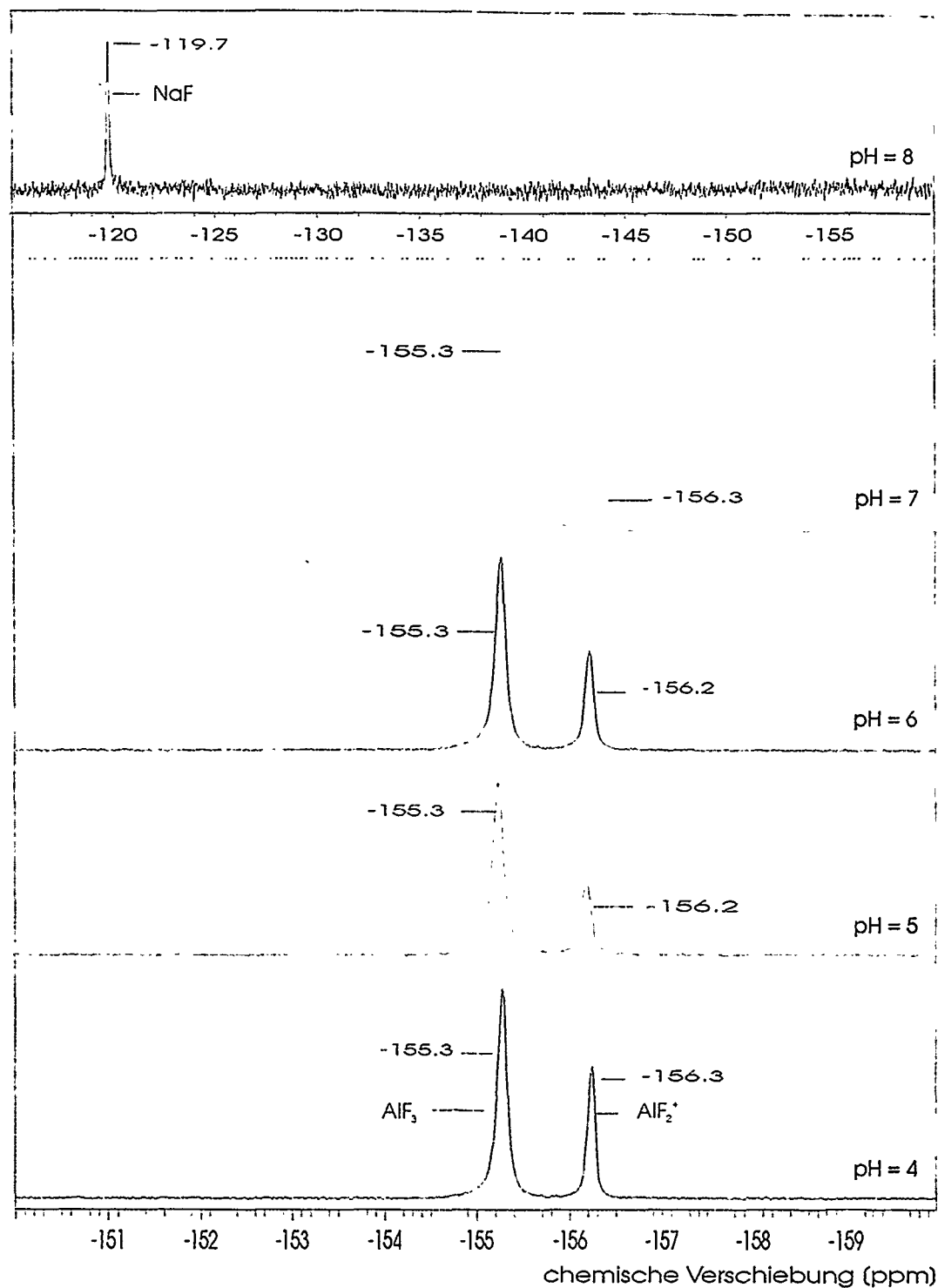
$AlF^{2+} = -156.5 \pm 0.5$ ppm $AlF_2^+ = -156.0 \pm 0.5$ ppm $AlF_3 = -155.0 \pm 0.5$ ppm
$AlF_4^- = -154.5 \pm 0.5$ ppm $NaF = -119.5 \pm 0.5$ ppm

1.20

titration of CaCO$_3$ with H$_2$SO$_4$, pH = 4,5 = const.
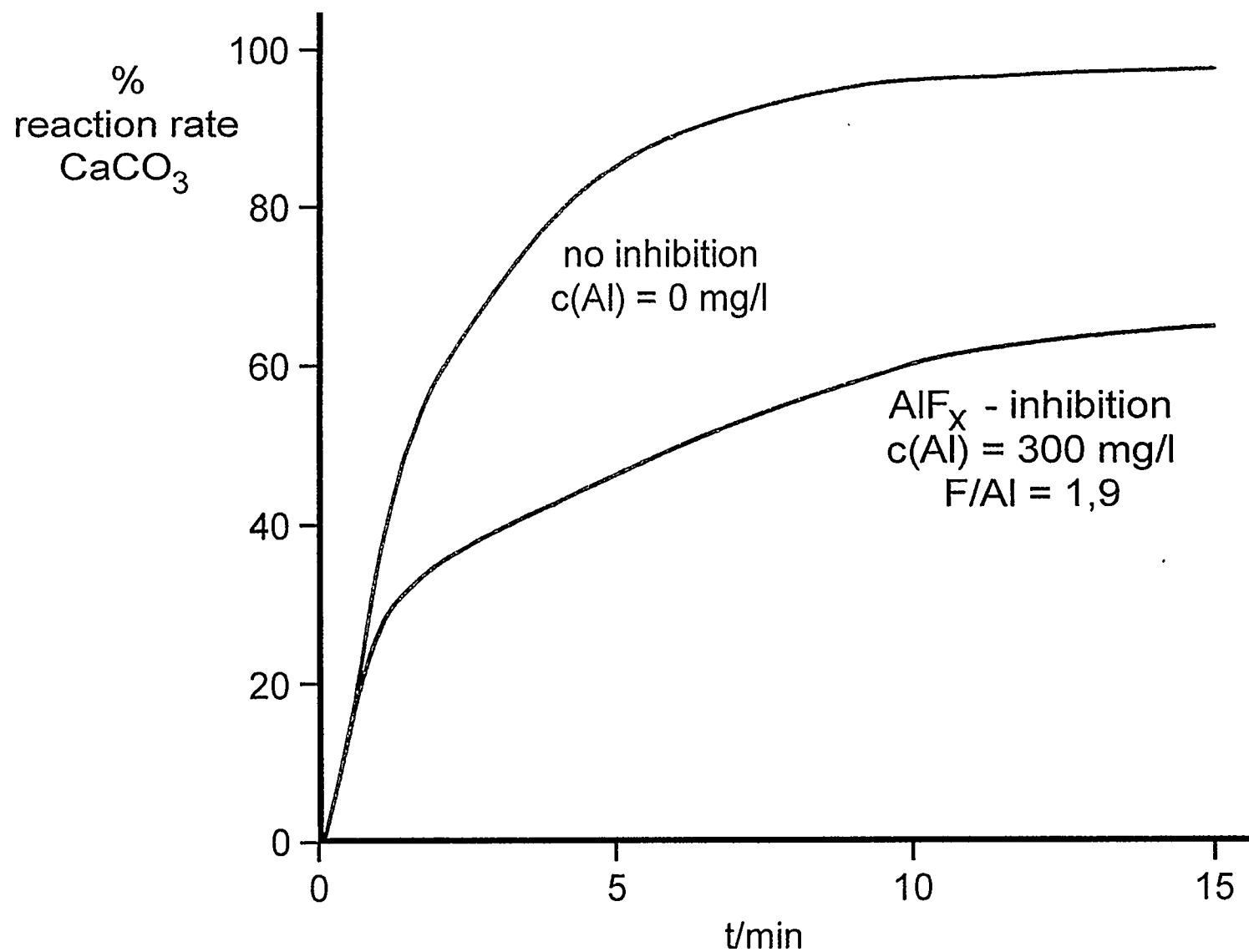
Fig. 7

titration of absorber liquid, pH 4,0 - 7,5 with NaOH

no buffering
c(Al) = 0 mg/l

AlF_x - buffering
c(Al) = 300 mg/l
F/Al = 2,4

ml NaOH ⟶

Fig. 8

Fig. 9

VKR 951 209

KB/Scho BL.F
Bahn 3 v. 15.05.96

Rea - Bahn 3, 350 ml
im Absorber berge mischt.

11:30 h, 2 ppm of antifoam added

200mg SO_2/m^3 n. REA
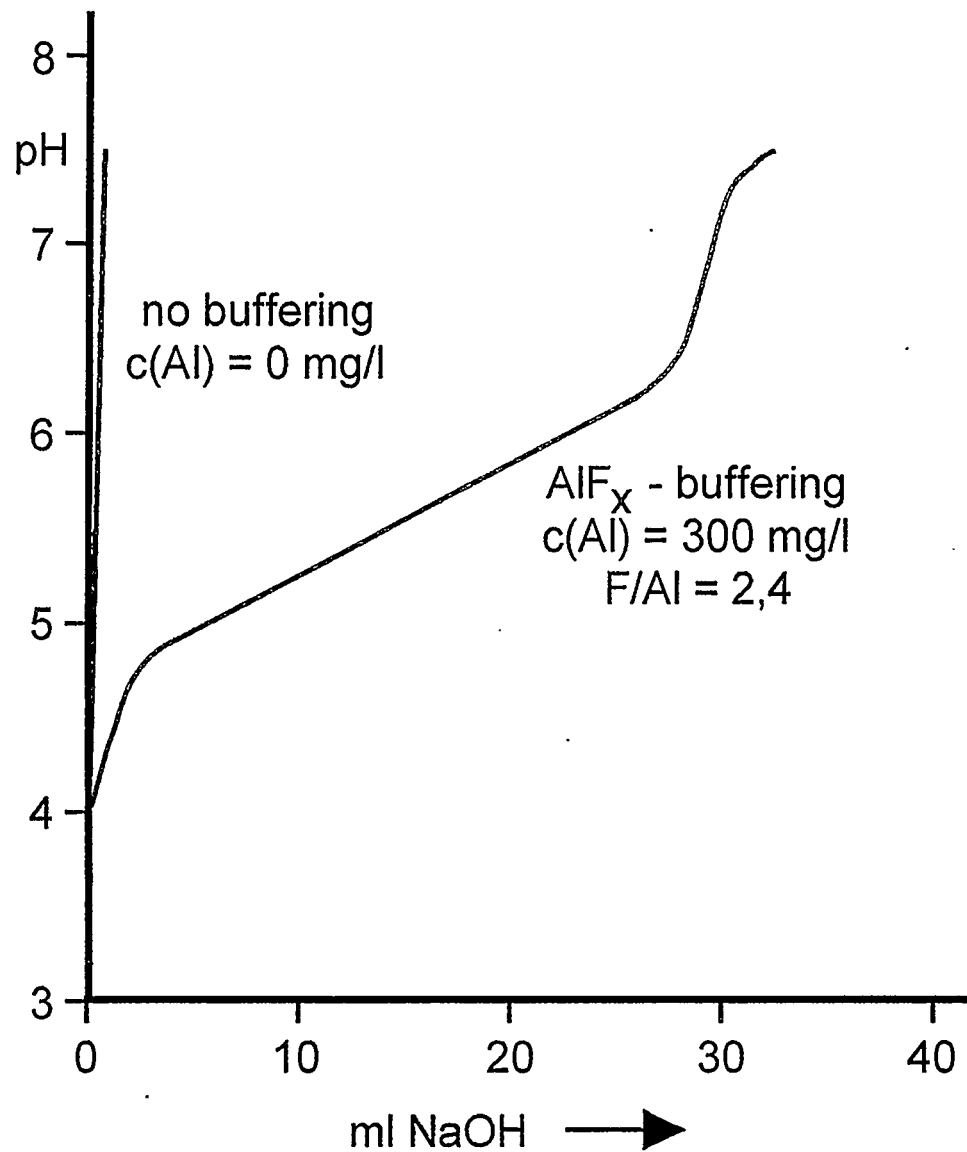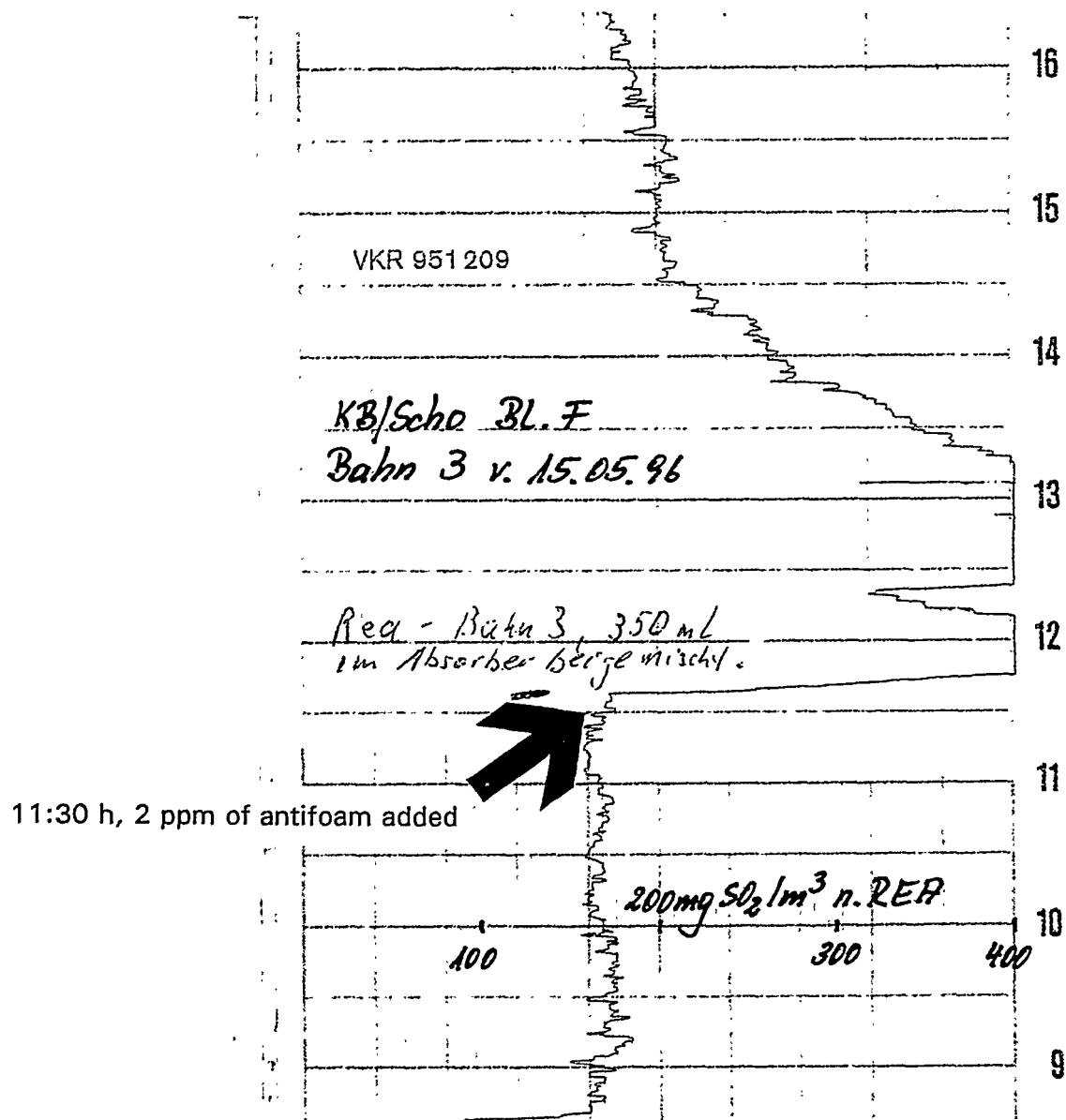
effect of antifoam on SO_2-clean gas
concentration, Scholven F, 15.05.1996

VKR

Analytik und Versuchswesen

TA

KB/Scho, Block E
NH3—Gehalte der E—Filterasche

Nachladung 3. Ebene
(KWH-Wabe) bei 9.271 Bh
Datum: 25.07.91

Nachladung 4. Ebene
(KWH-Wabe) bei 22.900 Bh
Datum: 01.08.93

Betriebsstunden
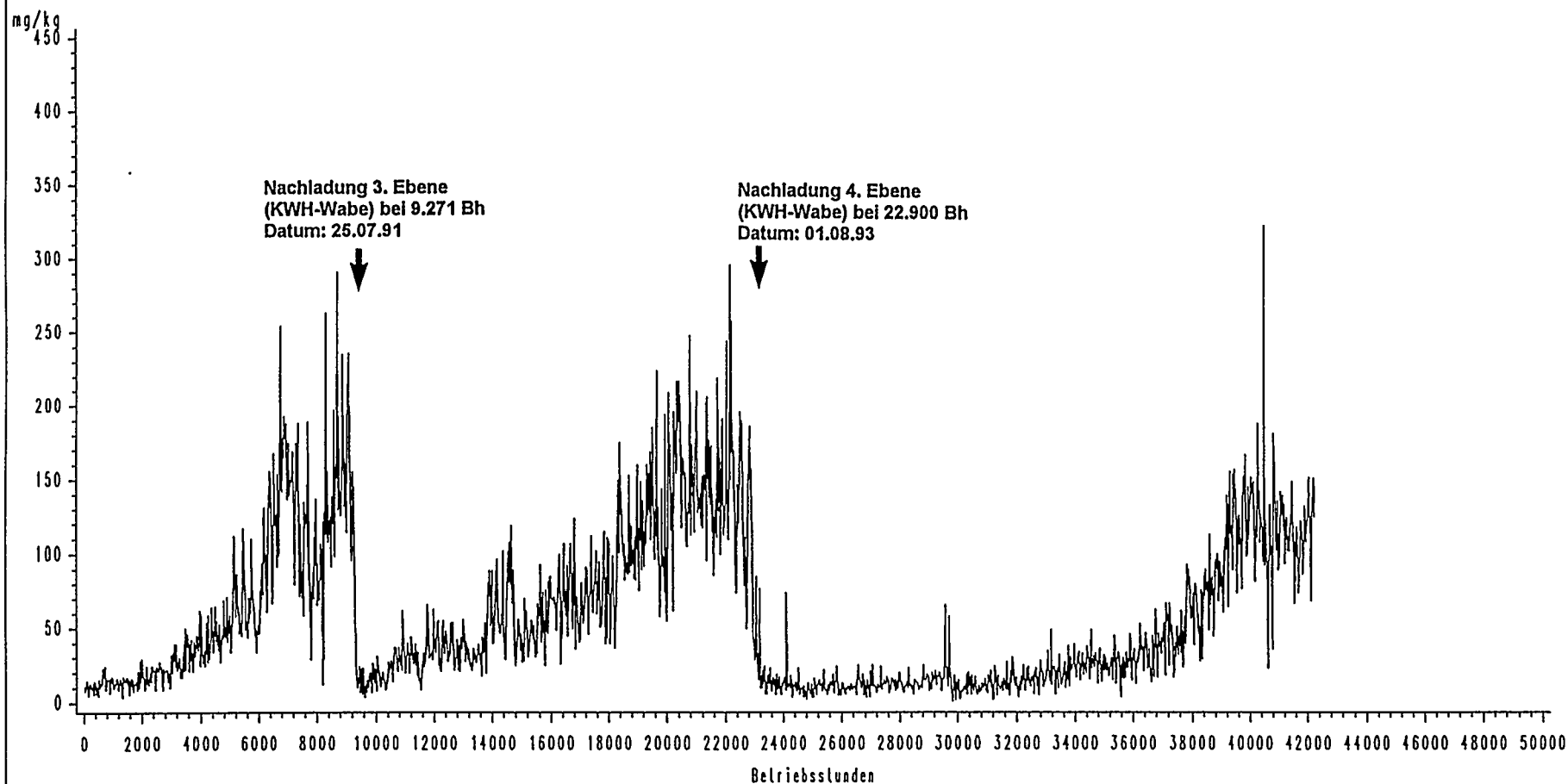
Abteilung : TA—B/weh
Datum   : 10.07.1996

Unterschrift:

Fig. 10

Fig. 11
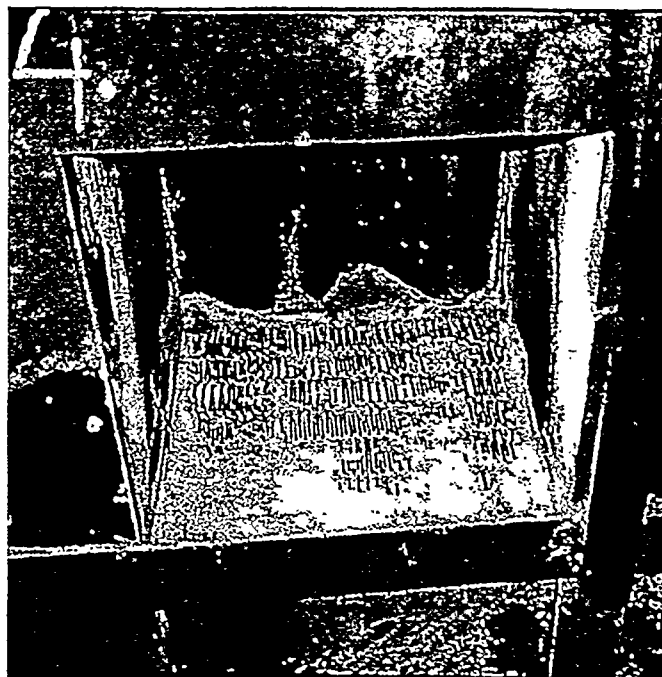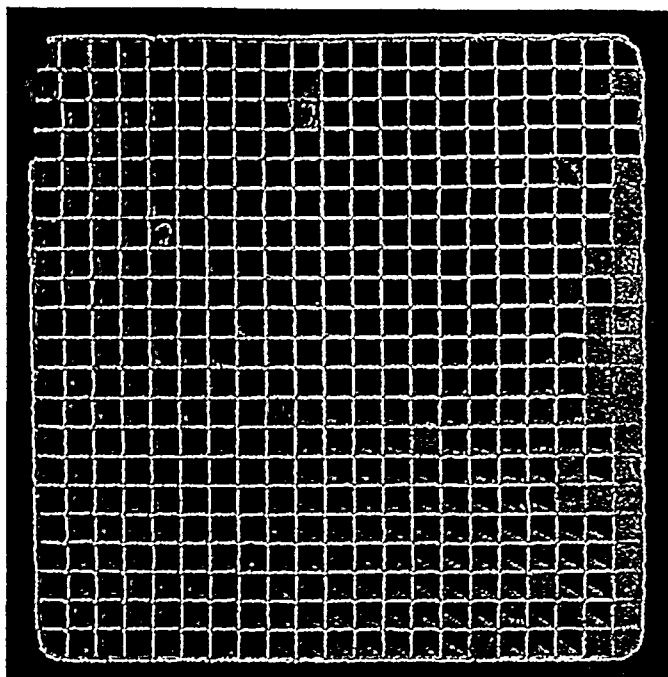
**fould ducts of honeycomb catalysts and
plugging of plate-type catalysts (piled cages)**

Fig. 12
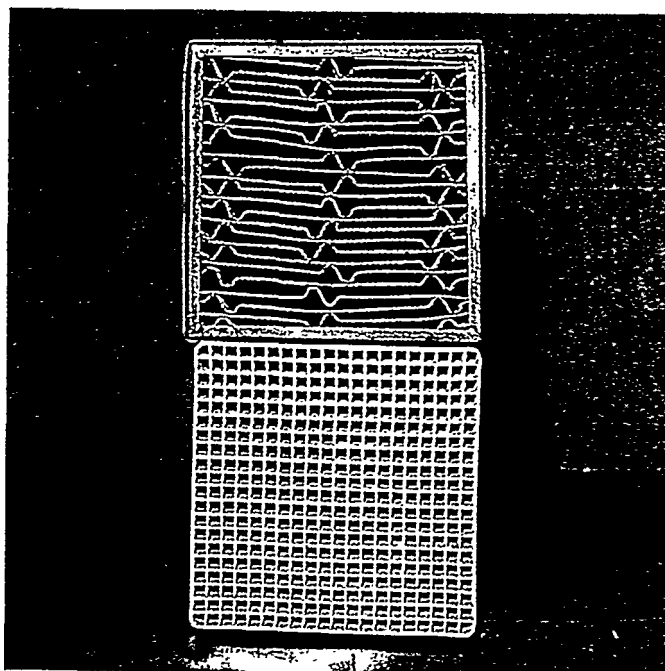
catalyst test elements for bench-scale reactor

Fig. 13

	∅		∅		∅
Waben	1,34	Waben	1,25	Waben	1,10
Platten	1,08	Waben	2,01	Waben	1,62
Platten	1,35	Platten	1,22	Platten	1,03
Platten	1,20	Platten	1,19	Platten	1,01
	4,97		5,67		4,76

10/91   5/92   4/93

erforderliches Mindestpotential
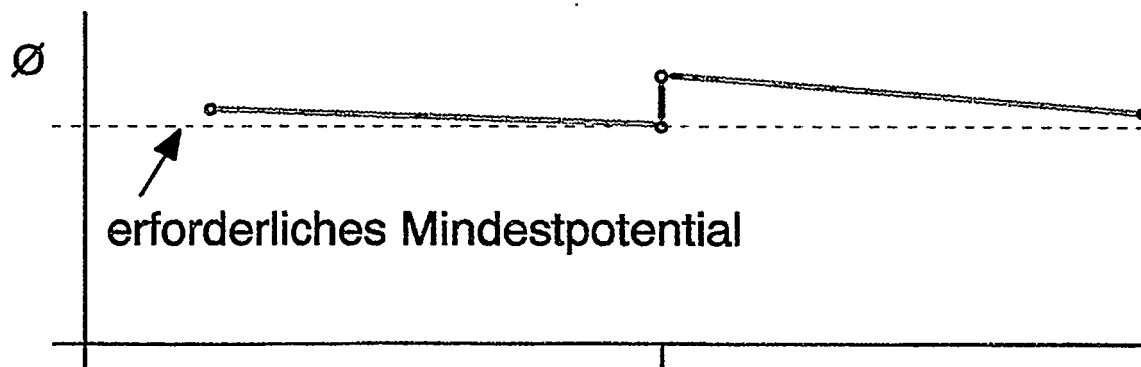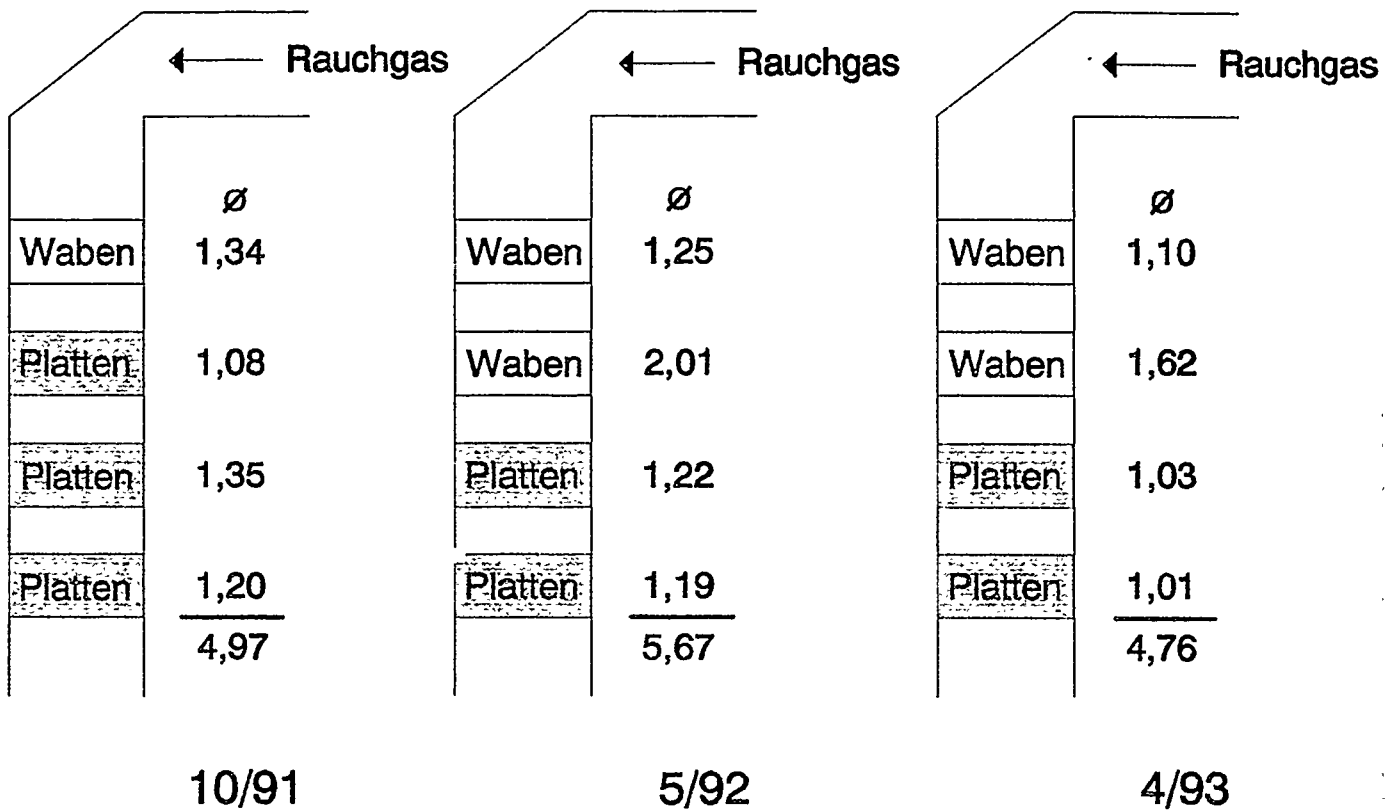
development of DENOX potential depending
on the layers in the course of time;
Buer district heat power plant

Fig. 14

ammonia

concentration

NO$_x$

NH$_3$
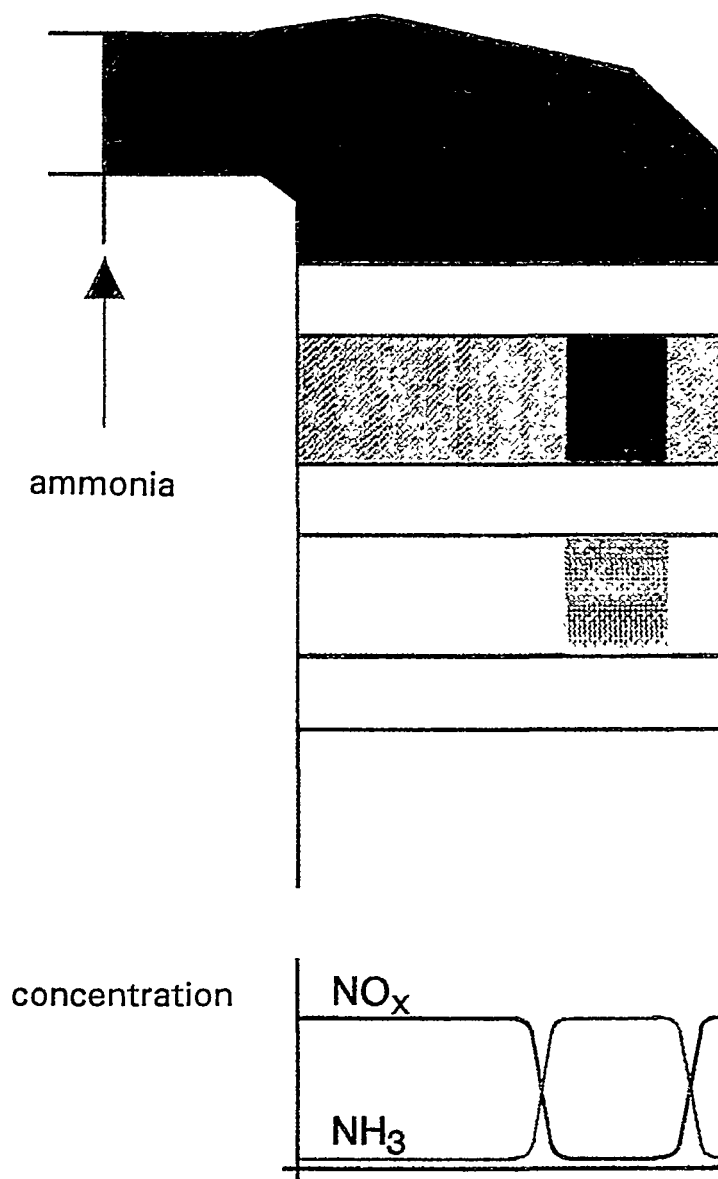
NH$_3$-slip by mal distribution

Fig. 15

NO$_x$
[mg/m³]

200

100

0

Y

X
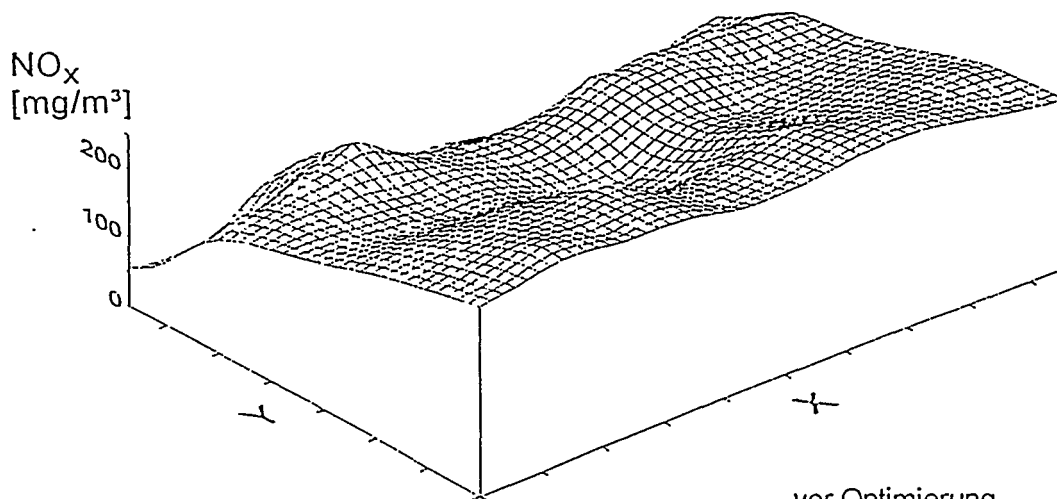
<u>vor Optimierung</u>

NO$_x$ im Mittel: 192 mg/m³ (i.N.tr.,6% O2)
Sigma (n-1):   57 mg/m³ (i.N.tr.,6% O2)
Variationskoeff.:   30,0 %

NO$_x$
[mg/m³]

200

100

0

Y

X
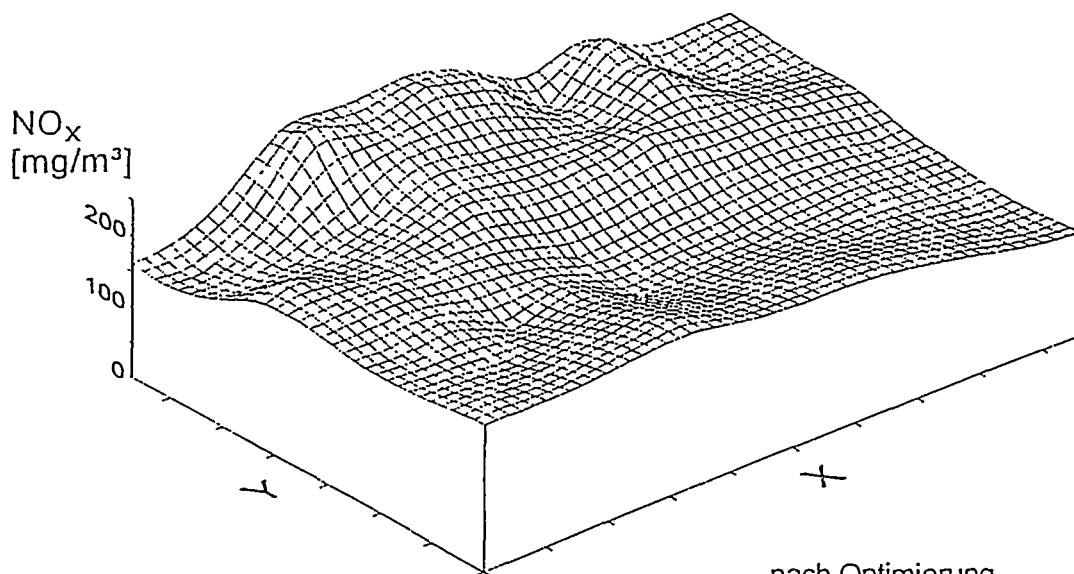
<u>nach Optimierung</u>

NO$_x$ im Mittel: 186 mg/m³ (i.N.tr.,6% O2)
Sigma (n-1):   31 mg/m³ (i.N.tr.,6% O2)
Variationskoeff.:   16,6 %

**NO$_x$-profile downstream SCR plant before
and after optimization of ammonia injection**

Converting SDAP into Gypsum in a Wet Limestone Scrubber

Fogh, F.
Fælleskemikerne/ELSAMPROJEKT A/S
Kraftværksvej 53
DK 7000 Fredericia
Denmark

ABSTRACT

The ELSAM power pool has an installed electrical capacity of approx. 5 GW_e, mainly firing import coal. The major base load units are equipped with desulphurization units and three different desulphurization technologies are used: the wet limestone gypsum process, the spray dry absorption process and a sulphuric acid process.

Gypsum and sulphuric acid are commercialized, whereas it has been difficult to utilize the spray dry absorption product (SDAP).

The main constituents of SDAP are calcium sulphite, calcium chloride, hydrated lime and impurities mainly originating from fly ash.

Sulphite can be oxidized into sulphate in acidic solution - the reaction is utilized in the wet limestone gypsum process - and the possibility of using any spare capacity in the wet limestone gypsum units to oxidize the sulphite content of SDAP into sulphate and produce usable gypsum has been investigated in the laboratory and in a 400 MW_e equivalent wet limestone unit.

Laboratory experiments showed that SDAP can be dissolved and oxidized at the slurry conditions of a wet limestone scrubber. The mass transfer of oxygen was found to be rate limiting. The laboratory results were confirmed in short duration experiments (2-4 hours) where SDAP was fed into a 400 MW_e equivalent wet limestone unit at a rate of 3.5 t/h .

The impact on the quality of the produced gypsum and the effect of the increased chloride and fly ash load on the wastewater plant has been addressed in a long-term (5 days) full-scale experiment. During the long-term test a reduced limestone reactivity , probably caused by the fly ash content of the SDAP, was observed. Apart from the implications caused by the reduced limestone reactivity, the SDAP was fully converted into gypsum and the gypsum quality was only marginally altered during the long-term test where up to 30% of the gypsum originated from the SDAP.

The limestone inhibition effect of the addition of SDAP is currently being studied in the laboratory in order to determine the effect of different SDAP types (plant/ coal sources) on limestone reactivity before further long-term full-scale tests are performed and permanent use of the process planned.

1   Introduction

The ELSAM power pool has an installed electrical capacity of approx. 5 GW_e, mainly firing import coal.

The major base load units with an equivalent capacity of 1.9 GW_e are equipped with desulphurization units, and an equivalent desulphurization capacity of about 1 GW_e is being constructed.

Three different desulphurization technologies are used:

- Wet limestone gypsum process (0.4 GW_e + 1 GW_e being constructed).
- Spray dry absorption process (1.2 GW_e).
- Sulphuric acid process (SNOX) (0.3 GW_e).

Gypsum and sulphuric acid are commercialized, whereas it has been difficult to utilize the spray dry absorption product (SDAP).

SDAP is produced at two power plants.

- Studstrupværket (MKS) in two 380 MW_e units.
- FYNSVÆRKET (FVO) in one 445 MW_e unit.

The total annual SDAP production capacity at these power plants is in the range of 300,000 t. However, in 1994 the actual SDAP production was 135,000 t, the majority of which had to be disposed of - partly as a noise barrier around the FVO coal yard.

It is estimated that approx. 20,000 t SDAP will be used as a sulphur fertilizer in 1995. Up to 50,000 t are estimated to be used as sulphur fertilizer in the future, but additional high tonnage applications are highly required.

2   Processes and Reactions

Two fundamental observations:

- One of the important chemical reactions that takes place in a wet desulphurization plant producing gypsum is the forced oxidation of sulphite species into sulphate.

- The sulphite content of the SDAP is the main obstacle against its useful application.

are the germ of the idea to use any spare capacity of a wet limestone scrubber for the forced oxidation of SDAP into gypsum.

The feasibility of such a process is the topic of an R&D effort launched by ELSAM and some of the findings are presented in the following.

2.1 SDAP Process and Product

SDAP is produced in the spray dry absorption (SDA) desulphurization process. The SDA process adopted in the ELSAM area uses slaked lime that is atomized and spray dried with hot (120-140°C) and ash free (less than 400 mg/Nm^3 particulate) flue gas.

SO$_2$ (and HCl) in the flue gas are absorbed in the atomized droplets of slaked lime. Simultaneously with the evaporation of water from the atomized droplets, chemical reactions take place and a fine (d$_{90}$<40 µm, d$_{50}$=15 µm), white and dry (1-2% H$_2$O) powder known as SDAP is produced and trapped in a bag filter. The overall chemical reactions are:

$$CaO(aq) + SO_2(g) + \tfrac{1}{2}H_2O(l) \rightarrow CaSO_3 \cdot \tfrac{1}{2}H_2O(s) \qquad (1)$$
$$2CaO(aq) + 2HCl(g) + H_2O(l) \rightarrow CaCl_2 \cdot Ca(OH)_2 \cdot H_2O(s) \qquad (2)$$

The reactions take place in alkaline (elevated pH) aqueous solution (droplets).

Apart from calcium sulphite and calcium chloride, SDAP also contains:

- Excess lime present as Ca(OH)$_2$ and CaCO$_3$.
- Gypsum due to a partial oxidation of SO$_2$ to SO$_3$ resulting in sulphates.
- Particulate matter originating from the flue gas (fly ash) and from the lime.

Typical SDAP analyses, content and standard deviations (weight basis) are given in table 1.

The main difference being that the chlorine content in the SDAP produced at MKS is higher than in the SDAP produced at FVO contrary to the content of insolubles.

	MKS	FVO
SO$_3^{2-}$ (sulphite)	37.5%±2.9%	39.6%±3.5%
SO$_4^{2-}$ (sulphate)	8.7%±3.0%	10.1%±1.6%
Cl$^-$ (chloride)	4.5%±0.6%	3.2%±0.6%
Ca(OH)$_2$ (excess lime)	6.3%±4.2%	4.5%±3%
Insolubles	≈0	2.8%

Table 1: SDAP analysis (content and standard deviation)

The reasons for this difference are that MKS uses saltwater as part of their process water in the SDA and that FVO uses a less efficient three-zone electrostatic precipitator (ESP) in front of the SDA.

The sulphite and sulphate contained in the SDAP does not dissolve in water and a sludge of SDAP in water has a pH above 10 due to the lime content. SDAP dissolves readily under acidic conditions.

The difficulties in finding useful applications for the SDAP are mainly associated with the sulphite content.

2.2 Symbiosis with the Gypsum Process

In the gypsum process SO_2 from the flue gas is absorbed in an aqueous slurry of limestone with a pH between 5 and 6. Under these conditions the absorbed SO_2 is present as hydrogen sulphite (HSO_3^-), which is readily oxidized to sulphate (SO_4^{2-}), and this is in turn combined with the calcium ions from the limestone and precipitated as gypsum. The important reaction in this context is the oxidation reaction :

$$HSO_3^-(aq) + \tfrac{1}{2}O_2(g) \rightarrow SO_4^{2-}(aq) + H^+(aq) \qquad (3)$$

This implies that it is possible to oxidize the sulphite contained in the SDAP by dissolving it under acidic conditions according to:

$$CaSO_3 \cdot \tfrac{1}{2}H_2O(s) + H^+(aq) \rightarrow Ca^{2+}(aq) + HSO_3^-(aq) + \tfrac{1}{2}H_2O(aq) \qquad (4)$$

followed by oxidation according to reaction (3). Because of the presence of calcium ions gypsum will precipitate.

A possible process setup would be an aerated tank fed with SDAP and acid combined with a slurry dewatering system to recover the gypsum. The equipment will be very similar to the slurry tank and slurry dewatering system of a wet desulphurization plant.

The idea to use any spare capacity of an existing wet FGD plant has emerged and is currently being investigated in order to evaluate the feasibility and to locate the pros and cons of the concept.

3 Project Setup and Progress

The project has until now included laboratory investigations, short duration full-scale tests and one long-term full-scale test. Results from these activities will be presented below.

Parallel to the technical investigations and tests, feasibility studies considering economic and practical issues have been made. These results are influenced by factors such as geography and legislation - ie. factors specific to the ELSAM area and hence not discussed further in this context.

3.1 Laboratory Investigations

The purpose of the laboratory experiments was to evaluate the kinetics of the combined SDAP dissolution and oxidation reactions at typical wet FGD conditions.

In the laboratory experiments, SDAP was converted in a 400 ml stirred and aerated reactor at 50°C. Excess SDAP and distilled water were added to the reactor making up

a saturated SDAP/water slurry which was subsequently aerated with an N_2/O_2 gas mixture at a constant pH.

The conversion rate (combined dissolution and oxidation rate) of the sulphite content in the SDAP was determined and the effect of pH (3.5-6.0), excess SDAP (1-16%), O_2 partial pressure (0.08-1.01 bar) and - to a certain extent aeration - was investigated.

The effect of the addition of manganese (known as an oxidation catalyst) was also investigated.

Sulphite conversion rates in the order of 10^{-5}-10^{-6} mol/l/s without addition of manganese were found; the same range of sulphite oxidation rate is found in wet FGD plants.

Without addition of manganese, the effect of pH, excess SDAP and aeration were limited but the O_2 partial pressure had a (positive) linear effect on the conversion rate.

Together with the observation of a very low value of dissolved oxygen in the slurry, it is concluded that the conversion rate is mainly limited by the mass transfer of oxygen and neither by the dissolution of SDAP nor the oxidation reaction itself.

It was observed that the conversion rate rises approx. one order of magnitude when adding manganese. Addition of manganese also resulted in conversion rate dependency of pH; the conversion rate was reduced at increased pH.

The purity of the produced gypsum was determined by TGA and found to be 92-97%.

3.2 Short Duration Full-Scale Tests

Based on the results of the laboratory experiments it was decided to perform full-scale experiments with direct addition of SDAP to the wet FGD plant at the 400 MW_e power plant I/S Vestkraft (VKE).

The wet FGD plant at VKE has been delivered by FLS Miljø according to the design of Mitsubishi Heavy Industries with a cocurrent absorption tower combined with a tank for forced oxidation. Limestone ($d_{90} < 45$ μm) is used as absorbent and wall board quality gypsum (<10% water and >94.5% gypsum) is produced.

The wet FGD plant is designed for a flue gas flow of 1.16×10^6 m_0^3/h with up to 2000 ppm SO_2 and 93.5% desulphurization.

The oxidation tank has a volume of approx. 2,000 m^3 and the normal content of solids (gypsum) is 20%. Oxidation air is introduced into the oxidation tank at 2.5-4 times the stoichiometric amount.

The slurry dewatering system has two sets of hydro cyclones and 3×50% vacuum band filters with gypsum wash.

The main objective of the short-duration full-scale experiments was to confirm the findings of the laboratory experiments regarding the possibility of oxidizing the sulphite in the SDAP and evaluate the impact on desulphurization.

Slurry with 35% SDAP was transported in a 25 m^3 silo tanker from FVO to VKE. At VKE the slurry was introduced as short-duration pulses (5-10 minutes) into the oxidation tank of the wet FGD plant by means of a pump submerged in the silo tanker.

During the experiments, an extended analysis programme was run focusing on sulphite in order to follow the oxidation. Sulphite was monitored in the oxidation tank, in the gypsum and in the overflow of the second set of hydro cyclones; the fine particles of the SDAP will end up in the overflow of the second set of hydro cyclones if they do not dissolve readily.

Table 2 shows the major process parameters of the four short-duration full-scale SDAP oxidation tests, and figure 1 shows the variation in pH and sulphite content in the oxidation tank and the SO_2 concentration in the stack during test #2.

Test	pH	Sulphur load (t/h)		Oxidation air (m_0^3/h)	Comments
		coal	SDAP*	(extra)	
#1	5.4	≈ 1.6	≈ 0.22 (+14%)	+2000	Low pH to facilitate SDAP dissolution. Additional air to ensure oxidation.
#2	5.6	≈ 1.6	≈ 0.20 (+13%)	+2000	Normal pH. Additional air to ensure oxidation.
#3	5.5 - 5.6	≈ 1.6	≈ 0.26 (+16%)	0	Normal pH. Normal air flow.
#4	5.5 - 5.6	≈ 1.6	≈ 0.56 (+35%)	0	Normal pH. Normal air flow. High SDAP feed rate.

* Sulphur load from the SDAP sulphite content.

Table 2: Short-duration full-scale SDAP oxidation tests.

When SDAP was introduced, the short-duration pulses were seen as pH peaks about 0.2 pH units high due to the excess lime content in the SDAP. Close examination of the corresponding SO_2 concentration in the stack shows a slight reduction during each pH peak.

Figure 1: SO_2 stack concentration, pH and slurry sulphite content during short duration full-scale SDAP test #2.

In this particular case the sulphite content was analysed once every hour and was found to remain at a level of approx. 140 mg/l except when samples were taken during an SDAP feed pulse. During an SDAP feed pulse, a sulphite content of about 200 mg/l was observed - levels of up to 1000 mg/l are acceptable with regard to the gypsum quality. This type of observation was carried out consistently in all four tests.

The sulphite content in the overflow from the second set of hydro cyclones and in the gypsum remained constant during all four tests.

The findings can be summarized as follows:

- SDAP can be dissolved in the absorber slurry of a wet FGD plant and converted into gypsum.

- An SDAP conversion capacity of at least 3.5 t/h was found during the short-duration full-scale tests at VKE.

- The excess lime content in the SDAP is at least partially active during the desulphurization process.

These changes did not influence the primary sedimentation step and the performance of the wastewater plant apart from the extra hydraulic load.

5   Conclusion

The laboratory experiments, the short duration full-scale tests and the long-term full-scale tests have all shown that it is possible to convert SDAP into gypsum in a wet limestone scrubber.

It is specifically concluded that:

with combustion of the solid fuels coal, straw and wood.

1.1   Solid Fuels

Coal, straw and wood are closely related. The precursor of coal was peat, which was formed by bacterial and chemical action on plant debris. Millions of years of heat and pressure metamorphosed the peat into various ranks of coal, from lignite to anthracite. Fuel compositions are often reported in two ways: by proximate analysis and ultimate analysis. Proximate analysis is the determination by standard methods of moisture, volatile matter, fixed carbon (the residue after the volatile matter has been driven out) and ash (inorganic residue after the fuel has been burned). Ultimate analysis is the determination of ash and the elemental constituents: carbon, hydrogen, nitrogen, oxygen, sulphur and chlorine. Both kinds of analysis are usually reported together with the high (including water condensation) and low heating values (MJ/kg) of the fuel. Calculation of the flue gas composition is based on the ultimate analysis. Table 1 shows the proximate and ultimate analyses of a number of fuels together with the stoichiometric amounts of air for combustion and the flue gas generated, which is seen to be almost independent of fuel type.

	Ultimate analysis as received					Proximate analysis daf						
Rank	Moisture	Ash	Volatiles	Fixed C	LHV	C	O	H	S	N	Air	Flue gas
	%wt	%wt	%wt	%wt	MJ/kg daf	%wt	%wt	%wt	%wt	%wt	Nm³/MJ	Nm³/MJ
ma	13.2	18.9	2.6	65.3	31.89	94.7	4.0	0.6	0.4	0.3	0.27	0.27
an	4.3	9.6	5.1	81.0	34.81	92.5	2.8	2.8	0.9	1.0	0.26	0.26

Figure 1: SO$_2$ stack concentration, pH and slurry sulphite content during short duration full-scale SDAP test #2.

In this particular case the sulphite content was analysed once every hour and was found to remain at a level of approx. 140 mg/l except when samples were taken during an SDAP feed pulse. During an SDAP feed pulse, a sulphite content of about 200 mg/l was observed - levels of up to 1000 mg/l are acceptable with regard to the gypsum quality. This type of observation was carried out consistently in all four tests.

The sulphite content in the overflow from the second set of hydro cyclones and in the gypsum remained constant during all four tests.

The findings can be summarized as follows:

• SDAP can be dissolved in the absorber slurry of a wet FGD plant and converted into gypsum.

• An SDAP conversion capacity of at least 3.5 t/h was found during the short-duration full-scale tests at VKE.

• The excess lime content in the SDAP is at least partially active during the desulphurization process.

3.3 The Need for Long-Term Full-Scale Tests

The possibility of converting SDAP into gypsum was shown in the short-duration full-scale tests but further investigations are needed due to the rudimentary SDAP feed system and the short duration (2-4 hours) of the tests.

Everything entering a wet FGD plant has to leave it either through the flue gas system, with the gypsum and/or through the wastewater plant. The residence time of flue gas born components is insignificant (minutes) compared to the residence time of gypsum and water born components (hours, days and even weeks). Table 3 lists typical residence times for chloride, gypsum and insoluble material in the wet FGD plant at VKE.

Component	Carrier stream	Conditions	Residence time
Gypsum	Gypsum	1% S in coal, 100% load 2% S in coal, 100% load	70 h (2^d22^h) 35 h (1^d11^h)
Chloride	Wastewater	0.1% Cl in coal, 100% load 0.4% Cl in coal, 100% load	350 h ($\approx 2^w$) 87 h (3^d15^h)
Insolubles (larger particles)	Gypsum		140 h (5^d19^h)

These changes did not influence the primary sedimentation step and the performance of the wastewater plant apart from the extra hydraulic load.

5 Conclusion

The laboratory experiments, the short duration full-scale tests and the long-term full-scale tests have all shown that it is possible to convert SDAP into gypsum in a wet limestone scrubber.

It is specifically concluded that:

- SDAP dissolves readily in the absorber slurry;
- the sulphite contained in the SDAP is totally oxidized;
- the gypsum quality is only marginally altered;
- the hydraulic load of the wastewater plant is increased as a result of the chloride contained in the SDAP;
- addition of SDAP can result in reduced limestone reactivity - probably caused by the fly ash content in the SDAP.

The future development of the concept to convert SDAP into gypsum in a wet limestone scrubber is linked to better understanding of the influence of the SDAP on the limestone reactivity.

Laboratory investigations regarding the influence of SDAP from different sources (EVO

2.1 SDAP Process and Product

SDAP is produced in the spray dry absorption (SDA) desulphurization process. The SDA process adopted in the ELSAM area uses slaked lime that is atomized and spray dried with hot (120-140°C) and ash free (less than 400 mg/Nm^3 particulate) flue gas.

SO$_2$ (and HCl) in the flue gas are absorbed in the atomized droplets of slaked lime. Simultaneously with the evaporation of water from the atomized droplets, chemical reactions take place and a fine (d$_{90}$<40 μm, d$_{50}$=15 μm), white and dry (1-2% H$_2$O) powder known as SDAP is produced and trapped in a bag filter. The overall chemical reactions are:

$$CaO(aq) + SO_2(g) + \tfrac{1}{2}H_2O(l) \rightarrow CaSO_3 \cdot \tfrac{1}{2}H_2O(s) \qquad (1)$$
$$2CaO(aq) + 2HCl(g) + H_2O(l) \rightarrow CaCl_2Ca(OH)_2 \cdot H_2O(s) \qquad (2)$$

The reactions take place in alkaline (elevated pH) aqueous solution (droplets).

Apart from calcium sulphite and calcium chloride, SDAP also contains:

- Excess lime present as Ca(OH)$_2$ and CaCO$_3$.
- Gypsum due to a partial oxidation of SO$_2$ to SO$_3$ resulting in sulphates.
- Particulate matter originating from the flue gas (fly ash) and from the lime.

Typical SDAP analyses, content and standard deviations (weight basis) are given in table 1.

The main difference being that the chlorine content in the SDAP produced at MKS is higher than in the SDAP produced at FVO contrary to the content of insolubles.

	MKS	FVO
SO$_3^{2-}$ (sulphite)	37.5%±2.9%	39.6%±3.5%
SO$_4^{2-}$ (sulphate)	8.7%±3.0%	10.1%±1.6%
Cl$^-$ (chloride)	4.5%±0.6%	3.2%±0.6%
Ca(OH)$_2$ (excess lime)	6.3%±4.2%	4.5%±3%
Insolubles	≈0	2.8%

Table 1: SDAP analysis (content and standard deviation)

The reasons for this difference are that MKS uses saltwater as part of their process water in the SDA and that FVO uses a less efficient three-zone electrostatic precipitator (ESP) in front of the SDA.

The sulphite and sulphate contained in the SDAP does not dissolve in water and a sludge of SDAP in water has a pH above 10 due to the lime content. SDAP dissolves readily under acidic conditions.

The difficulties in finding useful applications for the SDAP are mainly associated with the sulphite content.

2.2 Symbiosis with the Gypsum Process

In the gypsum process SO_2 from the flue gas is absorbed in an aqueous slurry of limestone with a pH between 5 and 6. Under these conditions the absorbed SO_2 is present as hydrogen sulphite (HSO_3^-), which is readily oxidized to sulphate (SO_4^{2-}), and this is in turn combined with the calcium ions from the limestone and precipitated as gypsum. The important reaction in this context is the oxidation reaction :

$$HSO_3^-(aq) + \tfrac{1}{2}O_2(g) \rightarrow SO_4^{2-}(aq) + H^+(aq) \qquad (3)$$

This implies that it is possible to oxidize the sulphite contained in the SDAP by dissolving it under acidic conditions according to:

$$CaSO_3 \cdot \tfrac{1}{2}H_2O(s) + H^+(aq) \rightarrow Ca^{2+}(aq) + HSO_3^-(aq) + \tfrac{1}{2}H_2O(aq) \qquad (4)$$

followed by oxidation according to reaction (3). Because of the presence of calcium ions gypsum will precipitate.

A possible process setup would be an aerated tank fed with SDAP and acid combined with a slurry dewatering system to recover the gypsum. The equipment will be very similar to the slurry tank and slurry dewatering system of a wet desulphurization plant.

The idea to use any spare capacity of an existing wet FGD plant has emerged and is currently being investigated in order to evaluate the feasibility and to locate the pros and cons of the concept.

3 Project Setup and Progress

The project has until now included laboratory investigations, short duration full-scale tests and one long-term full-scale test. Results from these activities will be presented below.

Parallel to the technical investigations and tests, feasibility studies considering economic and practical issues have been made. These results are influenced by factors such as geography and legislation - ie. factors specific to the ELSAM area and hence not discussed further in this context.

3.1 Laboratory Investigations

The purpose of the laboratory experiments was to evaluate the kinetics of the combined SDAP dissolution and oxidation reactions at typical wet FGD conditions.

In the laboratory experiments, SDAP was converted in a 400 ml stirred and aerated reactor at 50°C. Excess SDAP and distilled water were added to the reactor making up

a saturated SDAP/water slurry which was subsequently aerated with an N_2/O_2 gas mixture at a constant pH.

The conversion rate (combined dissolution and oxidation rate) of the sulphite content in the SDAP was determined and the effect of pH (3.5-6.0), excess SDAP (1-16%), O_2 partial pressure (0.08-1.01 bar) and - to a certain extent aeration - was investigated.

The effect of the addition of manganese (known as an oxidation catalyst) was also investigated.

Sulphite conversion rates in the order of 10^{-5}-10^{-6} mol/l/s without addition of manganese were found; the same range of sulphite oxidation rate is found in wet FGD plants.

Without addition of manganese, the effect of pH, excess SDAP and aeration were limited but the O_2 partial pressure had a (positive) linear effect on the conversion rate.

Together with the observation of a very low value of dissolved oxygen in the slurry, it is concluded that the conversion rate is mainly limited by the mass transfer of oxygen and neither by the dissolution of SDAP nor the oxidation reaction itself.

It was observed that the conversion rate rises approx. one order of magnitude when adding manganese. Addition of manganese also resulted in conversion rate dependency of pH; the conversion rate was reduced at increased pH.

The purity of the produced gypsum was determined by TGA and found to be 92-97%.

3.2 Short Duration Full-Scale Tests

Based on the results of the laboratory experiments it was decided to perform full-scale experiments with direct addition of SDAP to the wet FGD plant at the 400 MW_e power plant I/S Vestkraft (VKE).

The wet FGD plant at VKE has been delivered by FLS Miljø according to the design of Mitsubishi Heavy Industries with a cocurrent absorption tower combined with a tank for forced oxidation. Limestone ($d_{90} < 45$ μm) is used as absorbent and wall board quality gypsum (<10% water and >94.5% gypsum) is produced.

The wet FGD plant is designed for a flue gas flow of 1.16×10^6 m_0^3/h with up to 2000 ppm SO_2 and 93.5% desulphurization.

The oxidation tank has a volume of approx. 2,000 m^3 and the normal content of solids (gypsum) is 20%. Oxidation air is introduced into the oxidation tank at 2.5-4 times the stoichiometric amount.

The slurry dewatering system has two sets of hydro cyclones and 3×50% vacuum band filters with gypsum wash.

The main objective of the short-duration full-scale experiments was to confirm the findings of the laboratory experiments regarding the possibility of oxidizing the sulphite in the SDAP and evaluate the impact on desulphurization.

Slurry with 35% SDAP was transported in a 25 m^3 silo tanker from FVO to VKE. At VKE the slurry was introduced as short-duration pulses (5-10 minutes) into the oxidation tank of the wet FGD plant by means of a pump submerged in the silo tanker.

During the experiments, an extended analysis programme was run focusing on sulphite in order to follow the oxidation. Sulphite was monitored in the oxidation tank, in the gypsum and in the overflow of the second set of hydro cyclones; the fine particles of the SDAP will end up in the overflow of the second set of hydro cyclones if they do not dissolve readily.

Table 2 shows the major process parameters of the four short-duration full-scale SDAP oxidation tests, and figure 1 shows the variation in pH and sulphite content in the oxidation tank and the SO_2 concentration in the stack during test #2.

Test	pH	Sulphur load (t/h)		Oxidation air (m_0^3/h)	Comments
		coal	SDAP*	(extra)	
#1	5.4	≈ 1.6	≈ 0.22 (+14%)	+2000	Low pH to facilitate SDAP dissolution. Additional air to ensure oxidation.
#2	5.6	≈ 1.6	≈ 0.20 (+13%)	+2000	Normal pH. Additional air to ensure oxidation.
#3	5.5 - 5.6	≈ 1.6	≈ 0.26 (+16%)	0	Normal pH. Normal air flow.
#4	5.5 - 5.6	≈ 1.6	≈ 0.56 (+35%)	0	Normal pH. Normal air flow. High SDAP feed rate.

* Sulphur load from the SDAP sulphite content.

Table 2: Short-duration full-scale SDAP oxidation tests.

When SDAP was introduced, the short-duration pulses were seen as pH peaks about 0.2 pH units high due to the excess lime content in the SDAP. Close examination of the corresponding SO_2 concentration in the stack shows a slight reduction during each pH peak.

Figure 1: SO₂ stack concentration, pH and slurry sulphite content during short duration full-scale SDAP test #2.

In this particular case the sulphite content was analysed once every hour and was found to remain at a level of approx. 140 mg/l except when samples were taken during an SDAP feed pulse. During an SDAP feed pulse, a sulphite content of about 200 mg/l was observed - levels of up to 1000 mg/l are acceptable with regard to the gypsum quality. This type of observation was carried out consistently in all four tests.

The sulphite content in the overflow from the second set of hydro cyclones and in the gypsum remained constant during all four tests.

The findings can be summarized as follows:

- SDAP can be dissolved in the absorber slurry of a wet FGD plant and converted into gypsum.

- An SDAP conversion capacity of at least 3.5 t/h was found during the short-duration full-scale tests at VKE.

- The excess lime content in the SDAP is at least partially active during the desulphurization process.

3.3 The Need for Long-Term Full-Scale Tests

The possibility of converting SDAP into gypsum was shown in the short-duration full-scale tests but further investigations are needed due to the rudimentary SDAP feed system and the short duration (2-4 hours) of the tests.

Everything entering a wet FGD plant has to leave it either through the flue gas system, with the gypsum and/or through the wastewater plant. The residence time of flue gas born components is insignificant (minutes) compared to the residence time of gypsum and water born components (hours, days and even weeks). Table 3 lists typical residence times for chloride, gypsum and insoluble material in the wet FGD plant at VKE.

Component	Carrier stream	Conditions	Residence time
Gypsum	Gypsum	1% S in coal, 100% load 2% S in coal, 100% load	70 h (2^d22^h) 35 h (1^d11^h)
Chloride	Wastewater	0.1% Cl in coal, 100% load 0.4% Cl in coal, 100% load	350 h $(\approx2^w)$ 87 h (3^d15^h)
Insolubles* (larger particles) Insolubles* (fines)	Gypsum Wastewater		140 h (5^d19^h) 350 h $(\approx2^w)$

*Originating from limestone impurities and fly ash

Table 3: Typical residence times of gypsum, chloride and insolubles in the wet FGD plant at VKE.

Response to changes in the load of components that are associated with the gypsum and wastewater streams, eg. by addition of SDAP, is of first order (continuous stirred tank). This implies that 90% of the effect of a step change has occurred within 2.3 times the time constant (residence time), ie. the full impact on the gypsum quality caused by addition of SDAP is usually developed after one week of continuous addition of SDAP.

The gypsum quality is of main concern in this respect. The purity will not be altered, as long as the insoluble content in the SDAP is low and the sulphite content is properly oxidized. The dewatering properties and the size distribution might, however, be altered unfavourably with regard to the subsequent usage in wall board manufacturing.

The chloride content in the SDAP will mainly affect the performance of the wet FGD plant as an extra (hydraulic) load on the wastewater plant that may need to be upgraded.

The load of insolubles originating from fly ash and limestone at VKE is increased by the insoluble content in the SDAP. The insoluble content in the SDAP originates from the fly ash of the producing plant and the insoluble content of the lime used in the SDA plant.

A high content of insolubles in the SDAP might degrade the gypsum quality (larger particles) or affect the wastewater plant (fines) - it might even disturb the desulphurization process.

4   Long-Term Full-Scale Test Number One

A dry continuous SDAP feed system has been established and a long-term test with addition of SDAP from FVO to the wet FGD plant at VKE was made in week 2 of January 1996.

4.1   Test Conditions

During the five day test period a total of 230 t of SDAP, corresponding to an average sulphur load of 0.38 t/h, was added to the wet FGD plant at VKE.

The SDAP was taken from the daily production at FVO, which used a mixture of North American and South African coals during the test. The average composition (content and standard deviation) of the SDAP is given in table 4.

With a sulphur load of 0.93 t/h from the low sulphur Polish coals used at VKE in the test, approx. 30% of the gypsum produced would originate from the SDAP at the end of the test period.

SO_3^{2-} (sulphite)	$40.0\pm1.9\%$
SO_4^{2-} (sulphate)	$9.6\pm2.4\%$
Cl^- (chloride)	$3.6\pm0.3\%$
$Ca(OH)_2$ (excess lime)	$2.5\pm1.3\%$
Insolubles	$3.0\pm0.4\%$

Table 4: SDAP analysis (weight) during long-term test.

The wet FGD plant was initially run at pH 5.2 but pH was reduced to 4.6 during the test in an attempt to control the content of residual limestone in the gypsum.

4.2   The Desulphurization Process

During the test unexpected disturbances of the desulphurization process was encountered.

It was observed that after about 24 hours of addition of SDAP pH in the absorber was largely unaffected by large variations in the limestone feed rate - an indication of reduced limestone reactivity.

This resulted in large excess of limestone in the absorber and in the gypsum and pH was reduced to 4.6 in order to digest the excess limestone - a step with limited success.

The excess limestone was digested at first, but the reduced limestone reactivity caused the limestone control system to resume overdosing the FGD with limestone and the problem with an elevated excess of limestone in the absorber (and gypsum) was not solved.

Later investigations have shown that elevated levels of dissolved aluminium and fluoride were present in the absorber during the SDAP test. A dissolved aluminium content up to

40 mg/l and a dissolved fluoride content up to 200 mg/l were observed - the normal levels are below 3 mg/l for dissolved aluminium and below 20 mg/l for dissolved fluoride.

It is suggested that the reduced reactivity of the limestone was most probably caused by the inhibiting effect of aluminium fluoride complexes (AlF_n) as has been reported in the literature /1/.

It is assumed that the source of dissolved aluminium is the fly ash content of the SDAP, whereas the calcium fluoride particles (CaF_2) always present in a wet FGD plant (and in the SDAP) is the latent source of dissolved fluoride. (*The fluorine content of the coal is to a large extent present in the flue gas as hydrogen fluoride (HF) that is captured as particles of calcium fluoride (CaF_2) in the FGD plant.*)

4.3   The Gypsum Quality

Trends in the most important gypsum parameters during the long-term SDAP test are given in figures 2 and 3.
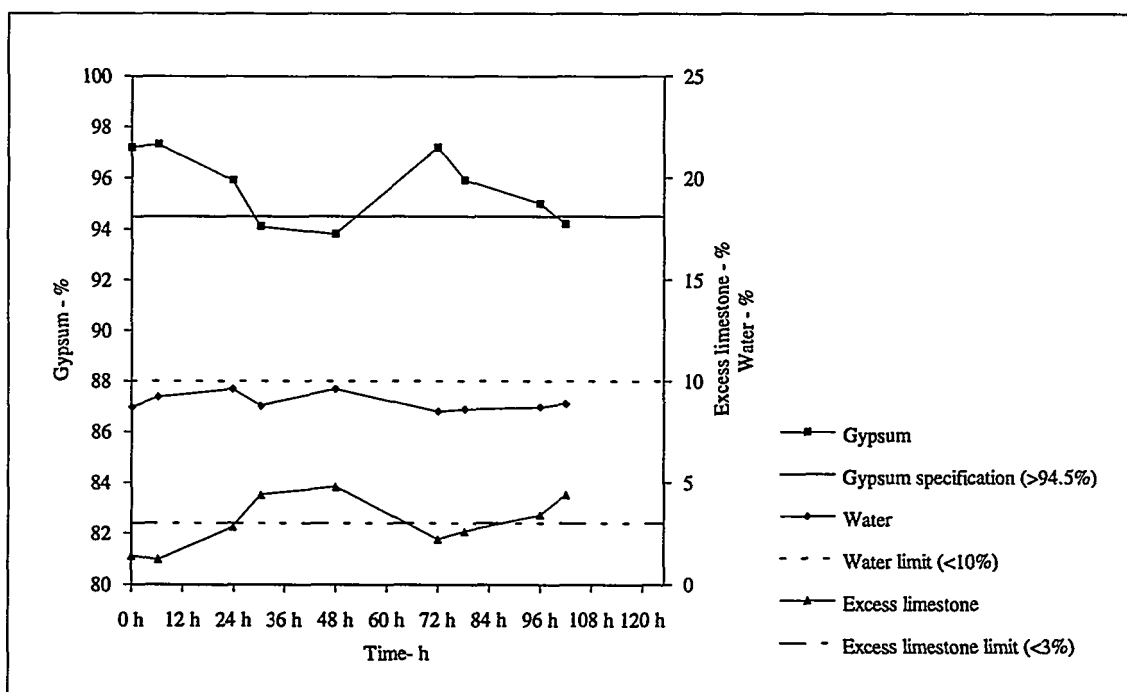
Figure 2: Trends in gypsum quality during the long-term full-scale SDAP test (week 2, 1996).

The upper limit of the water content in the gypsum was never exceeded during the SDAP test, whereas problems were encountered with the gypsum purity and the content of excess limestone. The sum of the gypsum purity and the content of excess limestone are almost constant, which strongly suggests that the reason is poor control of the limestone feeding caused by the above-mentioned reduced limestone reactivity.

2.10
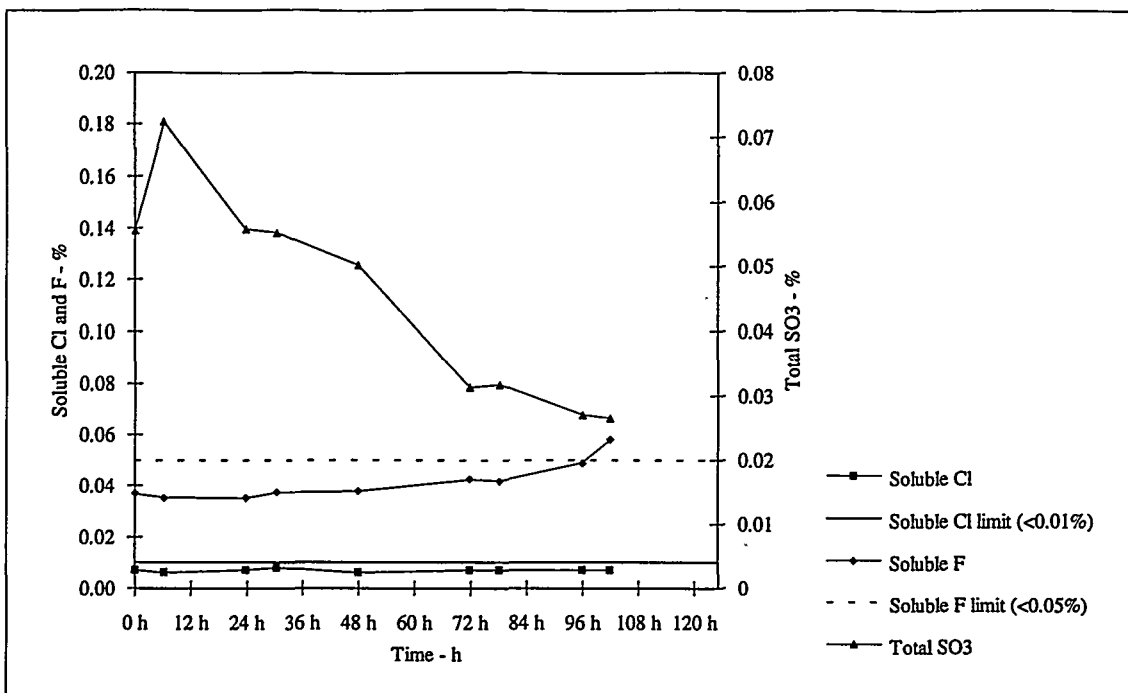
Figure 3: Trends in gypsum quality during the long-term full-scale SDAP test (week 2, 1996).

The total content of sulphite was far below critical values during the entire test and the observed reduction in the total sulphite content was caused by the induced pH drop from 5.2 to 4.6 - sulphite oxidation reaction is enhanced at lower pH.

No problems with the content of soluble chlorides in the gypsum was encountered during the SDAP test whereas the content of soluble fluoride in the gypsum exceeded the limit at the end of the SDAP test. The probable reason for this is the elevated content of dissolved fluorides in the absorber together with an insufficient wash procedure.

Particle size distributions of the gypsum were measured on a daily basis and showed an insignificant tendency to a more narrow distribution.

In summary the gypsum quality remained unaffected by the addition of SDAP apart from the implications caused by the reduced limestone reactivity.

4.4   Effects on Wastewater

The wastewater flow from the FGD plant at VKE had to be increased in order to handle the extra chloride contained in the SDAP and avoid an excessive rise in the chloride concentration in the absorber.

During the SDAP test the amount of dry matter in the primary wastewater stream was essentially constant (30 g/l), but the amount of insolubles in the dry matter increased from 15% to 25-30%.

2.11

These changes did not influence the primary sedimentation step and the performance of the wastewater plant apart from the extra hydraulic load.

5   Conclusion

The laboratory experiments, the short duration full-scale tests and the long-term full-scale tests have all shown that it is possible to convert SDAP into gypsum in a wet limestone scrubber.

It is specifically concluded that:

- SDAP dissolves readily in the absorber slurry;
- the sulphite contained in the SDAP is totally oxidized;
- the gypsum quality is only marginally altered;
- the hydraulic load of the wastewater plant is increased as a result of the chloride contained in the SDAP;
- addition of SDAP can result in reduced limestone reactivity - probably caused by the fly ash content in the SDAP.

The future development of the concept to convert SDAP into gypsum in a wet limestone scrubber is linked to better understanding of the influence of the SDAP on the limestone reactivity.

Laboratory investigations regarding the influence of SDAP from different sources (FVO, MKS and different coal sources) on limestone reactivity are initiated.

If the limestone inhibition problem can be more or less attributed to the fly ash content of the SDAP, long-term full-scale tests with SDAP from MKS with a very low fly ash content will be run in order to make a final demonstration of the feasibility of the process and evaluate the handling capacity for different SDAP products.

6   References

/1/   Farmer, R.W.; Jarvis, J.B.; Moser, R.; "Effects of Aluminium/Fluoride Chemistry in Wet Limestone Flue Gas Desulphurization"; Chem. Eng. Comm. 1989, Vol. 77, pp. 135-154.

COMBUSTION CHEMISTRY
– ACTIVITIES IN THE CHEC RESEARCH PROGRAMME

Kim Dam-Johansen, Jan E. Johnsson, Peter Glarborg,
Flemming Frandsen, Anker Jensen and Martin Østberg
Department of Chemical Engineering
Bldg. 229, Technical University of Denmark
DK-2800 Lyngby
Denmark

ABSTRACT

The combustion chemistry in the oxidation of fossil fuels and biofuels determines together with mixing and heat transfer the required size of a furnace, the emission of gaseous pollutants, and the formation of ash and deposits on surfaces. This paper describes technologies for solid fuels combustion and gives a summary of the fuels, the pollutant chemistry and the inorganic chemistry in combustion processes. Emphasis is put on the work carried out in the CHEC (Combustion and Harmful Emission Control) Research Programme.

1 Technologies

The choice of combustion technology in large scale heat and power plants depends on the fuel to be used, existing environmental legislation and financial considerations. In Denmark, most of the power production today is based on coal imported from a number of different countries [1]. Due to increasingly stringent legislation concerning emissions of sulphur dioxide, nitrogen oxides (NO_x) and other potentially harmful species and with restrictions on total carbon dioxide emissions, coal is expected to be partly replaced by biofuels and natural gas [2].

Danish natural gas resources are limited, and the annual surplus of biofuels available for power production may fluctuate significantly. New heat and power plants must therefore be flexible with respect to fuel type. This paper deals primarily

with combustion of the solid fuels coal, straw and wood.

1.1   Solid Fuels

Coal, straw and wood are closely related. The precursor of coal was peat, which was formed by bacterial and chemical action on plant debris. Millions of years of heat and pressure metamorphosed the peat into various ranks of coal, from lignite to anthracite. Fuel compositions are often reported in two ways: by proximate analysis and ultimate analysis. Proximate analysis is the determination by standard methods of moisture, volatile matter, fixed carbon (the residue after the volatile matter has been driven out) and ash (inorganic residue after the fuel has been burned). Ultimate analysis is the determination of ash and the elemental constituents: carbon, hydrogen, nitrogen, oxygen, sulphur and chlorine. Both kinds of analysis are usually reported together with the high (including water condensation) and low heating values (MJ/kg) of the fuel. Calculation of the flue gas composition is based on the ultimate analysis. Table 1 shows the proximate and ultimate analyses of a number of fuels together with the stoichiometric amounts of air for combustion and the flue gas generated, which is seen to be almost independent of fuel type.

Rank	Ultimate analysis as received				LHV	Proximate analysis daf					Air	Flue gas
	Moisture	Ash	Volatiles	Fixed C		C	O	H	S	N		
	%wt	%wt	%wt	%wt	MJ/kg daf	%wt	%wt	%wt	%wt	%wt	Nm³/MJ	Nm³/MJ
ma	13.2	18.9	2.6	65.3	31.89	94.7	4.0	0.6	0.4	0.3	0.27	0.27
an	4.3	9.6	5.1	81.0	34.81	92.5	2.8	2.8	0.9	1.0	0.26	0.26
sa	2.6	7.5	10.6	79.3	35.86	90.6	1.8	3.9	1.9	1.8	0.26	0.26
lvb	2.9	5.4	17.7	74.0	36.46	90.7	2.5	4.6	0.8	1.4	0.25	0.26
mvb	2.1	6.1	24.4	67.4	36.23	88.9	3.2	5.2	1.1	1.6	0.26	0.27
hvAb	2.3	5.2	36.5	56.0	35.28	84.8	7.0	5.7	0.8	1.7	0.25	0.26
hvBb	8.5	10.8	36.4	44.3	33.61	80.6	8.8	5.5	3.4	1.7	0.25	0.26
hvCb	14.4	9.6	35.4	40.6	33.07	78.6	9.5	5.6	5.0	1.3	0.25	0.27
subA	16.9	3.6	34.8	44.7	31.12	76.0	15.5	5.2	1.8	1.5	0.25	0.26
subB	22.2	4.3	33.2	40.3	30.40	73.4	18.7	6.0	0.6	1.3	0.25	0.26
subC	25.1	6.8	30.4	37.7	29.19	74.1	19.3	5.0	0.5	1.1	0.25	0.27
lig	36.8	5.9	27.8	29.5	28.42	70.9	21.4	5.0	1.6	1.1	0.25	0.26
Straw	6.3	4.3	78.5	18.4	18.64	49.7	43.9	6.2	0.1	0.0	0.25	0.28
Saw dust	13	0.4	70.9	15.6	19.10	50.7	42.8	6.4	0.0	0.1	0.25	0.29
Fir chips	39	0.3	50.1	11.0	19.00	50.6	43.0	6.3	0.0	0.1	0.25	0.28
Wood	27.0	0.8	-	-	18.50	50.8	39.8	6.4	0.1	2.8	0.27	0.31

Table 1: Composition of typical solid fuels and their stoichiometric requirements of combustion air and the amount of flue gas formed. Data are taken from different sources.

The sulphur and nitrogen content of the fuel is important for the emissions of sulphur dioxide and nitrogen oxides. The minerals, together with the combustion process, determine ash properties with respect to dust removal and the formation of deposits and/or agglomerates in the furnace or on heat transfer surfaces. The composition of inorganic constituents in a fuel is often reported as oxides but newer methods for a more detailed mapping of the composition exist [3].

Typical heating values and compositions of different fuels are shown in Figures 1 and 2 respectively.
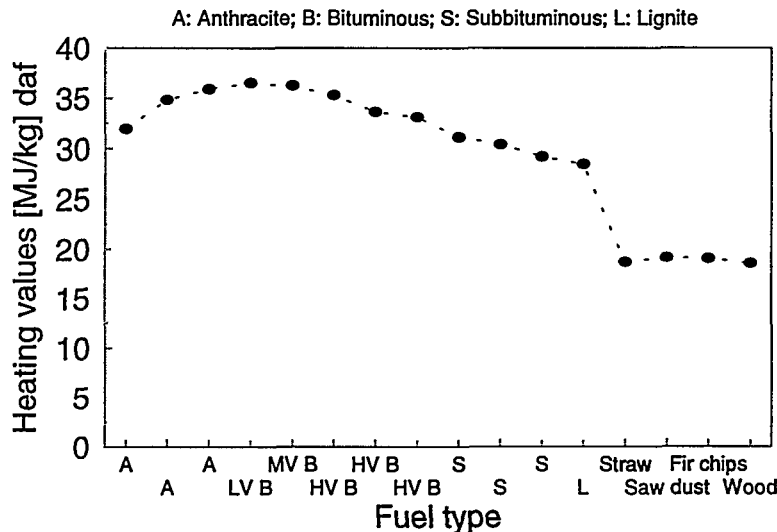
Figure 1: Heating values of various fuels.
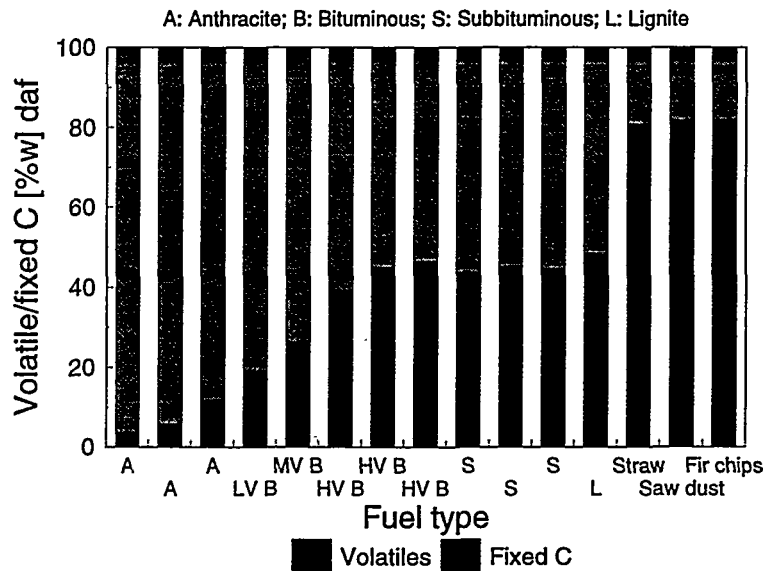
Figure 2: Volatile matter and fixed carbon in different fuels.

Solid fuels may be burned in a fuel bed supported on a grate or in suspension. The suspension fired systems comprise different types of entrained flow and fluid bed combustors. The fuel bed systems are usually relatively low–capacity whereas the entrained–flow systems are used in large plants.

1.2   Combustors

Previously the combustion of coal in fuel bed systems was common. In Denmark, these systems are now used almost exclusively for the combustion of biomass and waste. The fuel support usually consists of a travelling grate or a vibrating grate for primary air distribution and fuel transportation. Mechanical stokers are used for continuous fuel feed either to one end of a moving grate or by a spreader stoker. In spreader stoker systems some of the fuel is devolatilized and burned in suspension, and only the large and/or dense particles fall onto the grate. In both systems the large char particles burn on the grate in crossflow with a fraction of the combustion air fed to the system below the grate. This fraction is limited to avoid entrainment of fuel and ash particles and to reduce NO_x formation. Secondary air is injected above the grate. Figure 3 shows how a travelling grate overfeed stoker and a vibrating grate spreader stoker system works.
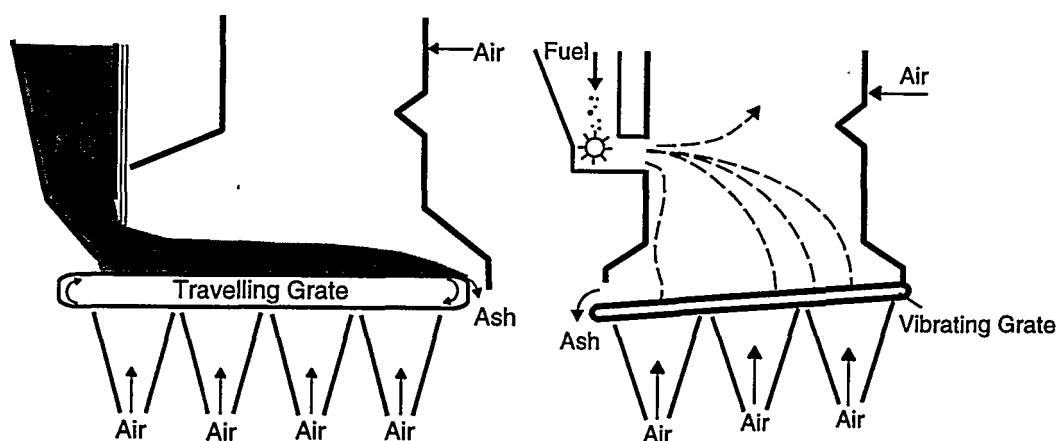
Figure 3: Schematic representation of a travelling grate overfeed and a vibrating grate spreader stoker system.

In a fuel bed, it is difficult to control the distribution of fuel and thus the mixing of the primary air and fuel. Poor mixing may result in local reaction conditions, leading to a higher rate of NO_x formation, unburnt carbon in the fly ash [4] and sintering of ash particles.

The mixing problems are at least partly solved in bubbling or circulating fluidized bed combustion (FBC) by injecting the fuel particles into a bed of non–combustible particles. The gas velocity through the bed is kept high enough to fluidize the bed material and ensure rapid mixing. In the circulating FBC unit, the particles are elutriated from the bed and sent back to the bottom of the riser by a hot particle separator. The non–combustible particles act as a heat source for ignition of the fuel and as a heat carrier by absorbing a significant fraction of the heat liberated by the combustion process and transferring it to heat transfer surfaces placed in the bed section or in an external particle cooler. As limestone injected to the bed reacts with sulphur dioxide to form calcium sulphate, the non–combustible particles may also act as a gas cleaning medium [5–9]. The air is usually separated into primary air introduced through a distributor plate in the bottom and secondary and perhaps tertiary air injected at higher levels. This leads to large reducing regions in the bed, which, combined with the relatively low combustion temperature of about 1123 K, leads to low NO_x emissions and often relatively high emissions of N_2O. Due to the heat capacity of the particles a variety of fuels ranging from biofuels rich in volatiles to antracite may be burned in FBC systems. Burning alkali–rich fuels such as straw may cause bed particle agglomeration problems, for example if potassium react with sand particles causing a decrease in the melting temperature of the ash. In Denmark, circulating fluidized bed technology has been tested intensively in connection with the combustion of coal–straw–wood mixtures [10–13].

Figure 4 shows a circulating fluidized bed combustor with an external particle cooler.
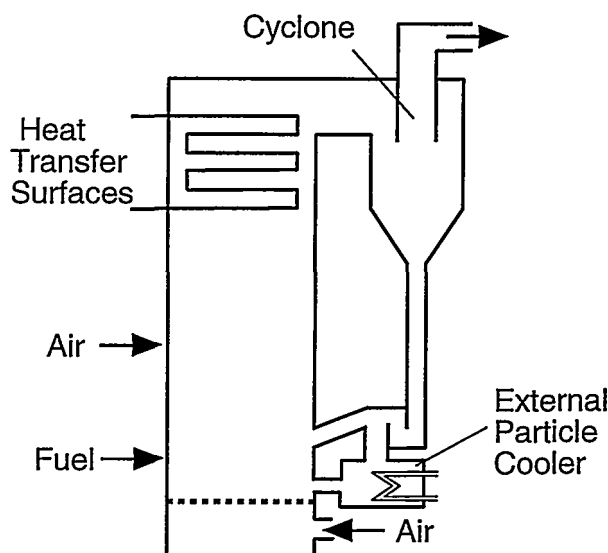
Figure 4: A circulating fluidized bed combustor with an external particle cooler.

Entrained flow combustors are used almost exclusively for pulverized coal, even though research on co–firing with, for example, bio–fuels has been initiated [14,15]. Grinding is used to keep coal particle size below 100 μm in order to secure a short burnout time. The particles are fed to burners placed in different configurations in the furnace: on one wall, on two opposite walls or in the furnace corners directed tangentially towards an imaginary circle in the furnace center. Previously, the burners were simple and designed to mix the coal and air as rapidly as possible to ensure a high degree of *turbulence*, high *temperatures* and lengthy reaction *times* ("the 3 T's"). This provided a good burnout, but NO_x emissions were also high. This is why the so–called "low–NO_x" burners were developed. In modern low–NO_x burners the air is separated into at least three flows: primary air which carries the coal, swirling secondary air fed to an annular ring around the primary air inlet, and tertiary air, the latter sometimes also with swirl and in some combustors over–fire air as well. The swirling secondary and tertiary air results in back–mixing in the near–burner zone, where devolatilization of fuel particles takes place. In this region, reducing conditions and relatively high temperatures prevail and the burnout air is slowly mixed in. This keeps NO_x emissions low.

Figure 5 shows the schematics of a pulverized fuel (PF) furnace and a modern low–NO_x burner. Table 2 lists some main characteristics of fuel bed, fluidized bed and entrained flow combustors.
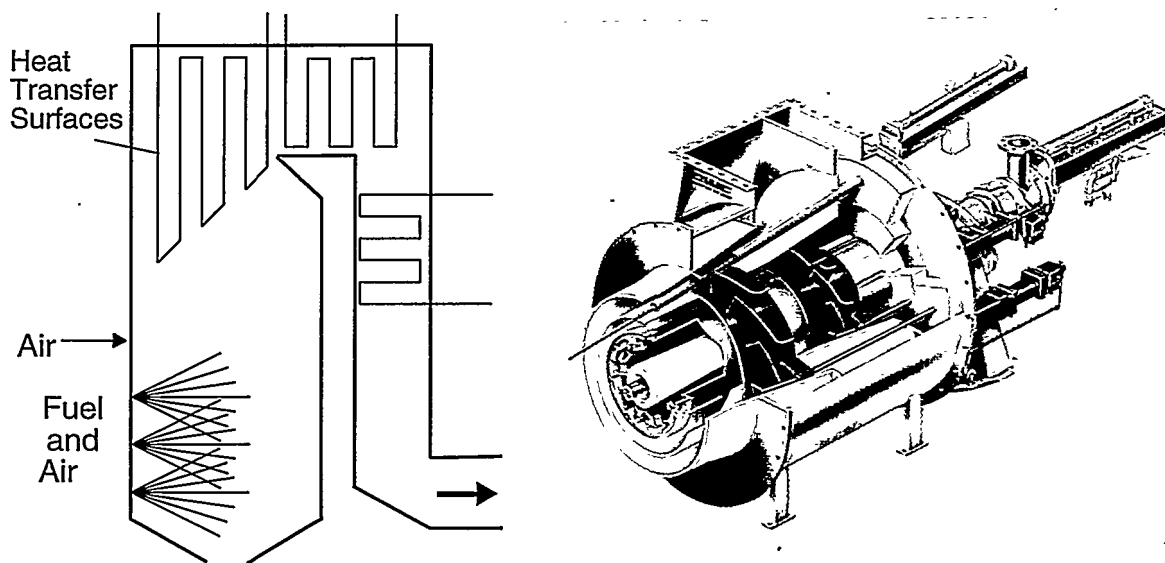
Figure 5: A furnace for combustion of pulverized fuel and a modern low–NO_x burner with primary, secondary and tertiary air.

Similar process steps occur in the combustion of solid fuel in the different sys-

Characteristics	Grate	BFBC	CFBC	PF
Capacity range, MW thermal	< 150	< 1000	< 600	< 1500
Combustion temperature, K	1373-1573	1073-1173	1073-1173	1373-1773
Gas velocity, m/s	4-6	1-2.5	4-6	5-10
Gas residence time, s	1-3	1-3	0.5-6	1-3
Excess air number, λ	1.3-2.5	1.2-1.4	1.2-1.3	1.1-1.3
Mean fuel particle size, mm	0.5-50	1-10	0.2-25	0.001-0.1
Mean bed material particle size, mm	-	0.5 - 3	0.15-0.3	-
Burnout time of fuel particles, s	1000-10000	1000-10000	500-10000	1-3
Volumetric heat release, MW/m^3	0.15-0.35	0.1-0.5	0.1-0.5	0.06-0.3
Cross section area heat release, MW/m^2	0.5-2.5	1-3	2-8	2-6.5
Burner region heat release, MW/m^2	-	-	-	0.6-3
Combustion efficiency, %	92-97	92-95	-	96-99
Combustion efficiency with ash recycling, %	-	97-99	97-99	-
Fly ash/Bottom ash ratio, %	60/40[a],35/65[b],15/85[c]	-	-	95/5[a],35/65[b]

[a] Bituminous coal
[b] Lignite
[c] Straw

Table 2: Characteristics of combustion process technologies. Adapted from Görner [16]. Data for ash split from Vuthaluru et al. [17].

tems. The particles are heated up and dried; this is followed by devolatilization, combustion of the volatiles and combustion of the residual char. These steps, as well as the formation of NO_x and ash components, are discussed in the following chapters.

2 Heating and Devolatilization

2.1 Heating of Coal Particles

The heating of fuel particles is important in pulverized fuel (PF) combustion. A fast heat–up is essential for the rapid release of volatiles needed to obtain a stable flame. In the hot furnace, a fuel particle is heated by convection and radiation. Assuming that there are no internal temperature gradients for the small particles used in PF combustion, the particle temperature (T_p) is determined from an energy balance [18]:

$$m_p \cdot C_p \cdot \frac{dT_p}{dt} = 4\pi \cdot R^2 \cdot (Q_c + Q_r) \qquad (1)$$

where m_p is the mass of the particle, C_p is the specific heat capacity of the particle, R is the particle radius (the particle is assumed to be spherical), t is time, and Q_c and Q_r are the heat fluxes the particle is subject to through convection and radiation respectively. The convective heat flux is given by

$$Q_c = \frac{Nu \cdot \lambda_g}{d} \cdot (T_g - T_p) = h \cdot (T_g - T_p) \tag{2}$$

where λ_g is the thermal conductivity of the gas, T_g the gas temperature and h the heat transfer coefficient. For the particle size range of interest in PF, the contribution from radiation may be neglected to a first approximation. Furthermore, the slip velocity between gas and particles is small, so the Nusselt number Nu is approximately equal to 2. Neglecting the radiative contribution, (1) and (2) can be solved to give the particle temperature as function of time:

$$T_p(t) = T_p(t = 0) + (T_g - T_p(t = 0)) \cdot (1 - \exp(-t/\tau_H)) \tag{3}$$

where τ_H is the characteristic time scale for heating by convection given by

$$\tau_H = \frac{\rho_p \cdot C_p \cdot d^2}{12 \cdot \lambda_g} \tag{4}$$

where ρ_p is the particle density. For a typical coal, $C_p = 1200$ J/(kg K), $\rho_p = 1500$ kg/m^3, and for $\lambda_g = 0.09$ W/(m K) one finds $\tau_H = 4$ ms for a 50 μm particle. Equation (4) shows that the heating time increases with the square of the particle diameter. The maximum heating rate occurs at $t = 0$ s and is of the order 10^5 K/s for a 50 μm particle. The heat–up time of coal particles can be controlled through the grinding process.

Experiments in full scale are being carried out with the aim of testing co–combustion of coal and straw [14,15]. The heat–up time of straw is longer than the heat–up time of finely ground coal particles. With high thermal fractions of straw, ignition problems have been observed in a 2.5 MW$_{th}$ semi–industrial furnace because the straw was not heated fast enough [15].

The analysis presented above is for particles with no internal temperature gradients. In combustion on grates or in fluidized beds, the fuel particle size is larger, and internal temperature gradients in the fuel particle may occur [19]. Furthermore, the fuel may not be dry when injected into the furnace, which results in a drying time. The equations which describe heat–up of a sphere with internal temperature gradients are [20]:

$$\rho_p \cdot C_p \frac{\partial T_p}{\partial t} = \frac{1}{r^2} \frac{\partial}{\partial r} \left(r^2 \lambda_p \frac{\partial T_p}{\partial r} \right) \tag{5}$$

$$\lambda_p \frac{\partial T_p(r = R)}{\partial r} = h \cdot (T_g - T_p(r = R) + \epsilon \cdot \sigma(T_w^4 - T_p^4(r = R)) \tag{6}$$

$$\frac{\partial T_p(r=0)}{\partial r} = 0 \qquad (7)$$

$$T_p(t=0) = T_{p0} \qquad (8)$$

where λ_p is the thermal conductivity of the solid and T_w is the temperature of the surroundings. In general, the above set of equations must be solved numerically, but if radiation is omitted and the physical properties are assumed to be constant, an analytical solution can be found [20]. Figure 6 illustrates the temperature profile at different times in a 5 mm particle being heated in a FBC system from 300 K to 1100 K and reveals significant temperature gradients. These temperature gradients may induce fragmentation of the fuel particles due to thermal stress.
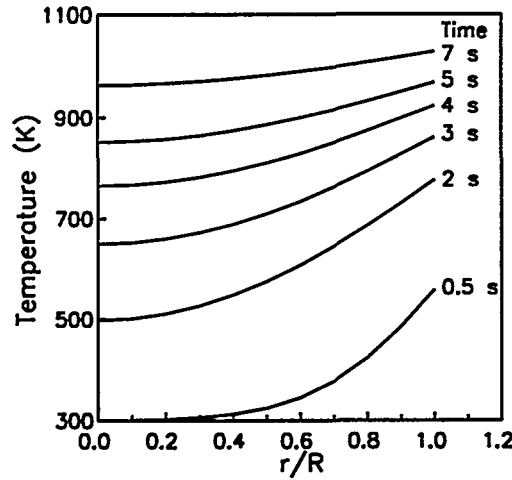
Figure 6: Temperature profiles in a 5 mm diameter coal particle heated in a FBC from 300 K to 1100 K. $Bi = h \cdot R/\lambda_p = 1.62$, $\lambda_p = 1.0$ W/(m K), $\alpha = \lambda_p/(\rho_p C_p) = 5.6 \cdot 10^{-7}$ m^2/s.

2.2 Coal Devolatilization

As the fuel particle is heated, it decomposes thermally, i.e. it devolatilizes, producing char and volatiles. Several reviews of coal devolatilization are available [18,21–23]. The volatiles consist of tar and light gaseous species, and may contain as much as 50% of the heating value of the fuel. The process of devolatilization is important for the flame stability in pulverized fuel combustion, and tar produces soot, which is important for radiation from flames. The amount and composition of volatiles depend mostly on the final temperature and the coal type, but also to a lesser extent on parameters such as particle size, heating rate and pressure

[21]. Solomon *et al.* [23] gave the following description of coal devolatilization. Before the primary devolatilization, low–temperature cross–linking takes place in low–rank coals with a high O content accompanied by evolution of H_2O and CO_2. During the primary devolatilization, weak bonds in the coal matrix are broken, producing fragments which evolve as tar if they are small enough to vaporize at the given temperature. The molecular fragments which are too large to vaporize, repolymerize and stabilize the evolving char matrix. Bituminous coals give the highest tar yields [24], because the low–temperature cross–linking in low–rank coals prevents the formation of molecular fragments and the initial degree of cross–linking in high–rank coals such as anthracite is too high for fragmentation to take place. After the breaking of weak bonds, the functional groups decompose, releasing CO_2, light gases and H_2O. This process requires hydrogen, and primary devolatilization ends when all donatable hydrogen atoms are depleted. During the secondary devolatilization of the char additional gases evolve: CH_4 from methyl groups, CO from ether linkages, H_2 from ring condensation and nitrogen is evolved from ring structures. The split of nitrogen in the coal into volatiles and char during devolatilization and the type of volatiles are important for NO_x and N_2O formation because the reactions of the different compounds are different.

Partitioning of coal nitrogen during devolatilization

The fraction of nitrogen released during devolatilization depends on the temperature, residence time and coal type. At low temperatures or residence times nitrogen is preferentially retained in the char [25]. The initial enrichment of nitrogen in the char is usually explained by the nitrogen being tightly bound in cyclic aromatic 5–ring (pyrrolic) and 6–ring (pyridinic) structures in the coal [26]. The initial enrichment of nitrogen in the char is greater for low rank coals [27,28] due to the initial loss of species not containing nitrogen. During secondary pyrolysis of char, at high temperatures or with long residence times, the nitrogen containing aromatic rings decompose releasing their nitrogen [29]. At temperatures above 2200 K and several minutes of residence time only carbon is left in the char [28]. Figure 7 shows the nitrogen concentration in char versus temperature. An enrichment of nitrogen in the 600–1200 K temperature range followed by depletion of nitrogen at high temperatures can be seen.

Volatile nitrogen species from coal devolatilization

The volatile nitrogen species formed during pyrolysis and the devolatilization of coal are mainly tar, HCN and NH_3 [29]. The pathways and selectivities for the formation of NO_x and N_2O from these species vary, so the amount and speciation of the volatile nitrogen are important factors. According to Niksa and coworkers [35–37], tar is the only volatile nitrogen containing product during primary devolatilization. At high temperatures, the nitrogen left in the char is released as HCN during secondary pyrolysis. The rate and amount of HCN release from

3.10
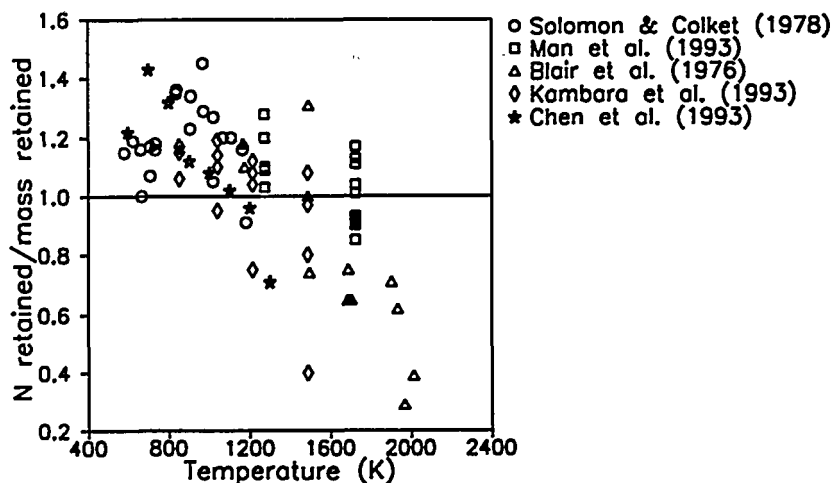
Figure 7: Relative concentration of nitrogen in char: the fraction of coal nitrogen in char divided by the fraction of coal as char after pyrolysis [30–34].

higher–rank coals is lower [38–40]. This is in agreement with the fact that high rank coals have more pyridinic nitrogen, which is more thermally stable than the pyrrolic nitrogen in lower–rank coals [29]. HCN is also released from tar during secondary reactions with soot formation, but some of the nitrogen becomes incorporated in the soot. Thus the HCN and tar yields observed depend on the extent of secondary decomposition of tar. At high temperatures the rate of soot formation from tar is very fast [41], which partly explains why HCN is the most important coal pyrolysis product at high temperatures such as those found in PF combustion [25]. The formation of NH_3 is less well understood. It appears that low–rank coals produce more NH_3 than high–rank coals [25,42,43].

There is not agreement in the literature whether NH_3 is formed from direct cleavage of $-NH_2$ groups in the parent fuel [42,43], by gas phase hydrogenation of HCN [42] or by intraparticle conversion of HCN to NH_3 [44–46]. Figure 8 summarizes HCN, NH_3 and tar–N yields as a function of temperature from coal pyrolysis experiments reported in the literature, including data from different equipment (fluidized bed, heated grid and pyroprobe). The particle sizes and particle heating rates were similar, less than 200 μm in all experiments and about 10^4 K/s, but there were important differences in gas residence time. The data of Freihaut and Seery [48] were obtained under vacuum conditions, where the extent of secondary tar reactions was small at temperatures below 1400 K. The tar–N yields range from 5 to 50%. This spread was mainly caused by differences in coal type and by temperature and residence time effects. The yields of HCN and NH_3 increased with increasing temperature. The highest yields were obtained by Kambara et al. [33] but their tar yields were very low (<5 wt.%) for all 20 coals, indicating severe tar cracking, which increases the yield of HCN. The three data points for

NH$_3$ from Kambara *et al.* [33], which are below 2%, were for a low–volatile coal.
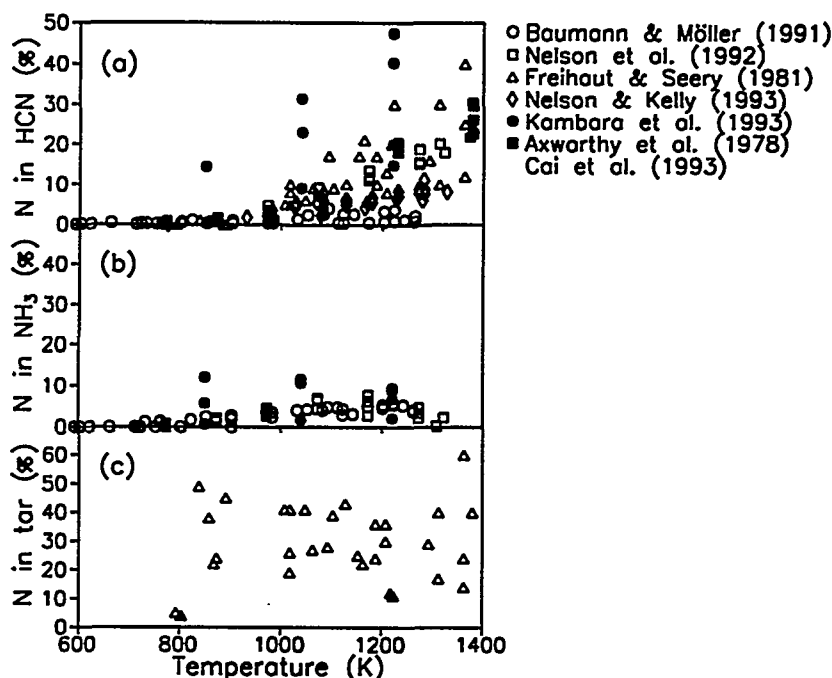
Figure 8: Percentage of coal nitrogen in volatile nitrogen species as a function of pyrolysis temperature in different experimental equipment. (a) HCN. (b) NH$_3$. (c) Tar. Data from [33,40,42,47–50].

The conclusion is that a significant part of the fuel–N is released as HCN, NH$_3$ and in the tar during coal devolatilization. The nitrogen may be released from the tar during its secondary cracking. The question of HCN conversion to NH$_3$ is yet to be resolved.

3 Homogeneous Reactions in Combustion

3.1 Combustion

The initial heat release in pulverized coal flames is controlled by three distinct chemical processes: primary devolatilization, secondary volatiles pyrolysis, and volatiles combustion. As discussed above, the products of the primary devolatilization include CO, CO$_2$, H$_2$O, light hydrocarbons and a large number of heavy hydrocarbons collectively known as tar. During secondary pyrolysis, the tar compounds simultaneously decompose by thermal cracking and condense into

soot [37]. Apart from the soot, the products of the secondary pyrolysis are mainly H_2, CO and C_2H_2 [51], at least at high temperatures.

The volatiles formed in primary and secondary pyrolysis oxidize in the gas film surrounding the particle [52]. The amount of hydrogen formed in secondary pyrolysis appears to be important for the volatile oxidation rate; due to its high reactivity, the presence of H_2 increases the flame speed by up to a factor of three [51]. The volatiles may burn in jets or in envelope flames surrounding the particle. During the volatiles combustion period, the gas phase temperature is much higher than the particle temperature. The elevated gas temperature due to this combustion accelerates the char heating and is thus very important for both ignition and flame stability.

It is difficult to propose a single global scheme for volatiles oxidation, since the volatiles are a mixture of combustible gases. Global rate expressions are available for a number of hydrocarbons [53], but care must be taken not to extrapolate these expressions outside their range of applicability. Usually, in computational fluid dynamics (CFD) models, the volatiles are presumed to react in a single global reaction to form carbon monoxide and water vapour, the rate of reaction being physically controlled by turbulent mixing. The carbon monoxide formed from volatile and char combustion is converted to carbon dioxide at a rate equal to the lesser of the mixing–controlled and chemically–controlled rates.

Recent model validations suggest that this simple approach is sufficient to describe the downstream region in pulverized coal combustion, but that modifications in the volatile matter combustion sub–model are necessary to describe the near–burner region satisfactorily [54,55]. Inadequacies in present model performances may arise from insufficient treatment of the oxidation kinetics or from poor knowledge of the turbulence/chemistry interactions.

The fact that the volatiles are a complex mixture of combustible gases, varying dependent on coal type and pyrolysis conditions and including a large number of heavy–weight aromatic compounds, makes it difficult to predict the oxidation behavior. However, as discussed above, there are some indications that the products of primary and secondary pyrolysis are mostly H_2, CO, and light hydrocarbons, since the heavy aromatic species condense rapidly into soot. In this case a volatiles oxidation model could be established based on the knowledge of the chemistry of C_1 to C_3 hydrocarbons [56]. Reliable elementary reaction mechanisms for these fuels are now emerging (e.g. [57,58]). Such detailed oxidation mechanisms are yet too complex to incorporate directly in CFD models, but they can be used as part of a simplified reactor modelling approach [59] or as the basis for establishing simplified oxidation schemes. Flame phenomena, which require a detailed description of the gas phase chemistry include formation and destruction of pollutants such as nitrogen oxides (see below), polyaromatic organic compounds and soot, but also flame stabilization and ignition/extinction.

Under fluidized bed conditions volatiles oxidation may take place in both the emulsion and bubble phases. The degree of volatiles oxidation in the bed depends on the temperature and the particle size of the bed material. Below a certain critical temperature, approximately 1100 K [60], little oxidation of coal volatiles occurs in the emulsion phase and ignition takes place in the bubbles and at the bed surface. Under these conditions, the gas phase chemistry is more or less quenched in the emulsion phase due to radical losses to the particle surfaces [60,61]. Similar effects have been postulated for pulverized coal flames at high solids concentrations [62]. At higher temperatures, volatiles oxidation occurs readily in the emulsion phase.

The heat transfer mechanisms in FBC are quite different from those of PF combustion, and the volatiles oxidation is not so important for ignition and flame stabilization. However, the gas–phase chemistry, which occurs to a significant extent above the dense bed, has probably a significant impact on pollutant emissions.

In fuel bed combustion, oxidation of the volatiles takes place in the freeboard over the grate. Depending on the specific design, volatiles oxidation may have significant influence on solid fuel ignition. In these units, the particle concentrations in the freeboard are fairly low, and gas–solid interactions are less important than in FBC. Typically the volatiles oxidation temperatures will lie between those of PF combustion and FBC.

3.2   Nitrogen Oxides

Although combustion modification has proven to be a viable method of reducing NO_x emissions from pulverized–coal–burning equipment, the full potential of these techniques has probably not yet been achieved because of a lack of reliable and efficient combustor modelling tools. One problem is that the pathways to formation and destruction of NO_x have not been fully explained.

Three different NO_x formation mechanisms have been identified in fossil fuel combustion (Fig. 9). Two of these mechanisms, *thermal* NO and *prompt* NO, are initiated by fixation of the molecular nitrogen in the combustion air, while the third, *fuel–NO*, involves conversion of nitrogen chemically bound in the fuel.

Thermal NO formation is initiated by the reaction

$$O + N_2 \rightleftharpoons NO + N, \tag{9}$$

followed by oxidation of the N atom to NO by reaction with OH or O_2. Because the $O+N_2$ reaction has a high activation energy, this mechanism is important at temperatures above 1800 K. Prompt NO, which is less temperature–dependent,
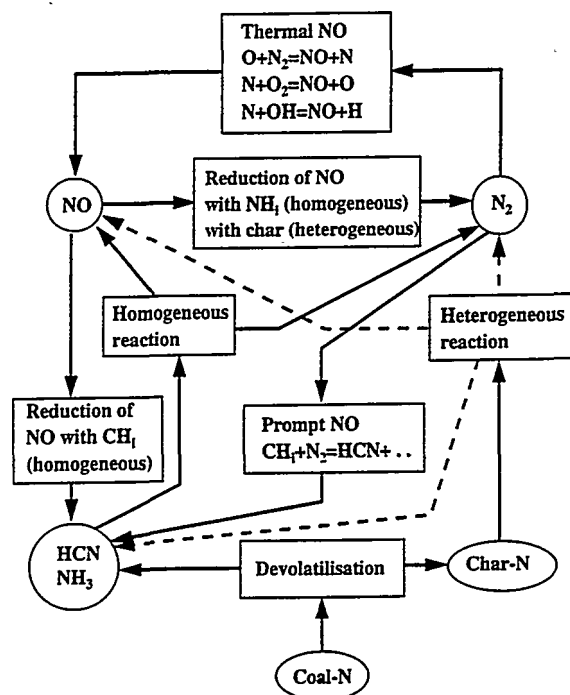
Figure 9: Formation and destruction of NO in coal combustion [63].

is initiated by the attack of hydrocarbon radicals on N_2, primarily

$$CH + N_2 \rightleftharpoons HCN + N. \tag{10}$$

Subsequently, HCN can be oxidized to NO through a sequence of elementary steps that involves intermediate cyanides and amines [64–66], or converted back to N_2 by the reaction of cyanide or amine radicals with NO. The detailed chemistry of these two mechanisms is fairly well established [64,65]. However, neither thermal NO nor prompt NO are very important in the combustion of fuels which contain significant amounts of bound nitrogen, such as coal.

Nitrogen oxides formed in coal combustion can be attributed mostly to fuel–NO ($\sim$ 80%). As discussed above, the coal–N may be partially devolatilized or retained in the char with the apportionment determined in part by the thermal exposure of the particles. The volatile–N consists mostly of tarry compounds which decay rapidly to HCN in the gas–phase. The homogeneous oxidation of HCN is presumed to be similar to that of prompt–NO, i.e. oxidation to NO via intermediate cyanides and amines or, depending on stoichiometry and fuel–N concentration, conversion to N_2 by the recombination of NO with another nitrogen containing species [62]. The remaining char–N can evolve at high temperatures as HCN and/or NH_3, depending on coal type, or undergo heterogeneous oxidation. NO once formed may be recycled by hydrocarbon radicals to cyanide or interact with the char or soot. This overall reaction sequence (Fig. 9) provides a useful

explanation of experimental trends, but more work is required to determine the rate–limiting processes.

Fluidized bed combustors and fuel bed units are characterized by intrinsically low NO_x emissions, mainly because of the low temperatures involved. In FBC, the high concentrations of solids and the staging of the combustion air also help minimize the conversion of fuel–N to NO. However, significant amounts of N_2O may be formed in these units. Both heterogenous (see below) and homogeneous pathways to N_2O may be significant. Knowledge about the homogeneous formation (with HCN as the main precursor) and destruction (dissociation, reaction with radicals) of N_2O is now well established, e.g. [66–69].

In the CHEC research programme there has been a great deal of activity over the years aimed at understanding and developing reliable modelling tools for the homogeneous nitrogen chemistry, both prompt and thermal NO formation [64,70], destruction of NO by reaction with hydrocarbon radicals [64,70–72], and the conversion/interaction of reactive nitrogen compounds [66–69,73–76] arising either from fuel–N conversion or from hydrocarbon attack on atmospheric N_2 (Fig. 9).

3.3 Other Gas–Phase Pollutants

Besides nitrogen oxides, the major homogeneous pollutants from fossil fuel combustion are sulphur oxides. During excess air combustion, fuel–bound sulphur is oxidized almost completely to sulphur dioxide (SO_2), with minor amounts of sulphur trioxide (SO_3) also formed. Because SO_x emissions can be controlled only with flue gas cleaning methods or sorbent addition, interest in homogeneous sulphur chemistry has been motivated partly by the interaction of sulphur species with fuel oxidation and nitrogen chemistry and partly by the adverse effects of a high SO_3/SO_2 ratio in the flue gas. Oxidation of SO_2 to SO_3 is undesirable in the combustion process, since the presence of SO_3 enhances corrosion problems and increases the probability of aerosol emissions. SO_3 is thermodynamically favoured at lower temperatures, but kinetic limitations/high gas cooling rates often prevent the attainment of SO_3/SO_2 equilibrium. The kinetic parameters controlling the SO_3/SO_2 ratio in the post–flame zone were recently investigated [77].

Another undesired emittant is carbon monoxide. Emissions of CO are usually an indication of poor combustion and are often attributed to inadequate mixing of burnout air. However, in some combustion systems CO is inherently difficult to control because of air staging, residence time/temperature limitations or fluctuations in the fuel reactivity (such as in waste incineration). Under these conditions the kinetic limitations for CO oxidation become important. Recent work [77–79]

has shown that species such as nitrogen oxides, sulphur oxides and halogenes, which are present in the flue gas in trace quantities, can have a significant impact on the CO oxidation rate. Nitric oxide generally promotes CO oxidation [78,79], while SO_2 [77] and HCl [78] inhibit oxidation.

4 Heterogeneous Reactions

4.1 Char Combustion

The rate of char combustion is low compared to the combustion of volatiles. In pulverized coal combustion, the time for devolatilization to take place is on the order of 0.1 second; for char burnout, the time is on the order of 1 second. In a fluidized bed combustor the corresponding orders are 10 and 1000 seconds ([80] and Table 2). Different mechanisms are important for the combustion of char, depending on the reaction temperature. At low temperatures, the chemical reaction limits the rate and at high temperatures external mass transfer is rate–limiting. In the intermediate regime, external mass transfer, chemical reaction and pore diffusion may influence the combustion rate, and so combustion of porous chars can be divided in three regimes [81] with transition zones in between [80]. Figure 10 shows the controlling mechanisms in a logarithmic plot of reaction rate versus reciprocal particle temperature.

Regime I
The rate of reaction is controlled by the rate of chemical reaction with no concentration gradients in the gas film or in the particle. The reaction rate is usually expressed as

$$r_c = kC_{O_2}^n \tag{11}$$

$$k = k_0 \exp(-E/RT), \tag{12}$$

where r_c is the intrinsic reaction rate of char combustion based on the char particle volume, mole $m^{-3}s^{-1}$. Combustion takes place uniformly, so the particle burns with a constant diameter and decreasing density. In this regime, the apparent activation E_a is equal to the activation energy E of the chemical reaction. The apparent reaction order with respect to O_2, m, is equal to the order of the chemical reaction n.

Regime II
Strong pore diffusion limitations. In this regime, the chemical reactions are fast enough to result in a steep O_2 concentration gradient in the particle. The apparent activation energy becomes half the value of the activation energy for the chemical reaction, and the apparent reaction order is m=(n+1)/2. There are changes in both size and density of the char particle during combustion.
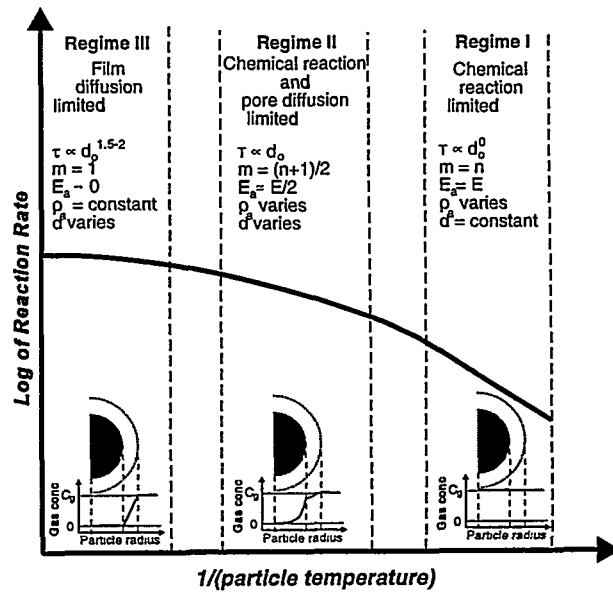
Figure 10: Arrhenius plot of reaction rate versus reciprocal particle temperature for combustion of a porous char particle. E_a and m are apparent activation energy and apparent reaction order respectively, d is the initial particle diameter, ρ_a is the particle density and τ is the burnout time. Modified from Hobbs *et al.* [80].

Regime III
The rate of combustion is controlled by the rate of O_2 transport through the gas film (external mass transfer, film diffusion). The apparent reaction order is 1 and the apparent activation energy is low because the influence of temperature on the mass transfer coefficient is small. The particle burns with a constant density and decreasing size.

Between these ideal regimes, there is a smooth transition as shown in Figure 10. The temperature of change between the regions depends on several parameters: especially the particle size but also the reactivity of the char and the pressure are important parameters. The general rate equation for char combustion with CO as a product and n=1 is [82]

$$r_c = \frac{C_{O_2}}{1/(k\eta) + V_p/(2k_g S_{ex})} \tag{13}$$

V_p and S_{ex} are the volume and external surface of the char particle respectively and k_g is the mass transfer coefficient. The effectiveness factor η for a first order reaction and spherical geometry is given by [83]

$$\eta = 3 \cdot \left(\frac{1}{\phi \cdot \tanh\phi} + \frac{1}{\phi^2} \right) \tag{14}$$

ϕ is the Thiele modulus defined as

$$\phi = \frac{d}{2} \cdot \sqrt{k/D_e} \qquad , \qquad (15)$$

In this simplified treatment, the effective diffusion coefficient, D_e, is assumed to be independent of the radial position, but in Regime II the porosity and D_e will change with position and time.

A large value for the Thiele modulus gives a low effectiveness factor, and it is seen that in the case of a large particle diameter (d) or a high value of k (i.e. a high reactivity or temperature) and a low effective diffusion coefficient, η will be low and the reaction will be in the strong pore diffusion regime, and eventually external mass transfer may be controlling. Table 2 shows burning rates for char in typical coal combustion systems. With the larger film diffusion controlled sizes used in grate firing, the reaction time varies with the initial diameter raised to a power of 1.5–2. In pulverized coal firing with char particle sizes below 100 μm, the chemical reaction was previously believed to be controlling [84]. However, with reactive fuels and high temperatures the rate is influenced by diffusion. Hurt and Mitchell [85] found film diffusion to be controlling at a gas temperature of 2000 K for a suite of ten US coals and with the most reactive coals diffusion–limited burning was observed at 1500 K. The use of low–NO_x technology moves the mechanism towards reaction control because of the lower combustion temperature.

In a fluidized bed using particle sizes from 0.5 to 7 mm Pillai [86] found that external mass transfer was controlling at 1283 K, but at a typical FBC temperature of 1148 K both chemical reaction and diffusion influenced the burnout time. At 1048 K the chemical reaction was controlling except for a very reactive char from Texas Lignite. Increasing the pressure from 1 to 5 bar when burning 0.7 mm coke particles at 1123 K changed the combustion regime from II to III (film diffusion) [87].

In fuel bed firing and pulverized coal combustion, the reaction time or char burnout time is an important parameter for design and operation because of the correlation with combustion efficiency and carbon burnout in the ash. In circulating fluidized bed combustion, the reaction time for the char is less important for operation, and the combustion efficiency is determined by the cyclone cut size diameter. A typical char content in a fluidized bed when burning bituminous coal is 1–3 wt% of the bed material, depending on operating conditions, but a variety of fuels can be burned in a given combustor. If the fuel is less reactive, the reaction time increases and so does the char content in the bed. In a 12 MW$_{th}$ circulating fluidized bed burning wood chips, bituminous coal and coke, 0.1, 2.2 and 12.0 wt% of char respectively were found in the solids at the bottom of the combustion chamber [88]. A decreasing combustion efficiency with decreasing fuel reactivity was observed. The char content may also be important for the

NO_x chemistry in FBC because of the simultaneous formation of NO and N_2O during char oxidation and the reduction of NO and N_2O by char or catalyzed by char.

The main gaseous products from the combustion of char particles are CO, CO_2, H_2O, SO_2, NO and N_2, but minor amounts of N_2O, NH_3 and HCN may also be formed. The sulphur is oxidized to SO_2 and a minor part of it may be oxidized to SO_3 and/or react with the mineral content of the char, e.g. to form $CaSO_4$, or K_2SO_4 if burning biomass [15]. Most of the nitrogen content is intrinsically oxidized to NO and perhaps N_2O, but may be reduced to N_2 in the pore system of the char [25]. In fixed bed char particle combustion, it was observed that the char–N conversion to NO decreased with increasing pressure from 1 to 5 bar in the case of 0.7 mm char particles [87]. This effect was explained by the film diffusion controlled combustion at higher pressures resulting in higher NO and CO concentrations in the pore system and thus a faster reduction of NO, because char is an active catalyst for the reduction of NO by CO, as explained below.

4.2   Nitrogen Chemistry

Figure 11 shows a simplified reaction scheme for the heterogeneous reactions in NO_x and N_2O formation and reduction. In general, heterogeneous reactions are of relatively greater importance at low temperatures because the activation energies are lower than the typical values for homogeneous gas phase reactions. In pulverized coal combustion, NO, NH_3, HCN, N_2O and other nitrogen–containing species react rapidly in the gas phase, and heterogeneous reactions are almost only of importance during char burnout. However, Peck et al. [62] concluded that radical recombination on soot surfaces influenced NO formation, and NO reduction by soot and char contributed to the reduction of NO in fuel–rich flames. At fluidized bed combustion temperatures and solids concentrations, heterogeneous catalytic and gas–solid reactions are important for the emission of NO and N_2O. The heterogeneous catalytic reactions for the conversion of fuel–nitrogen in FBC are complex, as illustrated in Figure 11. The mixture of solids in FBC usually consists of char, sand, ash and limestone, but sand and/or limestone may be absent. Char and calcined limestone have in general a high catalytic activity, but the activity of coal ash is dependent on the parent coal. The reaction rate of a given reaction depends on the type of catalyst, and different reactions have very different reaction rates over the same catalyst. The heterogeneous catalytic reaction rates may vary from negligible to extremely high rates, e.g. 5 to 6 orders of magnitude [25].

In FBC the volatile nitrogen species NH_3 and HCN may either be oxidized to NO and N_2 or reduce NO to N_2 depending on the conditions, i.e. the presence of catalysts, the O_2 concentration and the temperature. The NO and N_2O formed

DEVOLATILIZATION

AND   NO AND N_2O FORMATION AND REDUCTION

CHAR COMBUSTION

<div>

REACTION TYPE

		GAS-SOLID	CATALYTIC
$HCN + O_2$ → N_2, NO, (N_2O)			X
$NH_3 + O_2$ → N_2, NO, (N_2O)			X
$NO + CHAR$ → N_2		X	
$NO + O_2 + CHAR$ → N_2, N_2O		X	X
$N_2O + CHAR$ → N_2		X	
N_2O → N_2			X
$NO + CO$ → N_2			X
$NO + H_2$ → N_2, NH_3			X
$NO + NH_3$ → N_2			X
$N_2O + CO$ → N_2			X

CHAR-N → N_2, N_2O, NO, HCN, NH_3

COAL-N

VOLATILE-N → HCN, NH_3

</div>
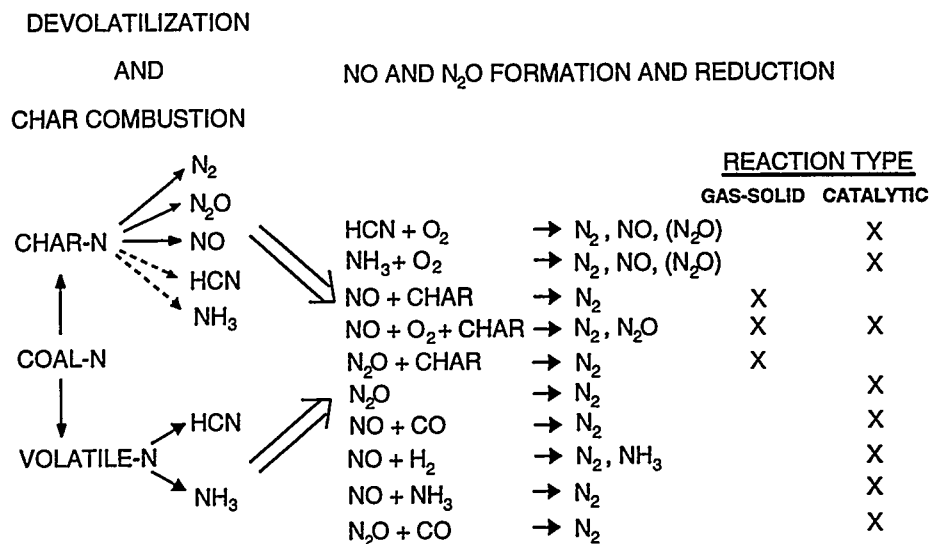
Figure 11: Simplified reaction scheme for coal devolatilization and the heterogeneous formation and reduction of NO and N_2O. Modified from Johnsson [25].

may be reduced in a number of heterogeneous gas–solid and catalytic reactions, as seen in Figure 11.

Table 3 shows a comparison of the catalytic activity of calcined limestones for the oxidation, decomposition and reduction of volatile nitrogen compounds [25]. The results are compiled from many references, and the variation range of the activity for a given reaction may be attributed to the use of different types of limestone [25]. The oxidation of HCN over calcined limestone is a very fast reaction compared to other gas–solid or heterogeneously catalyzed reactions in FBC. It is one to two orders of magnitude faster than the reduction of NO by char. The oxidation of NH_3 over calcined limestone is a slightly slower reaction than oxidation of HCN, and char has about the same activity as limestone in the oxidation of both components. Sulphation of limestone deactivates the catalyst, probably because of the combined effect of a loss of porosity and a lower catalytic activity of $CaSO_4$ [89,90].

In FBC limestone is usually added for sulphur retention, and in many cases an increase in NO emissions and a decrease in N_2O emissions are observed [25,29,91]. The increase in NO emissions is due to the fast catalytic oxidation of HCN and NH_3 to NO over calcined limestone. The lower N_2O emissions are partly due to a change in the HCN oxidation from a homogeneous route with high selectivity for N_2O formation [66,68] to a heterogeneous catalytic oxidation to NO, and partly due to N_2O decomposition over calcined limestone [91].

Reaction   **Rate Constant**

10^{-3} 10^{-2} 10^{-1} 10^{0} 10^{1}

<u>Oxidation</u>
$HCN + O_2 \rightarrow NO, N_2, (N_2O)$
$NH_3 + O_2 \rightarrow NO, N_2, (N_2O)$
<u>Decomposition</u>
$HCN \rightarrow N_2$
$NH_3 \rightarrow N_2$
$N_2O \rightarrow N_2$
<u>Reduction</u>
$NO + CO \rightarrow N_2, (N_2O)$
$NO + H_2 \rightarrow N_2, NH_3$
$NO + HCN \rightarrow N_2$
$NO + NH_3 \rightarrow N_2$
<u>Reduction by Char</u>
$NO + Char$
$N_2O + Char$

[a] Concentrations used in linearization of rate equations when necessary: NO, 500 ppmv ; N_2O, 100 ppmv; CO, 2 vol%; H_2, 0.5 vol%; NH_3, 400 ppmv; HCN, 100 ppmv, at 101.3 kPa
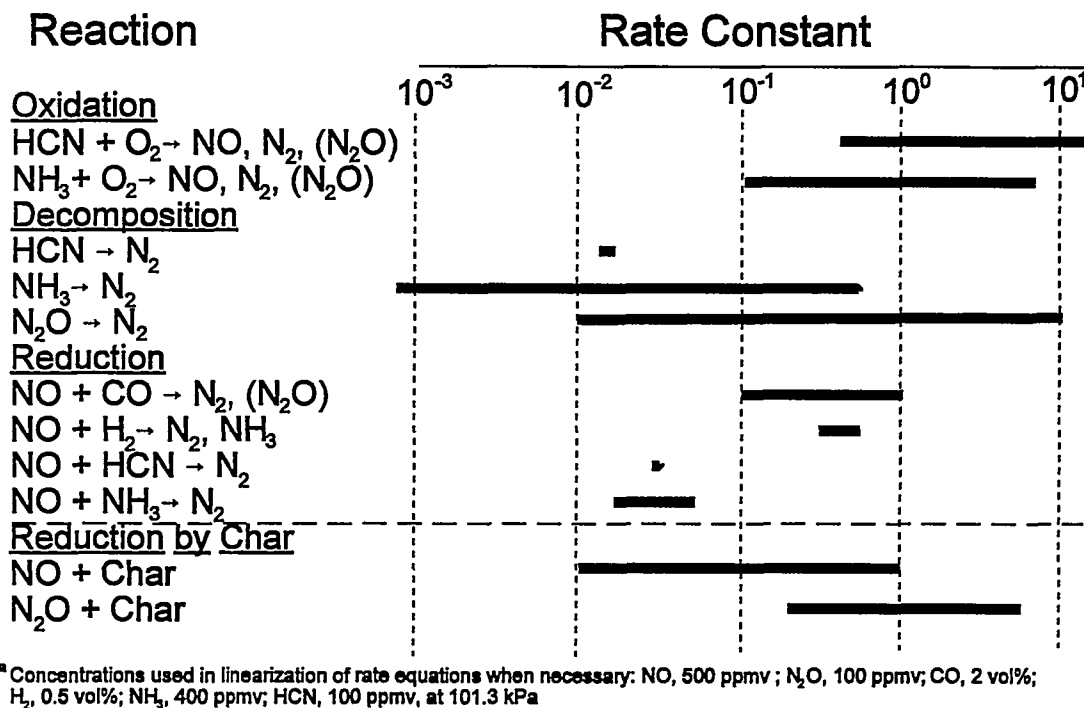
Table 3: Pseudo first order rate constants ($m^3 s^{-1} kg^{-1}$) for reactions catalyzed by calcined limestone at 1100 K[a]. The rate of NO and N_2O reduction by char is shown for comparison. Modified from Johnsson [25].

Existing detailed information about heterogeneous nitrogen chemistry and kinetics in fluidized bed combustion provides a better understanding of phenomena in full–scale plants and can be used to predict the influences of changes in design and operating conditions on the emissions of NO and N_2O. The first FBC models with a comprehensive kinetic model for the heterogeneous reactions showed the importance of char, limestone and ash for the fuel–N conversion to NO [92,93]. However, kinetic information about the heterogeneous reactions was scarce, and many activity studies have since been performed under the auspices of the CHEC research programme [29,89–91,94–100]. To perform reliable kinetic modeling, the wide variation in activity for different types of limestone and char seen in Table 3 necessitates known kinetic data for the specific solids in a given plant. Knowing the kinetics for the heterogeneous catalytic reactions made it possible to model full–scale plants. In all cases, the combination of experimental results from combustors and the measurement of kinetic data in laboratory experiments were used to set up and test FBC models for NO and N_2O formation and reduction [29,101–106].

To illustrate how mathematical modelling can be used to identify optimal operating conditions to produce a low emission of NO, the results from simulation

of the influence of air staging in a pressurized bubbling fluidized bed (PFBC) burning bituminous coal will be discussed.
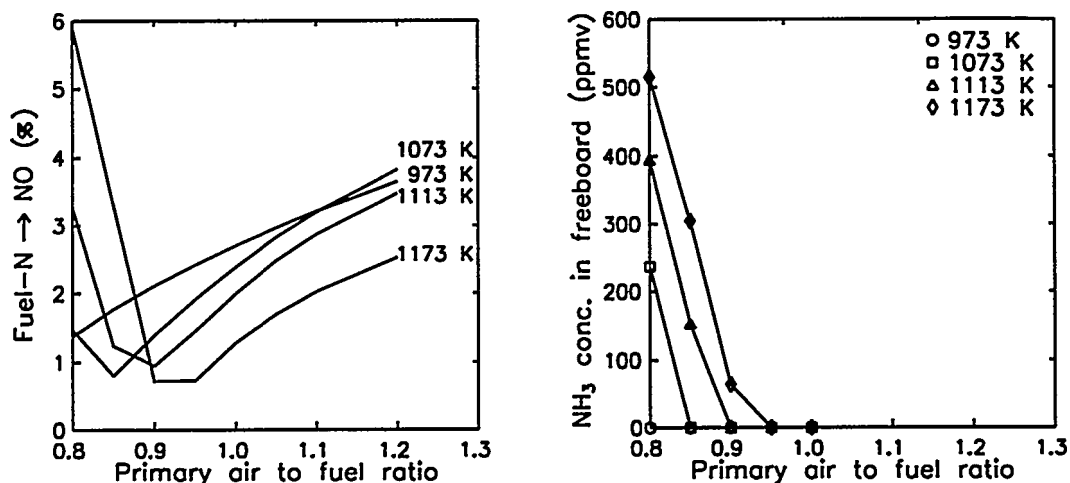
Figure 12: Influence of primary air to fuel ratio on a) the fuel–N conversion to NO in a bubbling pressurized fluidized bed combustor, and b) the concentration of NH$_3$ in the freeboard of a bubbling pressurized fluidized bed combustor after mixing with secondary air [104].

Figure 12a shows model results [29,104] on the influence of the primary air–to–fuel ratio on the conversion of fuel–N to NO at a fixed total air–to–fuel ratio of 1.2 at four different temperatures. There is a minimum in the conversion of fuel–N to NO at a primary air–to–fuel ratio of 0.85 to 0.9 for the three highest temperatures. The reason for the minimum is that at very low primary air to fuel ratios, a large fraction of the NH$_3$ released by coal devolatilization is not oxidized in the bed and NH$_3$ enters the freeboard, where some of it oxidizes to NO during secondary air addition. Figure 12b shows the NH$_3$ concentration in the freeboard after mixing with secondary air. The NH$_3$ concentration increases with temperature and decreasing primary air–to–fuel ratio, because O$_2$ is consumed faster in the bed under these conditions and less O$_2$ is available for oxidation. By increasing the primary air–to–fuel ratio, more NH$_3$ is oxidized in the bed where the NO formed can be reduced. Consequently, NO emissions initially decrease with increasing air to fuel ratio (Fig. 12a). At higher values of the primary air–to–fuel ratio, NO emissions increase with increasing primary air–to–fuel ratio because the oxidizing conditions in the bed results in lower CO and char concentrations and consequently a lower rate of NO reduction. At the lowest temperature of 973 K, no minimum is observed in Fig. 12a, and Fig. 12b shows that this is because all NH$_3$ is oxidized in the bed even at the lowest primary air–to–fuel ratio of 0.8. The reason is that the rates of the homogeneous combustion reactions are low and not all O$_2$ is consumed in the bed. Consequently, all NH$_3$ is oxidized in the

bed, where the NO produced may be reduced by char or catalytically by CO. A minimum in the NO emission during staged combustion has been observed experimentally under PFBC conditions [107,108] and under atmospheric FBC conditions [109]. The predicted value of the primary air–to–fuel ratio where the minimum is observed is in good agreement with experimental observations [107–109].

5   In–Furnace Reduction of Emissions

5.1   Nitrogen Oxides

Increasingly stringent NO_x emissions regulations are being implemented in a number of industrialized countries. These regulations have driven and continue to drive the development of NO_x emissions control techniques [110]. Approaches for controlling NO_x emissions from stationary sources can be divided into combustion modification techniques and post–combustion methods. These are reviewed elsewhere, for instance in [110]. A common and efficient combustion modification technique is the use of low–NO_x burners which employ aerodynamic staging of the combustion air to create fuel–rich regions that minimize conversion of fuel–N to NO and prevents thermal NO formation. Further NO reduction can be achieved by means of post–combustion methods such as the selective non–catalytic reduction of NO (SNCR), fuel staging/reburning, NO to NO_2 oxidation followed by NO_2 scrubbing, or the selective catalytic reduction of NO (SCR).

Apart from recent and ongoing work on low–NO_x burners [111] and FBC units, activities in the CHEC research programme have focused primarily on post–combustion reduction methods. A significant effort has been aimed at characterizing the SNCR process experimentally in laboratory scale [68,112–114], pilot scale [115], and full scale [116], as well as theoretically [73,76,117]. In this process, NO is removed in a temperature window at about 1250 K by injecting a selective reducing agent such as ammonia or urea downstream from the primary combustion zone. SNCR has proven to be an efficient method for controlling nitrogen oxide emissions in a number of combustion systems [116,118].

Another approach is to use fuel as a (non–selective) reducing agent. In reburning, part of the fuel (10–20%) is added downstream from the primary zone to create a fuel–rich region in which NO is converted to HCN and then to N_2 (see figure 9). Burnout air is then added to ensure complete combustion of the fuel. Natural gas has been used successfully as a reburn fuel in a number of full–scale demonstrations [119] and the feasibility of using coal is currently being investigated. Experimental and theoretical work [71,72,75] has contributed towards assessing the process potential and identifying optimum conditions.

The oxidation of nitric oxide to nitrogen dioxide by a combustible additive may constitute a promising NO_x control strategy if nitrogen dioxide can be removed economically for instance in existing wet scrubbers for flue gas desulphurization. Of the various agents tested [120], methanol has a particularly great potential for oxidizing NO. Oxidation takes place in a narrow temperature regime, typically 850–1050K. The technique has been tested in pilot scale with encouraging results [121]. The major drawback of the technique is that it may give rise to increased emissions of CO.

Fluidized bed and most fuel bed combustors are characterized by lower NO_x emissions than is the case with pulverized fuel firing. For this reason, comparatively little research has been devoted to developing and testing NO_x control strategies in fluidized bed combustion and secondary measures have been considered unnecessary in most cases. However, due to increasingly stringent legislation concerning nitrogen oxide emissions, as well as the significant amount of attention paid to nitrous oxide exhaust levels in FBC, it has become necessary to consider in–situ methods for controlling NO and N_2O.

SNCR is a possible means of controlling NO emissions in FBCs and this technology has been tested both on a laboratory scale and in large–scale fluidized bed combustors. The temperatures in FBC are typically below the optimum range for SNCR, but the presence of combustibles in the flue gas shifts the low temperature boundary for the SNCR reaction to even lower values, thereby promoting the process. Full–scale tests reported for various types of FBC systems [122–124] indicate that SNCR is feasible, provided that a proper location for injection of the reducing agent is found.

Nitrous oxide emissions may be more difficult to reduce without adverse effects on other emissions. A higher combustion temperature appears to be an efficient way to reduce N_2O. However, a higher bed temperature has significant adverse effects: NO emissions increase and sulphur capture becomes less efficient [88]. An alternative which has been tested in full scale [125] is secondary fuel injection. By injecting a fuel downstream from the combustion chamber, the radical pool is replenished and the flue gas temperature is increased, providing favorable conditions for the decomposition of N_2O. This process, which has a significant N_2O reduction potential, has now been well described theoretically and experimentally [125–127].

5.2   Sulphur Dioxide Retention on Limestone

Direct injection of limestone into a furnace may be used to reduce sulphur dioxide emissions. The main constituent in limestone is calcium carbonate which at high

temperatures undergoes fast calcination to form calcium oxide:

$$CaCO_3(s) \rightleftharpoons CaO(s) + CO_2(g). \qquad (17)$$
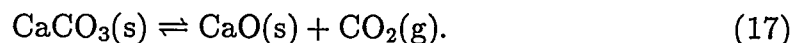
Calcium oxide can react with gaseous sulphur dioxide to form calcium sulphate under oxidizing conditions:

$$CaO(s) + SO_2(g) + 0.5O_2(g) \rightleftharpoons CaSO_4(s). \qquad (18)$$
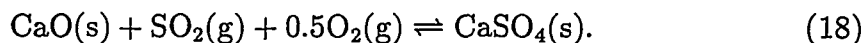
The calcium sulphate produced is predominantly in the form of anhydrite III, not anhydrite II (soluble anhydrite) as commonly assumed in the literature. The respective molar volumes of calcium carbonate, calcium oxide and calcium sulphate are approximately 36.9, 16.9 and 46.0 cm^3/mol. Thus significant volume changes occur in the solid phase in the course of the reactions and the initial physical texture of the limestone greatly influences the rate and ultimate degree of sulphation of different limestones [5–8,128].

In fuel–bed and entrained–flow combustors, the calcination and sulphation reactions take place in the freeboard in a once–through process with a residence time of only a few seconds. For this reason small limestone particles are used and often a relatively low degree of sulphation is obtained. These processes are usually only of relevance for retrofitting existing plants.

In fluidized bed combustion, particles have a much longer residence time. Larger limestone particles may be used and a higher degree of sulphation obtained. Comparison by Dam–Johansen and Østergaard [5] of more than 20 different types of limestone in two laboratory reactors and a coal–fired fluidized bed pilot plant showed that the sulphur capacity of limestones correlates closely with its physical texture and thus its geological age. Limestone can be divided into three categories according to its reactivity: the most reactive types are chalks with a porous, fine–grained texture of a relatively young geological age, whereas the least reactive are geologically old, crystalline calcites with a very low porosity. Types of intermediate reactivity are limestones of intermediate geological age with a porous, coarse–grained texture. Apart from these characteristics the attrition of limestone may also influence its sulphur capture capacity in practical combustors.

Extensive studies carried out at Chalmers University of Technology [129–131] and in the CHEC research programme [9,132] have shown that the sulphur retention process is more complicated than indicated by reactions (17) and (18). The complications are due to the existence of local reducing conditions in the bed primarily below the secondary air inlet. The local reducing conditions may lead to reductive decomposition of already–formed calcium sulphate or to the formation of calcium sulphide which again under oxidizing conditions may rapidly liberate sulphur dioxide as illustrated in Figure 13.

Thus the net sulphur emission from FBC with limestone injection is a result of a competition between the capture and release of SO_2, and the temperature

O_2

SO_2 — — CaO ← — → SO_2

O_2

$CaSO_4$ CaS

CO — — → CO_2

SO_2 ← — CaO — — → SO_2

CO_2 CO
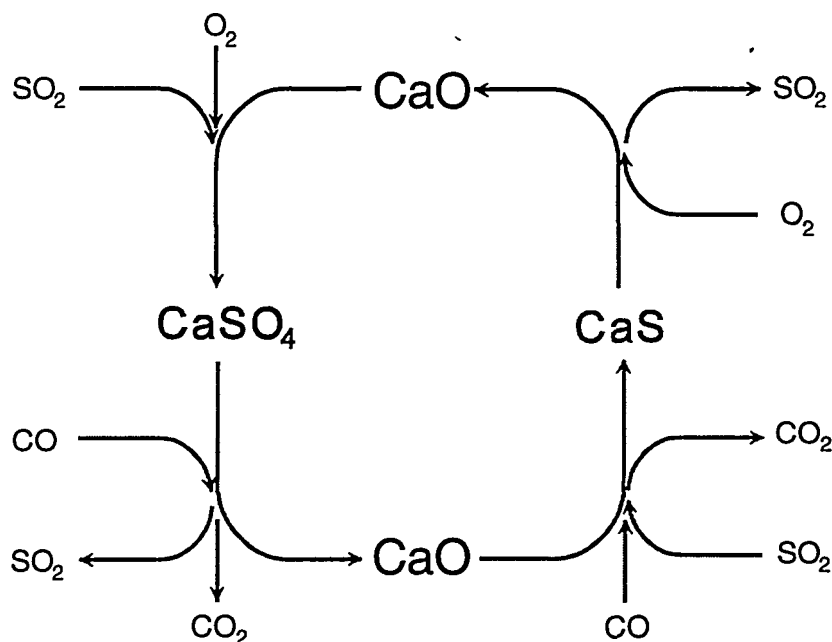
Figure 13: The mechanism of sulphur capture and release in FBC [9].

optimum observed for sulphur retention, about 1123 K, is mainly caused by this competion [9,132].

Calcined limestone acts as a solid reactant for sulphur species but is also an active catalyst for CO oxidation [133], for oxidation of nitrogen–containing compounds into NO and N_2O and for the reduction of NO and N_2O (see 4.2 above). These effects often result in an increased emission of NO if excess amounts of limestone are injected in order to secure a high degree of sulphur retention [134].

6   Mineral Transformations

6.1   Ash Formation and Transport

The elements contained in fossil fuels and biofuels can be grouped in three concentration levels [135,136]: 1) the major elements discussed previously (C, O, H, S and N) which form the organic matrix of the fuel, 2) the ash–forming elements, Al, Ca, Fe, K, Mg, Na and Si, present in the concentration range of about 1000 ppm to a few wt% on a dry fuel basis, and 3) trace elements, e.g. As, B, Cd, Cr, Hg, Pb, Se, Zn, and Cl, typically present in concentrations below 1000 ppmw on a dry fuel basis.

The ash–forming elements occur in fuels as internal or external mineral grains, simple salts such as Na_2SO_4 and KCl or associated with the organic matrix of the fuel (see Figure 14). In pulverized coal combustion, approximately 1 wt% of the inorganic metals is vaporized, while the rest remains in a condensed form as mineral inclusions [137].
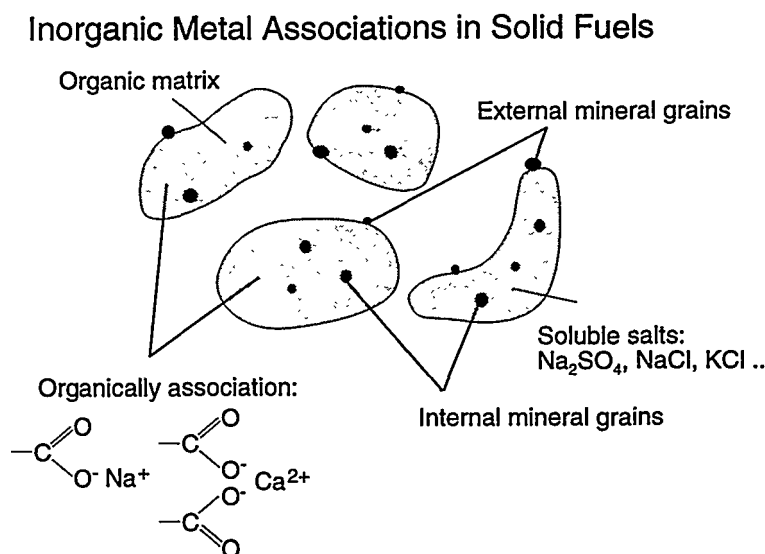
Figure 14: Inorganic metal associations in solid fuels.

Depending on the gas/particle temperature and redox conditions during coal particle heat–up, devolatilization and char burnout, these mineral inclusions will undergo phase transformations and approach each other to form a fly ash fraction: the residual ash (Figure 15). Laboratory experiments have shown that typically 3–4 residual fly ash particles are formed per coal particle [139]. The vaporized metal species may undergo several reactions: nucleation, coagulation, heterogeneous condensation and/or interactions with mineral inclusions in the burning char or residual fly ash particles, depending on the total specific surface area of the residual ash particles, the cooling rate of the flue gas, the redox conditions, and mixing in the gas phase. Local supersaturation with respect to certain chemical species such as $Na_2SO_4(g)$, KCl(g) and $K_2SO_4(g)$ may lead to the formation of submicron ash by homogeneous nucleation [137,140].

In a FBC unit burning a fuel such as straw, a high concentration of gaseous potassium species may be encountered. These potassium species may interact with the surface of the bed material to form low–melting eutectic mixtures, which in turn may lead to bed agglomeration and possibly even defluidization of the bed [141,142].

Vapours and fly ash particles may be deposited on heat transfer surfaces in the boiler through a number of mechanisms [143–145]: inertial impaction, ther-

Figure 15: Inorganic metal transformations in utility boilers [138].

mophoresis, condensation and chemisorption. Ash deposits may cause several operational problems (see Figure 16), e.g. changes in the heat uptake of the boiler [146], corrosion of heat transfer metal surfaces [147–149] and/or in extreme cases plugging of the convective pass of the boiler. This may cause unscheduled outages of the boiler and significant financial loss [150]. Thus, the ash forming elements in fuels constitute a potential operational and cost problem [136,151,152].

Although their abundance in fuels is very low, trace elements constitute a potential emission problem: they may cause biological and toxicological reactions in living creatures when emitted from combustion sources [135,153–155]. Trace elements may be vaporized during devolatilization. During flue gas cooling they may recondense on the surface of for example submicron fly ash particles [156,157]. These submicron particles are difficult to retain in a particulate removal device, e.g. an electrostatic precipitator. Some trace elements, such as B, Hg and Se may remain in the flue gas as vapours even at stack temperatures ($\sim$350 K) [158–160].

6.2 Ash Deposit Formation and Corrosion

Several CHEC activities concerning ash deposition and corrosion in thermal fuel conversion systems have been published. A brief introduction to these is given below.

With the use of probes for λ–type measurements, for particle and gas sampling

Figure 16: Ash deposit formed on a pendant superheater in a Danish power station [168].

and for alkali metal sampling, the fate of alkali metals has been investigated in a number of biomass and coal–biomass co–fired combustion systems [4,10,161–164].

A systematic comparison of fuel composition, fly ash, deposits and gas phase alkali metal concentrations was performed and a simple semi–empirical global equilibrium model was set up for a 20 MW$_{th}$ multi–circulating coal–straw co–fired fluidized bed combustor [10]. Alkali metal concentrations of 19 ppmv Na and 58 ppmv K were measured in the particle cooler, compared with 32 ppmv Na and 433 ppmv K in the riser section. Model results were found to correlate well with the experiments performed, except for the riser section, for which the model predicted higher concentrations of K than measured.

Larsen et al. [165] initiated a research project on mineral transformations and ash deposition in coal–fired utility boilers. As part of this project, Laursen et al. [166] performed deposition probe measurements at two Danish power stations firing coals of different ranks and origins. Deposits, fuel ash, bottom ash and fly ash were analyzed by Computer Controlled Scanning Electron Microscopy (CC-SEM) and Scanning Electron Microscopy – Energy Dispersive X–Ray Analysis (SEM–EDX). A model for empirical prediction of ash deposition propensities in PF fired utility boilers was developed by Frandsen et al. [167]. It is based on

the concept of combining a bulk ash chemistry index characterizing the chemical potential of a coal, e.g. the Na or the S content, with a plant parameter characterizing the combustion system (operation, furnace size and geometry, burner belt geometry and/or boiler configuration). Theoretical predictions showed that based on empirical modelling low slagging and/or fouling propensities are to be expected in most Danish power stations [167].

Recent full–scale measuring campaigns in a straw–fired stoker [4,164] and a down–fired furnace burning pulverized straw [163] showed gas phase alkali metal concentrations in the range of 1–60 ppmv Na and 100–420 ppmv K, depending on feedstock mixture and the absence or presence of a filter for particulate removal at the tip of the sampling probe. Use of deposition probes showed an extensive formation of deposits containing up to 40–70 wt% KCl [4,164].

Hansen *et al.* [14] initiated the two–year demonstration programme currently running at Unit No. 1 at the Midtkraft Studstrup power station. This campaign includes in–situ sampling of deposits on water/air–cooled probes; sampling of fly ash, flue gas and gas phase alkali metal species; and aerosols as well as temperature measurements. CHEC is involved in this project through the in–situ gas measurements, sampling of gas phase alkali metal species, and modelling efforts [14].

Hansen *et al.* [13] investigated the effect of variations in the boiler load on the reaction conditions in the loop seal of a Danish 80 MW_{th} Ahlström Pyroflow Circulating FBC. Tracer experiments and temperature measurements showed that the boiler changed from a circulating to a bubbling mode accompained by a decrease in the loop–seal temperature from 1173 K to 973 K, when the load was reduced from 100% to below 65%. Thus, the redox conditions and the chemistry and transport of S and Cl species in the system were strongly affected by variations in the boiler load.

Pedersen and coworkers [15,168,169] investigated the effect of co–firing of straw and coal on SO_2 and NO_x emissions. It was shown that SO_2 emissions decreased when straw was added to the feedstock mixture. This was due to either chemisorption of SO_2 on CaO and K_2O in the straw ash or a reaction between KCl and SO_2 in the gas phase to form $K_2SO_4(g)$, which may then condense on the surface of fly ash particles.

6.3   Trace Element Emissions

In 1986, the Danish Utilities Environmental Committee decided to perform mass balance measurements, including the trace elements, As, B, Cd, Cr, Hg, Ni, Pb and Se, at three Danish power stations equipped with different types of flue gas

desulphurization units. Sander [158] reported the main results and conclusions of this mass balance study.

Frandsen *et al.* [170,171] and Frandsen [172] performed an extensive theoretical study of the fate of 18 trace elements – including those mentioned above – in a pulverized–coal–fired boiler as a function of temperature and redox conditions. The equilibrium composition of a well–defined system at a constant total composition, constant pressure and constant temperature was calculated by minimizing the total Gibbs free energy of the system. This type of calculation provides valuable information about the equilibrium distribution of a particular element among and within fluid and crystalline phases in a chemically reacting system (Fig. 17).

Global Equilibrium Analysis (GEA)
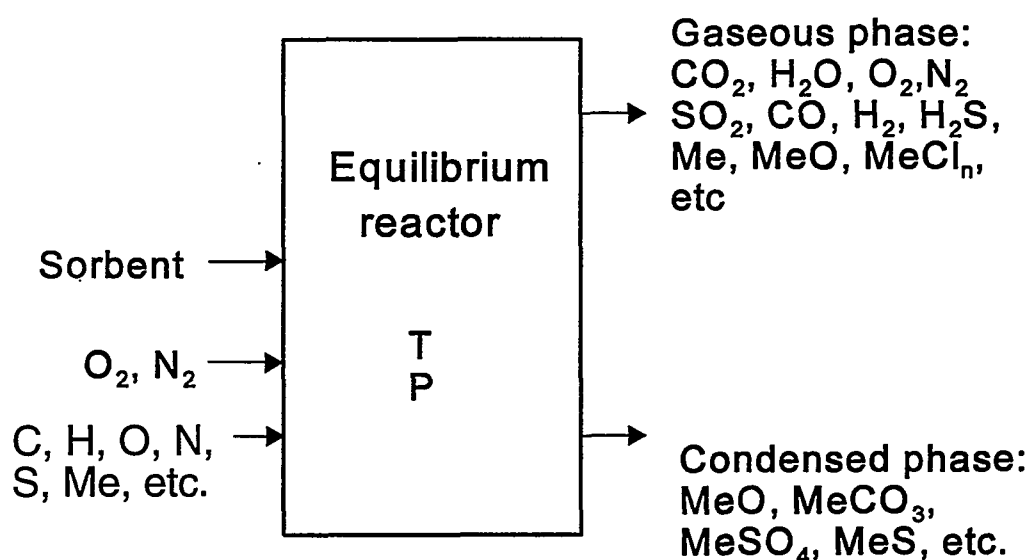
Figure 17: Model system for the Global Equilibrium Analysis of combustion systems.

Figure 18 shows the equilibrium distribution of mercury (Hg) in an oxidizing flue gas from the combustion of a bituminous Columbian coal. Calculations such as the one shown in Figure 18 for trace element partitioning in coal–fired power plants were compared with results from full–scale mass balance measurements for the trace elements As, B, Cd, Cr, Hg, Ni, Pb and Se. Model predictions correlated reasonably well with the measurements [170,172].

Frandsen *et al.* [173] compared output from four thermodynamic packages for the trace elements As, Cd, Cr, Hg, Ni, Pb and Se. Almost equal equilibrium distributions were obtained for the trace elements As, Hg and Se, while for other trace elements major differences in equilibrium distribution were observed, primarily
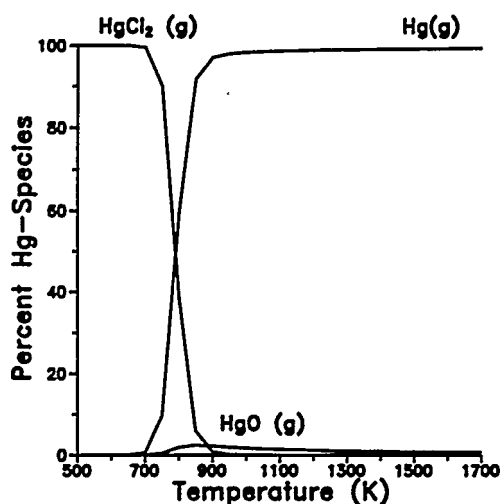
Figure 18: Equilibrium distribution of mercury (Hg) in a flue gas derived from the combustion of a bituminous Columbian coal [172].

due to differences in the thermodynamic data used in the various programmes.

Conclusions

In the Combustion and Harmful Emission Control (CHEC) research programme we work on many of the problems encountered with different technologies for combustion of fossil fuels and biofuels. Our projects cover characterization and pre–treatment of fuels, fuel oxidation and pollution chemistry including pollutant reduction in the furnaces, ash–formation, slagging, fouling and corrosion, and trace element chemistry as well as measuring techniques for process characterization. Experimentally we work with small laboratory scale reactors, in pilot plants, and in full scale boilers, often in co–operation with the Danish Utilities, and our experimental work is closely connected to theoretical modelling and data base development.

Acknowledgements

References

[1] Elsam, Beretning og regnskab, 1995.

[2] Dam–Johansen, K.; "Clean and Efficient Energy Systems for the Future". Dansk Metal/Institut for Kemiteknik, DTU, 1995.(In Danish).

[3] Steadman, E.N., Erickson, T.A., Folkedahl, B.C., and Brekke, D.W.; "Coal and Ash Characterization: Digital Image Analysis Applications", In *Inorganic Transformations and Ash Deposition During Combustion*, S.A. Benson (Ed.), Proc. Eng. Found. Conf., Palm Coast, FA, March 10–15, 1991.

[4] Michelsen, H. P.; "Results of Deposit Measurements at Rudkøbing KVV", CHEC Report No. 9603, 1996.

[5] Dam–Johansen, K. and Østergaard, K.; "High–Temperature Reaction Between Sulphur Dioxide and Limestone. I. Comparison of Limestones in Two Laboratory Reactors and a Pilot Plant." *Chem. Eng. Sci.* **46**, 827, 1991.

[6] Dam–Johansen, K. and Østergaard, K.; "High–Temperature Reaction Between Sulphur Dioxide and Limestone. II. An Improved Experimental Basis for a Mathematical Model." *Chem. Eng. Sci.* **46**, 839, 1991.

[7] Dam–Johansen, K., Hansen, P.F.B., and Østergaard, K.; "High–Temperature Reaction Between Sulphur Dioxide and Limestone. III. A Grain–Micrograin Model and Its Verification." *Chem. Eng. Sci.* **46**, 847, 1991.

[8] Dam–Johansen, K. and Østergaard, K.; "High–Temperature Reaction Between Sulphur Dioxide and Limestone. IV. A Discussion of Chemical Reaction Mechanisms and Kinetics." *Chem. Eng. Sci.* **46**, 855, 1991.

[9] Hansen, P.F.B., Dam–Johansen, K., and Østergaard, K.; "High–Temperature Reaction Between Sulphur Dioxide and Limestone. V. The Effect of Periodically Changing Oxidizing and Reducing Conditions." *Chem. Eng. Sci.* **48**, 1325, 1993.

[10] Hansen, L.A., Michelsen, H.P., and Dam–Johansen, K.; "Alkali Metals in a Coal- and Biomass–Fired CFBC – Measurements and Thermodynamic Modeling", *Proc. 13th Int. Conf. on FBC*, pp. 39–48, ASME, 1995.

[11] Rasmussen, I. and Clausen, J.C.; "The Elsam Strategy of Firing Biomass in CFB Power Plants", *13th International Conference on Fluidized Bed Combustion*, pp. 557–564, K.J. Heinschel (Ed.), ASME, 1995.

[12] Lin, W., Weinell, C.E., Dam–Johansen, K., and Hansen, P.F.B.; "Measurements of Particle Recirculation Rate with Radioactive Tracer Particles in a Large Scale Circulating Fluidized Bed Boiler", *Proc. 3rd Int. Symp. on Coal Comb. Sci. Techn.*, Beijing, P.R. China, Sept. 18–21, 1995.

[13] Hansen, P.F.B., Lin, W., Dam–Johansen, K., and Henriksen, N., "Can Superheater Corrosion during Co–Combustion of Straw and Coal in a CFB–Boiler be Reduced?", *Proc. 5th Int. Conf. on CFBs*, Beijing, P.R. China, May 28–31, 1996.

[14] Hansen, P.F.B., Andersen, K.H., Wieck–Hansen, K., Overgaard, P., Rasmussen, I., Frandsen, F. J., Hansen, L. A., and Dam–Johansen, K.; "Co–Firing Straw and Coal in a 150 MW$_e$ Utility Boiler: In–Situ Measurements", *Biomass Usage for Utility and Industrial Power*, Proc. Eng. Found. Conf., Snowbird, UT, USA, April 28 – May 3, 1996.

[15] Pedersen, L.S., Morgan, D.J., van de Kamp, W.L., Christensen, J., Jespersen, P., and Dam–Johansen, K.; "Effects on SO$_x$ and NO$_x$ Emissions by Co–Firing Straw and Coal", to be presented at the Finnish–Swedish Flame Days, Naantali, Finland, September 3–4, 1996.

[16] Görner, K.; *Technische Verbrennungssysteme*, Springer–Verlag, 1991.

[17] Vuthaluru, H.B., Eenkhoorn, S., Kiel, J.H.A., and Veringa, H.J.; "Trace Element Emissions – Literature Review", Energieonderzoek Centrum Holland (ECN), Report No. ECN-C-94-096, 1994.

[18] Wall, T.F.; "The Combustion of Coal as Pulverized Fuel through Swirl Burners", *Combustion Treatise, Principles of Combustion Engineering for Boilers*, C.J. Lawn (Ed.), Chapter 3, Academic Press, 1987.

[19] Tomeczek, J. and Kowol, J.; "Temperature Field Within a Devolatilizing Coal Particle", *Can. J. Chem. Eng.* **69**, 286, 1991.

[20] Jensen, A.; "Heating of Coal Particles in Fluidized Bed Combustion", CHEC Report No. 9106, 1991.

[21] Howard, J.B.; "Fundamentals of Coal Pyrolysis and Hydropyrolysis", *Chemistry of Coal Utilization*, M.A. Elliott (Ed.), Chapter 12, pp. 665–784, John Wiley & Sons, New York, 1981.

[22] Gavalas, G.R.; *Coal Pyrolysis*, Elsevier, 1982.

[23] Solomon, P.R., Serio, M.A., and Suuberg, E.; "Coal Pyrolysis: Experiments, Kinetic Rates and Mechanisms", *Prog. Energy Combust. Sci.* **18**, 133, 1992.

[24] Freihaut, J.D., Zabielsky, M.F., and Seery, D.J.; "A Parametric Investigation of Tar Release in Coal Devolatilization", *Nineteenth Symposium (International) on Combustion*, pp. 1159–1167, The Combustion Institute, 1982.

[25] Johnsson, J.E.; "Formation and Reduction of Nitrogen Oxides in Fluidized Bed Combustion", *Fuel* **73**, 1398, 1994.

[26] Davidson, R.M.; "Nitrogen in Coal", *IEA Coal Research*, Report No. IEAPER/08, 1994.

[27] Baxter, L.L., Mitchell, R.E., Fletcher, T.H., and Hurt, R.H.; "Nitrogen Release during Coal Combustion", *Energy Fuels* **10**, 188, 1996.,

[28] Pohl, J.H. and Sarofim, A.F.; "Devolatilization and Oxidation of Coal Nitrogen", *Sixteenth Symposium (International) on Combustion*, pp. 491–501. The Combustion Institute, 1976.

[29] Jensen, A.; "Nitrogen Chemistry in Fluidized Bed Combustion of Coal", Ph.D thesis, Department of Chemical Engineering, The Technical University of Denmark, 1996.

[30] Solomon, P.R. and Colket, M.B.; "Evolution of Fuel Nitrogen in Coal Devolatilization", *Fuel* **57**, 749, 1978.

[31] Man, C.K., Pendlebury, K.J., and Gibbins, J.R.; "Laboratory Measurement of N Release Under Combustion Conditions and Comparison with Plant NO_x Formation", *Fuel Proc. Technol.* **36**, 117, 1993.

[32] Blair, D.W., Wendt, J.O.L., and Bartok, W.; "Evolution of Nitrogen and Other Species during Controlled Pyrolysis of Coal", *Sixteenth Symposium (International) on Combustion*, pp. 475–489, The Combustion Institute, 1976.

[33] Kambara, S., Takarada, T., Yamamoto, Y., and Kato, K.; "Relation between Functional Forms of Coal Nitrogen and Formation of NO_x Precursors during Rapid Pyrolysis", *Energy Fuels* **7**, 1013, 1993.

[34] Chen, Y., Matsuda, H., and Hasatani, M.; "Behaviors of Coal–N Release during Coal Pyrolysis", *Proceedings of the International Conference on Coal Science*, K.H. Michaelian (Ed.), pp. 55–58, Butterworth Heinemann, 1993.

[35] Chen, J.C. and Niksa, S.; "Coal Devolatilization during rapid Transient Heating. 1. Primary Devolatilization", *Energy Fuels* **6**, 254, 1992.

[36] Chen, J.C. and Niksa, S.; "Suppressed Nitrogen Evolution from Coal Derived Soot and Low–Volatility Coal Chars", *Twenty–Fourth Symposium (International) on Combustion*, pp. 1259–1276, The Combustion Institute, 1992.

[37] Chen, J.C., Castagnoli, C., and Niksa, S.; "Coal Devolatilization during Rapid Transient Heating. 2. Secondary Pyrolysis", *Energy Fuels* **6**, 264, 1992.,

[38] Niksa, S.; "Predicting the Evolution of Fuel Nitrogen from Various Coals", *Twenty–Fifth Symposium (International) on Combustion*, pp. 537–544, The Combustion Institute, 1994.

[39] Niksa, S.; "FLASHCHAIN Theory for Rapid Coal Devolatilization Kinetics. 6. Predicting the Evolution of Fuel Nitrogen from Various Coals", *Energy Fuels* **9**, 467, 1995.

[40] Nelson, P.F. and Kelly, M.D.; "Effects of Coal Characteristics on the Release of Coal Nitrogen as NO_x Precursors", *Proceedings of the International Conference on Coal Science*, K.H. Michaelian (Ed.), pp. 140–143, Butterworth Heinemann, 1993.

[41] Haussmann, G.J. and Kruger, C.H.; "Evolution and Reaction of Coal Fuel Nitrogen during Rapid Oxidative Pyrolysis and Combustion", *Twenty–Third Symposium (International) on Combustion*, pp. 1265–1271, The Combustion Institute, 1990.

[42] Baumann, H. and Möller, P.; "Pyrolysis of Hard Coals Under Fluidised Bed Combustor Conditions", *Erdöl Kohle–Erdgas Petrochem.* 44, 29, 1991.

[43] Phong–Anant, D., Wibberley, L.J., and Wall, T.F.; "Nitrogen Oxide Formation from Australian Coals", *Combust. Flame* 62, 21, 1985.

[44] Bassilakis, R., Zhao, Y., Solomon, P.R., and Serio, M.A.; "Sulfur and Nitrogen Evolution in the Argonne Coals: Experiment and Modeling", *Energy Fuels* 7, 710, 1993.

[45] Hämäläinen, J.P. and Aho, M.J.; "Effect of Fuel Composition on the Conversion of Volatile Solid Fuel–N to N_2O and NO", *Fuel* 74, 1922, 1996.

[46] Wójtowicz, M.A., Zhao, Y., Serio, M.A., Solomon, P.R., and Nelson, P.F.; "Modeling of Hydrogen Cyanide and Ammonia Release during Coal Pyrolysis", *Coal Science and Technology*, J.A. Pajares and J.M.D. Tascón (Eds.), 24, pp. 771–774, Elsevier, Amsterdam, 1995.

[47] Nelson, P.F., Buckley, A.N., and Kelly, M.D.; "Functional Forms of Nitrogen in Coals and the Release of Coal Nitrogen as NO_x Precursors (HCN and NH_3)", *Twenty–Fourth Symposium (International) on Combustion*, pp. 1259–1267, The Combustion Institute, 1992.

[48] Freihaut, J.D. and Seery, D.J.; "Evolution of Fuel Nitrogen during the Vacuum Thermal Devolatilization of Coal", *J. Am. Chem. Soc., Div. Fuel Chem.* 26, 18, 1981.

[49] Axworthy, A.E., Dayan, V.H., and Martin, G.B.; "Reactions of Fuel–Nitrogen Compounds Under Conditions of Inert Pyrolysis", *Fuel*, 57, 29, 1978.

[50] Cai, H.-Y., Güell, A.J., Dugwell, D.R., and Kandiyoti, R.; "Heteroatom Distribution in Pyrolysis Products as a Function of Heating Rate and Pressure", *Fuel* 72, 321, 1993.

[51] Cho, S., Marlow, D., Niksa, S.; "Burning Velocities of Multicomponent Organic Fuel Mixtures Derived from Various Coals", *Combust. Flame* 101, 399, 1995.

[52] Annamalai, K., and Ryan, W.; "Interactive Processes in Gasification and Combustion – II. Isolated Carbon, Coal and Porous Char Particles", *Prog. Energy Combust. Sci.* 19, 383, 1993.

[53] Dryer, F.L.; *Fossil Fuel Combustion*, Chapter 3; W. Bartok, and A. Sarofim (Eds.), John Wiley and Sons, New York, 1991.

[54] Truelove, J.S., and Holcombe, D.; "Measurement and Modelling of Coal Flame Stability in a Pilot–Scale Combustor", *Twenty–Third Symposium (International) on Combustion*, pp. 963–971, The Combustion Institute, 1990.

[55] Visser, B.M., Smart, J.P., van de Kamp, W.L., and Weber, R.; "Measurements and Predictions of Quarl Zone Properties of Swirling Pulverised Coal Flames", *Twenty-Third Symposium (International) on Combustion*, pp. 949–955, The Combustion Institute, 1990.

[56] Cho, S., and Niksa, S.; "Elementary Reaction Models and Correlations for Burning Velocities of Multicomponent Organic Fuel Mixtures", *Combust. Flame* **101**, 411, 1995.

[57] P. Glarborg and S. Hadvig; "Development and Test of Chemical Kinetic Model for Combustion of Natural Gas", *NGC–rapport, Forbrændingsteknik og Miljø*, Nordisk Gasteknisk Center, Marts 1991.

[58] Tan, Y., Dagaut, P., Cathonnet, M., Boettner, J.C., Bachman, J.S., and Carlier, P.; "Natural Gas and Blends Oxidation and Ignition: Experiments and Modeling", *Twenty-Fifth Symposium (International) on Combustion*, pp. 1563–1569, The Combustion Institute, 1994.

[59] Pedersen, L.S., Glarborg, P., and Dam–Johansen, K.; "Simplified Modelling of Pulverized Coal Flames", Proceedings of the 3'rd Nordic SO_x –NO_x Conference, CHEC Report No. 9610, 1996.

[60] Hesketh, R.P., and Davidson, J,F.; "Combustion of Methane and Propane in an Incipiently Fluidized Bed", *Combust. Flame* **85**, 449, 1991.

[61] Hayhurst, A.N.; "Does Carbon Monoxide Burn Inside a Fluidized Bed? A New Model for the Combustion of Coal Char Particles in Fluidized Beds.", *Combust. Flame* **85**, 155, 1991.

[62] Peck, R.E., Glarborg, P., and Johnsson, J.E.; "Kinetic Modeling of Nitrogen Oxide Formation in One–Dimensional Pulverized Coal Flames", *Combust. Sci. Techn.* **76**, 81, 1991.

[63] Pedersen, L.S.; "Low–NO_x Burners", M.Sc. thesis, Department of Chemical Engineering, Technical University of Denmark, 1995 (in Danish).

[64] Glarborg, P., Miller, J.A., and Kee, R.J.; "Kinetic Modeling and Sensitivity Analysis of Nitrogen Oxide Formation in Well-Stirred Reactors", *Combust. Flame* **65**, 177, 1986.

[65] Miller, J.A., and Bowman, C.T., "Mechanism and Modeling of Nitrogen Chemistry in Combustion", *Prog. Energy Combust. Sci.* **15**, 287, 1989.

[66] Glarborg, P., and Miller, J.A.; "Mechanism and Modeling of Hydrogen Cyanide Oxidation in a Flow Reactor", *Combust. Flame* **99**, 475, 1994.

[67] Johnsson, J.E., Glarborg, P., and Dam–Johansen, K.; "Thermal Dissociation of N_2O at Medium Temperatures", *Twenty-Fourth Symposium (International) on Combustion*, pp. 917–923, The Combustion Institute, 1992.

[68] Hulgaard, T., and Dam–Johansen, K.; "Homogeneous Nitrous Oxide Formation and Destruction under Combustion Conditions.", *AIChE J.* **39**, 1342, 1993.

[69] Glarborg, P., Johnsson, J.E., and Dam–Johansen, K.; "Kinetics of Homogeneous Nitrous Oxide Decomposition", *Combust. Flame* **99**, 523, 1994.

[70] Glarborg, P., Lilleheie, N., Byggstøyl, S., Magnussen, B., Kilpinen, P., and Hupa, M.; "A Reduced Mechanism for Nitrogen Chemistry in Methane Combustion", *Twenty–Fourth Symposium (International) on Combustion*, pp. 889–898, The Combustion Institute, 1992.

[71] Kilpinen, P., Glarborg, P., and Hupa, M.; "Reburning Chemistry – A Kinetic Modeling Study", *Ind. Eng. Chem. Res.* **31**, 1477, 1992.

[72] Alzueta, M.U., Glarborg, P., and Dam–Johansen, K.; "Low Temperature Interactions between Hydrocarbons and Nitric Oxide: An Experimental Study.", *Combust. Flame*, accepted for publication.

[73] Glarborg, P., Dam–Johansen, K., Miller, J.A., Kee, R.J., and Coltrin, M.E.; "Modeling the Thermal DENO$_x$ Process in Flow Reactors. Surface Effects and Nitrous Oxide Formation.", *Int. J. Chem. Kin.* **26**, 421, 1994.

[74] Glarborg, P., Kristensen, P.G., Jensen, S.H., and Dam–Johansen, K.; "A Flow Reactor Study of HNCO Oxidation Chemistry", *Combust. Flame* **98**, 241, 1994.

[75] Kristensen, P.G., Glarborg, P., and Dam–Johansen, K.; "Nitrogen Chemistry during Burnout in Fuel-Staged Combustion" *Combust. and Flame*, accepted for publication.

[76] Miller, J.A. and Glarborg, P.; "Modeling the Formation of N$_2$O and NO$_2$ in the Thermal De-NO$_x$ Process", Gas–Phase Chemical Reaction Systems: Experiments and Modeling 100 Years after Bodenstein, *Springer Series in Chemical Physics*, in press

[77] Glarborg, P., Kubel, D., Dam–Johansen, K., Chiang, H.–M., and Bozzelli, J.W.; "Impact of SO$_2$ and NO on CO Oxidation under Post–Flame Conditions", *Int. J. Chem. Kin.*, accepted for publication

[78] Roesler, J.F., Yetter, R.A., and Dryer, F.L.; "Kinetic Interactions of CO, NO$_x$ and HCl Emissions in Post–Combustion Gases.", *Combust. Flame* **100**, 495, 1995.

[79] Glarborg, P., Kristensen, P.G., Kubel, D., Hansen, J., and Dam–Johansen, K.; "Interactions of CO, NO$_x$ and H$_2$O under Post–Flame Conditions", *Combust. Sci. Techn.* **110–111**, 461, 1996.

[80] Hobbs, M.L., Radulovic, P.T. and Smoot, L.D.; "Combustion and Gasification of Coals in Fixed–Beds", *Prog. Energy Combust. Sci.* **19**, 505, 1993.

[81] Laurendeau, N.M.; "Heterogeneous Kinetics of Coal Char Gasification and Combustion", *Prog. Energy Combust. Sci.* **4**, 221, 1978.

[82] Levenspiel, O.; *Chemical Reaction Engineering*, John Wiley & Sons, New York, 1972.

[83] Froment, G.F. and Bischoff, K.B.; *Chemical Reactor Analysis and Design*, John Wiley & Sons, New York, 1990.

[84] Essenhigh, R.H.; "Fundamentals of Coal Combustion", in *Chemistry of Coal Utilization*, pp. 1153–1312, Elliott, M.A. (Ed.), John Wiley & Sons, New York, 1981.

[85] Hurt, R.H. and Mitchell, R.E.; "Unified High–Temperature Char Combustion Kinetics for a Suite of Coals of Various Rank", *Twenty–Fourth Symposium (International) on Combustion*, pp. 1243–1250, The Combustion Institute, 1992.

[86] Pillai, K.K.; "The Influence of Coal Type on Devolatilization and Combustion in Fluidized Beds", *J. Inst. Energy* 54, 142, 1981.

[87] Brodén, H., Andersson, S.E., Leckner, B., and Johnsson, J.E.; "Combustion of Metallurgical Coke – Experiments and Mathematical Modelling", *Nordic Seminar on Solid Fuel Reactivity*, Gothenburg, November 24th, 1993.

[88] Åmand, L.–E. and Leckner, B.; "Reduction of N_2O in a Circulating Fluidized–Bed Combustor", *Fuel* 73, 1389, 1994.

[89] Hansen, P.F.B., Dam–Johansen, K., Johnsson, J.E. and Hulgaard, T.; "Catalytic Reduction of NO and N_2O on Limestone during Sulfur Capture under Fluidized Bed Combustion Conditions", *Chem. Eng. Sci.* 47, 2419, 1992.

[90] Kiil, S., Bhatia, S.K., and Dam–Johansen, K.; "Modelling of Catalytic Oxidation of NH_3 and Reduction of NO on Limestone during Sulphur Capture", *Chem. Eng. Sci.* 51, 587, 1996.

[91] Jensen, A., Johnsson, J.E. and Dam–Johansen, K.; "Formation of Nitric Oxide and Nitrous Oxide From Heterogeneous Oxidation of Hydrogen Cyanide at Fluidized Bed Combustion Conditions", *12th International Conference on Fluidized Bed Combustion*, pp. 447–454, L. Rubow and G. Commonwealth (Eds.), ASME, 1993.

[92] Johnsson, J.E.; "A Kinetic Model for NO_x Formation in Fluidized Bed Combustion", *10th International Conference on Fluidized Bed Combustion*, pp. 1111–1118, A.M. Manaker (Ed.), ASME, 1989.

[93] Johnsson, J.E.; "Modeling of NO_x Formation in Fluidized Bed Combustion", *Fluidization*, pp. 435–442, J.R. Grace, L.W. Shemilt and M–A. Bergougnou (Eds.), Engineering Foundation, 1989.

[94] Johnsson, J.E. and Dam–Johansen, K.; "Formation and Reduction of NO_x in a Fluidized Bed Combustor", *11th International Conference on Fluidized Bed*, pp. 1389–1396, E.J. Anthony (Ed.), ASME, 1991.

[95] Lin, W., Johnsson, J.E., Dam–Johansen, K., and van den Bleek, C.M.; "Interactions Between NO_x Emission and Desulphurization in FBC", *12th International Conference on Fluidized Bed Combustion*, pp. 1093–1100, L. Rubow and G. Commonwealth (Eds.), ASME, 1993.

[96] Lin, W., Johnsson, J.E., Dam–Johansen, K., and van den Bleek, C.M.; "Influence of Sulfur Capturing Sorbents on Nitrogen Chemistry in Pressurized Fluidized Bed Combustion of Coal", *Proceedings of the 1993 International Conference on Coal Science*, pp. 554–555, 1993.

[97] Lin, W., Johnsson, J.E., Dam–Johansen, K., and van den Bleek, C.M.; "Interaction between Emissions of Sulfur Dioxide and Nitrogen Oxides in Fluidized Bed Combustion", *Fuel* **73**, 1202, 1994.

[98] Lin, W., Dam–Johansen, K., and van den Bleek, C.M.; "Kinetics of Catalytic Formation of NO_x from NH_3 over CaO Based Sorbents during Fluidized Bed Combustion of Coal", *The 8th International Conference on Coal Science*, pp. 783–786, 10–15 Sept., Oviedo, Spain, 1995.

[99] Hansen, P.F.B. and Dam–Johansen, K.; "Limestone Catalyzed Reduction of NO and N_2O under Fluidized Bed Combustion Conditions", *12th International Conference on Fluidized Bed Combustion*, L. Rubow and G. Commonwealth (Eds.), ASME, 1993.

[100] Johnsson, J.E. and Dam–Johansen, K.; "Reduction of N_2O over Char and Bed Material from CFBC", *13th International Conference on Fluidized Bed Combustion*, pp. 859–869, K.J. Heinschel (Ed.), ASME, 1995.

[101] Johnsson, J.E., Åmand, L.-E. and Leckner, B.; "Modelling of NO_x Formation in a Circulating Fluidized Boiler", *Circulating Fluidized Bed Technology III*, pp. 405–410, P. Basu, M. Horio, and M. Hasatani (Eds.), Pergamon Press, Oxford, 1991.

[102] Jensen, A., Johnsson, J.E., Andries, J., Laughlin, K., Reed, G., Mayer, M., Baumann, H. and Bonn, B.; "Formation and Reduction of NO_x in Pressurized Fluidized Bed Combustion of Coal", *Fuel* **74**, 1555, 1995.

[103] Jensen, A. and Johnsson, J.E.; "A Model for NO_x Emissions from FBC", *Fluidization VIII*, Tours, France, May 14–19, 1995.

[104] Jensen, A. and Johnsson, J.E.; "A Parameter Study of a Model for NO_x Emissions from PFBC", to be presented at the *Finnish–Swedish Flame Days*, September 3–4, 1996.

[105] Johnsson, J.E., Åmand, L.-E., Dam–Johansen, K., and Leckner, B.; "Modelling N_2O Reduction in a Circulating Fluidized Bed Boiler", *The Fifth International Conference on CFB*, Beijing, China, May 28–31, 1996.

[106] Johnsson, J.E., Åmand, L.-E., Dam–Johansen, K., and Leckner, B., "Modelling N_2O Reduction and Decomposition in a Circulating Fluidized Bed Boiler", *Energy Fuels*, accepted for publication.

[107] Minchener, A.J. and Kelsall, G.J.; "The Control of NO_x Emissions from PFBC Systems", *J. Inst. Energy* **63**, 85, 1990.

[108] Hippinen, I., Lu, Y., and Jahkola, A.; "The Effect of Combustion Air Staging on Combustion Performance and Emissions in PFBC", *12th International Conference on Fluidized Bed Combustion*, L. Rubow and G. Commonwealth (Eds.), ASME, 1993.

[109] Valk, M., Bramer, E.A. and Tossaint, H.H.J.; "Optimal Staged Combustion Conditions in a Fluidised Bed for Simultaneous Low NO_x and SO_2 Emissions Levels",

10th International Conference on Fluidized Bed Combustion, pp. 995–1001, A.M. Manaker (Ed.), ASME, 1989.

[110] Bowman, C.T.; "Control of Combustion–Generated Nitrogen Oxide Emissions: Technology Driven by Regulation", *Twenty–Fourth Symposium (International) on Combustion*, pp. 859–878, The Combustion Institute, 1992.

[111] van der Lans, R.P., Glarborg,P., and Dam–Johansen, K.; "Influence of Process Parameters on Nitrogen Oxide Formation in Pulverized Coal Burners", submitted for publication.

[112] Duo, W., Dam–Johansen, K., and Østergaard, K.; "Widening the Temperature of the Thermal DeNO$_x$ Process. An Experimental Investigation.", *Twenty–Third Symposium (Int.) Combustion*, pp. 297–303, The Combustion Institute, 1990.

[113] Kasuya, F., Glarborg, P., and Dam–Johansen, K.; "The Thermal DeNO$_x$ Process: Influence of Partial Pressures and Temperature", *Chem. Eng. Sci.* **50**, 1455, 1995.

[114] Kjærgaard, K., Glarborg, P., Dam–Johansen, K., and Miller, J.A.; "Pressure Effects on the Thermal DeNO$_x$ Process", *Twenty–Sixth Symposium (International) on Combustion*, accepted for publication.

[115] Jødal, M., Nielsen, C., Hulgaard, T., and Dam–Johansen, K.; "Pilot Scale Experiments with Ammonia and Urea as Reductants in Selective Non–Catalytic Reduction of Nitric Oxide", *Twenty–Third Symposium (Int.) Combustion*, pp. 237–243, The Combustion Institute, 1990.

[116] Jødal, M., Lauridsen, T.L., and Dam–Johansen, K.; "NO$_x$ Removal on a Coal–Fired Utility Boiler by Selective Non–Catalytic Reduction", *Env. Progr.* **11**, 296, 1992.

[117] Glarborg, P., Dam–Johansen, K., and Miller, J.A.; "The Reaction of Ammonia with Nitrogen Dioxide in a Flow Reactor: Implications for the NH$_2$+NO$_2$ Reaction.", *Int. J. Chem. Kin.* **27**, 1207, 1995.

[118] Lyon, R.K.; "Thermal DeNO$_x$: Controlling Nitrogen Oxides Emissions by a Non–Catalytic Process", *Environ. Sci. Technol.* **21**, 231, 1987.

[119] Glarborg, P., Karll, B., and Pratapas, J.M.; "Review of Natural Gas Reburning. Initial Full Scale Results", *Nineteenth World Gas Conference*, Milano, June 20–23, 1994.

[120] Hjuler, K., Glarborg, P., and Dam–Johansen, K.; "Mutually Promoted Thermal Oxidation of Nitric Oxide and Organic Compounds", *Ind. Eng. Chem. Res.* **34**, 1882, 1995.

[121] Pont, J.N., Evans, A.B., England, G.C., Lyon, R.K., and Seeker, W.R.; "Evaluation of the CombiNO$_x$ Process at Pilot Scale." *Env. Progr.* **12**, 140, 1993.

[122] Braun, A., Bu, C., Renz, U., Drischel, J., and Köser, J.K.; "Emission of NO and N$_2$O from a 4 MW Fluidized Bed Combustor with NO Reduction", *11th International Conference on Fluidized Bed*, pp. 709–717, E.J. Anthony (Ed.), ASME, 1991.

[123] Leckner, B., Karlsson, M., Dam–Johansen, K., Weinell, C.E., Kilpinen, P., and Hupa, M.; "The Influence of Additives on Selective Non–Catalytic Reduction of NO with NH_3 in Circulating Fluidized bed Boilers", *Ind. Eng. Chem. Research* **30**, 2396, 1991.

[124] Andries, J., Verloop, C.M., and Hein, K.R.G.; "Influence of Operating Conditions and mmonia Injection on the Emission of Nitrogeneous Gases from Pressurized Fluidized Bed Combustion of Coal", pp. 795–802, *12th International Conference on Fluidized Bed Combustion*, L. Rubow and G. Commonwealth (Eds.), ASME, 1993.

[125] Leckner, B. and Gustavsson, L.; "Reduction of N_2O by Gas Injection in CFB Boilers", *J. Inst. Energy* **64**, 176, 1991.

[126] Gustavsson, L., Glarborg, P., and Leckner, B.; "Modeling of Chemical Reactions for N_2O Reduction", *Combust. Flame*, accepted for publication.

[127] Rutar, T., Kramlich, J.C., Malte, P., and Glarborg, P.; "Nitrous Oxide Emissions Control by Reburning", *Combust. Flame*, accepted for publication.

[128] Dam–Johansen, K.; "Sulphur Dioxide Reduction on Dry Lime", Ph.D. thesis, Department of Chemical Engineering, Technical University of Denmark, 1987 (in Danish).

[129] Lyngfelt, A. and Leckner, B.; "Sulphur Capture in Fluidized Bed Boilers – the Effect of Reductive Decomposition of $CaSO_4$", *Chem. Eng. J.* **40**, 59, 1989.

[130] Lyngfelt, A. and Leckner, B.; "SO_2 Capture in Fluidized Bed Boilers – Re–emission of SO_2 due to Reduction of $CaSO_4$", *Chem. Eng. Sci.* **44**, 207, 1989.

[131] Lyngfelt, A. and Leckner, B.; "Sulphur Capture in Fluidized Bed Combustors – Temperature Dependence and Lime Conversion", *J. Inst. Energy* **62**, 62, 1989.

[132] Hansen, P.F.B.; "Sulphur Capture in Fluidized Bed Combustors", Ph.D. thesis, Department of Chemical Engineering, Technical University of Denmark, 1993.

[133] Dam–Johansen, K., Åmand, L–E., and Leckner, B.; "Influence of SO_2 on the NO/N_2O Chemistry in Fluidized Bed Combustion. 2. Interpretation of Full–Scale Observations Based on Laboratory Experiments.", *Fuel* **72**, 565, 1993.

[134] Åmand, L.-E., Leckner, B., and Dam–Johansen, K.; "Influence of SO_2 on the NO/N_2O Chemistry in Fluidized Bed Combustion. 1. Full–Scale Experiments." *Fuel* **72**, 557, 1993.

[135] Swaine, D. J.; *Trace Elements in Coal*, Butterworth and Co., London, U.K., 1990.

[136] Benson, S.A., Jones, M.L., and Harb, J.N.; "Ash Formation and Deposition", In: *Fundamentals of Coal Combustion – For Clean and Efficient Use*, L.D. Smoot (Ed.); Coal Science and Technology, Vol. 20; Elsevier, Amsterdam, 1993.

[137] Flagan, R.C. and Friedlander, S.K.; "Particle Formation in Pulverized Coal Combustion – A Review", D.T. Shaw (Ed.); *Recent Developments in Aerosol Science*; John Wiley & Sons, New York, USA, 1978.

[138] National Center for Excellence on Air Toxics; 1st Annual Kickoff Meeting, Energy & Environmental Research Center, University of North Dakota, Grand Forks, ND, May 24–25, 1994.

[139] Sarofim, A.F. and Helble, J.J.; "Mechanisms of Ash and Deposit Formation" In: *The Impact of Ash Deposition on Coal Fired Power Plants*, J. Williamson, F. Wigley (Eds.), Proc. Eng. Found. Conf., Solihull, England, June 20–25, 1993; Taylor & Francis Ltd., London, U.K., 1994.

[140] Christensen, K.A.; "The Formation of Submicron Particles from the Combustion of Straw", Ph.D. Thesis, Dept. Chem. Eng., Techn. Univ. of Denmark, 1995.

[141] Frandsen, F.J.; "Fate of Inorganic Metals in FBCs", CHEC Report No. 9404, 1994.

[142] Krusholm, G.; "Combustion of Straw in Fluid Bed – A Litterature Study", CHEC Report No. 9507, 1995 (in Danish).

[143] Baxter, L.L., Abbott, M.F., and Douglas, R.E.; "Dependence of Elemental Ash Deposit Composition on Coal Ash Chemistry and Combustor Environment", In: *Inorganic Transformations and Ash Deposition During Combustion*, S.A. Benson (Ed.), Proc. Eng. Found. Conf., Palm Coast, FA, USA, March 10–15, 1991; 1992.

[144] Rosner, D.E., Konstandopoulos, A.G., Tassopoulos, M., and Mackowski, D.W.; "Deposition Dynamics of Combustion–Generated Particles: Summary of Recent Studies of Particle Transport Mechanisms, Capture Rates and Resulting Deposit Microstructure/Properties"; In: *Inorganic Transformations and Ash Deposition During Combustion*, S.A. Benson (Ed.), Proc. Eng. Found. Conf., Palm Coast, FA, USA, March 10–15, 1991; 1992.

[145] Baxter, L.L.; "Ash Deposition During Biomass and Coal Combustion: A Mechanistic Approach", *Biomass Bioener.* 4, 85, 1993.

[146] Wall, T.F., Bhattacharya, S.P., Zhang, D.K., Gupta, R.P., and He, X.; "The Properties and Thermal Effects of Ash Depositions in Coal Fired Furnaces: A Review", In: *The Impact of Ash Deposition on Coal Fired Power Plants*, J. Williamson, F. Wigley (Eds.), Proc. Eng. Found. Conf., Solihull, England, June 20–25, 1993; Taylor & Francis Ltd., London, U.K., 1994.

[147] Harb, J.N. and Smith, E.E.; "Fireside Corrosion in PC–Fired Boilers", *Prog. Energy Combust. Sci.* 16, 169, 1990.

[148] Jacobson, N.S., McNallan, M.J., and Kreidler, E.R.; "High Temperature Reactions of Ceramics and Metals with Chlorine and Oxygen"; *High Temp. Sci.* 27, 381, 1990.

[149] Ahila, S. and Iyer, S.R.; "Fire–Side Corrosion of Superheaters and Reheaters in Coal Fired Boilers", *Tool & Alloy Steels* 26, 45, 1992.

[150] Borio, R.W., Levasseur, A.A., Chow, O.K., and Miemiec, L.S.; "Ash Deposition: A Boiler Manufacturers Perspective", In: *Inorganic Transformations and Ash Deposition During Combustion*, S.A. Benson (Ed.), Proc. Eng. Found. Conf., Palm Coast, FA, USA, March 10–15, 1991; 1992.

[151] Raask, E.; *Mineral Impurities in Coal Combustion*, Hemisphere Publishing Company, Washington, USA, 1985.

[152] Couch, G.; "Understanding Slagging and Fouling during PF Combustion", *IEA Coal Research*, Report No. IEACR/72, London, U.K., 1994.

[153] Clarke, L.B. and Sloss, L.L.; "Trace Elements – Emissions from Coal Combustion and Gasification", *IEA Coal Research*, Report No. IEACR/49, London, U.K., 1992.

[154] Swaine, D. J. and Goodarzi, F.; *Environmental Aspects of Trace Elements in Coal*, Kluwer Academic Publishers, Dordrecht, The Netherlands, 1995.

[155] Davidson, R.M. and Clarke, L.B.; "Trace Elements in Coal", *IEA Coal Research*, Report No. IEAPER/21, London, U.K., 1996.

[156] Kauppinen, E.I., and Pakkanen, T. A.; "Coal Combustion Aerosols – A Field Study", *Env. Sci. Techn.* **24**, 1811, 1990.

[157] Linak, W.P. and Wendt, J.O.L.; "Trace Metal Transformation Mechanisms during Coal Combustion", *Fuel Proc. Techn.* **39**, 173, 1994.

[158] Sander, B.; "Measurements of Trace Element Mass Balances in Coal–Fired Power Plants Equipped with Different Types of FGD Systems", *Proc. 2nd Int. EPRI Conf. on Managing Hazardous Air Pollutants*, Washington D. C., July 13–17, 1993.

[159] Meij, R.; "Trace Element Behavior in Coal–Fired Power Plants", *Fuel Proc. Techn.* **39**, 199, 1994.

[160] Weber, G.F.; Ness, S.R., Miller, S.J., Brown, T.D., and Schmidt, C. E.; "A Summary of Utility Trace Element Emissions Data from the DOE Air Toxics Study", *Proc. EPRI/DOE Int. Conf. on Managing Hazardous and Particulate Air Pollutants*, Toronto, Ontario, Canada, August 15–17, 1995.

[161] Hansen, L.A. and Michelsen, H. P.; "Multi Circulating Fluidized Bed Combustion of Biofuels and Coal – Measurements and Thermodynamic Modeling", CHEC Report No. 9407, 1994.

[162] Hansen, P.F.B., Bank, L.H., and Dam–Johansen, K.; "In–situ Measurements in Fluidized Bed Combustors: Design and Evaluation of Four Sample Probes"; *Proc. 13th Int. Conf. on FBC*, ASME, 1995.

[163] Michelsen, H. P.; "Results of Deposit Measurements during Straw Firing at the Kyndby Power Station", CHEC Report No. 9604, 1996.

[164] Michelsen, H.P., Larsen, O.H.; Frandsen, F.J., and Dam–Johansen, K.; "Deposition and High Temperature Corrosion in a 10 MW Straw Fired Boiler", *Biomass Usage for Utility and Industrial Power*, Proc. Eng. Found. Conf., Snowbird, UT, USA, April 28 – May 3, 1996.

[165] Larsen, O.H., Laursen, K., and Frandsen, F.J.; "Danish Collaborative Project on Mineral Transformations and Ash Deposition in PF–Fired Boilers and Related Research Projects", *Applications of Advanced Technology to Ash–Related Problems*, Proc. Eng. Found. Conf., Waterville Valley, NH, USA, July 16–21, 1995.

[166] Laursen, K., Frandsen, F. J., and Larsen, O. H.; "Slagging and Fouling Propensity: Full–Scale Test at Two Power Stations in Western Denmark"; *Applications of Advanced Technology to Ash–Related Problems*, Proc. Eng. Found. Conf., Waterville Valley, NH, USA, July 16–21, 1995.

[167] Frandsen, F.J., Dam–Johansen, K., Laursen, K., and Larsen, O.H.; "Prediction of Ash Deposition Propensities at Two Coal–Fired Power Stations in Denmark", *Proc. 12th Int. Ann. Pittsburgh Coal Conference*, Pittsburgh, PA, September 11–15, 1995.

[168] Pedersen, L.S., Michelsen, H.P., Hansen, L.A., and Kiil, S.; "Full Scale Co–Firing of Straw and Coal", CHEC Report No. 9503, 1995.

[169] Pedersen, L.S., Michelsen, H.P., Kiil, S., Hansen, L.A., Dam–Johansen, K., Kildsig, F., Christensen, J., and Jespersen, P.; "Full–Scale Co–Firing of Straw and Coal", *Fuel*, accepted for publication.

[170] Frandsen, F.J., Dam–Johansen, K., Rasmussen, P., and Sander, B.; "Trace Elements from Combustion: Thermodynamic Equilibrium Approach and Full–Scale Measurements – A Comparative Study", *Proc. Swedish–Finnish Flame Days*, Gothenburg, Sweden, September 7–8, 1993.

[171] Frandsen, F.J., Dam–Johansen, K., and Rasmussen, P.; "Trace Elements from Combustion and Gasification of Coal – An Equilibrium Approach", *Prog. Energy Combust. Sci.* **20**, 115, 1994.

[172] Frandsen, F.J.; "Trace Elements from Coal Combustion", Ph.D.–Thesis, Dept. Chem. Eng., Techn. Univ. of Denmark, 1995.

[173] Frandsen, F.J., Erickson, T.A., Kühnel, V., Helble, J.J., and Linak, W.P.; "Equilibrium Speciation of As, Cd, Cr, Hg, Ni, Pb, and Se in Oxidative Thermal Conversion of Coal – A Comparison of Thermodynamic Packages", *Proc. 3rd Int. Symp. on Gas Cleaning at High Temperatures*, Karlsruhe, Germany, September 18–20, 1996.

BIOFUEL PROPERTIES AND COMBUSTION EXPERIENCES

Bo Sander
Fælleskemikerne/ELSAMPROJEKT
Kraftværksvej 53
DK-7000 Fredericia
Denmark

ABSTRACT

In Denmark the electric utility groups ELSAM and ELKRAFT are, due to government demands, obliged to utilise large amounts of biomass for power production. By the year 2000, 1,200,000 tonnes of straw and 200,000 tonnes of wood chips will be used annually.

This paper gives an overview of the fuel properties of Danish straw and wood chips compared with coal. It is shown that straw has a much higher content of potassium and chlorine than wood chips and coal and this causes a number of serious technical problems in power production plants. Therefore, it has been investigated whether it is possible to reduce the content of potassium and chlorine in straw from the field.

Cultivation trials have been carried out in the growing seasons of 1993, 1994 and 1995. In the first year it was investigated how different cultivation factors influence the chemical composition of straw. In the two following years the aim was to study how the chlorine supply from fertilizers influences the straw composition and it was shown that the chlorine content of straw can be reduced by using chlorine-free fertilizers.

Use of straw as a fuel in existing pulverized coal-fired units may be accomplished by co-firing straw and coal in the boiler or by establishing a separate grate-fired boiler for straw and wood chips which supplies steam to the steam turbine of the coal-fired power plant. This paper describes some of the experiences with emissions, residues and deposit formation which have been gained for these types of plants in Denmark.

1. INTRODUCTION

In Denmark the electric utility groups ELSAM and ELKRAFT are, due to government demands, obliged to utilise large amounts of biomass for power production. By the year 2000, 1,200,000 tonnes of straw and 200,000 tonnes of wood chips will be used annually representing an amount of energy of approx. 19 PJ. This corresponds to approx. 6% of the annual energy consumption in the power plants in Denmark.

As the first step in realising the plans for biomass utilisation, ELSAM has three large-scale power plants for biofuels under construction or in the planning process. In these projects three different technologies will be demonstrated:

* Co-firing of straw and coal in pulverized coal-fired units.

* Separate grate-fired boiler for straw and wood chips supplying steam to a coal-fired parent plant.

* Co-firing of straw, wood chips and coal in circulating fluidised bed combustion.

This paper gives an overview of the fuel properties of Danish straw and wood chips and describes some of the experiences with emissions, residues and deposit formation in biomass-fired boilers which have been gained in the past.

2. FUEL DATA FOR STRAW AND WOOD CHIPS.

Straw and wood chips are the most abundant biofuels in Denmark. Table 1 gives an overview of the chemical composition of Danish cereal straw and wood chips. The table includes water content, heating value, content of ash and volatiles and elemental composition. The ash content is measured at an ash temperature of 550°C. For each parameter the table gives a typical value of the biofuel supplied and the range of variation which has been observed for samples analysed. The fuel data of rape straw are similar to those of cereal straw except that the content of calcium is higher (0.8-1.6 weight-%) and the content of silicon is lower (<0.2%).

The table shows some clear differences between the fuel data for straw and wood. The lower heating value on water and ash free basis is slightly higher in wood than in straw, but due to the higher water content in wood chips, the lower heating value as received is highest for straw. It is seen that the content of ash-forming and gaseous

pollutant-forming elements is higher in straw than in wood. The most important fact is that the content of potassium and chlorine in straw is an order of magnitude higher than that in wood chips. In power production plants, fuels with a high content of potassium and chlorine cause a number of serious technical problems such as increased corrosion of superheaters, increased slagging and fouling, increased deterioration rates of SCR catalysts for NO_x-reduction, and in the co-firing concepts with coal the utilisation of fly ash for cement and concrete production is impeded.

Water content and heating value		Straw		Wood chips	
	Unit	Typical	Variation	Typical	Variation
Water content	Weight-%	14	8-23	45	20-60
Lower heating value as received	MJ/kg	14.9	12.3-16.9	9.5	5.9-15.9
Lower heating value, water and ash free	MJ/kg	18.6	18.0-19.0	19.5	18.5-20.5

Chemical composition	Straw		Wood chips	
Unit: Weight-% on dry basis	Typical	Variation	Typical	Variation
Ash	4.5	2-7	1.0	0.3-6
Volatiles	78	75-81	81	70-85
Hydrogen, H	5.9	5.4-6.4	5.8	5.2-6.1
Carbon, C	47.5	47-48	50	49-52
Nitrogen, N	0.7	0.3-1.5	0.3	0.1-0.7
Sulphur, S	0.15	0.1-0.2	0.05	<0.1
Chlorine, Cl	0.4	0.1-1.1	0.02	<0.1
Silicon, Si	0.8	0.1-1.5	0.1	<1.1
Aluminium, Al	0.005	<0.03	0.015	<0.1
Iron, Fe	0.01	<0.03	0.015	<0.1
Calcium, Ca	0.4	0.2-0.5	0.2	0.1-0.9
Magnesium, Mg	0.07	0.04-0.13	0.04	<0.1
Sodium, Na	0.05	<0.3	0.015	<0.1
Potassium, K	1.0	0.2-1.9	0.1	0.05-0.4
Phosphorus, P	0.08	0.03-0.2	0.02	<0.1

Table 1.   Fuel data for Danish cereal straw and wood chips.

Imported coal is the main fuel for central power plants in Denmark today and figure 1 shows a comparison of the content of some key components in straw, wood chips and coal. Sulphur and nitrogen are important for SO_2 and NO_x-emissions and chlorine and alkalies are important in connection with the above-mentioned technical problems.

Coal has a higher heating value than straw and wood, and in order to make a proper comparison, the contents have been calculated on a lower heating value basis. The figure shows that biofuels have a much lower content of sulphur than coal and that the content of nitrogen is comparable in straw and coal but lower in wood. It is also observed that the content of chlorine and alkalies is comparable in wood and coal but much higher in straw.
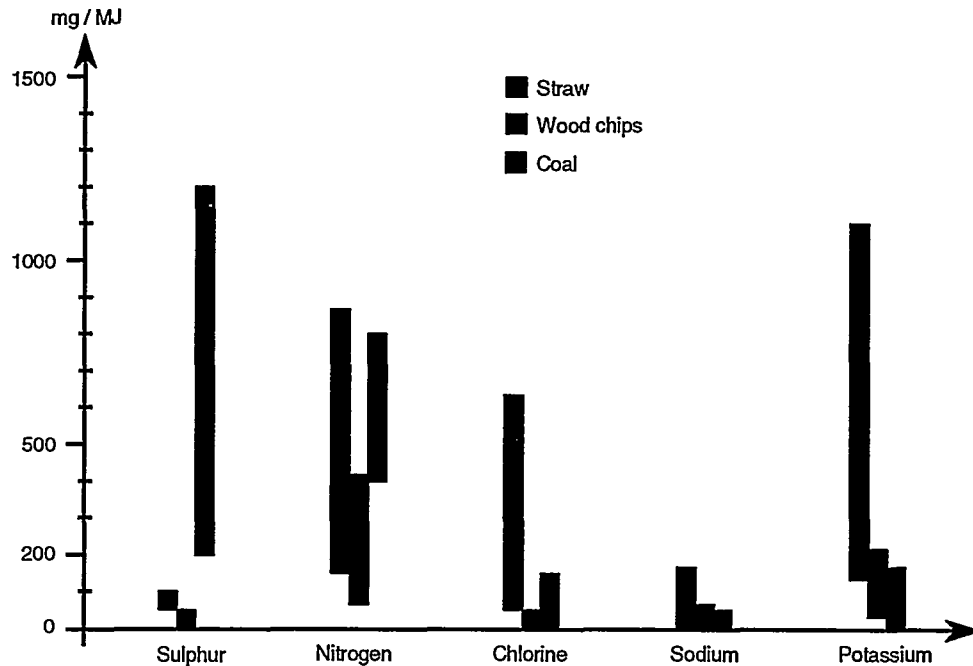
Figure 1.   Range of content of some key components in straw, wood chips and coal on the basis of the lower heating value.

3.   IMPROVEMENT OF STRAW FUEL QUALITY.

The extreme properties of straw with respect to the content of potassium and chlorine are a major obstacle for an efficient utilisation of straw as a fuel for power production and therefore an R&D-project has been carried out with the aim to investigate the possibilities of improving the fuel quality of straw by reducing the content of potassium and chlorine. The participants in the project were the Biotechnological Institute, the Danish Agricultural Advisory Centre, the Danish Institute of Plant and Soil Science and ELSAM/ELKRAFT.

Phase one of the project was carried out in the growing season of 1993 and the aim was to study how cultivation factors influence the straw composition /1/. 89 samples of straw were collected from 38 farmers throughout Denmark, covering the major types of soil and species. Furthermore, 58 samples of straw and 12 samples of grain were collected at the Rønhave Experimental Station. The analysis programme included the content of ash, Cl, K, Na and Ca in all samples, Si, Al, Fe, Mg and P in most samples and the heating value and content of volatiles, S, Cd, C, N, H, cellulose, lignin and pentosan in selected samples. The results of this programme are the major source of the data given in table 1.

The content of cadmium, Cd, was measured in 24 samples and varied between 0.06 and 0.29 mg/kg on dry basis. No significant differences between species were found.

3.1 Comparison of Species.

Table 2 shows a comparison of the content of Si, Ca, K and Cl in straw of the following species: winter barley, spring barley, wheat, rye and winter rape. The data show that the composition of cereal straw species is quite similar. The only major difference is seen for Si where there is a statistically significantly higher content in wheat than in the other cereal species. As mentioned above rape straw has a low content of Si and a high content of Ca. The content of K and Cl is, however, similar to that of cereal straw.

Species	Number of samples	Si		Ca		K		Cl	
		Mean	STD	Mean	STD	Mean	STD	Mean	STD
Winter barley	10	0.29	0.20	0.40	0.06	0.90	0.34	0.41	0.32
Spring barley	26	0.46	0.23	0.43	0.08	0.86	0.30	0.37	0.18
Wheat	33	0.90	0.40	0.33	0.09	1.00	0.44	0.41	0.29
Rye	10	0.35	0.21	0.27	0.05	0.97	0.15	0.24	0.10
Winter rape	10	0.04	0.06	1.16	0.27	0.78	0.42	0.35	0.22

Table 2.   Content of some inorganic components in five straw species.
Unit: Weight-% on dry basis.
STD: Standard deviation.

Table 3 shows the content of cellulose, hemicellulose and lignin in the samples of the five straw species. Rye has a higher content of cellulose than the other species but beyond that no significant differences are observed.

Species	Number of samples	Cellulose	Hemicellu- lose	Lignin
Winter barley	3	46	23	15
Spring barley	8	45	22	16
Wheat	5	45	24	16
Rye	2	51	21	17
Winter rape	2	45	19	18

Table 3.   Content of cellulose, hemicellulose and lignin in straw.
Unit: Weight-% on dry basis.

3.2   Comparison of Varieties.

It is of interest to evaluate whether the content of potassium and chlorine can be reduced by the choice of variety. Table 4 shows mean values for the content of K and Cl in some varieties of spring barley, wheat and rye. Each set of samples for a given species has been grown on the same test site and therefore differences between varieties are not caused by effects of the growing conditions.

Species/variety	Number of samples	K	Cl
Spring barley			
Collie var.	13	0.80	0.38
Digger var.	13	0.92	0.37
Wheat			
Haven var.	11	1.05	0.42
Pepital var.	11	0.79	0.29
Sleipner var.	11	1.14	0.51
Rye			
Marder var.	5	0.92	0.21
Petkus II var.	5	1.02	0.21

Table 4.   Content of K and Cl in varieties of spring barley, wheat and rye.
Unit: Weight-% on dry basis.

4.6

The data in table 4 show no differences between the investigated varieties for spring barley and rye, but for wheat Pepital has a lower content of K and Cl than Haven and Sleipner. A detailed analysis of the data has shown that the deviations observed between the varieties of wheat are statistically significant.

3.3   Influences of Growing Conditions.

The data collected have also been used to investigate the influence of the growing conditions on the chemical composition of straw. The data set shows no relation between the soil type and the content of K and Cl. On the other hand, there is a clear tendency to increase the content of Si and decrease the content of N with increasing content of clay in the soil. No relation has been observed between the chemical composition of straw and the geographical location of the field.

It has also been tested whether the data set shows any correlation between the fertilizer dose and the chemical composition of straw. The amount of K supplied to the field varied between 0 and 170 kg/ha. The content of K in the straw varied between 0.2 and 1.9% on dry basis, but no correlation was found between K supplied and the content of K in straw. This means that also trials with zero supply of K may give high contents of K in straw due to the generally high amount of K in Danish agricultural soil. The amount of N supplied to the field varied between 70 and 210 kg/ha and the content of N in straw was in the range of 0.4 and 1.7% on dry basis. Also in this case no relation was observed between the amount supplied with fertilizer and the content in straw was observed. It is concluded that in practice the effect of the fertilizer dose on the chemical composition of straw is overridden by other factors of which the weather conditions are probably the most important.

A positive correlation is observed between the content of K and Cl in straw for all species and the data for wheat are shown in figure 2. This relation is probably due to the fact that in normal cultivation practice K is supplied as KCl and that Cl follows the uptake of K by the plant. It is noticed that there is always a surplus of K compared to Cl in the straw and that there seems to be a minimum level of K in wheat straw of 0.2 - 0.3%.
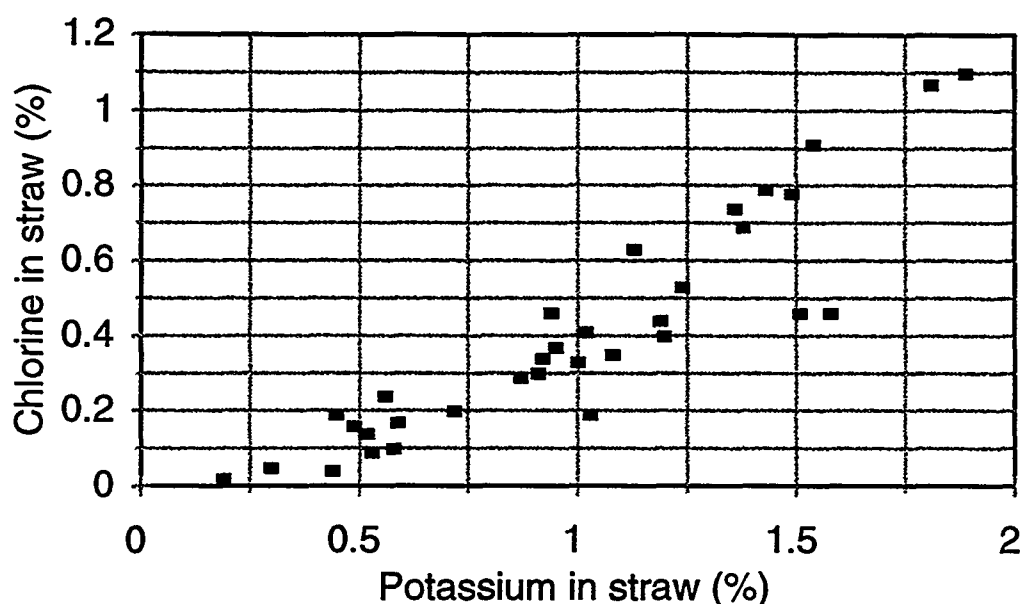
Figure 2.   Content of potassium and chlorine in wheat straw.
                 Unit: Weight-% on dry basis.

In the field trials at Rønhave Experimental Station it was investigated whether the type or dose of pesticide applied has any influence on the chemical composition of straw. The test included two varieties of each of the five species. Six different types of pesticides were applied. There was not found any clear relation between pesticide application and chemical composition of straw.

Straw lying on the field between harvest and baling is often subject to rainfall and the effect of rainfall on the chemical composition of wheat and barley straw has been investigated. Straw lying on the field after harvest has been sampled and analysed at regular intervals and at the same time the accumulated rainfall has been measured. Figure 3 shows the leaching of Cl, K and Ca from barley straw. It is seen that 100 mm of rain reduces the content of Cl to a very low level. The leaching of K closely follows Cl but keeps a minimum level of approx. 0.2% in accordance with the results shown in figure 2. The content of calcium is not affected by rainfall. The results of leaching of wheat straw were quite similar to the results of barley.
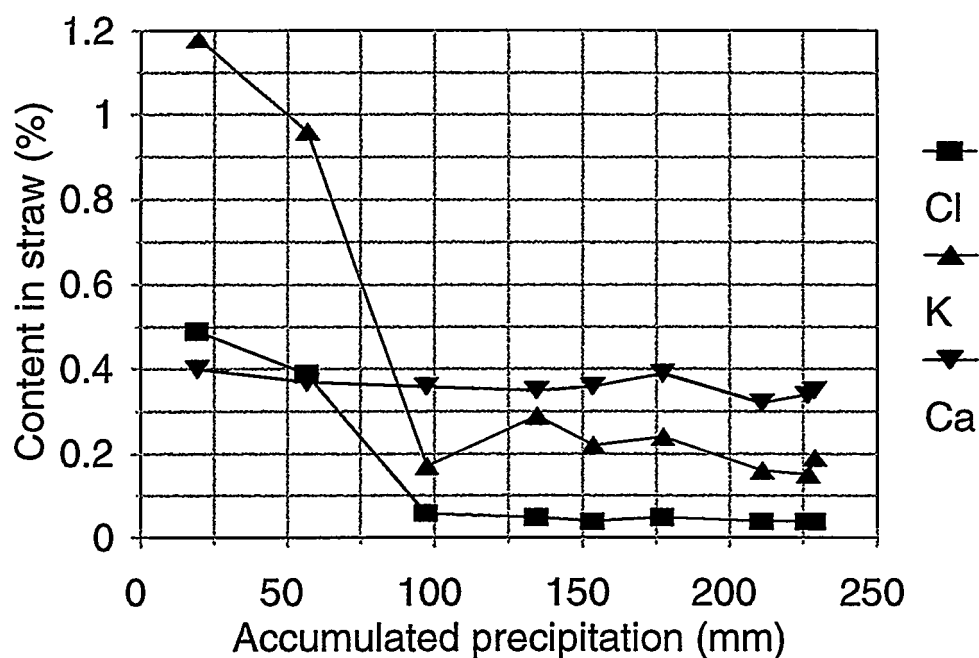
Figure 3. Leaching of barley straw lying on the field.

4. COMPARISON OF STRAW AND GRAIN

In order to achieve a large long-term reduction of CO_2-emissions, it might be necessary to supplement the biomass from surplus straw and wood chips with energy crops. One of the relevant types of energy crops is cereal whole crops, and in order to evaluate the fuel quality of this biofuel, samples of grain and straw from Rønhave were analysed. Figure 4 shows a comparison between the content of some key components in straw and grain.

It is clear from figure 4 that grain has a much lower content of ash, K, Ca, Si and Cl than straw but also a significantly higher content of nitrogen and phosphorus.
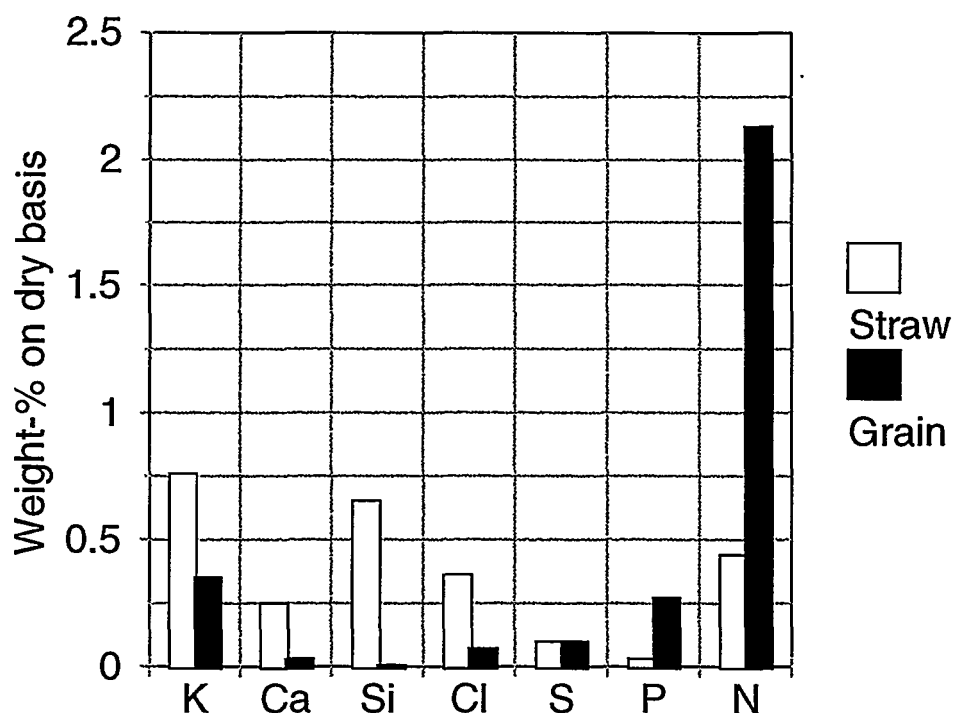
Figure 4.   Comparison of straw and grain composition for winter wheat.

5.   CULTIVATION TRIALS WITH CHLORINE-FREE FERTILIZER.

Potassium fertilizer is normally supplied as KCl. Mass balances for uptake of chlorine in the growing season show that chlorine from fertilizers is a major source of chlorine. It has therefore been investigated if the application of chlorine-free fertilizers will reduce the content of chlorine in straw. In practice this is done by applying K_2SO_4 instead of KCl as potassium fertilizer.

In phase two of the project cultivation trials have been established on different soil types in the growing season of 1994 at three farmers and at Rønhave Experimental Station /2/. Five or six different fertilizer combinations were applied in each trial. The results show that the chlorine content in straw is significantly reduced when the chlorine dose from the fertilizer is reduced. However, the chlorine level in the straw samples at normal chlorine dose was below the typical level for straw. This is

probably due to rainfall just before harvest which leaches chlorine from the straw. Therefore, new cultivation trials with chlorine-free fertilizers have been carried out in the growing season of 1995 where the content of K and Cl in straw has been monitored at regular time intervals /3/. Figures 5 and 6 show how the content of chlorine in straw from four varieties of triticale varies during the growing season with and without supply of chlorine in the fertilizer. The chlorine content in straw was very high in 1995 due to an unusually dry summer. It is, however, clear from figures 5 and 6 that chlorine-free fertilizers significantly reduce the content of chloride in straw and that rainfall leaches chlorine from the standing crop.

Monitoring chlorine in straw
Fertilizer: 100 kg K, 91 kg Cl
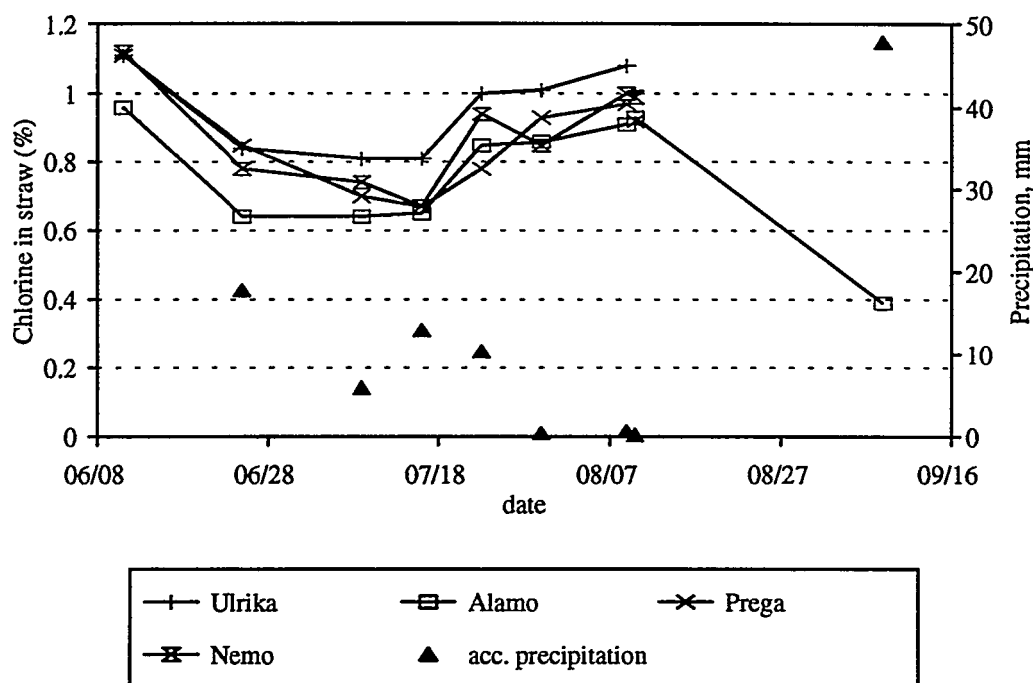
Figure 5.   Chlorine in four varieties of triticale straw during the growing season. Chlorine dose: 91 kg/ha.

Monitoring chlorine in straw
Fertilizer: 100 kg K, 0 kg Cl
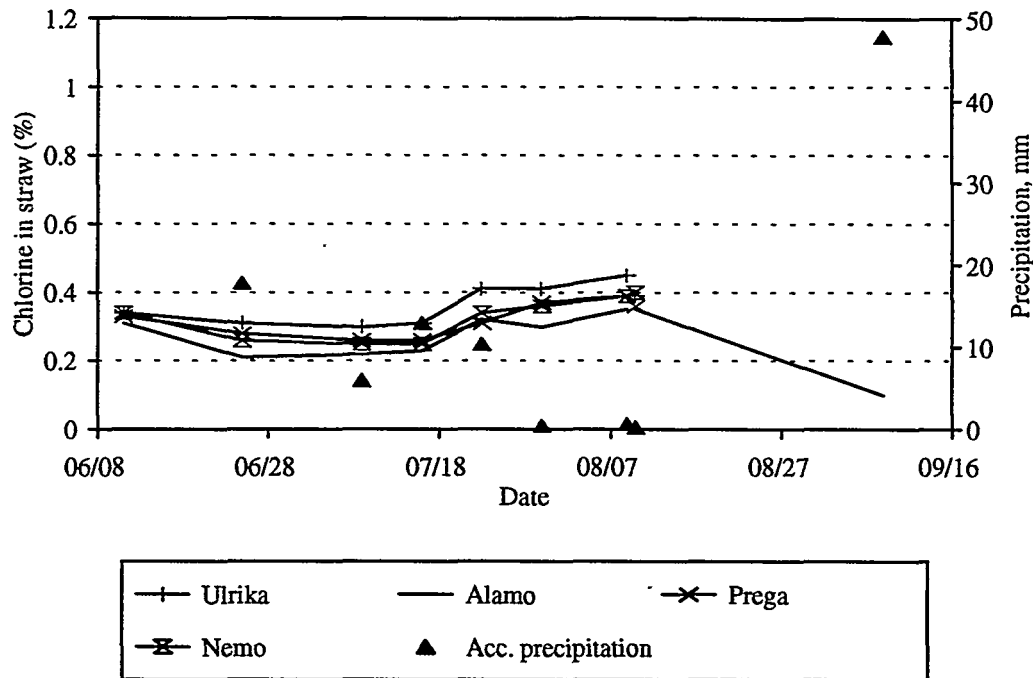
Figure 6.   Chlorine in four varieties of triticale straw during the growing season. Chlorine dose: 0 kg/ha.

The amount of sulphur added to the field is significantly increased by supplying K_2SO_4 instead of KCl. Selected samples have been analysed for the content of sulphur and it is concluded that an increased sulphur supply does not increase the content of sulphur in the straw.

7.   CO-FIRING OF STRAW AND COAL IN PULVERIZED COAL-FIRED UNITS.

In order to investigate the feasibility of co-firing straw and coal in pulverized coal-fired units, a test program was carried out from October 1993 to March 1994 on Vestkraft Power Plant, unit 1 /4/. During the test period 15,000 tonnes of straw was co-fired with 63,000 tonnes of coal. The maximum straw share applied on energy basis was 25%.

Vestkraft Power Plant, unit 1, is a 125 MW_e pulverized coal-fired power plant equipped with 12 burners at the boiler front. Two of the burners were reconstructed

for straw-firing. The straw was chopped and transported by air to the burners through 450 mm pipes.

The boiler was operated at about the same content of O_2 in the flue gas as applied for coal-firing and no significant increase was observed in unburned carbon in the fly ash. The straw burners were recorded on video during operation and the flame temperature was measured. It was shown that due to the high amount of air supplied to the straw burners, no stable flame was established and the temperature in the straw burner zone was low and unstable. An attempt to reduce the amount of transportation air was not successful since the straw capacity could not be maintained.

Co-firing of straw did not increase the need for soot blowing in the boiler and no increased formation of deposits was observed on boiler tubes, superheaters or air preheater. However, slagging occurred around the straw burners.

The influence of co-firing straw on emissions and the composition of residual products was investigated during the measuring campaigns /5/. Coal, straw, bottom ash, fly ash and flue gas were sampled in each test period which had a duration of approx. 5½ hours. Chemical analyses included Si, Al, Fe, Ca, Mg, K, Na, Ti, S, Cl, P and quality parameters for industrial utilisation of fly ash. The flue gas content of O_2, CO, SO_2, NO_x, HCl and dust was measured. 12 tests were carried out, 4 of which were coal reference measurements.

Two coal types were applied during the tests: COCERR - a Columbian coal with a lower heating value of 24 MJ/kg, an ash content of 11% and a sulphur content of about 0.8% and RUKUZN - a Russian coal with a lower heating value of 24 MJ/kg, an ash content of 13% and a sulphur content of about 0.4%. The major part of the straw applied was from wheat with a water content of between 15 and 19% and an ash content of about 4%.

On the basis of mass flows and chemical analyses of fuels and residual products the retention of sulphur and chlorine in the fly ash has been calculated. The results of co-firing straw with COCERR coal are shown in figure 7.
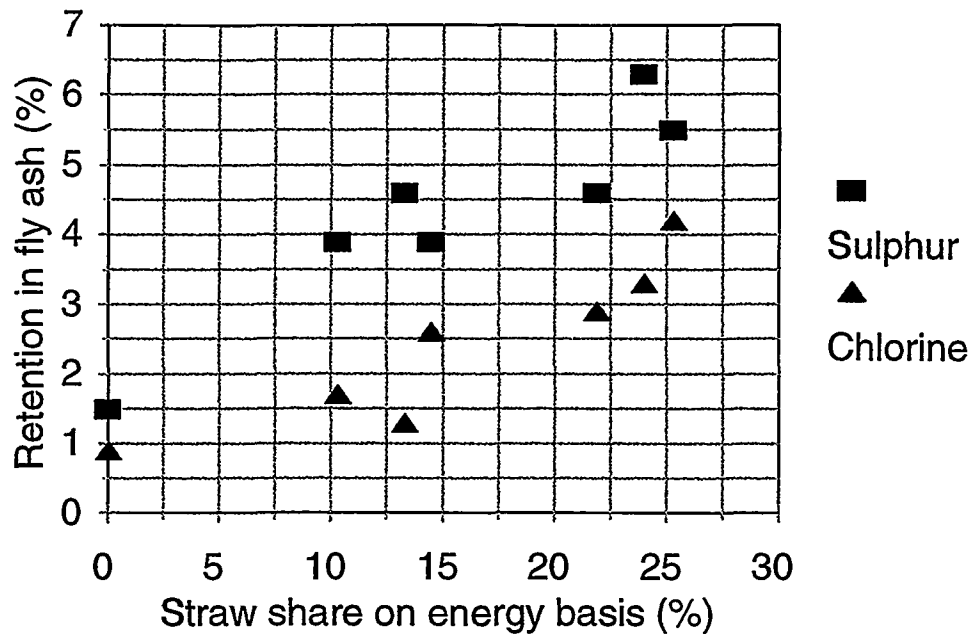
Figure 7.   Retention of sulphur and chlorine in the fly ash when co-firing straw and COCERR coal.

The retention is here defined as the fraction of the content of sulphur and chlorine in the fuels which ends up in the fly ash. It is observed that the retention of sulphur and chlorine in the fly ash increases with increasing straw share but that it is still well below 10%.

The limited retention of sulphur and chlorine in the fly ash means that it is primarily the differences in the content of sulphur and chlorine between coal and straw which affect the emissions of SO_2 and HCl. As seen in figure 1 straw has on a lower heating value basis, a much lower content of sulphur and a much higher content of chlorine than coal, ie., co-firing of straw will result in reduced concentration of SO_2 and increased concentration of HCl in the flue gas from the boiler. This was confirmed by the emission measurements during the combustion tests.

The emission of NO_x from the boiler was measured during the test periods. Figure 8 shows the NO_x-emission in mg/MJ as a function of the straw share. The NO_x-emission is reduced by 25-30% by co-firing straw and the results of two coal types are quite similar. The reduction of the NO_x-emission is significantly higher than the reduction of the fuel-nitrogen due to co-firing of straw. A lower furnace temperature and

4.14

liberation of NO_x-reducing gas species during straw combustion probably contribute to the additional NO_x-reduction observed.
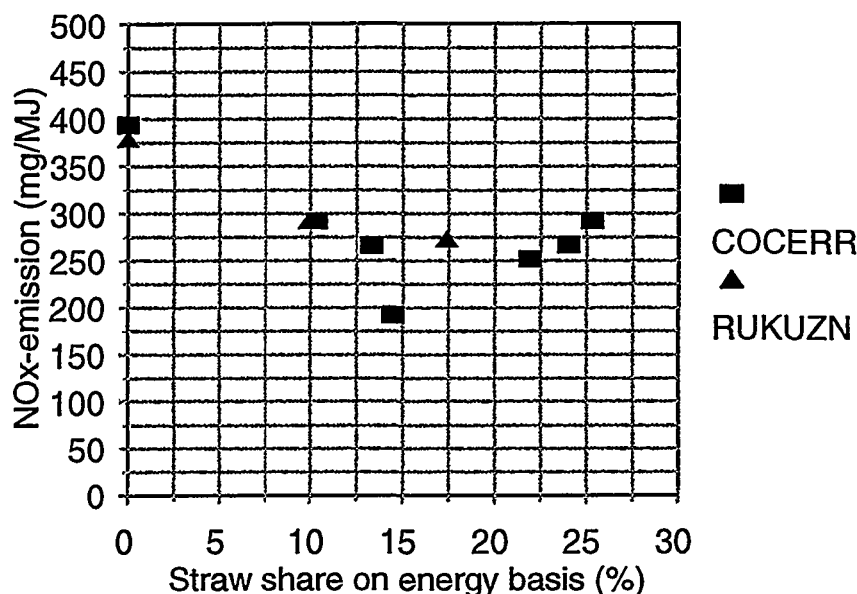
Figure 8. NO_x-emissions for co-firing coal and straw.

NO_x-reduction by means of the SCR technology is an integrated part of modern coal-fired power plants and by inserting catalyst elements in the flue gas duct during the test period, the deactivation of SCR catalysts when co-firing straw has been investigated. After exposure for 250 hours under high-dust conditions at a temperature of 280-290°C, the SCR test elements had lost 25% of the initial catalytic activity. This is an extremely high deactivation rate which will make it impossible to co-fire straw in boilers with high-dust SCR. However, more tests under better controlled conditions and with different catalyst types should be performed before a final conclusion can be made.

As utilisation of fly ash from coal-fired boilers has a high priority due to environmental considerations, the investigation of the influence of co-firing straw on the fly ash quality was an important part of the test program. The cement and concrete industries are the main consumers for industrial utilisation of fly ash in Denmark and strict quality requirements for fly ash must be met for these applications. Due to the high content of potassium in straw, cf. figure 1, and the increased retention of sulphur and chlorine in the fly ash, cf. figure 7, the most critical fly ash quality parameter for co-firing straw is the content of alkali, SO_3 and Cl. Table 5 shows how this parameter is influenced by the maximum straw share of 25% on energy basis.

	COCERR coal	COCERR coal + 25% straw
Equivalent Na_2O total (%)	2.1	3.4
Equivalent Na_2O available (%)	0.7	1.6
Equivalent Na_2O water-soluble (%)	0.3	0.3
SO_3 (%)	0.4	1.0
Cl (%)	<0.005	0.05

Table 5.   Fly ash quality parameters measured at 0 and 25% straw share. Equivalent Na_2O: Na_2O + 0.658 K_2O.

As expected the content of alkali, SO_3 and Cl in the fly ash increases significantly when straw is applied as fuel. Taking into consideration the variations in the composition of coal ash and the content of potassium in straw, it will in general not be possible to meet the quality requirements for fly ash to be applied as raw material in cement production at straw shares higher than 10% on energy basis. Fly ash as a substitute for cement in concrete production has less stringent quality requirements but the maximum allowable straw share will be limited to less than 20% for this application. However, more data are necessary in order to give a more accurate estimate of the limiting straw shares for fulfilment of the quality requirements for fly ash.

It is interesting to note from table 5 that the content of water-soluble alkali in the fly ash does not increase when straw is co-fired with coal. This means that the increased content of potassium in the fly ash cannot be present as chlorides or sulphates as seen in 100% straw-fired boilers but is more likely associated with silicates in the fly ash. In accordance with this observation it was found by means of XRD measurements that SO_3 in the fly ash was present mainly as $CaSO_4$.

Based on the results of the co-firing tests at Vestkraft Power Plant, unit 1, ELSAM decided to rebuilt the 150 MWe coal-fired unit 1 of Studstrup Power Plant as a demonstration plant for co-firing of straw in pulverized coal-fired units. The plant was commissioned at the end of 1995 and an extensive demonstration program has been initiated. The demo program includes investigations of emissions, FGD and DeNOx plants, composition of residues, deposit formation and corrosion rates. One of the features of the new plant is the installation of a newly developed combined

straw and coal burner. The plant will have an annual straw consumption of 50,000 tonnes.

8. SEPARATE GRATE-FIRED BOILER FOR STRAW AND WOOD CHIPS.

As an alternative to co-firing of biofuels in coal-fired boilers, ELSAM has decided to establish a 40 MW$_e$ separate grate-fired boiler for biofuels which delivers steam to the steam turbine of a coal-fired parent plant. In this plant the main boiler is straw-fired and the steam temperature is limited to 480°C in order to avoid unacceptable corrosion rates. The steam temperature is increased to 540°C in a separate wood chip-fired superheater in order to match the steam conditions in the coal-fired power plant. The plant is under construction at Sønderjyllands Højspændingsværk and will be in commercial operation at the beginning of 1998. The annual consumption of biofuel will be 120,000 tonnes of straw and 30,000 tonnes of wood chips.

Decentralized power plants based on straw-firing have been in operation in Denmark for some years and combustion tests have been made at two of these plants - located in Haslev and Slagelse - with well-defined straw qualities in order to investigate the relation between the composition of straw and emissions, residue compositions and deposit formation /6/. The plant in Haslev is equipped with a so-called "cigar"-burner where combustion of whole straw bales takes place at the front. The Haslev plant has a capacity of 5 MW$_e$. At the plant in Slagelse shredded straw is combusted on a grate. This plant has a capacity of 8 MW$_e$. The combustion trials included four tests on the Haslev plant and eight tests on the Slagelse plant. The measuring program included sampling and analysing of straw, bottom ash and fly ash, emissions of O_2, CO, SO_2, HCl, NO_x and CO_2, aerosol concentration in the flue gas, insertion of deposition probes and temperature measurements.

The range of the mean flue gas concentrations during each test is given in table 6.

	Haslev	Slagelse
O_2 (%)	8.1-8.7	6.7-7.4
CO (ppm)	120-210	30-380
SO_2 (ppm)	1-49	1-57
HCl (ppm)	9-98	1-100
NO_x (ppm)	170-210	140-217

Table 6.   Range of mean values of flue gas emissions on dry basis.

For SO$_2$ and HCl a large variation in the emission data is observed and it was investigated whether this behaviour was related to the content of sulphur and chlorine in the straw. The relation between HCl-emission and chlorine in straw is shown in figure 9.
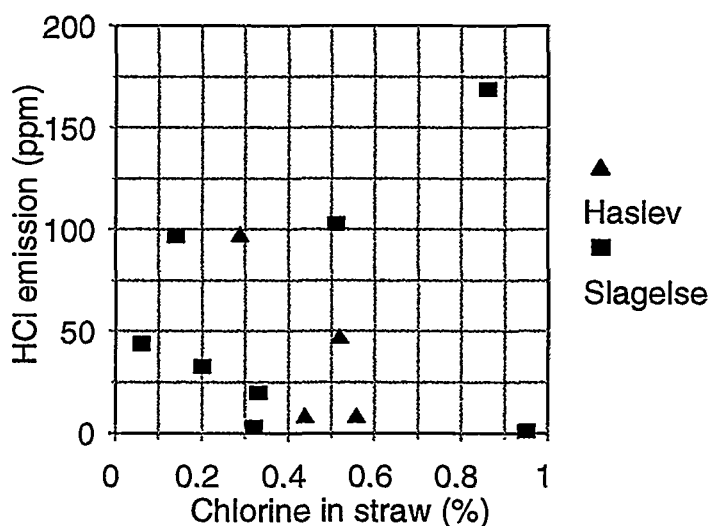
Figure 9.   HCl-emission vs. Cl in straw in straw-fired boilers. Dry basis.

It is clear from figure 9 that the emission of HCl is not correlated with the content of chlorine in straw and similarly we find no correlation between the emission of SO$_2$ and the content of sulphur in straw. However, there seems to be a relation between the emission of HCl and the emission of SO$_2$ as shown in figure 10. Apparently combustion conditions which results in high levels of SO$_2$ also promote high levels of HCl. However, it is not known which fuel characteristics of the straw that favour high or low emissions of SO$_2$ and HCl.
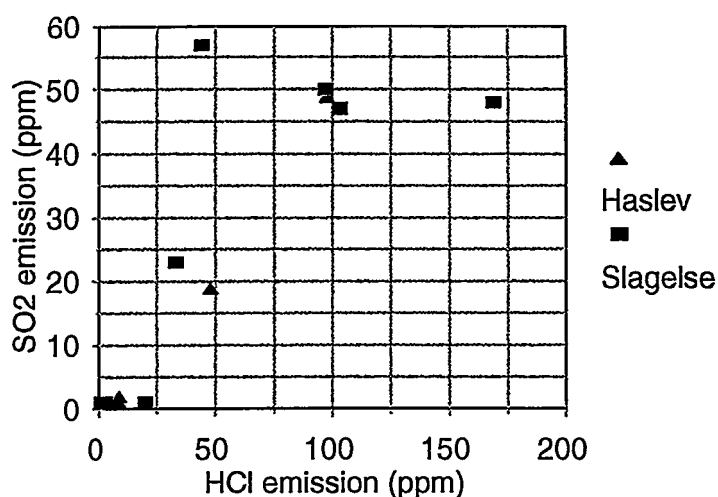
Figure 10.   Emissions of SO_2 vs. HCl for straw-fired boiler. Dry basis.

Concentrations of aerosols in the flue gas were measured just before the filter for removal of particles. The measuring methods applied are described by Christensen et al /7/. The aerosol particle fraction has a typical mean diameter of about 0.4 μm and is composed of KCl and to a lesser extent of K_2SO_4. The aerosols are formed by condensation of gaseous potassium salts which are liberated in the combustion process. The aerosol concentrations can therefore be interpreted as a measure of the gas phase alkali concentration in the boiler. The fraction of potassium in the straw which is liberated as a gas during combustion varies from 4 to 32% and this means that the aerosol concentration may become very high. Figure 11 shows the aerosol concentration as a function of the content of potassium in the straw and it is seen that aerosol concentrations of more than 2000 mg/Nm^3 occur. This is a much higher level than normally seen for coal combustion aerosols.

Based on the measurements of aerosol concentration and composition and emissions of HCl and SO_2, it was proposed /7/ that the sulphation reaction

$$2KCl + SO_2 + H_2O + \tfrac{1}{2}O_2 \rightleftharpoons K_2SO_4 + HCl$$
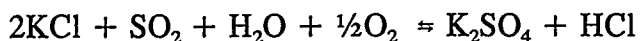
is the main reaction which governs the concentration level of K, S and Cl containing species in the flue gas. The concentrations measured fit well with an assumption of a "quenched equilibrium" of this reaction at about 800°C.

4.19
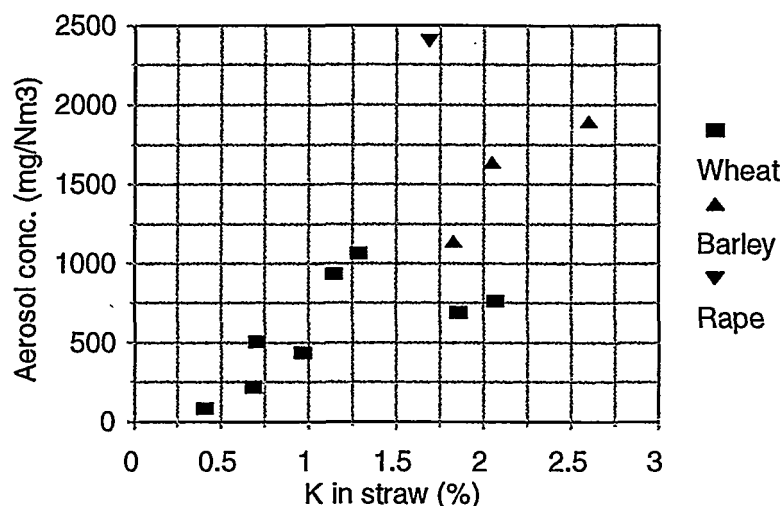
Figure 11.   Relation between K in straw and aerosol concentration in the flue
                  gas before particle removal. Dry basis.

The vaporization and condensation of potassium compounds at straw-firing has a
significant influence on the composition of bottom ash and fly ash. Table 7 shows the
range of content of the main elements in ash samples from the combustion tests.

	Bottom ash	Fly ash
Si	21-32 %	1-16 %
Ca	6-11 %	1-6 %
K	9-20 %	22-51 %
S	0-1 %	2-4 %
Cl	0-3 %	12-33 %

Table 7.   Element concentration in bottom and fly ash samples (excl. rape
                 straw).

Fly ash is highly enriched in K, S and Cl whereas the bottom ash is enriched in the
nonvolatile elements Si and Ca. Rape is excluded from the table as rape straw has a
very low content of Si and a high content of Ca. The fly ash typically constitutes 10-
30% of the total ash production in straw-fired boilers.

Straw-fired boilers are frequently exposed to extensive deposit formation in the
furnace and the convective passes. Deposits are formed by a combination of conden-
sation of gaseous potassium compounds and impaction of fly ash particles. In the

4.20

combustion tests at the plants in Haslev and Slagelse deposition probes have been inserted in order to investigate the relation between deposit formation and fuel composition. The probes were air-cooled in order to control the surface temperature at about 510°C and were placed at two positions: in the upper part of the furnace and in the superheater section. After each test the deposits were collected and the deposition rate was calculated. Selected samples were analysed for chemical composition. Figures 12 and 13 show the relation between the deposition rate in the furnace and in the superheater section and the content of potassium in the straw.
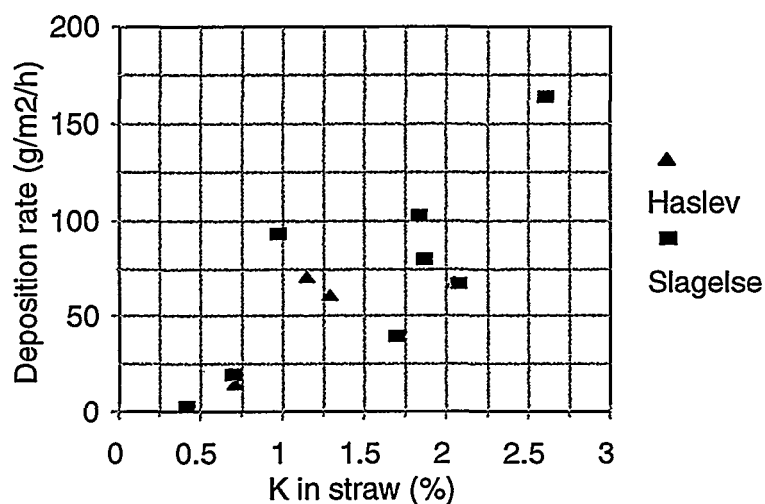
Figure 12.   Deposition rate in top of furnace.
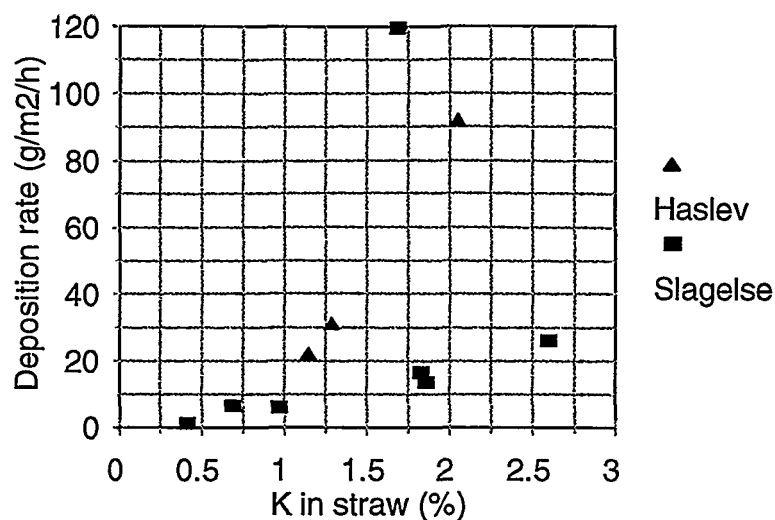
Figure 13.   Deposition rate in superheater section.

The deposition rates in the furnace and in the superheater section increase with increasing content of potassium in the straw. This is probably due to the increased concentration of gaseous potassium compounds at high potassium levels in the straw as shown by the aerosol measurements in figure 11. The single point with an exceptionally high deposition at the Slagelse plant is for the combustion test with rape. This is in accordance with figure 11 which shows that combustion of rape straw results in exceptionally high aerosol concentrations.

The deposition rates are higher in the furnace than in the superheater section. This may be explained by higher impaction of fly ash particles and a higher rate of condensation of potassium compounds. This is supported by figure 14, which shows the content of K, Cl and SO_4^- in the aerosol, in the furnace deposits and in the superheater deposits for one of the combustion tests at the Slagelse plant. It is seen that the residual part of the deposits that consists of Si and Ca compounds is higher in the furnace deposits than in the superheater deposits. Another interesting aspect of figure 14 is that the sulphate/chloride-ratio in the deposits are higher than in the aerosols. This is an indication of sulphation of KCl deposited on the probes and this reaction may of importance for the corrosion rate of the superheaters due to the liberation of gaseous HCl in the deposits.
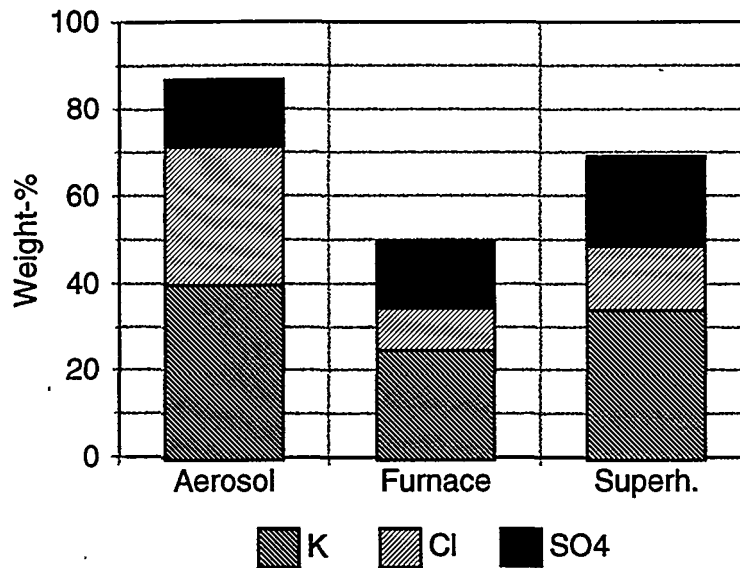
Figure 14.   Content of potassium, chloride and sulphate in aerosol, furnace deposits and superheater deposit for one of the combustion tests at the Slagelse plant.

9.   CONCLUSION.

By means of field trials the possibilities of improving the fuel quality of straw by reducing the content of potassium and chlorine have been investigated. The data obtained have shown that

*   there is no correlation between the content of potassium and chlorine in straw and soil type, nitrogen and potassium fertilizer dose, pesticide dose and geographic location;

*   the content of potassium and chlorine depends on the variety;

*   rain in the harvest period leaches significant amounts of potassium and chlorine from straw;

*   application of chlorine-free fertilizes reduces the content of chlorine in straw but the chlorine level is also dependent on the rainfall in the harvest period - a dry summer gives a high content of chlorine in straw;

*   grain has a lower content of ash, K, Ca, Si and Cl than straw but a higher content of P and N.

Co-firing of straw and coal in pulverized coal-fired units has been tested in full scale in a preliminary test programme at Vestkraft Power Plant, unit 1, and the results have shown that at co-firing of straw

* the emission of SO_2 and NO_x from the boiler is reduced;

* the emission of HCl is increased;

* a limited retention of sulphur and chlorine in the fly ash is observed;

* the deactivation rate of high-dust SCR is increased;

* the industrial utilization of the fly ash is impeded due to the increased content of alkali;

* the main part of chlorine from straw is converted to HCl in the flue gas.

These results will be further investigated in an extensive demonstration programme at the co-combustion plant at Studstrup Power Plant, unit 1, commissioned at the end of 1995.

Emissions, residue composition and deposit formation in separate straw-fired boilers have been studied at two decentralized power plants in Haslev and Slagelse and the results have shown that

* there is no correlation between the emissions of SO_2 and HCl and the content of sulphur and chlorine in straw;

* a significant fraction of the content of potassium and chlorine in the straw is evaporated as KCl during combustion;

* the vaporization of potassium results in very high concentrations of aerosols consisting of KCl and K_2SO_4 in the cooled flue gas.

* the fly ash is highly enriched in K, S and Cl, whereas the bottom ash is enriched in Si and Ca;

* the deposition rates in the furnace and in the superheater section are high and increase with increasing content of potassium in the straw;

* deposited KCl is sulphated by reaction with SO_2 from the flue gas.

10. REFERENCES.

1. Bioteknologisk Institut, "Undersøgelser af halms kemiske sammensætning - med relation til forbrænding og forgasning", november 1994.

2. Bioteknologisk Institut, "Klorfri kontra klorholdige gødningers indflydelse på klorindholdet i halm", august 1995.

3. KONCEPTOR, "Kornarter som energiafgrøde - forbedring af brændselskvaliteten", august 1996.

4. Kierkegaard Petersen, S.C. & Hansen, K.E., "Co-firing of straw in pulverized coal-fired boiler Vestkraft unit 1", P94-035, september 1994.

5. Sander, B., "Halmtilsatsfyringsforsøg på Vestkraft, blok 1. Målekampagner vedrørende restprodukter og emissionsforhold", EP94/595, juli 1994.

6. Stenholm, M., Jensen, P.A. & Hald, P., "Biomasses brændsels- og fyringskarakteristika. Fyringsforsøg", dk-Teknik/Risø, april 1996.

7. Christensen, K.A., Stenholm, M. & Livbjerg, H., "The Formation of Submicron Aerosol Particles, HCl and SO_2 in Straw-Fired Boilers", to be published in J.Aer.Sci.

Degradation mechanisms of organic rubber and glass flake/vinyl ester linings in flue gas desulphurization plants

By Rudolf Weber
Allianz-Centre for Technology GmbH
Krausstr. 14
85737 Ismaning
Germany

1. Abstract

In recent years, there have been reports in numerous publications about damage to rubber and glass flake coatings in flue gas desulphurization plants. The pattern of damage has been described and attempts have frequently been made to determine and explain the cause of the damage. Oxidation/hydrolytic changes were generally observed as the damage mechanisms. In addition, blistering occurs in both the chloroprene coatings in the absorbers and in the glass flake coatings in clean gas ducts. This blistering may be considered as the end of the useful life and leads to cost-intensive and time-intensive repair and restoration measures. The present state of knowledge suggests that the blistering is mainly due to osmotic processes preceded by permeation processes and with permeation processes superimposed on them. Among other things, the reports describe the permeation behaviour of water and other flue gas constituents; the blistering in chloroprene rubber coatings and glass flake coatings is explained by means of the knowledge gained.

2. Introduction

In the retrofitting with flue gas desulphurization plants introduced in Germany in the Eighties for the purpose of reducing SO_2, it was mainly the lime or limestone methods which were employed. The surfaces in contact with the flue gases were in unalloyed steel and were protected from corrosion by rubberizing or coating. The damage which is currently occurring leads prematurely to cost-intensive and time-intensive repair and restoration measures. Because of this damage, intensive efforts are being made to determine

the causes. The present article describes the current state of knowledge concerning some damage mechanisms which have been found during laboratory investigations.

3. Rubber coatings

3.1 Application locations and the conditions met by the coatings

The absorbers and also, in some cases, the flue gas ducts are frequently coated with rubber. The essential difference between power stations fired with hard coal and those fired with brown coal is the absorber temperature and, therefore, the saturation humidity occurring. Because of the water content in brown coal (between 52 and 60 %) and the high untreated gas temperatures (between 120 and 190 °C), temperatures of between 65 and 70 °C, accompanied by a saturation humidity of between 250 and 320 g/m³ occur in the absorber. In contrast, the hard coal has a water content of 6 %. This give an untreated gas temperature between 90 and 170 °C and a humidity of between 60 and 75 g/m³. Because of the temperature and humidity of the untreated gas, the absorber temperature is between 45 and 50 °C and the saturation humidity is between 100 and 130 g/m³. Table 1 shows the results of analyses of the inlet and clean gas condensates and compares brown coal and hard coal. These results should be considered as an indication of trend because of the sampling arrangements /7/.

| Komponenten | Braunkohle | | | | | | Steinkohle | | | | | |
| | Rohgas | | | Reingas | | | Rohgas | | | Reingas | | |
	min.	max.	$\overline{X}$	min.	max.	$\overline{X}$	min.	max.	$\overline{X}$	min.	max.	$\overline{X}$
pH	2,0	2,55	2,3	2,6	3,5	3,0	0,8	2,0	1,3	2,1	2,6	2,4
Leitfähig-keit mS/cm	1,66	4,28	3,5	0,28	0,90	0,6	15,9	46,4	31	0,85	12,8	10,5
Na mg/l	<0,5	<0,5	<0,5	<0,5	0,9	0,55	0,07	70	15,5	0,03	30	6,0
K mg/l	<0,25	<0,25	<0,25	<0,25	<0,25	<0,25	0,025	30	5,4	0,02	15	2,8
Ca mg/l	<0,1	5,8	1	<0,1	3,2	1,4	0,01	30	14,5	<0,1	11	2,8
Mg mg/l	<0,1	0,2	0,11	<0,1	0,4	0,14	0,01	8,3	2,2	<0,01	2,5	0,7
Al mg/l	<0,1	0,3	0,13	<0,1	0,6	0,2	0,13	5	2,5	<0,1	1	0,75
Si mg/l	<0,1	1,1	0,4	<0,1	2,6	0,7	2,5	187	77	0,5	34	15,6
Fe mg/l	<0,1	0,9	0,34	<0,1	2,8	0,6	<0,1	0,3	0,2	<0,1	1,0	0,4
Cl mg/l	128	193	144	2	15	4,7	825	3260	2126	3	196	64
NO₃ mg/l	<1	4,7	2,0	1,5	7	4,5	3	46	25	2,7	584	88
SO₄ mg/l	76	420	267	18	120	7,0	305	1670	915	21	1880	660
F mg/l	0,6	21,5	6,4	<0,5	1	0,6	52	430	240	50	400	57
Br mg/l	—	—					<1	20	10	0,4	6	2

Table 1   Untreated condensate/clean gas condensate band width, comparing brown coal and hard coal /7/

3.2 Rubber coating systems employed

Generally speaking, rubber strips with a thickness of between 3 and 5 mm are bonded onto the steel surface which has been abrasively blasted (degree of rust removal SA 2 1/2, DIN 55 928/4) and primed. The following are used as the rubber coating materials[1]:

➢ Synthetic rubber on the basis of polychlorinated butadiene (CR) blended with styrol-butadiene rubber (SBR) in the ratio (80:20);

➢ Halogenated butyl rubber, such as brominated butyl rubber (BIIR);

➢ Chlorinated butyl/polychlorinated butadiene blend (CIIR/CR);

3.3 Cases of damage observed and their mechanisms /8-11/

Blistering (Fig. 1), and also high levels of moisture behind the whole of the coating, have appeared after only relatively short operating periods of a few thousand operating hours, mainly in the case of chloroprene.
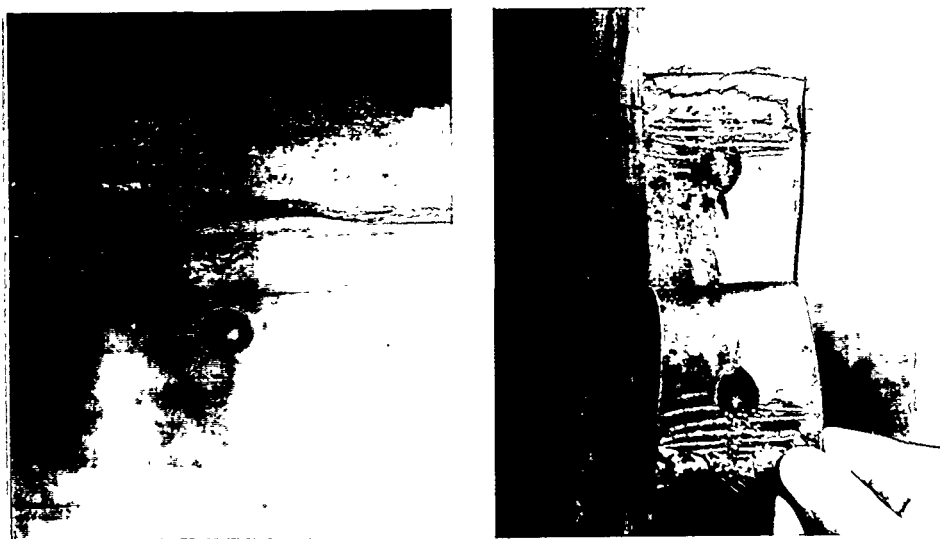
Fig. 1   Blisters - doming of the rubber sheet away from the base

---

[1]   CR elastomeric poly(chloroprene) (ANSI/ASTM); polychlorinated butadiene elastomer

SBR elastomeric copolymer from styrene and butadiene (ANSI/ASTM); styrol-butadiene rubber

BIIR brominated elastomer from isobutene and isoprene; brominated isobutyl-isoprene elastomer

CIIR postchlorinated elastomeric copolymer from isobutene and isoprene (ANSI/ASTM); chlorinated isobutyl-isoprene elastomer

Further damage mechanisms observed were oxidative/hydrolytic changes to the rubber coatings. These led to cracking, the release of carbon black and loss of mechanical properties such as extension and tear resistance.

Cases of damage due to excessive temperature and lack of adhesion have appeared in addition to the above damage features.

3.4 Blistering

The blisters were always filled with a high salt content solution. The local separations necessary were always located in the bonding agent layer between the rubber coating and the steel base. Numerous investigations were carried out in order to explain the blistering. At the present state of knowledge, the investigations suggest that it is mainly osmotic processes which are involved, these being preceded by permeation processes and with permeation processes superimposed on them.

3.4.1 Blister fluid

Table 2 gives, as an example, a survey of blister fluids in hard coal and brown coal installations compared with a condensate sample from a brown coal installation. No difference in principle in the composition can be recognized. The fundamentally similar composition for similar rubber coating material is unambiguous evidence of the same damage mechanism which, because of the lower temperature to which the coating is subjected, is displaced in time in the case of the hard coal installation although it still appears to the same extent.

	Steinkohle		Braunkohle		Kondensat +54 m
pH-Wert	7,5			4,8	2
Leitfähigkeit	34800			28200	5470
Blei	<5	45	3	19	3
Calcium	540	465		355	153
Magnesium	2000	1890	1700	1860	60
Aluminium			16	<1	8
Mangan				15	2
Eisen	1600	836	600	260	9
Natrium	190	410	310	5	60
Kalium	295	280	500		
Zink	31	167	300	5	
Chlorid	2680	8130	10040	6910	140
Sulfat	6900	1112	2600	1340	1420
Sulfit				<5	0,2
Nitrat	60	<5		<10	118
Fluorid		<5		<2	5
Bromid	<10	16		9	3
Formiat	230	268	350		
Acetat	<250	175	300		
Kieselsäure				<50	30

Table 2   Typical composition of blister fluids (conductivity in µS/cm, information on the ion contents in mg/l).

In all the blister fluids, the magnesium content found is substantially higher than the calcium content - the opposite to what is found in the condensate. The iron proportions vary widely; this can be explained by the pH values and the age of the blisters. An astonishing feature is a relatively high sodium and calcium content and a high zinc content. These cations can only originate from the sheet and/or the bonding agent. The chloride proportion is very much higher than it is in the condensate; the sulphate contents are approximately the same. A striking feature is the proportion of low carboxylic acids, in particular formic acid and acetic acid, which can only be explained in terms of hydrolytic and oxidative reactions.

3.4.2   Diffusion of ions

Tests on a 0.5 mm thick sheet of neoprene showed that no water-soluble constituents of the washer suspension can permeate the sheet in ional form. The neoprene sheet has semi-permeable properties and only permits water molecules to pass from the suspension. With respect to the blister fluids, this means that all the ions demonstrated must originate

from the sheet and/or the bonding agent. Penetration due to mechanical damage or faults in the sheet or from the occurrence of in-line pores can be excluded because all the blisters are under positive pressure and may therefore be regarded as having sealed pores.

3.4.3 Changes in the surface zone

X-ray micro-analyses across the section on several samples from chloroprene coated installations (Fig. 2) demonstrated that there is chlorine impoverishment at the surface and that sulphur enrichment due to the effect of the suspension is only present in the surface regions. On the one hand, this shows that chloroprene is attacked thermally and hydrolytically, which leads to the separation of chlorine or hydrogen chloride. On the other hand, it can be deduced from the sulphur distribution that the sheet is not uniformly penetrated by sulphate from the flue gas or the suspension, as would be the case if the sulphate content had to be explained by suspension diffusing into it.
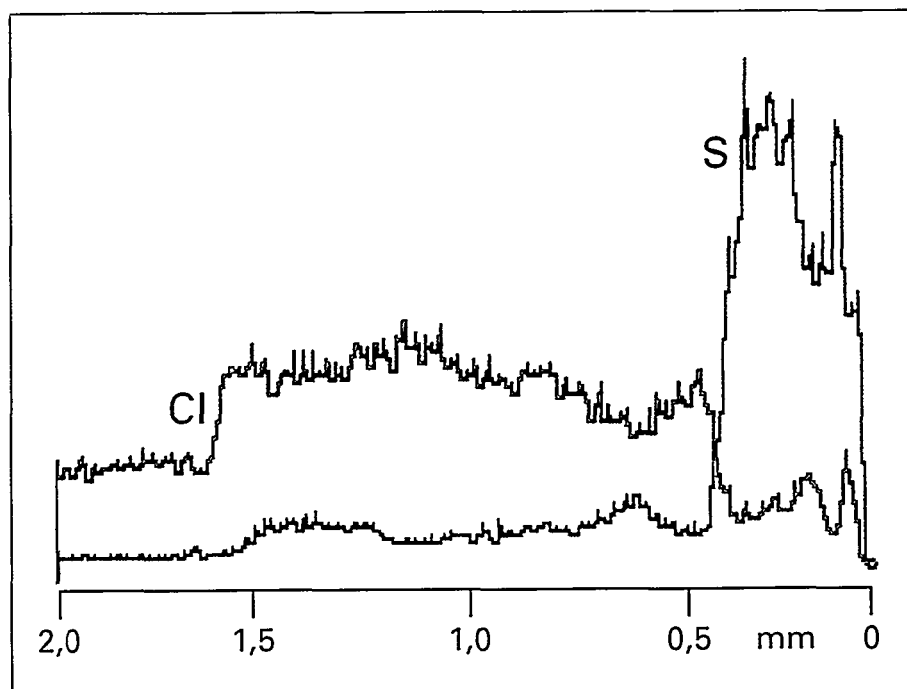
Fig. 2   Distribution of the elements sulphur S and chlorine Cl over the cross-section of a chloroprene sheet subject to operating conditions.

3.4.4 Water absorption

For systematic comparison of the water absorption, five different rubber sheets were tested in the new condition for 80 days under the same conditions in deionized water and

in suspension at 70 °C (Fig. 3). The sheets in chloroprene F5 and F6 have a higher water absorption than the sheets in butyl rubber F7 to F9. At the end of the test, the water absorption had not reached saturation in any of the materials tested. The very high absolute value of the water absorption (up to 18 % by mass) in 80 days corresponds very well with the data given in the literature.
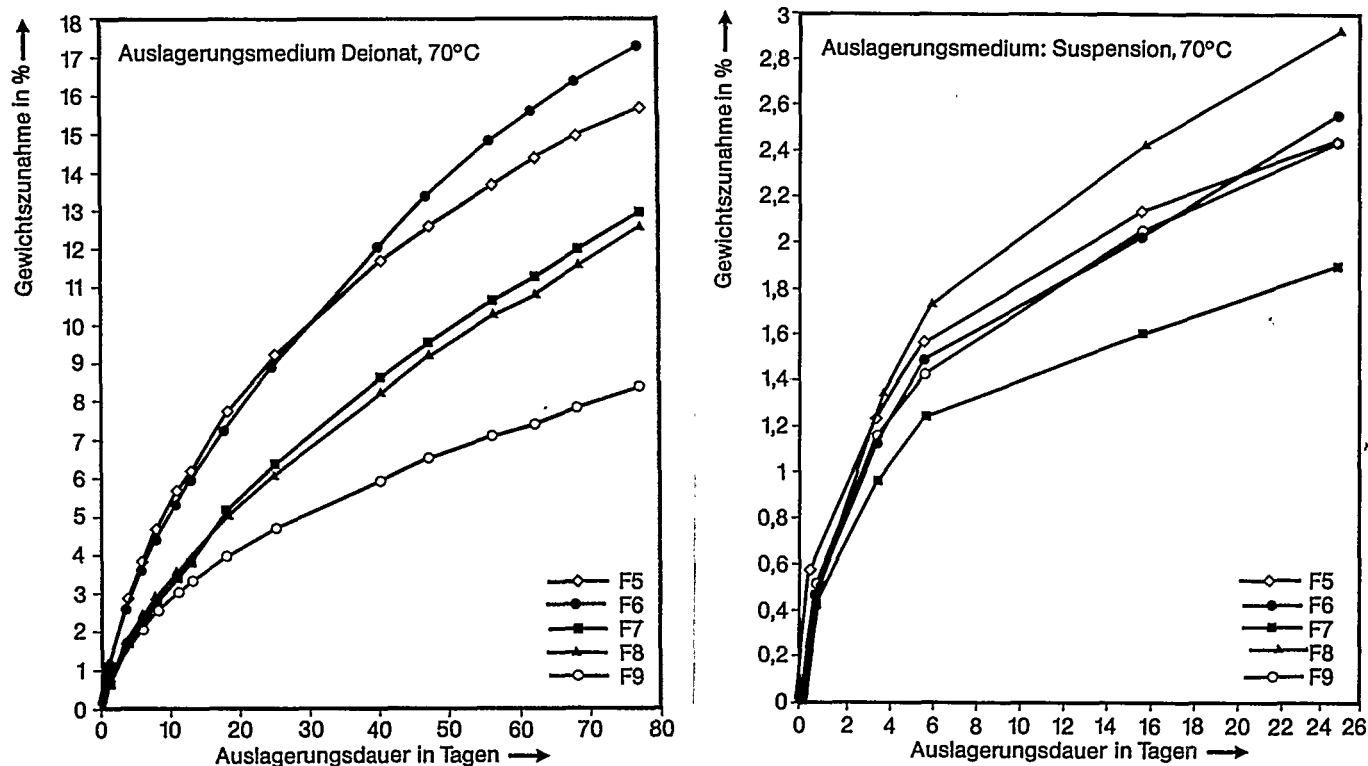
Fig. 3a   Water absorption of different rubber sheets (F5, F6: chloroprene; F7, F8, F9: butyl rubber), increase in mass in percent.

It follows that the rubber sheets investigated absorbed substantial quantities of water within a very short period, i.e. that water can penetrate as far as the steel base or to the layer of bonding agent after a short period.

The water absorption is reproducible and depends on temperature. The fact that the water absorption must be due to osmosis is shown by the reduction in the water absorption when ageing takes place in suspensions; this may be attributed to the salts dissolved in the suspension.

5.6

3.4.5 Salt elutability

As an example, Fig. 4 gives the proportions which can be eluted from 2 of the 10 rubber sheets investigated, shown as a function of the temperature to which they were subjected. A striking feature in the case of all the chloroprene rubbers is the rapidly increasing content of lead and chloride with increasing temperature; this may be attributed to the higher water solubility of lead chloride. There is, overall, a very high level of water-soluble salts, in particular sulphates, formates and acetates. Although the proportion of chloride due to temperature is lower in the case of the types based on chlorinated rubber, it is still noticeably demonstrable and the total proportion of the salts at 70 °C must still be described as substantial. Brominated butyl rubbers behave similarly to chlorinated rubber materials. A commercial polyisobutyl (Rhepanol) is shown as an example of a product with low elution. The elutable constituents from chloroprene materials which had already been in use for 10,000 operating hours had a higher formate and acetate content than the types which had not been subjected to use.
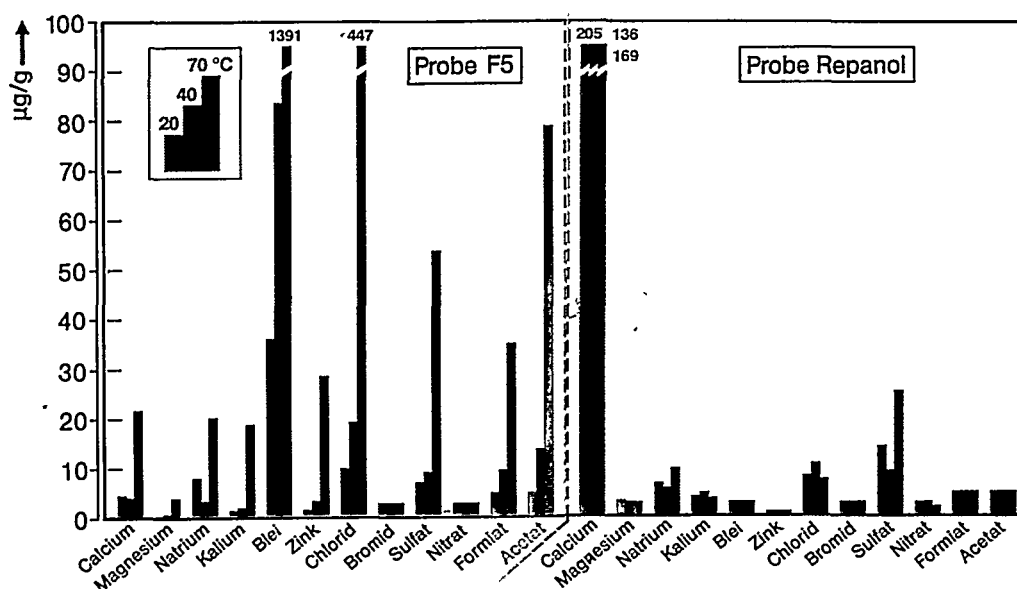
Fig. 4   Elutability of water-soluble salts from rubber sheets (F5: chloroprene, Rhepanol: polyisobutylene).

3.4.6 Bonding systems

Some bonding agents were also subjected to similar ageing tests (pH value 2, 70 °C). Under these conditions, the bonding agents behave in a similar manner to the sheets, i.e. it is mainly chloride and lead which are released. The bonding agent systems contain all

the constituents which can be eluted in water and whose solubility increases with temperature in a weakly acid environment. As a supplement to the elutable constituents from the sheets, they therefore provide a sufficiently large reservoir for water-soluble and acid-soluble salts, which is the condition for osmosis.

3.4.7 Blisters due to osmosis

For this investigation, a 0.5 mm thick rubber sheet was bonded to both glass plates and steel plates, local accumulations of different salts being added to the layer of bonding agent. Liquid-filled blisters occurred between the sheet and the base material at these locations because of the effect on the rubber sheet of water vapour at 70 °C. The size of the blister depends on the type of salt.

3.4.8 Permeation by water vapour

For the systematic investigation of the permeation behaviour of water vapour, pure chloroprene (F5), chloroprene with 20 % styrol-butadiene rubber (F6) and chlorinated butyl rubber with chloroprene (F7) were compared with two samples of butyl rubber (F8 and F9), a commercial polyisobutyl (Rhepanol) and a commercial chloroprene (neoprene). The result is given in Fig. 5. It is clear that the chloroprene types F5 and F6 exhibit a markedly higher diffusion conduction coefficient than chlorinated butyl rubber or brominated butyl rubber - at least in the temperature range around 70 °C. The water absorption capacity of the sheets (Fig. 3) shows that substantial quantities interact with the rubber coating.

Diffusionsleitkoeffizient in g/cm · s · bar

F5; 3,25 mm dick
F6; 3,15 mm dick
F7; 3,00 mm dick
F8; 3,00 mm dick
F9; 4,00 mm dick
Rhepanol; 1,40 mm dick
Neopren; 3,00 mm dick

Wasserdampftemperatur in °C

Diffusionsleitkoeffizient von Wasserdampf
für verschiedene Kautschukfolien

© 1992 | **Allianz** Ⓜ
2.1/79
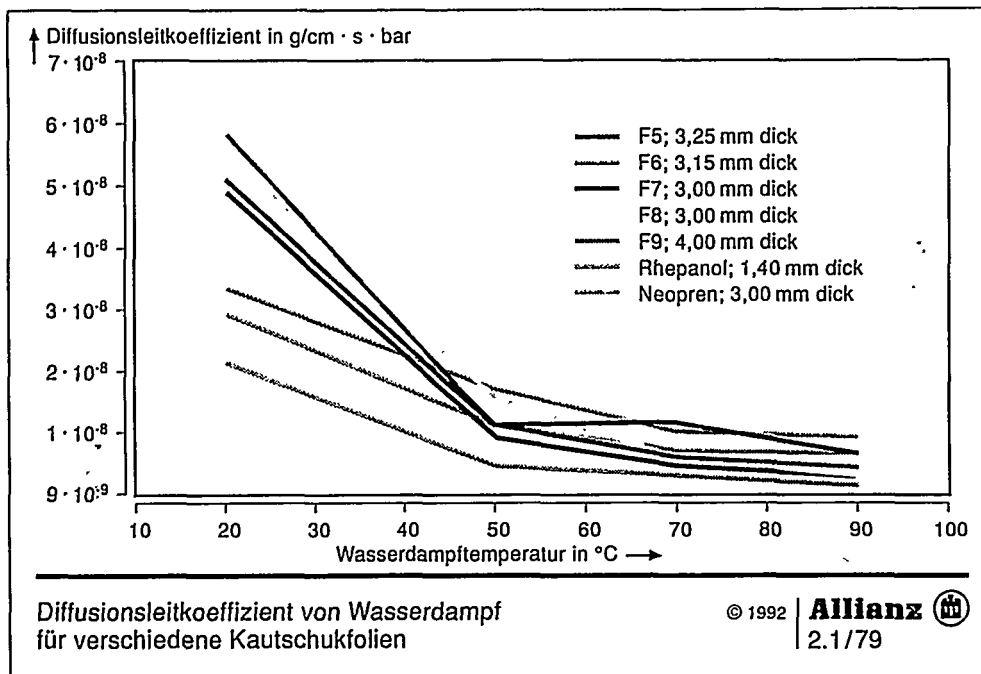
Fig. 5   Diffusion conduction coefficient of water vapour for various rubber
                sheets.

3.4.9 Permeation by sulphur dioxide

Fig. 6 shows the permeation flow densities for sulphur dioxide as a function of the SO_2 partial pressure and the temperature in the case of neoprene and butyl rubber. With neoprene, there is a marked increase in the permeation flow density as a function of partial pressure and temperature - in a manner similar to the water vapour permeation - whereas, in the case of butyl rubber, the permeation flow density is substantially less and is practically independent of temperature and pressure. Relatively high partial pressures were used for all the tests in order to obtain quantifiable and reproducible results in tolerable periods of time.

Diffusionsstromdichte in g/m² · d

Legend:
- Neopren
- Butylkautschuk
- ▨ ■ T = 70 °C
- ▲ △ T = 50 °C
- T = 20 °C

X-axis: SO₂-Partialdruck in bar →

SO₂-Diffusionsstromdichte in Abhängigkeit von der Konzentration und der Temperatur

© 1992 | **Allianz** ⊕ | 2.1/80
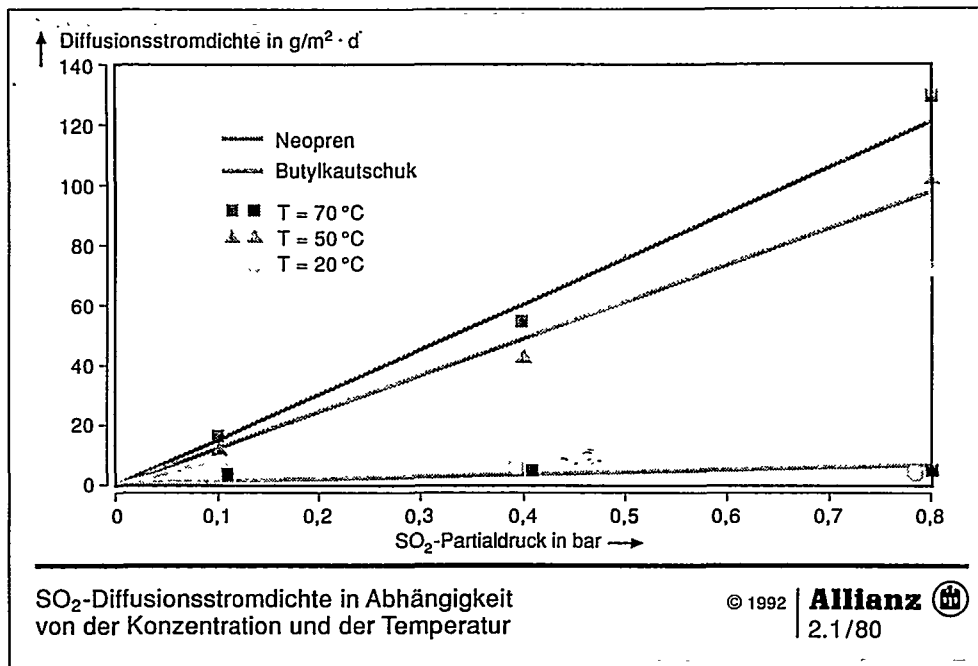
Fig. 6   SO₂ diffusion current density as a function of partial pressure and temperature.

3.4.10 Permeation by hydrogen chloride

In the case of neoprene, substantial permeation by hydrogen chloride occurred after an initial inhibition of permeation, which may be associated with solubility or with saturation of the sheet. It is also conceivable that hydrogen chloride initially reacts with typical oxidic constituents such as zinc oxide and magnesium oxide. Fig. 7 shows the way in which the hydrogen chloride diffusion flow depends on the partial pressure, with the SO_2 permeation flow shown as a comparison. In the case of the butyl rubber sheet, no permeation of hydrogen chloride could be found under the same test conditions.

Diffusionsstrom in g/d

SO₂ und HCl-Durchlässigkeit in Abhängigkeit vom Partialdruck bei Neopren

© 1992 **Allianz** Ⓐ
2.1/85
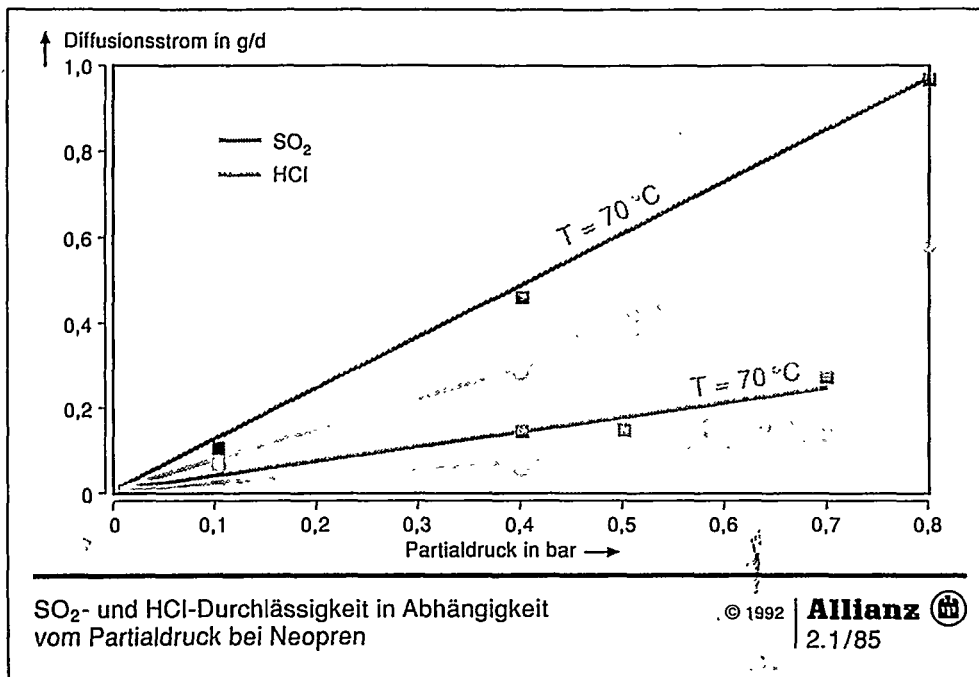
Fig. 7   SO$_2$ and HCl permeability of neoprene as a function of partial pressure.

3.4.11 Permeation by sulphur trioxide

The tests with SO$_3$ again showed that permeation rates between 3 and 5 g/m^{2}d occur at partial pressures of between 0.01 and 0.03 bar for both neoprene and butyl rubber. At higher partial pressures (Fig. 8), 86 g/m^{2}d was reached in the case of neoprene and 6.5 g/m^{2}d in the case of butyl rubber. In the case of sulphur trioxide, it was found that destruction of the rubber matrix by cracks and embrittlement took place relatively rapidly because of the strong oxidation effect.
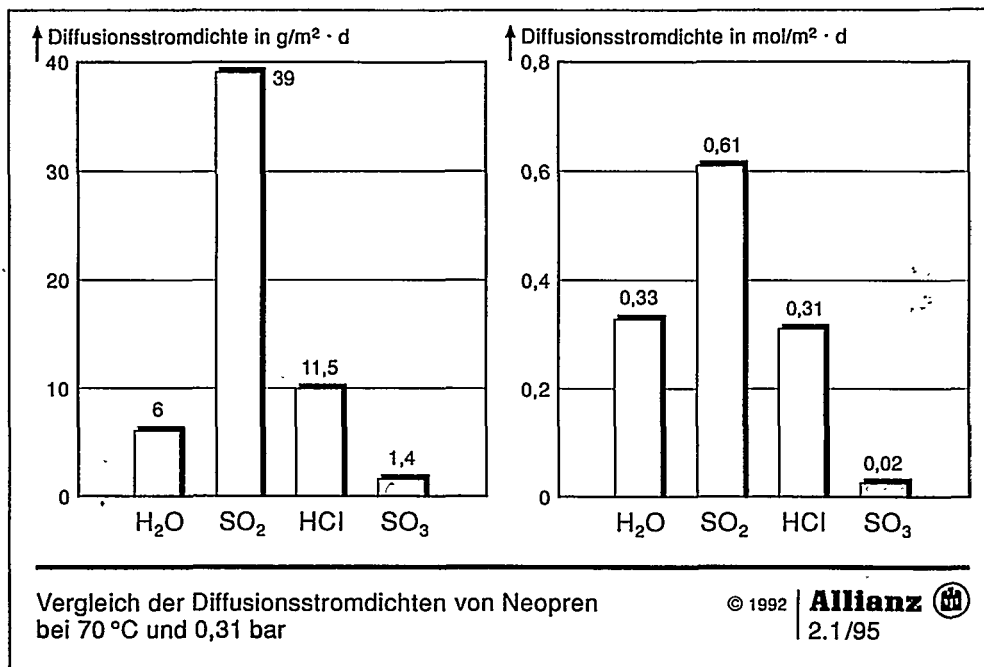
Fig. 8   Comparison of the diffusion current density of various gases for neoprene
at 70 °C and 0.31 bar.

3.4.12 Permeation by sulphur dioxide under the action of water

During the permeation tests using sulphur dioxide and various humidities, it was found
that the presence of water vapour substantially increases the permeation rates in the case
of both neoprene and butyl rubber (Fig. 9).
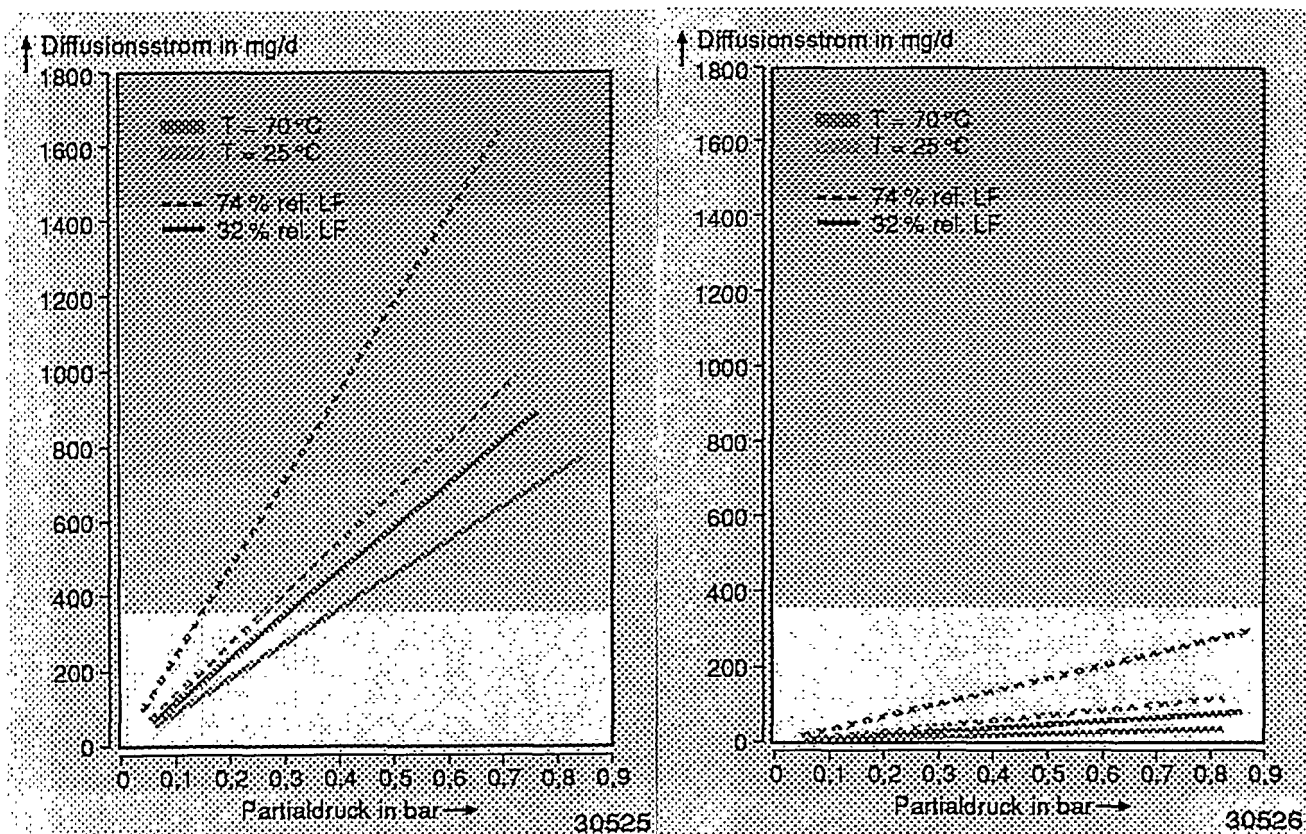
Fig. 9   SO₂ diffusion current as a function of partial pressure and relative humidity.

4.   Coatings

4.1   Application locations and the conditions to which the coatings were subjected

Coatings containing glass flakes and based on vinyl ester and unsaturated polyester resin are often employed in flue gas ducts in the clean gas region behind the washer. In some cases, however, they are also employed in the untreated gas region before the flue gas has been cleaned. In the clean gas region, the temperature in the case of brown coal installations is approximately 70 °C; it is approximately 45 °C in the case of hard coal installations. The clean gas is then saturated with water. When used in the untreated gas region, temperatures in excess of 90 °C and low SO_3 contents are to be expected.

4.2   Coating systems employed

The coatings containing glass flakes are applied to the steel surface, which has been abrasion blasted (degree of rust removal SA 2 1/2) and primed, by means of spatulas or by

the airless spraying method. The total layer thickness, which is applied in several coats, is approximately 3 mm in the case of the coatings applied by spatula and is approximately 1.5 mm in the case of the spray coatings. The glass flakes align themselves parallel to the surface and increase the length of the diffusion paths (Fig. 10). The synthetic resin binder employed may consist of an unsaturated polyester (UP) or various vinyl ester types (VE).
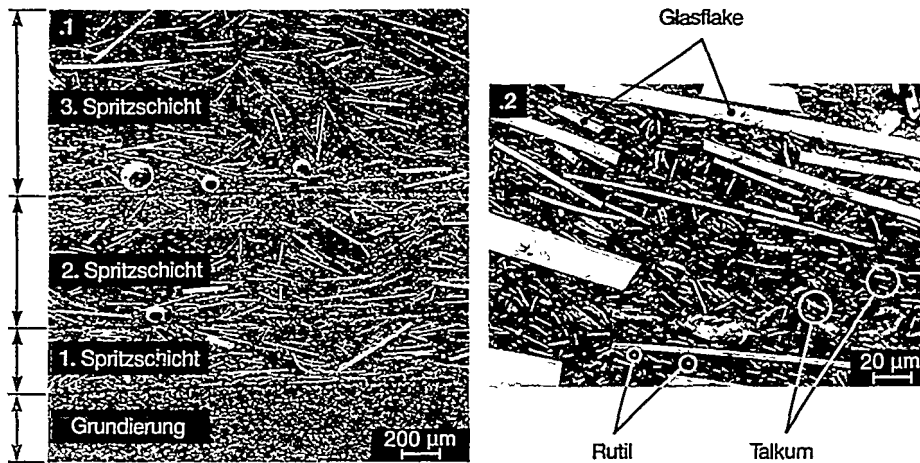
Fig. 10   Typical structure of a coating.

4.3   Cases of damage observed and their mechanisms /11-16/

In the case of the unsaturated polyester, blistering generally occurs in the clean gas ducts of brown coal installations after short operating periods of some 1,000 operating hours (Fig. 11). The marked blistering may then be considered as the end of the useful life and generally leads to cost-intensive and time-intensive restoration measures.
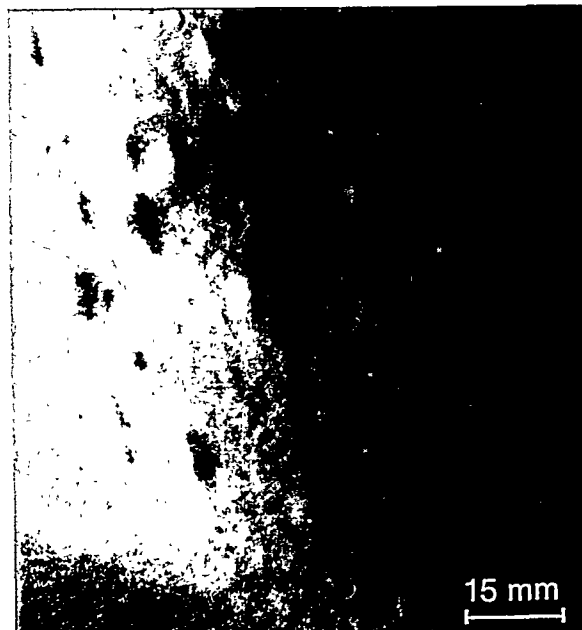
Fig. 11   Blisters in a glass flake/
               unsaturated polyester
               coating of a clean gas duct.

In the case of ducts for untreated gas, particularly in installations fired with refuse and heavy oil, thermo-oxidative removal (and therefore destruction of the synthetic resin base) occurs after short operating periods when the vinyl ester types are employed.

4.4 Blister damage pattern

The blisters (Fig. 12) start from the glass flakes embedded parallel to the surface in the coating. The blister is always tautly inflated by an aqueous salt solution. With a diameter of more than 10 mm, they can be clearly recognized and grow with operating time. Numerous investigations have been carried out to explain the blistering. As can be seen from the investigations, the current view suggests osmotic processes which are preceded by permeation processes and have permeation processes superimposed on them.

1 mm
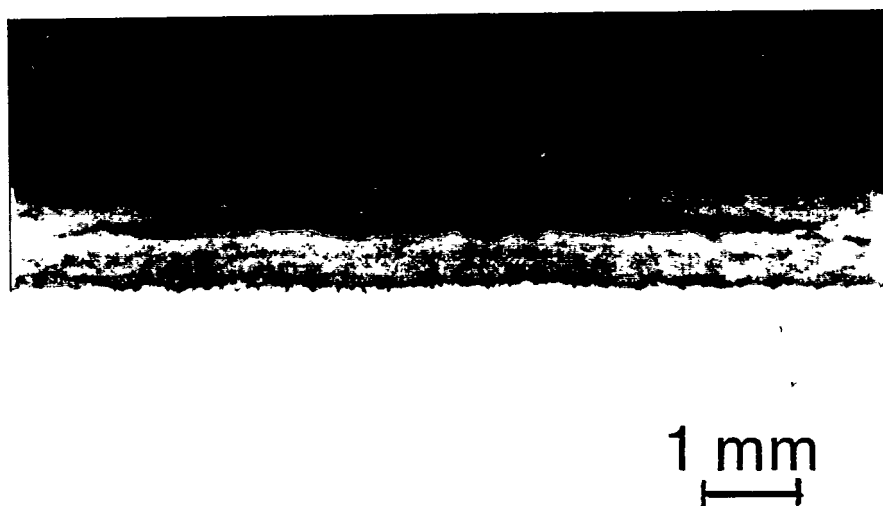
Fig. 12   Cross-section through a blister. The separation is located in the centre of the second sprayed coat.

4.4.1 Blister fluid

The composition (in terms of concentration) of the blister fluid depends on the coating system, in particular on the resin binder. The fluid is an aqueous solution of sodium salts and hydrolysis and oxidation products of the resins (Table 4).

Organische Bestandteile	Konzentration in ppm
Fumarsäure (trans-Butendisäure, HOOCCH=CHCOOH)	5500
Essigsäure (CH_3COOH)	1600
2-Ethylhexansäure ($C_8H_{16}O_2$)	800
2-Methoxyethanol ($CH_3OCH_2CH_2OH$)	400
1-Methyldodecylbenzol ($C_{19}H_{27}$)	200
Nicht identifizierte organische Bestandteile	etwa 13 000
	etwa 22 000
Anorganische Bestandteile	
Natrium (Na^+)	5000
Kalium (K^+)	20
Chlorid (Cl^-)	60
Nitrat (NO_3^-)	< 10
	etwa 5100
Wasseranteil (H_2O in %)	etwa 90
pH-Wert	7,4

Table 3   Analysis of a blister fluid from an unsaturated polyester coating.

4.4.2   Diffusion of ions

Tests with 1.2 mm thick sheets of unsaturated polyester and vinyl ester coatings containing glass flakes showed that no water-soluble constituents of the clean gas permeate in ional form through the coating film. Only water molecules can pass. With respect to the blister fluid, this means that the ions and organic constituents found must come from the coating. Penetration via mechanical damage or faults, such as chains of pores, are excluded because all the blisters are under positive pressure and can therefore be regarded as having sealed pores.

4.4.3   Water absorption

The correctly applied coatings absorb substantial quantities of water when in contact with water or water vapour (Fig. 13a). The increase in weight can reach several percent, depending on the coating system and the temperature.
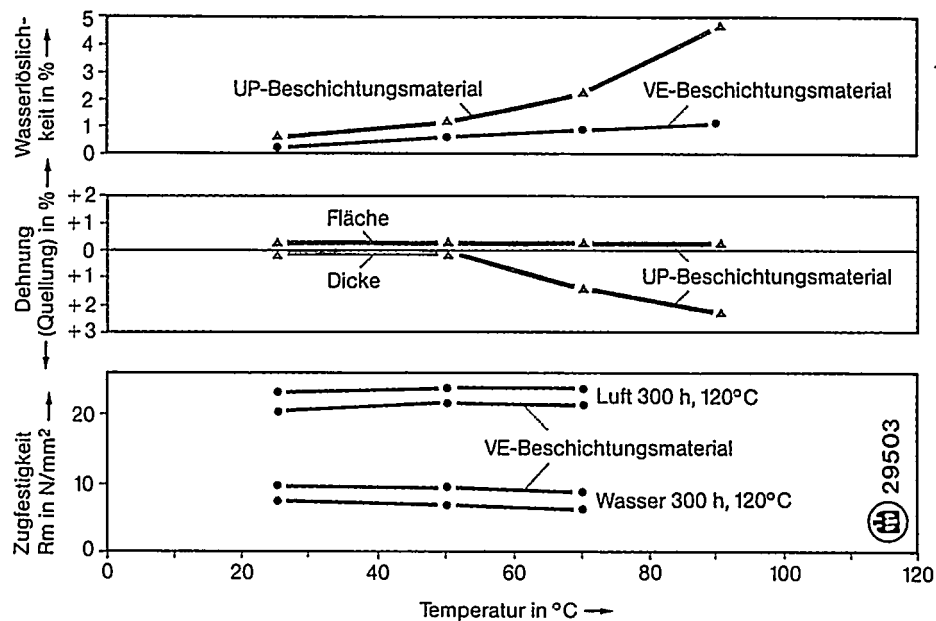
Fig. 13   Water absorption, expansion due to swelling and change in strength in the case of glass flake coatings (sheet thickness approximately 1 mm).

Anisotropic swelling takes place in parallel with the absorption of water (Fig. 13b). It is interesting to note that there is a substantial increase in thickness between 50 and 70 °C.

The mechanical strength figures fall simultaneously with the water absorption and the swelling (Fig. 13c). Whereas, for example, the tensile strength Rm does not show any reduction after 300 hours of ageing in dry air, the figures drop irreversibly by 70 % when the material is exposed to water. Losses which are even greater and are specific to the medium are found in the case of the adhesion strength testing.

4.4.4   Permeation by water

The tests with a vinyl ester coating based on a Novolak acrylate showed that the diffusion conduction coefficient is only slightly affected by temperature but is affected by the selection of the filler materials (Fig. 14).
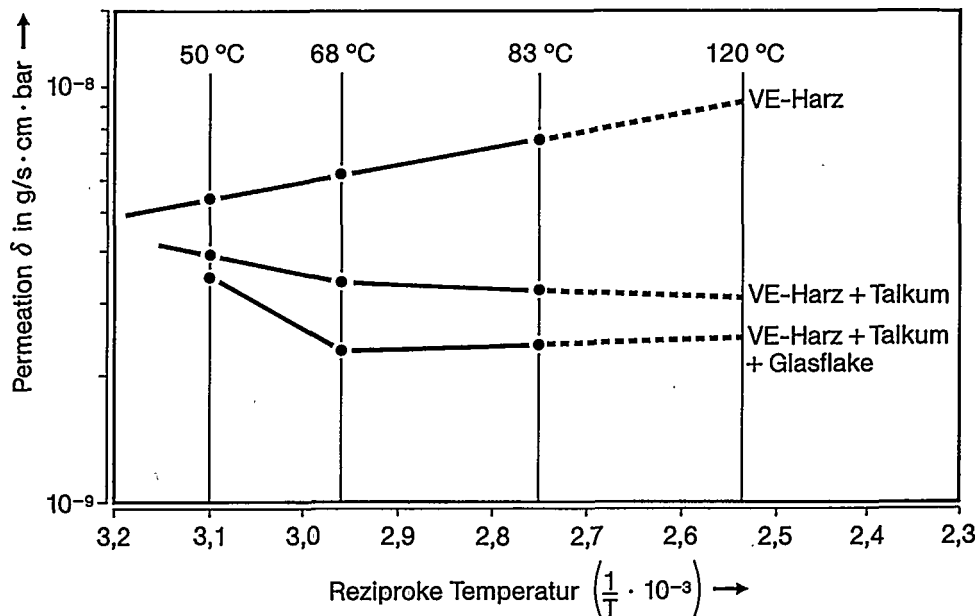
Fig. 14   Variation of water diffusion with temperature and type of filler material.

4.4.5   Structural changes due to the effect of water

As is shown by comprehensive microfractographic investigations, the following changes or damage to the resin/glass flake composite occur due to the water diffusing in and being absorbed.
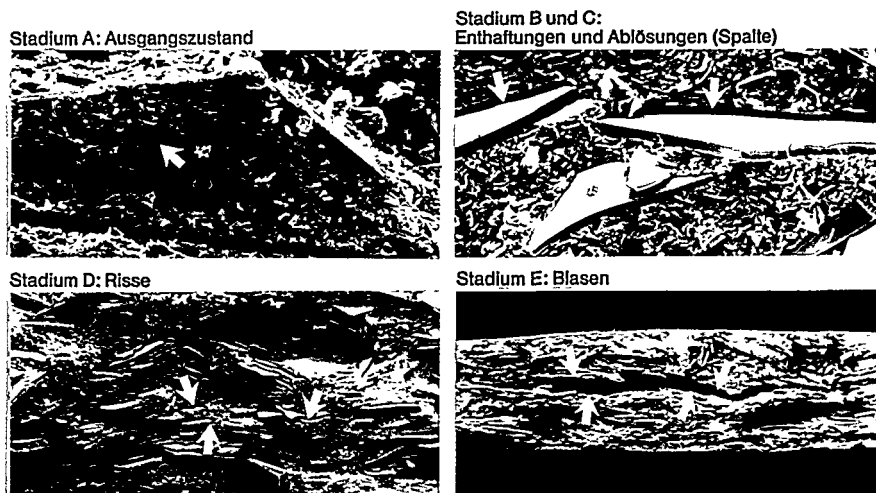
Fig. 15   Electron microscopic representation of the change with time of the fracture structure (Stages A to E) in the coating film due to the action of water.

Stage A:

Initial or unaffected condition (Fig. 15). In the fracture pattern, resin residues adhere to the protruding glass flakes. The glass flakes are still solidly embedded in the resin matrix.

Stage B + C:

Initial failure of adhesion and separations (gaps) occur between the resin and the glass flakes (Fig. 15). No resin residues adhere to the glass flakes.

Stage D:

The resin matrix between the individual glass flakes is completely penetrated by cracks (Fig. 15). The separations between the glass flakes and the resin matrix have coalesced.

Stage E:

Gaping cracks, which can be recognized macroscopically by doming (blistering) on the surface of the coating, occur preferentially along the glass flakes due to further crack growth (Fig. 15).
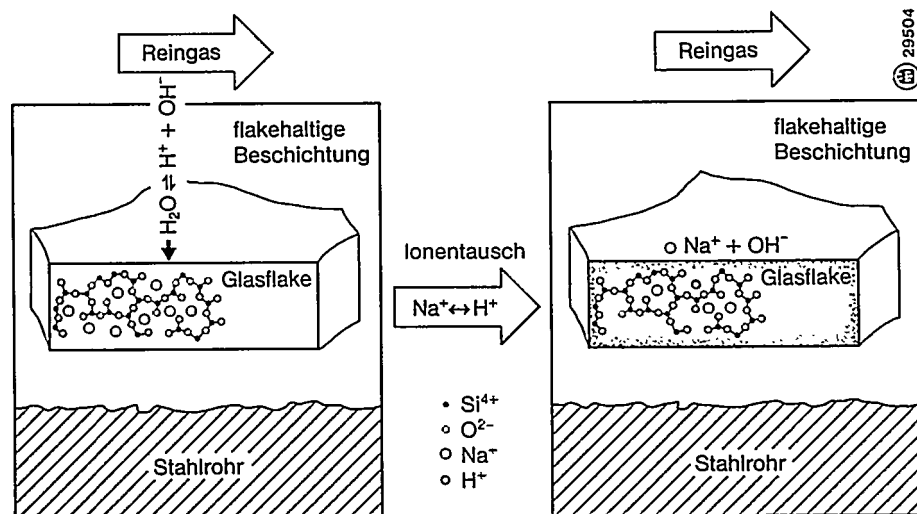
Fig. 16   Reaction of the absorbed water with the glass flakes (diagrammatic).

Fig. 16 attempts to explain the structural changes by means of a diagrammatic representation. Water diffuses through the water-permeable synthetic resin matrix to the glass flake/resin phase boundary. At this point, sodium ions of the glass flakes are preferentially exchanged for hydrogen ions. A gel-type surface layer with highly alkaline fluid can then appear on the glass. In parallel with this, compounds due to hydrolysis and oxidation processes associated with the synthetic resin can dissolve in the liquid film.

Ageing tests with vinyl ester and unsaturated polyester resins in water at increased temperatures show that substantially more hydrolysis and oxidation products occur in the case of unsaturated polyester resins than occur with vinyl ester resins. In consequence, the unsaturated polyester resin matrix is substantially less resistant to the action of water than the vinyl ester resin matrix. This fact can be explained by means of the structural formulae of the two different resins (Fig. 17). The ester groups are susceptible to hydrolysis. In consequence, the resistance to water is determined by the position of the ester groups in the molecular chain of the resin. If the ester groups are present throughout the molecular chain (see up to bisphenol A fumaric acid polyester), then it is less resistant than resins in which the double linkages are present at the end of the molecular chain (see vinyl ester).
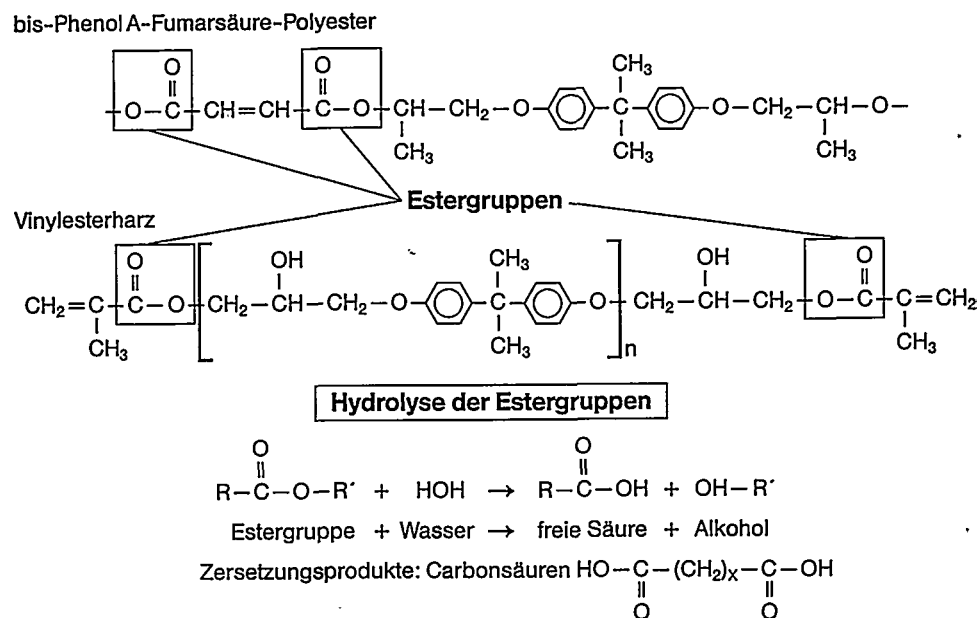
Fig. 17   Position of the ester groups for different resins and diagrammatic representation of the hydrolysis of an ester group.

5.20

The resulting drop in electrolyte concentration between the condensate on the coating surface and the boundary layer between the glass flakes and the resin matrix ensures subsequent diffusion of water to this boundary surface, whatever the water vapour partial pressure.

The osmotic diffusion of water causes a hydrostatic pressure to occur between the resin matrix and the glass flakes.

The formation of gel layers causes a loss of adhesion between the glass flakes and the resin matrix. A multiplicity of bubble-type micro-separations occur which then coalesce.

The positive pressure in the gaps and the restraints on thermal expansion and swelling lift the synthetic resin matrix completely. Unification of such gaps on the glass flakes causes macro-cracks parallel to the surface. The resin matrix located between the glass flakes tears apart under high tensile stresses.

4.4.6 Summary

The current state of knowledge suggests that the blistering which has appeared, both in the case of chloroprene coatings in absorbers and in the case of glass flake coatings in the clean gas ducts, is essentially due to osmotic processes which are preceded by permeation processes and on which permeation processes are superimposed. The blistering may be regarded as the end of the useful life and can lead to cost-intensive and time-intensive repair and restoration measures. For this reason, installations with such corrosion protection systems should be regularly examined and inspected for fault locations and rusting behind the coating in order, where necessary, to permit the introduction of repair and restoration measures in good time.

5.   References

/1/   G. H. Wagner: Rauchgasentschwefelung - eine Herausforderung an die Werkstofftechnik. Werkstoffe und Korrosion 40 (1989) S. 703-715.

/2/ Fenner, J. und Schedlitzki, D.: Gummierungen als Korrosionsschutz in Rauchgas-entschwefelungsanlagen. VGB Kraftwerkstechnik 71 (1991) H. 1, S. 916-920.

/3/ Fenner, J. und Schedlitzki, D.: Gummierungen als Korrosionsschutz in Rauchgas-entschwefelungsanlagen (Teil II). VGB Kraftwerkstechnik 73 (1993) H. 6, S. 544-550.

/4/ Möllmann, A. und Lacour, D.: Überwachung von organischen Korrosionsschutz-systemen in REA zur Abschätzung der Restlebensdauer. VGB Kraftwerkstechnik 73 (1993) H. 2, S. 153-158.

/5/ Möllmann, A. und Kamp, W.: Gummierungen und Beschichtungen in Rauchgas-entschwefelungsanlagen. VGB Kraftwerkstechnik 72 (1992) H. 11, S. 1011-11020.

/6/ Möllmann, A.: Betriebserfahrungen mit Innengummierungen und Beschichtungen in Rauchgaswäschern und Rauchgaskanälen. VGB Kraftwerkstechnik 70 (1990), H. 1, S. 77-87.

/7/ Willmes, O. und Glaser, W.: Materialangriff an Gummierungen und Beschichtun-gen. VGB Kraftwerkstechnik 72 (1992) H. 9, S. 805-822.

/8/ Grupp, H. und Kase, H.J.: Ermittlung der Ursache von Schäden an Gummierun-gen in Rauchgasentschwefelungsanlagen. Der Maschinenschaden 64 (1991) H. 1, S.10-18.

/9/ Grupp, H. und Mohr, G.: Diffusionsverhalten verschiedener Gummiqualitäten in REA gegen Bestandteile von Rauchgasen. Der Maschinenschaden 65 (1992), H. 6, S.209-217.

/10/ Werkstoff- und Beschichtungsprobleme in Rauchgasentschwefelungsanlagen. Be-richt der Diskussionstagung im Allianz-Zentrum für Technik in Ismaning am 4./5. Juni und 9./10.Oktober 1991. Allianz Bericht Nr. 25 (1992), Allianz Versi-cherungs-AG, München.

/11/ Schmitt, G. und Kuron, D.: Korrosion in Abfasreinigungsanlagen und Schornstei-nen. Tagungsbuch zum 6. Korrosionum 1993. Verlag Irene Kuron, Bonn.

/12/ Kase, H.-J.: Prüfung fehlerhafter Glasflakebeschichtungen und ihre Deutung für die Praxis im REA-Betrieb. VDI-Berichte Nr. 674, 1988, S.309-327.

/13/ Effertz, P.-H. und Kase, H.-J.: Prüfung von Vinylester-Glasflakebeschichtungen auf ihr Temperaturwechselverhalten und ihre Wasserdampfdurchlässigkeit. Im Tagungsband: Werkstoffprüfung 1987.

/14/ Effertz, P.-H. und Weber, R.: Blasenbildung in Glasflake-Kunstharzbeschichtun-gen bei Einsatz in Rauchgasentschwefelungsanlagen. VGB Kraftwerkstechnik 70 (1990) Heft 12, S. 1045-1049.

/15/ Effertz, P.-H. und Weber, R.: Prüfung der Wasser- und Wasserdampfbeständig-
keit von glasflakehaltigen Polyesterbeschichtungen. Im Tagungsband: Werkstoff-
prüfung 1990, S. 317-324.

/16/ Kase, H.-J. und Weber, R.: Eignungskriterien für Kunstharzbeschichtungssyste-
me in Rauchgasentschwefelungsanlagen. Der Maschinenschaden 64 (1991)
Heft 1, S. 19-23.

Lifetime Evaluation Of Superheater Tubes Exposed To Steam Oxidation, High Temperature Corrosion And Creep

Niels Henriksen
ELSAMPROJEKT A/S
Fælleskemikerne
Kraftværksvej 53
7000 Fredericia
Denmark

Ole Hede Larsen
I/S FYNSVÆRKET
Fælleskemikerne
Havnegade 120
5000 Odense C
Denmark

Rudolph Blum
I/S FYNSVÆRKET
Fælleskemikerne
Havnegade 120
5000 Odense C
Denmark

Abstract

Advanced fossil fired plants operating at high steam temperatures require careful design of the superheaters. The German TRD design code normally used in Denmark is not precise enough for the design of superheaters with long lifetimes. The authors have developed a computer program to be used in the evaluation of superheater tube lifetime based on input related to tube dimensions, material, pressure, steam temperature, mass flux, heat flux and estimated corrosion rates. The program is described in the paper.

As far as practically feasible, the model seems to give a true picture of the reality.

For superheaters exposed to high heat fluxes or low internal heat transfer coefficients as is the case for superheaters located in fluidized bed environments or radiant environments, the program has been extremely useful for evaluation of surface temperature, oxide formation and lifetime.

The total uncertainty of the method is mainly influenced by the uncertainty of the determination of the corrosion rate. More precise models describing the corrosion rate as a function of tube surface temperature, fuel parameters and boiler parameters need to be developed.

1. Introduction

The development of coal-fired power plants especially in Japan and Europe is going in the direction of improving the efficiency by increasing the steam data. The Danish electricity utility consortium ELSAM has a leading role in this development. In 1993 ELSAM commissioned Unit 3 at Vestkraft Power Plant (260 bar, 560°C / 560°C) with a unit efficiency in condensation mode of 45.3% [1] and two units are currently under construction: Unit 3 at Skaerbaek Power Plant (gas-fired) and Unit 1 at the power plant Nordjyllandsvaerket (coal-fired) both with steam data 290 bar, 580°C/580°C/580°C; the latter with a unit efficiency of 47% [2]. However, development does not stop here,

ELSAM is continuously exploring possibilities of increasing steam pressure and temperature and the next target will be plants pushing the efficiency up to 50%.

High steam pressures and temperatures call for improved materials and water chemistry. The requirements to the materials are good creep properties and good corrosion properties, and the steel industry in Europe and especially in Japan have already developed several suitable superheater steels [3].

This paper discusses the considerations which ELSAM have gone into with regard to the ability to verify the design of a new boiler and to predict the lifetime of boiler tubes.

In Denmark the design of superheaters is based on the German TRD design code (Technischen Regeln für Dampfkesseln). According to this code, the design temperature is 30°C above the steam temperature. The development of ELSAM's new boiler concepts has made it clear that this design requirement is often unsatisfactory. For some of the boiler steels the high steam temperatures result in very fast steam side formation of oxide, which may lead to considerably elevated metal temperatures and hence faster degradation of the steel.

As an alternative to the TRD design criteria, ELSAM has produced a simple calculation program to be used for estimating the lifetime of superheaters. The program has turned out to be an extremely useful tool when comparing different material solutions for superheaters in design studies, evaluating boilers and in connection with remaining lifetime investigations. A similar program is currently being developed for the purpose of estimating the lifetime of evaporator tubes; however, the calculations for this purpose are much more complex. This issue will be described in a separate paper to be published later.

Simple, but practically useful models have been developed and the material data needed could for the most part be found in available literature. Normally, the boiler data needed are fairly easily accessible or can be computed without much difficulty.

The calculation program has been constructed after a model described by Horgan [4]. This model assumes the lifetime of superheater tubes to be restricted by creep and fireside high temperature corrosion. Compared to the program developed by Horgan, our program has been extended with further algorithms and has the possibility of

making calculations with 20 different superheater steels instead of only the 2.25% Cr/1%Mo steel-P22.

2. Tube Lifetime

Normally, the lifetime of a superheater tube is limited, as the tubes degrade on a continuous basis due to fireside corrosion, creep and steam side oxidation. All degradation processes are highly temperature dependent. Steam side oxidation is responsible for a gradually increasing temperature over the whole service period due to the growth of an oxide layer with low heat conductivity.

2.1 Corrosion

Fireside corrosion of a tube exposed to combustion gas is caused by oxidation, molten salt corrosion or direct attack of the corrosive gasses in the flue gas. For ordinary coal combustion, corrosion is usually caused by oxidation and molten sulphate: when the temperature of the sulphate mix reaches the melting point the corrosion rate increases significantly. At a temperature above the dew point of the corrosive substances the corrosion will decrease to a level where corrosion is solely oxidation, although oxidation at this high temperature level still is considerable. The effect of the described mechanism is illustrated in fig. 1.

Figure 1: Corrosion versus temperature.

Unfortunately, no precise model has yet been developed describing the rate of high-temperature corrosion as a function of eg. surface temperature, gas temperature, fuel mix, flue gas residence time in boiler, etc. In the program a constant corrosion rate is used, which of course has some impact on the precision of the results.

2.2 Creep

Creep is a material degrading process highly dependent on temperature and stress, where the material destabilizes and the strength decreases with increased service time resulting in permanent plastic deformation. Creep data are available for all normal superheater steels up to 100,000 hours service time or more at temperatures relevant to boiler application. The 100,000 hour creep rupture strength reduced with a safety factor forms the basis in codes used for designing superheater tubes.

2.3 Oxidation

Steam oxidation turns the surface layer of the steel into oxides. The oxygen needed for oxidation and oxide growth is supplied from the oxygen contained in the steam and dissociation of the steam, thus resulting in the formation of oxygen ions diffusing through the oxide film to the steel. At the surface of the steel, metallic iron oxidizes forming iron ions (Fe^{2+}, Fe^{3+}). Part of these iron ions react with the oxygen ions in situ and the remaining Fe^{2+} diffuses out through the oxide film. In the course of this process, Fe^{2+} is partly converted into Fe^{3+} and iron oxides are formed in a reaction with the inwardly diffusing oxygen ions.

The formation of a dense layer of magnetite has a markedly restrictive impact on the diffusion which impedes further oxidation, and therefore the oxidation rate often approaches a parabolic growth law. If the alloy contains either chromium or silicon, Cr will form either a spinel layer with iron or a pure Cr-oxide film or for silicon a purely silicon oxide film on the metal surface. The homogeneous pure oxide films constitute very effective barriers against further oxidation, thus resulting in a lower oxidation constant or an oxide growth law, which is cubic rather than parabolic. Small fluctuations in the content of Cr and Si may cause large changes to the oxidation constant and will often explain the relatively large scatter attached to the determination of oxide constants [5].

Pure Cr-oxides are formed in austenitic steels, but when the Cr-content exceeds approx. 22%, but they are also formed in 18% Cr steels with small grain size. Such films are particularly efficient in impeding further corrosion, the growth of the oxide film will follow the growth law of a higher order rather than that of a parabolic one [6].

3. Calculation Program

In a simple approach the lifetime of a superheater tube is consumed, when the hoop stress exceeds the rupture stress at the average service temperature of the material. This is illustrated in fig. 2 as the intersection between the hoop stress curve and one of the stress rupture curves representing the average service temperature of the tube material. This rather simple approach has been used in ELSAM for lifetime evaluation before our computer program was developed. As the temperature changes with time due to internal oxidation of the tube and the stress changes due to inside oxidation and outside corrosion, more precise calculation of the lifetime requires a stepwise calculation.

Figure 2: Example of creep rupture strength curves and hoop stress curve for a superheater tube.

The program uses a stepwise calculation with time steps of typically 100-1000 h, the hoop stress is calculated according to equation (1) and the rupture time $t_{rupture}$ is calculated according to (2). As mentioned the time dependent corrosion reduces the outside radius (r_3) causing higher hoop stress. The higher hoop stress affects the rupture time, which gradually reduces for each time step.

$$\sigma = P(\frac{r_2 + r_3}{2(r_3 - r_2)})$$
(1)

$$t_{rupture} = A \cdot \sigma^{-n}$$
(2)

Where equation 2 can be derived from the well-known Norton creep law [7] and the Monkman Grant equation [8] and:

n   =   The Norton exponent
r_2 =   Distance from centre to tube inner surface, [m]
r_3 =   Distance from centre to tube surface,[m]
A   =   Constant

P =   Pressure $[N/mm^2]$

$\dot{\varepsilon}_{min}$ =   Secondary creep rate

σ =   Hoop stress $[N/mm^2]$

$t_{rupture}$ =   Time to rupture [hours]

$$\dot{\varepsilon}_{min}=B\sigma^n \tag{3}$$

$$\dot{\varepsilon}_{min}\cdot t_{rupture}=C \tag{4}$$

The temperature dependent Norton constant "n" and the constant "A =C/B " can be derived from equation 5 and 6.

$$n=\frac{\ln 10^5-\ln 10^4}{\ln\sigma_{rupture(10^4)}-\ln\sigma_{rupture(10^5)}} \tag{5}$$

$$A=10^5\cdot\sigma^n_{rupture(10^5)} \tag{6}$$

Where:

$\sigma_{rupture}(10^4)$ =   Rupture stress at 10^4 hours, $[N/mm^2]$

$\sigma_{rupture}(10^5)$ =   Rupture stress at 10^5 hours, $[N/mm^2]$

After each time step (Δt_i), the accumulated consumed lifetime fraction (LTF) defined by equation (7) is calculated.

$$LTF=\sum\left(\frac{\Delta t_i}{t_{rupture_i}}\right) \tag{7}$$

$$t_{life}=\sum\Delta t_i \text{ ,when } LTF=1 \tag{8}$$

For each time step the temperature in the middle of the material (T_{middle}) is calculated and $t_{rupture}$ can be calculated. The total lifetime (t_{life}) is found by summing each time step until LFT = 1. If the 0.2% proof stress ($R_{0.2}$) of the steel is exceeded, the lifetime is defined as being consumed, and LFT is given a higher value than 1 and $t_{lifetime}$ is calculated as already described.
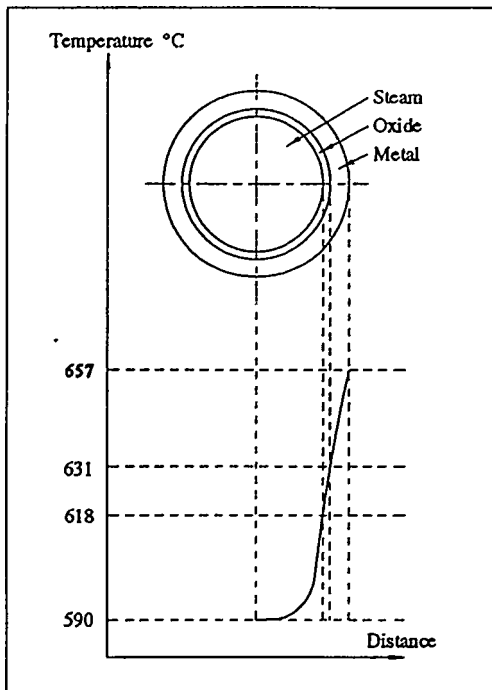
Figure 3. Temperature increase across a tube wall.

With time the temperature in the tube will increase due to steam side oxide formation, as the oxide film constitutes a significant resistance against the heat transfer. This process is self-supporting as higher material temperatures lead to higher oxidation rate.

Apart from its impact on corrosion and creep, steam side oxidation may in itself constitute a problem. Thick magnetite films may exfoliate causing blocking of the superheater tubes and valves resulting in reduced flow and elevated pressure drop. Furthermore, magnetite particles may cause erosion of the turbines.

The heat transfer across a tube wall from the fireside surface of the tube to the medium within the tube is illustrated in fig. 3 above.

The differences in temperatures between the fireside surface of the tube and the steam temperature can be found by means of equation (9):

$$T_{surf} - T_{steam} = Q_{outside} (\frac{r_{30}}{r_{20}})(\frac{r_1}{\lambda_{metal}} \ln \frac{r_3}{r_2} + \frac{r_1}{\lambda_{oxide}} \ln \frac{r_2}{r_1} + \frac{1}{\alpha_{inner}}) \tag{9}$$

Where:

r_1 =   Distance from centre to oxide inner surface, $r_1 = r_2 - 2.1x$, [m]
r_2 =   Distance from centre to tube inner surface, $r_2 = r_{20} + x$, [m]
r_{20} =   Distance from centre to tube inner surface at time = 0, [m]
r_3 =   Distance from centre to tube surface, $r_3 = r_{30} - ct$, [m]

r_{30} =	Distance from centre at time = 0. [m]
c =	Corrosion rate, [m]
x =	Material loss due to oxidation. [m]
$Q_{outside}$ =	Heat flux at the outer surface, [W/m^2]
T_{steam} =	Temperature of steam,[°C]
T_{surf} =	Temperature at metal surface,[°C]
α_{inner} =	Inner heat transfer coefficient,[W/m^2·K]
λ_{metal} =	Thermal conductivity of metal [W/m·K]
λ_{oxide} =	Thermal conductivity of oxide [W/m·K]

The individual parameters used in the program will be discussed in the following and the uncertainty of the parameters themselves will be estimated. The estimated uncertainty of the individual parameters will be used in a sensitivity analysis (section 4) where the uncertainty of the model is analysed. For the sensitivity analysis the following examples have been selected: the final superheaters of ELSAM's new USC-units and a hypothetical example of a final superheater of a PFBC-plant with the superheaters located in fluidized bed environment.

Reference data:	Unit	PF-USC	PFBC-USC
Inside diameter, [$2 \cdot r_{20}$]	mm	22	22
Thickness, [$(r_{30}-r_{20})$]	mm	8	8
Material		347H FG	347H FG
Pressure, [P]	bar	295	295
Corrosion rate, [c]	mm/10^5	2	2
Steam temperature, [T_{steam}]	°C	590	590
Heat transfer coefficient, steam side, [α_{inner}]	kW/m^2·K	5	5
Heat conductivity, metal, [λ_{metal}]	W/m·K	24.9	24.9
Oxide conductivity,[λ_{oxide}]	W/m·K	1.0	1.0
Heat flux, outer surface, [$Q_{outside}$]	kW/m^2	25	80

Table 1. Reference data.

3.1 Heat Flux, $Q_{outside}$.

The difference between the temperatures of steam side and fireside surface of a tube is proportional to the heat flux. The heat flux of a PF-boiler is highly dependent on the location of the superheaters in the boiler. The heat flux will also vary from one type of boiler to another, in the sense that the heat flux in the superheaters of a PFBC-boiler is higher than in a PF-boiler, cf. table 2.

Heating Surface	PF-USC kW/m²	PFBC-USC kW/m²
Final Superheater	20-30	80-100

Table 2. Typical heat flux of the final superheater of a pulverised coal-fired (PF-USC) unit and a PFBC (CFB-USC) unit with evaporator and final superheater located in the fluidised environment.
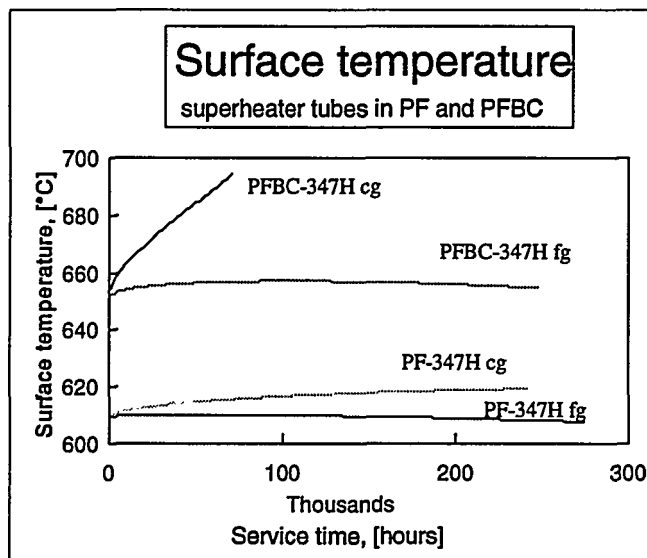
Figure 4: The development in surface temperature of a superheater tube: of AISI 347H fine-grained (fg) in a PF and a PFBC boiler and the normal AISI 347H (coarse-grained, cg) in a PF and a PFBC boiler. All input is in agreement with table 1.

Fig. 4 illustrates the calculated lifetime and surface temperature. The figure clearly reveals the differences in surface temperatures due the differences in heat flux for a tube of the same material (AISI 347H fine grained) and dimensions. The surface temperature of the PFBC tube is approx. 40°C higher than the corresponding PF tube.

For a tube with lower oxidation resistance the high heat flux has a dramatic influence on the development in surface temperature and tube lifetime as illustrated with the 347H coarse-grained tube.

The heat flux values mentioned are the average heat flux for the heating surface. Across the heating surface itself, the heat flux will always vary as gas temperature, flue gas flow rate and steam temperature will differ across the heating surface. The average heat flux of the convection pass is estimated to fluctuate ±10%.

3.2 Thermal conductivity of the steel, λ_{metal} .

The thermal conductivity of a certain steel is normally listed in the data sheet. The value is considered to be rather accurate with an estimated uncertainty of $\pm 5\%$. The impact of the variations of metal thermal conductivity on the total result is only marginal.

The thermal conductivity is dependent on steel type according to the following table 3:

Steels	Heat Conductivity [W/m·K]
Ferritic	35-39
Ferritic/martensitic	26-28
Austenitic:	21-22

Table 3. Thermal conductivity of typical superheater steels at 500-600°C.

3.3 Steam Side Heat Transfer Coefficient, α_{inner}.

The steam side heat transfer coefficient varies notably with the pressure, temperature and flow velocity of the steam. Hence the heat transfer coefficient is considerably lower in the final reheater than in the high-pressure superheater and again in the evaporator. The steam side heat transfer coefficient has great influence on the steam oxidation, as the temperature in the interface between steel and oxide film increases with a falling steam side heat transfer coefficient.

As example of the heat transfer coefficients dependency on pressure and temperature some of the data from ELSAM's coal-fired CHP plant Nordjyllandsvaerket, under construction, are supplied.

Heating surface:	Steam side heat transfer coefficient, α_i [W/m²·K]
Evaporator (420°C, 325 bar)	33000
Superheater outlet (290 bar)	5000
1st reheater outlet (97 bar)	1700
2nd reheater outlet (24 bar)	750

Table 4. Steam side heat transfer coefficients of the superheaters in Nordjyllandsvaerket's Unit 3 (290 bar, 580°C/580°C/580°C).

Table 5 illustrates how the steam side heat transfer coefficient of the of the second reheater in a double reheating PF-USC design affects the temperature and thickness of the oxide layer compared to the final superheater in the same design. The low steam side heat transfer coefficient in the second reheater results in a thicker magnetite layer and higher surface temperatures compared to the final superheater.

Parameter	Unit	Outlet second reheater	Outlet final superheater
Magnetite thickness, 10^5 h	μm	106	70
Magnetite thickness, $2*10^5$ h	μm	152	101
Surface temperature, 10^5 h	°C	637	610
Surface temperature, $2*10^5$ h	°C	638	609

Calculation input, superheater: AISI 347H FG, Ø 38x8 mm, T_{steam} = 590°C, P= 295 bar, α_i = 5000 W/m²·K, corrosion rate: 1mm/100,000 hours, Q_{outer} = 25 kW/m².
Calcualtion input reheater:AISI 347H FG, Ø 44x4 mm, T_{steam} = 590°C, P= 23 bar, α_i = 750 W/m²·K, corrosion rate: 1mm/100,000 hours, Q_{outer} = 25 kW/m².

Table 5. Impact of low steam side heat transfer coefficient on temperature and oxide in the second reheater and the final superheater in a double reheating PF-USC design.

The steam side thermal conductivity coefficient is computed by means of an approximation from Haussen [9], also comprising Nusselt's, Prandl's and Reynold's numbers. The overall uncertainty of the steam side thermal conductivity coefficient is estimated to be in the range of ±20%.

3.4 Tube Dimensions (r_{20} and r_{30})

The tube dimension primarily influences tube strength and only slightly the heat transfer. Variations in tube dimension could be considered as a negative/positive corrosion safety.

Tube radius normally varies $\pm 2\%$. Wall thickness will normally vary $\pm 5\%$.

3.5 Corrosion Rate, c.

As mentioned earlier, the corrosion rate depends on surface and flue gas temperatures as well as composition of ash layer and flue gas and on construction details [10].

There are no exact approximations to be used when estimating the corrosion rate correlated with temperature, composition of flue gas/ash and alloy, which makes it necessary to use empirical data, which are not specially related to any of the above-mentioned parameters. CEGB [11] has constructed an approximation (see equation 8), which could form the basis of further work:

$$c=0.4 \cdot D \cdot E (T_{gas}/1000)^2 ((T_{surf}-550)/100)^2 (Cl-0,06) \tag{10}$$

In equation 10, c is the corrosion rate (nm/h), D and E are constants dependent of material and construction details, T_g is the fluegas temperature, T_m is the metal surface temperature and Cl is the chlorine content in the fuel. The Cl term in equation 10 is based on a strong correlation between Cl and Na. In our opinion this term should be replaced by a term including the concentration of water soluble alkali metals in the ash after bomb combustion. [11] In order to do that there is a need for larger internationally oriented projects to determine the constants involved with reasonable precision. This is an evident choice for future high temperature corrosion research within the power plant sector, as the corrosion rate is a very uncertain but significant factor.

During the past 25 years ELSAM have taken out tube samples on a routine basis from 10CrMo910 (P22) superheaters of all our plants operating at 540°C. According to this data the normal corrosion rate for coal-firing with imported coals is 1-2mm/100,000 h. In rare cases rates of 3-4mm/100,000 h are found for individual tubes related to

temperatures exceeding the design temperature due to incorrectly designed superheaters. In the calculations a constant corrosion rate are used based on the mentioned data.

As already mentioned the corrosion rate is indeed a very uncertain factor, the uncertainty being in the range of $\pm$ 50% in connection with coal-firing. In connection with more aggressive fuels, the uncertainty will often be even more pronounced.

3.6 Steam Oxidation

The thickness of the oxide film is a variable factor depending on material, temperature and time. As the thermal conductivity of the oxide film is lower than the thermal conductivity of the steel, the oxide film acts as an efficient thermal barrier contributing significantly to the temperature rise in a tube. In superheater tubes the oxide film is formed by self-oxidation only, as opposed to evaporator where deposited oxides contributes to the layer.

As already mentioned oxide film growth follows a parabolic growth law as given in equation no. 11, which applies to most superheater materials. Concurrent with the increase of steam data for PF-USC plants, austenitic superheater steels with high oxidation and corrosion resistance are required. These steels form a very compact oxide film with a diffusion restricting impact on the penetrating oxygen, and the oxide growth probably follows a cubic growth law. In spite of this the authors have so far chosen a more conservative standpoint assuming a parabolic growth law for these steels, until the range of materials forming the basis of the research has increased considerably.

$$x^2 = k(T) \cdot t \tag{11}$$

Where:

k(T) =   Oxidation constant [mm^2/h], dependent on temperature (T)
t   =   Time [h]
x   =   Material loss due to oxidation. [m]

Extensive studies of available literature have revealed oxidation constants for practically all superheater steels [12-16]. Data originate from tests conducted under isothermal conditions in order to assure well-defined constants. For each steel there is a rather high uncertainty for oxidation constants primarily caused by variations in

alloy composition of especially Si but also other alloying elements giving high corrosion resistance. Also experimental inaccuracies in the determination of the constants may be important.
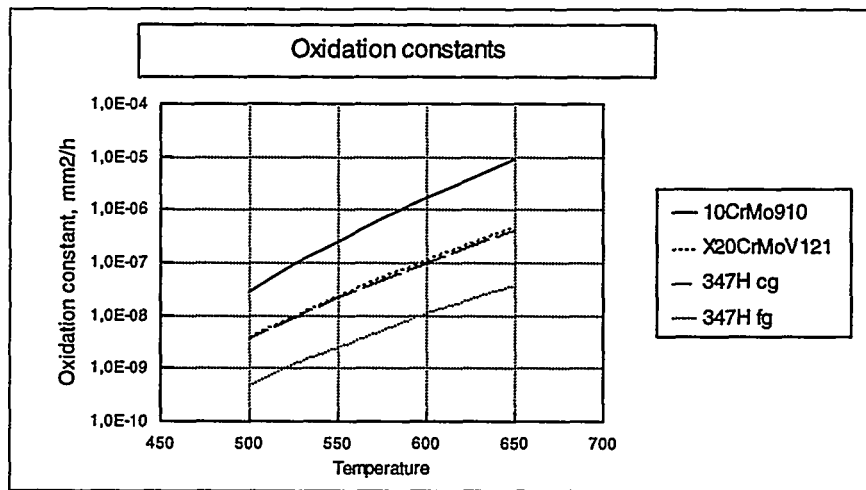
Figure 5: Oxidation constants for 10CrMo910, X20CrMoV121, AISI 347H and AISI 347H fine grained.

In fig. 5 oxidation data for the steels 10CrMo910 (P22), X20CrMoV121, AISI 347H and AISI 347H fine-grained used in the model are listed. The data used in the model is based on data from the literature and steel suppliers, a small selection of data is mentioned in [12-16].

From the scatter of the literature data on the oxidation constant for each steel, an uncertainty of ±50% is considered to be reasonable. For some steels - especially highly alloyed austenitic steels - there are only very few data, which might lead to even more pronounced uncertainties.

A side effect of a growing oxide layer is that it after some time reaches a critical thickness, where spalling of the oxide layer starts. Extensive spalling can cause problems with turbine erosion blocking of tubes and valves and should therefore be avoided.

Spalling of oxides is not yet part of our work, but hopefully it will be possible to obtain data for various steels.

As a criterion for the assessment of an acceptable oxide film, data from Japanese literature is used demonstrating that for austenitic steels spalling starts at magnetite thicknesses in the range of 100-200 μm [21], but for ferritic steels at thicknesses of approx. 500 μm. The latter finding is consistent with our findings based on ELSAM's own old superheater tubes. In our opinion the magnetite film of austenitic tubes should not exceed 125-150 μm during the first 100,000 h, and for ferritic tubes it should not exceed 500 μm.

In ELSAM's new USC-PF boilers the oxide spalling criteria have been used in the selection of superheater steels, where it has been necessary to use fine-grained 347H instead of normal 347H, although this steel has sufficient creep strength.

3.7 Thermal Conductivity of the Oxide Film, λ_{oxide}

As already mentioned the oxide film consist of a matrix of magnetite with pores filled with steam. The thermal conductivity of the oxide film will therefore be a function of the thermal conductivity of the magnetite as well as of the steam.

The thermal conductivity (λ_{magn}) of magnetite is temperature (T) dependent and has been defined by Mikk [17] who obtained a material with a porosity in the range of 8-10% by sintering magnetite powder. The approximation of the magnetite thermal conductivity is:

$$\lambda_{magn} = 4.133 - 0.852 \cdot 10^{-2} T + 0.757 \cdot 10^{-4} T^2 \tag{12}$$

For haematite a similar approximation has been defined, where (λ_{heam}) is the thermal conductivity of haematite:

$$\lambda_{haem} = 13.215 - 0.375 \cdot 10^{-1} T + 0.379 \cdot 10^{-4} T^2 \tag{13}$$

On the basis of the thermal conductivity of magnetite and the medium as well as the porosity of the oxide film, it is possible to determine the thermal conductivity of the porous layer. A number of the references [18-20] give approximations of the thermal conductivity of porous magnetite films. Fig. 6 illustrates the thermal conductivity as a function of the porosity calculated using the approximations of these authors.
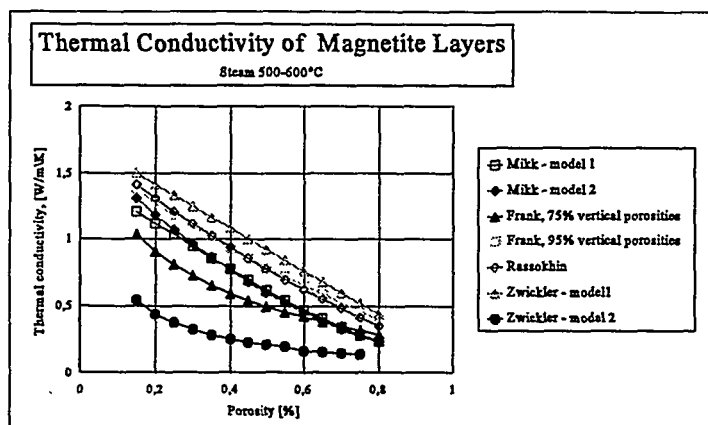
Figure 6: Thermal conductivity of porous magnetite layers.

The uncertainty of the thermal conductivity is dependent on the porosity. According to examinations of tube samples the porosity of the magnetite film found on superheater tubes is in the range of 10-20%. The porosity of the self-oxidising film found on evaporator tubes is of the same order, whereas the porosity of deposited oxide is 65-75%.

According to Mikk [17] the uncertainty of magnetite's conductivity is below 5%. Therefore the uncertainty of the thermal conductivity of the oxide layer in a superheater tube could be limited to ±20%.

3.8 Mechanical Strength

In the calculations average values for the creep rupture strengths have been used without any safety factors in our calculations. In cases where the minimum value of the 0.2% proof stress ($R_{0.2}$) is lower than the creep rupture strength, the rupture strength has been chosen as the intersection point between the average creep rupture stress curve and the curve for the minimum value of the 0.2% proof stress ($R_{0.2}$). This data is easily available from table works. A 10-15% scatter of the mechanical data is not unlikely due to differences in heat treatment and small variations in alloy composition.

Normally, we observe that materials are better than average, but in a few cases the opposite has also been observed.

3.9 Other Parameters

Until now we have not mentioned the uncertainty of pressure and temperature in a well-designed superheater. Both parameters will vary very little, temperature: ±2% and pressure: ±1% .

We have therefore not included sensitivity calculations of these parameters in this paper.

4. Total Uncertainty of the Model

The uncertainty of the calculation program has been evaluated by performing a sensitivity analysis with reference examples of the final superheaters of a PF boiler and a PFBC boiler. The input data of the references are given in table 1. Each parameter has been given a variation from its minimum value to its maximum value, the impact on the result are listed in tables 6 and 7. The range of variations of the individual parameters are what the authors believe are realistic for normal full load boiler operation.

PF-USC	Deviation from reference value (274000 hours). Lifetime [1000 hours]		Deviation from reference value (70 μm) Magnetite thickness at 10^5 hours, [μm]		Deviation from reference value (610°C). Temperature at 10^5 hours, [°C]	
	Min.	Max.	Min.	Max.	Min.	Max.
Heat flux ±10%	+1	0	-1	+1	-4	+2
Heat transfer coefficient ±20%	+0	+1	+3	-1	+2	-2
Tube radius ±5%	-19	+20	0	+1	-1	+1
Corrosion rate ±50%	+269	-90	0	0	0	-1
Oxidation constant ±50%	+2	-1	-21	+31	-2	+11
Oxide thermal conductivity ±20%	0	0	+1	0	+1	-2
Mechanical strength ±15%	0	0	0	0	0	0

Table 6. Sensitivity analysis of the model on a tube from the final superheater of a PF-USC boiler.

PFBC-USC	Deviation from reference value (247000 hours). Lifetime [1000 hours]		Deviation from reference value (97 μm). Magnetite thickness at 10^5 hours, [μm]		Deviation from reference value (657°C). Temperature at 10^5 hours, [°C]	
	Min.	Max.	Min.	Max.	Min.	Max.
Heat flux ±10%	+15	-15	-5	+5	-7	+8
Heat transfer coefficient ±20%	-20	+13	+11	-5	+9	-5
Tube radius ±5%	-13	+13	-2	+3	-3	+3
Corrosion rate ±50%	+147	-66	0	0	+4	-3
Oxidation constant ±50%	+17	-23	-31	+48	-4	+7
Oxide thermal conductivity %20%	-13	+9	+3	-3	+4	-2
Mechanical strength ±15%	-37	+26	0	0	0	0

Table 7. Sensitivity analysis of the model on a tube from the final superheater of a PFBC-USC boiler.

The uncertainties of calculations of lifetime, magnetite thickness and temperature show that corrosion rate due to the large uncertainty has a very large impact on the result. The oxidation also has a large uncertainty, but has less impact on the uncertainty of the final result.

The uncertainty of the results in the PFBC case are generally higher than in the PF case due to the higher heat flux in the PFBC boiler, which magnifies the uncertainty of the individual parameters. An exception for this is the influence of the corrosion rate, where the variation has a higher impact of the lifetime of PF superheater tubes than the PFBC tubes. This could be explained by the degradation mechanism of the tubes. The superheater tubes in the PF boiler consumes lifetime only by corrosion, and ends its lifetime by exceeding the defined rupture criteria - the 0.2% proof stress, whereas PFBC tubes degrades by a combination of creep and corrosion. It should be remembered that the fine-grained 347H was selected as superheater material in the PF boiler in order to avoid oxide spalling and not for the higher creep strength of this

material, where the normal 347H version would have been sufficient if only the creep strength had to be considered.

The parameters used in the model are divided into 3 groups according to uncertainty. The uncertainty of the first group is regarded as acceptable, whereas the uncertainty of the data in the third group is unacceptable and in future research work ELSAM will concentrate on minimizing this uncertainty. The parameters of the second group should be improved by asking boiler suppliers for more precise data.

1. Low uncertainty (<10%): Tube dimensions, metal heat conductivity, pressure, and temperature.

2. Medium uncertainty (10-50%): Heat flux, internal heat transfer coefficients, mechanical strength and oxide heat conductivity.

3. High uncertainty (>50%): Oxidation constant and corrosion rate.

5. Verification of the Model

Samples are taken from ELSAM's units on a continuous basis and in rare cases bursted superheaters tubes are received for investigation. The findings resulting from these investigations are used to verify the model or make minor adjustment. Of course it is a problem to get the data required to verify the model with newer alloys and materials exposed to high material temperatures, and hence some uncertainty will have to be accepted for these data. However, when feeding the model with oxide data, we have made an effort to use data giving conservative results; highly contributory to this conservative practice is our assumption that the oxidation follow a parabolic growth law, although in reality it is probably cubic.

In order to verify the model in a more systematic way, data achieved from the on-going Brite-Euram USC Superheater project BRE CT 93-0600 will be used. In the Brite-Euram three test superheater loops are installed in the steam generator of unit 3, Vestkraft Power Station. Nine different materials - from the conventional X20CrMoV12 via the new modified ferritic/martensitic steels to austenites - are tested at steam temperatures ranging from approx. 500 to 620°C. The three test loops are identical, but duration of exposure time will vary, the longest duration being 40,000

hours. The experiment will provide detailed information about the oxidation and corrosion behaviour of the tested steels.

6. Conclusion

A program for superheater tube life evaluation has been developed by the authors which program has to the full proved its worth in the assessment of new power plant concepts. Superheater tube lifetime are evaluated based on input regarding dimension of tubes, material, pressure and temperature of the steam, mass flow, heat flux and estimated corrosion rates.

As far as practically feasible, the program seems to give a true picture of reality.

The program has shown that magnetite build-up has a significant impact on tube life for some superheater applications, for example superheaters exposed to high heat fluxes and steam temperatures as well as superheaters located in fluidized or radiant environment. Also the second reheater in a double reheating USC design could be critical due to high steam temperature and low internal heat transfer coefficient.

The most significant uncertainty of the input data to the program is found for corrosion rate. At high corrosion rates magnetite growth is often of relatively minor importance, and hence the corrosion rate alone is decisive to the lifetime of the materials. At the moment corrosion rate is estimated on the basis of experience from an existing coal-fired unit, but there is a need for developing more precise expressions for the corrosion rates as a function of surface temperature of the tube and parameters describing boiler and fuel.

Symbols.

c =	Corrosion rate, [nm/h]
$k(T)$ =	Oxidation constant [mm²/h], dependent on temperature (T)
n =	The Norton exponent
r_1 =	Distance from centre to oxide inner surface, $r_1 = r_2 - 2.1x$, [m]
r_2 =	Distance from centre to tube inner surface, $r_2 = r_{20} + x$, [m]
r_{20} =	Distance from centre to tube inner surface at time = 0, [m]
r_3 =	Distance from centre to tube surface, $r_3 = r_{30} - c$, [m]
r_{30} =	Distance from centre at time = 0. [m]
t =	Time [h]
$t_{rupture}$ =	Time to rupture [h]
t_{life} =	Lifetime of the tube [h]
x =	Material loss due to oxidation. [m]
A =	Constant
B =	Constant
C =	Constant
Cl =	Chlorine content in coal [%wt]
D =	Constant
E =	Constant
LTF=	Life time fraction
P =	Pressure [N/mm²]
$Q_{outside}$ =	Heat flux at the inner surface, [W/m²]
$R_{0.2}$ =	0.2% proof stress [N/mm²]
T =	Temperature [K]
T_{gas} =	Temperature of flue gas,[°C]
T_{steam} =	Temperature of steam,[°C]
T_{surf} =	Temperature at metal surface,[°C]
α_{inner} =	Inner heat transfer coefficient,[W/m²·K]
Δt =	Time step, [h]
$\acute{\varepsilon}_{min}$ =	The secondary creep rate
λ_{haem} =	Thermal conductivity of haematite [W/m·K]
λ_{magn} =	Thermal conductivity of magnetite [W/m·K]
λ_{metal} =	Thermal conductivity of metal [W/m·K]
λ_{oxide} =	Thermal conductivity of oxide [W/m·K]
σ =	Hoop stress [N/mm²]
$\sigma_{rupture}(10^4)$ =	Rupture stress at 10^4 hours, [N/mm²]
$\sigma_{rupture}(10^5)$ =	Rupture stress at 10^5 hours, [N/mm²]

References.

1. S. Lindhard and A. Lind-Hansen. Vestkraft power Plant, Unit 3. Experience gained during commissioning and initial operation. Proceedings of VGB-conference, Fossil-fired Power Plants with Advanced Design Parameters, June 1993.

2. Sven Kjaer. Die zukünftigen 400-MW-ELSAM-Blöcke in Aalborg und Skærbæk. Proceedings of VGB-conference, Fossil-fired Power Plants with Advanced Design Parameters, June 1993.

3. R. Blum. Materials Development for Power Plants with Advanced Steam Parameters - Utility Point of View. The Cost-501 Conference "Materials for Advanced Power Engineering 1994, Liege.

4. G. Horgan and K. Leavy. Abschätzung des Kriechverhaltens von Überhitzern und Zwischenuberhitzern in modernen Dampferzeugern mit Hilfe eines Computers. VGB Kraftwerkstechnik 68, pp.760-768, (1988).

5. W.M.M. Huijbregts. Bespreking van de in de literatuur vermelde oxidatiesnedheden van ferrietische Cr-stahle in overhitte stoom. KEMA 60064-SO 89-3036, 1989 .

6. N. Otsuka and H. Fujikawa. Scaling of Austenitic Stainless Steels and Nickel Base Alloys in High-Temperature Steam at 973K. Corrosion, 1991,Vol. 47 (4), pp. 240-248

7. F.H. Norton. Creep of Metals at High Temperatures. McGraw-Hill Book company, New York, 1927.

8. F.C. Monkman, N.J. Grant. Proc. ASTM 56, 1956, p. 593.

9. FDBR Handbuch. Wärme und Strömungstechnik. Fachverband Dampfkessel-, Behälter und Rohrleitungsbau E.v., 1972.

10. H. Breucker und L. Stadie. Steinkohlebefeurte Dampferszeuger für Kraftwerke mit hohen Dampfzuständen. VGB Kraftwerstechnik 63 (1), 1983, pp.29-37.

11. Abbott M.F., Cambell J.A.L., Doane E.P. Utility Experience Burning High-Chlorine Illinois Coals. Power-Gen America '94, Orlando, December 7-9, 1994.

12. M.I. Manning and E. Metcalfe. Oxidation of Ferritic Steels in Steam. BNES 1978, pp. 378-382.

13. F.Eberle and J.L. McCall. Electron-Microprobe Study of Scale Formations on Cr-Mo Superheater Tubing After Long-Time Exposure to 2000 Psi Steam of 1100 F and 1200 F. Journal of Engineering for Power. April 1965, pp. 205-209.

14. P.-H. Effertz und H. Meisel. Verzunderung warmfester Stahle in Hochdruckdampf nach langen Betriebszeiten. Allianz-Berichte für Betriebstechnik und Schadenverhütung, 16 (1971), pp. 52-60.

15. Y. Sawagari et al. Development of the Economical 18-8 Stainless Steel (Super 304H) Having High Elevated Temperature Strength for Fossil-fired Boilers. The Sumitomo Search, 48, Jan. 1992.

16. A. Iseda. Development of New 12% cr Steel Tubing (HCM12) for Boiler Application. Sumitomo Search, 40, 1989

17. I.R. Mikk et al. Experimental Determination of the Coefficient of Thermal Conductivity of Skeleton Material of Iron Oxide Deposits, Thermal Engineering, 27, pp.106-108, (1980)

18. R. Frank. Der Maschinenschaden 58(1985), heft 4, p. 160-164.

19. N. G. Rassokhin et al. Thermal Conduction of Deposits of Iron Oxides. Thermal Engineering, 20, pp.16-18, (sept. 1973)

20. R. Zwickler. Der Einfluss poröser Eisenoxidablagerungen auf den Warmeübergang bei überkritischen Drücken. VGb Speisewassertagung, pp.5-13 (1966).

21. Y. Nakabayashi et al. Japanese developments in high temperature steam cycles. High Temperature Materials for Power Engineering 1990, Liege (COST 501 and 505). Proceedings, Part 1, pp.313-342.

ASH DEPOSITION AND HIGH TEMPERATURE CORROSION AT COMBUSTION OF AGGRESSIVE FUELS

Ole Hede Larsen

Fælleskemikerne

I/S FYNSVÆRKET

Havnegade 120

5000 Odense C

Denmark

Niels Henriksen

Fælleskemikerne

ELSAMPROJEKT A/S

Kraftværksvej 53

7000 Fredericia

Denmark

ABSTRACT

In order to reduce CO_2 emission, ELSAM is investigating the possibilities of using biomass - mainly straw - for combustion in high efficiency power plants. As straw has very high contents of chlorine and potassium, a fuel with high corrosion and ash deposition propensities has been introduced. ELSAM has investigated 3 ultra supercritical boiler concepts for combustion of straw alone or together with coal: 1) PF boilers with a relatively low share of straw, 2) CFB boilers with low to high share of straw and 3) vibrating grate boilers with 100 % straw. These investigations has mainly been full-scale tests with straw fed into existing boilers.

Corrosion tests have been performed in these boilers using temperature regulated probes and in-plant test tubes in existing superheaters. The corrosion has been determined by detailed measurements of wall thickness reduction and light optical microscopic measurements of the material degradation due to high temperature corrosion. Corrosion mechanisms have been evaluated using SEM/EDX together with thermodynamical considerations based on measurements of the chemical environment in the flue gas.

Great differences were found in the corrosion mechanisms for superheaters in PF boilers and the CFB boilers fired with almost the same share of straw and at the same material temperatures. For co-combustion in the PF boiler the corrosion mechanism is similar to normal coal-firing and the corrosion rate is only moderately affected. In the CFB boiler, a distinctly different corrosion mechanism showed a more direct action of chlorine-type gases originating from KCl condensed on the tubes and the corrosion rate was found to be many times higher than in the PF boilers. In strawfired vibrating grate boilers, the same type of corrosion as in CFB boilers was observed and the corrosion rates were similar to or higher than in the CFB boiler. For PF boilers higher alloyed materials reduce the corrosion rate. The same observation was not found in the CFB boiler and in the vibrating grate boiler.

Ash deposition is problematic in CFB boilers and in strawfired boilers, especially in years with high potassium and chlorine content of the straw. This ash deposition also is related to condensation of KCl and can probably only be handled by improved cleaning devices.

1. Introduction

The power generating capacity in Denmark is mainly based on coal combustion. Coal can be a troublesome fuel with respect to ash deposition and high temperature corrosion, but generally this can be solved by fuel selection or blending as many coals of world-wide origin are available.

Anyhow the fuel situation is constantly changing. One of the most recent changes is an increased use of biomass - especially straw - for electricity production. As straw is characterised by very high concentrations of chlorine and potassium [1], a fuel with high corrosion and ash deposition propensities has been introduced.

The introduction of biomass for electricity production is one of the means for reaching the goals set up in the Danish Energy Plan - that is a 20% reduction of the CO_2 emissions by 2005 compared to the 1988-level. In order to reduce CO_2 emissions by 20% and still maintain coal as the major fuel, it is important to maintain a highly efficient electricity generation and to include biomass, as biomass is considered to be a 100% renewable source of energy.

The newest and future power plants within the ELSAM area have steam parameters of 250 bar/560°C/560°C and 290 bar/580°C/580°C/580°C giving efficiencies of 45 and 47 % based on LHV, respectively. The same efficiencies and hence, steam data are aimed for at biomass combustion.

Due to the high alkali and chlorine content of straw, especially high-temperature corrosion of superheater tubes, and also ash deposition, could be limiting factors for efficient use of this fuel.

ELSAM has therefore set up an R&D programme with the aim of co-firing straw and coal or straw alone at existing units and initiating the development of new technologies capable of firing large amounts of straw, with attention to ensuring high efficiency and maintaining high fuel flexibility.

2. Concepts for Combustion of Straw

ELSAM is investigating 3 ultra supercritical (USC) boiler concepts for combustion of straw and coal: 1) co-combustion in pulverized fuel (PF) boilers with a relatively low share of straw; 2) co-combustion in circulating fluidized bed (CFB) boilers with low to high share of straw and 3) single straw firing in a vibrating grate boiler.

2.1 The USC-PF Concept

At co-combustion in a USC-PF boiler, the major change is that some of the burners are modified for coal and strawfiring. The critical part with respect to high temperature corro-

sion and ash deposition is the convective pass superheaters, where 580°C steam temperatures occur.

The USC-PF concept has been investigated at full-scale tests at **Vestkraft Unit 1** (VKE1). VKE1 is a 125 MW$_{el}$ (330 MW$_{th}$) natural circulation front-fired PF boiler with four burners in three levels (figure 1). Two of the mid-level burners were replaced with straw burners for the test. Steam parameters are 170 bar /540°C/540°C.

At present, ELSAM is carrying out corrosion tests at another PF boiler, Unit 1 at Studstrup Power Plant (MKS1) with steam parameters 165 bar/540°C/540°C, a naturally circulating boiler. This boiler has been reconstructed for co-combustion of coal and straw (up to 20% straw). At this boiler corrosion tests with durations of up to 2,500 h with a larger number of test probes and built-in tubes as well as a more comprehensive investigation of the corrosive environment is in progress. The total test period will include 1996 and 1997.

2.2   The USC-CFB Concept

In a USC-CFB boiler the primary superheaters will be located in the corrosive environment of the convective pass and the final superheater will be located in the fluidized ash cooler environment, where no or very low content of corrosive species might be expected. The critical parts with respect to ash deposition is the convective pass, whereas corrosion may occur in both convective pass and in the ash cooler, if corrosive species are present here.
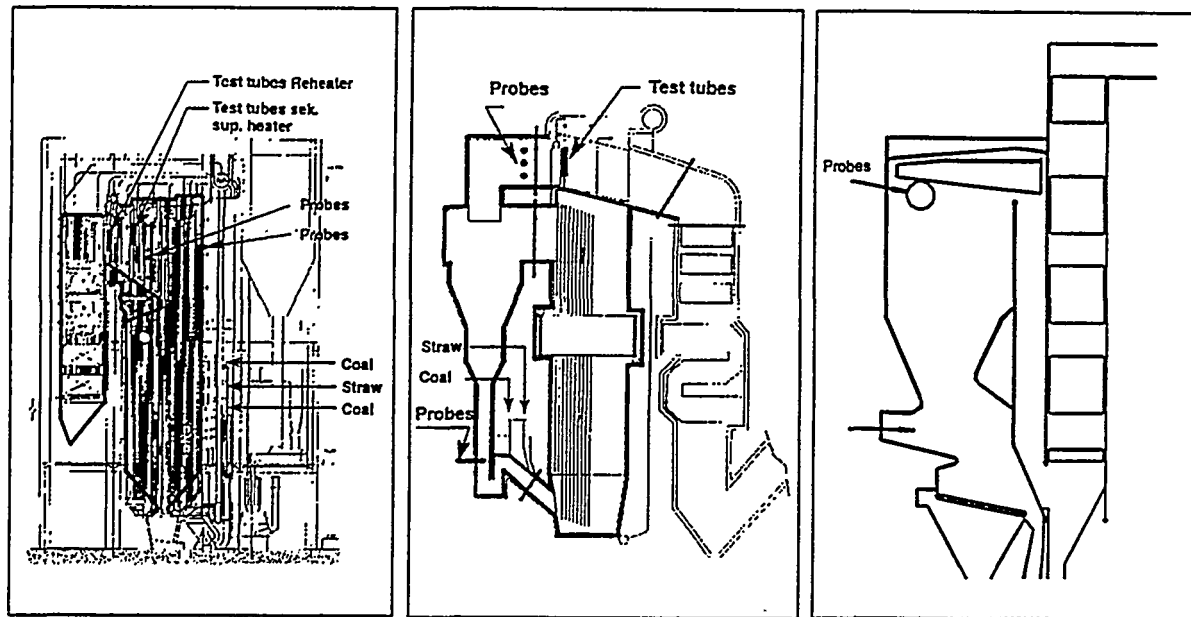

Figure 1.   Boilers used for full-scale tests. From left: Vestkraft Unit 1, Grenaa CFB, Rudkøbing CHP

The USC-CFB concept has been investigated at full-scale tests at **Grenaa CFB**, which is a 17 MW$_{el}$ (80 MW$_{th}$) CFB boiler made by Ahlstrom (figure 1). Coal and straw are mixed with circulated ash and limestone and is fluidized with combustion air at approx. 850°C in the combustion chamber. The particles are separated from the flue gas in two parallel cyclones, with the ash returning to the fluidized combustion chamber via two fluidized loop seals and the flue gas is leaving through the convective pass. Grenaa CFB has no external ash cooler and the steam parameters are 92 bar/505°C.

ELSAM has planned to build a 100 MW$_{el}$ CFB boiler in Aarhus for co-combustion of coal and biomass and with steam temperatures of 580°C. Superheating up to 500°C for the superheaters located in the convective pass is foreseen, whereas the final superheating up to 580°C will take place in superheaters located in the fluidized ash cooler. Straw may contribute with as much as 60%. In order to limit corrosion a project has been scheduled to influence the corrosive environment in an external ash cooler.

2.3   The USC-Vibrating Grate Boiler Concept

The primary superheating takes place in the convective pass of a strawfired vibrating grate boiler, whereas the final superheating will have to take place in a separate boiler fed with less aggressive fuel, for example wood or coal. The critical part with respect to ash deposition and high temperature corrosion is the convective pass superheaters in the strawfired boiler.
The USC-vibrating grate boiler concept has been investigated at full-scale test at **Rudkøbing CHP**, which is a 2.3 MW$_{el}$ (11 MW$_{th}$) vibrating grate boiler fed with 100 % shredded straw (figure 1). Steam parameters are 60 bar/450°C.

A vibrating grate boiler for straw firing is under construction at the power plant Enstedværket (I/S Sønderjyllands Højspændingsværk) at Åbenrå. This boiler will have steam temperatures of 470°C and the final superheating to 540°C takes place in a separate boiler fuelled with wood. At this plant corrosion tests also are planned.

2.4   Other Concepts

ELSAM is also looking into the possibilities for introducing a pre-treatment of the straw in order to reduce its impact on corrosion and ash deposition. If successful, the pre-treated straw will no longer be regarded as an aggressive fuel.

3.   Full Scale Tests

The test programme includes long term full scale test firings with investigations of high temperature corrosion supplemented with investigation of fuel, ash, deposits and flue gas compositions.

Full-scale tests have been carried out at the abovementioned PF-boiler **Vestkraft Unit 1**, the CFB boiler **Grenaa CFB** and the vibrating grate boiler **Rudkøbing CHP**.

7.4

Corrosion tests were carried out by means of temperature controlled probes for simulation of relevant steam temperatures. Probes were located in the convective passes of all three boilers, and further probes in the loop seal of the CFB boiler were used as a simulation of superheaters located in separate fluidized ash coolers. As a supplement and as references to the probes, also test tubes built in the existing superheaters were used in the PF-boiler and CFB-boiler convective passes. The locations of probes and test tubes in the boilers are shown in figure 1.

The relevant test data can be found in table 1. The tests were carried out with various shares of straw and coal reference corrosion tests were performed as well, although the vibrating grate boiler tests were only with 100 % straw.

The probes used were developed by ELSAMPROJEKT A/S for this purpose. The probes were cooled with pressurized air in regimes with low heat flux and with pressurized air as well as water in regimes of high heat flux. The outer part of the probes consist of exchangeable test rings of various superheater candidate materials, and rings containing thermocouples are also situated in various positions at the probes. These rings are pressed together by an external spring thus forming an airtight seal. The metal temperature is controlled by regulating the pressurized air flow on the basis of readings of one thermocouple. The longitudinal and circumferential temperature profiles are calculated on the basis of the other thermocouple readings, all are compiled in a computer during the tests.

Boiler	Vestkraft Unit 1			Grenaa				Rudkøbing
Type	PF			CFB				Grate
Size MW$_{el}$	125			17				2.3
Location	Convective pass			Convective pass		Loop seal		Conv. pass
T$_{steam}$ °C	540-580			460-540		560-590		490-580
T$_{metal}$ °C	570-620			480-570		630-665		520-630
Test serie	1	2	3	1	2	3	4	1
Duration h	1250	500	250	500	1000	400	1500	500-3000
Share of straw	10 %	10 %	0 %	50 %	50 %	15 %	0 %	100 %
Straw % Cl	0.25	0.25	-	-[1]	0.16	0.30	-	0.38
% K	0.75	0.75	-	-[1]	0.49	0.98	-	1.00
Coal % Cl	0.02	0.02	0.02	-[1]	0.02	0.02	0.02	-
% K	0.25	0.25	0.25	-[1]	0.25	0.25	0.25	-

1) No data available

Table 1. Test data for full-scale tests at Vestkraft Unit 1, Grenaa CFB and Rudkøbing CHP

Material	C	Cr	Ni	Mo	Si	Other
10CrMo910	0.10	2¼	-	1.0	<0.5	Mn
X20CrMoV121	0.20	12	0.5	1.0	<0.5	V; Mn
X8CrNiMoNb1616	0.08	16	16	1.8	<0.02	Nb
AISI 347H CG	0.07	18	12	-	<0.75	Mn; Nb
AISI 347H FG	0.07	18	12	-	<0.75	Mn; Nb
Sanicro 31HT	0.07	21	31	-	<1	Al; Cu; Ti
AC66	0.06	27	32	-	<0.3	Nb; Mn; Al; Ce
Sanicro 28	0.01	27	31	3.5	<1	Cu; Mn
Fecralloy	0.015	20	0.2	0.1	0.5	5 Al; Mn; N

Table 2.   Materials for corrosion tests

In some tests, a 14-thermocouple probe without test samples has been exposed in the same positions as the corrosion probes in order to establish a more precise temperature profile of the probe.

The test tubes were welded into the existing superheaters, preferably in the last part of the final superheater, where the steam temperature is highest and well documented.

A list of tested materials can be found in table 2. Test pieces were used in both as-received, machined and preoxidized conditions in order to evaluate impact of surface condition on corrosion. The preoxidation was carried out on machined samples in air at 600°C for 200 hours.

4.   Analysis of tested Materials

Detailed measurements of wall thickness in various identified positions of test rings and test tubes were performed before the tests. After exposure, the rings and tubes were cut in exactly the same positions as the preexposure measurements and wall thickness were remeasured in the same positions. Material losses due to corrosion were calculated in these defined positions of the test rings and tubes (figure 2).

In cases with a low corrosion rate, the results of the described method are very inaccurate, as the difference in pre- and post-exposure wall thickness is very small and therefore the method is supplemented with measurements of oxide thickness. This method utilises the

fact that the thickness of the topotactical oxide layer generally corresponds to the extent of corrosion, provided that no exfoliation or chemical attack of this layer has occurred [2].

Besides the material loss, also the depth of other material deteriorations as selective corrosion, grain boundary corrosion and pitting was measured in a light optical microscope.

Total corrosion in each position was calculated as the sum of material loss and the thickness of the deteriorated zone with internal selective corrosion. The highest four figures out of eight averaged double measurements of corrosion were averaged and the corresponding metal temperatures were calculated by interpolation between thermocouple readings. Each thermocouple reading is an arithmetic time average of the temperatures measured during exposure. Exposure times lasted between 250 and 3,000 hours (table 1).

The test pieces including ash deposits were investigated by scanning electron microscopy with energy dispersive analysis by X-ray (SEM/EDX) in order to acquire more detailed information for evaluation of corrosion mechanisms.

Also analysis of fuels, ashes, ash deposits and gases were performed in order to contribute to the understanding of corrosion mechanisms.
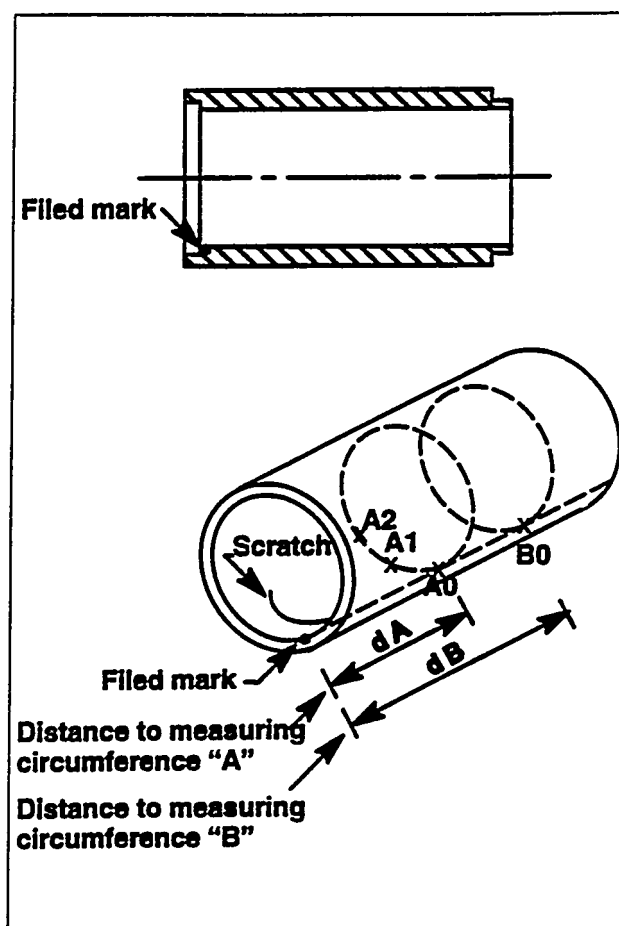

Figure 2. Measurement of material loss on test tubes

5.   Results

Analysis of the samples revealed large qualitative and quantitative differences in corrosion resulting from co-combustion of coal and straw in the PF boiler and in the CFB boiler, whereas there are many similarities in corrosion between co-combustion of coal and straw in the CFB boiler and strawfiring in the vibrating grate boiler.

5.1   Qualitative Results

The exposed samples from the PF boiler generally showed an even outer metal surface covered with oxide and some ash deposits. No degradation of the remaining metal and generally no pitting were observed. Samples from the coal reference corrosion tests and from the test with coal/straw co-combustion showed the same general appearance (figure 3).

The samples from the CFB generally showed more uneven metal surfaces, sometimes covered with oxide and ash. The oxide layers often were very irregular, porous, cracked and often partly exfoliated. Many of the CFB samples showed degradation of the remaining metal described as a selective corrosion, whereby mainly Cr is removed from the metal. This was the case for both the samples from the convective pass and from the loop seal. The selective corrosion was especially observed in the austenitic materials, whereas the ferritic/martensitic materials only showed very little of this degradation, although the latter were generally found to have a higher degree of material loss. Selective corrosion was found in samples from all tests with straw, but was not observed in the coal reference corrosion test (figure 4).

The samples from strawfiring in the vibrating grate boiler showed the same general appearance as the convective pass samples from the CFB-boiler, that is severe selective corrosion and exfoliation (figure 5) especially at the high metal temperatures.

Selective corrosion as observed from the CFB and vibrating grate boilers, was characterised by a selective removal of mainly chromium, and to a minor extent iron, and the remaining metallic phase was hereby enriched in nickel. In some cases this selective corrosion was mainly found to occur as grain boundary corrosion, leaving the inside of the grains largely unaffected. In other cases, it was found to occur as a general selective corrosion, where also the inside of the grains was largely depleted mainly of Cr.

The removed Cr is often found in the form of chromium oxide, sometimes very pure and at other times together with iron oxide as a spinel. These oxides can be situated in the degraded zone between partly degraded metal grains. In other cases the Cr and Fe had been transported to the metal surface forming layers of oxides and leaving the degraded metal zone rather porous.

In many cases chlorine is found near the corrosion front in the degraded metal zone. In this zone, chlorine is only present together with metal components such as Cr and Fe. Other

ash components such as alkalies have never been found in this zone. Therefore we assume that Cl occurs as chlorides and/or oxychlorides of chromium and iron.

Exfoliation of oxide layers often occurred and in cases with intense selective corrosion, cracks through the degraded metal zone were also observed.

Figure 3.   SEM micrograph of AISI 347H samples exposed in the PF boiler Vestkraft Unit 1. Left: coal combustion 250 hours, 620°C. Right coal/10 % straw 500 hours, 620°C
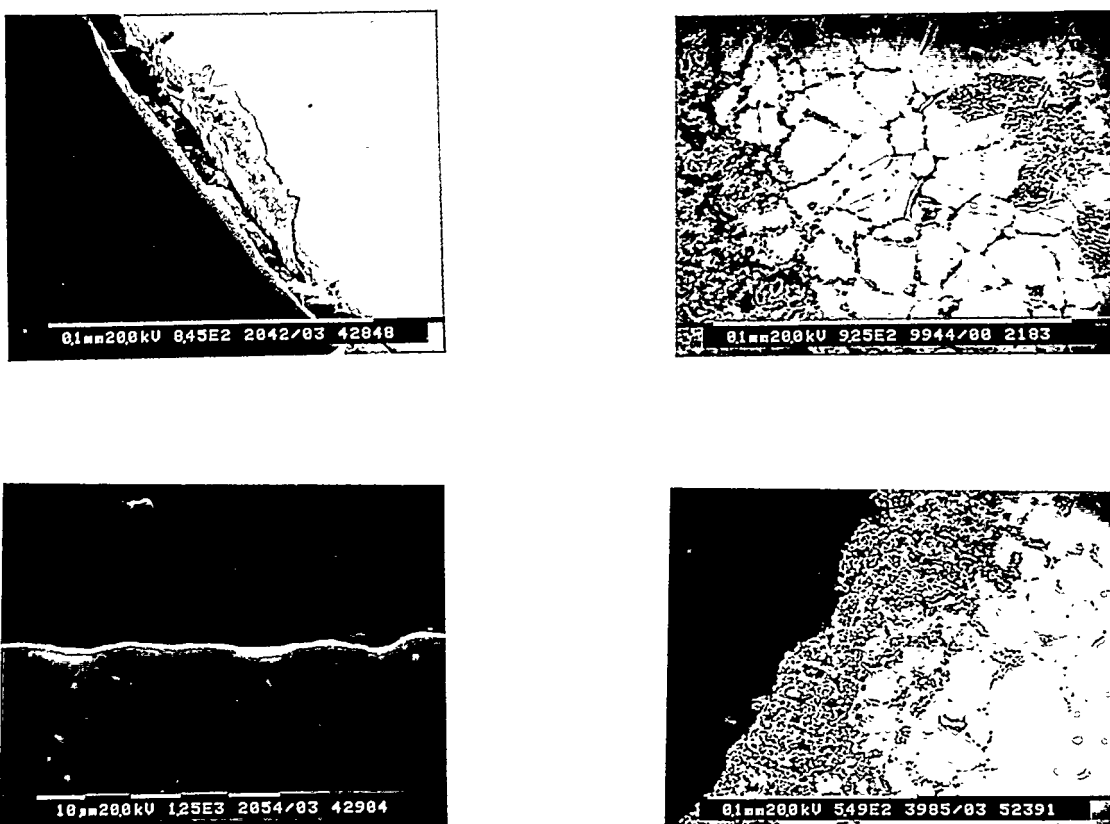

Figure 4.   SEM micrograph of AISI 347H samples exposed in the CFB boiler Grenaa CFB. Left: coal combustion 250 hours. Right coal/50 % straw 1,000 hours. Top: convec tive pass, 530°C. Bottom: loop seal, 660°C.
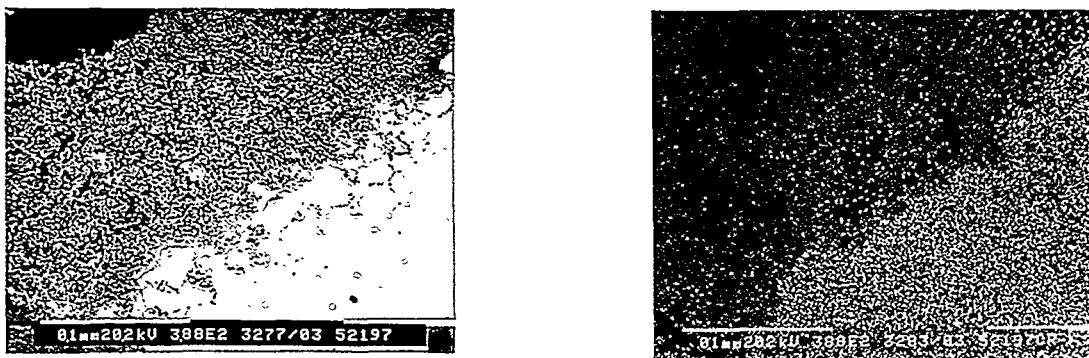
7.9

Figure 5. SEM micrograph of AISI 347H samples exposed in the vibrating grate boiler Rudkøbing CHP. 1,700 hours, 580°C. Right: distribution of Cr

5.2 Quantitative Results

Some of the quantitative results are shown in figure 6. In the calculation of the corrosion rates of the materials tested in the PF boiler, it is assumed that the corrosion follows a parabolic law. In the CFB boiler and the vibrating grate boiler, a linear dependence of the corrosion as a function of time is assumed, as the oxide layer does not offer efficient protection of the underlying metal. In principle the growth of the oxide layer might follow a parabolic law, but frequent exfoliation implies that the growth approaches a linear expression.

The quantitative results exhibit large differences between the boilers. In the PF boiler the corrosion rate is rather low by coal combustion and the corrosion rate is unaffected or slightly increased, when adding approx. 10% straw to the coal. At the most the corrosion rate is increased by a factor 1.5. Within the range of material temperature tested (560-630°C), there is only a moderate increase in the corrosion rates with increasing temperature for the tested materials as illustrated with X20CrMoV121 in figure 6.

In the CFB boiler the corrosion rates also are low at coal combustion and comparable to those of the PF-boiler. When adding straw to the fuel in the CFB boiler, the corrosion rates are markedly increased. This increase is variable and within 5-20 times in the convective pass and 2-10 times in the loop seal.

The temperature dependence of the corrosion rate illustrated in figure 6, shows that the corrosion rate increases with temperature for materials operating in the convective pass at material temperatures in the range of 440-580°C. In the loop seal, where corrosion tests have been carried out at 550-690°C, the level of corrosion was high, but had a decreasing tendency at increasing temperatures.

In the vibrating grate boiler, corrosion rates similar to or higher than the CFB convective pass, are observed. As compared to coal firing in PF and CFB boilers, the corrosion rate is increased 2-20 times. It is also clear from figure 6, that there is a strong temperature dependence on corrosion, with markedly increased corrosion rates at higher temperatures.
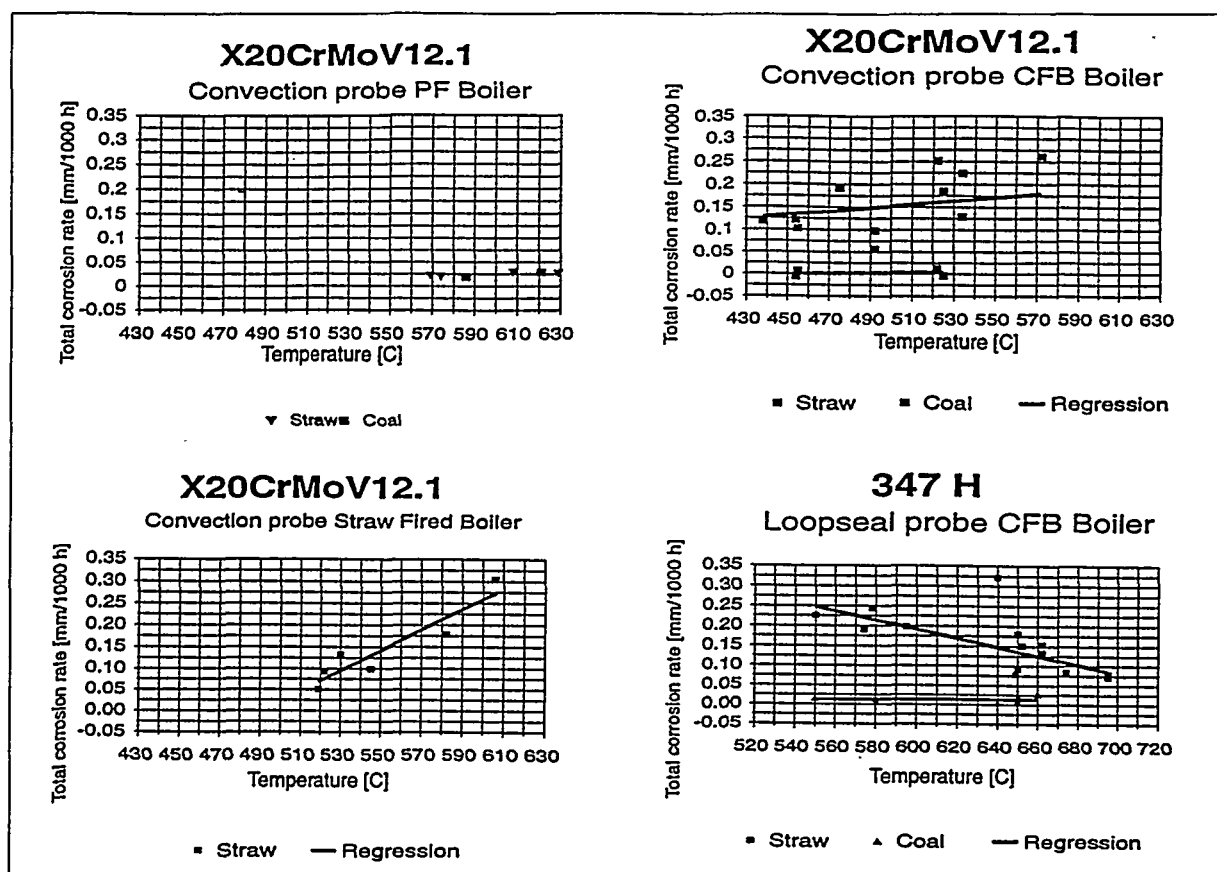
X20CrMoV12.1
Convection probe PF Boiler

Total corrosion rate [mm/1000 h]

0.35
0.3
0.25
0.2
0.15
0.1
0.05
0
-0.05

430 450 470 490 510 530 550 570 590 610 630
Temperature [C]

▼ Straw ■ Coal

X20CrMoV12.1
Convection probe CFB Boiler

Total corrosion rate [mm/1000 h]

0.35
0.3
0.25
0.2
0.15
0.1
0.05
0
-0.05

430 450 470 490 510 530 550 570 590 610 630
Temperature [C]

■ Straw ■ Coal — Regression

X20CrMoV12.1
Convection probe Straw Fired Boiler

Total corrosion rate [mm/1000 h]

0.35
0.30
0.25
0.20
0.15
0.10
0.05
0.00
-0.05

430 450 470 490 510 530 550 570 590 610 630
Temperature [C]

■ Straw — Regression

347 H
Loopseal probe CFB Boiler

Total corrosion rate [mm/1000 h]

0.35
0.30
0.25
0.20
0.15
0.10
0.05
0.00
-0.05

520 540 560 580 600 620 640 660 680 700 720
Temperature [C]

■ Straw ▲ Coal — Regression

Figure 6.   Total corrosion rate for X20CrMoV121 as a function of metal surface temperature in the three boiler concepts with coal, coal+straw and straw

5.3   Effects of Material Quality

The impact on the type of material also differs for the three boilers. In the PF boiler, higher alloyed materials showed decreasing corrosion rates as would be expected and the alloying impact on the corrosion rate is comparable to the alloying impact on the steam oxidation rate.

For the CFB and vibrating grate boiler test samples, higher Cr content in ferritic/martensitic materials reduces corrosion as would be expected. For the austenitic materials the reverse is found to be the case, i.e. higher Cr content associated with high Ni content often gives a higher corrosion rate. Especially selective corrosion is high for some of the higher alloyed austenitic materials, and of the materials investigated Sanicro 31 HT (W.stoff.nr. 1.4876) - similar to Alloy 800H - was most prone to selective corrosion.

In figure 7 the regression lines are shown for various materials exposed in the convective pass and the loop seal of the CFB boiler. The corrosion rates for all materials are rather high and will normally be considered unacceptable from a practical point of view. Only a marginal effect on life time can be achieved by the use of higher alloyed materials. and it must be considered more economically to use lower alloyed materials. The same argument counts for the vibrating grate boiler.
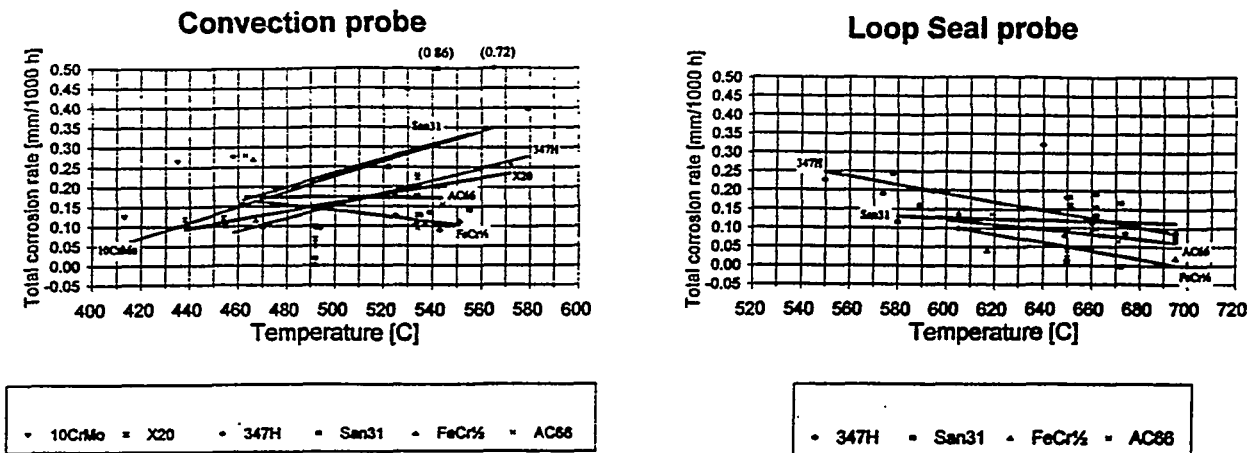
Figure 7. Comparison of corrosion rates of different test materials. 10CrMo: 10CrMo910; X20: X20CrMoV121; 347H: AISI 347H; San31: Sanicro 31HT; FeCr½: FeCralloy

For all cases the preexposure surface conditions of samples was found to have no impact on corrosion. Tubes used in the as-received condition showed larger variations in material loss, which relates to the relatively large circumferential variations in wall thickness. In many cases this variation is larger than the metal loss to be measured. Samples used in machined or in machined and oxidized conditions have nearly no circumferential thickness variations, and the measurement of material loss is correspondingly more precise.

5.4 Fuel, Ash and Flue Gas Analysis

Fuel analyses show that the chlorine and potassium contents of the straw were comparable in the PF and CFB tests with a 10-15% straw share and the vibrating grate test, i.e. approx. 0.3% Cl and 0.8-1.0% K on a dry basis, whereas the chlorine and potassium content was lower in the CFB test with 50% straw share (table 1).

In the PF boiler addition of straw with higher content of K and Cl have resulted in higher potassium content in the fly ash, but the major part of the K is insoluble and probably occurs as silicates. The Cl-content in fly ash has not been increased and the concentration is negligible. Ash deposits on the corrosion probe samples looked very similar at coal and at co-combustion of coal and straw. Ash deposition analyses carried out by ENEL [3] have shown low rates of deposition with coal alone and at co-combustion of coal and straw. Flue gas analyses showed that almost all Cl is emitted from the stack as HCl. Flue gas concentrations have been increased from 20 ppm to 60-75 ppm when adding straw to the coal.

7.12

In the CFB boiler ash deposition analyses have revealed high rates of deposition proportional to the share of straw. Ash deposition analyses carried out by ENEL [3] indicates high content of KCl and $CaSO_4$ in the convective pass deposits and in the fly ash. In the loop seal selective chloride corrosion is observed, although only minor amounts of chlorine is found in the loop seal ash (approx. 0.01% Cl). Due to the high mass flux and a relatively low fluidisation air flow high partial pressures of chlorine compound are possible and could explain the characteristic corrosion phenomena. Analysis have shown, that the oxidation conditions in the loop seal are very dependent on the load, with generally reducing conditions during full load and varying oxidising and reducing conditions at part load.

In the vibrating grate boiler also high deposition rates are observed and the deposits from the convective pass and the fly ash is rich in soluble K and Cl. SEM-analysis of deposits show, that these generally are composed of fly ash particles and large amounts of condensed KCl [4].

Experience has shown, that ash deposition varies from one year to another. In the winter season of 1995/96, ash deposition has been extreme for strawfired boilers and co-fired CFB boilers and caused loss of availability and loss of efficiency. The straw of this winter season has high content of potassium and chloride.

6. Discussion

The distinct differences in corrosion features between the boilers show that very different corrosion mechanisms are involved.

Tests have been performed on a PF boiler and a CFB boiler, with almost the same Cl and alkali concentrations in the fuel, but anyway no selective corrosion was observed in the PF boiler, whereas severe selective corrosion occurred in the CFB. This implies that it is the reaction pathways of various forms of Cl and alkali, rather than the concentration of Cl and alkali in the flue gas, that are decisive to corrosion.

6.1 PF Boiler

In the PF boiler there were no differences in the appearance of samples from combustion with and without co-combustion with straw, which leads to the conclusion that the corrosion mechanism is the same in both cases. The dominating degradation process then presumably is oxidation and perhaps some alkali sulphate melt corrosion.

The corrosion rate was unaffected or slightly increased, when adding 10 % straw to the coal. An increase in the corrosion might be attributed to higher release of volatile potassium encountered when co-firing with straw, as this can lead to higher rate of formation of alkali-iron sulphates on the metal oxide surface [5].

On the other hand, the major part of potassium in the fly ash was not water soluble, but probably occur as silicates. As potassium is in a soluble form in straw, this indicates, that this potassium reacts with silicates, probably silicate melts, in the flame. This potassium then will not be available for forming corrosive sulphates on the tubes surfaces.

The corresponding chlorine will form gaseous HCl or Cl_2, which will follow the flue gas and leave the boiler. There is no observation of Cl-containing agents near the metal and consequently no indication of Cl contributing directly as a corrosive agent. Therefore the increase in HCl and the Cl_2 partial pressure in the flue gas (from 20 ppm to 60-75 ppm) is not sufficient to provoke selective corrosion.

Chlorine might have an indirect impact on corrosion as a liberating agent of silicate bound alkali in the coal [6], but the observations does not substantiate this. On the contrary, volatile potassium seem to be catched by the silicates. Whether these silicates originate from the coal ash or straw ash is not yet determined.

The major reasons for these reactions are probably the high combustion temperature, high heat-up rate and relatively high SO_2 partial pressure, which favour conversion of the K and Cl content of straw to inert silicates and HCl and small amounts of K_2SO_4.

6.2   CFB Boiler

In the CFB there was markedly selective corrosion when co-firing with straw, but no selective corrosion at all without straw in the fuel fired, the latter being similar to coalfiring in the PF-boiler.

At selective corrosion mainly chromium, and to some extent iron, was removed from the metal grains and especially from the grain boundaries leaving these areas enriched in nickel. This chromium and iron has formed oxides, which are situated between the degraded metal grains or at the degraded metal surface. Also some chloride or oxychlorides of Cr and Fe are present, mainly at the corrosion front and at the base of the oxide layers. In many cases, large part of the degraded zone is porous with no oxide present. Solid or liquid components from the flue gas, such as alkali chlorides or sulphates, have never been found in this zone. The only flue gas component found in this zone is Cl, which occurs in connection with chromium and iron.

From these observations, it can be concluded that melt corrosion is not the direct corrosive mechanism in the selective corrosion, as this would leave some of the corrosive media in the degraded zone. Instead a gas-phase corrosive agent is implied, and as metal chlorides are found at the corrosion front, it seems plausible that gaseous HCl and/or Cl_2 are the corrosive agents. As the flue gas concentration of these species is lower than in the PF boiler, where no selective corrosion occur, another mechanism of creating a higher partial pressure of HCl or Cl_2 has to be found in the deposits on the tubes.

In the CFB fly ash most potassium is found in the form of KCl. In CFB boilers, combustion takes place at much lower temperatures, approx. 850°C, lower heat-up rates and lower

SO_2 partial pressure, the latter due to in-bed desulphurization. These conditions are not favourable for incorporation of potassium in insoluble silicates and major sulfation in the flue gas, although K_2SO_4 is the thermodynamic stable type of K.

Instead potassium to a large extent forms gaseous KCl, of which a part will condense on the superheater tubes, as also the deposit analysis showed. Some of this KCl will, due to the long residence time, react with flue gas SO_2 and O_2 forming potassium sulphate, K_2SO_4, and the chlorine is released as HCl or Cl_2, see reaction 1 [6, 7, 8]. KCl is also capable of reacting with the oxides hereby releasing HCl and Cl_2 (see reaction 2).

As these reactions take place in the deposits, it will give rise to very high concentrations of various types of gaseous chlorine near the metal surface - much higher concentrations than the average concentration of chlorine in the flue gas. These higher concentrations of chlorine on the metal surface are sufficient to provoke selective corrosion.

$$2KCl + SO_2 + O_2 \rightarrow K_2SO_4 + Cl_2 \tag{1}$$

$$2KCl + Fe_2O_3 + \tfrac{1}{2}O_2 \rightarrow K_2Fe_2O_4 + Cl_2 \tag{2}$$
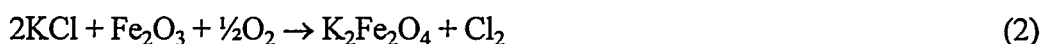
The gaseous chlorine reacts with the metal components, primarily Cr, forming chromium chlorides and chromium oxychlorides. These reactions (3 and 4) take place at the metal surface, where oxygen partial pressure is very low. As the reaction products are volatile at the existing temperature/oxygen partial pressure, the metal chlorides vaporize and move outwards. Here a higher oxygen partial pressure prevails and the metal chlorides oxidize to metal oxide, hereby releasing gaseous chlorine to renewed reaction with metal chromium (see reaction 5). In this way a small amount of chloride can act as a catalyst and result in severe corrosion.

This reaction mechanism also might explain the increasing corrosion rate with temperatures at the probes located in the convective pass. The higher the temperature the higher is the partial pressure of metal chlorides and again the rates of diffusion. A prerequisite is a sufficiently high gaseous chlorine partial pressure, which is supplied from the in-deposit sulphation of KCl.

$$Fe_{(s)} + Cl_{2\,(g)} \rightarrow FeCl_{2\,(s,g)} \tag{3}$$

$$Cr_{(s)} + Cl_2 \rightarrow CrCl_{2\,(s,g)} \tag{4}$$

$$2FeCl_{2\,(g)} + 1\tfrac{1}{2}O_2 \rightarrow Fe_2O_{3\,(s)} + Cl_{2\,(g)} \tag{5}$$

Although melt corrosion is not responsible for the selective corrosion, it might play an important role for the total corrosion rate. At the relevant tube surface temperatures, no melt will form from KCl and K-sulphate. When the selective corrosion from other reactions has started and produced metal chlorides, these chlorides can form low-melting eutectica with KCl, which will be melted at the relevant tube surface temperature. Such melted compounds might dissolve the oxide layers on the tube surface, hereby increasing

the corrosion rate. Melt corrosion might this way be the rate determining process of corrosion, although it can not be concluded from the observations.

The severe selective corrosion observed in the loop seal was not expected, as the KCl was expected to vaporize and leave the boiler with the flue gas. Anyhow it seems, that part of the KCl can be found as melt after combustion, and in the particle-rich environment this melt will probably stick to particle surfaces and hence be transported to the loop seal via the cyclone. In the loop seal part of this melt might be transferred to the tube surface, where it probably solidifies. In the loop seal SO_2-concentration will be low, and therefore sulphation of the deposited KCl is not probable. Another possibility is the reaction between KCl and Fe, Cr-oxide, producing metal ferrates and chlorine gas, but SEM/EDX-analyses do not seem to indicate any significant presence of these ferrates on the metal surfaces.

The mechanism of releasing gaseous types of chlorine in the loop seal therefore remains unclear, but anyway must be related to the KCl deposited on the tubes. The decreasing corrosion rate at higher surface temperatures in the loop seal might be attributed to more KCl vaporizing from the tube surface.

In order to reduce corrosion in the ash coolers, a project has been scheduled at Grenaa CFB for influencing the corrosive environment herein, as mentioned in chapter 2.2.

6.3 Vibrating Grate Boiler

In the vibrating grate boiler, the same type of selective corrosion as in the CFB at co-combustion of coal and straw was observed. Also the same general arguments as for the convective pass of a CFB boiler counts for the vibrating grate boiler. Supply of sulphur to the boiler by fuel is higher in the CFB boiler, but is due to in-bed desulphurization reduced to the same level as in the strawfired boiler. Deposits from the strawfired boiler are richer in KCl and lower in Ca-sulphates, but the general reactions leading to selective corrosion probably are the same - that is presumably in-deposit sulphation described in reaction 1 and the subsequent reactions 3-5.

In strawfired boilers, also melt corrosion from metal chloride - KCl eutectic melts is probable and might be the major explanation for the markedly temperature effect on corrosion.

Corrosion probes taken out at different times showed different deposit compositions. In some cases, significant concentrations of sulphate occurred, thus supporting the in-deposit sulphation theory, whereas deposits at other times showed very low sulphate content.

Therefore it seems likely, that factors such as variations in fuel composition and combustion characteristics affect deposit chemistry and therefore also has impact on corrosion.

Anyhow the results suggest, that high corrosion rates are inevitable at high metal temperatures and hence at high steam temperatures, but the absolute level of corrosion might be somewhat affected by process conditions and fuel composition.

7.16

Ash deposition will occur, whenever the fuel has high alkali and chloride content, as these components will form vaporized KCl, which will condense on tube surfaces. The bulk of deposits generally are KCl. The only way to reduce the impact of deposition on plant operation, then is to reduce the strength building in the deposits. This strength building in these deposits seem mainly to be controlled by deposition and sintering/melting of Ca-silicates. Ca-silicates are present mainly in the outer part of deposits, where deposit temperatures approaches the flue gas temperature.

The best way to reduce strength building then is to make frequent cleaning, for example by soot blowing, hereby avoiding the high deposit temperatures. Especially soot blowing in the furnace is important, as removal of deposits here, will reduce the flue gas temperature in the convective pass.

7.   Conclusion

In order to reduce CO_2 emission, ELSAM is investigating the possibilities of using biomass - mainly straw - for combustion in high efficiency power plants. As straw has very high contents of chlorine and potassium, a fuel with high corrosion and ash deposition propensities has been introduced.

ELSAM has carried out corrosion tests with corrosion probes and test tubes in a 125 MWel pulverized coal-fired boiler at co-combustion with up to 20% straw; in an 17 MWel circulating fluidized bed boiler at co-combustion coal and straw with straw making up approx. 50% of the fuel fired and in a 2.3 MWel vibrating grate boiler at 100 % strawfiring.

In the PF boiler the corrosion test showed no or only a slight increase in corrosion when co-firing coal and straw compared to coal-firing only.

In the CFB boiler there was found to be a large difference in the rates of the corrosion between coal-firing only and co-combustion of coal and straw. The corrosion rates when co-firing coal and straw were up to 2-25 times higher than the corrosion rates encountered for coal-firing only. Corrosion rates were high for all tested materials.

In the vibrating grate boiler, also high corrosion rates, similar to and higher then the CFB, was observed. Also here corrosion rates were high for all materials.

The large difference between the corrosion rates in a PF boiler on one side and a CFB boiler when co-firing coal and straw and a strawfired vibrating grate boiler on the other side, can be explained by a large condensation of KCl on the superheater tubes in the case of CFB and vibrating grate. This condensation is followed by reactions leading to high partial pressure of highly corrosive chlorine gasses at the tube surface. In the PF boiler heat up rate and combustion temperatures are much higher than in a CFB boiler and the vibrating grate boiler and chlorine will be bound as HCl, leaving the boiler with the flue gasses.

Combustion of straw in PF boilers seems possible provided that the share of straw is limited. The maximum limit is still unknown. Combustion of straw in a CFB boiler and in a vibrating grate-boiler at high steam parameters is associated with serious corrosion. As corrosion could not be reduced significantly by the use of higher alloyed materials, modifications of design is needed or replacement of the superheaters has to be accepted.

High ash deposition rates in CFB boilers and in vibrating grate boilers are also related to condensation of KCl and must be handled by improved cleaning devices.

8. References

[1]   Sander, B.: Fuel Data for Danish Biofuels and Improvement of the Quality of Straw and Whole Crops. Proc. 9th European Bioenergy Conference, Copenhagen, June 24-27, 1996.

[2]   Effertz, P.-H. and Wiume, D.: Mechanismen und Schadenformen der Hochtemperaturkorrosion an Überhitzerrohren Steinkohlenbefeuerte Grosskessel. Der Maschinenschaden 50(3), 93-102 (1977).

[3]   Baldacci A. et al.: Fireside Fouling during Coal/Biomass Co-firing in a Circulating Fluidized Bed Combustor and a Pulverized Coal Power Plant. Report APAS Clean Coal Technology Programme 1992-1994.

[4]   Michelsen, H.P., Larsen, O.H., Frandsen, F. & Dam-Johansen, K.: Deposition and High Temperature Corrosion in a 10 MW Straw Fired Boiler. Proc. Engineering Foundation Conf. "Biomass Usage for Utility and Industrial Power", Snowbird, Utah, USA, April 28- May 3,   1996.

[5]   Rask, E.: Mineral Impurities in Coal Combustion. Behavior, Problems, and Remedial Measures. Hemisphere Publishing Corporation, Washington, 1985.

[6]   Latham, E., Meadowcroft, D.B. and Pinder, L.: The effects of coal chlorine on fireside corrosion. Stringer & Banergee (eds.): Chlorine in Coal. Elsevier Science Publ., Amsterdam, 225-246, 1991.

[7]   Spiegel, M. and Grabke, H.J.: Hochtemperaturkorrosion des 2.25Cr-1Mo-Stahls unter simulierten Müllverbrennungsbedingungen. Materials and Corrosion 46, 121-131, 1995..

[8]   Husemann, R.U.: Korrosionserscheinungen und deren Reduzierung an Verdampfern und Überhitzerbauteilen in kommunalen Müllverbrennungsanlagen. VGB Kraftwerkstechnik 72, 10, 918-927, 1992.

COAL-FIRED POWER PLANTS AND THE CAUSES OF HIGH TEMPERATURE CORROSION

J E Oakey and N J Simms
British Coal Corporation
Coal Technology Development Division
Stoke Orchard
Cheltenham
Glos
UK

and

A B Tomkings
ERA Technology Ltd
Cleeve Road
Leatherhead
Surrey
UK

ABSTRACT

The heat exchangers in all types of coal-fired power plant operate in aggressive, high temperature environments where high temperature corrosion can severely limit their service lives. The extent of this corrosion is governed by the combined effects of the operating conditions of the heat exchanger and the presence of corrosive species released from the coal during operation. This paper reviews the coal-related factors, such as ash deposition, which influence the operating environments of heat exchangers in three types of coal-fired power plant - conventional pulverised coal boilers, fluidised bed boilers and coal gasification systems. The effects on the performance of the materials used for these heat exchangers are then compared.

1. Introduction

Coal has been the major fuel for heat and power generation in many countries around the world since the industrial revolution. Although, its continued use is threatened by environmental concerns that have come to prominence over the past two decades, it is widely recognised that coal will continue to be an important fuel in developed countries due to the lack of economically viable alternatives[1]. Further, its use will expand in the coal-rich countries of the Far East and other less developed regions to underpin their rapid economic development. In order to minimise the environmental impact of this inevitable situation, research activities have focused on technologies to reduce the

production of the harmful emissions from existing coal-fired plant and the development of new high efficiency systems which can meet the challenging environmental targets while producing power at economic prices. One of the major constraints on the efficiency of coal-fired plant results from the limitations of the materials used in heat exchangers.

High temperature corrosion is an important mechanism which can substantially reduce the service life of heat exchangers. The severity of the corrosion damage is related to the operating conditions of the heat exchanger concerned together with the abundance of corrosive species in the local environment. These species will arise from the coal used and from any additional feedstocks or additives injected to reduce emissions. This paper briefly reviews the potentially aggressive contaminants in coals and their release in three types of coal-fired plant and then discusses the impact they have on high temperature corrosion in heat exchangers in such systems.

2. Coal Constituents and Their Release

2.1 Coal Constituents

Coals are complex, heterogeneous materials comprising a mixture of organic matter (macerals) and associated mineral matter. This mineral matter originates from two main sources. It was either present in the structure of the plant matter which, over millions of years has led to the formation of the coal macerals, so-called inherent mineral matter, or it was laid down amongst the coal-bearing strata from other sources, eg the soils in which the coal forming plants were growing, so-called adventitious mineral matter. The relative amounts of these two forms of mineral matter present in a power station coal depends on the location from which it is mined and the degree of cleaning the coal has undergone during its preparation for sale. For the hard, bituminous coals used in most types of power plant around the world, the inherent mineral matter is typically only 3-6% of the total coal whereas the adventitious minerals, which are less well bound into the coal substance and are therefore more readily removed from the coal during cleaning, can vary from a few % up to more than 50% of the coal substance.

The wide range of minerals found in coals[2] comprise common clays (kaolinite, illite, monmorillonite, etc), quartz, feldspars, carbonates (calcite ($CaCO_3$), ankerite, siderite (Fe_2CO_3), etc), sulphates (gypsum ($CaSO_4.2H_2O$), barytes, etc), sulphides (pyrites (FeS_2), sphalerite (ZnS), etc) and rutile (TiO_2). This is by no means an exhaustive list but serves to illustrate the complex mix of constituents that pass through coal-fired plant.

In addition to the mineral matter, the organic coal matter contains various other 'inorganic' constituents such as S and Cl; in UK coals, the latter, which varies in concentration up to >0.5%, arises from saline ground-waters which have filtered through the coal bearing strata. Na and several other cations (eg Mg) also arise from saline ground-waters in UK coals; this Na represents well over 90% of that present in the coal and so the Cl content of a coal is a reasonably good indicator of a coal's Na

content. Some further Na, and most of the K in coal, are present in clay minerals (mainly illite) from which they are not easily released.

2.2 Release and Impact on Corrosion Mechanisms

High temperature corrosion mechanisms are influenced by a wide range of factors and the complex environments resulting from coal combustion/gasification processes make separating cause and effect very difficult. Component life is maximised when the alloys used can develop stable, protective oxide scales and so the factors that destabilise these scales are the 'causes' of excessive high temperature corrosion. The formation of stable oxide scales is promoted in strongly oxidising environments (usually characterised by the partial pressure of oxygen (pO_2)).

During combustion or gasification, the volatile, high hydrogen components of the coal macerals are evolved and burn readily. The more unreactive components require more aggressive conditions (higher temperatures/better oxidants) to initiate their combustion or gasification which may not be achieved in some systems leaving unconsumed carbon in the 'ash' residues, hence resulting in a potential loss in efficiency. Therefore, the relative amounts of reactive and unreactive coal constituents will impact on the rates of coal reactions occurring in the regions close to the points of coal injection into a coal-fired process. Combining this effect with the variations in operating parameters required for load following and the introduction of special injectors to reduce harmful emissions, eg low NO_x burners in pulverised coal plants, will cause the environment experienced by heat exchange surfaces located in these regions to vary considerably. The reactions of the organic coal matter largely dictate the oxidising potential (pO_2) of the gas produced. The pO_2 will also be influenced by the moisture content of the coal which in some high pressure systems may even be fed as a water-borne slurry. Indeed, recent studies have suggested that the presence of steam in heat exchanger environments in gasifiers promotes the formation of oxide scales in ways other than its impact on the pO_2 of the gas[3].

The decomposition of the coal's organic material also dictates the carbon activity (a_c) of the product gases which directly influence the potential of the gas to cause carburisation of the heat exchanger materials. Reducing environments arising in gasification systems and O_2-deficient (sub-stoichiometric) combustion in other systems can lead to a_c values ≥ 1 which mean that the gas will 'dump' carbon under suitable circumstances. Kinetic considerations usually restrict the extent to which this occurs in practice.

Sulphur contents of coals vary widely, but all will lead to the presence of some S - bearing gases in both combustion and gasification environments. There is therefore a competing tendency for heat exchanger materials to form sulphides/sulphates as well as, or in place of, oxides under suitable conditions. These conditions are largely dictated by the sulphur partial pressure (pS_2) (or the sulphur oxide partial pressure (pSO_x)) in the environment. When sulphides are thermodynamically stable in the environment, their rate of growth far exceeds that of competing oxides and severe sulphidation, or oxidation/sulphidation can occur.

The pS_2 or pSO_x in the combustion/gasification environment is controlled by the release of S from the coal and the extent of any competing S capturing reactions, such as those when S sorbent materials (eg limestone) are added to the system to reduce SO_x emissions from the plant. The S in the organic coal matter is readily released during combustion/gasification whereas that in sulphide and sulphate minerals is only released under conditions which cause these minerals to decompose. In oxidising, combustion environments most sulphates are stable and, for example, any S present in gypsum in the coal will remain bound in this Ca-phase although it will degrade to anhydrite ($CaSO_4$) through the loss of its water of crystallisation. Conversely, sulphides are stable in reducing environments and so their decomposition to release S is more likely in combustion than gasification systems.

The high temperature corrosion scales observed in coal-fired plants usually comprise mixtures of oxides and sulphides/sulphates indicating that they operate under conditions that, at one time or another, favour both oxidation and sulphidation reactions. The tendency for an alloy to form oxide or sulphide scales is traditionally presented in a thermodynamic phase stability diagram, an example of which is shown in Figure 1[4]. By marking the expected range of pO_2 and pS_2/pSO_x on this type of diagram, this approach allows the thermodynamically stable phases for each of the elements present in an alloy to be determined. Unfortunately, this does not give a complete picture of the situation in coal-fired plant as the kinetics of the corrosion reactions and the accessibility of corrodent species also have to be considered. However, in attempting to understand, and hence control, the causes of high temperature corrosion it is certainly important to know what effect plant operating conditions have on the pO_2 and pS_2/pSO_x in the heat exchanger environment.

From this position one then has to consider the impact that other characteristics of the environment may have on the corrosion mechanisms/rates. These include the presence of Cl (or HCl) in the gaseous environment and the effects of deposition of solid or liquid phases onto the heat exchanger surfaces.

The Cl present in coal is released readily HCl[5,6] at temperatures around 260°C. The presence of HCl in the gas can influence directly on the oxidation/sulphidation mechanisms and may lead to the formation of chlorides in the corrosion products. In general, the presence of HCl in the environment is recognised as nearly always leading to more severe damage although the reasons for this effect are often far from clear. As a result, however, high Cl content coals have a bad reputation.

The presence of high HCl levels in the coal combustion/gasification zone also encourages the formation of high concentrations of stable chloride vapour phases (eg NaCl, $FeCl_2$, $ZnCl_2$ etc)[7] which are thermodynamically favoured in reducing environments and will condense onto cooled surfaces below their dewpoints. Once deposited, these may form low melting point phases with other deposit or scale constituents leading to molten salt corrosion and significantly increased wastage rates.

The other main coal constituents which are recognised to play a significant part in high temperature corrosion are the alkali metals. When released into the gas phase as

chlorides, or other simple salts, the Na and K in coals readily condense onto cooled heat exchanger surfaces below their respective dewpoints. Dewpoints are dependent on the concentration of salt in the vapour phase and the process conditions; for alkali salts they are usualy in the range 600 - 800°C. In combustion systems, as in gas turbines, these salts are mostly found in deposits as sulphates, the thermodynamically stable form at the surface temperatures concerned. As such they act to flux underlying oxide scales forming low melting point phases (eg iron pyrosulphates) which lead to molten salt corrosion. In doing so, they act to transfer S-species from the gas phase to the underlying alloy leading to an increased potential for sulphidation to occur. The loosely bound Na which originates from saline ground-waters is readily released as volatile species during combustion/gasification[8]. Some K is also readily released during combustion /gasification although the majority remains bound in the ash residue derived from illite clay. At very low surface temperatures (<300°C) little deposition occurs as the alkali salts form solid particles as they pass through the surface boundary layers which do not adhere as easily to the surfaces as moltem droplets.

Finally, the residual ash phases produced during combustion/gasification reactions can also impact on heat exchanger corrosion. These phases are mostly derived from clays and other unreactive coal constituents and are essentially inert in terms of their individual potential to cause corrosion. However, they can act in several important ways to influence the corrosion mechanisms. Depending on the system and the relative temperatures of the heat exchangers, inert ash particles can cause substantial fouling by solid or molten slag deposits. These will have the effect of shielding the metal surfaces from the gaseous environment, reduce heat transfer and modify the environment local to the metal surface where the corrosion reactions are occurring, potentially reducing the pO_2. Deposits of this type are usually removed at regular intervals by 'sootblowing' to maintain thermal output from the heat exchanger leading to the heat exchanger materials experiencing variable conditions.

The deposits that form in coal-fired plant comprise a variety of constituents from the coal as described above. Over time very complex deposit structures can develop, with distinct layering of the different phases. They will also contain residual char left in the gas or carbon dumped from non-equilibrium gases which will add to the reducing potential of the deposit or may even burn on the heat exchanger surfaces if the surrounding environment becomes more oxidising.

The following section considers three different types of coal-fired plant and explains how the various coal constituents influence the high temperature corrosion observed in practice. Details of all the corrosion mechanisms involved are beyond the scope of this paper.

3. Coal Behaviour and Corrosion in Operating Coal-fired Plant

3.1 Pulverised Coal Combustion

Pulverised coal combustion is the best established technology for electricity generation from coal, having undergone continuous development since its first introduction early this century. Coals of typically 15-20% ash are ground to <75μm to provide a fine coal feed for these systems. Detailed descriptions of pulverised coal boiler systems are available elsewhere[9].

3.1.1 Furnace Walls
Pulverised coal burners produce a controlled flame with a very high temperature (in excess of 1600°C) in a cooled chamber of water walls which form the evaporator section of the steam circuit. The operating conditions for the furnace wall (or water wall) tubes are generally not highly corrosive. Although the gas temperature is very high the water wall is typically made using carbon steel tubes. The use of this material is possible because these tubes contain a mixture of steam and water (below 350°C) which keeps the metal temperature below 450°C. This means that the metal is operating under a high heat flux.

The high flame temperatures cause nearly all the mineral particles in the finely ground feed coal to melt and slag deposits form continuously on the furnace walls. The characteristics of the ash particles produced and the slag deposits have been described elsewhere[10]. However, the fact that the coal minerals are melted in the coal flame means that a significant amount of the trace metals and alkalis released at the high combustion temperatures are re-captured in the molten ash particles.

It is generally accepted that accelerated corrosion rates in furnace wall tubes are due to localised reducing conditions caused by the combustion dynamics of the boiler. Excess air levels leading to 3-4% residual O_2 in the flue gas are generally used in firing such boilers to reduce the risk of accelerated corrosion but it is still possible to generate local sub-stoichiometric conditions. In these areas there may be up to 10% CO in the atmosphere and any S will be present as H_2S (rather than the SO_2 or SO_3 formed under oxidising conditions). Under these conditions the scale formed on the metal will be a mixture of sulphide and oxide. Although few direct measurements have been made, evidence for the existence of reducing conditions is provided by the presence of free carbon in the scale on the metal.

Clarke and Morris[11] have reported on direct measurements of furnace gas composition at positions in the side and back walls of a front wall fired 120 MW$_e$ boiler. The sample positions included areas known to have high corrosion rates. Sampling points in areas of high corrosion (>150 nm/h) typically had low O_2 levels, high CO levels and, in some cases, high H_2S levels. The results are reproduced in Table 1.

In the UK (where coal Cl content is high) it has been found that a content of more than 0.1-0.2% Cl may increase corrosion rates. Cl contents may be in excess of 0.8% in UK coals and so much research was carried out by the CEGB to better understand the

effects of Cl in coal combustion environments. In tests to determine the rate of Cl release from pulverised coal it was determined that the Cl is almost completely dissipated within 300 ms from quite large (300 μm) particles at 1100°C[6]. This is shorter than the transit time from the burners to the side wall in pulverised coal fired boilers. Hence the Cl is present as a gaseous species by the time the burning coal air mixture reaches the side and back walls of the furnace.

Attempts have also bee made to quantify the effects of Cl on corrosion rates[12]. A linear dependence of corrosion rates on Cl content was derived for older plant producing 100 bar steam:

Corrosion rate (nm/h) = 1380 Cl - 290

(where Cl is the Cl % content of the coal)

No such relationship has been derived for the later 160 bar steam plant. It has been suggested that this results from the higher metal temperatures (up to 75°C). Under these conditions corrosion can be promoted by Cl, or in the absence of Cl, where local reducing conditions occur

On furnace wall tubes the wastage due to corrosion is distributed over the front radiant face, as shown in Figure 2. Under normal circumstances the mild steel tubes typically used in this application form a protective oxide forms, comprising layers of magnetite (Fe_3O_4) and haematite (Fe_2O_3) (Figure 3). However, where accelerated corrosion occurs (under reducing conditions), the morphology becomes more like that shown in Figure 4. A non-protective layer of Fe_2O_3 forms with islands of FeS. Intergranular attack of the underlying metal is common and the ash layer over the oxide surface contains Fe sulphides and particles of unburnt coal. . For the rapid corrosion of furnace walls largely to form Fe_2O_3 and FeS, it has been suggested that the presence of H_2S is necessary[12]. The stable form of S at the furnace gas temperatures is SO_x, not H_2S which is more stable at the metal temperature of the furnace walls. Consequently, for H_2S to form and influence the corrosion rates, it has been suggested that thick deposits must be present in order to create a suitable micro-environment beneath.

The effect of Cl in the coal is to make oxides thicker and more porous[12], ie less protective. Cl does not become a major constituent of the corrosion scale but is often found at the scale metal interface. It is believed that the Cl has a fluxing action forming iron chlorides at the scale metal interface (often related with intergranular attack of the metal) which are subsequently destabilised to form sulphide and oxides. This may happen at the scale:gas interface or after outward diffusion of gaseous chlorides through the scale. Cl thus released is free to react further with the metal.

Methods used to combat furnace wall corrosion have included varying operating parameters and bleeding air through the walls in order to lessen the occurrence of reducing conditions. However, it has been found that, under some circumstances, the most economical alternative is to use a more corrosion resistant material. Experience with alternative materials has shown that the ferritic steels with Cr contents up to 9% do

not perform significantly better and the corrosion morphologies are much the same. Materials such as 310 stainless steel (ss) tend to form protective Cr-rich oxide scales and are much more resistant to accelerated corrosive attack. However, even this material may fail through intergranular attack after prolonged periods[13] due, it is believed, to the slow rate of Cr diffusion to the metal surface. If 310 ss is to be used to improve the fireside corrosion resistance of furnace wall tubes then it must be used as a cladding because of its poor resistance to stress assisted cracking on the water side.

3.1.2 Superheater/Reheater Tubes

Compared with the furnace walls the conditions for superheater and reheater tubes are very different. Metal temperatures are higher and heat fluxes are lower. For example, in the coal fired plant built in the UK in the 1960s generating 565°C/160 bar steam, flue gas temperatures range from 900 to 1150°C in the superheaters and reheaters and metal temperatures of up to 650°C are possible. There is little localised variation in gas conditions, since the fuel is completely combusted by the time it reaches these sections of the boiler. Clarke and Morris[13] have reported a typical flue gas composition: N_2 15% CO_2, 9% H_2O, 3.5% O_2, 500-2000 ppm SO_2, 50 ppm CO, 50-500 ppm HCl (measured at the air heater inlet).

Corrosion in superheaters and reheaters is enhanced by the coal ash deposits which form on the tubes. It is the conditions prevailing beneath these deposits which promote corrosion. Alkali salts (Na and K sulphates) in the deposits react with the surface oxides on superheater and reheater tubes to form molten sulphates/pyrosulphates and so lead to rapid corrosion rates. At the temperatures which prevail at the scale surface, Na and K sulphates are not normally molten, but the corrosion rates found in practice can only be attributed to the presence of a molten phase[14]. The precise mechanism is not fully understood, but one suggestion is that the sulphates react with the scale in the presence of SO_3 to form mixed sulphates which are molten. For example SO_3 may react with iron oxide:

$$Fe_2O_3 + 3\ SO_3 = Fe_2(SO_4)_3$$
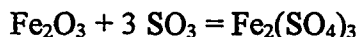
It is clear from the flue gas analysis reported by Clarke and Morris (see above) that SO_3 is not a major constituent. It is most likely that this species forms within the deposit[15]. The characteristic bell shaped curve of corrosion dependence (Figure 5) has now been widely reported by investigators of fireside corrosion in PF boilers[16]. The corrosion rate increase is due to the wide melting range of the sulphates on the tube surface and the consequently increasing amount of molten salt with temperature. However, this reaches a peak at a metal temperature around 670°C above which it is believed the stability of metal ions (iron and chromium) in the molten sulphate decrease).

The presence of Cl in the environment is known to influence the corrosion rate[12], although its precise role is not understood since chloride containing phases are not always observed in the corrosion products. (As the Cl content of a coal is usually a good indicator of the Na content and Na salts are known to be involved in the corrosion mechanisms, the role of Cl may be partly co-incidental.) Knowledge of the nature of Cl in coal (discussed in section 2), and its method of release as HCl suggests that the Cl

acts in a gaseous fluxing of the corrosion process. It has also been observed[12] that the Cl assists with the release of K from non-volatile phases in coal promoting the deposition of the more aggressive mixed Na/K sulphates on the metal surfaces. The resulting corrosion rate dependence on coal Cl content is linear following the expression:

$$R = KLB \ (Cl - a) \ (T_m - b)^c \ (T_g - d)^e$$

Where K, a, b, c, d, e are empirically derived constants

Cl is the coal Cl content in wt %
T_m is the surface metal temperature
T_g is the gas temperature
L is the leading tube factor (unity for non-leading tubes)
B is the alloy factor

In the superheater and reheater sections of pulverised coal fired boilers tube wastage due to corrosion occurs on two flats either side of the face immediately facing the gas flow, as show in Figure 6. The face towards the gas flow tends to be protected by a build up of ash deposits. However, either side of this there is a gas flow over the surface and deposit layers are thinner leading to higher metal temperatures and consequently higher corrosion rates. A typical corrosion morphology is shown schematically in Figure 7. The oxide layer on the metal surface may combine with the alkali sulphates deposited to form molten mixed sulphates and lead to rapid metal wastage.

The effect of Cl is generally to make scales thicker and more porous although, as with furnace wall tubes, the precise mechanism is not clear. It may be due to the outward diffusion of volatile metal chlorides or to the formation of a more defective oxide scale[17]. It is clear that the gaseous HCl formed during the burning of coal penetrates to the scale metal interface, since this is where Cl has been observed in microstructural studies of corroded tubes.

The tube materials typically used in these sections of the boiler are the Cr-Mo steels (1¼Cr - ¼Mo, 2¼Cr-1 Mo, 5Cr-½Mo, 9Cr-1Mo) or austenitics for higher rated boilers (AISI 304, 316, 321, 347). Where corrosion is particularly severe co-extruded tubing has been used. This comprises a highly corrosion resistant grade, such as 310ss or 50Cr-50Ni extruded as an outer layer over a more creep resistant grade such as Esshete 1250 or Alloy 800H.

3.2 Fluidised Bed Combustion

Fluidised bed combustion (FBC) systems operate at lower temperatures than pulverised coal boilers to avoid the melting of the ash particles arising from the coals mineral matter, to enable limestone addition to capture most of the SO_x emitted during combustion and to lower the NO_x generated during combustion. Low bed temperatures also act to reduce the release of alkali phases which could lead to hot corrosion damage

if the flue gas from the system is used directly to power a gas turbine. Both bubbling and circulating bed systems have been developed to commercial scale[18]. Bed temperatures are typically in the range 800 - 950°C depending on the type of combustor. A typical flue gas composition for a pressurised FBC is given in Table 2. To take full advantage of the high heat transfer rates achievable in bubbling fluidised beds, both evaporators and superheaters are located within the bed of these systems which are operated at low fluidising velocities, ie <3m/s. The high particle transfer velocities used in the circulating systems preclude the use of heat exchange surfaces located within the active bed and so either conventional gas pass heat exchangers or a supplementary low velocity fluidised bed are used.

The 'low' velocity bubbling beds have still proven to be aggressive to in-bed heat exchange surfaces even though they were originally thought to be benign because of the low impact velocities involved. The environments in these beds are essentially oxidising; as with all combustion systems the air introduced is controlled to optimise combustion efficiency by targeting a specific flue gas oxygen level. Within the bed itself, however, the gases rise in bubbles leading to a two-phase structure to the bed with gas-rich bubbles and a gas-lean dense phase[19]. Thus, the gaseous environment around any in-bed heat exchange tubing may be expected to oscillate between the pO_2s of these two phases. While the pO_2 of the bubble phase will be high and similar to that of the flue gas leaving the combustor bed, the pO_2 of the dense phase has been measured using various types of 'oxygen' sensors to be 10^{-10} atm or lower but has not been found to vary with the passage of bubbles[20]. In addition, the rising bubbles in the bed cause the surrounding particles in the dense phase to be forced against the tubing leading to high abrasive forces. Thus the overall environment is conducive to a combined abrasion/corrosion process.

As a result, low temperature evaporator surfaces (eg <300°C) often suffer severe wastage (rates of >1mm/1000h have been experienced [18,21,22]) and a wide range of engineering remedies (eg fins, shields, coatings, etc) have been tried to reduce the problem. However, it has been shown that with careful alloy selection and control of operating conditions, 'protective oxide scales can develop which restrict the wastage rates to acceptable levels of <50μm/1000h[23]. An example of a 'protective' scale is shown in Figure 8. Under FBC condition continuous, layered oxide scales of Fe/Cr spinels develop on low alloy steels which are often thickest on the bottom surface of the tubing which is subject to abrasive wear from the bed material.

The formation of deposits on heat exchanger tubing at high temperatures may actually help to reduce metal wastage as they act to separate the bed particles from the metal/oxide scale surface thus reducing the risks from wear/corrosion interactions. The abrasive nature of the fluidised bed also tends to restrict the deposit thicknesses so that they have minimal impact on heat transfer.

The type and extent of deposition observed in practice depends on the coal used and the temperature of the heat exchange surface involved[24]. Deposits of ash particles form on surfaces above about 450°C due to the sintering of the fine ash particles derived mainly from the inherent mineral matter in the coal; the adventitious minerals tend to remain

8.10

intact and act as the bed material in many cases. Other constituents of the deposits come from any minerals that degrade at the operating temperatures of the FBC such as the limestone added to retain sulphur released from the coal; this will lead to $CaSO_4$ rich deposits. Overall, the balance of elements found in FBC deposits is broadly similar to those present in the minerals introduced with the coal. The exception to this occurs with coals which release high levels of vapour phase species, such as Na, during combustion which deposit readily below their dewpoints.

Even at the lower combustion temperatures used in FBC systems, considerable quantities of Na species may be released from high Na-content coals (often also high Cl coals) unless the levels are constrained by competing Na-capturing reactions. Clays are well known as alkali capturing materials and special, active clays are being developed to reduce the alkali levels in flue gases upstream of gas turbines in some coal-fired combined cycle systems[25]. This effect also occurs to a lesser extent in FBCs where reduced levels of Na are found in deposits from coals with high ash and therefore high clay contents. The release of K species from illite is less favoured under FBC conditions and so little is found in deposits. When they do deposit in FBCs, both Na and K form sulphates, the thermodynamically stable form when sufficient SO_x is present in the gas phase. Where these are reduced by the introduction of a sulphur sorbent, then chlorides are the stable alkali salts and these have been found in deposits in such circumstances. They have also been found in deposits formed close to coal feed points where the local environment is reducing in character.

The effects of deposits on high temperature corrosion in FBCs are complex[24]. Firstly, if they are dense and impervious (as found on in-bed superheater surfaces at 650°C), they restrict gas access to the underlying surfacing thus reducing the pO_2. At the same time they provide a ready source of S, particularly deposits from systems with limestone addition, leading to a possibly increased pS_2 at the underlying surface. An example of a deposit covered superheater alloy from an FBC using a limestone S sorbent is shown in Figure 9. Oxidation/sulphidation has occurred on the underlying alloy surface. As FBC deposits are nearly always solid, very few instances of liquid phase development leading to molten salt corrosion have been observed. However, a study by British Coal[5] using two different high Cl coals without a limestone sorbent to reduce the SO_x level in the bed revealed that molten Na_2SO_4:NaCl rich deposits could occur on surfaces at 650°C (the eutectic melting point for this phase system is 627°C). This unusual occurrence led to much more severe molten salt corrosion similar to the superheater corrosion observed with high Cl coals in some UK power stations. However, in the case of FBCs, it is not yet clear whether Cl in the environment enhances corrosion, other than through its connection with the Na content of the coal.

3.3 Coal Gasification

A wide range of designs have been developed for gasifying coal to produce a combustible fuel gas. Two types of design are essentially developments from pulverised coal and fluidised bed combustion systems.

An example of the former which is broadly analagous to a high pressure, pulverised coal boiler is Shell's entrained flow gasifier which is now being demonstrated at the 250MW$_e$ commercial scale at Buggenum in The Netherlands. This plant gasifies a fine coal feed with oxygen in a water-cooled reactor where the gasification reactions occur at ~1500°C and 28 bar. The raw fuel gas from this reactor is quenched with recycled fuel gas, reducing its temperature to 900°C, before it passes into a gas cooler which acts as part of the evaporator in a conventional steam circuit (heat recovery steam generator). The fuel gas leaves this cooler at ~300°C, is scrubbed and burned to drive a gas turbine.

The latter type of gasifier employs a spouted fluidised bed operating at ~950-1000°C and 25 bar, with air as the gasifying agent. British Coal has developed a variant of this type which is now known as the 'Air Blown Gasification Cycle (ABGC)[26]. In this system the objective is to partially gasify the coal and to burn the residual char in a supplementary combustor. In this system a fuel gas cooler reduces the raw gas temperature to ~400-600°C before the gas is passed through hot gas cleaning systems and on to the gas turbine. The fuel gas cooler forms part of the steam system along with the heat exchangers in the char combustor and the heat recovery steam generator.

In both gasification systems the major gas components (H_2, H_2O. CO, CO_2, CH_4, etc) are in equilibrium at the point where the gas leaves the gasifier vessel[27]. Examples of gasifier exit gas compositions are given in Table 3. Because of the short residence time for the gas in the system the composition remains 'frozen' through the downstream components. Gas phase corrosion has been shown to be dominated by the balance between pO_2 and pS_2. In the oxygen blown entrained flow gasification system this leads to pO_2 and pS_2 values of 10^{-35} and 4×10^{-13} respectively in the gas cooler at 400°C. In the ABGC, the combination of using air as the gasifying agent (giving the fuel gas a significant N_2 content) and the removal of most of the H_2S by limestone additions to the bed leads to a far less aggressive environment in the downstream gas cooler: the pO_2 and pS_2 values in the gas cooler at 400°C are 10^{-33} and 9×10^{-15} respectively.

The type of corrosion damage experienced by gas cooler tubing is shown in Figure 10 which shows the complex oxidation/sulphidation occurring in pilot plant studies at British Coal. However, this damage is significantly less than that experienced in some oxygen blown systems which, as indicated above, operate with much lower pO_2s and higher pS_2s. From laboratory studies alone the effect of this change in gas chemistry potentially lead to an increase in corrosion rate of 5 orders of magnitude as the predominant corrosion mechanism changes from oxidation to sulphidation as shown in Figure 11[28]. The introduction of high levels of HCl further increases the corrosion rate[29]. This topic is under active investigation in many laboratories: some recent work has suggested that absolute gas steam content may have an additional effect on corrosion rates[3].

In the entrained flow oxygen blown gasifier, the mineral matter present in the coal is melted in the gasifier vessel and 50-80% of it leaves the base of the gasifier as a slag. In the ABGC, the lower gasification temperature leaves much of a coal's mineral matter intact; melting of the ash is avoided to minimise the risk of agglomeration. The coarse ash passes from the bed with the residual char to the combustor along with spent

limestone sorbent which is added to the bed to reduce the H_2S level in the fuel gas. In both cases, the remainder of the ash, residual carbon and sorbent products (in ABGC case) pass with the fuel gas to the gas cooler where they contribute to the deposits formed on the tubing..

The combination of the high gas temperatures and the composition of the fuel gases means that many metal species will be volatilised from the coal minerals (eg Pb, Cd, Zn, Fe, As, etc). For the entrained gasifier, it has been reported that the levels in the gas phase are likely to approach the equilibrium vapour pressures of these species with the remainder retained within the molten ash particles[30]. In both systems, along with the alkali vapour phase species, these species are likely to exist in the gas phase as chlorides (the HCl content of the gas will depend on the coal but is likely to be high enough for chlorides to be the predominant gas phase form) and will condense out onto the heat exchange surfaces in the gas cooler below their respective dewpoints as mixtures of chlorides and sulphides[31,32]. The exact composition of the condensate will depend largely on the dewpoints of the components in the fuel gas and the metal temperature but Pb and Zn are usually found as sulphides, Fe as sulphides and chlorides and Na and K as chlorides. At low metal temperatures it is also possible to drop below the NH_4Cl dewpoint although efforts are made to avoid this due to the potential risk of significant blockages developing in the gas cooler.

The high carbon activity of the fuel gas, combined with the carbon rich deposits (especially in the ABGC), mean that carburisation is also a potential concern in fuel gas coolers[33,34].

The role of complex mixtures of deposit phases and their interaction with the underlying oxide/sulphide scales is unclear other than their impact on aqueous downtime corrosion where the compositions and hydroscopic nature of the deposits can cause localised damage an order of magnitude more severe than the 'high' temperature corrosion occurring at normal operating conditions.

The environments in all gasifier fuel gas coolers are very corrosive and current designs are limited to metal temperatures of 400°C and lower depending on the corrosion potential of the fuel gas, the service life required from the heat exchange tubing and the steam requirements of the particular cycle.

4. Conclusion

This concise review of the environments of the heat exchanger in three distinct types of coal-fired plant illustrates that there are many common factors leading to the corrosion damage observed. The environments produced are highly dependent on the behaviour of the coals during the combustion/gasification processes. These environments contain a diverse range of potentially aggressive contaminants which can act either chemically or physically (in the case of fluidised bed combustion) to disrupt the development of simple protective oxide scales on the alloys and coatings commonly used for heat exchanger construction.

5. Acknowledgements

6. References

1 'Clean Coal Technology - Options for the Future', IEA/OECD, Paris (1993).

2. Jenkins, R G and Walker Jr, P L , 'Analysis of Mineral Matter in Coal', in Analytical Methods for Coal and Coal Products, Volume II, Chapter 26, edited by Karr, Academic Press Inc, (1978).

3. Bakker, W T, 'Effect of Gasifier Environment on Materials Performance', Proc of the First International Workshop on Materials for Coal Gasification Power Plant, Petten, The Netherlands, 14-16 June (1993).

4. R Perkins, 'Thermodynamic Phase Stability Diagrams for the Analysis of Corrosion Reactions in Coal Gasification and Combustion Atmospheres', EPRI Report FP-539, December (1977).

5. Oakey, JE, Minchener, AJ and Hodges, NJ, 'The Use of High Chlorine Coals in Industrial Boilers', Chlorine in Coal, Ed. J Stringer and D D Banerjee, Elsevier Science (1991).

6. Gibb, W, 'The Nature of Cl in Coal and Its Behaviour', in Coal Resistant Materials for Coal Conversion Systems, Ed D B Meadowcroft and M I Manning, 25-45, Applied Science, London (1983).

7. 'Trace Elements - Emissions from Coal Combustion and Gasification', IEA Coal Research, IEACR/49, July (1992).

8. Gibb, W and Angus, J G, 'The Release of Potassium from Coal During Bomb Combustion', J Inst Energy, Vol 56, 149 (1983).

9. 'Modern Power Station Practice', Pergamon (1971).

10. Raask, E, 'Mineral Impurities in Coal Combustion' Hemisphere Publishing (1985)

11. Clark, F and Morris, C W, 'Combustion Aspects of Furnace Wall Corrosion', in Coal Resistant Materials for Coal Conversion Systems, Ed D B Meadowcroft and M I Manning, 47-61, Applied Science, London (1983).

12. Latham, E P, Meadowcroft, D B and Pinder, L,'The Effects of Coal Chlorine on Fireside Corrosion', Chlorine in Coal, Ed. J Stringer and DD Banerjee, Elsevier Science (1991).

13. Brooks, S, Meadowcroft, D B, Morris, C W and Flatley, T,'A Laboratory Evaluation of Alloys Potentially Resistant to Furnace Wall Corrosion', in Coal Resistant Materials for Coal Conversion Systems, Ed D B Meadowcroft and M I Manning, 121-136, Applied Science, London (1983).

14. Cutler, A J B, Flatley, T and Hay, K A, 'Fire-side Corrosion in Power Station Boilers', CEGB Research 12-26, October (1978).

15. Latham, E P, Flatley, T and Morris, C W,' Comparative Performance of Superhaeted Steam Tube Materials in Pulverised Fuel Fired Plant Environments', in Coal Resistant Materials for Coal Conversion Systems, Ed D B Meadowcroft and M I Manning, 137-158, Applied Science, London (1983).

16. Stringer, J and Wright, I G, 'Current Limitations of High Temperature Alloys in Practical Applications', Oxidation of Metals, Vol 44, Nos 1/2, August (1995).

17. Cutler, A J B et al, 'Laboratory Measurements of the Corrosion of Superheater Materials in Atmospheres Simulating the Combustion of High Chlorine Coals', in Coal Resistant Materials for Coal Conversion Systems, Ed D B Meadowcroft and M I Manning, 137-158, Applied Science, London (1983).

18 . Rademakers, PLF, Lloyd, DM and Regis, V, 'AFBC's: Bubbling, Circulating and Shallow Beds', High Temperature Materials for Power Engineering (1990)..

19. Stringer, J, Minchener, A J and Lloyd, DM, 'The Effect of Process Variables on Hot Corrosion in Fluidised Bed Combustors', Materials Performance, Vol 23, No 6, 29-36, June (1984).

20. Mortimer, AG and Reed, GP, 'Development of a Robust Electrochemical Oxygen Sensor', Sensors and Actuators B 24-25, 328-335(1995).

21. Oakey, J and Minchener, A J, 'Erosion and Corrosion in Advanced Coal Fired FBC Systems', Proc 3rd Int Symposium on High Temperature Corrosion and Protection of Materials, Les Embiez, France, 25-29 May (1992).

22. Simms, N J and Oakey, J E, 'Protective Oxides in Coal-fired Combined Cycle Power Systems, Materials at High Temperatures, 75-80, Vol 13, No 2 (1995).

23. Meadowcroft, DB, Montrone, ED, Oakey, JE and Stott, J, 'Experiences of Combatting Tube Bank Wastage in the Grimethorpe PFBC', Proc Institute of Energy Conference, FBC and the Environmental Challenge, London 1991, 105-114.

24 . Oakey, JE, Minchener, AJ and Stringer, J,'Ash Deposition in Atmosheric Pressure Fluidised Bed Combustion Systems', J Inst Energy, March 1990, 208-219.

25. Fantom, I R, 'Measurement and Control of Alkali Meatl Vapours in Coal-derived Fuel Gas', Gas Cleaning at High Temperatures, Symposium at the University of Surrey, Ed Seville and Clift, Blackie (1993).

26. Dawes, S G, Mordecai, M, Brown, D and Burnard, G K, 'Air Blown Gasification Cycle' Proc 13th Int Conf on FBC, Orlando, Florida, May (1995).

27. John, R, 'Predicting Corrosion of High Temperature Process Plant' Proc. Conf. Life Prediction of Corrodible Structures, NACE, 23-26 September (1991).

28. Tiearney Jr, T C and Natesan, K, J Mater. for Energy Systems, Vol 1, 16 (1980).

29. Gohil, D D, Saunders, S R J and Bennett, M J, 'The Behaviour of Fecralloy Steels in Coal Gasification Atmospheres Containing Hydrogen Chloride', High Temperature Materials for Power Engineering, Part I, 189-198 (1990).

30. Thompson, D and Argent, B B, 'The Application of Thermochemocal Techniques to the Prediction of Equilibria Relevant to Coal Utilisation and the Nature of By-products', ECSC Final Report on Contract EC/861 (1996).

31. van Liere, J, Bakker, WT and Bolt, N,'Buggenum Coal Gasification Plant - Supporting Research on Construction Materials and Gasification Slag', VGB Kraftwerkstechnik 75 (1995), No 1.

32. Bakker, WT and Perkins RA, 'Beyond Mixed Oidant Corrosion - Corrosion Phenomena in Gasifiers',Proc Conf on Corrosion, Erosion and Wear, Berkeley 1990, NACE (1991).

33. Oakey, J, Simms, NJ, Fantom, IR and Nicholls, JR,' Materials Issues in Air Blown Gasification Combined Cycle Systems', Materials for Power Engineering, Part II,1453-1466 (1994).

34. 'Materials and Components', No. 118, October (1995).

35. Simms, N J , Norton, J F and Lowe, T M, 'Alloy Corrosion in Coal Gasification Systems', Proc 3rd Int Symposium on High Temperature Corrosion and Protection of Materials, Les Embiez, France, 25-29 May (1992).

Table 1 Gas analyses from various points on the side and back walls of a front wall fired 120 MW boiler (after Clarke and Morris[11])

	Units	Sample Point Number										
		1	2	3	4	5	6	7	8	9	10	11
GAS												
O_2	%	10.8	4.1	nil	1.2	nil	nil	1.1	8.9	8.6	6.2	6.1
CO	%	0.02	0.02	4.2	0.8	2.7	4.3	0.61	0.03	0.06	0.005	0.03
SO_2	vpm	490	800	900	1200	800	1000	1600	600	400	700	1000
H_2	%	nil	nil	1.08	0.20	0.70	1.23	0.12	nil	nil	nil	nil
H_2S	ppm	nil	nil	>300	trace	trace	nil	nil	nil	nil	nil	nil
HC	vpm	nil	nil	6	6	2	nil	nil	nil	nil	nil	nil
HCl	ppm	150	265	377	303	385	470	410	287	230	239	225
HCl_c	ppm	159	246	425	316	407	425	404	266	267	320	286
SOLID												
Combu-stibles	%	2.9	8.2	14.6	50.8	24.5	42.3	12.4	2.5	2.4	5.7	7.8
Cl	%	0.11	0.03	0.13	0.15	0.21	0.13	0.15	0.03	0.07	0.08	0.10
S	%	0.59	0.49	0.50	0.48	0.77	0.60	0.46	0.28	0.27	0.42	0.33

At sample points 2, 3, 4, 5, 6 and 7 high corrosion rates (>150 nm/h) were experienced. HC is total hydrocarbon gases concentration. HCl_c is the calculated concentration of HCl based on coal composition.

Table 2 Example of PFBC Gas Composition

Gas Species	Units	PFBC Gas Composition
O_2	%	3 - 6
CO_2	%	12 - 15
H_2O	%	3 - 6
N_2	%	balance
HCl	vppm	<400
SO_x	vppm	100 -200

8.18

Table 3 Gasifier Gas Compositions

Gas Species	Units	Oxygen Blown Entrained Slagging Gasifiers			Air Blown Gasifier
		Dry Feed[#]	Slurry Feed[+]	Fluidised Bed[=]	Fluidised Bed
CO	%	62 - 64	35 - 45	30 - 40	15 - 20
CO_2	%	2 - 4	10 - 15	10 - 15	5 - 8
H_2	%	27 - 30	27 - 30	24 - 28	10 - 15
H_2O	%	0 - 3	15 - 25	11 - 20	5 - 12
N_2	%	1 - 5	0 - 2	0 - 2	40 - 50
CH_4	%	n/a	n/a	3.5	2 - 4
H_2S [*]	vppm	2000 - 12000	2000 - 12000	2000 - 12000	300 - 5000
NH_3	vppm	200 - 500	2000 - 5000	200 - 500	500 - 1500
HCl [*]	vppm	50- 1000	50 - 1000	50 - 1000	50 - 500

[*] Dependent on coal S and Cl content
[#] eg Texaco Gasifier
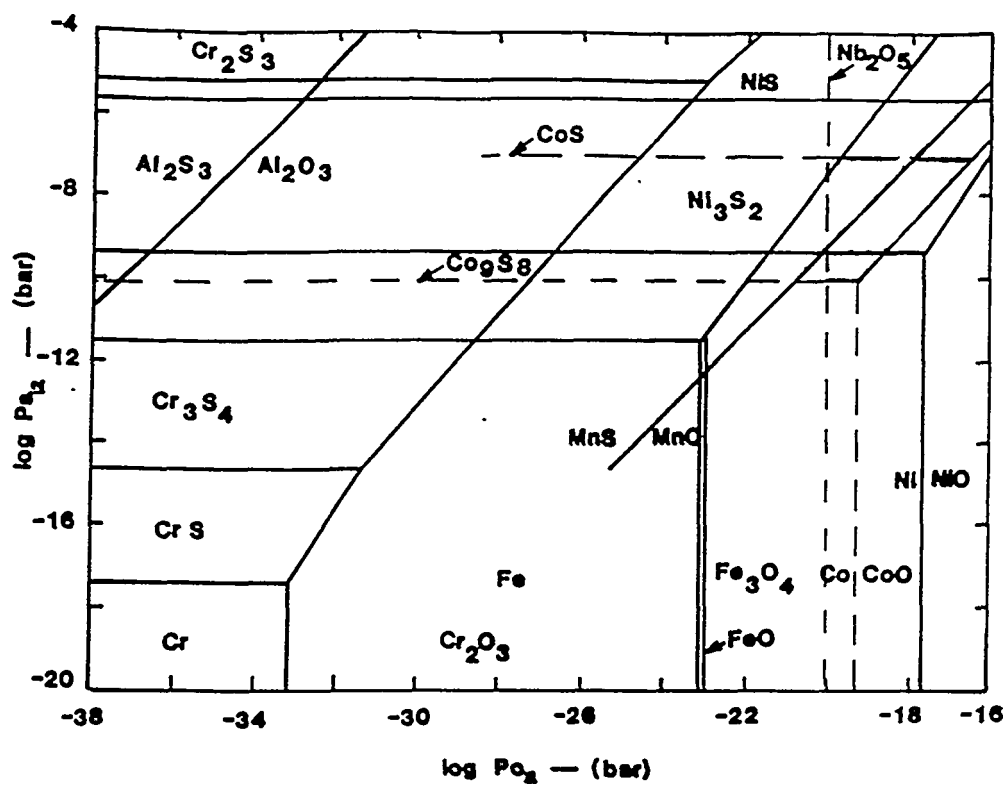[+] eg Shell Gasifier
[=] eg High Temperature Winkler Gasifier

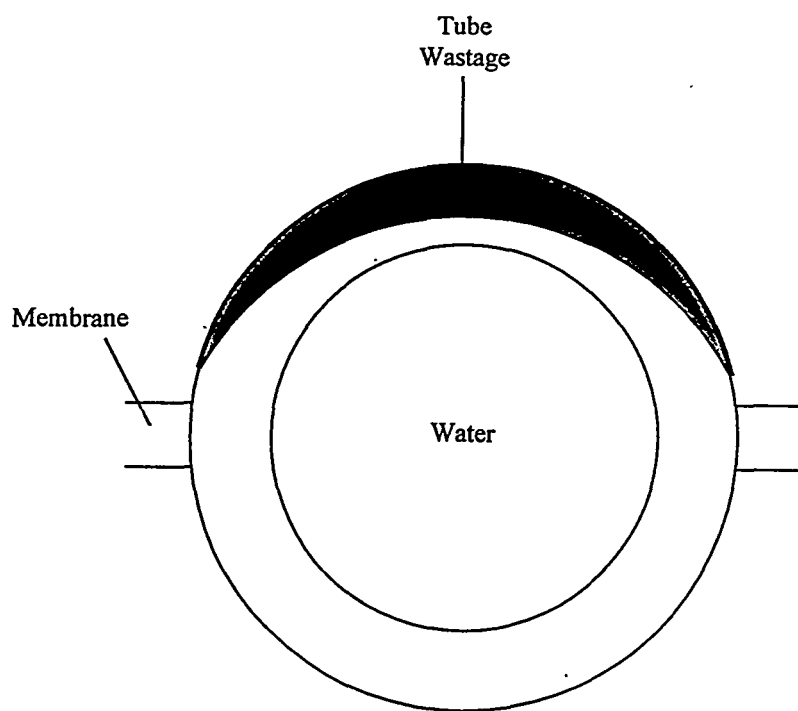Figure 1 Example of pS_2, pO_2 phase stability diagram at 650°C[35]

Figure 2 Distribution of metal wastage on pulverised coal fired furnace wall tubes (After Cutler et al[14])
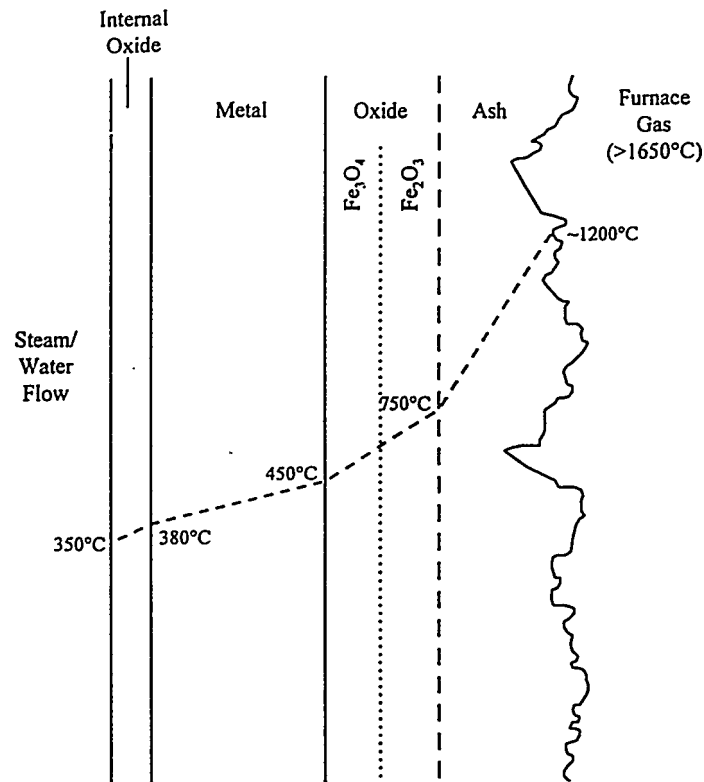
Figure 3 A schematic diagram showing the temperature profile and protective oxidation of mild steel tubes in pulverised coal fired furnace walls (After Cutler et al[14])
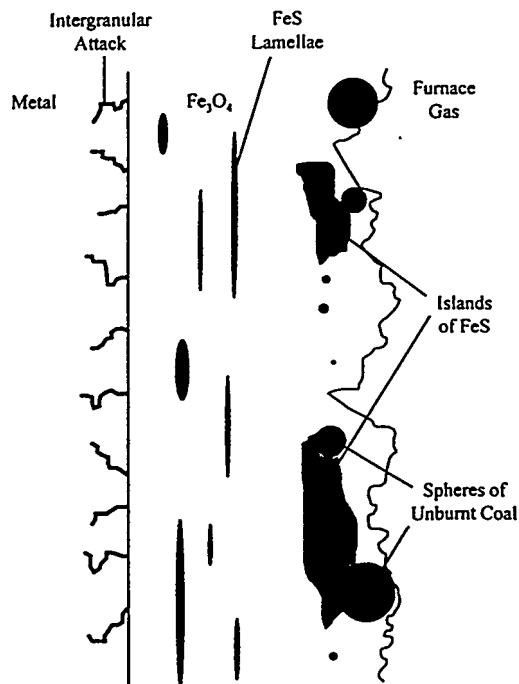

Figure 4 A schematic diagram showing the damage morphology occurring under accelerated corrosion of mild steel tubes in pulverised coal fired furnace walls (After Cutler et al[14])
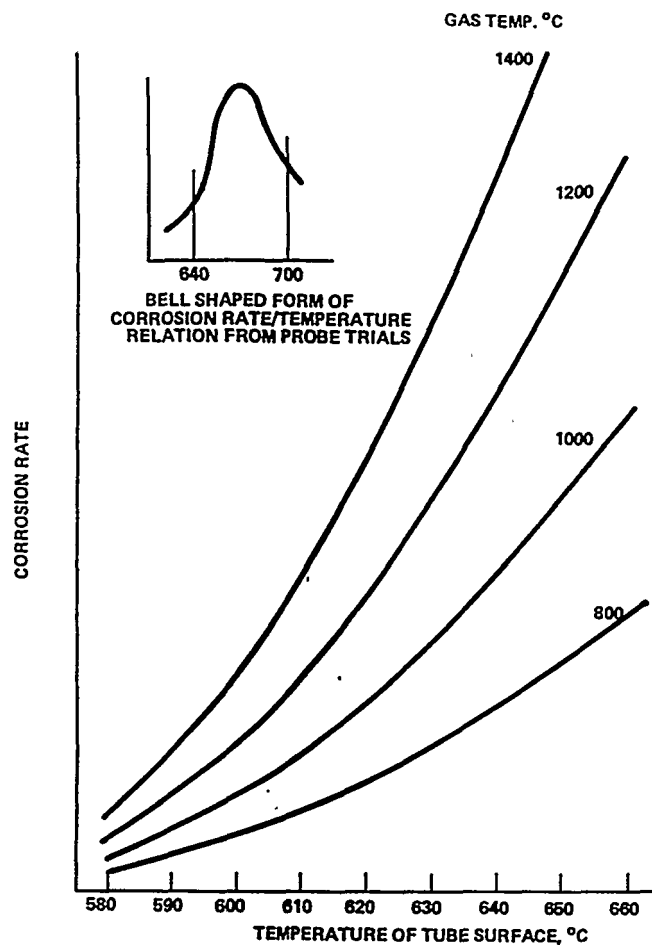
GAS TEMP. °C

Figure 5 The dependence of corrosion rate on metal temperature beneath molten sulphate deposits at various furnace gas temperatures. The inset shows the characteristic bell shaped curve of corrosion dependence of which the main graph illustrates only a portion (After Cutler et al[14])
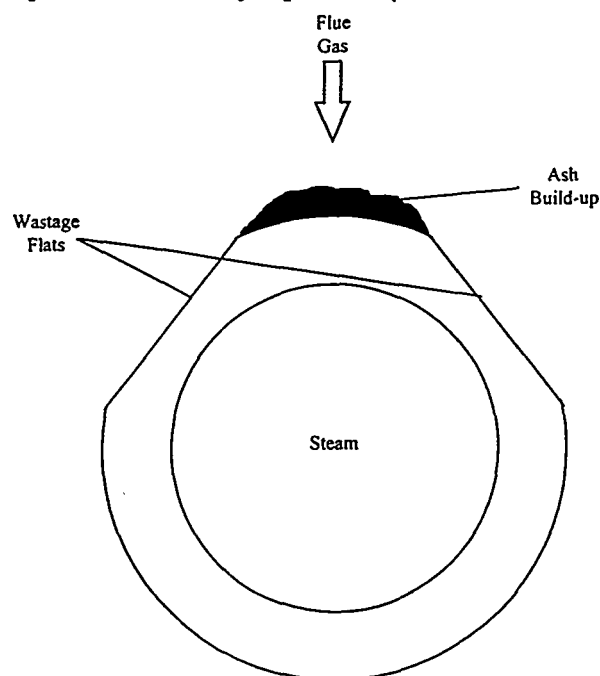

Figure 6 Wastage profile for pulverised coal fired superheater and reheater tubing (After Latham et al[26])
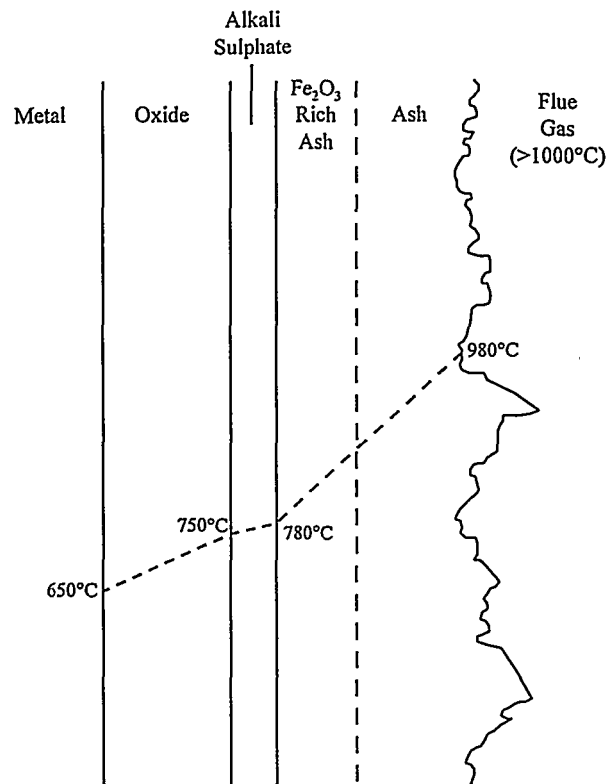
Figure 7 A schematic diagram showing the damage morphology occurring under accelerated corrosion of pulverised coal fired superheater and reheater tubes (After Cutler et al[17])
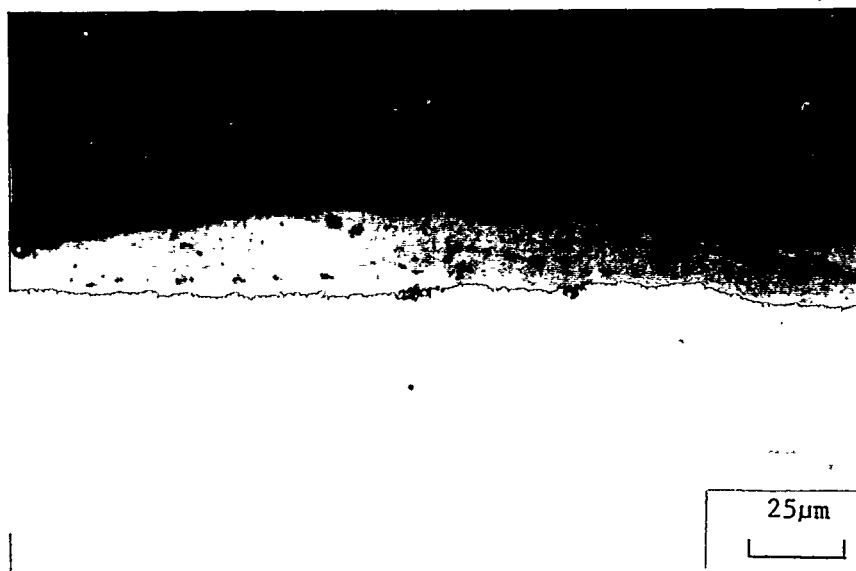

Figure 8 Example of Protective Scale Formed on a Low Alloy Steel on an FBC Evaporator Tube
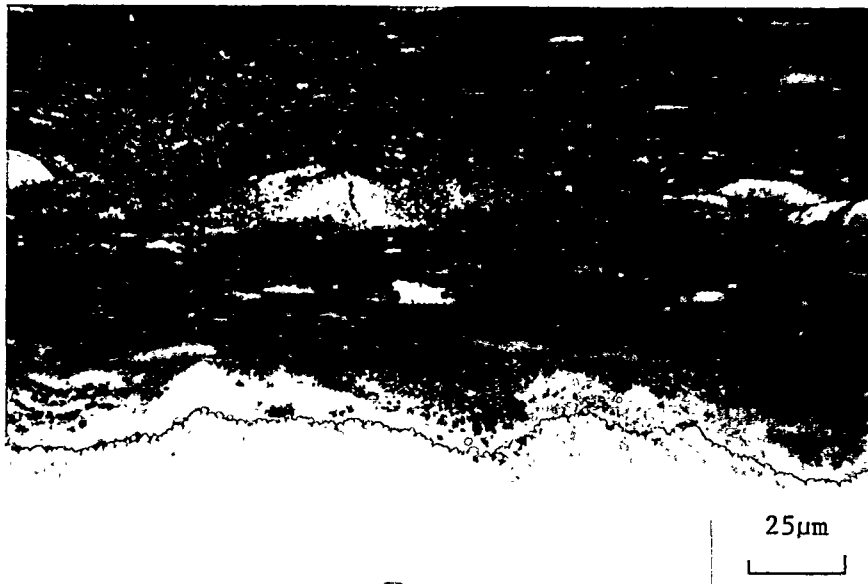
Figure 9 Example of a Superheater from a FBC (operated using a Limestone Sulphur Sorbent) showing Deposit Formation and Underlying Corrosion Damage
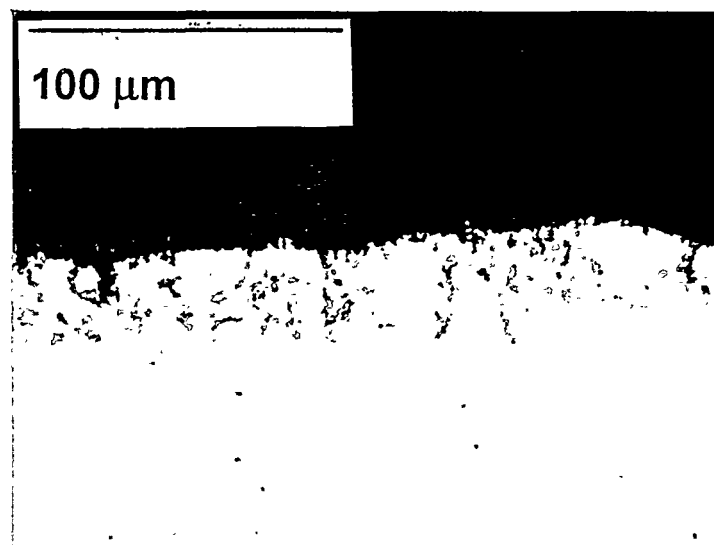

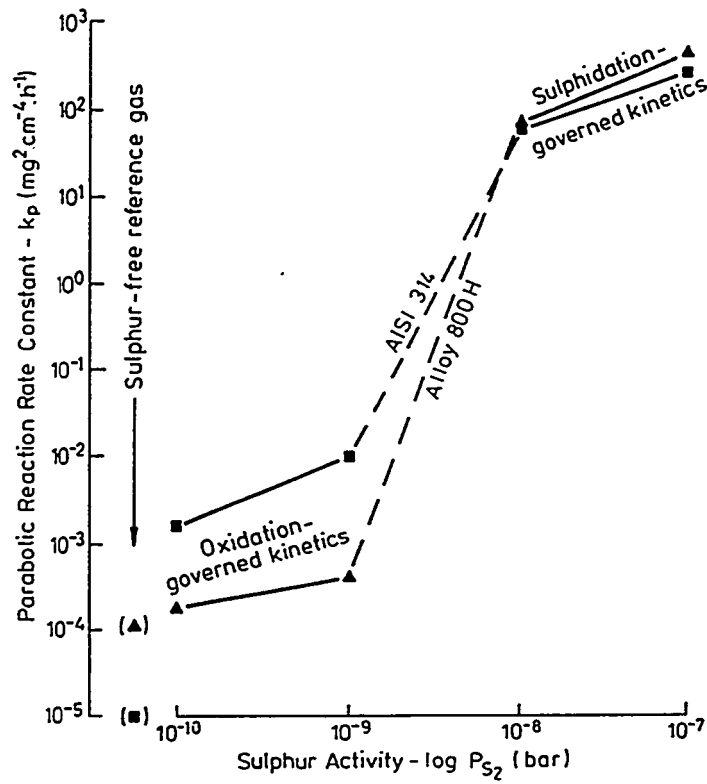Figure 10 Example of Corrosion Damage Produced by Exposure to Coal Gasification Gases

8.24

Figure 11 Effect of Changes in Sulphur Partial Pressure (pS$_2$) on Corrosion Rates in Laboratory Simulated Coal Gasification Gases[28]

Development Tendencies in Cycle Chemistry
of Fossil Fired Power Plants

Karol Daucik
Fælleskemikerne
Skærbækværket
7000-Fredericia
Denmark

Abstract
The development of cycle chemistry during the past 50 years is described and the main tendencies are pointed out. Improvement of cycle purity is the most dominant evolution, which introduces more freedom with respect to pH and redox potential control. Units with once-through boilers have profited most from this development. The development of boiler water chemistry in drum boilers also tends towards higher purity and less chemicals, which raises possibilities for oxygenated treatment.

1. Introduction

Power cycle chemistry has been and is used to improve the performance of power plants. The most substantial improvement can be achieved for units with deteriorated design. Nevertheless, the right solution is the improvement of the design. The real task of cycle chemistry is the optimization of the well-designed units.

In other words, chemistry is often used to make poorly designed equipment running at costs lower than the costs of a redesign.

Because of this interference between the installation design and chemistry, chemistry has been developed differently throughout the world.

The problems of cycle chemistry are in general the same as they were 50 or more years ago, i.e. deposition and corrosion. However, the problems appear to be somewhat more sophisticated as well as design is more sophisticated.

Apart from the influence on the designers, the only instrument a chemist has is the control of chemical parameters. This instrument has many "strings" and only a harmonic use of them will result in suitable tuning, which together with the tuning of other specialists' instruments gives the pleasant "melody" of a well-operating plant in the long term.

The corrosion and deposition problems are most commonly related to some acute difficulties affecting plant reliability or plant efficiency. The general effects on the lives of the components and on maintenance are often forgotten or just suppressed.

The corrosion and deposition problems are most commonly related to some acute difficulties affecting plant reliability or plant efficiency. The general effects on the lives of the components and on maintenance are often forgotten or just suppressed. However, the significance of these effects is increasingly dominant in the economic evaluation of modern power units.

Table 1 shows the main conditioning types used in the past 50 years. The development of the conditioning for boiler water is shown in table 2 and the development of the conditioning for once-through boilers is illustrated in table 3. The history of cycle chemistry is different in various countries. However, there are some general tendencies which can be recognized through a discussion of main chemical kontrol parameters.

Table 1 - Characteristics of Feed and Boiler Water Treatment							
Abbr	Type of treatment	Feed Water			Boiler Water		
		NH_3 mg/L	N_2H_4	O_2 μg/L	PO_4^{3-} mg/L	Na/P ratio	NaOH free
PT_1	Coordinated Phosphate Treatment	0.5-1	+	< 5	2 - 10	< 3	+
PT_2	Congruent Phosphate Treatment	0.5-1	+	< 5	2 - 10	< 2.8	0.00
PT_3	Equilibrium Phosphate Treatment	0.5-1	+	< 5	1 - 2	> 3	10
HT_1	Hydroxide Treatment $+N_2H_4$	0.5-1	+	< 5	-	-	0.5 - 4
HT_2	Hydroxide Treatment N_2H_4	0.5-1	-	< 20 (< 100)	-	-	0.5 - 4
AVT_1	All Volatile Treatment	0.5-2	+	< 5	-	-	-
AVT_2	All Volatile Treatment	0.5-2	-	< 20	-	-	-
OT	Oxygenated Treatment	1 - 2	-	30-250	-	-	-
COHAC	Comb.Oxyg.Hy-draz.Ammonia Cond.	0.8-1	(+)	20-30	-	-	-

Corrosion and deposition in the water/steam cycle can be observed through chemical analysis and controlled by chemical means. The tools of chemical control are :

- Control of purity
- Control of pH
- Control of redox potential O_2, oxygen scavengers

Table 2 - Boiler Water Treatment in Drum Boilers					
Decade	**1950**	**1960**	**1970**	**1980**	**1990**
Denmark Great Britain Ireland South Africa Hong Kong	PT HT_1	PT_1 PT_2	PT_2 HT_1	HT_1 HT_2	HT_1 HT_2
Italy		PT_1	PT_2	AVT	AVT
Australia		PT_1 PT_2	PT_2 HT_1	HT_1 AVT	HT_1 AVT cohac
Germany	PT HT_1	PT_1 PT_2	PT_1 PT_2 HT_1	PT_1 HT_1 HT_2 AVT	PT_2 HT_1 HT_2 AVT
USA	PT HT_1	PT_1 PT_2	PT_1 PT_2	pt_1 PT_2 AVT	pt_1 PT_2 pt_3 ht_1 AVT ot
Canada		PT_1 PT_2	PT_1 PT_2	PT_1 pt_3	pt_2 PT_3

Table 3 - Water Treatment in Once-Through Boilers				
Decade	**1960**	**1970**	**1980**	**1990**
Western Europe	AVT_1 -	AVT_1 ot	$AVT_{1,2}$ OT cohac	AVT_2 OT cohac
Russia	AVT_1 -	AVT_1 ot	AVT_1 OT	AVT_1 OT
USA	AVT_1	AVT_1	AVT_1	AVT_1 OT
Japan	AVT_1	AVT_1	AVT_1	AVT_1 OT
South Africa	AVT_1	AVT_1	AVT_1	AVT_1 OT

Bold type   Dominant practice
Ordinary type   Few units - pilot tests

2. Control of purity

Purity control was the very first answer to the early problems of power generation concerning deposits in boilers due to hardness in make-up water. In the first stage hardness was eliminated by softening, but corrosion problems originating from salt contents of softened water called upon the "new" post-World War II technology - demineralization of make-up water. At that time many people believed that problems with deposition would disappear. There was nothing left in the water except for what had been added on purpose. However, these people did not understand the nature of separation processes being basically equilibrium processes, which means that there will always be something left.

Despite the fact that the chemical properties of the traces of impurities left in water do not change with time, the requirements on water purity were tightened throughout time. This is a result of several factors; first of all the load on materials is changing when installations for higher pressures and temperatures are designed. Besides, the demand for higher reliability and economic improvement resulted in great efforts to optimize all parts of power generation - even chemistry. The Silica "story" is very illustrative of this development. Until the dependence of silica's solubility in saturated steam on the pressure was recognised, the situation among power plant technicians was chaotic.

This development continues. Smaller and smaller traces are hunted to avoid troubles which could disturb safety or reliability or shorten lifetime.

3. Control of pH

The importance of boiler water pH control has been recognized from the very early stage of power generation. Addition of sodium hydroxide to boiler water was then the usual way to increase pH, resulting in lower corrosion rates. However, exaggeration of the dose and/or inappropriate design of the boiler often resulted in local increases of pH to values at which iron's amphoteric nature provided another type of attack on steal. This experience initiated an extensive aversion against boiler water conditioning with sodium hydroxide. In many countries sodium hydroxide was abandoned and phosphate was introduced as the new miracle aid. Phosphate did solve the actual problem of grooving and caustically initiated stress corrosion cracking, but it caused other problems too, which may not be that dramatic, but are still unpleasant and inconvenient. Hide-out at high load and return at low load were some of them. It is very difficult to control the "right" phosphate concentration as it changes all the time, and a relatively complicated analytical procedure for phosphate does not make the job any easier. The latest investigations even indicate that phosphate contributes to the higher solubility of the protective layer on steel.

Ammonia and hydrazine have been used for pH control of feedwater and condensate for a long time, so why not use it for boiler water as well? The classical All Volatile Treatment (AVT) was introduced. The only disadvantage of this treatment is the significantly lower pH in boiler water than in feed water or condensate due to high volatility of ammonia. Actually, a volatile base is needed, but with a somewhat lower volatility than for ammonia. This would provide very effective protection not only for the boiler, but also for the low pressure turbine, where early condensation takes place, concentrating almost every impurity in steam in the very first droplets of condensate. It would be convenient to ensure high pH in these droplets. Morpholine and other organic amines have been tried, but succeeded only in nuclear plants due to lower temperature of their steam. Organic amines decompose at higher temperatures to a number of organic acids contributing to the acidity of early condensate. In fossil plants this decomposition is excessive, and very few fossil plants operating at lower temperatures use organic amines.

However, AVT treatment became quite popular after it was recognized that the lower pH in boiler water must be compensated by higher purity. Table 4 shows a comparison of some guidelines for purity of boiler water at AVT and solid alkalized treatment.

Action level	N	1	2	3
Table 4 - Guidelines for Boiler Water Purity (16 MPa/20 MPa) Acid Conductivity (μS/cm)				
EPRI* AVT	<0.7 <0.22	>0.7 >0.22	>1.5 >0.43	>3 >0.84
VGB AVT	<5 <3			>5 >3
EPRI* Phosphate	<30 <10.7	>30 >10.7	>60 >21.3	>120 >42.5
VGB Solid Alk.	<50			>50
GOM 92*	<14.4			>14.4
Denmark	<15	>15		>50

* calculated values from chloride/sulphate specifications

Disadvantages of phosphate treatment and AVT brought some new initiatives to the agenda. The problems of caustic treatment were reevaluated and caustic treatment was reintroduced particularly after genuine research in Great Britain.
It became a dominant treatment in almost all British-influenced parts of the world and some of the European countries have adopted the caustic treatment as well.

The essential condition for success of caustic treatment is a real circulation in all parts in contact with boiler water. Actually it is not an unreasonable condition for either boilers with natural circulation or for boilers with forced circulation. The ironic thing is that the fear of failure due to caustic concentration is much more pronounced in England, where the reintroduction of caustic treatment started, than in countries which took results and just applied them. The English guidelines recommend dosing of caustic soda depending on the chloride concentration up to the same level as other users of the caustic treatment apply continuously. This means that according to English Guidelines the free caustic concentration should be lowered when there is no inleakage of chloride. The only reason for lowering the caustic level is the risk of caustic damage. However, other users of caustic treatment assume that the risk of caustic damage is the same, if not higher, during chloride inleakage. If circulation in the boiler is sufficient during chloride inleakage, it is surely sufficient during operation with pure boiler water. Thus, the same caustic concentration is required all the time, which is considerably easier to run and control.

However, according to recent information phosphate treatment will come back. Particularly for combined cycles with multistage steam generators, phosphate treatment is recommended by some manufacturers. The reason seems to be the safety at

chemical control failure rather than better performance under well-controlled chemical conditions. However, this logic is not quite consistent; the appropriate chemical control of caustically treated boiler water is very easy to establish on the basis of extremely reliable measurements of specific and acid conductivity, whereas control of phosphate treatment requires skilled chemists. The more risky, but better, protective method is so easy to control that it is often preferable. The risk is reduced to a degree where the benefit is justified. This is particularly true for utilities where high standard chemical control is customised.

4. Control of redox potential

From the early stage the necessity of controlling the redox potential was based on simple logic. It was a well-known fact that corrosion is due to steel oxidation. Thus, elimination of oxygen will naturally suppress corrosion. Later it was recognised that the protection of steel is a question of quality of an oxide protective surface layer. The reducing conditions at low oxygen concentration and low redox potential promote the formation of magnetite layers, which are reasonably stable, but in water environment rather porous and under certain conditions rather soluble.

In the seventies a new kind of protection was introduced independently in Germany and Russia. This protection was based on hematite stability at a somehow higher redox potential and lower pH than usually used for the classical magnetite type of protection. The higher redox potential was achieved by controlled addition of oxygen or hydrogen peroxide. This oxidized treatment was quite successful, but for once-through boilers only.

Pourbaix has qualitatively characterized the situation in a pH - Redox Potential diagram. The Pourbaix diagram has successfully been used to justify all possible different types of water conditioning. However, it only describes the conditions under which different iron compounds are most stable in thermodynamic terms. It does not quantify the equilibrium between this stable compound under certain conditions and all the less stable compounds. In other words, it does not describe the solubility of the compound in question; and the solubility of the dominant oxide is one of the most important parameters for the stability of the protective layer. The porosity of the oxide layer is the second most important parameter for the protection of steel. However, the porosity is most probably dependent on the solubility and other conditions at the formation process of oxide layer.

The protective oxide layer on steel surfaces in contact with water at the so-called oxygenated treatment is less soluble and less porous than the layer at so-called alkaline treatment at low redox potentials. It is therefore generally experienced that better protection of steel operating at moderately elevated redox potentials (oxygenated treatment) results in reduction of iron transport to the boiler.

5. Interaction of control parameters

It is very often forgotten to emphasize that the most important precondition for the positive experience with oxygenated treatment is high purity of the water with respect to anionic contaminants (low acid conductivity). The requirement on acid conductivity makes a well-operated condensate polisher a necessity for the units on oxygenated treatment. For a long time this requirement was the main reason why only once-through boilers were converted to oxygenated treatment. Boiler water of drum boilers concentrates impurities, and the acid conductivity here is far above the values normally expected at economizer inlet of once-through boilers (0.1 $\mu S/cm$). However, these two terms are not comparable. The boiler water should be compared with the last droplet of water in the evaporator of a subcritical once-through boiler. But nobody ever dreamed of measuring this value. Calculations show that at the stage of the evaporation process where still 1 % is in liquid phase the acid conductivity would be approx. 2 $\mu S/cm$ (25 °C), a value easily achievable in boiler water at AVT or caustic treatment. The tests made with oxygenated treatment on several drum boilers throughout the world indicate that these two situations are comparable with respect to the protection of evaporator construction materials.

In this discussion about the importance of redox potential we somehow ended in a discussion about the purity of water. This is of course due to the fact that all three main parameters affecting the steel protection - purity, pH and redox potential - are interdependent and an optimization of them must be carried out for each installation specifically. However, there is also a qualitative difference between controlling the purity of the system and the other two primary parameters - pH and redox potential. pH and redox potential can be controlled by dosage of chemicals, while purity is controlled by optimization of purification processes and removal of accumulated contaminants by special procedures. The control of purity level is therefore a more long-term strategic process. Thus, control of pH and redox potential must be adapted to the purity level achieved in the particular stage of development. The dependence !of relative protection quality on acid conductivity and oxygen concentration is illustrated in figure 1. The figure is based on extensive experiences with steel and not on any scientific investigation. On the figure lines are drawn for minimum pH, which have to be used for protection. It illustrates that the purer water is the more relaxed pH and oxygen have to be controlled.

These considerations have significant importance particularly at oxygenated treatment. Any conversion of a unit from AVT treatment to oxygenated treatment must be based on previous achievement of high purity conditions. And when the purity deteriorates during operation at oxygenated treatment, it is necessary at some point to change conditioning to alkaline treatment with low redox potential, because this conditioning is less sensitive to contamination. This means that the damage caused by impurities is less dramatic at high pH and low redox potential, nevertheless it is a damage.

9.8

6. Conclusion

The main tools of chemical control of water/steam cycle are the control of purity, pH and redox potential. There is a relatively broad range within which these parameters can be operated with good results. The particular choice of conditions is dependent on a number of specific factors attributed to the particular unit.

The range of control is illustrated in figure 1. It appears that no specific area is dedicated to alkaline treatment, nor is any area dedicated to oxygenated treatment. These two types of treatment are not of significant difference with respect to their basic chemical nature, as only the amount of hematite on the surface of magnetite is different. The difference is more or less based on the efforts to reach the chosen conditions. In one case the oxygen is removed with all economically avaliable means, whereas in the other case oxygen is added. There are many examples of these two efforts being realized. The oxygen is just there, fluctuating in moderate concentrations without any particular desire to keep it constant. Because of the physical design of the system it does not exceed some broad, acceptable limits.

The most important factor for the chemical protection of water/steam cirquit is the purity of the water. The pH and oxygen has to be optimized according to the water purity standards and the physical factors of the particular unit.

Figure 1

Parameters effecting quality of protective layer
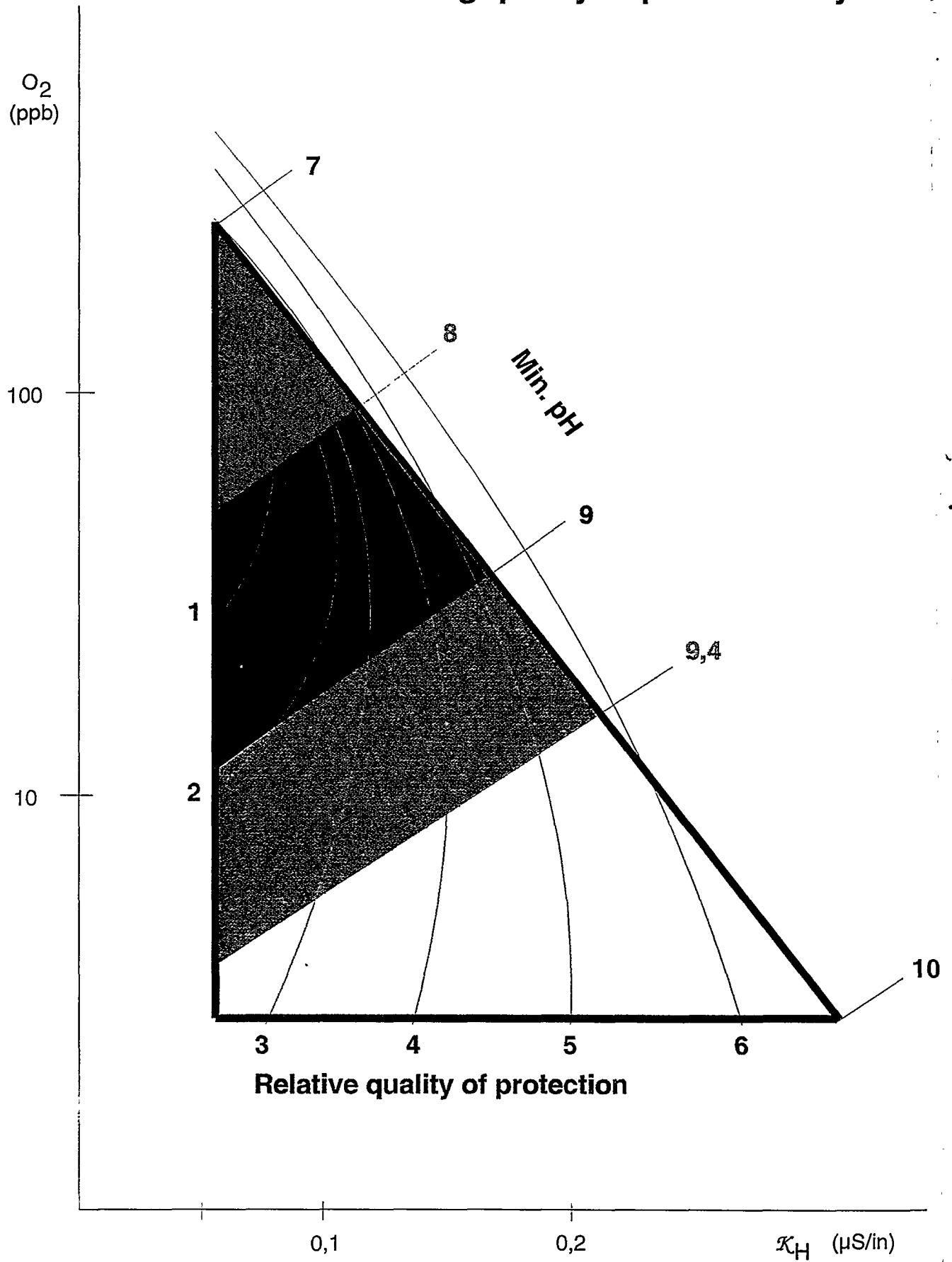
LOCAL ENVIRONMENTAL CONDITIONS AND THE STABILITY OF PROTECTIVE LAYERS ON STEEL SURFACES

Albert Bursik
Kornstrasse 47A
P.O. Box
68806 Neulussheim
Germany
and
Jørgen Peter Jensen
Department of Chemical Engineering
Technical University of Denmark
2800 Lyngby
Denmark

ABSTRACT
Local environmental conditions determine whether the protective layers on steel surfaces are stable. With unfavorable local environmental conditions, the protective layers may be subject to damage. Taking the cation conductivity of all plant cycle streams <0.2 μS/cm for granted, an adequate feed-water and - if applicable - boiler water conditioning is required to prevent such damage. Even if the mentioned conditions are met in a bulk, the local environmental conditions may be inadequate. The reasons for this may be the disregarding of interactions among material, design, and chemistry. The paper presents many possible mechanisms of protective layer damage that are directly influenced or exacerbated by plant cycle chemistry. Two items are discussed in more detail: First, the application of all volatile treatment for boiler water conditioning of drum boiler systems operating at low pressures and, second, the chemistry in the transition zone water/steam in the low pressure turbine. The latter is of major interest for the under-standing and prevention of corrosion due to high concentration of impurities in the aqueous liquid phases. This is a typical example showing that local environmental conditions may fundamentally differ from the overall bulk chemistry.

1. Plant Cycle Materials

Many different materials are in contact with operating medium (water, steam or super-critical fluid) in plant cycles of fossil-fired power stations. Chemists must take all specific properties of all plant cycle materials into consideration when looking for the optimum plant cycle chemistry. This task would be very simple, if a plant cycle consisted of one single material or at least of materials of one single group. Unfortu-nately, the opposite is true. The use of different materials or rather of different groups

of materials with different behaviors in contact with operating medium renders the selected plant cycle chemistry only a compromise.

1.1 Iron-Based Materials

Iron-based materials represent the most important group of materials that is used in fossil plant cycles. In many units, iron-based materials are applied in all plant cycle components and tubing except the condensate tubing. Several units erected in the last decade use iron-based materials even for the condensate tubing.

1.2 Non Iron-Based Materials

Among non iron-based materials, the following groups of materials are the most important:

- Copper and copper alloys (pure copper, red brass, Muntz metal, admiralty, aluminum bronze, aluminum brass, low silicon and high silicon bronzes, and copper/nickel alloys),
  used, e.g., for condenser tubing and for tubing of a few heaters operating at temperatures lower than 50 °C (for example, gland exhaust condenser). In many older units, copper or copper alloys have been used for the low-pressure and high-pressure heater tubing.
- Titanium,
  which is used more and more for the condenser tubing at units with seawater or brackish water cooling. The last two rows of low-pressure turbine blades are made of titanium in several units.
- Aluminum,
  which is used, e.g., for the tubing in air-cooled condensers.
- Nickel-chromium and nickel-chromium-iron,
  for use in highly aggressive or high temperature environment.
- Cobalt alloys,
  which are very often applied as hard facing materials, e.g., in boiler feed pump low flow valves, feed water and attemperation water control valves, and others.
- Synthetic materials,
  as ion exchangers and polypropylene yarn (both used in condensate polishing installations), elastomers used as gaskets and seals (vitons, Teflon, buna-N rubber, butyl rubber, neoprene, etc.), leak seal additives, and many other BOP synthetic materials.
- Other materials,
  as hard carbon with antimony impregnation and tungsten carbide with metallic nickel or cobalt binder (slip ring seals), chromium (chrome-plated steel in boiler feed pump wearing rings), and other BOP materials.

2.   Behavior of Iron-Based Materials in Plant Cycle

The extent of the use of non iron-based metallic materials in modern high-pressure plant cycles has been reduced to minimum. In major plant cycle components, out of non iron-based materials, only copper alloys and titanium (water-cooled condensers) or aluminum (air-cooled condensers) are applied for tubing. For this reason, this paper focuses on the behavior of iron-based materials in plant cycle conditions.

2.1   Condensate and Feedwater Train

Two groups of materials are used for the tubing of low-pressure and high-pressure heaters:

- Non alloyed and low-alloyed carbon steels.
- Stainless steels (austenitic, ferritic, and austenitic-ferritic steels).

In the low temperature region (about up to 200 °C), the protective magnetite layer forms only very slowly on the surface made of non alloyed and low-alloyed steel. The very thin magnetite film is covered with a thicker but loose and porous layer that can easily be wiped off. For this reason, such a layer can be damaged locally with unfavorable flow conditions, e.g., with a high turbulence. The dissolution of iron (the actual corrosion) still remains diffusion-controlled.

In pure water (cation conductivity <0.2 μS/cm), the dissolution process can be inhibited by an adequate treatment or conditioning. Two treatments are conceivable: the pH increase and the addition of oxidants. The combination of both treatments, the simultaneous application of both volatile alkali and oxygen is very popular mainly in cycles with once-through boilers. Detailed information on all three treatments can be found in the literature [1-3].

As expected, stainless steels applied in condensate and feedwater trains for low-pressure heater tubing are not subject to failures related to the damage of passive layers protecting stainless steels against corrosion.

In the high temperature region, a magnetite layer forms spontaneously on surfaces made of non-alloyed or low alloyed steel. For this reason, the corrosion of high-pressure heater tubing made of non-alloyed or low alloy steel, in general, is never a problem.

Under certain environmental conditions (flow, chemistry, and material), oxide and oxide hydrate films on carbon steel surfaces can be damaged by erosion/corrosion (flow-accelerated corrosion). This phenomenon may occur either in water or in a water/steam mixture. Recently, a compilation of present knowledge on flow-accelerated corrosion in power plants was published [4].

2.2   Water-Touched Boiler Tubes

As a rule, water-touched boiler tubes are made of non alloyed and low-alloyed steels (e.g., carbon steel and carbon-molybdenum steel). Under temperature conditions in the boiler system, the magnetite protective layer forms spontaneously on the tube surface. Nevertheless, an ingress of contaminants (e.g., cooling water, air, or chemicals from the make-up demineralizer or condensate polisher) and the corrosion product transport from condensate and feedwater train into the boiler can markedly influence the local environment on the surface of boiler tubes.

Boiler water of natural and forced circulation boilers must be conditioned to ensure that the dissolution of the protective layer is kept at a minimum. In this way, the internal iron species transport within the boiler is diminished. VGB Guidelines prefers the sodium hydroxide conditioning and all volatile treatment (AVT) [1]; in the United States several variations of phosphate treatment [5] and AVT [2] are the standard practice. Recently, oxygenated treatment [3] has been applied. As to the sodium hydroxide treatment, caustic gauging and stress corrosion cracking that occurred in the past give reason to be suspicious of this treatment in the United States. The fact that the international experience with this treatment was recently reviewed is promising.

Table 1 lists the boiler tube failure (BTF) mechanisms that are directly influenced or exacerbated by plant cycle chemistry.

2.3   Steam-Touched Boiler Tubes

Steam-touched boiler tubes (in superheaters and reheaters) are made either of non alloyed or low-alloy steels or of austenitic stainless steels. The formation of a protective duplex layer on the steam-touched surface of non alloys and low-alloys steels obeys the parabolic formation law. Ferritic steels often form laminated or multilaminated oxide layers tending to exfoliation.

Steam-touched boiler tube failures are rarely influenced by the local environment on the surface of those tubes. Table 2 lists the few steam-touched BTF mechanisms that are directly influenced or exacerbated by plant cycle chemistry.

2.4   Turbine

The turbine parts are made of relatively corrosion-resistant metals (12% chromium, in some cases austenitic steel or titanium). Nevertheless, blades, discs, and rotors manufactured of iron-based materials just mentioned are often subject to damage. Factors that cause or contribute to failures include both the components' design and the environmental (cycle chemistry-related) conditions. The blade and disk cracking are the major causes of turbine (= units) forced outages. The failure mechanisms that are influenced by cycle chemistry are pitting, corrosion fatigue, and stress corrosion.

10.4

Mechanism	Nature of Chemistry Influence
Hydrogen damage	Deposits formed from excessive feedwater corrosion products combined with a source of acidic contamination.
Caustic gauging	Deposits formed from excessive feedwater corrosion products combined with a source of caustic.
Acid phosphate corrosion	Deposits formed from excessive feedwater corrosion products combined with a source of phosphate
Chemical cleaning damage	Excessive deposits in waterwalls lead to chemical cleaning; process errors lead to tube damage.
Corrosion fatigue	Poor water chemistry, shutdown or lay-up practices, and improper chemical cleaning worsen contribution of the environment to causing damage.
Supercritical waterwall cracking	Excessive internal deposits lead to increased tube metal temperatures; exacerbates mechanism.
Fireside corrosion	Excessive internal deposits lead to increased tube metal temperatures; exacerbates mechanism.
Short-term overheating	Plugging of waterwall orifices by feedwater corrosion products.
Erosion/corrosion of economizer inlet headers	Attack by reducing feedwater conditions.
Pitting (economizer)	Improper lay-up.

Table 1:   BTF Mechanisms in Water-Touched Tubes that are Influenced by Cycle Chemistry [7].

Mechanism	Nature of Chemistry Influence
Long-term overheating (creep)	If caused by restricted steam flow as a result of contaminant deposits, debris, etc.
Short-term overheating	Blockage from improper chemical cleaning of superheater and reheater or of waterwalls.
Stress corrosion cracking (SCC)	Variety of bad environment influences, most directly related to chemistry control and practices.
Pitting (reheater)	Carryover of Na_2SO_4 or improper lay-up.
Chemical cleaning damage	Poor chemical cleaning practice.

Table 2:   BTF Mechanisms in Steam-Touched Tubes that are Influenced by Cycle Chemistry [7].

Recently, an extensive state-of-art review of knowledge concerning the chemistry and corrosive effects of turbine steam containing impurities was published [8]. The aspects covered here are impurity concentration mechanisms, distribution and effects of oxygen, liquid-vapor chemical transport (vaporous carry-over), steam flow and moisture nucleation, and effects of steam chemistry on droplet nucleation.

3.   Local Environment Conditions and the Stability of Protective Layers

The basic tasks of cycle chemistry are to prevent or minimize the ingress of contaminants into the cycle and to reduce the corrosion and deposition within the cycle by an adequate feedwater and - if applicable - boiler water conditioning. For these reasons, the chemistry surveillance is essential. Unfortunately, not even the best monitoring of the 'bulk chemistry' supplies any information on actual local environmental conditions in the critical areas of plant cycles in which the concentration of contaminants or conditioning chemicals may occur. It is important to stress that not the 'bulk chemistry' but the actual local environmental condition (local environment) affects the stability of protective layers.

3.1   Material Selection - Components' Design and Processing - Chemical Properties of Operating Fluids

In discussing the effects of the local environment, the interactions among the material selection, the components' design and processing, and the chemical properties of operating fluids must not be disregarded. Disregarding only a single aspect of this 'magic triangle' *Material-Design-Chemistry* will cause trouble. The daily practice in power stations supplies many impressive examples.

We assume that both the material selection and the design issues are appropriately taken in consideration. What about the third aspect of our triangle *Material-Design-Chemistry*? What type of chemistry are we talking about when dealing with the critical areas of plant cycles? It is certainly not the 'bulk chemistry' but the local environment. This defines whether the operating fluid in contact with the respective protective layers or the metal (metal selection) under local conditions (influence of design) is corrosive or not.

In section 4 (Examples), we will address two areas. The first is the AVT application for boiler water treatment of drum boiler systems operating at low pressure (e.g., at 60 bar). This question may be important for waste heat recovery steam generators or for low-pressure steam generators of combined cycles. The second task deals with the actual local environment conditions on the surface of the last blade rows of a low-pressure turbine. These blades are in contact with the first condensate.

10.6

3.2 Chemistry-Influenced Damage of Protective Layers

Out of all possible chemistry-related mechanisms of protective layer damage resulting in failures only the most important are listed here.

3.2.1 *Hydrogen Damage*

Hydrogen damage is caused by the reaction of iron carbides in the boiler tube steel with hydrogen produced as a result of corrosion reactions, particularly those taking place in low pH water [9].

$$Fe_3C + 2\,H_2 \rightarrow 3\,Fe + CH_4 \tag{1}$$

Hydrogen damage occurs preferentially under deposits where acidic cycle contaminants concentrate and locally lower the pH of concentrated boiler water.
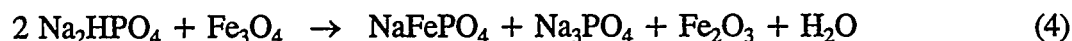
3.2.2 *Caustic Gauging*

Caustic gauging is caused by the reactions of concentrated sodium hydroxide with protective layer (2) and steel (3):

$$Fe_3O_4 + 4\,NaOH \rightarrow 2\,NaFeO_2 + Na_2FeO_2 + 2\,H_2O \tag{2}$$

$$Fe + 2\,NaOH \rightarrow Na_2FeO_2 + H_2 \tag{3}$$
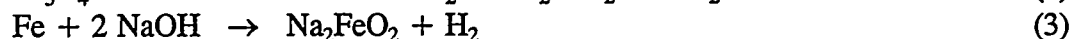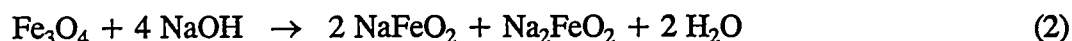
Caustic gauging, too, occurs under boiler tube deposits since sodium hydroxide may concentrate there with a factor $> 1,000$.

3.2.3 *Acid Phosphate Corrosion*

Acid phosphate corrosion is the third important type of the under-deposit corrosion leading to BTF. The reactions among the concentrated acidic phosphates and magnetite (4), (5) or steel (6) are probably the cause of acid phosphate corrosion [10]:

$$2\,Na_2HPO_4 + Fe_3O_4 \rightarrow NaFePO_4 + Na_3PO_4 + Fe_2O_3 + H_2O \tag{4}$$

$$3\,NaH_2PO_4 + Fe_3O_4 \rightarrow 3\,NaFePO_4 + \tfrac{1}{2}\,O_2 + 3\,H_2O \tag{5}$$

$$2\,Na_2HPO_4 + Fe + \tfrac{1}{2}\,O_2 \rightarrow NaFePO_4 + Na_3PO_4 + H_2O \tag{6}$$

3.2.4 *Corrosion Fatigue*

Corrosion fatigue occurs by the combined actions of cyclic loading and a corrosive environment. The primary occurrence is on the water-side in waterwalls and economizer tubing, usually located near attachments or restrains [9]. The importance of proper design (restriction of strain level in protective layer during operation) and proper chemistry during operation and lay-up (avoidance of oxide film damage) stresses again the inevitable coordination among material and design issues and plant cycle chemistry.

3.2.5 *Stress Corrosion Cracking*

Stress corrosion cracking (SCC) is the initiation and growth of cracks in a susceptible material by simultaneous exposure to stress and an adverse chemical environment [11]. This corrosion mechanism can occur in different plant cycle components, e.g., in

austenitic superheater tubes and in turbine components. Austenites are not the only materials susceptible to SCC. In many cases, also ferritic materials may be subject to SCC. Out of the possible plant cycle contaminants and conditioning chemicals, sodium hydroxide and chlorides are the most dangerous.

3.2.6 *Flow-Accelerated Corrosion*

Flow-accelerated corrosion (erosion/corrosion) is the next example of the triangle *Material-Design-Chemistry* importance. Only a combination of these three aspects leads to flow-accelerated corrosion damage:

- Material sensitive against erosion/corrosion.
- Design making a local heavy increase of mass transfer possible.
- Characteristics of operating fluid (e.g., pH and redox potential).

The erosion/corrosion occurs locally if the oxide layer growth is slower than the oxide layer dissolution intensified by a mass transfer increase.

3.3 Concentration of Impurities in Turbines

Concentration of impurities and/or of certain conditioning chemicals causes many corrosion problems in turbines. In each case, the damage of the passive oxide layer on the surface of a turbine component is a result of the concentration process and local environmental conditions. Here, not only the operational conditions but also those during lay-up are to be considered.

The presence of chemicals in steam is based on a liquid to vapor chemical transport. This includes both the mechanical and chemical carry-over. The possible concentration mechanisms in turbines are [8]:

- Deposition from superheated steam.
- Evaporation on hot surfaces.
- Concentration in condensed phases.
- Concentration on oxides.

In many turbine locations, there exists conditions which make the passive layer damage possible as a result of concentration processes. In no case the actual local environmental condition is identical with the 'bulk steam chemistry'. This is true for both the operation and the lay-up.

4. Examples

4.1 Waste Heat Recovery Steam Generators

4.1.1 Task Description
The poor design of several waste heat recovery steam generators contributes to serious corrosion problems. The originally intended boiler water treatment is the sodium hydroxide conditioning (≈ 1 mg/l NaOH in the boiler water). Due to circulation problems, the sodium hydroxide concentrates locally in some parts of the boiler system what results in BTF. For this reason, the application of AVT in waste heat recovery steam generators is analyzed for drum boilers operating around 60 bar.

4.1.2 Theoretical Basis
In AVT, ammonia is used for the conditioning of water by raising the pH and thereby minimizing the corrosion. The protecting layer of iron oxides on the boiler tubes consists predominantly of magnetite (Fe_3O_4). This analysis of minimizing the corrosion of boilers is therefore based on minimizing the solubility of magnetite. Comprehensive high temperature experimental studies of Sweeton and Baes [12] and Tremaine and LeBlanc [13] have provided most of the available data concerning the solubility of magnetite. In this work, the thermodynamic equilibrium constants estimated in [13] are adopted.

According to [13], the following iron species were present in the aqueous solution at the experimental conditions, Fe^{2+}, $Fe(OH)^+$, $Fe(OH)_2(aq)$, $Fe(OH)_3^-$, $Fe(OH)_3(aq)$, and $Fe(OH)_4^-$. The solubility of magnetite is a function of pH and the hydrogen fugacity if iron complexation reactions with impurities and conditioning chemicals can be ignored at a given temperature and pressure.

Since the solubility minimum with respect to pH is not a strong function of the hydrogen fugacity and hematite has been observed in the protective layer in many units, the hydrogen fugacity may be close to the equilibrium conditions for magnetite/hematite. If nothing else is stated below, the hydrogen fugacity is estimated from the magnetite/hematite equilibria.

Figure 1 shows the logarithm of the total moles of iron species per kg water at saturation (solubility of magnetite) as a function of the feedwater pH at 25 °C. The feed water pH is the pH of the solution before it comes into contact with the magnetite. Sodium hydroxide and hydrochloric acid was used to fix the pH. The hydrogen fugacity is 0.18 bar. Any iron chloride complex has been ignored. A similar plot produced by Tremaine and LeBlanc served as the basis for most guidelines for the feedwater pH at 25 °C almost regardless of the used pH-buffer.

4.1.3 Results of Calculations
In following, the optimal concentration of the pH-buffer with respect to minimal solubility of magnetite will be investigated for the different feedwater treatments. The use of different pH buffers which give the same pH at 25 °C will result in different

pH values for the solutions at elevated temperatures. It is therefore easier to analyze the effect of buffer systems by showing the solubility of magnetite as a function of the pH at the temperature (saturation pressure) of the solution. The black lines in Figure 2 illustrate the solubility of iron species at pressures from 40-80 bar as a function of the pH at the temperature of the solutions. The solid lines marked with symbols in Figure 2 correspond to the feedwater pH values (25 °C) of 7, 8.5, 9.1, 9.6, and 10 (feedwater conditioned with ammonia) to illustrate the effect of using AVT. It is observed in Figure 2 that an ammonia concentration corresponding to a feedwater pH higher than 10 (at 25 °C) is needed at 60 bar in order to be at the magnetite solubility minimum. At higher pressures, the pH range at which the solubility is close to the minimum is larger than at low pressures, and it is observed that the solubility increases with increasing pressure.

In order to provide guidance for utilities, a more informative graph may be a plot of the pH at the solution temperature where the acceptable pH ranges are shown corresponding to a solubility of magnetite that may be less than plus 10%, 20%, or 30% of the concentration of iron species at the solubility minimum vs. the boiler pressure.

Figure 3 shows that the solubility of magnetite increases from a concentration 10% larger than at the solubility minimum to a concentration 30% larger than at the solubility minimum when the pH of the boiler water at the actual temperature is changed by about 0.25 to 0.5 pH units. This result is consistent with Figure 2 where the solubility of magnetite is shown as a function of the pH of the boiler water. In Figure 3, the lines with open symbols show feedwater pH (at 25 °C) of 7, 8.5, 9.1, 9.6, and 10 set by ammonia dosing. Increasing concentration of ammonia in the feedwater results in higher pH values at higher temperatures (and pressures). However, ammonia concentrations corresponding to pH values at 25 °C covering a range of 3 pH units (from 7 to 10) result in a pH range less than one pH unit at elevated temperatures (Figure 3). Because ammonia is such a weak alkaline substance at high temperature, the effect on the pH of the boiler water when adding relatively large amounts of ammonia into the feedwater is limited. It is observed in Figure 3 where no impurities are present in the boiler water that an ammonia concentration in the feed water corresponding to pH (at 25 °C) =10 will enter the "+10%" acceptable pH range only close to 65 bar.

Solid alkali treated drum boilers where the boiler water contains sodium hydroxide and ammonia is recommended in [1]. Sodium hydroxide is dosed directly into the drum. Ammonia is added to prevent corrosion in condensate and feedwater train and during steam condensation. In Figure 4 and 5, the boiler water pH (at temperature) is shown as a function of the boiler pressure, the feedwater pH (at 25 °C) increased by an appropriate ammonia, and the constant sodium hydroxide concentration in the boiler water. The solid black lines with closed symbols indicate where the concentrations of iron species are 10%, 20%, and 30% larger than at the solubility minimum. The dotted lines indicate the location of the solubility minima with respect to pH. The lines with open with white symbols indicate different concentrations of ammonia in the feedwater. The gray lines with closed gray symbols are estimated

values for chloride concentrations of 10^{-5} mole/kg HCl in the boiler water at different ammonia concentrations in the feedwater. Figure 4 and 5 show that higher concentrations of sodium hydroxide are needed in order to operate at the optimal pH with respect to the solubility minimum for low pressure boilers than for boilers operating at higher pressures. At sodium concentrations corresponding to 1-2 mg/kg NaOH (Figure 4 and 5), the boiler water pH at temperature is not very sensitive to the concentration of impurities. However, mechanical and chemical carry-over of sodium hydroxide to the steam phase can result in potential corrosion problems in boilers and turbines.

4.1.4 *Discussion*

The operation of drum boilers with operating pressures ≤80 bar on AVT (ammonia) without any additional boiler water treatment results in an increased iron species transport within the waterwalls due to magnetite dissolution. This is true also for the operation with feedwater pH (25 °C) of 10. An increased iron species transport may cause deposition on heated surfaces which is a precursor of many corrosion mechanisms. For this reason, boiler water treatment with solid alkali (e.g., sodium hydroxide) is required.

Sodium hydroxide is an adequate conditioning chemical for those boilers. It ensures that the pH at temperature is set in the range of minimum magnetite solubility. With this boiler water conditioning even traces of acidic contaminants (10^{-5} mole/kg HCl in the boiler water) do not markedly influence the pH at temperature.

In many cases, drum boilers with operating pressures ≤80 bar are successfully operated on AVT (ammonia) without any additional boiler water treatment. The assumption is that in such cases a feedwater solid alkali contamination (e.g., from makeup) has contributed to an increased pH at temperature.

4.2   First Condensate in Low-Pressure Steam Turbines

The chemistry in the water/steam transition zone in the low pressure turbine is of major interest for the understanding and prevention of corrosion due to high concentration of impurities in the aqueous liquid phase. The driving force for achieving high concentrations of solutes under these conditions is the chemical potential of each of the species. At chemical equilibrium, there are no driving forces to change the concentrations of the species in the phases. Estimations based on chemical equilibrium for species with very small (< <1) distribution factors therefore represent maximum values for the concentrations of these species (electrolytes) in the condensed phase in a dynamic system.

Svoboda et al. [14] have constructed an early condensate collector where superheated steam is cooled to obtain a partial condensation. They measured the solute concentration of the anions in the condensate and the concentration of ammonia in both phases. The ratio of ammonia in both phases was independent of the condensation fraction of the steam. Surprisingly, the ratio of ammonia was 2-3 times lower than the values

reported in [15]. Svoboda et al. made the important observation that the concentration of the solutes increases with decreasing condensation fraction. In Figure 6, the concentration of the solutes in the condensate is shown at 105 °C as a function of condensation percentage for steam entering the low pressure turbine with a composition of 1 μg/kg chloride, 0.65 μg/kg sodium and 1 mg/kg ammonia calculated by STEAMCYC [16]. Figure 6 shows that basically all salts enter the early condensate and successive partial condensation dilutes the solutes. Unfortunately, Svoboda et al. were only able to reduce the condensation degree to 2%, so evidence that very high concentration can be achieved when very pure steam is expanding and cooled in a turbine-like environment is still missing. Analysis of water from condensate traps of wells from vapor-dominated geothermal fields indicates that high salinity solutions can build up in crevices [17]. Serious problems, such as pitting and stress corrosion cracking of turbine blades in condensation areas are typical problems of vapor-dominated geothermal systems [18].

Simple calculations can be made on whether chloride is a major threat by causing acid attack when the early condensate is formed. At low pH, the charge balance equation for the condensate can be approximated as

$$[Cl] \approx [H^+] + [Na^+] + [NH_4^+] \tag{7}$$

Assuming unit activity coefficients for the solutes the above equation can be rewritten as

$$[Cl] \approx [H^+] + [Na^+] + [NH_3 (v)] \cdot [H^+] / (K_{NH_3} K_h) \tag{8}$$

where K_{NH_3} is the partitioning constant for ammonia [15] and K_h is the hydrolysis constant for ammonium (19).

Multiplying (8) with the proton concentration gives

$$[H^+] \cdot [Cl] \approx [H^+] \cdot ([H^+] \cdot (1+[NH_3 (v)] / (K_{NH_3} \cdot K_h)) + [Na^+]) \tag{9}$$

Substituting (9) with the expression for the partitioning constant for HCl, K_{HCl} [19], gives

$$[HCl (v)] \approx K_{HCl} \cdot [H^+] \cdot ([H^+] \cdot (1+[NH_3(v)] / (K_{NH_3} \cdot K_h)) + [Na^+]) \tag{10}$$

It should be noted that if the concentration of sodium is negligible the concentration of HCl in the vapor phase increases with 2 orders of magnitude when the pH of condensate is lowered by one pH unit. Assuming that the early condensate is formed at 100 °C, pH (100 °C)=3 and [NH$_3$ (v)]=1.0 mg/kg; a HCl concentration in the steam of 79 μg/kg results.

5. In Conclusion

The stability of protected layers which form on water-touched and steam-touched surfaces of plant cycle materials is vital for a smooth plant cycle operation. Looking at the interaction between plant cycle materials and operation fluids, not the 'bulk chemistry', but the actual local environmental condition determines whether the protected layer will be damaged or not. The local environmental condition does not only mean the chemical composition immediately on the protective layer surface. All design-related parameters as, e.g., temperature, flow velocity and its patterns, heat flux and stresses must be considered when discussing the actual environmental conditions. The *Material-Design-Chemistry* interactions during operation and during lay-up (the latter is very often disregarded) are of substantial importance for trouble-free power plant operation.

6. Literature

[1]   VGB Guidelines for Boiler Feedwater, Boiler Water and Steam of Steam Generators with a Permissible Operating Pressure >68 bar. VGB Kraftwerkstechnik GmbH, Essen. VGB-R 450 L e (1996).

[2]   Cycle Chemistry Guidelines for Fossil Plants: All-Volatile Treatment. Electric Power Research Institute, Palo Alto, CA. EPRI TR-105041 (1996).

[3]   Cycle Chemistry Guidelines for Fossil Plants: Oxygenated Treatment. Electric Power Research Institute, Palo Alto, CA. EPRI TR-102285 (1994).

[4]   Chexal, B. et al.: Flow-Accelerated Corrosion in Power Plants. Electric Power Research Institute & Electricité de France (1996).

[5]   Cycle Chemistry Guidelines for Fossil Plants: Phosphate Treatment for Drum Units. Electric Power Research Institute, Palo Alto, CA. EPRI TR-103665 (1994).

[6]   Ball, M.: Sodium Hydroxide for Conditioning the Boiler Water of Drum-Type Boilers. Electric Power Research Institute, Palo Alto, CA. EPRI TR-104007.

[7]   Dooley, B. and McNaughton, W.: Boiler Tube Failures: Theory and Practice. Volume 1: Boiler Tube Fundamentals. Electric Power Research Institute, Palo Alto, CA. EPRI TR-105261-V1 (1996).

[8]   Turbine Steam, Chemistry, and Corrosion. Electric Power Research Institute, Palo Alto, CA. EPRI TR-103738 (1994).

[9]   Dooley, B. and McNaughton, W.: Boiler Tube Failures: Theory and Practice. Volume 2: Water-Touched Tubes. Electric Power Research Institute, Palo Alto, CA. EPRI TR-105261-V2 (1996).

[10]   Dooley, R.B. and Paterson, S.: Phosphate Treatment: Boiler Tube Failures Lead to Optimum Treatment. Proceedings of the International Water Conference 55 (1994), pp. 420-428.

[11]   Dooley, B. and McNaughton, W.: Boiler Tube Failures: Theory and Practice. Volume 3: Steam-Touched Tubes. Electric Power Research Institute, Palo Alto, CA. EPRI TR-105261-V3 (1996).

[12] Sweeton, F. H. and Baes, C.F. Jr.: The Solubility of Magnetite and Hydrolysis of Ferrous Ion in Aqueous Solutions at Elevated Temperatures. J. Chem. Thermodynamics 2 (1970), pp. 479-500.

[13] Tremaine, P.R. and LeBlanc, J.C.: The Solubility of Magnetite and the Hydrolysis and Oxidation of Fe^{2+} in Water to 300 °C. J. Sol. Chemistry 9 (1980), pp. 415-442.

[14] Svoboda, R., Sandmann, H., Romanelli, S., and Bodmer, M.: Investigations on the Early Condensate in Steam Turbines. White H.J. Jr. et al. (Editors): Physical Chemistry of Aqueous Systems - Proceedings of the 12th International Conference on the Properties of Water and Steam, pp. 720-729 (1995).

[15] Palmer, D.A. and Simonson, J.M.: Volatility of Ammonium Chloride over Aqueous Solutions to High Temperatures. J. Chem. Eng. Data 38, pp. 465-474 (1993).

[16] Jensen, J. P., Palmer, D.A., and Simonson, J.M.: Volatility Measurements of Dissolved Substances from Aqueous Solutions and their Application for Plant cycles (in German). VGB Kraftwerkstechnik 75, pp. 152-157 (1995).

[17] Truesdell, A.H., Haizlip, J.R., Armannsson, H., and D'Amore, F.: Origin and Transport of Chloride in Superheated Geothermal Steam. Geothermics 18, pp. 295-304 (1989).

[18] Andreussi, P., Corsi, R., Guidi, M., and Marini, L.: Theoretical Prediction of Physical and Chemical Characteristics of the "First Drop" of Condensate from Superheated Geothermal Steam. Implications for Corrosion and Scaling in Turbines. Geothermics 23, pp. 233-255 (1994).

[19] Thiessen, W.E. and Simonson, J.M.: Enthalpy of Dilution and the Thermodynamics of NH_4Cl(aq) to 523 K and 35 MPa. J. Phys. Chem. 94, pp. 7794-7800 (1990).

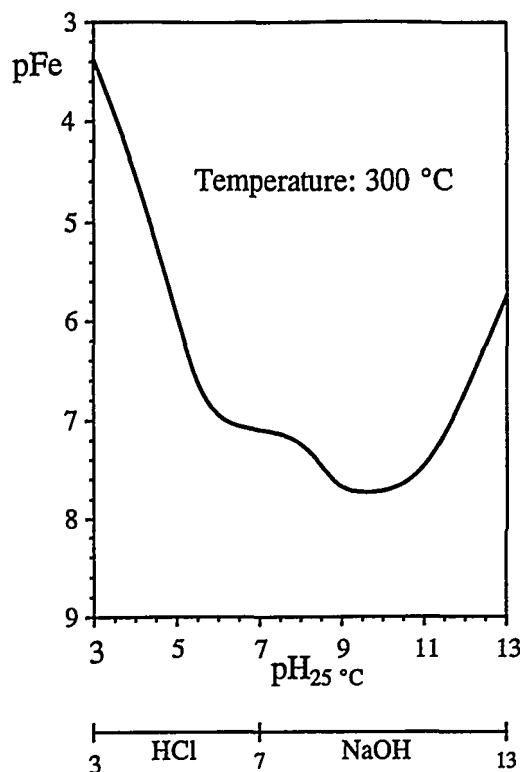**Figure 1:** Solubility of magnetite as a function of pH at 25 °C (pH buffered with HCl or NaOH) [13].

$pK = -\log[m(Fe,sat)]$; $m(Fe)$ in mole/kg.

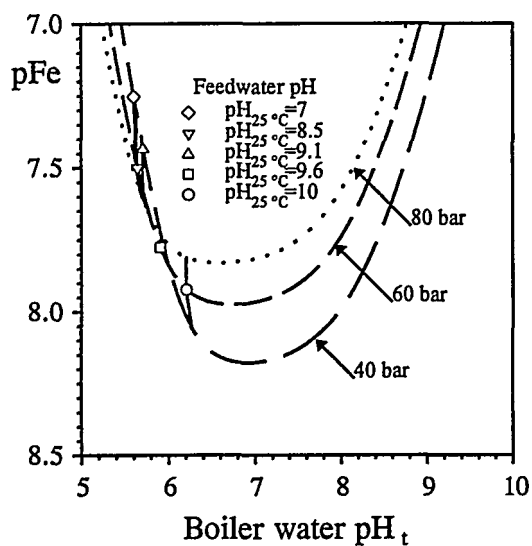**Figure 2:** Solubility of magnetite at saturation pressures of 40, 60, and 80 bar versus pH at temperature (pH_t).

$pK = \log[m(Fe, sat.)]$; $m(Fe)$ in mole/kg.

<u>Comment.</u> The actual boiler water pH at temperature (pH_t) is given as a function of feedwater pH at 25 °C ($pH_{25\,°C}$) for AVT without any additional solid alkali dosing.

10.15
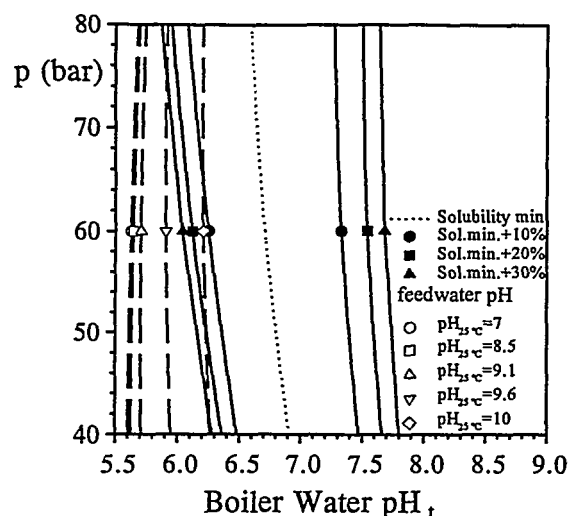
Figure 3: Boiler pressure (p) versus boiler water pH at temperature (pH$_t$).

AVT without any solid alkali dosing into the boiler water.

Comment. The dotted line corresponds to the magnetite solubility minimum. Solid black lines with closed symbols indicate concentrations of iron species 10%, 20%, and 30% larger than at the solubility minimum. The dashed lines with open symbols indicate the actual boiler water pH at temperature (pH$_t$) corresponding to the respective feedwater pH at 25 °C (pH$_{25\ °C}$).
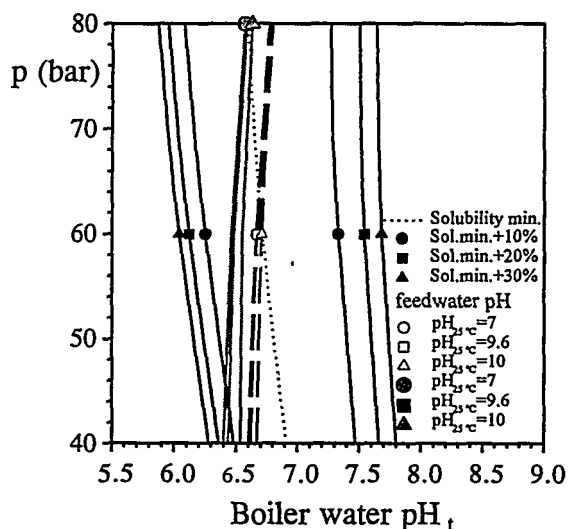
Figure 4: Boiler pressure (p) versus boiler water pH at temperature (pH$_t$).

AVT with an additional sodium hydroxide dosing into the boiler water (1 mg/kg NaOH).

Comment. The dotted line corresponds to the magnetite solubility minimum. The solid black lines with closed symbols indicate concentrations of iron species 10%, 20%, and 30% larger than at the solubility minimum. The dashed lines with open symbols indicate the actual boiler water pH at temperature (pH$_t$) corresponding to the sodium hydroxide concentration (1 mg/kg) and to the respective feedwater pH at 25 °C (pH$_{25\ °C}$). The gray lines with closed gray symbols correspond to the conditions of the dashed black lines plus a chloride concentration of 10^{-5} mole/kg HCl in the boiler water.
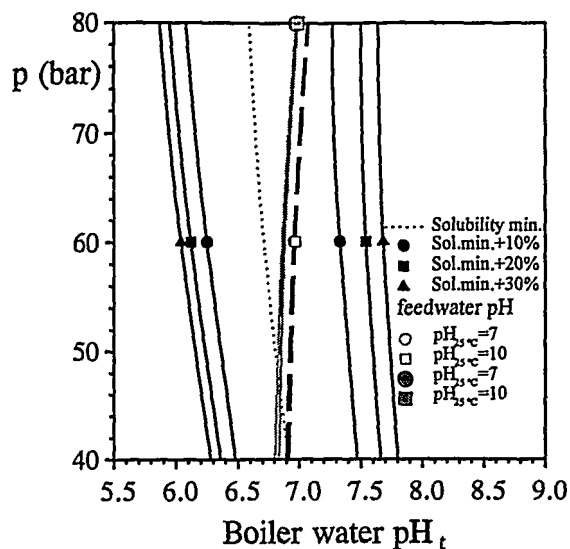
10.16

Figure 5: Boiler pressure (p) versus boiler water pH at temperature (pH$_t$).

AVT with an additional sodium hydroxide dosing into the boiler water (2 mg/kg NaOH).

Comment. See Figure 4, Comment; the sodium hydroxide concentration in boiler water amount to 2 mg/kg NaOH.
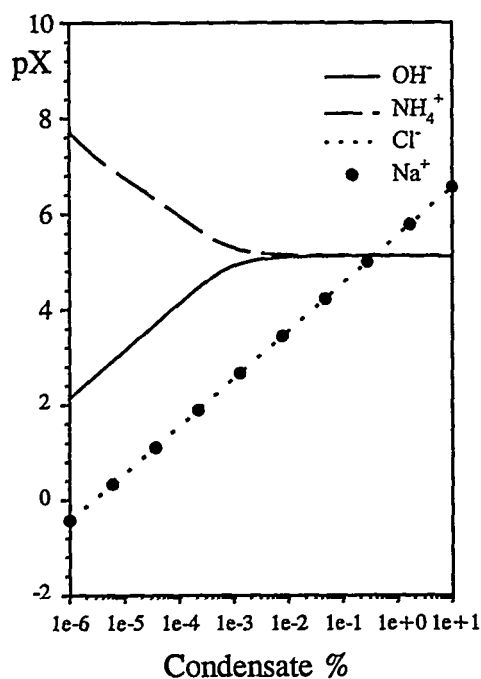

Figure 6: Concentration of the solutes in the condensate at 105 °C as a function of condensation percentage for steam entering the low pressure turbine.

pX = -log[m(I)];
m(I) in mole/kg;
I .... individual specie.

Comment. AVT (ammonia content 1 mg/kg NH$_3$); steam contaminants: 1 μg/kg chloride, 0.65 μg/kg sodium.

CHEMICAL AND MECHANICAL CONTROL OF CORROSION PRODUCT TRANSPORT

Ole Hede Larsen
Fælleskemikerne
I/S FYNSVÆRKET
Havnegade 120
5000 Odense C
Denmark

Rudolph Blum
Fælleskemikerne
I/S FYNSVÆRKET
Havnegade 120
5000 Odense C
Denmark

Karol Daucik
Fælleskemikerne
I/S SKÆRBÆKVÆRKET
Skærbæk
7000 Fredericia
Denmark

ABSTRACT

The corrosion products formed in the condensate and feedwater system of once-through boilers are precipitated and deposited inside the evaporator tubes mainly in the burner zone at the highest heat flux. As these deposits are heat insulating, deposition lead to increased oxidation rate and increased metal temperature of the evaporator tubes, hereby decreasing tube lifetime. This effect is more important in the new high efficiency USC boilers due to increased feedwater temperature and hence higher thermal load on the evaporator tubes. As there until now has been no material solution to that, the only way to reduce the load on the evaporator tubes is to minimise corrosion product transport to the boiler.

Two general methods for minimising corrosion product transport to the boiler have been evaluated through measurement campaigns for Fe in the water/steam cycle in supercritical boilers within the ELSAM area. One method is to reduce corrosion in the low temperature condensate system by changing conditioning mode from alkaline volatile treatment (AVT) to oxygenated treatment (OT). The other method is to filtrate part of the condensate with a mechanical filter at the deaerator. The results show, that both methods are effective at minimising Fe-transport to the boiler, but changing to OT has the highest effect and should always be used, whenever high purity condensate is maintained. Whether mechanical filtration also is required, depends on the boiler, specifically the load on the evaporator.

A simplified calculation model for lifetime evaluation of evaporator tubes has been developed. This model has been used for evaluating the effect of corrosion product transport to the boiler on evaporator tube lifetime. Conventional supercritical boilers generally can achieve sufficient lifetime by AVT and even better by OT, whereas all measures to reduce Fe-content of feedwater, including OT and mechanical filtration, should be taken, to ensure sufficient lifetime for the new boilers with advanced steam data - 290 bar/580°C and above.

1. Introduction

This paper concern the water/steam cycle of once-through boilers. Corrosion in some way occurs in all parts of this system, as the construction materials are not thermodynamic stable in water/steam. Corrosion products of relevance here, are those led by the feedwater to the boiler. These products are formed from the turbine outlets, through different heat exchangers and the condensate system to the economizer.

Materials in this system are mainly steel and Cu-alloys. Corrosion products are mainly Fe and Cu, although no copper is present in new boiler generations as seawater condensers are Ti-tubed and heat exchangers are made of steel. This corrosion gives two types of problems: 1) corrosion gives leakages and 2) corrosion products are transported to and deposited in the boiler tubes. This paper relates to the latter aspect.

Deposition of corrosion products lead to increased metal temperatures and this is especially significant in the newer generation high efficiency boilers with higher feedwater temperatures.

2.   Consequences of Corrosion Product Transport

Corrosion products, that is Fe-compounds in the new boiler generations, formed in the low temperature system are transported to the economizer and the evaporator tubes. These products are then precipitated and deposited on the tube inner surfaces mainly as iron oxides and -oxyhydroxides, Fe_3O_4, Fe_2O_3 and $FeOOH$. Deposition occurs from the entrance to the boiler until all liquid water has turned to steam, but the major part of deposition occurs in the zone of high heat flux near the location of the boiling point, or pseudophase transition point in the case of supercritical boilers [1].

This affects the boiler in two ways: 1) deposition can give rippled oxide surfaces leading to increased pressure drop in the evaporator and hence lower efficiency and 2) deposition gives thicker oxide layers and hence higher insulating effect leading to higher metal temperatures and increased material degradation in the form of hydrogen embrittlement and creep degradation. These effects may lead to requirements of acid cleaning of the evaporators, which is time-consuming and costly or if not detected in time, lead to major exchange of furnace wall.

The material temperature, which is the major factor for material degradation, depends on the temperature of the medium in the tubes and the temperature increase over the laminar boundary layer, the oxide layers and the tube wall - Henriksen et al. [2]. The temperature increase over the oxide layer increases as oxide thickness increases and consequently also the metal temperature increases during boiler lifetime.

The oxide layers are formed as a combination of selfoxidation of the steel and deposition of iron oxides from the feedwater [3]. While the latter in general remain constant during boiler lifetime, the selfoxidation is dependant on the oxide formation temperature and the protectiveness of the oxide layer. If oxide formation temperature is constant, the protectiveness of the oxide layer will cause the selfoxidation to follow a parabolic growth rate, that is with a decreasing rate during lifetime. Anyhow, as oxide layer grow due to selfoxidation and deposition, the oxide formation temperature increases and consequently also the rate of selfoxidation increases. The combined effect is dependent on a number of factors, where the heat flux, medium temperature and oxide heat conductivity are the most important.

As we are looking on the new generation boilers, the medium temperature effect is important, as feedwater temperature is increased for achieving high efficiency [4]. These boilers have spirally wound evaporators, where the burner zone have the highest heat flux, highest rate of iron oxide deposition and furthermore the lowest heat conductivity of the oxide layer, as deposited iron oxide has a high porosity [5]. These factors all tend to increase metal temperature. Also the top of the spiral tubes has high metal temperature due to high medium temperature, but in this place heat flux is lower and no iron oxide deposition occurs.

The only way to reduce the temperature load on the tubes in the burner zone, apart from constructional measures, is to minimise the transport of corrosion products to the boiler or remove the deposits by acid cleaning.

Two principal types of measures against corrosion product transport to the boiler are relevant:

- Minimise corrosion in the low temperature condensate system
- Removal of corrosion products from feedwater before entering the boiler

3. Measures against Formation of Corrosion Products

The corrosion products are formed in the low temperature condensate system from the turbine outlets, through heat exchangers and the condensate system to the economizer. Corrosion of materials in this system depends on a number of factors such as material, water purity, water conditioning and water temperature.

Considering the new generation boilers, where design leads to the highest temperature exposure of the evaporator tubes, different steels are used as materials of construction. Titanium tubing of the seawater cooled condensers is the only exception. No Cu-alloys are present. As Ti-tubes generally are not affected by corrosion, the only relevant corrosion products are Fe-compounds from corrosion of steels. Heat exchanger tubes are in an increasing degree made of stainless steels, on which corrosion in the relevant environment is insignificant. Some heat exchanger tubes and other parts such as mantles and pipes are made of mild steel. Corrosion of mild steel is dependent on water temperature, purity and water conditioning.

According to the guidelines used in the ELSAM system, the target for water purity is defined by an acid conductivity less than 0,1 µS/cm at 25°C. To further minimise corrosion of steels, water conditioning as either alkaline volatile treatment (AVT) or oxygenated treatment (OT) is used. Careful control of purity and appropriate conditioning is the only way to minimise the formation of corrosion products.

The traditional conditioning type is AVT, where the oxygen content is kept at minimum and the magnetite solubility is reduced by adding NH_3 to the condensate in concentration appr. 700-1000 µg/kg. AVT also offers some protection against salts in

the system and therefore this conditioning type is always used at start/stop and whenever the acid conductivity constantly exceeds 0,15 μS/cm.

When the salt content is low, a better protection against corrosion in the condensate system is offered by using OT conditioning. Details and experiences with OT are given in many publications [6]. By OT less NH_3 - appr. 150 μg/kg is added to the condensate and the iron solubility is reduced by forming a thin hematite layer on the top of the magnetite layer on tube surfaces. The hematite layer, which has a very low solubility, is formed by adding oxygen to the condensate in concentrations 50-200 μg/kg. In the boilers referred to, the oxygen is dosed just before and/or just after the deaerator.

At the first change from AVT to OT, generally a period of increased acid conductivities in the water/steam cycle is observed. This might be explained by redistribution of salts due to changing solubilities and by oxidation of organic material in the oxygenating environment. However, different boilers respond differently. At one plant, the introduction of OT was carried out over a long period, as much oxygen was lost through leaking deaerator valves. In this case only weak increases in acid conductivity was observed, whereas another boiler, where shift to OT was fast, more markedly increases in acid conductivity was observed, although for a shorter period. The type of ion exchange resin in the condensate polishing plant might also play a role as a contributor for organic materials. High release of leachables tend to create more acid conductivity from CO_2 in the condensate system at OT, whereas these leachables are oxidized at higher temperatures at AVT.
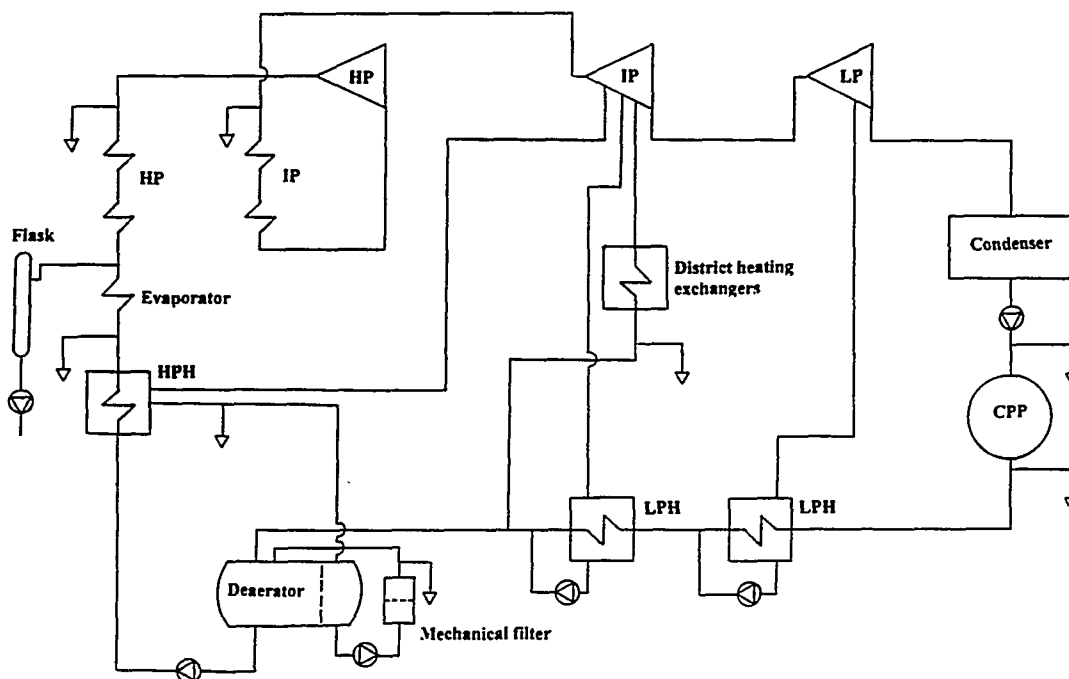

Figure 1. Sketch of typical water/steam cycle with sampling points indicated.

4. Measures against Corrosion Product Transport to Boiler

Hindering the corrosion products to enter and deposit in the boiler can be done by filtering all or part of the water entering the boiler or by discarding impure water.

All the relevant boilers in Denmark are equipped with continuously full-flow condensate polishing plants (CPP) consisting of cation and mixbed for maintaining high quality feedwater. The condensate polishing plant always treat the main condensate, but in special situations also the other condensates - hot condensate from district heating exchangers, high pressure heaters (HPH)-condensate etc. - can be discontinuously treated. Very impure condensate can also be discarded, but naturally this is feasible for very short periods only.

In addition to that, some boilers have mechanical filters installed at the deaerator for continuos filtration of some of the impure condensate streams or in some cases even all the condensate. A typical case is shown in figure 1, where the deaerator is separated in two parts with limited water exchange. The impure condensate streams such as from high pressure heaters and air heaters are led to one part of the deaerator, and from this side a stream is pumped through a mechanical filter to the other part of the deaerator, from where water is led to the feedwater pumps. Filters with different pore sizes are used on the various power plants. Pore sizes are ranging from 1 to 50 µm, where the optimum size probably is in the range 1-5 µm.

5 Evaluation of Measures

The measures taken will differ in different phases of boiler lifetime, where the following phases are most relevant:

- Plant commissioning and early operational period
- Start/stop of the plant
- Normal operation of the plant

5.1 Plant Commissioning and early operational Period

At commissioning and the first period hereafter, it is known, that the iron content of condensate/feedwater is high. Measurements made at commissioning of Vestkraft Unit 3 (VKE3) in 1992 showed Fe-concentrations at generally 10-20 µg/kg with a few peaks up to 50 µg/kg, for the first 2 and 3 months of steam production for main condensate after condensate pumps and feedwater at economizer inlet respectively.

In this period only AVT conditioning was used, as the requirements for using OT - very high purity water - was not achieved. The only possible mean of reducing corrosion product transport in this phase is to filter the impure condensate streams as discarding the water for such a long period of time is not feasible.

The VKE3-plant has a mechanical filter as described above. Condensate from the high pressure heaters, which is led to the "impure" end of the deaerator, showed high Fe-concentrations, often higher than 100 µg/kg. No measurement on the Fe retention was made, but there was clearly build-up of ΔP over the filter, which necessitated frequent back washing. During back washing, high content of corrosion products could be observed, which demonstrates, that a high amount of Fe has been removed from the condensate. Also the condensate polishing plant was used for partial cleaning of the condensate in order to reduce the load on the mechanical filter.

So even not quantified, a substantial amount of corrosion products can be removed with a mechanical filter during the commissioning and the early operational period.

5.2 Start/stop of the Plant

Also at start/stop of the plant, AVT has to be used, as salts are redistributed in the system, thus disenabling OT conditioning and only filtration or discarding water is possible.

Also in this case only few measurements are available. Midtkraft Studstrup Unit 3 and 4 (MKS3 and 4), also have mechanical filters at the deaerators. Measurements from cold-starts show Fe-concentrations in the impure condensate decreasing from 600 µg/kg at start to 200 µg/kg 2-4 hours later. Measurements also showed, that less than 10 % of this Fe was removed in the filter. The filter pore size of 50 µm is apparently to high.

Anyhow the measurements show, that there is a large potential for removal of Fe from the condensate at start up and this could probably be achieved with a mechanical filter with smaller pore size in the range of 1-5 µm.

5.3 Normal Operation of the Plant

During normal operation, the water purity is generally high, with acid conductivity less than 0,1 µS/cm, and therefore it is possible to use OT conditioning for minimising Fe-uptake in the condensate system. Also mechanical filters are used at normal operation.

Both measures has been evaluated during a large measurement campaign at Fynsværket Unit 7 (FVO7), a supercritical boiler 400 MW; steam data 250 bar/540°C/540°C. This plant also has a mechanical filter at the deaerator, where the main condensate is led to the pure water side and condensate from high pressure heaters, air heaters and a heat exchanger for flue gas reheating are led to the "impure" side, from where condensate is pumped through the filter to the pure side. Fe-measurements has been made on most important streams through a period running on AVT conditioning and in a subsequent period, after turning to OT conditioning.

A simplified sketch of the water/steam cycle is shown in figure 1, where HPH-condensate is the only "impure" condensate shown. The sampling points are also

11.6

indicated. Most of the sampling equipments are designed for isokinetical sampling. Samples are generally taken twice a week during normal operation and all samples are analysed for total Fe-concentration. At the same time NH_3 concentration in HP-steam was measured and O_2 concentration of feedwater is continuously monitored.

The iron content was on an acceptable level during the AVT period, but showed a clear reduction after turning to OT-conditioning, as seen in the hot condensate from district heating exchangers (figure 2) and feedwater at economizer inlet (figure 3).
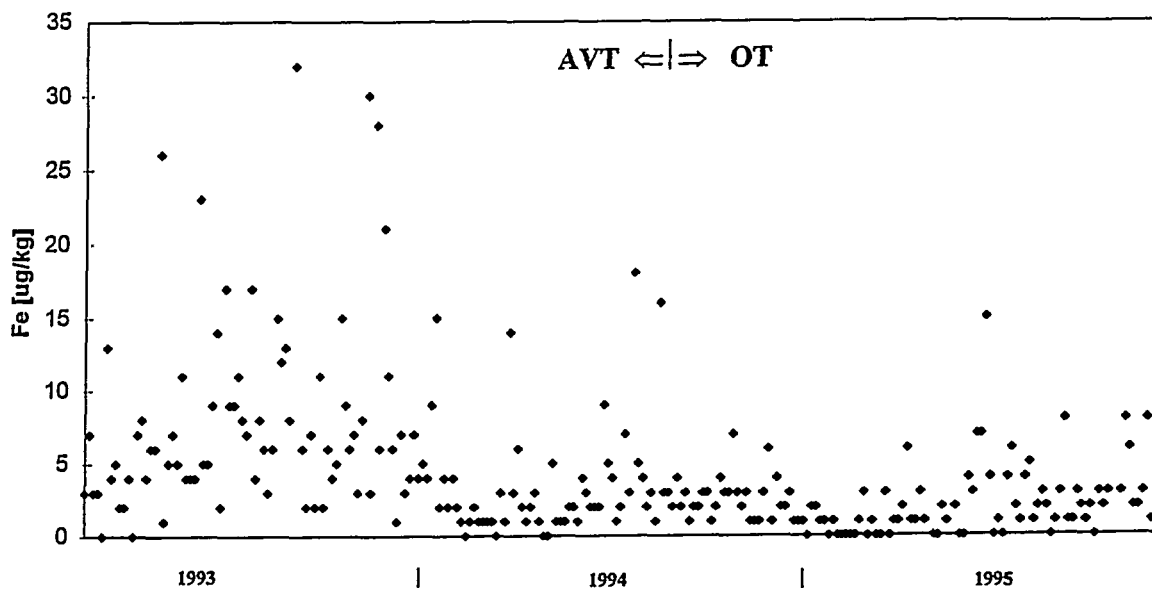

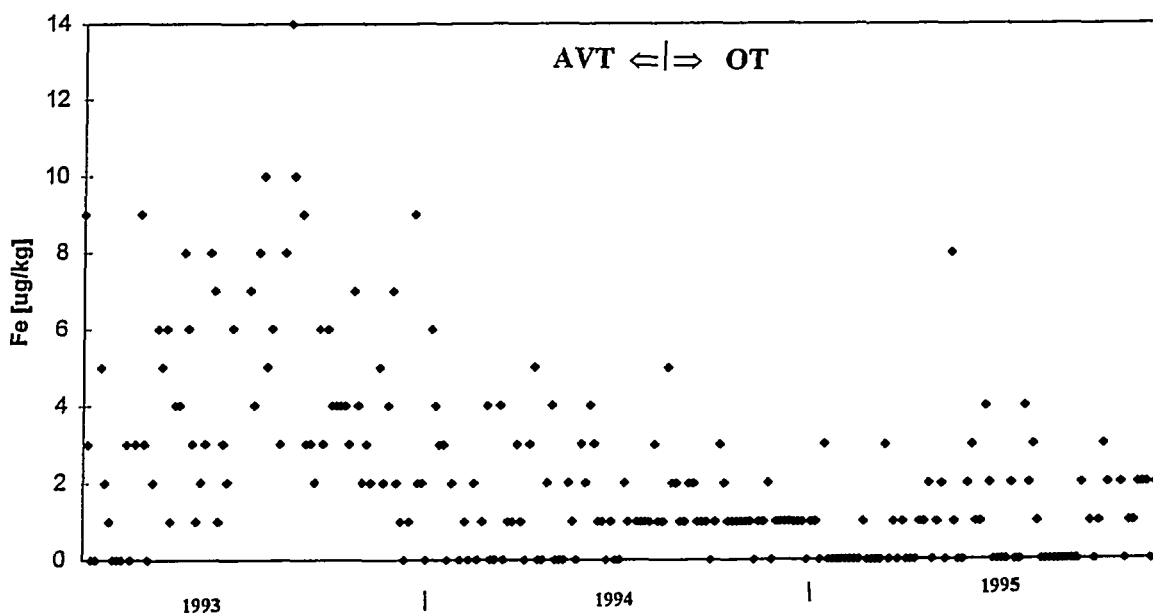**Figure 2.** Fe-concentrations in the hot condensate from district heating exchangers

Figure 3. Fe-concentrations in feedwater at economizer inlet

11.7

The largest reduction in Fe-content occur in the condensate from the high pressure heaters (figure 4). At AVT, this condensate had relatively high Fe-concentrations - 8 µg/kg in average, but at introduction of OT, the Fe-concentrations immediately decreased to 0-2 µg/kg. This gives the advantages of decreasing corrosion in the heat exchanger, decrease Fe-contribution to the feedwater and in general lowering the deposition of iron oxides in critical components as valves. At AVT, the regulating valve for the discharge of HPH-condensate to the deaerator was frequently blocked up by magnetite deposits and cleaning had to be done each 2-3 month. Figure 5 show the disassembled valve after 2 month of AVT conditioning. After the introduction of OT, the valve has been in operation for 2 years without need for cleaning.
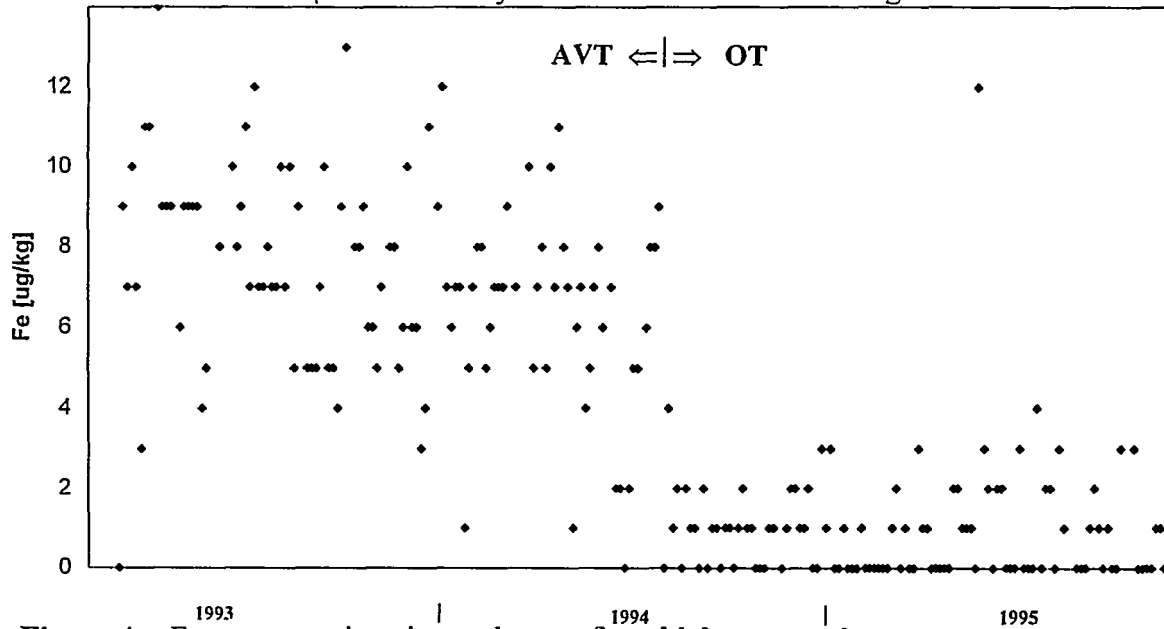

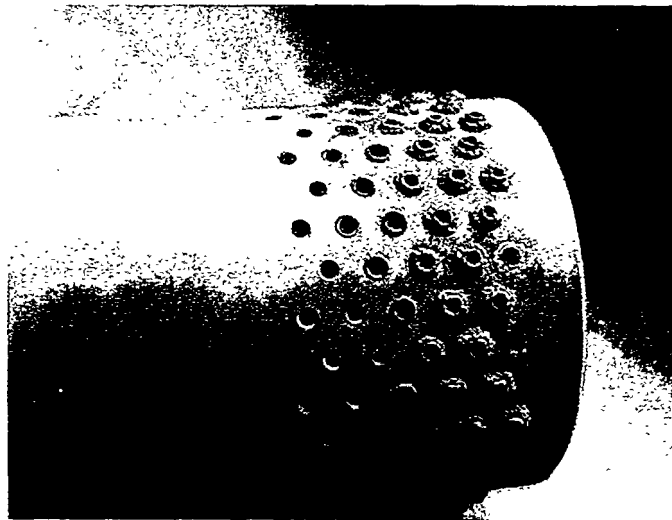**Figure 4.**   Fe-concentrations in condensate from high pressure heaters

Figure 5.   Discharge valve for HPH-condensate after 2 month of AVT conditioning
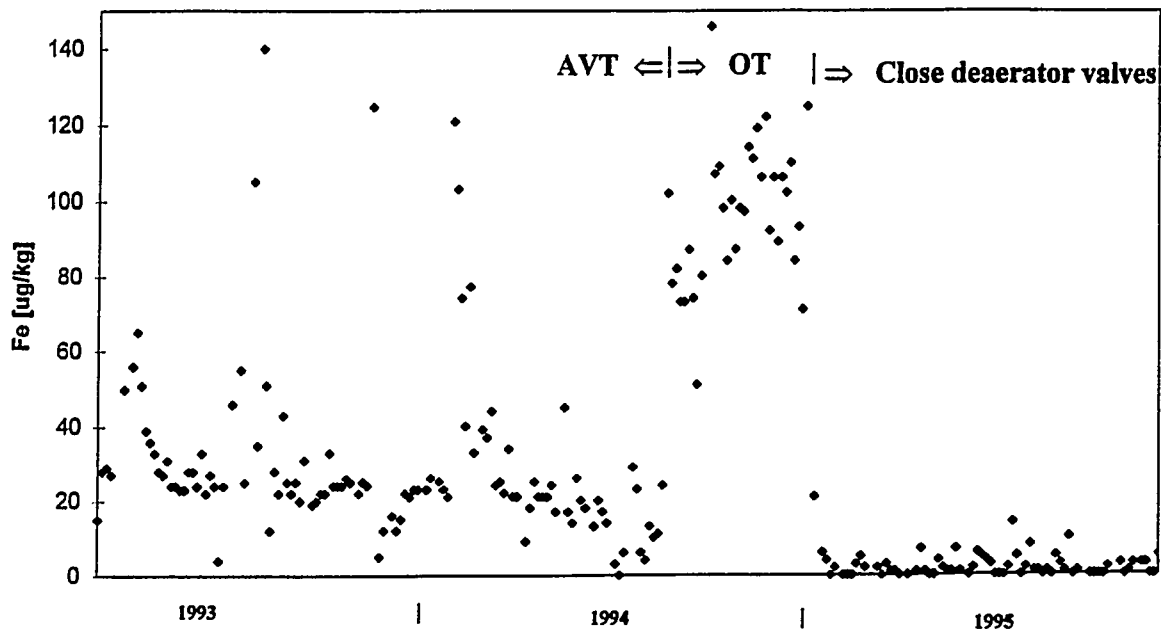
11.8

Figure 6. Fe-concentrations in condensate from flue gas reheater heat exchanger

A curious effect of OT was observed on condensate from the flue gas reheater heat exchanger, as it showed a significant increase in Fe-content, when turning to OT (figure 6). It was found, that this probably could be related to the deaeration to the condenser, whereby most of the oxygen is lost. As the NH_3 concentration also is low, only poor corrosion protection is offered. This problem was then solved by closing the deaerator valves (and opening them shortly periodically), and as can be seen in figure 6, the Fe-concentration hereafter is reduced to a very low level.

It might here be inferred, that also the other heat exchangers that are deaerated to the condenser, should lose the oxygen and hence give increased corrosion. There are several reasons, why this does not occur. Firstly the other heat exchangers have tubes of stainless steel and only the mantle is made of mild steel, whereas the flue gas reheater heat exchanger is tubed with mild steel. Another reason is that the other heat exchangers are not as efficiently deaerated as the mentioned, which might be explained by the smaller size or the opening position of deaerator valves.

Table 1 shows the average values of Fe-measurements for each of the periods AVT and OT. The OT period has been divided in two periods for the streams affected by the period with high Fe-concentration in flue gas reheater heat exchanger. Table 1 shows, that the Fe-concentrations has been reduced with 40-80 % by change from AVT to OT, except for the main condensate, where the reduction is smaller. Most important is the feedwater, where the Fe-concentration is reduced with 65 %, that is, the transport of corrosion products to the boiler has been reduced to one third of the original level.
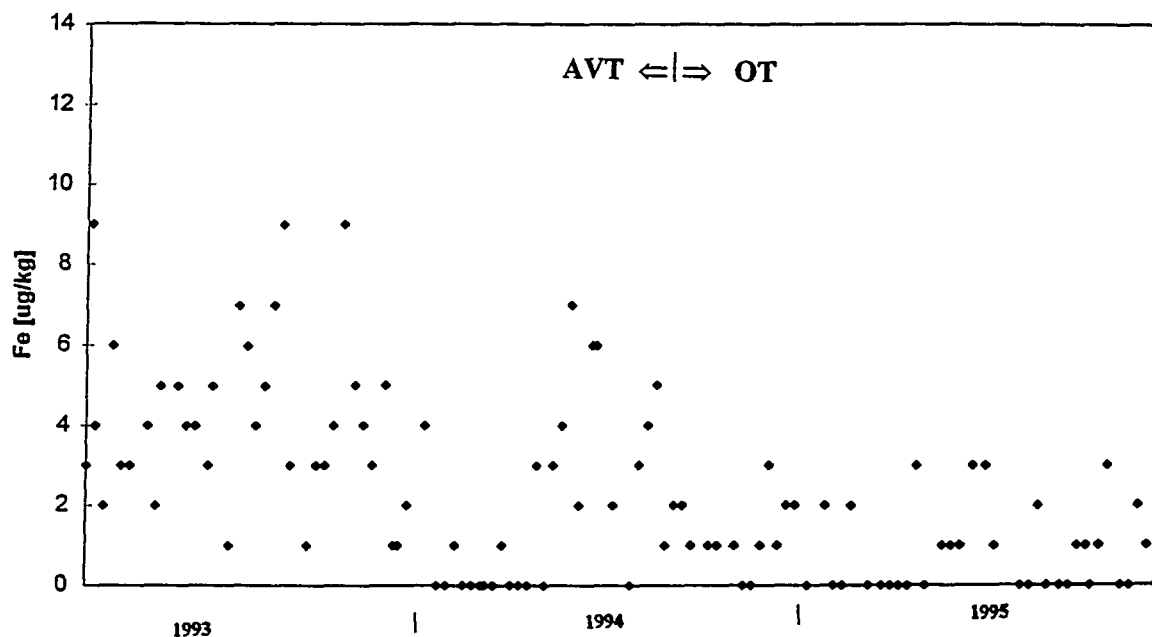
Figure 7. Fe-concentrations in effluent from the mechanical filter

	AVT	OT	
Main condensate after pumps	7.6	8.2	
After CPP	2.3	1.4	
Hot cond. after district heating exchanger 1	6.0	2.4	
Hot cond. after district heating exchanger 2	4.0	2.4	
Feedwater at economizer inlet	3.0	1.0	
HPH condensate	7.7	1.0	
Cond. from flue gas reheater exchanger	32.8	32.8	2.2
After mechanical filter	3.6	1.0	0.8

Table 1. Average values of Fe-measurements for each of the periods AVT and OT

An investigation of the efficiency of the mechanical filter at AVT and OT has been performed based on the abovementioned results. The Fe-concentration of water to the filter is calculated from Fe-analysis of HPH-condensate and flue gas reheater condensate constituting 96 % and 2 % of the flow respectively. The remaining 2 % is air heater condensate, which could not be analysed. To illustrate the effect of this condensate, two different levels of Fe were assumed in the calculations. The Fe-concentration in the effluent from the filter was analysed and a substantial reduction was observed after change to OT (figure 7).

	Flow (kg/s)	AVT		OT a		OT b	
Fe-concentrations (µg/kg)							
HPH condensate	56.0	7.7		1.0		1.0	
Flue gas reh. cond.	1.3	32.8		32.8		2.2	
Air heater cond.	1.3	10.0	50.0	10.0	50.0	10.0	50.0
From mechanical filter	58.6	3.6		1.0		0.8	
Fe-flow (µg Fe/s)							
To mechanical filter	58.6	487	539	112	164	72	124
From mechanical filter	58.6	211		59		47	
Removed in mech. filter		276	328	53	105	25	77
Fe removed in mechanical filter							
in % of Fe to mech. filter		57	61	48	64	35	62
in kg/year		7.3	8.7	1.4	2.8	0.7	2.0
Fe-flow to the boiler (kg/year)							
+ mechanical filter		16.8	16.8	5.6	5.6	5.6	5.6
÷ mechanical filter		24.1	25.5	7.0	8.4	6.3	7.6
Fe-concentration in feedwater to the boiler (µg/kg)							
+ mechanical filter		3.0	3.0	1.0	1.0	1.0	1.0
÷ mechanical filter		4.3	4.6	1.3	1.5	1.1	1.4

The OT period has been divided in two periods (a and b) for the streams affected by the period with high Fe-concentration in flue gas reheater heat exchanger. For each period two different levels of Fe-concentration (10 and 50 µg/kg) of the air heater condensate were assumed in the calculations.

Table 2. Calculated Fe-balance at the deaerator - mechanical filter at FVO7.

The results are shown in table 2. At AVT the cleaning efficiency for Fe is appr. 60 %. At OT the efficiency is 50-60 %, when some of the condensate still has high Fe-concentration and 35-60 % when condensates are more pure. The calculated efficiency is very dependent on the assumed Fe-concentration in the air heater condensate, especially at OT, where the total Fe-level is lowest. So it seems, that the cleaning efficiency is the same at AVT and OT, but perhaps decreased somewhat at OT, in cases where the "impure" condensates have very low Fe-concentrations. This possible decrease does not seem related to any change of the form of corrosion products due to the oxygenating chemistry but instead to the general lower Fe-concentrations gained by the oxygenating chemistry. In that case, increases in Fe-concentrations of different causes during OT conditioning will result in increasing filter efficiency.

The effect of OT-conditioning and filtration of some of the condensates on the Fe-supply to the boiler also can be seen from table 2. At AVT, mechanical filtration reduce [Fe] in feedwater from 4.5 to 3 µg/kg. This is further reduced to 1µg/kg by introducing OT, but if filtration was omitted, [Fe] in feedwater would be 1.1-1.5 µg/kg.

Evidently, the highest effect on minimising Fe-supply to the boiler is related to change from AVT to OT, but still the effect from the mechanical filter is significant. As OT also is economically attractive due to less chemicals and less regeneration of ion exchange resins, this conditioning should be used, whenever a high standard of water quality is maintained. Whether a mechanical filter also is recommended, depends on the boiler, specifically the load on the evaporator as will be discussed in chapter 6.

Before that, some observations and further experiments on OT conditioning will be discussed.

An experiment was set up, with the aim of investigating the optimum O_2-concentration for OT conditioning. The idea was to use the flue gas reheater heat exchanger, as the Fe take up due to corrosion herein reacted promptly on opening/closing deaerator valves, hereby changing the O_2-concentration of the steam/condensate, as seen in figure 6. At the experiment, the deaerator valves were gradually changed and $[O_2]$, $[NH_3]$, $[Fe]$ and conductivity of the condensate measured.

The results are shown in figure 8. The experiment did not give all the required results, but anyway show interesting features. In top of the figure, the valve position is illustrated (VOP). First the valves were closed, whereby $[O_2]$ varies between 20 and 80 $\mu g/kg$ and the $[Fe]$ is low - 0-2 $\mu g/kg$. Hereafter the valves were opened fully and instantaneously the $[O_2]$ drops to <1 $\mu g/kg$. It is interesting here to note, that $[Fe]$ remain low for one month before increasing to > 50 $\mu g/kg$.
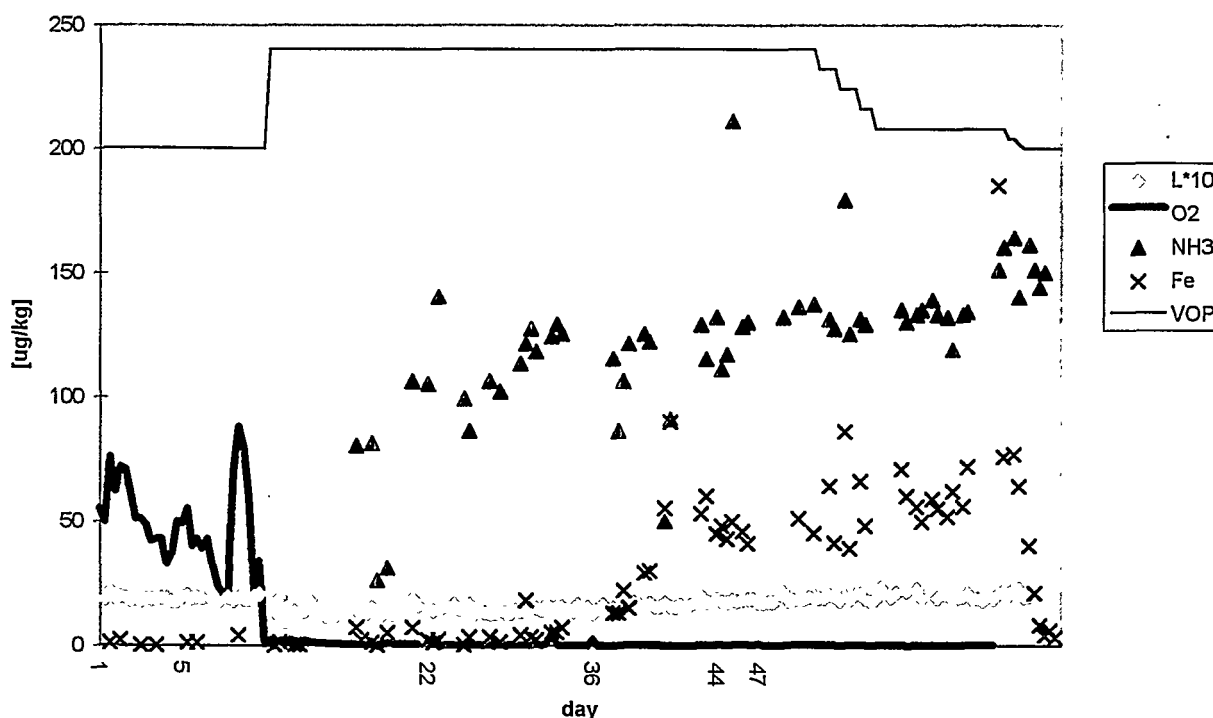
Deaerator valves are closed at VOP = 200 and full open at VOP = 240. L*10 = conductivity (25°C)*10

Figure 8.   Results from experiment with the flue gas reheater heat exchanger

This illustrates the high protectiveness of the hematite layer as it takes one month to destroy this layer after turning from OT to the more corrosive conditions with low [NH$_3$] and low [O$_2$].

Later the deaerator valves were gradually closed in order to gradually increase [O$_2$]. Unfortunately the oxygen monitor failed just at the end of this operation and the exact time of [O$_2$]-increase can not be seen directly, but is very close to the valves being totally closed. At this time also a small increase in [NH$_3$] is observed. At this time, the [Fe] drops to < 5 μg/kg within one or two days.

It can be concluded, that it takes very short time to build a protective hematite layer upon introduction of oxygen, but the protective layer remain stable for a long time, even when the corrosive environment is changed by removing oxygen without increasing alkalinity.

This also mean, that the protective layers also will remain stable during short periods of more corrosive environment at changing from OT to AVT at start/stop.

Another point to consider is, that although the low Fe-concentrations in the water/steam cycle at OT as shown in table 1 are reasonable consistent, there are periods or events where higher Fe-concentrations occur, even though the [O$_2$] and [NH$_3$] in the system are correct and the acid conductivity is low. There can be different reasons for this.

One explanation could be, that if the condensate polishers, especially the cation filter, are fouled with corrosion products, they might start to release Fe during operation. This can usually be helped with more frequent and more efficient cleaning of the filters, f.ex. by enhanced airscrubbing or prolonged HCl-soaking at regeneration.

Another potential mechanism for having periods with increased Fe uptake in the condensate system is the deaeration from heat exchangers to the condenser as the situation described above with the flue gas reheater heat exchanger. Even though most modern heat exchangers have stainless steel tubes, the mantle and pipes often are mild steel and corrosion is possible.

Former measurements of oxygen content of the different condensate streams showed relatively large variations in [O$_2$], that is from 5 to 100 μg/kg although [O$_2$] in feedwater were quite stable at 150-200 μg/kg. These variations seems partly related to load, but also other factors are determining. Therefore these heat exchangers are exposed to an environment, that is alternating protecting (high [O$_2$]) and aggressive (low [O$_2$]). However the Fe-analysis did not show increased Fe-uptake in the periods with low [O$_2$].

This can probably be explained from the results given in figure 8 - that is, it is fast to build the protective hematite layers but it takes a long time to destroy them. Only when running at very constant operating conditions that promotes constant low O$_2$-concentration, the corrosion will increase.

6. Discussion of Relevance for different Boiler Generations

For conventional supercritical boilers - 250 bar/540°C - evaporators are usually made of 1 % Cr-steels, and the thermal exposure is generally on such level, that sufficient lifetime can be realised, when the level of corrosion products in the feedwater is relatively low.

In the new generation ultra supercritical (USC) boilers - 290 bar/580°C - the thermal exposure on the evaporator is significantly increased due to higher feedwater temperature. Until now, there has not been new better steels to solve this problem and the only solution is to achieve feedwater with very low concentration of corrosion products.

The results given above, show which levels of Fe-concentration in the feedwater to the boiler can be achieved by different means, that is mainly OT conditioning and mechanical filtration and some other measures at commissioning and start/stop. It will always be advantageously to use OT instead of AVT, provided that a high standard of water quality is maintained, and turning to OT also has the highest impact on reducing Fe-transport to the boiler. On the other hand, it is not as simple to evaluate, whether mechanical filtration should be recommended, as it is costly and even though the efficiency is maintained, the absolute effect is less at OT than at AVT, as the Fe-concentration is lowered beforehand.

Therefore the need for reduction of Fe-transport to the boiler should be evaluated. As has already been discussed in chapter 2, this need arises from the fact, that Fe in feedwater make deposits in the evaporator tubes, which give rise to increased metal temperatures and reduced lifetime. The future boilers operate at higher steam temperatures and therefore also the feedwater temperature increases, thereby increasing thermal exposure of evaporator tubes.

Due to the higher steam temperatures in the advanced boilers, a calculation model for lifetime evaluation of superheater tubes described in [2] has been developed and is going to be extended to include evaporator tubes. By now, a simplified model has been made for evaporator tubes, including deposition of iron oxides from feedwater. The deposition of corrosion products from feedwater, the finwall construction and the one-sided heat affection makes the situation more complicated for evaporator tubes than for superheater tubes. The team behind [2] are in progress of developing a more sophisticated model for evaporator tubes, which is also being "calibrated" on tube samples from boilers, but until that, the existing model can be used at least to give indications of the real conditions.

Two generations of boilers has been evaluated. A is a conventional supercritical boiler, with steam data 250 bar/540°C/540°C and B is the new USC-boiler with steam data 290 bar/580°C/580°C/580°C. The major difference with respect to evaporator lifetime is the medium temperature at the burner zone, which is appr. 390°C and 420°C for the two boilers respectively - that is a difference on 30°C. Also other factors as pressure and

tube dimensions differs in the two boilers, whereas factors as heat flux and water/steamside heat transfer coefficient are almost equal. Heat conductivity is assumed to be lower for the deposited oxide than oxide formed by selfoxidation, due to higher porosity [5]. The material is 13CrMo44 in both boilers.

For both these boilers, lifetime calculations has been made with 3 different levels of Fe-concentrations in the feedwater. The distribution of deposited corrosion products is not precisely known and will probably vary from boiler to boiler. Therefore the Fe-concentration of feedwater can not be directly transformed to deposition rate in the evaporator tubes, although it seems reasonable to assume a linear correlation between [Fe] in feedwater and deposition rate.

In the effort of developing a more advanced model, this deposit distribution in different boilers is evaluated by investigating evaporator tube samples. From our general experience, the water quality usually achieved at our plants with Fe-concentrations in feedwater in the range of 1-3 µg/kg, gives rise to deposition in the range of 25-100 µm/100,000 hours, although these figures are very uncertain.

Therefore the lifetime calculations has been made with deposition rates of 25, 50 and 100 µm/100,000 hours. The in-data and results are shown in figure 9.
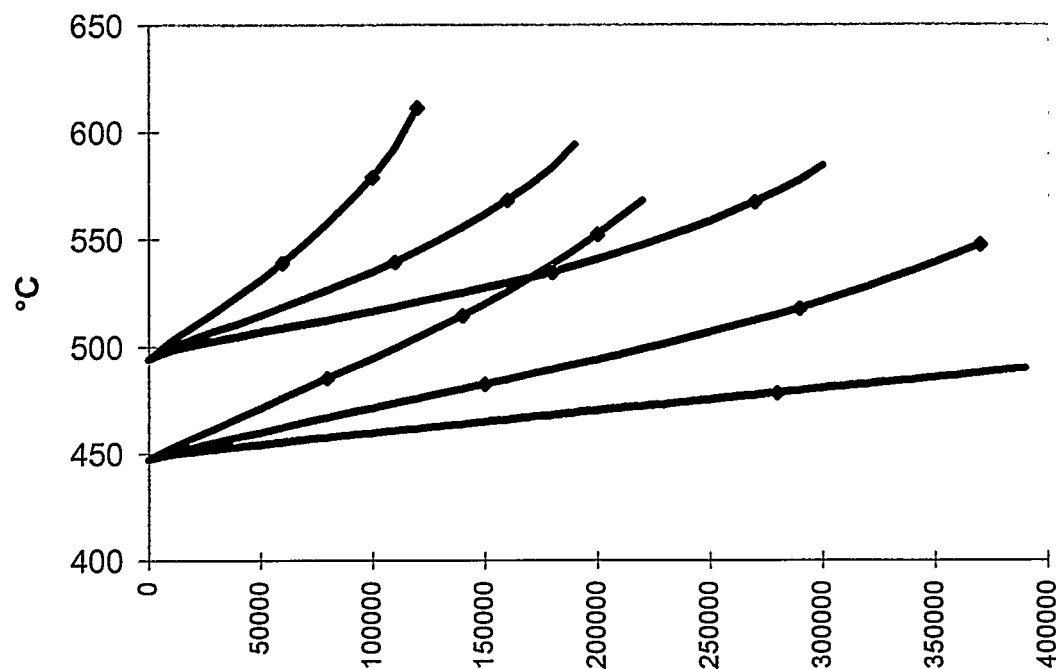
Steam data: A: 250 bar/540°C/540°C; B: 290 bar/580°C/580°C/580°C. Medium temperature in burner zone: A: 390°C; B: 420°C. Tube dimensions: A: 42.4*6.3 mm, B: 30*7.1 mm. Pressure: A: 285 bar, B: 310 bar. Heat flux: 240 kW/m^2. Inside heat transfer coefficient: 33 kW/m2/K. Inner oxide heat conductivity 1.5 W/m/K. Outer oxide heat conductivity 0.75 W/m/K. Corrosion rate 0.5 mm/100,000 h. Deposition rate: 25 (green), 50 (blue) and 100 (red) µm/100,000 h. Marks on the curves indicate oxide thicknesses of 100 µm each.

Figure 9. Results from lifetime calculations for the two boilers A (upper 3 curves) and B (lower 3 curves). Metal surface temperature versus operational hours

11.15

For each boiler, the development in tube surface temperature during lifetime is calculated. For a given boiler, an increased Fe-concentration of feedwater gives increased surface temperatures and consequently shorter lifetime. Also there is a tendency for curving upwards at the higher deposition rates, which is due to the highly insulating effect of the porous deposit layers giving rise to higher rate of selfoxidation. This curving-upwards is most severe for boiler B, because the absolute temperature is higher and therefore the effect on selfoxidation also is higher.

The results show, that a lifetime of 200,000 hours can be realised for boiler A with a deposition rate of 100 μm/100,000 hours, whereas the deposition rate has to be reduced to 50 μm/100,000 hours for achieving the same life time for boiler B.

Even though this model is somewhat simplified, it illustrates very well the importance of reducing Fe-transport to the boiler especially when looking at future boilers with increased steam and feedwater temperatures.

Boilers A - 250 bar/540°C - may well be getting sufficient lifetime with the Fe-transport reduction gained by OT, whereas getting sufficient lifetime with boiler B - 290 bar/580°C - all measures to reduce the iron content in the feedwater should be taken. For both boilers, a mechanical filter is very relevant during commissioning and the first period of operation hereafter, as Fe-concentrations are high. Also Fe deposited in the early stage takes more lifetime of the tubes, than later formed deposits.

The conclusion here is, that even at relatively moderate increases in feedwater temperature for achieving higher efficiency of boilers, the need for minimising Fe-transport to the boiler increases significant. This is especially true, as long as we are restricted to use the 1% Cr-steels for evaporators. Newly developed 2¼ % Cr and especially 12 % Cr-steels for membrane walls can reduce the requirements for Fe-concentration in feedwater, but at the same time, the material cost increase.

7.   Conclusions

Corrosion product transport from the condensate system to the boiler of once-through boilers can be minimised by changing from AVT to OT conditioning, whereby corrosion is reduced or by partial mechanically filtration of feedwater.

The quality with respect to concentration of corrosion products, i.e. Fe, in feedwater gained from these measures has been evaluated during measurement campaigns at a supercritical boiler Fynsværket Unit 7.

At AVT conditioning, Fe-concentration in feedwater can be reduced from 4.5 μg/kg to 3 μg/kg by partially cleaning of feedwater with a mechanical filter.

A larger reduction can be achieved by changing to OT, whereby Fe-concentration can be reduced to 1.4 μg/kg and even lower to 1 μg/kg when also using mechanical

filtration. Filtration also reduces the load from the impure feedwater at commissioning, early period of operation and starts/stops.

An experiment on a heat exchanger shows the high quality of the protective hematite layer as this layer forms very quickly when adding oxygen, whereas it takes one month to destroy the protective layer after removal of oxygen.

A program for lifetime calculation has been used for an evaluation of the effect of corrosion products on temperature exposure of evaporator tubes in different generation boilers. The higher feedwater temperatures in the new USC-boilers makes the evaporator tubes more sensitive to deposition of corrosion products from feedwater.

These evaluations show, that by AVT conditioning, acceptable Fe-concentrations in feedwater and sufficient lifetime can be realised for supercritical boilers with steam data 250 bar/540°C.

OT conditioning give significant reduction in Fe-content in feedwater and hereby increases the safety margin for convential supercritical boilers.

For boilers with more advanced steam data - 290 bar/580°C and above - all measures to reduce Fe-content of feedwater, including OT conditioning and mechanical filtration, should be taken, to ensure sufficient lifetime.

8.   References

[1]   Heitmann, H.G. & Thomas, D.: Der Einfluß der Eisenoxide im Speisewasser von Durchlaufkesseln. VGB-Speisewassertagung 1966, p. 14-23.

[2]   Henriksen, N., Larsen, O.H. & Blum, R.: Lifetime evaluation of superheater tubes exposed to steam oxidation, high temperature corrosion and creep. Proc. Int. Conf. Power Plant Chemical Technology 1996 (This proceeding), 22p.

[3]   Straubert, K. & Bursik, A.: Schichtbildung und Metallauflösung in heißwasserdurchströmten Stahlrohren. VGB Kraftwerkstechnik 66, Heft 11, Nov. 1986, p. 1077-1080.

[4]   Blum, R.: Materials Development for Power Plants with Advanced Steam Parameters - Utility Point of View. Proc. COST-501 Conf., Materials for Advanced Power Engineering, 3-6 Oct. 1994, Liége, Belgium, Part I, p. 15-30.

[5]   Frank, R.: Rohrreißer im Verdampferbereich durch Überschreiten der Warmfestigkeit infolge innerer Belagbildung. Der Maschinenschaden 58, 1985, Heft 4, p. 160-164.

[6]   Effertz, P.-H., Hickling, J., Heinz, A. & Mohr, G.: Die kombinierte Ammoniak-/Sauerstoff-konditionierung von Wasser-/Dampf-kreisläufen in Kraftwerken. Tagungsbericht des Allianz-Workshops im Allianz-Zentrum für Technik. Ismaning   bei Munchen, 8./9. November 1982, 44pp.

DEVELOPING THE OPTIMUM BOILER WATER AND FEEDWATER TREATMENT FOR FOSSIL PLANTS

Barry Dooley
Electric Power Research Institute
3412 Hillview Avenue
Palo Alto, California 94303
USA

ABSTRACT

Over the last two years a new set of cycle chemistry guidelines has been developed for each of the treatments used in fossil plants. These revisions have been based on research conducted over the last ten years, much at the international collaborative level. By careful selection and optimization of the boiler water and feedwater treatments, it will be possible to accrue large financial, maintenance, availability and performance improvements.

1. Introduction

Over the last 10 years EPRI has structured much of its cycle chemistry research towards upgrading the Interim Consensus Guidelines[1]. These guidelines, which were the first comprehensive cycle chemistry guidelines in the U.S., were issued in 1986 in an effort to reduce the increasing availability and performance losses due to cycle chemistry.

Based on some of the most serious problems (Table 1 highlights, for example, those boiler tube failure mechanisms influenced by cycle chemistry[2]), it is now realized that developing the optimum boiler water and feedwater treatment is of the highest importance in plant availability. Specifically this has come down to two basic concerns: a) limiting the quantity of feedwater corrosion products entering the boiler, and b) preventing impurities ingressing to, and concentrating on, the boiler waterwalls.

To accomplish this, it was recognized in 1988, as a result of the international monitoring program[3], that major research was needed to understand the following deficiencies prior to being able to address these two basic concerns:

- Volatility of salts in steam. Historically the "ray diagram" has provided a rough estimate for determining vaporous carryover from the boiler water. But it was

confirmed from plant monitoring that chloride and sulfate concentrations can be two orders of magnitude higher in the steam than shown in the "ray diagram". Ten international organizations have supported work to re-evaluate the partitioning constants for the most important salts, acids and bases in thermal plants and the latest results are shown in Figure 1.

Table 1

Boiler Tube Failure Mechanisms in Water-Touched Tubes that are Influenced by Cycle Chemistry

Mechanism	Nature of Chemistry Influence
Hydrogen damage	Excessive feedwater corrosion products form excessive deposits and combine with a source of acidic contamination.
Caustic gouging	Excessive feedwater corrosion products form deposits and combine with a source of caustic.
Acid phosphate corrosion	Excessive feedwater corrosion products form deposits and combine with a source of phosphate.
Chemical cleaning damage	Excessive feedwater deposits in waterwalls lead to chemical cleaning; process errors lead to tube damage.
Corrosion fatigue	Poor water chemistry, shutdown or lay-up practices, and improper chemical cleaning worsen contribution of the environment to causing damage.
Supercritical waterwall cracking	Excessive feedwater deposits lead to increased tube metal temperatures which exacerbate mechanism.
Fireside corrosion	Excessive feedwater deposits lead to increased tube metal temperatures.
Short-term overheating	Plugging of waterwall orifices by feedwater corrosion products.
Erosion/corrosion of economizer inlet headers	Attack by reducing feedwater conditions.
Pitting (economizer)	Stagnant, oxygenated water formed during shutdown.

- Steam chemistry and corrosion in the phase transition zone. The first phase of work in this area resulted in a state-of-knowledge document[4] which brought together information on steam chemistry, moisture nucleation, early condensate and depositions. This led to the formation of an international collaboration of 23

organizations that has performed detailed monitoring of these areas in operating turbines.

- Many utilities in the U.S. experienced phosphate hideout and boiler water pH instability when following the information on Congruent Phosphate Treatment (CPT) in the ICG[1]. Also, an increasing number of utilities have experienced serious internal corrosion (attributed to acid phosphate corrosion) of the boiler waterwalls and subsequent boiler tube failures when using this phosphate chemistry[2]. The sodium iron phosphate compound, maricite, has been found to be a magnetite-phosphate reaction product associated with cases of serious corrosion, and a distinguishing difference from caustic gouging. Research in the U.S. and Canada has led to two new phosphate treatment ranges for equilibrium phosphate treatment (EPT) and phosphate treatment (PT) as shown in the control range diagram (Figure 2)[5].

The international collaborative research in these areas illustrates the importance of the problems. It has also allowed the cycle chemistry community to move ahead quickly in revising the operating guidelines.

In the U.S. over the last two years, a new set of cycle chemistry guidelines have been developed using the completed and on-going research, as well as the experience gained over the last 10 years:

- Phosphate Treatment Guidelines to cover phosphate treatment (PT) and equilibrium phosphate treatment (EPT)[5]

- Oxygenated treatment for once-through and drum units[6]

- All-Volatile treatment for once-through and drum units[7]

A further document has been prepared which summarizes the worldwide experience with caustic treatment for drum boilers[8]. This treatment is currently utilized in over 50,000 MW of drum boilers successfully at concentrations up to 2 ppm NaOH.

The next step has involved developing procedures for selecting which of the five drum boiler water treatments, and which feedwater treatment are most appropriate for each unique unit condition. A new document has been assembled, which integrates the approach for U.S. utilities[9]. This paper provides a brief summary.

2. Feedwater Treatment

The primary purpose of feedwater treatment is simply to deliver, to the economizer inlet, feedwater with the minimum impurities and corrosion products for *all* operating

regimes. It is the most important part of the cycle, currently the least maintained, highly complex and dependent on the system metallurgy. Table 2 delineates the plant problem areas that relate to the generation and transport of feedwater corrosion products for all-ferrous and mixed metallurgy systems. Flow accelerated corrosion (or erosion-corrosion) not only is a major generator of corrosion products but is also a major safety problem in the industry[10],

For both all-ferrous and mixed metallurgy feedwater systems, the feedwater treatment always needs to be all-volatile which means that ammonia is combined with the use of hydrazine or an alternate oxygen scavenger. As a rule none of the new organic feedwater chemicals (alkalizing agents and/or oxygen scavengers) are desirable or needed in utility fossil cycles. The basic EPRI philosophy is to keep the cycle chemistry simple and minimize chemical additions to the cycle.

Table 2

Generation of Feedwater Corrosion Products by Corrosion and
Erosion-Corrosion, and the Major Unit Transport and Deposition Problem
Areas for All-Ferrous and Mixed Metallurgy Systems

Generation	Transport and Deposition
a) All-Ferrous Metallurgy Systems	
• Low/high pressure heater • Deaerator • Economizer Inlet • Feedwater Piping	• Boiler deposits and increased boiler pressure drop • Ripple magnetite formation on the waterwalls of once-through units • At least five boiler tube failure mechanisms • Frequent need for chemical cleaning • Boiler feedpump fouling • Orifice fouling
b) Mixed Metallurgy Systems	
• Low/high pressure heater • Condenser	• HP turbine deposits • Boiler deposits and increased boiler pressure drop • At least five boiler tube failure mechanisms • Frequent need for chemical cleaning • Orifice fouling • Superheater deposits

A summary of the feedwater chemistry limits for all-ferrous and mixed metallurgy systems is shown in Table 3. Also shown on this table are the desirable and achievable feedwater corrosion product levels; these are the real goals of any feedwater

optimization program, as experience has shown that the problems enumerated in Table 2 will not occur or be minimized if a utility keeps below these values. For mixed metallurgy systems it is clear that reducing conditions are required, whereas for all-ferrous systems an oxidizing environment or a regime without an oxygen scavenger is preferred.

Table 3

Comparison of Normal Cycle Chemistry Limits at the
Economizer Inlet for AVT Feedwater and Oxygenated Treatment

Cycle Chemistry Parameter	$AVT^{5,7}$ (mixed metallurgy)	$AVT^{5,7}$ (all-ferrous)	Oxygenated Treatment $(OT)^6$ (all-ferrous)
pH	8.8-9.1	9.2-9.6	8-8.5[a] 9-9.5[b]
Ammonia, ppm		0.5-1.0	0.02-0.07[a]
Cation conductivity (μS/cm)	<0.2	<0.2	<0.15
Fe, ppb	<10 (<5)	<5 (<2)	<5 (<1)
Cu, ppb	<2 (<2)		
Oxygen, ppb	<5	1-10	30-150[a] 30-50[b]

Notes: a) For once-through units   b) for drum units
Values in parenthesis represent the achievable and desirable levels of feedwater corrosion products

2.1   Mixed Metallurgy Feedwater Systems

The *feedwater treatment dilemma* for mixed metallurgy feedwater cycles is that the optimum pH for corrosion control of copper alloys is lower (8.5-9.0) than the optimum pH for carbon and low alloy steels (>9.5).

Depending on the extent of the use of copper alloys, i.e., condenser—LP feedwater heaters—HP feedwater heaters, the following feedwater treatments could be selected:

Treatment	Conditions
oxygenated	condensate polishers, Cu in condenser only
all-volatile with:	
ammonia	all situations, condensate polisher preferred
morpholine cyclohexylamine	must be evaluated prior to continuous use
other amines	application restricted to cycles with lower pressure drum boilers only. Must be evaluated. Little experience.

The feedwater treatments using amines are often (but not always) combined with an oxygen scavenger; most frequently hydrazine or carbohydrazide. Which of these feedwater treatments and what oxygen scavenger and what concentrations should be used can only be determined by field testing and unit specific optimization (Section 2.1.2).

2.1.1 Growth of Copper Oxides in Feedwater and Their Transport

Although it is not likely that the oxides which form on the variety of copper-based feedwater materials (brass, Cu-Ni, Ni-Cu) will be the same, some general understanding does exist. This was recently discussed in an international conference in Piacenza[11].

Both cuprous (Cu_2O) and cupric (CuO) oxides can form under feedwater conditions, with cuprous oxide essentially being the barrier (protective) layer adjacent to the metal surface. The outer cupric oxide, CuO (or $Cu(HO)_2$), is formed by oxidation of the cuprous ions. Formation of the cuprous oxide is preferred at lower reducing potentials, whereas with higher potentials (oxidizing) the growth is predominantly CuO. This supports the continued use of a reducing agent such as hydrazine. However, recent work[12] has suggested that an oxidizing environment will preferentially form CuO which has a lower solubility than Cu_2O. It is not clear yet whether less than 2 ppb of copper can consistently be maintained at the economizer inlet under all operating regimes with such as oxidizing treatment.

Much recent field experience in the U.S. has shown that even if the oxygen level is kept low (<5 ppb), then elimination of the reducing environment (hydrazine) has led to serious copper deposition problems in the HP turbine.

The reason for the preferential deposition of copper and its oxides at the inlet of the HP turbine is a sharp drop of their solubility in superheated steam under the steam expansion conditions at the HP turbine inlet[13]. Cupric oxide is more soluble in superheated steam than cuprous oxide, which is more soluble than copper; again supporting the need to keep the feedwater under a reducing environment.

12.6

2.1.2 Optimization and Benefits

To ensure minimum corrosion and flow-accelerated corrosion (erosion-corrosion) in the feedwater system, and minimum deposition of copper within the boiler and HP turbine, experience has indicated that the copper levels at the economizer inlet should be less than 2 ppb (Table 3). This can only be achieved and maintained through experimentation with different water treatment chemicals at different concentrations in conjunction with a detailed monitoring program. Figure 3 shows a road map methodology for optimizing feedwater treatments for mixed metallurgy (copper and iron) feedwater systems where optimum pH control (8.8-9.1) is a compromise of the optimum corrosion protection for each metal.

The optimization consists of three general steps:

a) A review of current water treatment, sampling and monitoring, design, operation, materials, and experience.

b) Implementation of changes when required, including changes of water treatment, operation, and material replacement.

c) Verification of the effects of the implemented changes. In this verification step, the water and steam chemistry will be compared to the recommended limits in the appropriate EPRI guidelines[5][7].

The monitoring campaign which is part of Steps 2 and 6 on Figure 3 should include:

- Varying Operating Conditions—base load, startup and shutdown
- Steam Chemistry—cation conductivity, sodium, chloride, silica and sulfate
- Feedwater Chemistry—cation conductivity, chloride, corrosion products (Fe, Cu), oxygen, pH, and oxidizing-reducing potential (ORP)
- Operation of Condensate Polishers

Step 3 consists of a series of tests to determine the proper scavenger levels. The tests should utilize the monitoring system instrumentation (Step 2) while reducing the hydrazine (or alternative) dosage. Particular note should be made of dissolved oxygen levels, quantities of corrosion products, and the oxidizing/reducing potential (ORP). The latter is particularly important with mixed metallurgy feedwater systems because as indicated above a reducing environment is required for the copper containing alloys.

The choice of oxygen scavenger is also involved here. This includes safety as well as optimized reaction rates and concern for the alternate behavior of any thermal decomposition products and their effects in other parts of the cycle. Carbohydrazide, for example, decomposes to hydrazine and carbon dioxide.

Particular attention should be paid to the fact that there can be a long time (as long as six months has recently been observed in the U.S.) between changes in feedwater chemistry (ORP) and corrosion product transport. Thus careful planning is needed for accurate extended tests.

Although industry experience has shown that the maximum reduction of corrosion product transport in fossil utility cycles can only be obtained by eliminating chemical control compromises caused by the use of mixed metal feedwater systems, application of these optimization procedures suggests the following benefits can accrue:

- increased time between boiler chemical cleans and elimination of the need to chemically clean HP turbines
- easier chemical cleans with reduced copper deposits
- increased life and improved availability of feedwater heaters
- reduced number of boiler tube failures due to under-deposit mechanisms (hydrogen damage, acid phosphate corrosion and caustic gouging)
- safer boiler tube failure weld repairs

2.2 All-Ferrous Feedwater Systems

Compared to the mixed metallurgy systems, feedwater treatment for all-ferrous systems is much simpler. In cycles with all-ferrous alloys, the following feedwater treatments could be selected:

Treatment	Conditions
oxygenated	condensate polishers
all-volatile with:	
ammonia	all situations, condensate polisher preferred.
amines	applications restricted to cycles with lower pressure drum boilers only. Must be evaluated. Little experience.

All-volatile treatment with ammonia is often combined with the use of hydrazine or another oxygen scavenger. In many cases, the application of an oxygen scavenger is not required[14]. It has been shown that reducing or eliminating the dosing results in a decrease of feedwater total iron content.

The feedwater treatments using amines are often (but not always) combined with an oxygen scavenger; most frequently hydrazine or carbohydrazide.

Which of these feedwater treatments should be used and whether an oxygen scavenger should be used at all, can only be determined by field testing.

When the feedwater is constructed of only all-ferrous materials the objectives of chemistry optimization are achieved either by selection of a pH value that is high enough to reduce generation of corrosion products in the plant cycle (pH>9.5) or by using an oxygenated treatment. With both alternatives, controlling impurity ingress by *condenser leaks* and *air in-leakage* is essential as well as very quickly reaching the normal guideline values during and after each startup.

2.2.1 Oxygenated Treatment

While elevated pH is the basis of AVT, oxygenated treatment (OT) uses oxygenated high-purity water to minimize corrosion and erosion-corrosion in the feedwater train. Oxygen, hydrogen peroxide, and air have historically been used as oxidants; currently oxygen is the primary choice[6]. The feedwater oxygenated treatment key parameters are summarized in Table 3.

For the application of oxygenated treatment in units with once-through and drum boilers, there is one indispensable prerequisite that the cation conductivity must be less than 0.15µS/cm (at 25°C) in the condensate, feedwater, and steam. An added prerequisite for drum boilers is that the cation conductivity in the boiler water (downcomer) must be less than 1.5µS/cm (at 25°C).

The basis of the success of OT depends on the formation of a layer of ferric oxide hydrate (FeOOH) on the surface and within the pores of the magnetite oxide layer. This is illustrated in Figure 4.

2.2.2 All-Volatile Treatment

The basis of AVT is an elevated pH in all plant cycle streams. The most common alkalizing agent used in AVT is ammonia. Originally, the ammonia dosing was always combined with the hydrazine feed. Investigations performed in the last two years show that reducing and even eliminating hydrazine feed minimizes the corrosion product generation[14]. Figures 5 to 6 show some of these results for all-ferrous systems in drum and once-through cycles. As a result, the recently revised feedwater AVT parameters which are summarized in Table 3 reflect a less rigid requirement for oxygen, and an implication that running with less than one ppb of oxygen could in fact be harmful and dangerous from a flow accelerated corrosion viewpoint[10].

2.2.3 Optimization and Benefits

Since 1991, over 70 once-through units have been converted to OT in the U.S. It was expected that the penetration for drum units would be slower and directed towards specific problems such as flow accelerated corrosion. All oxygenated units easily achieve much less than one ppb iron at the economizer inlet during normal operation. Only slightly elevated levels occur during startup periods, compared to many hundreds

of ppb when operating on AVT. The well published benefits of running on OT have also been achieved by these units.

Of course, not all units can be converted to OT, but many utilities have now recognized that the use of an oxygen scavenger for the last 20 or more years has been superfluous in all-ferrous systems. Whether the oxygen scavenger is retained or not, the overriding objective should be to achieve less than 2 ppb of iron at the economizer inlet for non-oxygenated units.

As with the mixed metallurgy systems, this can only be achieved and maintained through experimentation and a monitoring campaign. A road-map approach similar to that shown in Figure 3 has been developed for all-ferrous systems[9].

Even a cursory glance at Table 1 provides an immediate indication of the importance of the iron levels to boiler tube availability problems. Also OT has eliminated all the problems in Table 2a, with most being eliminated or reduced by operation without an oxygen scavenger. Some of the other accrued benefits included:

- reduced number of maintenance days for a unit (up to 2 days have been saved on annual overhauls)
- faster startup times
- increasing continuous running hours
- easier dismantling of equipment
- avoidance of generation of corrosive and scale forming decomposition products of feedwater impurities and treatment chemicals
- improved environmental discharges

3.   Boiler Water Treatment

The primary purposes of the boiler water treatment are to ensure that the steam has minimum impurities to protect the turbine, and that the treatment can neutralize any contaminant ingress to prevent concentration and ultimate boiler tube failures.

There are currently five choices for boiler water treatment for drum cycles:

- Equilibrium Phosphate Treatment (EPT) (See Figure 2)
- Phosphate Treatment (PT) (See Figure 2)
- All-Volatile Treatment (AVT)
- Caustic Treatment (CT)
- Oxygenated Treatment (OT)

A comparison of the limits for key cycle chemistry parameters between the boiler chemistry control methods is shown in Table 4. This example is for normal operating conditions in a 2500 psi boiler.

Table 4

Comparison of Normal Cycle Chemistry Limits
for Four Drum Boiler Water Chemistries

Cycle Chemistry Parameter	Phosphate Treatment [5] (PT)	Equilibrium Phosphate Treatment [5] (EPT)	Caustic Treatment [8] (CT)	All-Volatile Treatment [7] (AVT)
Na, ppm	1.5	0.85	1.5	0.7
Cl, ppm	0.9	0.028	0.4	0.028
SO_4, ppm	1.6	0.028	0.5	0.028
SiO_2, ppm	0.13	0.13	0.2	0.13
pH	9.3	9.0-9.7	9.4-9.6	
Na: PO_4	>2.8	>2.8		
PO_4, ppm	>2.5	<2.5		
NaOH, ppm			1.0-1.5	
Cation Cond. $\mu S/cm$			≤ 8.0	≤ 1.5

Note: Values are normal operating limits for a coal-fired 2500 psi boiler with reheat.

The limits for feedwater for these treatments are similar to one another and, therefore, the choice of the boiler water chemical conditioning, largely reflects the tolerance to ingress of impurities, out-of-specification operation, type of boiler, maximum heat flux, and the amount of blow-down required. One of the major influencing factors is the cooling water for the plant.

EPRI has recently developed an approach for selecting the optimum treatment[9]. Some of the key steps in this process include:

• Base line monitoring to determine if a unit is suitable for conversion and whether any serious problems exist with the current treatment (hideout with phosphate treated boilers, boiler tube failures, etc.).

- Analysis of how the design and operational features of the unit may affect the choice of alternative methods of boiler water treatment. Guidance on the typical effects of design on the various methods of treatment (AVT, PT, EPT and CT) are given in Table 5. A similar table of operational factors has also been developed. These tables can be used to provide some initial screening of the alternatives. Oxygenated treatment is not included on these tables and is considered as a special case of AVT.

- Consideration of whether a condensate polisher is in the cycle and whether feedwater contamination events are significant. If the answer to the former is yes then AVT or OT (after chemical cleaning) are logical choices. If the answer to the latter is a) positive then CT or PT are choices or b) negative then EPT is a possible route.

4.0   Concluding Remarks

While most utilities in the U.S. could meet the limits within the Interim Consensus Guidelines published in 1986, a number of problem areas were identified in the intervening years. The recent production of individual guidelines for phosphate treatments, all-volatile treatment and oxygenated treatment, as well as an initial compilation of limits for caustic treatment, should help utilities overcome the problems. The selection and maintenance of the optimum treatment for boiler water and feedwater will provide further guidance.

However, the continuing research in the areas of volatility, solubility, deposition and steam chemistry will fine tune both the limits and the optimum treatment over the next few years. One major outcome will be a tightening of the steam limits to ensure that the production of the first condensate droplets and any deposition on blade surfaces will not contribute to failure mechanisms.

With this greater understanding of the interface of the cycle and cycle chemistry, it is also envisaged that a large number of utilities will be able to control their unit's cycle chemistry with an expert system/advisor connected to a few key instruments around the cycle.

5.0   Acknowledgments

Table 5

Typical Effects of Design on the Suitability of
Various Methods of Boiler Water Treatment

		AVT	PT	EPT	CT
Pressure*					
Low		Possible	Yes	Yes	Possible
Medium		Possible	Yes	Yes	Yes
High		Yes	Possible	Yes	Possible
Carryover+					
Low		Yes	Yes	Yes	Yes
Medium		Yes	Possible	Possible	No
High		Yes	No	No	No
Boiler Circulation					
Natural		Yes	Yes	Yes	Yes
Assisted		Yes	Yes	Yes	Yes
Heat Flux#					
Low		Yes	Yes	Yes	Yes
High		Yes	No	No	No
Feedwater Materials					
All ferrous		Yes	Yes	Yes	Yes
Ferrous/copper		Yes	Yes	Yes	Yes
Cooling Water					
Acid forming (sea water)		Possible	Yes	Yes	Yes
Alkaline forming (fresh)		Yes	Yes	Yes	Possible
Acid forming (fresh)		Possible	Yes	Yes	Yes
Cooling Towers		No	Yes	Possible	Possible
Condensate Polishing					
With condensate polishing		Yes	Yes	Yes	Yes
Without polishing		No	Possible	Possible	Possible
Instrumentation/Control					
EPRI recommended instruments		Yes	Yes	Yes	Yes
Insufficient instruments		No	Possible	No	No
Makeup Volume Required, % of Total Steam Flow (exclusive of startup/shutdown)					
High	>5%	No	Yes	No	No
Medium	1-5%	Possible	Yes	Possible	Possible
Low	<1%	Yes	Yes	Yes	Yes
Adequacy of Boiler Makeup Quality and Capacity (including startup and shutdown)					
Sub-standard		No	Possible	No	No
Marginal		No	Yes	Yes	Possible
Adequate		Yes	Yes	Yes	Yes

Notes: Yes—a recommended method of conditioning

Possible—depending on circumstances

No—not recommended

Sub-standard—can meet quality at normal makeup flow requirements only; requires borrowing from sister units for above normal sootblowing, blowdown, or component flushing.

Marginal—can meet quality requirements for usual makeup flow requirements but must reduce production seasonally because of reduced intake water quality (including temperature)

Adequate—can meet quality requirements throughout the year and has sufficient capacity to supply both high sootblowing requirements and substantial flushing during shutdown and startup.

*Low=typically <1500 psig (100 bar), High=typically >2400 psig (160 bar)
+Low=typically <0.1% carryover, High=typically >0.3% carryover
#Low=typically coal fired plant, High=typically oil & gas fired plant

6.0 References

1. *Interim Consensus Guidelines on Fossil Plant Cycle Chemistry.* Electric Power Research Institute, Palo Alto, California. CS-4629. June 1986.

2. R.B. Dooley and W.P. McNaughton, *Boiler Tube Failures: Theory and Practice.* Electric Power Research Institute, Palo Alto, California. EPRI Book TR-105261, 1996.

3a. *Monitoring Cycle Water Chemistry in Fossil Plants—Vol. 2, International Practices in Fossil Fuel Units.* Electric Power Research Institute, Palo Alto, California. EPRI GS-7556. December 1992.

 b. O. Jonas and B. Dooley, *International Water Treatment Practices and Experiences",* Proceedings International Water Conference 51 (1990).

4a. O. Jonas, N. Rieger and B. Dooley, *Turbine Steam, Chemistry, and Corrosion.* Electric Power Research Institute, Palo Alto, California. EPRI TR-103738. August 1994.

 b. O. Jonas, B. Dooley and N. Rieger, *Steam Chemistry and Turbine Corrosion— State of Knowledge.* 54th International Water Conference, 1993. Pittsburgh. IWC-93-51.

 c. N. Rieger, B. Dooley, T. McCloskey and O. Jonas, *State of Knowledge for Nucleating Flow in Nozzles and Steam Turbine Stages.* ASME JPGC, Kansas City, October 1993.

5. R.B. Dooley, A. Aschoff and F.J. Pocock, *Cycle Chemistry Guidelines for Fossil Plants: Phosphate Treatment for Drum Units.* Electric Power Research Institute, Palo Alto, California. EPRI TR-103665. December 1994.

6. A. Bursik, R.B. Dooley and B. Larkin, *Cycle Chemistry Guidelines for Fossil Plants: Oxygenated Treatment.* Electric Power Research Institute, Palo Alto, California. EPRI TR-102285. December 1994.

7. R.B. Dooley, A. Aschoff and F.J. Pocock, *Cycle Chemistry Guidelines for Fossil Plants: All-Volatile Treatment.* Electric Power Research Institute, Palo Alto, California. EPRI TR-105041, April 1996.

8. M. Ball and R.B. Dooley, *Sodium Hydroxide for Conditioning the Boiler Water of Drum-Type Boilers*. Electric Power Research Institute, Palo Alto, California. EPRI TR-104007. January 1995.

9. R.B. Dooley, M. Ball, A. Bursik, O. Jonas, F.J. Pocock and J.K. Rice, *Selection and Optimization of Boiler Water and Feedwater Treatments for Fossil Plants*. Electric Power Research Institute, Palo Alto, California. EPRI TR-105040. To be published winter 1996.

10. B. Chexal, J. Horowitz, R. Jones, B. Dooley and C. Wood, *Flow Accelerated Corrosion in Power Plants*. Electric Power Research Institute, Palo Alto, California. EPRI Book TR-106611, 1996.

11. *The Interaction of Non-Iron Based Materials with Water and Steam*. ENEL/EPRI/VGB International Conference. Proceedings. To be published 1997.

12. G. Perboni, V. Scolari and R. Zoppetti, *Electrochemical Monitoring of Copper Release from Low Pressure Heaters*. In reference 11.

13. F.J. Pocock and J.F. Stewart, *Solubility of Copper and Its Oxides in Superheated Steam*. J. Eng. for Power, 1963.

14. R.B. Dooley, J. Mathews, R. Pate and J. Taylor, *Optimum Chemistry for All-Ferrous Feedwater Systems: Why Use an Oxygen Scavenger?*, 55th Annual Meeting, International Water Conference, Pittsburgh, PA, October 1-Nov. 2, 1994.
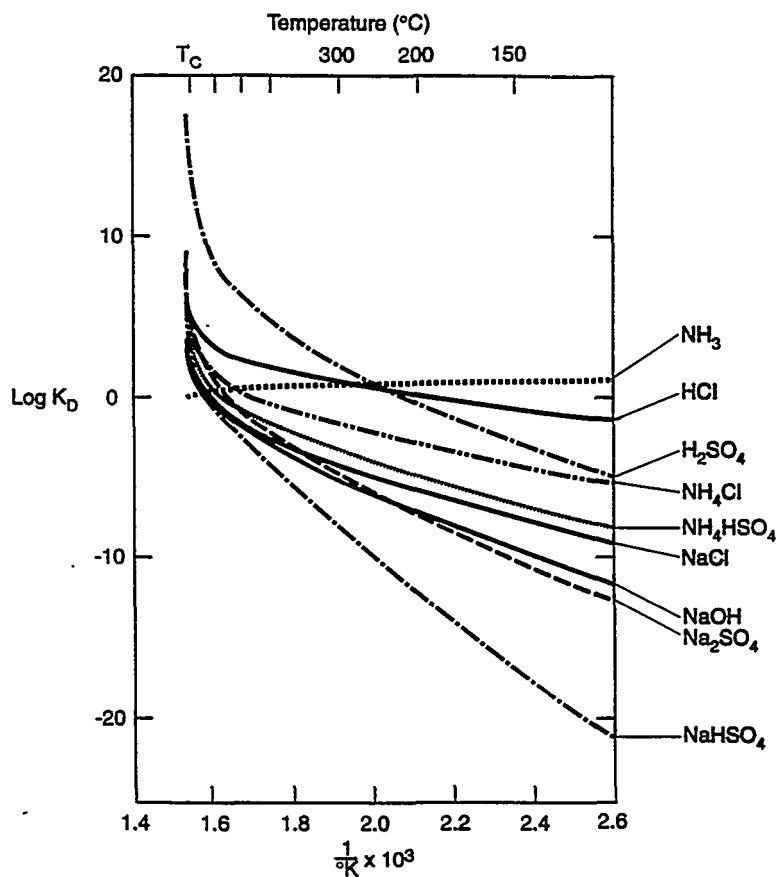
Fig. 1   Partitioning Constants K $_D$ for Common Boiler Water Salts,
Acids and Bases Represented by Mathematical Functions of
the Reciprocal of Temperature in Kelvin up to the Critical
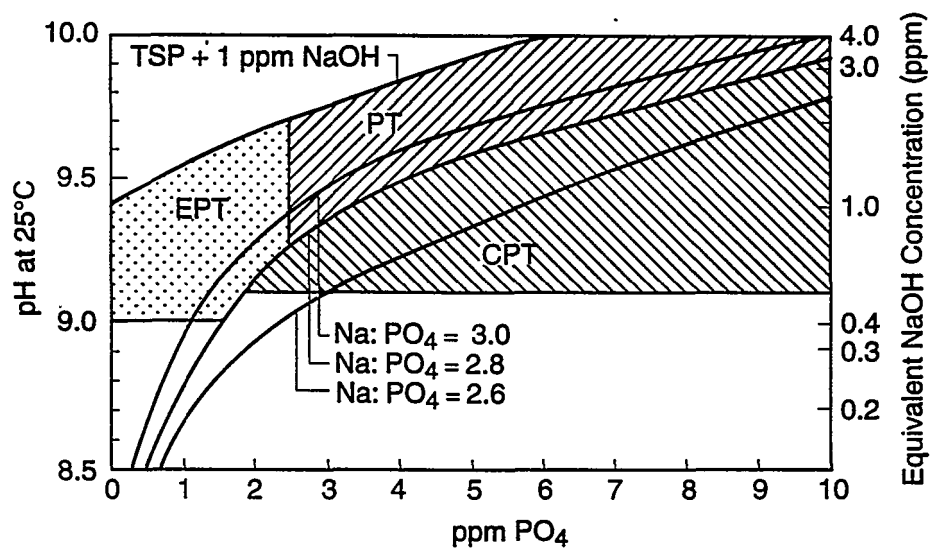Temperature of Water, Tc.

Fig. 2   Schematic of Operating Ranges of Boiler Water on Equilibrium
Phosphate Treatment (EPT), Congruent Phosphate Treatment (CPT)
and Phosphate Treatment (PT). It should be noted that "Na:PO$_4$" is a
molar ratio determined from the phosphate-pH relationship. It is not
an analytical ratio. The CPT is shown to its maximum Na:PO$_4$ molar
ratio of 2.8; the normal operating range from the ICG is below
the Na:PO$_4$ molar ratio of 2.6.

Step 1

Review design and
materials experience.
Review current
treatment, sampling
and monitoring.

— No current
problems

Continue use of
current treatment

No problems but
possible economic
savings

Step 2

Baseline
monitoring

Low level of
corrosion products

Implementation

Step 3

Water chemistry
optimization (pH,
ammonia/amine,
oxygen scavenger)

Step 4

Design and
materials changes

Step 5

Operation

Step 6

Monitoring to
compare with
baseline

Step 9

Long-term plans

Step 7

Normal operation
and monitoring

Step 8

Continual check of
chemistry

Fig. 3   Road-Map for Optimizing Feedwater Treatment for Mixed Metal
Systems (Cu/Fe).
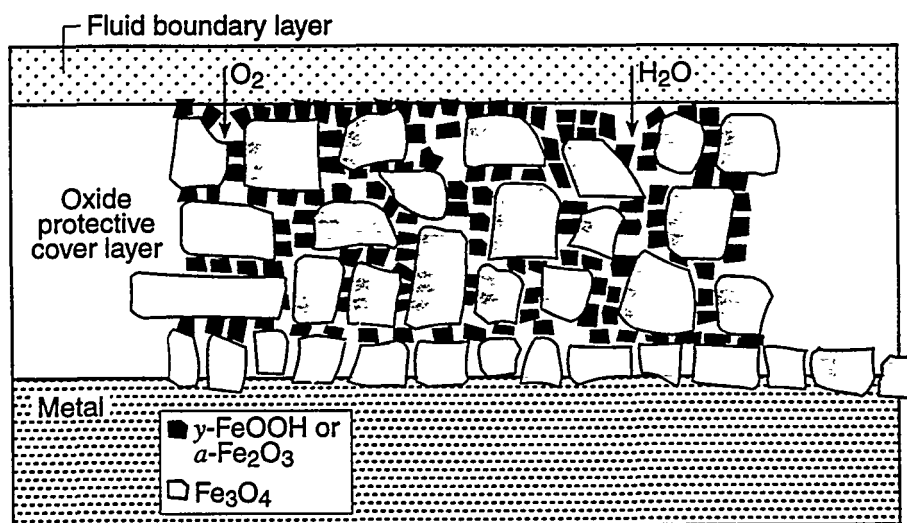
Fig. 4   Schematic Representation of Oxide Formed on Iron-Based
Feedwater Surfaces During Operation with OT.

12.17
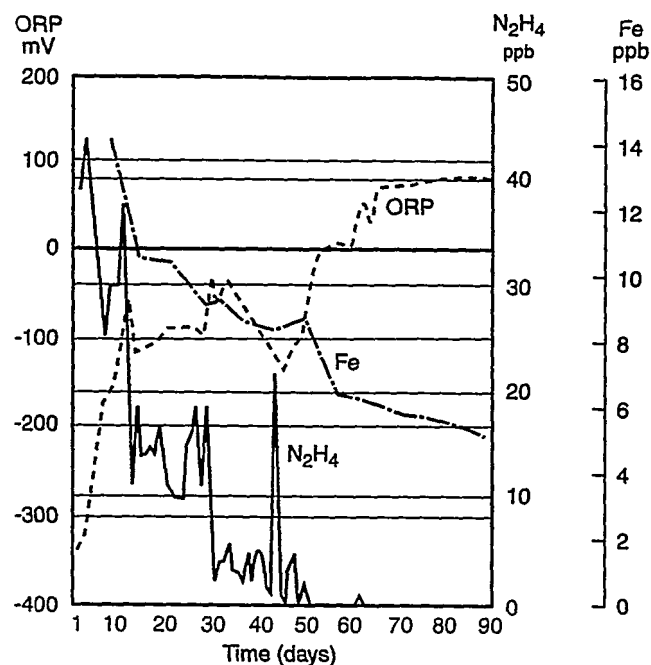
Fig. 5   Change in Oxidizing Reducing Potential (ORP) and Feedwater Iron
Levels (Fe) at the Economizer Inlet when Hydrazine (N_2H_4) is
Gradually Reduced on a 600MW Drum Unit with an All-Ferrous
Feedwater System.
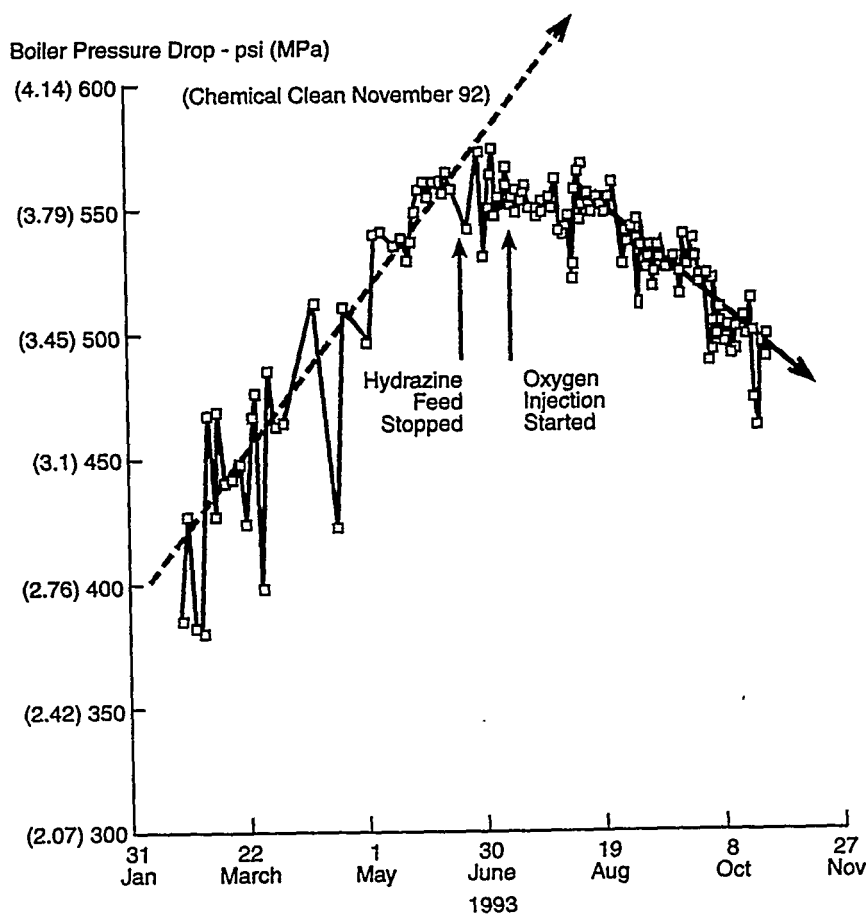
Fig. 6   Change in Boiler Pressure Drop Increase When Hydrazine is
Eliminated and Also When Oxygen is Injected. (1165MW Once-
Through Unit with an All-Ferrous Feedwater System.)

12.18

METHODS USED BY ELSAM FOR MONITORING PRECISION AND ACCURACY OF ANALYTICAL RESULTS

Jan Hinnerskov Jensen
Sønderjyllands Højspændingsværk/Fælleskemikerne
Flensborgvej 185
6200 Aabenraa
Denmark

ABSTRACT

Performing round robins at regular intervals is the primary method used by Elsam for monitoring precision and accuracy of analytical results. The first round robin was started in 1974, and today 5 round robins are running. These are focused on: boiler water and steam, lubricating oils, coal, ion chromatography and dissolved gasses in transformer oils. Besides the power plant laboratories in Elsam, the participants are power plant laboratories from the rest of Denmark, industrial and commercial laboratories in Denmark, and finally foreign laboratories. The calculated standard deviations or reproducibilities are compared with acceptable values. These values originate from ISO, ASTM and the like, or from own experiences. Besides providing the laboratories with a tool to check their momentary performance, the round robins are very suitable for evaluating systematic developments on a long term basis. By splitting up the uncertainty according to methods, sample preparation/analysis, etc., knowledge can be extracted from the round robins for use in many other situations.

1. The Laboratories

All power plants in Elsam have their own laboratory for operational control. Examples of the analyses performed are: iron in boilerwater, check of on-line conductivity analysers, determination of calorific value in coal and analysis of total acid number in lubricating oils. For the execution of this task, the laboratories are provided with equipment such as spectrophotometers, calorimeters and furnaces.

Beside this task, each laboratory has a so-called "co-ordinated speciality", which is a group of analyses that only one or two of the laboratories are doing on behalf of all the power plants in Elsam (with exception of Midtkraft). At the moment the specialities are allocated as shown in table 1.

Table 1	
Laboratory	**Speciality**
Vendsysselværket (NVV)	Oils (lubricating, transformer)
Aalborgværket (NVA) and Skærbækværket (SV)	Ion exchange resins, Trace contaminants in water/steam-curcuit
Vestkraft (VK) og Fynsværket (FV)	Metallurgy
Sønderjyllands Højspændingsværk (SH)	Fuels and Environment

The arrangement with the co-ordinated specialities is to be regarded as an alternative to an actual central laboratory.

2. Quality Assurance

Quality assurance (QA) of the analytical work on the laboratories is made internally and externally. The internal QA is typically done by running control cards, using internal standards and certified reference materials. The responsibility for this effort is placed at the laboratory itself. To develop the QA and to gain as much information as possible from the work, Fælleskemikerne ("the joint chemists") are running a course for the laboratory staff. The aim of the course is that the laboratories should be able to estimate the uncertainty of their analytical results.

Due to the physical separation of the laboratories which in many areas make the same analyses, there is a need for QA between the laboratories. To obtain this QA, Fælleskemikerne have conducted round robins for several years. It is the extend and benefits of these round robins that will be described more closely in the following.

3. Round Robins

3.1. Boiler Water and Steam

This round robin is focused on the control of the purity and the chemical treatment of the water/steam-curcuit in boilers.

The round robin on water started in 1974 and has continued nearly unchanged until today. The participants are the 8 power plant laboratories in Elsam. In turn, the laboratories distribute the samples, which are made of ultra pure water (UPW) added a known amount of standard. Because of conflicting demands to the conservation of the measurerants, the samples only contain one substance. Each month two samples containing the same analyte in different concentrations are sent out. It is up to the distributing laboratory to decide the concentration levels. The analytes included are ammonia, copper, iron and silica. The laboratories make a single determination on two different days.

13.2

3.1.1 Treatment of Results

The results from the round robin are tested for outliers, and the grand mean and standard deviation (SD) in and between the laboratories are calculated. The total SD is compared with an acceptable value and the grand mean is compared with the true value. A graphic check of the laboratories is made in which the acceptable SD is used to calculate confidence levels. Enclosure 1 is showing an example of a round robin report.

The acceptable values for SD originate from ASTM and Standard Methods[#], but have all been tightened due to our own evaluation. In the beginning only spectrophotometric methods were used, but now also AAS and electrochemical techniques are used by the laboratories. The applied methods are indicated, so that a comparison is possible.

To evaluate systematic deviations (trends), the relative SD (RSD) is calculated. It is defined as the achieved SD in % of the true value. Also the recovery, defined as the grand mean in % of the true value, is calculated. Enclosure 2 is showing RSD and recovery as a function of time and concentration for copper. RSD is increasing with decreasing concentration, while the recovery seems to be independent of the concentration.

The values for precision and trueness are obtained in synthetic samples, so they do not take into account any interferences. As the round robin, however, is addressed towards boiler water and steam, considerable interferences will rarely occur in practice.

3.2. Lubricating Oils.

This round robin is focused on the operational control of lubricating oils in turbines.

The round robin started in 1984 with 7 participants. Today 11 laboratories are participating, of which 9 are power plants. Four times a year 3 oils, new or in operation, are distributed. This work is carried out by 3 of the participating laboratories. There are no specific demands for sample preparation.

The laboratories are analysing density, viscosity, total acid number (TAN) and water content. Determinations are made in double at one day.

3.2.1. Treatment of Results

Statistics on the results is made in accordance with ISO 5725 part 2. Firstly, the SD at the single laboratory is tested following Cochrans outliertest. Secondly, the means from the laboratories are tested using Grubbs outliertest. Finally, the grand mean (X), repeatability (r) and reproducibility (R) are calculated. In the report to the participants, the achieved values are compared to acceptable values from ASTM. Enclosure 3 is an example of a front page from a round robin report. Since 1995 the report also includes a so-called "TREND-analysis". An example is given in enclosure 4. In the TREND-analysis the deviation of the single laboratory in % from the grand mean is shown in a bar graph. The round robin numbers are given on the x-axis.

[#]Standard Methods for the Examination of Water and Wastewater. Published by APHA, AWWA, WEF.

For each of the 4 round robins in 1991, an extra calculation was made. For each analysis the results were divided into groups according to the used equipment, and for each group of results X, r and R were calculated. For example, the results for viscosity were split up in two groups. One group using glass capillary viscometers, and one using rotation viscometers. The conclusion was that RSD for rotation viscometers was 2-5 times the RSD for capillary viscometers, but the grand means were not significantly different.

3.3. Coal

This round robin is focused on the analyses performed in relation to the import and use of coal.

This round robin started early in the 80's with 9 participants. This number has varied throughout the years and is at the moment 14. The power plant laboratories in Elsam have participated since the start, while the power plants in the eastern part of Denmark joined the round robin in 1990. The last participants are industrial coal users and commercial impartial laboratories. As for the last-mentioned it is a demand from the Danish Accreditation Authorities that they participate in the round robin to maintain their accreditations. Finally, coal suppliers have had laboratories participating for a short period of time.

Until 1990 only analysis samples were distributed. In this case the entire sample preparation is done at the distributing laboratory. Since 1990 analysis and laboratory samples have been sent out in turn. When receiving a laboratory sample, the laboratories have to do some sample preparation themselves before the final determinations.

3.3.1. Preparation of Samples for the Round Robin
Preparation and distribution of analysis samples are done by 3 of the participating laboratories. An analysis sample consists of 100 g coal with a particle size of 0.2 mm. Since no true values are given, no specific demands have been set up for the selection of the initial amount of coal to the sample preparation - but typically it will be a laboratory sample. The critical point is to ensure that the coal is homogeneous after crushing to 0.2 mm, before the final division. Before sending out the analysis samples, the distributing laboratory analyses the ash content in all the samples. This step is called "homogeneity test".

Preparation and distribution of laboratory samples are done by one of the participating laboratories. A laboratory sample consists of 10 kg coal with a particle size of 10 mm. This type of coal sample is the out-put from the mechanical sample units used for sampling coal delivered to Elsam by ship. The preparation of the laboratory samples to analysis samples at the individual laboratories is usually done by crushing, dividing and subsequent crushing to 0.2 mm.

At the time when it was decided to distribute laboratory samples, nearly 20 laboratories were participating. A divider for the preparation of 20 samples of 10 kg each was not available on the market. A test was made at Sønderjyllands Højspændingsværk (SH) on a

smaller divider. This divider had a stationary cone and a hopper with a rotating spout. The hole circumference was split up into 8 outlets of equal size. The result of the test was positive, and a larger divider with 20 outlets was ordered. Because of a demand on the width of the outlets of 3 times the particle size of the coal, the dimensions on the divider became considerable. The test for homogeneity mentioned earlier is indeed necessary for the preparation of laboratory samples to the round robin. It is, however, a problem that to determine the ash content you have to "destroy" the samples. Therefore a procedure was developed resulting in 2 sets of 20 samples. 400 kg coal originating from the stockpiles at SH were divided to give 20 samples of 20 kg. Then each sample was divided in a manual rifle giving 2 samples of 10 kg. One set was sent out, on the other SH made a test for homogeneity, that is, they had to prepare and analyse all 20 laboratory samples.

The obtained SD in the ash content of the samples in the homogeneity test was not acceptable in the beginning. Investigations showed that manual riflling of coal with a particle size of 10 mm was introducing a large uncertainty. As a consequence, the procedure was changed to eliminate the riflling. This was done using two steps of division. Later the sampling of the 400 kg coal was moved from the stockpiles to the mechanical sampling unit when sampling from a ship. Together these two changes have lowered the SD in the ash content to an acceptable level, see enclosure 5.

The great amount of work for SH preparing the samples and making the test for homogeneity resulted in a last change of the procedure. Now 3 sets of laboratory samples are made by two subsequent divisions of 600 kg coal. This gives us two sets of samples to send out in the round robin and one set for homogeneity test covering both round robins.

The participating laboratories all determine moisture, ash, volatile matter, sulphur and calorific value. Four of the laboratories also determine swelling index and fusibility of ash. Results on analysis samples are given on a dry basis to estimate the analysis uncertainty itself. Results of laboratory samples are reported on a "as received" basis, by which the daily work, from receiving a laboratory sample to reporting the results, is reflected.

3.3.2. Treatment of Results

The statistical treatment of the results is, like the round robin for lubricating oils, made according to ISO 5725 part 2, which implies test for outliers and calculation of grand mean (X), repeatability (r) and reproducibility (R). Enclosure 6 is showing an example of a front page from a round robin report, including the result of the homogeneity test, X, r and R achieved in the round robin and finally acceptable values of r and R from ISO-standards. Failing anything better, the acceptable values from ISO are used for both round robins, but it is important to notice that ISO only is giving values for analysis samples. Because of the sample preparation, the round robin on laboratory samples will give higher values of R. For each of the participants two TREND-analyses are made, one for analysis samples and one for laboratory samples. The TREND-analysis is showing the deviation from the grand mean with an upper and lower critical limit based on the acceptable value of R.

3.3.3. Benefits

In table 2 the acceptable values for R from ISO are listed together with an average of R obtained in the round robin in the years 1994-1996.

Table 2					
Analysis	Standard	Acceptable value	$R_{analysis}$	$R_{lab.}$	$R_{lab.}/R_{analysis}$
Moisture (%)	ISO 589	*	0.47	0.69	1.5
Ash (%)	ISO 1171	A < 10 %: 0.30	0.26	0.61	2.3
		A > 10 %: 0.03*A	0.32	0.72	2.2
Volatile (%)	ISO 562	V > 10 %: 0.04*V	1.17	1.50	1.3
Sulphur (%)	ISO 351	0.10	0.16	0.16	1.0
Calorific value (J/g)	ISO 1928	300	251	482	1.9
Calorific value (J/g)				343	1.4

* No value in ISO. A value of 1.00 is used.

The achieved values for R in analysis samples are satisfying. The exception is sulphur which is the only analysis in which different methods are used.

As mentioned earlier, there are no acceptable values for R in laboratory samples. Instead of this, the ratio between R in laboratory and analysis samples is calculated, giving a number greater or equal to 1, as expected. Not surprising, the maximum ratio is found in ash, as this parameter is the most sensitive to errors in the sample preparation. Because of the direct relationship, also the calorific value has a high ratio. Calculated on dry-ash-free basis, the ratio is considerably lower.

Whether the increase in R was due to increased random errors or to systematic errors at some of the laboratories has been evaluated by means of the TREND-analysis schemes. The conclusion is that systematic errors are predominant at few laboratories. The size of the error is depending on the homogeneity of the coal type. Enclosure 7 is showing an example of a TREND-analysis in laboratory samples. The laboratory had a large systematic error for ash content until round robin 4/95. After an examination of the sample preparation leading to changes in the procedure, an improvement is evident.

In the absence of a true value, the round robin cannot give an estimate for the trueness. One of the laboratories in Elsam is participating in the round robin of analysis samples run by CT&E. The aim is to create a link and make traceability to laboratories outside Denmark. The trueness on laboratory samples can to some extent be evaluated by comparison with results from the coal suppliers.

In table 3 the average values for R achieved in the round robin on analysis samples are listed again. This time they are compared with similar values from round robins in Australia and USA (CT&E).

Table 3			
Analysis	Denmark	Australia	USA *
Moisture (%)	0.47		0.41
Ash (%)	0.30	0.25	0.28
Volatile (%)	1.17	0.84	1.49
Sulphur (%)	0.16	0.06	0.11
Calorific value (J/g)	251	350	268

* Results for coal with sulphur contents > 4% are not included.

Besides giving the laboratories a tool for their QA, the round robins are providing Fælleskemikerne with information usable in other connections.

Example 1: Fælleskemikerne participate in the working groups on coal within ISO. The present acceptable value for R on sulphur (0.10 %) in table 2 originates from the ISO-standard 351. By this method the coal test sample is burned, the evolved gasses are absorbed and the final determination is a titration. As the majority of the laboratories today use "automatic" equipment such as LECO, with IR-detection directly on the gasses, a new ISO-standard is in preparation, which again implies a new acceptable value for R. Enclosure 8 shows the achieved values for R on sulphur as a function of the sulphur content in the round robin samples. From this it is our opinion that the acceptable value of 0.10 % independent of concentration is unrealistic low. The first proposal in the new working draft is $R = 0.05 + 0.06 \cdot S$. The proposal is indicated with a line in enclosure 8. The idea to let the acceptable value increase with increasing sulphur content is in good agreement with our results. That we still in most cases have too high values of R, can to some extent be explained by the use of different methods, although LECO is predominant.

Example 2: The results from the homogeneity tests and the results on ash from the round robins provide a good basis for an evaluation of the homogeneity of the different types of imported coal. By testing of sampling and sample preparation equipment this knowledge is used to choose inhomogeneous coals such as Colombian or Polish coal. The use of Australian coals, which according to our experience is very homogeneous, could lead to a false confidence.

3.4. Ion Chromatography

This round robin is split in two concentration levels. One for the ppb-range, focused on the water/steam-curcuit, water treatment plant and the like, plus one for the ppm-range focused on slurry in desulphurization plants, water in district heating pipes and the like.

The round robin on Ion Chromatography (IC) was established in 1992 when nearly all Danish power plant laboratories had purchased IC-equipment. In the round robin in the ppb-range, 12 laboratories are currently participating, including 3 Swedish, 1 Finnish, 1 German and 1 UK laboratory. In the round robin in the ppm-range 8 laboratories participate, primarily the Danish power plants themselves.

In the ppb-range two samples with known contents of fluoride, chloride and sulphate are sent out in each round robin. The samples are prepared from ultra pure water and standards. The water used for dilution is making up a blind sample. The very first round robin in the ppb-range was a test to decide if it was possible to prepare and distribute samples in these low concentrations and still obtain usable results. The conclusion was positive, but the sample preparation requires great care.

In the ppm-range two samples with known contents are distributed together with a third sample of slurry or district heating water.

All samples are analysed for fluoride, chloride and sulphate on two different days.

3.4.1. Treatment of Results

The results are treated according to ISO 5725 part 2, starting with tests for outliers and calculating grand mean (X), SD in the laboratories (S_0) and total SD (S_t). The trueness is estimated by comparison of X with the true value. In the round robin in the ppm-range the obtained values for S_0 and S_t are compared with acceptable values.

Since no acceptable values are given in analytical standards such as ASTM or ISO, the acceptable values in table 4 are derived from the results of the round robins executed in 1993 and 1994. Results of dilution water and natural samples are not included.

Table 4				
Maximum acceptable standard deviations				
Analyte	**Single lab.**		**Total**	
	S_0 (ppm)	Conc. (ppm)	S_t (ppm)	Conc. (ppm)
Fluoride	0.10 * C	C < 4	0.11 * C	C < 4
	0.40	4 < C < 15	0.44	4 < C < 15
Chloride	0.03 * C	C < 6	0.05 * C	C < 6
	0.18	6 < C < 15	0.30	6 < C < 15
Sulphate	0.02 * C	C < 15	0,4 * C	C < 25
	0.30	15 < C < 25		

The acceptable values were derived from the data available at that time. This means that it may be necessary to re-evaluate the acceptable values when more experiences are gained. Enclosure 9 shows an updated graphical presentation of values for S_t, together with the acceptance limits from 1994. A revision of the acceptable values seems to be necessary in the near future for at least fluoride and chloride.

In table 5 the ranges of recovery for the samples with known concentrations are listed. Only values from the round robins performed in 1995 and 1996 are included.

Table 5						
Round Robin	Fluoride		Chloride		Sulphate	
	Recovery (%)	Conc.	Recovery (%)	Conc.	Recovery (%)	Conc.
ppb-range	95 - 105	2 - 13	95 - 100	2 - 20	90 - 110	3 - 25
ppm-range	95 - 105	1 - 12	97 - 103	1 - 18	97 - 100	3 - 25

The trueness, expressed as recovery, is good.

3.5. Dissolved Gas Analysis

This round robin is focused on the operational control of transformers by monitoring the dissolved gasses in the oils.

In 1993 and 1994, four round robins were carried out with 8 participating laboratories from 8 different countries. After a break in 1995, the round robin is now continued with laboratories from 5 countries. Three round robins a year are planned.

The samples originate from transformers in operation. Because of the volatility of hydrogen and carbon monoxide, the sampling is done using gastight syringes. Before the final detection, each laboratory has to extract the gasses from the oil. How large the uncertainty introduced by this pre-treatment is, compared to the total uncertainty, is not known, but it is most likely the largest single contributor.

The laboratories determine hydrogen, methane, ethane, ethene, ethyne, carbon monoxide and carbon dioxide. The development in the amounts of the gasses and the relationship between the gasses are used for monitoring the condition of the transformers.

3.5.1. Treatment of Results
The report to the participants contain all results listed in a table together with the results in bar graphs for each gas. Finally, each laboratory gets a bar graph showing its performance in relative deviation from the grand mean. The acceptable values for reproducibility are not so clearly stated as for example in the case of coal. The conclusion of the round robins run so far is, however, that the laboratories have a repeatability well under the desired, but considerable systematic differences between laboratories occur. The monitoring of a transformer by DGA therefore ought to be done by the same laboratory.

3.6. Summary

Table 6 summarizes some of the features from the 5 round robins.

Table 6								
Round Robins	**Analyses**	**Participants**		**RR's yearly**	**Prec. (estim.)**	**True. (estim.)**	**Accept. values**	**Trend-analysis**
		Total	**Foreign.**					
Boiler Water and Steam	Cu, SiO_2, Fe, NH_3	8	No	12	Yes	Yes	ASTM, StM, own	No
Lubrica-ting oils	Dens., visc., TAN, water	11	No	4	Yes	No	ASTM	Yes
Coal	M, A, V, S, CV	14	Yes	10	Yes	No	ISO	Yes
IC	F^-, Cl^-, SO_4^{2-}	12	Yes	4	Yes	Yes	Own	No
Transfor-mer oils	Dissolved gasses	5	Yes	3	Yes	No	IEC	No

4. Conclusion

Performing round robins at regular intervals is very important for Elsam in the monitoring of precision and trueness of analytical results.

The achieved values for uncertainty are good estimates because of the use of natural samples from the operation of the plants, and because the round robins are run continuously, so that they become part of the daily work in the laboratories.

Besides providing the laboratories with a tool to check their momentary performance, the round robins are very suitable for evaluating systematic developments on a long term basis.

In some cases the round robins can replace certified reference materials, which still are available to a limited extent only.

By splitting up the uncertainty according to methods, sample preparation/analysis etc., knowledge can be extracted from the round robins for use in many other situations.

Lab. nr	Method	Sample A µg/l			Sample B µg/l		
		Day 1	Day 2	Average	Day 1	Day 2	Average
1 VK	PVA 204.2	2	4	3	14	15	14.5
2 SV	Elec.chem.	4.5	4.5	4.5	13.5	13.2	13.4
3 MKS	AAS	4	5	4.5	14	14	14
4 NVA	Elec.chem.	4.9	4.9	4.9	15.2	15.4	15.3
5 SV	PVA 204.2	5	5	5	16	16	16
6 SH	PVA 204.2	4.7	5.4	5.1	16.4	15.5	16.0
7 SH	AAS	5.3	5.3	5.3	15.3	15.3	15.3
8 FV	PVA 204.2	8	6	7	18	17	17.5
9							
Grand mean				4.9			14.9
True concentration				5			15
S (acceptabel standard deviation)				1.2			1.6
So (standard deviation in single lab.)				0.8			0.4
S1 (standard deviation between lab.)				1.0			1.3
St (total standard deviation)				1.2			1.4

Sample B
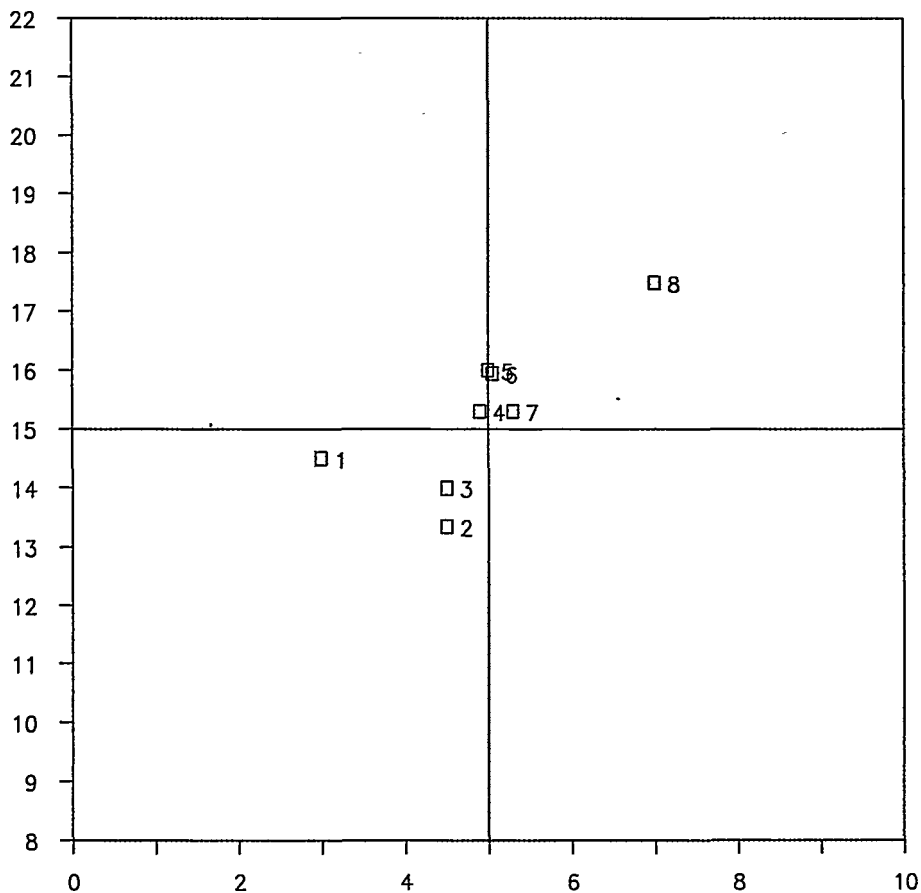
Confidens interval : > 95 % ☐ > 99 % ☐ **Sample A**

Remarks : If the results from the laboratories 1 and 8 are omitted for sample A, St will drop to 0,4.

Jan Hinnerskov

13.11

Round Robin, water.
Copper.

Precision. RSD (%).	Year						
	89	90	91	92	93	94	95
0 - 5	10 12		22 28	20 23	12	10 22 15	9 31 24 15
5 - 10	14		17		17	19	
Conc. 10 - 15			7 17	12		12 5	7 7 9
15 - 20	6	13		6	10		
20 - 30	5		10		9	8 7	
30 - 40	9	9		8 6			

Trueness. Recovery (%).	Year						
	89	90	91	92	93	94	95
0 - 5	106 100		103 92	124 110	107	106 100 110	94 106 98 105
5 - 10	89		77		92	104	
Conc. 10 - 15			97 96	104		100 106	94 97 99 110
15 - 20	102	104		102	104		
20 - 30	102		96		96	102 103	
30 - 40	100	101		104 99			

13.12

FÆLLESKEMIKERNE
JHJ/jhj

Round Robin, lubricating oils 4/95

Your ID-number : _____ .

The samples was distributed by NVV and analysed by ASV, dk-TEKNIK, FMK, FV, KBC, KYV, MKS, NVV, SH, STV, SV and VK. The laboratories have analysed as follows :

- density (g/cm³)
- viscosity (cSt v. 40°C)
- total acid number (mg/g)
- water content (mg/kg)

The distributed samples are :

oil A :	GRXP 150	New
oil B :	HLP 46	New
oil C :	Castrol Perfecto 46t	In operation

Results

All results are shown in enclosure 1, 2, 3 and 4. Grand mean (X), repeatability (r) and reproducibility (R) are calculated and listed in the tabel. In the statistical treatment 10 results were identified as outliers.

	ROUND ROBIN 4/95			ASTM	
	X	**r**	**R**	**r**	**R**
Oil A					
Density (g/cm³ at 40°C)	0,8798	0,0004	0,0024	---	---
Viscosity (cSt at 40°C)	152	5	24	2	11
TAN (mg/g)	0,50	0,03	0,16	0,03	0,14
Water (mg/kg)	39	5	53	26	96
Oil B					
Density (g/cm³ at 40°C)	0,8622	0,0002	0,0022	---	---
Viscosity (cSt at 40°C)	45,8	1,2	6,7	0,7	3,4
TAN (mg/g)	0,46	0,02	0,11	0,03	0,13
Water (mg/kg)	82	7	90	37	139
Oil C					
Density (g/cm³ at 40°C)	0,8615	0,0007	0,0020	---	---
Viscosity (cSt at 40°C)	46,8	0,6	6,7	0,7	3,4
TAN (mg/g)	0,11	0,02	0,06	0,01	0,05
Water (mg/kg)	40	7	65	26	97

TREND-analysis for NN
Deviation from grand mean (%)
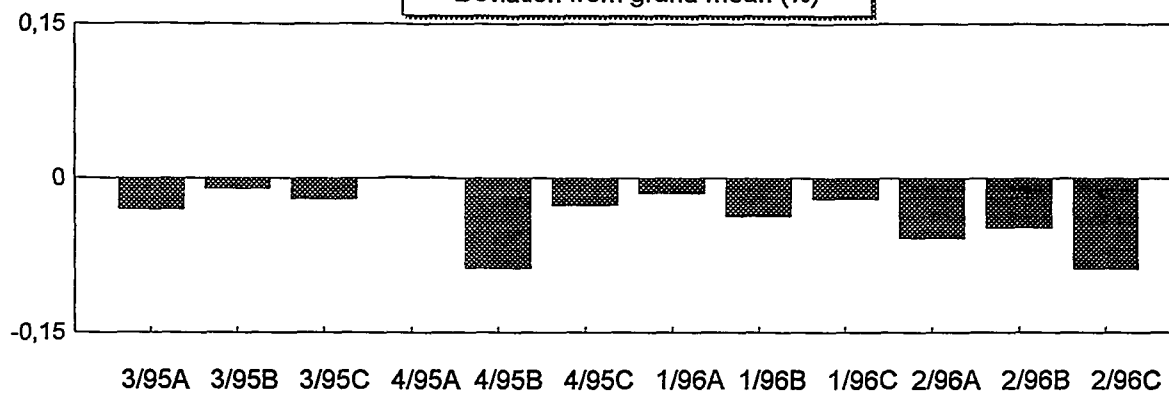
Enclosure 4

Density

0,15 — 0 — -0,15

3/95A 3/95B 3/95C 4/95A 4/95B 4/95C 1/96A 1/96B 1/96C 2/96A 2/96B 2/96C

Viscosity

10-22 cSt

15 — 0 — -15

1/95A 2/95B

Viscosity

32-68 cSt

15 — 0 — -15

1/95B 1/95C 2/95A 3/95C 4/95B 4/95C 1/96C 2/96A 2/96B

Viscosity

100-320 cSt

15 — 0 — -15

2/95C 3/95A 3/95B 4/95A 1/96A 1/96B 2/96C

13.14
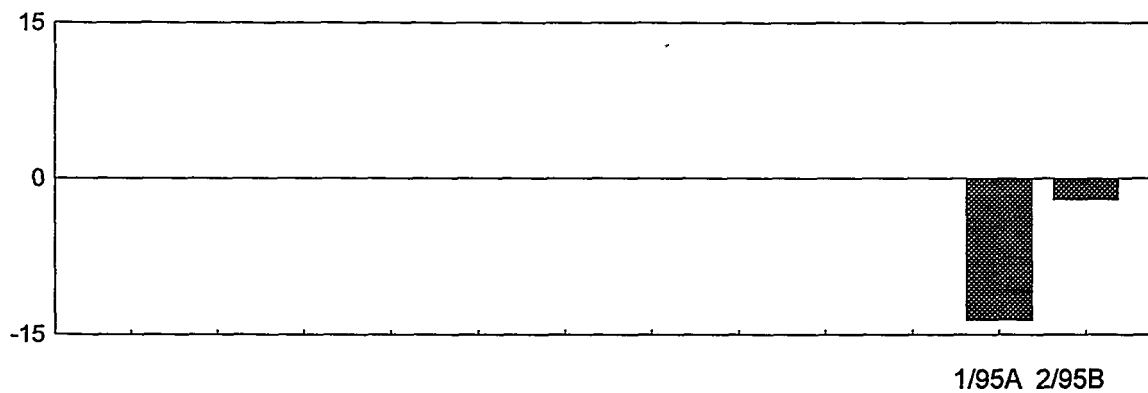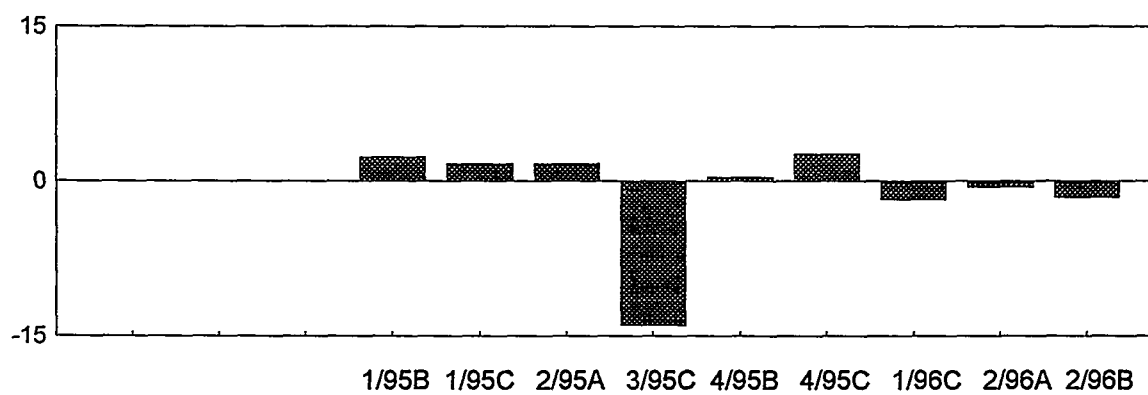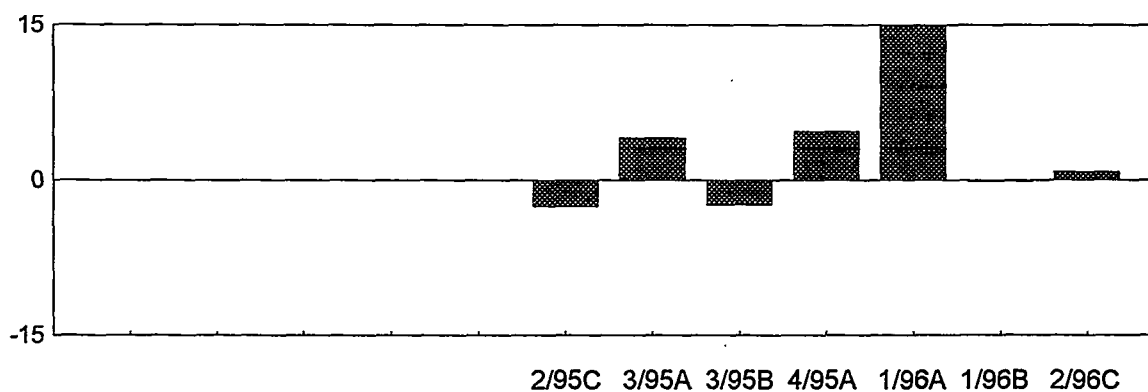
Test for homogenity of round robin samples.
Standard deviation, ash content (%).

Coal type	Coal from stockpile		Coal from ship	
	Manual riffle used		Manual riffle used	
	Yes	No	Yes	No
Australia		0,09	0,06 0,07 0,11	
Colombia		0,15 0,16 0,26	0,12 0,16	0,1
US	0,28 0,33 0,39			0,05 0,05
South Africa				0,06

FÆLLESKEMIKERNE
JHJ/jhj

Round Robin, coal 5/96.

Your ID-number : _____ .

Analysis samples distributed by KBC week 23. Polish coals (PODUFF).

Test for homogenity (% ash, dry basis) :

13,96	14,21	14,24	14,29	14,39
14,02	14,23	14,24	14,31	14,45
14,18	14,23	14,27	14,32	14,47
14,19	14,23	14,27	14,35	

Standard Deviation = 0,12.

Achieved and Acceptable Values for Precision				
	Round Robin 5/96		ISO	
	r	R	r	R
Moisture (%)	0.09	0.41	0.50	1.00
Ash (%)	0.16	0.36	0.29	0.43
Volatile matter (%)	0.33	1.70	0.98	1.31
Sulphur (%)	0.04	0.17	0.05	0.10
Calorific value (J/g)	103	200	120	300
Swelling index	0.5	0.2	1.0	0.5
Fusibility of ash				
Deformation temp. (°C)		70		80
Hemisphere temp. (°C)		110		60
Flow temp. (°C)		150		80

The statistical treatment 1 result (CV) was identified as an outlier.

Comments.
The two lowest results for ash are close to be outliers according to Grubb's test. The test for homogenity on the distributed samples is however showing a relative high SD, not least due to 2 samples with low ash contents. As the two laboratories at the same time are reporting high results on calorific value, it indicates that the measured ash contents are correct.

If the two highest results on sulphur are omitted, the reproducibility is only 0,12.

13.16

TREND-analysis for NN
Laboratory samples

	9/93	1/94	3/94	5/94	7/94	2/95	4/95	6/95	8/95	10/95	2/96	4/96
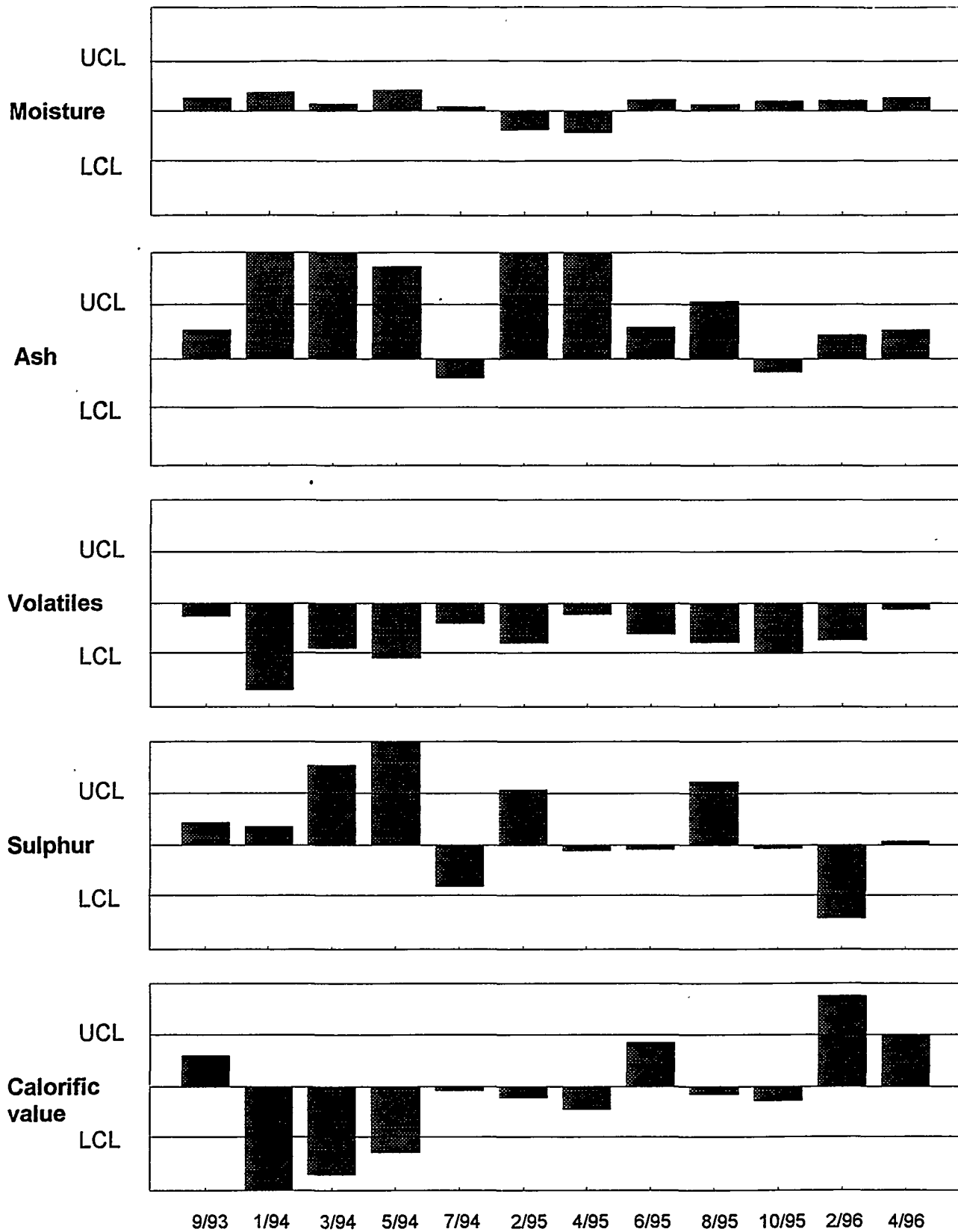
Relationship between sulphur content and reproducibility
Round robins 1994 - 1996, analysis samples
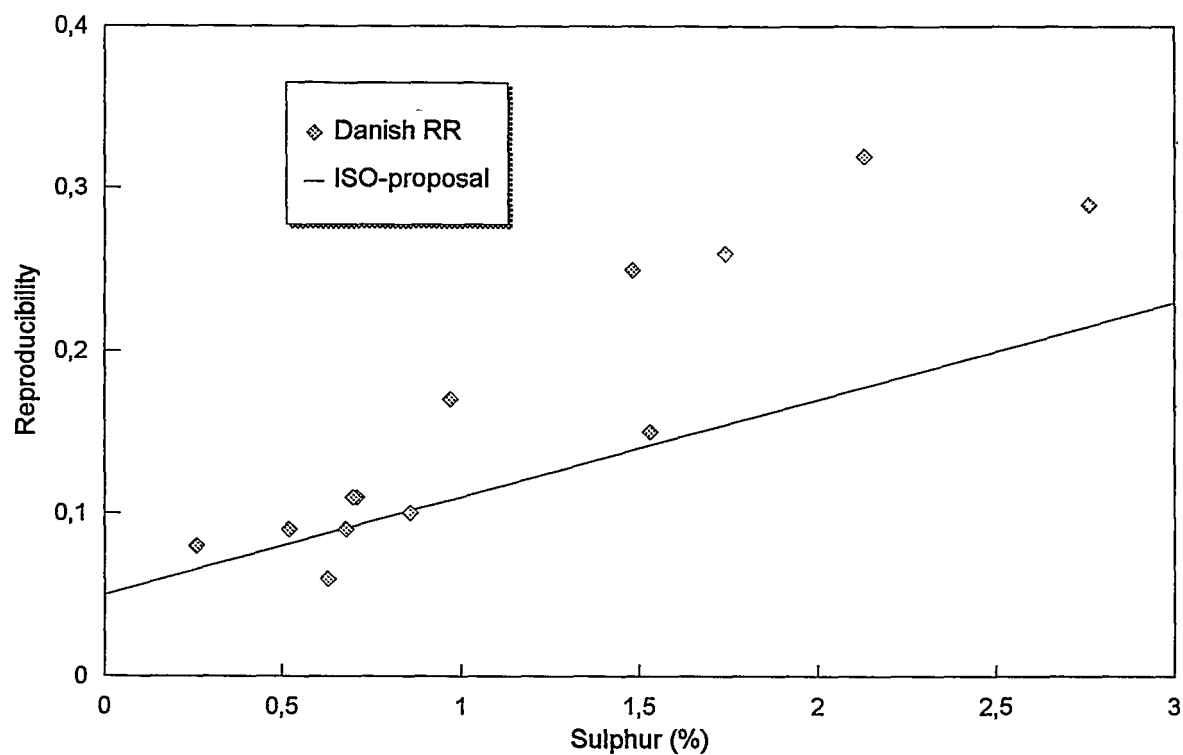
Round robins 1994 - 1996, laboratory samples

13.18

Fluoride (ppm)

Chloride (ppm)

Sulphate (ppm)
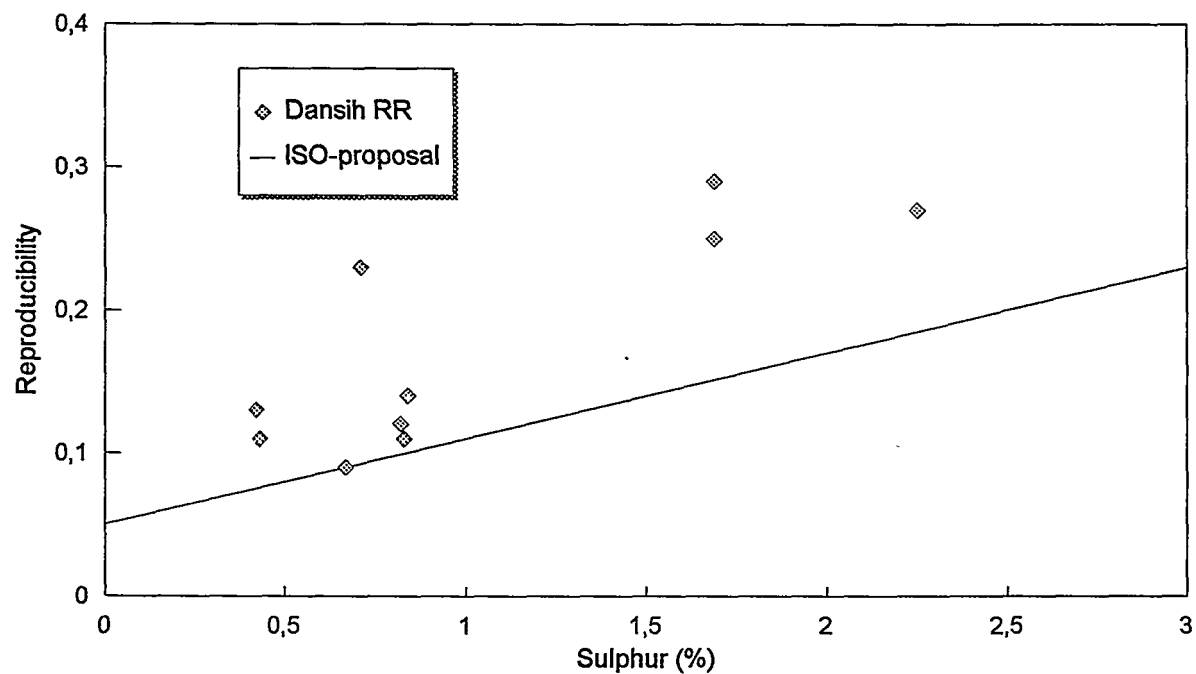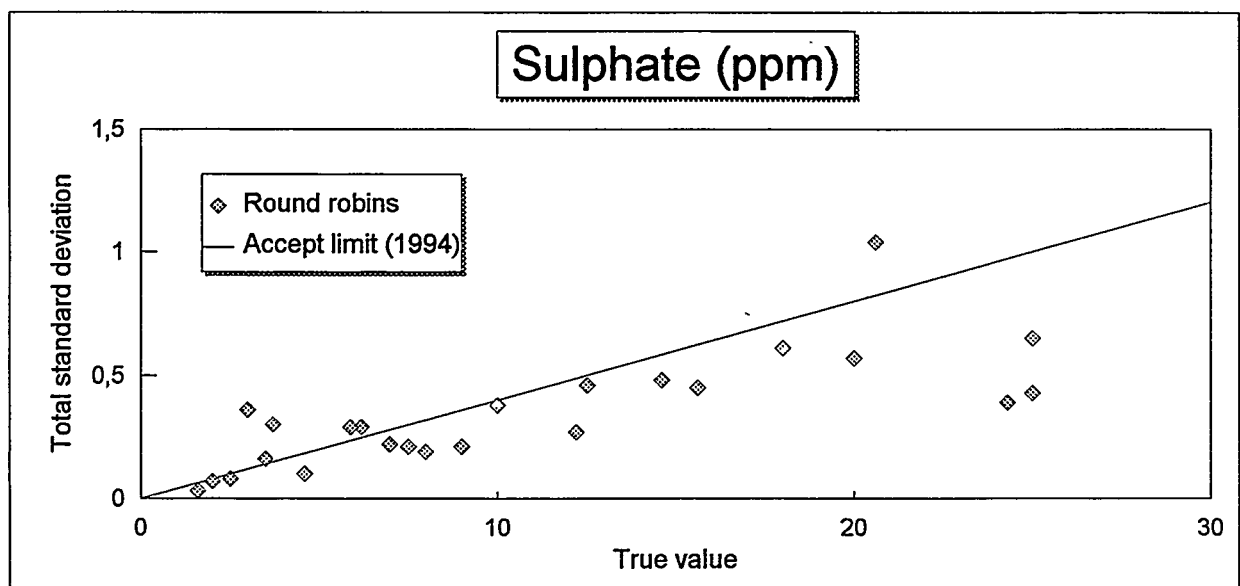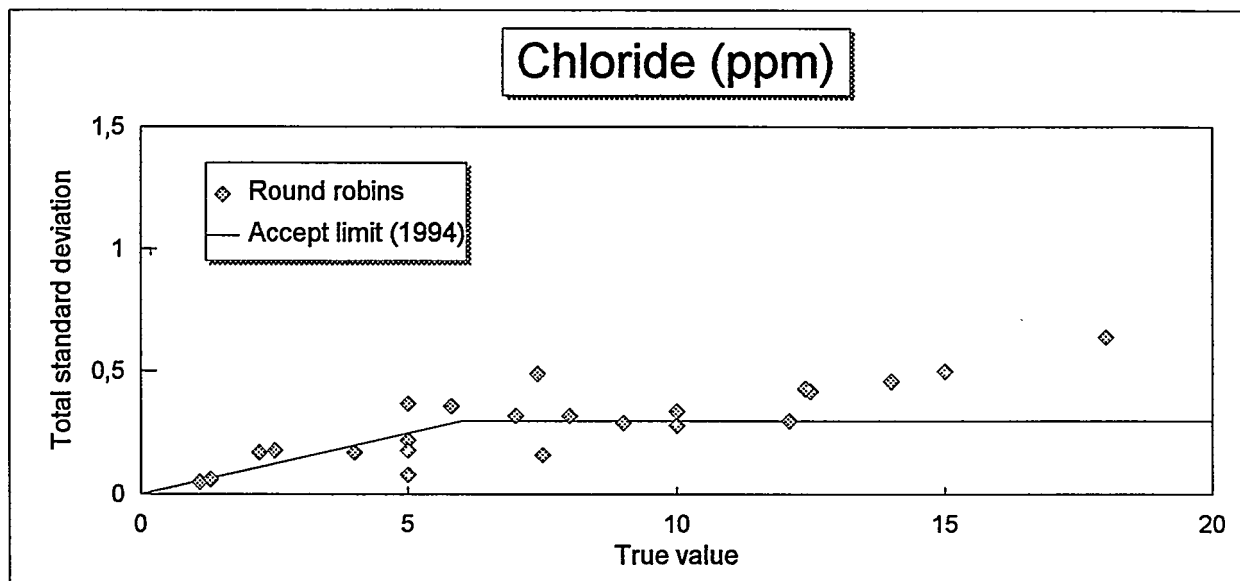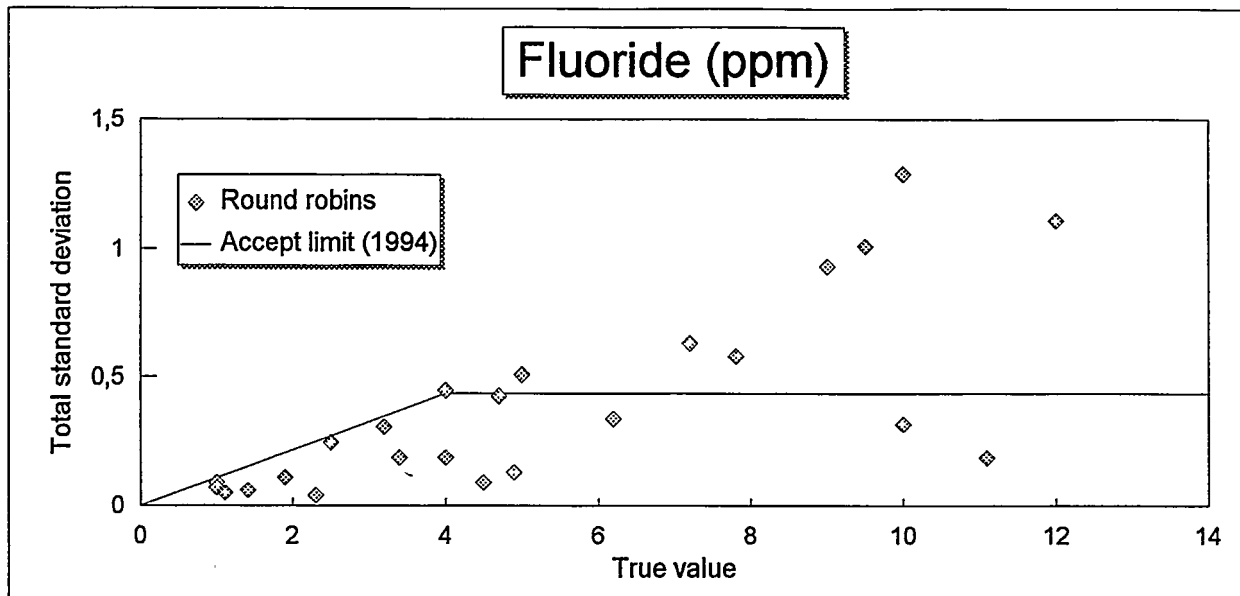
On-Line Ion Chromatography at Ringhals Nuclear Power Plant

Staffan Redén
Vattenfall
Ringhals
S-43022 Väröbacka
Sweden

Rickard Halldin
Vattenfall
Ringhals
S-43022 Väröbacka
Sweden

ABSTRACT

In 1981 Ringhals Nuclear Power Plant identified a demand for more accurate methods to determine low concentrations of ions in ultra pure water. Therefore the method - Ion Chromatography developed by Dionex Inc., USA - was of great interest for us.

The first instrument purchased was a "Model 16". The development of the technique was slow but compared with the ordinary analytical methods available at that time, the abilities were outstanding.

In 1984, the next generation of instrument from Dionex was purchased. It was the model 2000i with the self regenerating suppressor column, the "Fiber Suppressor". This technique gave us the ability to test the system for an on-line application. The first study in 1985 was with process water from the reactor coolant of the BWR unit. The results from the study showed the demand for such a configuration due to the risk of contamination of the sample.

In 1988, we bought the first non Dionex equipment, an Ion Chromatograph from Shimadzu. The type of instrument had a couple of advantages such as price, ease of handling, and size. The main disadvantage was the poor stability resulting in a detection limit of only 1 ppb of sulfate, chloride etc.

Due to requirements for much higher purity of the process water and the make-up water, we were forced to develop a much more accurate method to determine the concentration of impurities.

The demands for detection limits were now in the ppt range. Therefore a new generation of Dionex equipment, the 4000-series, was bought. The first system was purchased in 1989. At the end of 1990, the detection limit in high purity water was 5-10 ppt for chloride and sodium and approximately 50 ppt for sulfate.

Since then we have further developed the technique for a more stable environment and an optimized date acquisition system.

The future seems to advance to less complicated equipment built for the very application it is supposed to work in, not a general configuration.

The paper will be handed out at the conference

On-Line Ion Chromatography at Ringhals Nuclear Power Plant

Presented at the "Power Plant Chemical Technology 1996"
September 4 - 6, 1996 in Kolding, Denmark.

In 1981 Ringhals Nuclear Power Plant identified a demand for more accurate methods to determine low concentrations of ions in ultra pure water. Therefore the "new" method - Ion Chromatography developed by Dionex Inc., USA, was of grate interest for us.

The first instrument purchased was a "Model 16". The development of the technique was slow but compared with the present ordinary analytical methods available, it´s abilities were outstanding.

In 1984, the next generation of instrument from Dionex was purchased. It was the model 2000i with the new self regenerating suppressor column, the "Fiber Suppressor".·
This new technique gave us the ability to test the system for an on-line application.
The first study, which·occured in 1985, was with process water from the reactor coolant of the BWR-unit.
The results from the study showed the demand for such a configuration due to the risk of contamination of the sample.

In 1988 we bought the first non Dionex equipment, an Ion Chromatograph from Shimadzu.
The type of instrument had a couple of advantages such as price, easy to handle and size.
The main disadvantage was the poor stability which gave us the ability to a detection limit of only 1 ppb of sulphate, chloride etc.

Due to requirements for much higher purity of the process water and the make-up water we were forced to develop a much more accurate method to determine the concentration of impurities.
The demands for detection limits was now in the ppt range.
Therefore a new generation of Dionex equipment, the 4000-series, was bought.
The first system was purchased in 1989 and the development was started.
The problem with analysing at these low levels of impurities is the calibration, this was however solved with the use of a calibrated loop.
In the late 1990, the detection limit in high purity water was 10 ppt for chloride and sodium and approximately 50 ppt for sulphate.
The development took place at the deminplant at unit 3

Today we are still using the equipment, used for the study. It is now operating continuously on the deminplant at unit 3, since the demand for a detection limit for low levels of ppt is not valid anymore, the chromatograph is now operating with a simpler configuration.We are also using the same configuration on the on-line chromatographs on the blowdown system at unit 3 and 4 where the matrix is on of 2-3 ppm of ammonia and 6-8.ppm boric acid. This matrix reduces the lifetime of the columns and of course the "potential" for low detection limit is not as good as on the deminplant.

The future seems to advance to less complicated equipment with system built for the very application it is supposed to work in, not a general configuration.

On-line Ion Chromatography at Ringhals Nuclear Power Plant

Presented by

Staffan Redén

at the

"Power Plant Chemical Technology 1996"
September 4-6 in Kolding, Denmark.

VATTENFALL
RINGHALS

On-line Ion Chromatography at Ringhals?

- Why measure so low levels?
- Why Ion Chromatography?
- Why on-line?

VATTENFALL
RINGHALS

Part of crack, broken open.
Ringhals 3, max depth 637µm, 7mm long, EC-detected.
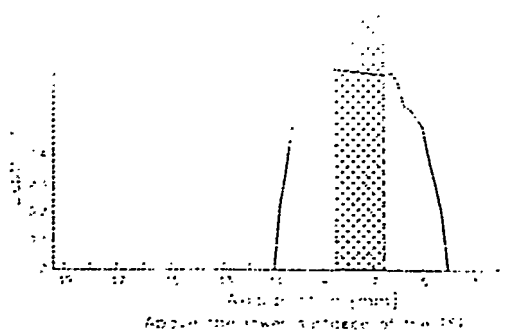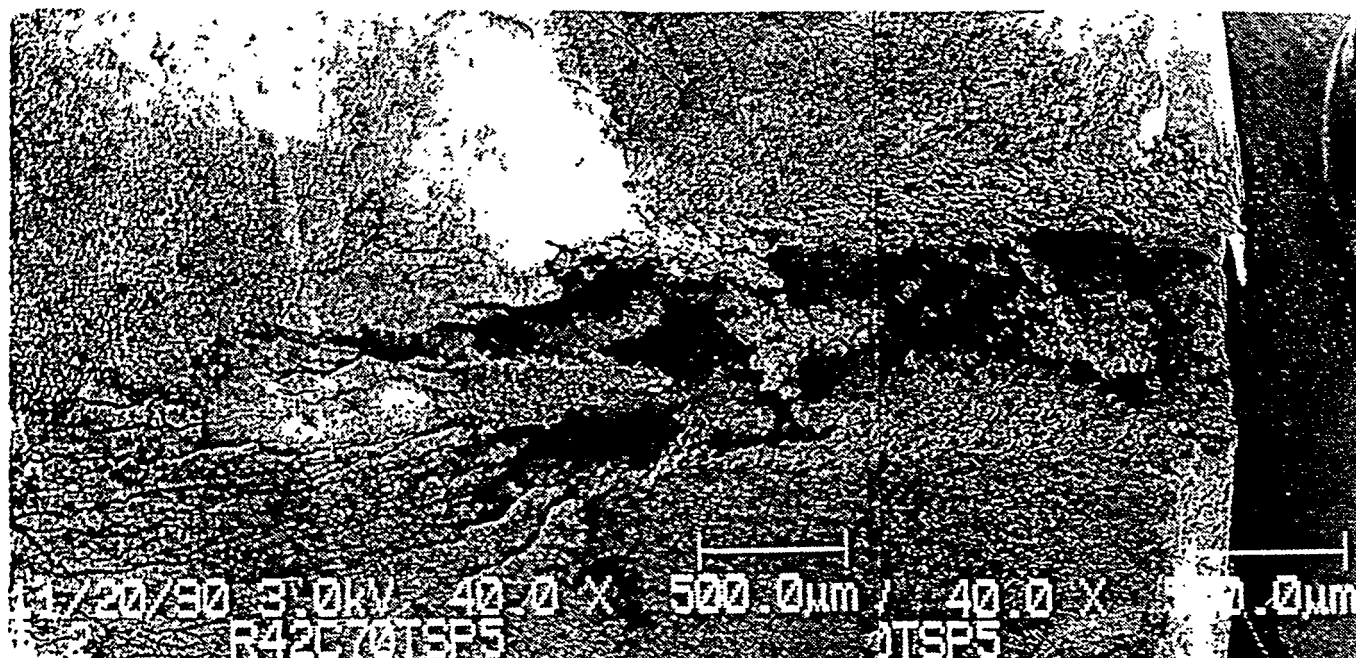
Crevice chemistry vs. analyses of pulled tubes

* Optical microscopy: crack size and morphology

* SEM + EDS + AES: Element distribution in deposits

* AES: Concentration profiles for oxide and deposits

* XRD: Phase identification of deposits

◄ Correlation ►

* Calculation of concentrated soak data

   MULTEQ code ➠ pH, liquid composition
                              precipitates (deposits)

Crevice chemistry

Crevice inventory

Redox potential
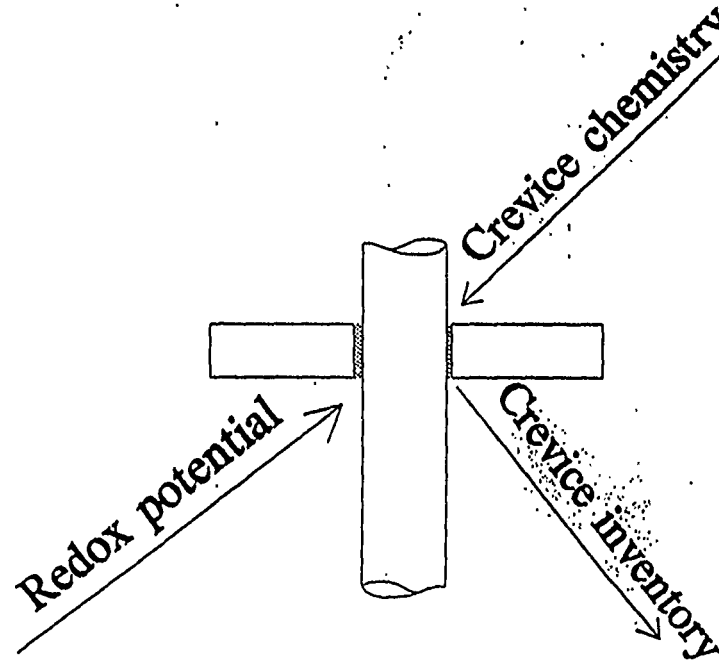
* Mößbauer spectroscopy

   Relative proportions of Fe(II) and Fe(III)

* SG hot soaks

* Soaks of pulled TSP-sections

On-line Ion Chromatography at Ringhals yesterday

- **1981**   **Dionex Model 16**
- **1984**   **Dionex 2000**
- **1985**   **First "on-line" study**
- **1988**   **Schimadzu**
- **1989**   **Dionex 4500i**
- **1990**   **ppt range, On-line on the deminplant**
- **1992**   **Dionex 4500 On-line on Unit 4**
- **1993**   **Dionex 4500 On-line on Unit 3**

VATTENFALL RINGHALS

On-line Ion Chromatography at Ringhals

Sample from the blowdown system

Controlsample

Standardsolutions

Samplevalve

STDvalve

Eluent   Eluent
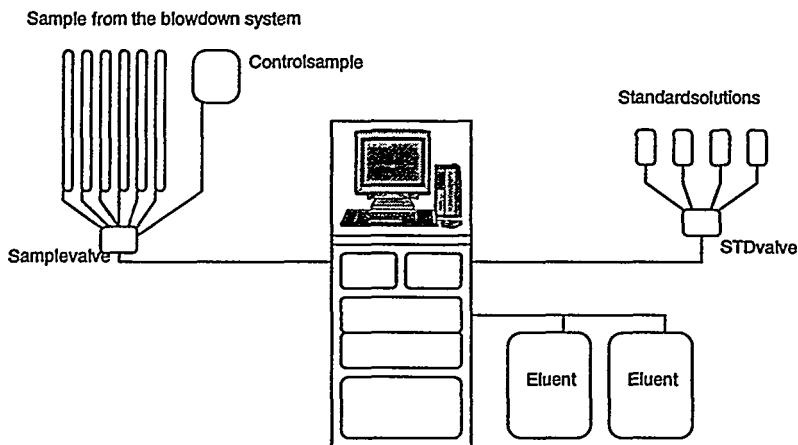
VATTENFALL RINGHALS
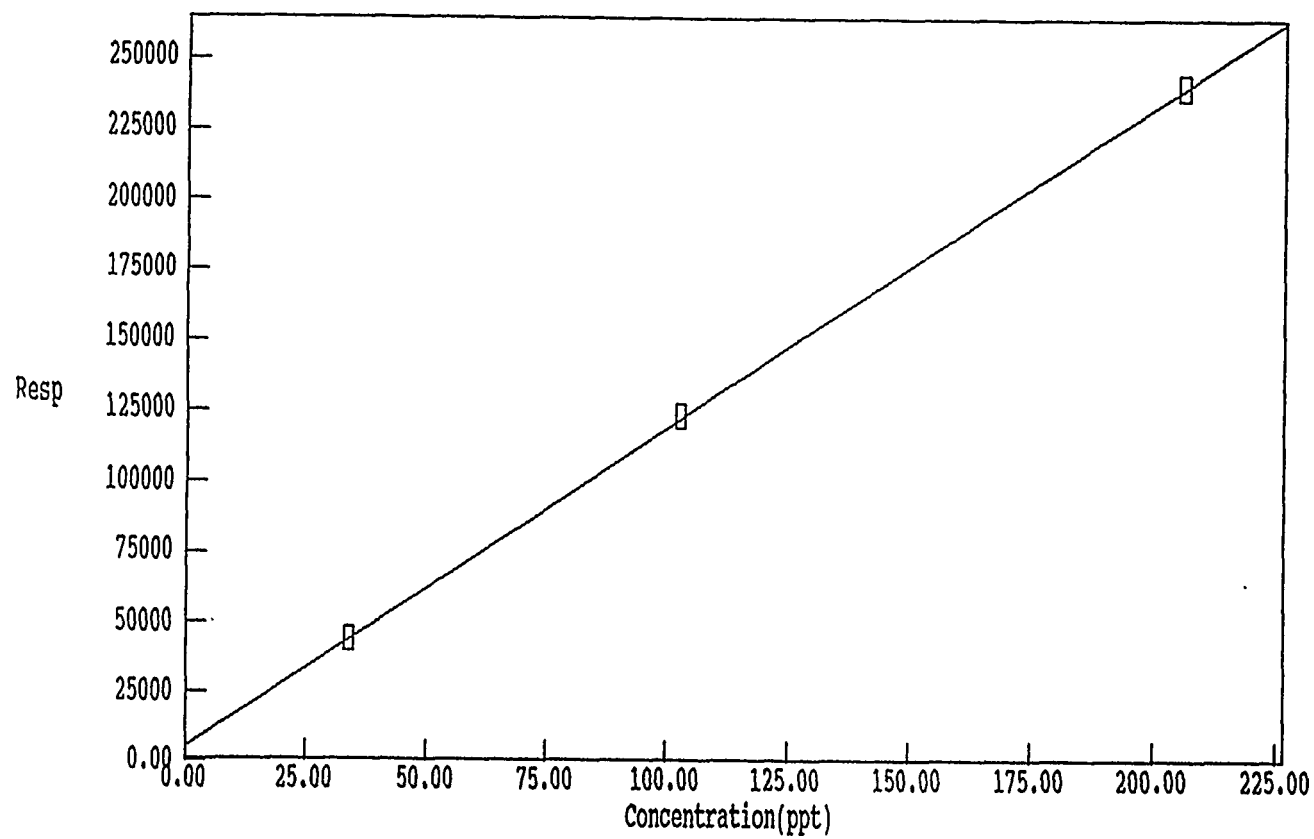
Component: Cl
Fit Type: Linear
r²: 0.999988
Conc = Resp * 0.0008756 + -4.777
Resp = Conc * 1142 + 5455
Standardization: External
Calibration: Height
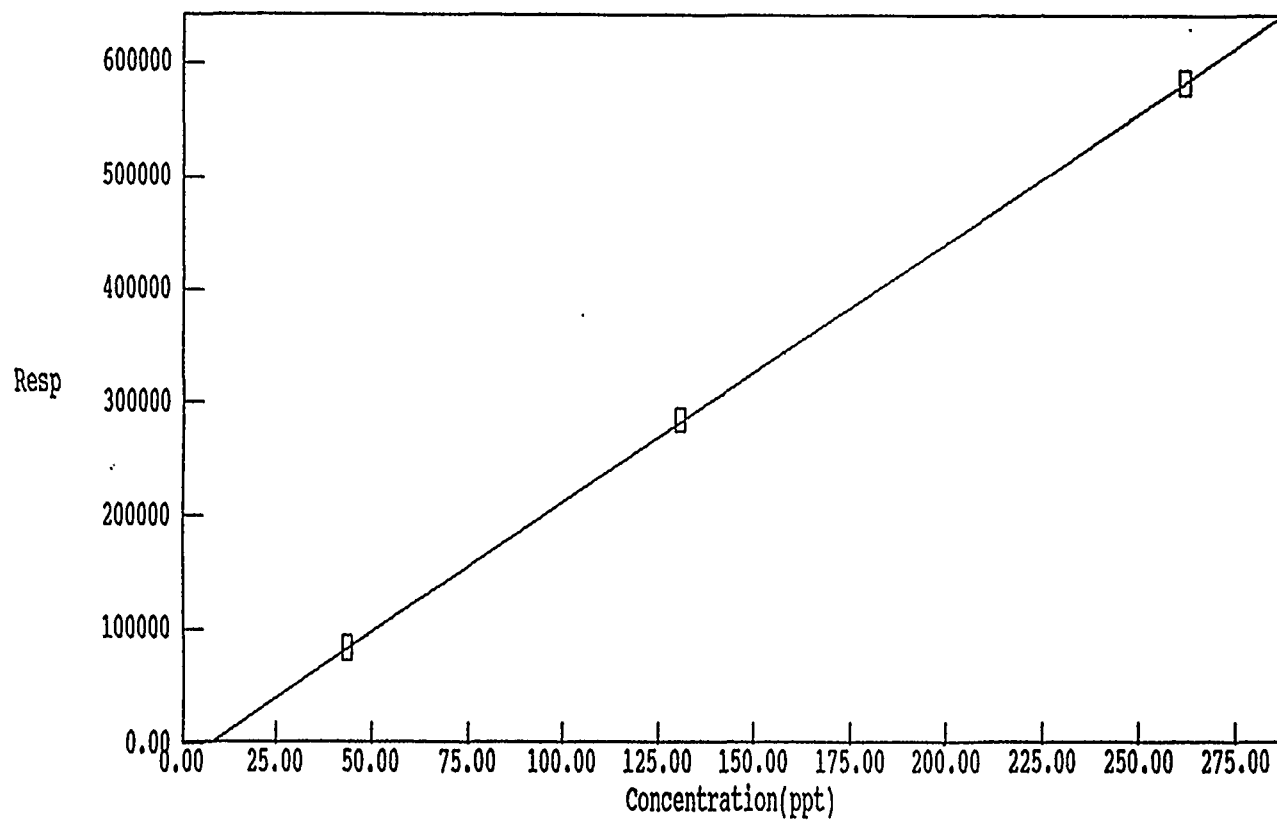
Component: NA
Fit Type: Linear
r²: 0.999984
Conc = Resp * 0.0004364 + 7.355
Resp = Conc * 2291 + -16850
Standardization: External
Calibration: Height

On-line Ion Chromatography at Ringhals
Equipment in use today

Instrument	Dinoex 4500i
Software	AI-450
Eluentpump	GPM/AGP
Regenerentpump	Watson Marlow 101U
Sample valve	VICI Valco ESF 12P
STD valve	Rheodyne 5703

On-line Ion Chromatography at Ringhals

Columns and Eluents

Instrument	System	Column		Eluent	Flow (ml/min)	Regenerant	Sample volume (ml)	Loop (µl)
Deminplus	Anion	Conc.	TAC-2	0.3 mM NaHCO3	1,0	H2SO4	20	38
		Guard	AG12A	2.7 mM Na2CO3				
		Sep.	AS12A					
		Suppr.	ASRS-1					
	Cation	Conc.	CG-12	20 mM MSA	1,0	Water	20	45
		Guard	CG-12					
		Sep.	CS12					
		Suppr.	CSRS-1					
BD	Anion	Precol.	ATC-1	80 mM NaOH	1,0	Recycle	10	30
		Conc.	AG4A					
		Guard	AG10					
		Sep.	AS10					
		Suppr.	ASRS-1					
	Cation	Precol.	CTC-1	20 mM MSA	1,0	Recycle	5	25
		Conc.	CG-12					
		Guard	CG-12					
		Sep.	CS12					
		Suppr.	CSRS-1					

VATTENFALL
RINGHALS
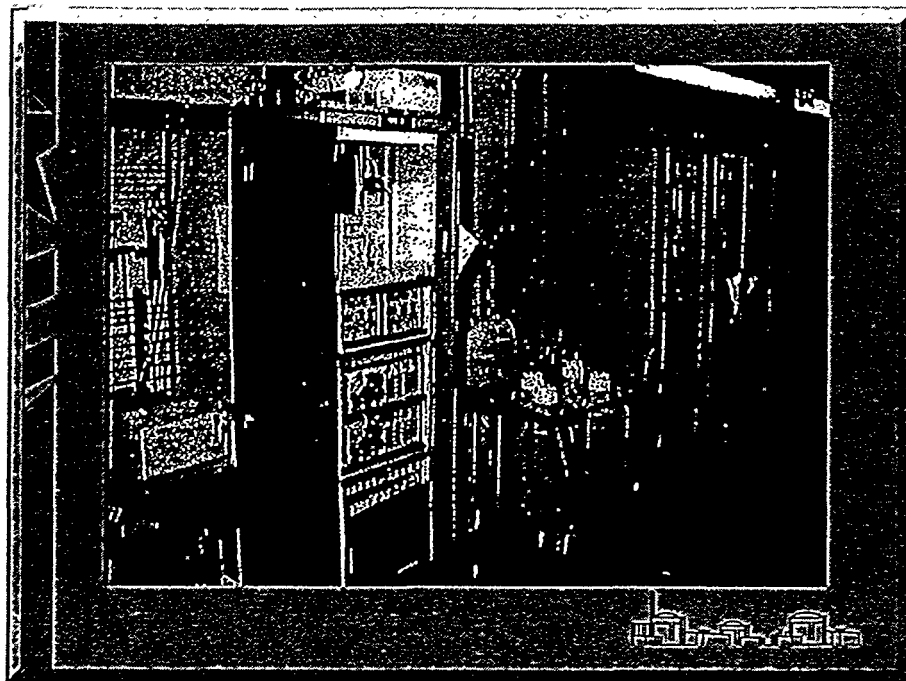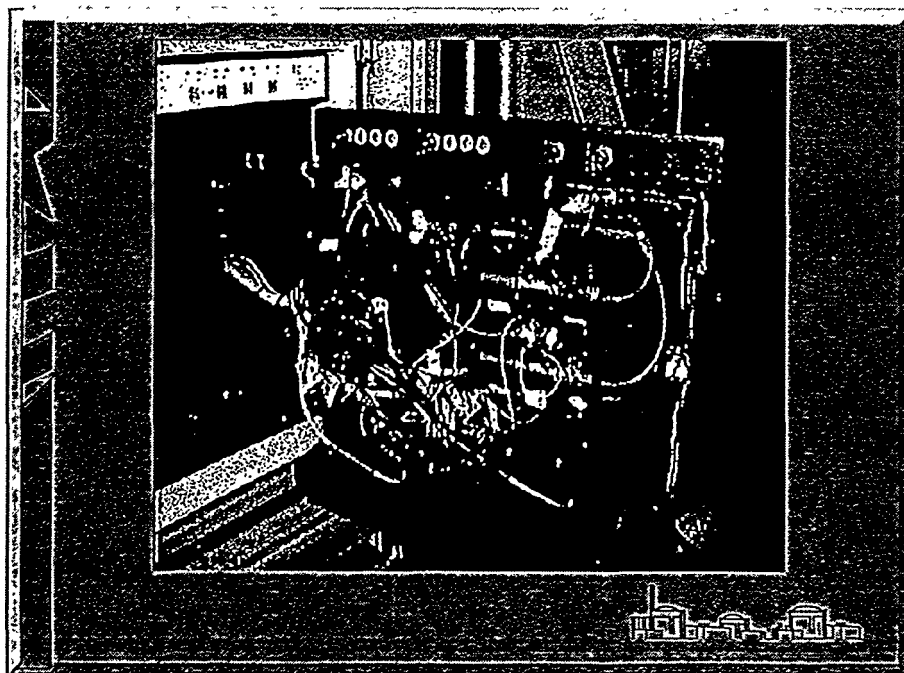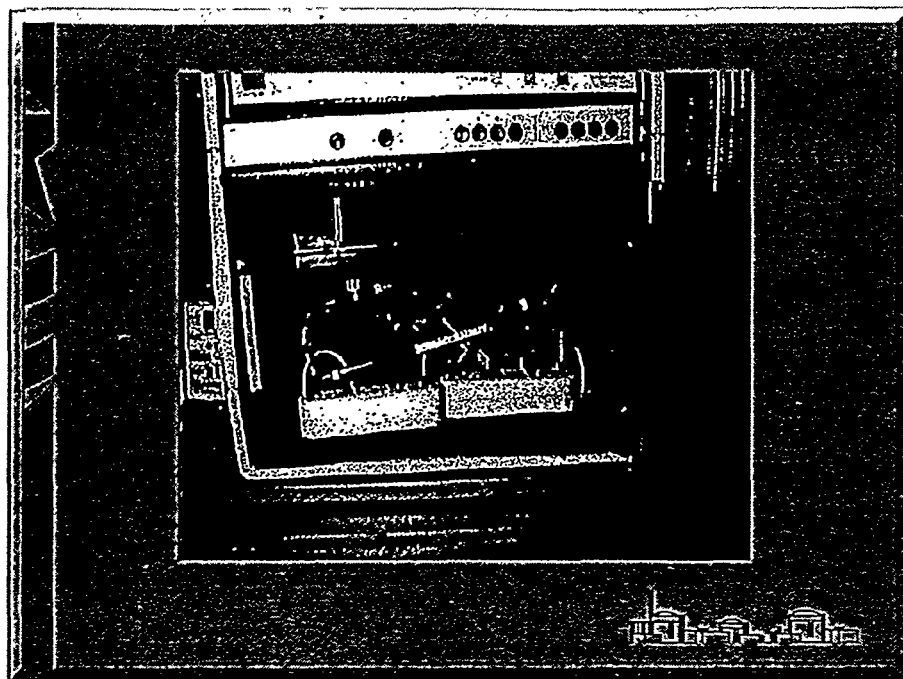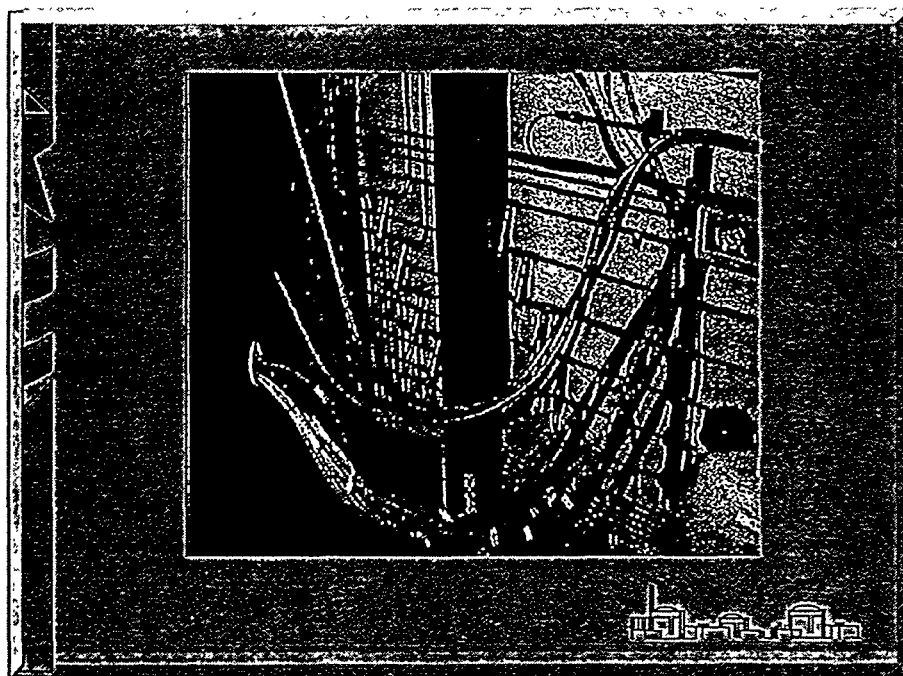
VATTENFALL
RINGHALS

VATTENFALL
RINGHALS

VATTENFALL
RINGHALS
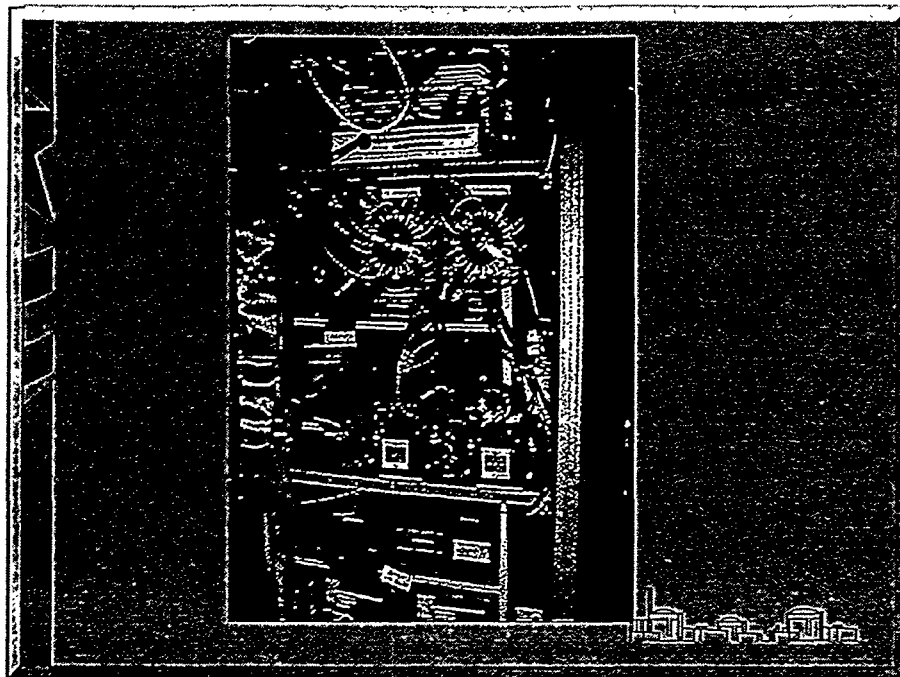
VATTENFALL
RINGHALS
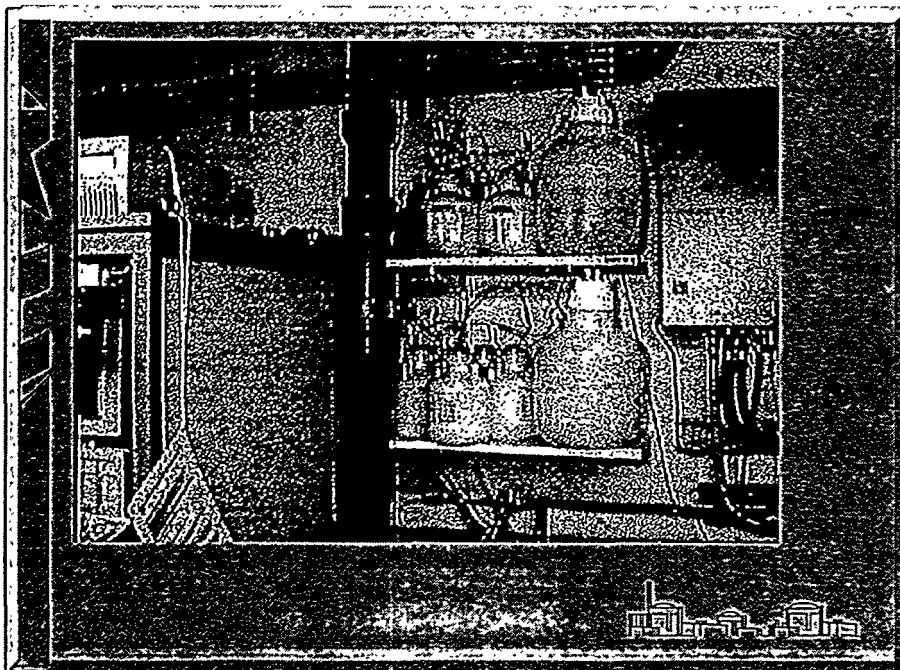
VATTENFALL
RINGHALS

On-line Ion Chromatography at Ringhals today

- On-line operating for 6 years
- Reducing costs
- Optimising the maintaince

VATTENFALL RINGHALS

On-line Ion Chromatography at Ringhals tomorrow

- Less complicated instruments on-line
- Data acquisition to Plant Chemistry Data System

VATTENFALL RINGHALS

On-line Ion Chromatography at Ringhals questions?

On-line Ion Chromatography at Ringhals

You are welcome to visit Ringhals for a closer look at our On-line Ion Cromatographs

EXPERIENCES WITH ELECTROCHEMICAL ANALYSIS OF COPPER AT THE PPB-LEVEL IN SALINE COOLING WATER AND IN THE WATER/STEAM CYCLE

Karsten Thomsen
I/S Nordjyllandsværket
Postbox 51
DK-9310 Vodskov
Denmark

ABSTRACT

Determination of trace amounts of copper in saline cooling water and in process water by differential pulse anodic stripping voltammetry combined with an UV-photolysis pretreatment is described. Copper concentrations well below 1 µg/L may be analysed with a precision in the order of 10% and a high degree of accuracy. The basic principles of the method are described together with three applications covering analysis of cooling and process water samples. The analysis method has been applied to document the adherence of environmental limits for the copper uptake of cooling water passing brass condensers, to monitor the formation of protective layers of iron oxides on the cooling water side of brass condensers, and to study the transport of copper in water/steam cycles with heat exchangers and condensers of brass materials.

1. Introduction

Routine determinations of trace amounts of copper by means of electrochemical stripping analysis have been performed at two ELSAM laboratories since 1993. The method was introduced to meet the analytical challenges that we faced at that time. In connection with an environmental approval of one of the power stations, the local authorities requested weekly measurements to assure that the copper uptake of the cooling water from the brass condensers was less than 2 µg/L. Another incident tricked an increased interest in copper in the water/steam cycle. In 1989, a turbine at one of the older units experienced a significant power loss due to deposits consisting mainly of copper oxide on the high pressure turbine blades[1]. The sources of the copper were the heat exchangers of brass materials in the water/steam cycle such as the low pressure heaters and the condenser. It was clear that other units could potentially suffer from the same problem, and a couple of measuring campaigns were conducted to locate the major source of copper and to optimize the conditioning of the feedwater with respect to copper release. However, it was realized that the spectrophotometric method used for copper determination was not sufficiently sensitive below 3 µg/L

to give reliable conclusions. Thus, a new method for copper was needed both for samples of cooling water and of the water/steam circuit. The characteristics of the method should be as follows:

- Precision and accuracy should be sufficiently good that it would be meaningful to evaluate copper uptakes of less than 2 µg/L in both types of samples.

- A quantification limit around 0,1 µg/L was needed.

- The method should be able to tolerate the high salt content of the saline cooling water samples.

- Because of the low copper levels, any pretreatment of the samples had to introduce only minimal dilution.

- Since the method would be used for routine measurements, it should not be too involved or time-consuming.

From preliminary tests, we concluded that digestion of organic matter in the samples by means of UV-photolysis and subsequent quantification of copper by differential pulse anodic stripping voltammetry (dpasv) had the potential to fulfil these demands, and the necessary instrumentation was purchased by two laboratories.

Electrochemical stripping analysis, which preconcentrates the heavy metals in a mercury phase by electrolysis and subsequently quantifies the analytes in a voltammetric or potentio-metric re-oxidation step, is not commonly used in industrial laboratories. However, the methods have a long history in research and environmental laboratories, and there is an abundant literature describing principles and applications which has been summarized by Wang[2]. Instrumentation that is well-suited for even the most demanding tasks is commercially available such that the basis for routine applications of the methods is present. For such purposes, the DIN-standard covering the techniques is relevant[3]. Compared to the commonly used atomic absorption spectrometric methods for heavy metals, electrochemical stripping analysis is limited with respect to the range of analytes because only the elements forming amalgams with mercury can be analysed. Application of the electrochemical methods is advantageous in some cases, especially with samples containing high amounts of salts, and because lower detection limits and uncertainties may be obtained. Furthermore, the instrumentation is far less in price than atomic absorption instrumentation that can operate at comparable concentration levels.

This paper describes the basic principles of the dpasv technique, the performance of the method, and a few applications in practise.

15.2

2. Experimental

2.1 Sampling

2.1.1 Samples for environmental monitoring

The samples for monitoring the cooling water uptake of copper at power station SVS were collected at three sample points (inlet block 1, inlet block 2, and common outlet) by means of automated sampling devices (Aquasampler HCV 500, Struers, Copenhagen, Denmark) which collected 10 L of sample over a 24 h period. The day for sampling was chosen randomly in each week. The samples were collected in rinsed containers of polyethylene or polypropylene. A portion of the sample was subsequently filtered through a 0,45 μm membrane filter and conserved by addition of nitric acid (suprapure quality) to pH around 2.

2.1.2 Samples for corrosion control of brass condensers

The samples of cooling water from unit NVA were collected in acid-cleaned polyethylene containers from sampling lines placed immediately ahead or after each half section of the condenser. The samples were conserved by addition of hydrochlorid acid (suprapure quality) to a pH between 1,7 and 2,0.

2.1.3 Samples of process water

Samples from the water/steam circuit were taken through sampling devices designed to give isokinetic sampling and connected to short sampling lines with coolers placed immediately after the sampling devices. The samples were collected in acid-cleaned high density polyethylene containers exclusively used for this purpose and conserved by addition of nitric acid (suprapure quality) to a pH in the interval from 1,7 to 2,0.

2.2 UV-photolysis

Organic matter in samples of cooling water was destroyed by photolysis in presence of hydrogen peroxide by means of an UV-digester (UV-digester 705, Metrohm, Herisau, Switzerland). The UV source was a 500 W high pressure mercury lamp with 50 W intensity in the UV-region between 200 and 280 nm. The samples were irradiated in quartz tubes with a capacity of 10 mL each. Prior to the digestion, 0,100 mL of hydrogen peroxide (32%, p.a. quality) was added to each tube. The samples were photolyzed for 1 h, and the cooling water flow was adjusted to give a temperature between 90 and 95 °C.

Samples from the water/steam circuit could in most cases be analysed directly. Occasionally, some samples (especially those taken in or after the condensate polishing plant) contained organic trace contaminants that interfered with the determination of copper such that UV-photolysis was necessary for these samples also.

2.3 Differential pulse anodic stripping voltammetry

The electrochemical measurements were performed by a microprocessor-based, programable instrument controlling an electrode stand (VA-processor 693 and VA-stand 694 respectively, Metrohm, Herisau, Switzerland). The electrodes used were a mercury

electrode operated as a hanging mercury drop electrode (HMDE), a reference electrode (Ag/AgCl/3 M KCl), and a platinum rod counter electrode. The drop size used was very low - typically less than 0,5 mm in diameter.

The samples were initially stirred and de-aerated by purging with nitrogen for 5 min. Next, the preconcentration was performed by electrolysis at -800 mV between 30 and 300 s depending on the copper level in the sample. Stirring was then turned off, and the sample allowed to become quiescent during a 10 s waiting period. The anodic scan was initiated at -600 mV (cooling water) or -300 mV (process water) to avoid scanning potential regions without signal and was stopped at 0 (cooling water) or 150 mV (process water). The parameters defining the potential waveform during the scan were: Step period, 200 ms; step height, 6 mV (*i.e.* average scan rate 30 mV/s); pulse duration, 40 ms; pulse height, 50 mV; sampling periods, 20 ms. Each cycle of preconcentration and stripping was performed with a fresh mercury drop.

2.4   Quantification

The copper content of the samples was quantified by means of standard addition. Following the initial measurement of the sample, addition of a small volume of standard (0,020 to 0,100 mL) and subsequent measurement was repeated twice. The height of the copper peak above a linear background was used as the analytical response. The size of the standard addition was adjusted such that the peak height was roughly doubled by the first addition - this could be done automatically by the VA-processor using an approximately constant sensitivity in similar samples. The standard contained 1,000 mg/L copper and was prepared from a Titrisol standard (Merck). It was added by a dosing pump (Dosimat 685, Metrohm, Herisau, Switzerland) controlled by the VA-processor.

3.   Principles of the method

3.1   UV-digestion

The organic material in the samples must be removed prior to the electrochemical analysis - otherwise it will accumulate on the mercury surface and give rise to interference effects such as small or missing signals, non-linear concentration dependence, or distorted background curves. The task was performed by UV-photolysis after addition of a small amount of hydrogen peroxide (1 % v/v) to the acidified samples. The temperature was kept around 95 °C during the photolysis which typically lasted 1 h. The samples were irradiated batchwise (11x10 mL) in quartz tubes.

In this process, mineralisation takes place in radical reactions initiated by hydroxy radicals formed from hydrogen peroxide under UV-radiation. The hydroxy radicals are strong oxidants which non-specifically attack organic compounds and initiate the degradation. The use of UV-digestion as a pretreatment step for analysis of environmental samples has recently been reviewed by Golimowski and Golimowska[4], and further information about the radical mechanisms, UV-lamps and instrumentation, and applications may be found in this paper.

15.4

The main advantages of UV-digestion compared to other methods are the minimal dilution introduced to the samples and the low amounts of chemicals added. When operating at concentration levels around 1 μg/L in the original samples, even moderate dilution may bring the concentration near the quantification limit of the technique and introduce a contamination from the background level of the chemicals. The technique is not suited for samples with very high contents of organic matter due to incomplete degradation, but we have not encountered any problems in that direction sofar.

3.2   Electrochemistry

The electrodes and other remedies contacting the sample during analysis are schematically shown in figure 1. The working electrode is a hanging mercury drop electrode (HMDE) which consists of a pressurized mercury reservoir connected to a thin capillary. When a needle valve controlling the capillary is opened briefly, mercury flows and forms a tiny drop hanging under the capillary. Each mercury drop is used for a single preconcentration-stripping cycle and is then detached by a light knock on the capillary. The potential of the HMDE is controlled relative to the reference electrode by a potentiostat. This device controls the potential via a feed-back loop, such that the potential drop between the counter and working electrodes is varied until the potential drop between the reference and the working electrodes reaches the proper value. This regulation lasts only a few microseconds, and the potentiostat - practically speaking - always makes the potential of the working electrode equal the input signal at any time. The output signal from the potentiostat corresponds to the current flowing between the counter and working electrodes at any time. If electron transfer processes between the working electrode and species in solution (faradaic processes) take place at the given potential, they will be experienced as a current in this circuit.

Besides the electrodes, two thin teflon tubes for purging gas and addition of standard and a stirring rod are placed in the sample cup. The samples are de-aerated prior to analysis because oxygen is electroactive in the same potential region as the heavy metals and would give rise to a large background current if present.

The microprocessor in the instrument operates the mercury electrode, feeds the potentiostat with input signals, records the output signal when relevant, and controls the purging gas, stirring rod, and the dosing pump with standard. Sequences of these operations are gathered in small programmes and all together form a complete analysis procedure.

The potential vs. time scheme of a measuring cycle is outlined in figure 2a. In the preconcentration step, the potential of the HMDE is held at a cathodic potential between -1100 and -500 mV for a given period of time (deposition time, t_{dep}) which typically last between 30 and 300 s. The sample is stirred to obtain maximum mass transfer to the electrode surface. Because the potential of the electrode is more negative than the apparent redox potential of the heavy metals, they are accumulated in the mercury drop due to electrolysis. Using copper as example, the process is:

$$Cu^{2+}_{aq} + 2e^- \rightarrow Cu_{Hg}$$
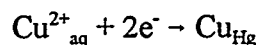
Copper ions in solution are reduced at the electrode surface and form elemental copper which dissolves in the mercury phase forming an amalgam. In this way, heavy metals like zink, cadmium, lead, copper, and a few others may be preconcentrated in the mercury drop even from samples containing only trace amounts. If the the mass transfer conditions are kept constant, the amount of heavy metal accumulated is within certain limits proportional to both the concentration of metal ions in the sample and to the deposition time. The last proportionality allows the sensitivity of the technique to be adjusted according to the concentration level of the sample.

Next, the accumulated metals are quantified in a stripping step, in which the potential of the HMDE is scanned in the positive (anodic) direction. The scan may be started at values more positive than the electrolysis potential to avoid scanning potential regions without useful information. When the potential reaches the vicinity of the apparent redox potentials of the metals, re-oxidation takes place and metal ions in solution are formed again, for instance:

$$Cu_{Hg} \rightarrow Cu^{2+}_{aq} + 2e^-$$
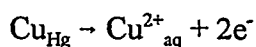
The electrons tranferred in the process give rise to an increased current flowing between the electrodes, and a curve of current vs. potential (*i.e.* a voltammogram) shows a peak corresponding to the re-oxidation of a given metal, see figure 2b. The peak will be centered around the apparent redox potential for the metal, and the size of the peak - either measured as the peak height or peak area - will be related to the amount of metal accumulated and through the proportionality also to the original concentration of metal ions in the sample.

In the differential pulse voltammetric technique, the potential is not varied linearly with time in the scan - instead a waveform with a steadily increasing base potential and a pulse is repeated continuously. In figure 2a, a few replicas of the potential waveform are indicated in the scan, and it is shown in detail in figure 3. Each waveform lasts 200 ms of which the pulse is applied for 40 ms. The current is actually sampled only in the last 20 ms prior to the pulse and in the last 20 ms of the pulse. The difference between the average current at the pulse level and at the base potential is assigned to the base potential in the voltammogram. The base potential is increased by 6 mV for each repetition of the waveform and the pulse height is 50 mV. Of course, the values of these parameters are not fixed, but we have found this set to give optimum sensitivity and fastest possible scan rate without distortion of the copper peak[5]. The main advantage of the pulsed waveform is compensation of background currents recorded together with the faradaic currents in a linear potential scan. The ions in the interface between electrode and solution (the electric double layer) act as a capacitor that must be charged or decharged whenever the potential is changed. Following a potential step, the charging current decays much more rapidly than the current from faradaic processes. This means that the current samples taken after a waiting period of at least 20 ms in the differential pulse technique will reflect faradaic processes to a much higher degree than the corresponding current recorded in a linear scan. Far from the apparant redox potential of a heavy metal, the two current samples will be almost equal and the difference close to zero. In the vicinity of the apparant redox potential the current flowing at the pulse potential will be much larger than the current at the base potential, such that the difference will be considerable. The difference drops off again as the mercury phase is depleted for the metal being re-oxidized.

15.6

The concentration of heavy metal in the original sample is quantified by means of the standard addition technique. The concentration is calculated from the peak heights recorded in the unspiked sample, in the sample spiked with a certain amount of standard, and in the sample spiked with the double amount of standard. For optimum determination of the concentration, the peak height should be roughly doubled by the first addition. Since one year ago, the amount of standard added has been calculated automatically from the peak height obtained in the unspiked sample. This is can easily be done, because the slopes of the calibration curves are approximately constant in samples of same type such as cooling water or process water[5]. However, the sensitivity depends on the matrix and on the temperature of the samples, such that the more accurate results are obtained by the standard addition technique.

Figure 4 shows a determination of copper in process water, and the inset shows the corresponding standard addition curve giving a concentration of 0,7 µg/L in the sample. The deposition time was in this case 100 s. This type of measurement is performed in diluted nitric acid, in which the nitrate ions have a low tendency of forming complexes with cupric ions. Thus, the electrochemical reaction in the stripping step may be described by:

$$Cu_{Hg} \rightarrow Cu^{2+}_{aq} + 2e^-$$
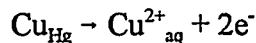
The peak potential for the copper in this medium is approximately +50 mV. Figure 5 shows the determination of copper in the coastal seawater used as cooling water. Here, the peak potential of the copper signal is much more negative (approximately -150 mV) due to the high levels of chloride. Chloride ions form very strong complexes with cuprous ions, and reactions like:

$$Cu_{Hg} + Cl^- \rightarrow CuCl + e^-$$
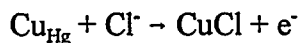
becomes favorable in media with high chloride content. In the determination of copper in seawater samples, the two reactions overlap and give rise to broader copper peaks than in nitrate media. Nevertheless, the peak height is proportional to the copper concentration as seen from the standard addition curve in the inset of figure 5. In the example, a deposition time of 100 s was used, and the copper concentration was found to 1,3 µg/L. The extra peak in the voltammogram at -380 mV is due to the background level of lead in the cooling water (1-2 µg/L).

4.   Analytical performance

The analytical performance of the method has been evaluated by internal quality control at the laboratories and by participation in round robins. For the cooling water, the internal quality control has mostly been performed with spiked inlet samples because of a lack of suitable reference materials. The precision of the method at low copper levels has been evaluated from the double determinations performed weekly over several months. Both laboratories have participated in the round robins for copper in process water running regularly within the ELSAM laboratories. Since most of the laboratories use spectrophotometric methods for this analysis, the copper levels in the samples have been higher than 3

μg/L. Below this level, the performance has been evaluated by analysis of spiked samples of ultrapure water, which has a background level of copper typically less than 0,1 μg/L. The results of these investigations are summarized in table 1.

Table 1 - Analytical performance of the method					
Sample	Cooling water			Process water	
Conc. level (μg/L)	1-20	0,4-1,9	20	0,5-4,0	3-30
Precision[a]	<13%	0,14 μg/L	1,8 μg/L (or 9%)	0,07 μg/L or <7%[e]	0,25
Systematic error[b]	None	Not inv.	None	-3%	None
Linearity[c]	$R^2 = 0,992$	Not inv.	Not inv.	$R^2 = 0,997$	$R^2 = 0,992$
Degrees of freedom[d]	7	30	10	65	18
Source of data	Round robin	Weekly determinations	Internal quality control	Internal quality control	Round robins

a   The precision is stated as 2 times the relevant standard deviation or relative standard deviation.
b   "None" means that a systematic error could not be demonstrated at the 95% confidence level.
c   The squares of the correlation coefficient in regressions of measured vs. true concentrations are given.
d   Minimum degrees of freedom in calculation of statistics.
e   Whichever figure is the largest.

The data for the round robin with cooling water samples covers only one of the laboratories. The other laboratory had a positive systematic error in this test which was due to a slight non-linearity of the calibration curve for the highest concentrations. Presumeably, the non-linearity was caused by the combination of high concentrations and a long deposition time which made the copper amount in the mercury phase approach the saturation level. With lower deposition time, the calibration curves were linear, and we concluded that samples with more than 10 μg/L copper should be analysed with a short deposition time of 30 s.

A small systematic error was also demonstrated for the analysis of process water with copper concentrations below 4 μg/L. The series of measurements was performed prior to the introduction of the automatic adjustment of the amount of standard added in the quantification procedure. Whether this improvement has solved the problem, still needs to be tested.

Quantification limits are not stated in the table because they are so dependent on the deposition time used. Practical experience shows that in cooling water samples, copper levels down to 0,4 μg/L may easily be analysed with a 100 s deposition time. With the same deposition time, copper amounts down to 0,1 μg/L have been determined in process water samples.

Generally speaking, the performance of the method is satisfactory taking the trace levels in account, and the method fulfils the requirements with respect to uncertainty.

5. Applications

5.1 Environmental monitoring

Since 1994 the copper uptake of the cooling water passing the brass condensers at the power station SVS has been followed by weekly measurements. Samples were taken in the cooling water inlets of the two units (B1 and B2) and in the common cooling water outlet during a 24 h period by means of automated sampling devices. The purpose of the measurements was to check that the uptake was below a limit of 2 µg/L imposed by the local authorities.

Figure 6 shows the copper concentrations in the three samples and the calculated uptake during 1995 and the first part of 1996. In general, the concentrations in the three samples tracked each other rather closely at a level around 1 µg/L, and the uptake varied around zero. Exceptions from this were seen in mid-1995 after the overhaul of the two units when the condensers released somewhat higher amounts of copper.

The distribution of the uptake values during the period is shown in figure 7. Approximately 78% of the values falls in the interval from -0,5 to 0,5 µg/L, and only 4% is larger than 2 µg/L. The uptake values less than -1 µg/L, which must be characterized as artifacts, amounts to less than 3% of the total number. These values typically stemmed from the situations which gave the spikes in figure 6. Thus, it may be concluded that the copper uptake of the cooling water is well below the specified limit except in extraordinary situations such as start up of an unit after overhaul.

5.2 Corrosion control of brass condensers

In Denmark, brass condensers are generally protected against corrosion at the cooling water side of the tubes by a layer of iron oxides formed by dosing ferrous sulphate to the inlet. The ferrous ions are oxidized by oxygen in the cooling water and precipitate as oxides. Once in a while, the protective layer must be removed and a new formed, either because of cracks in the layer formed from drying up in the overhaul period or because the heat exchange efficiency of the condenser has become too low. Measurements of the copper uptake of the cooling water is an effective means to follow the formation of the protective layer and to evaluate the amount of copper released to the environment during the process.

Figure 8 shows an example from the unit NVA. The old layer was initially removed by applying carborundum balls in the Taprogge system which made the copper uptake increase to a level between 30 and 40 µg/L. In the following period, ferrous sulfate was dosed three times daily for a period of 1 hour following a practice that had worked in other situations. The amount of ferrous sulphate dosed corresponded to a concentration of 0,5 mg/L in the cooling water. This made the copper uptake decrease to a level around 10 µg/L and then stabilize. This indicated that the protective layer was not complete, possibly because

bacterial films had formed on part of the tube surfaces, such that further dosing would not improve the situation. The condenser tubes were then polished with carborundum balls once more, which immediatly increased the corrosion rate and thus the copper uptake level. Next, the dosing of ferrous sulphate was increased to six times daily with an amount corresponding to 1 mg/L of iron. This treatment made the copper uptake drop to below 10 μg/L within 3 days and to below 2 μg/L within 7 days. When 2 μg/L was reached, the sampling frequency was reduced to once a week. The total amount of copper released to the environment was estimated to 400 kg which was close to the amount allowed pr. year by the authorities.

The formation of a good protective layer depends on several variables that influence the oxidation kinetics of ferrous ions (pH, temperature, and oxygen and chloride content of cooling water) and the deposition rate of iron oxides at the tube surfaces (surface condition, dosing point, suspended and organic matter in cooling water). Some of these variables are or can be kept constant from time to time, but the others will have the effect that a procedure that worked once will not necessarily work as well next time. Thus, we find it appropiate to monitor the process by means of the copper uptake in the cooling water.

5.3   Copper removal by the condensate polishing plant

Since the first incident in 1989, we have observed deposits of mainly copper oxide on several high pressure turbine which has focused the attention on copper transport in water/steam cycles with brass heat exchangers and condensers. A mass balance which has been set up for an unit with low pressure heaters, district heating exchangers, and condenser of brass materials has been reported elsewhere[1]. As a part of this, we studied the removal of copper in the condensate polishing plant (CPP) consisting of a cation filter in series with a mixed-bed filter. Typically, the major part of the incoming copper - at levels around 2 μg/L - was removed by the cation filter whereas the mixed-bed filter consequently did not take copper up. However, there was indications that a regenerated CPP did not function as well during the first 7-10 days (or approximately 10% of the total cycle length) after start up. Later measurements confirmed that during this period of time, the fraction of the incoming copper removed by the cation filter gradually increased from 30% to the 60-80% level normally seen. This made us look at the release of copper from the cation filter during regeneration, and we found that copper ions were released more slowly than the ammonium ions. The cation resin of the mixed-bed filter was regenerated with the last part of the acid coming from the cation filter, and the late release of copper from that filter meant that the level peaked when the acid was directed to the mixed-bed filter. Following the normal procedure, incomplete regeneration of the cation filter could be the consequence of the slow release of copper from the cation exchangers. The inactivity of the mixed-bed filter in the removal of copper could be due to the high levels of copper ions in the regeneration acid hindering release of copper from the cation resin. In order to test these two suppositions, the regeneration procedure was changed such that the cation filter was first regenerated by the usual amount of acid, but without diversion of acid to the mixed-filter. The cation filter was then flushed with demineralized water and regenerated once more using 50% of the usual amount of acid which was also led through the cation resin of the mixed-bed filter. The behaviour of a CPP regenerated in this way is illustrated in figure 9. The concentrations of

copper in the condensate ahead of the CPP, after the cation filter, and after the mixed-bed filter over a period of 11 days after start up is shown in the figure.

It is clear from the figure that the cation filter rinses the condensate down to a level around 0,75 µg/L copper right from start up. The function of the mixed-bed has not improved since the copper contents of the condensate after the cation filter and after the mixed-bed filter still track each other closely. Thus, the changed regeneration procedure is only beneficial for the function of the cation filter.

6.   Conclusion

Three years of experiences with dpasv analysis of copper combined with UV-photolysis as pretreatment has shown that the method is well suited for routine applications in power plant laboratories. The method has proven to fulfil the requirements listed in the introduction, and it operates with a high degree of accuracy and a precision around 10% even at very low concentrations.

The method has been a valuable tool for the laboratories and has allowed us to document the copper uptake of cooling water, to monitor the formation of protective layers of iron oxides on brass condenser tubes, to set up a mass balance for copper in the water/steam cycle, and to study the removal of copper by a condensate polishing plant in detail.

7.   References

1)   K. Thomsen, K. Daucik, "Deposits on turbines in relation to the use of copper alloys in the water/steam cycle", ENEL/EPRI/VGB International Conference - Interaction of non-iron based materials with water and steam, Piacenza, Italy, June 11-13 1996

2)   J. Wang, "Stripping Analysis", VCH Publishers, Inc., Deerfield Beach, Florida, 1985.

3)   DIN 38 406, Teil 16, "Kationen (Gruppe E) - Bestimmung von 7 Metallen (Zink, Cadmium, Blei, Kupfer, Thallium, Nickel, Cobalt) mittels Voltammetrie", (in german)

4)   J. Golimowski, K. Gomowska, "UV-photooxidation as pretreatment step in inorganic analysis of environmental samples", Analytica Chimica Acta **325** (1996) 111-133

5)   T.A. Aarhaug, "Cu-analyser med Metrohm VA693 ved NVA-laboratoriet, uke 32-35", Nordjyllandværket 30.08.1995, Internal report, (in norwegian).
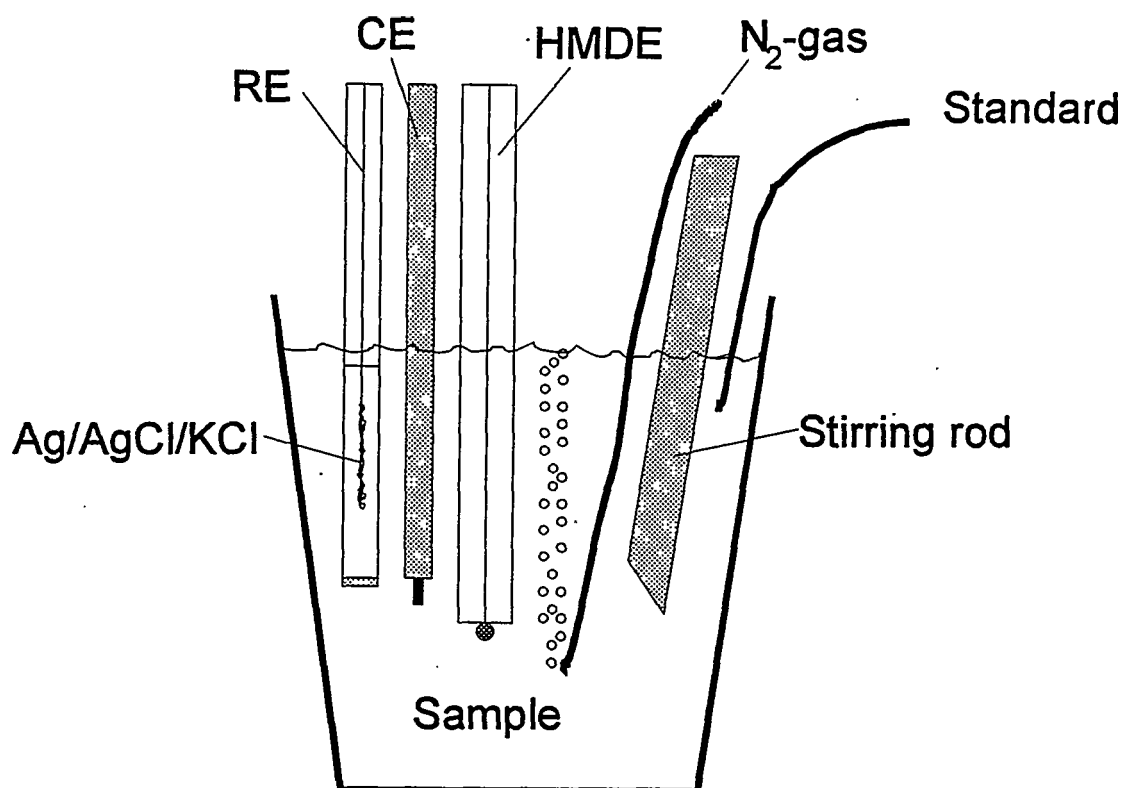
Figure 1. Experimental setup for dpasv. The electrodes are a Ag/AgCl reference electrode (RE), a platinum counter electrode (CE), and a hanging mercury drop electrode (HMDE) as working electrode. Oxygen is removed from the sample by purging with nitrogen gas, and the sample is stirred by a rotating stirring rod. Small amounts of standard may be added by a dosing pump.
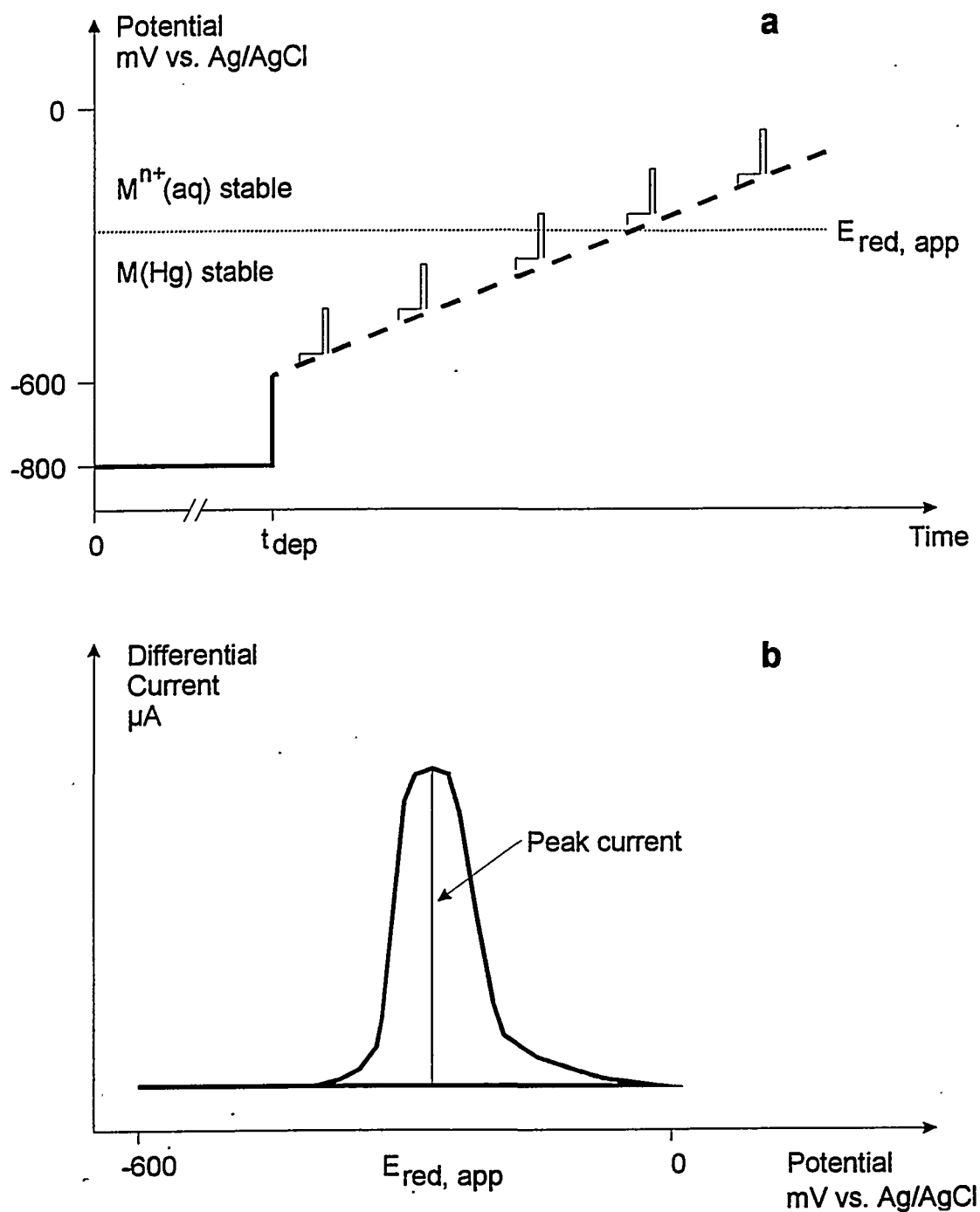
Figure 2. a: Potential vs. time scheme for dpasv showing the deposition and stripping steps. During the potential scan, a potential waveform with a gradually increasing base potential and a pulse is applied. A few replicas of the waveform is shown. **b:** Voltammogram in which the differential current is plotted vs. the base potential.

15.13
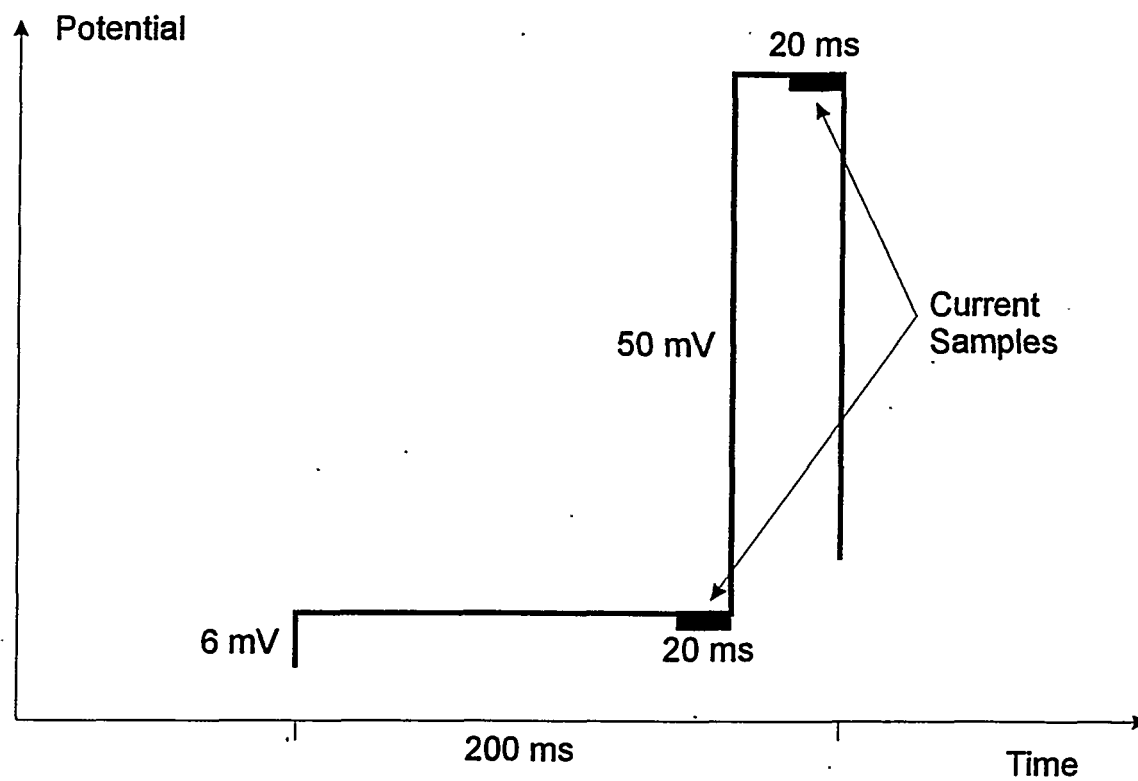
Figure 3. Potential waveform of dpasv. The differential current is formed as the difference between currents at the pulse and base potential levels. The currents are sampled in two 20 ms periods just prior to the application and removal of the pulse.
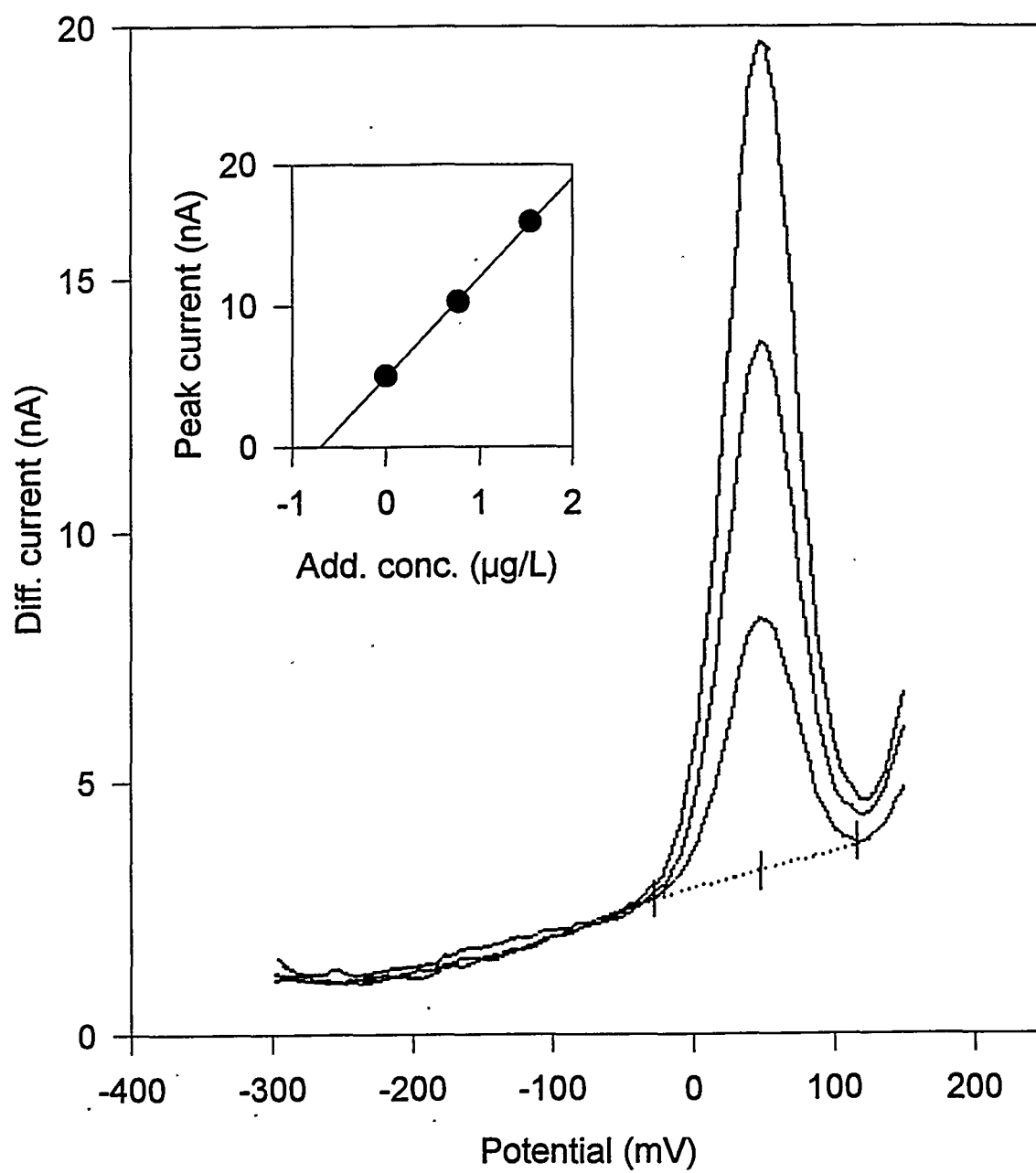
Figure 4. Determination of copper in process water. From the standard addition plot, the concentration of copper is evaluated to 0,7 µg/L.
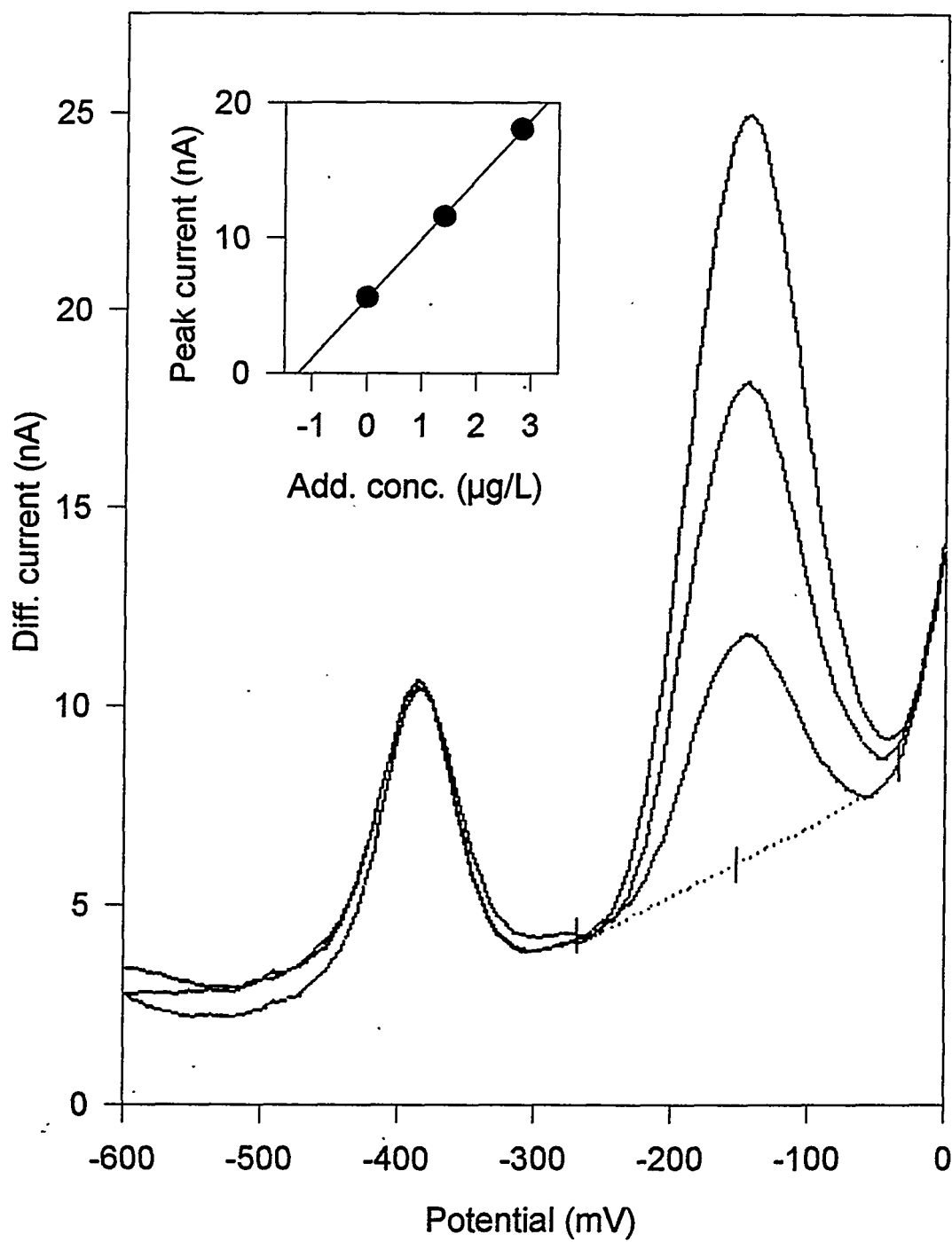
Figure 5. Determination of copper in saline cooling water. From the standard addition plot, the concentration of copper is evaluated to 1,3 µg/L.

15.16
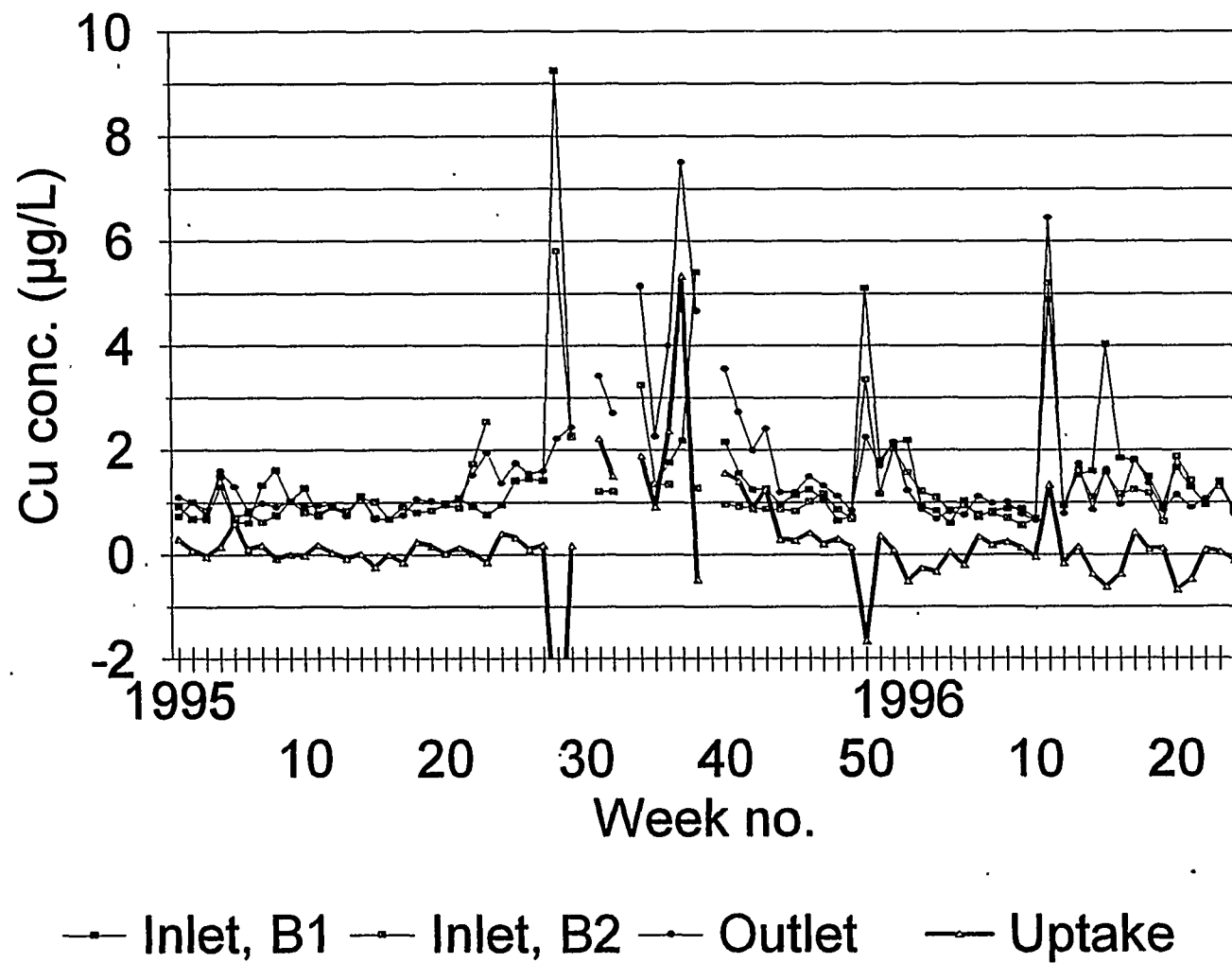
Figure 6. Weekly measurements of copper in cooling water and calculated uptake values (thick line) at SVS.
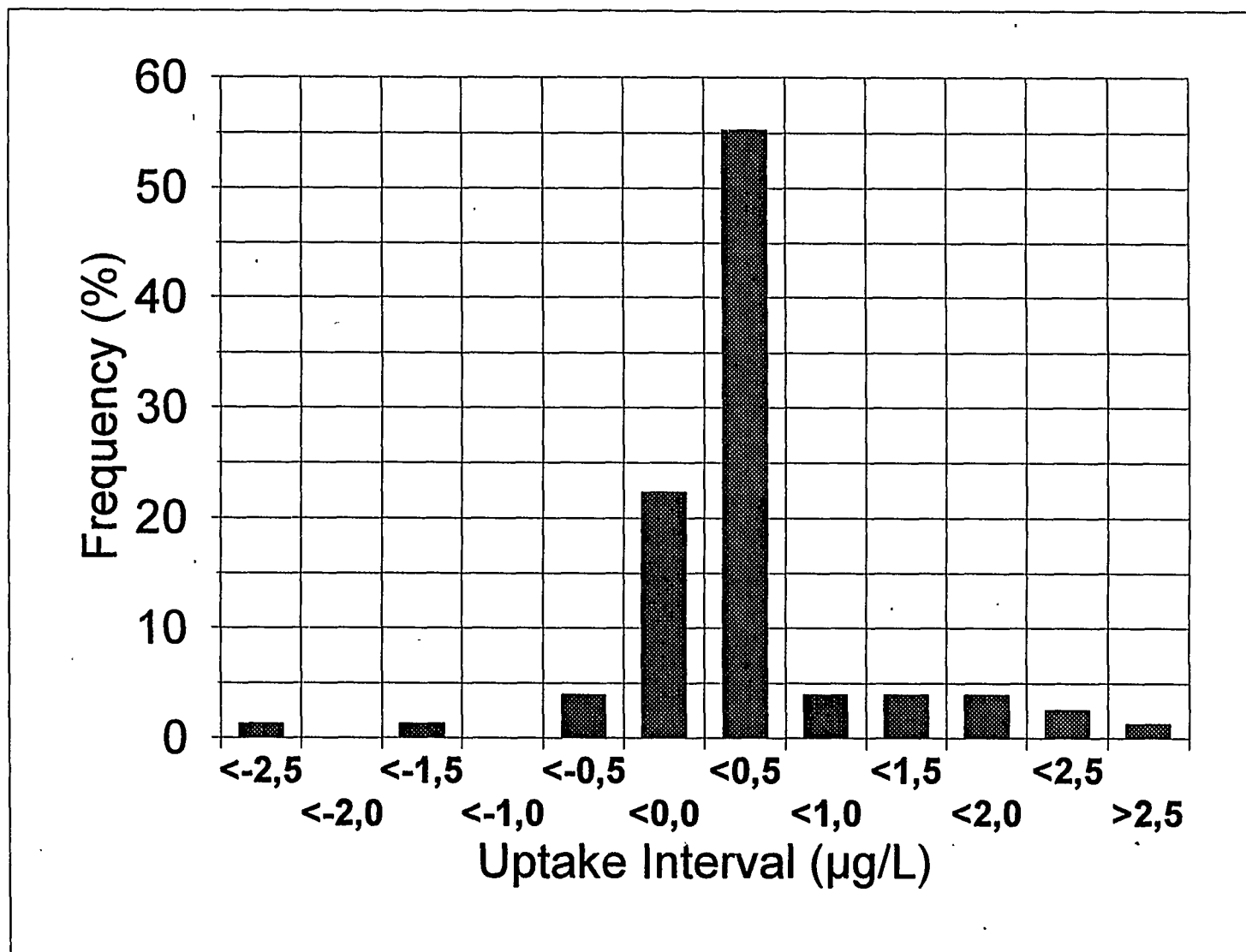
Figure 7. Distribution of copper uptake values for cooling water during 1½ year of weekly measurements.
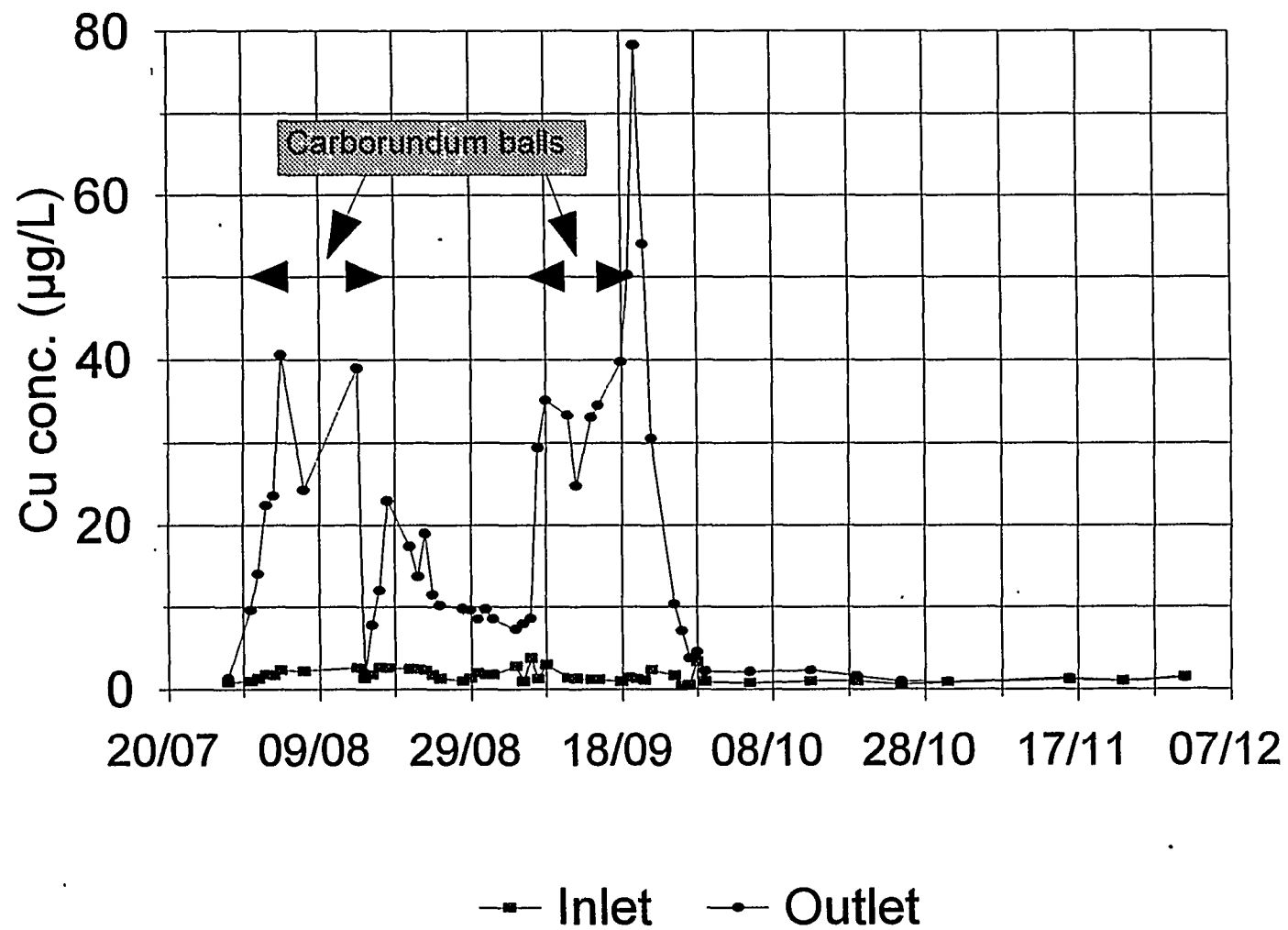
Figure 8. The formation of a protective layer on the condenser tubes monitored by copper measurements.
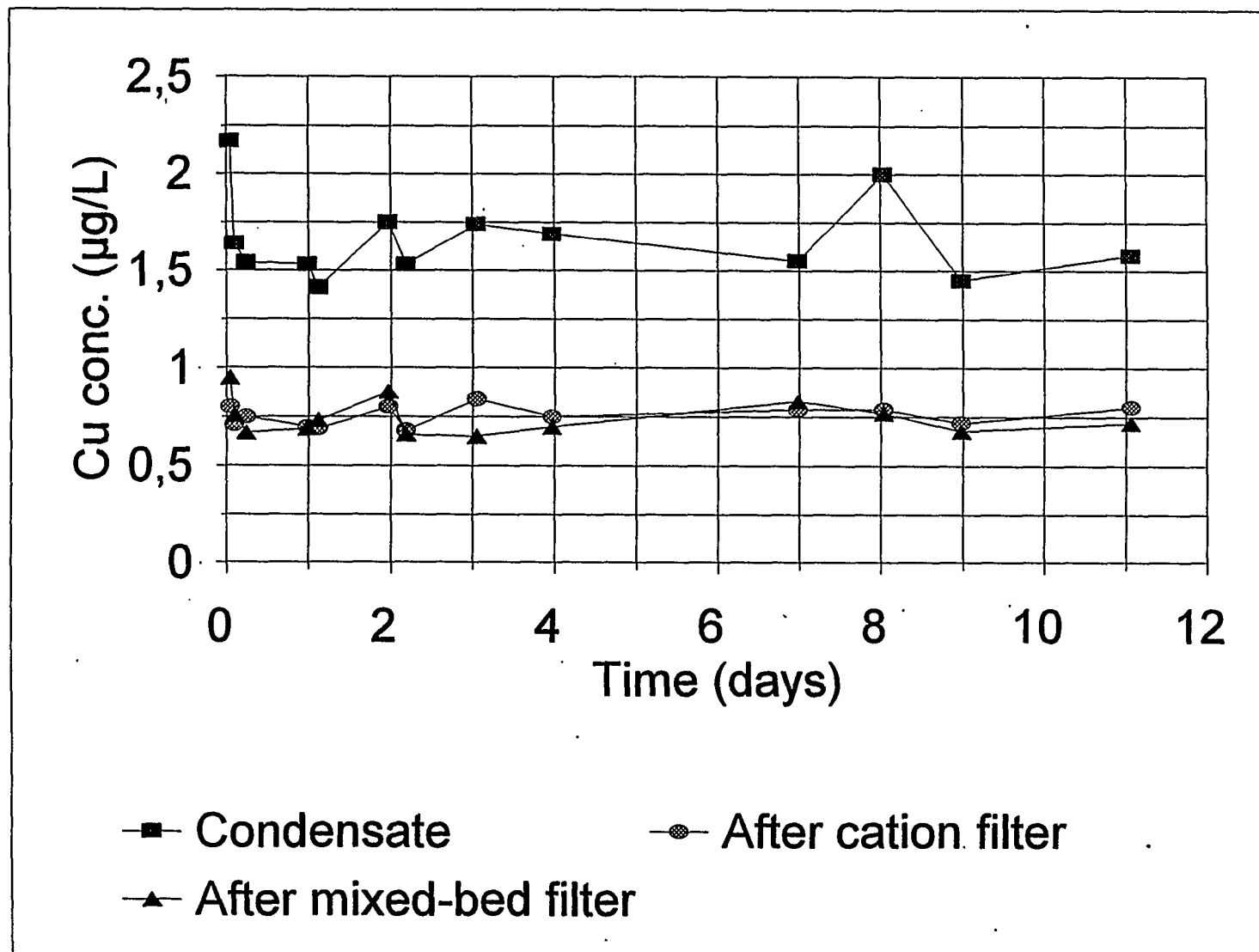
Figure 9. Copper removal by cation and mixed-bed filters in a regenerated CPP after start up.

How Tests of Lubricating and Transformer Oils became Part of Power Plant Chemistry in Denmark

Hans Møller
I/S Nordjyllandsværket
Postbox 51
DK 9310 Vodskov
Denmark

Abstract

Lubricating, hydraulic and transformer oils based on refined crude oil are used in nearly all power station components, such as gear, turbines, hydraulic stations, feed pumps and transformers. The function of these components totally depends on the condition of the oils and their properties. Seen from this point one may wonder why examination and evaluation of oils did not become part of the power station chemistry within the ELSAM utility area until during the middle of the eighties.

We started to examine the properties of lubricating oils at the time when several steam turbines experienced serious problems with formation of deposits in their hydraulic control circuits. This work was intensified in connection with the significant number of CHPs and wind turbines erected within the Danish electricity sector during the past 10 years or so.

The majority of the CHPs are natural gas fired turbines or motors, equipment which severely stresses the lubricating oil. In collaboration with KEMA, the Netherlands, we have carried through with a large examination of lubricating oils in gas turbines and we have found suitable oil types.

The measurement of dissolved gases in transformer oil is a well-known technique for diagnosing the conditions of transformers. A gas chromatography laboratory was established in 1992. Today this lab performs routine analyses on the approx. 1200 transformers installed in the ELSAM utility area. Besides, the lab examines the general properties of the transformer oil.

The objectives of our work with lubricating and transformer oils have been to link together the laboratory measurements with operational experience. Only by doing this is it possible to utilize the laboratory measurements in a correct way. It must be remembered that the main part of all oil specifications concerns the properties of new oils. Only very little is published about the requirements concerning used oils.

It is the opinion of the Joint Chemists that the oil specifications and analysing programmes mentioned in the guidelines of the Original Equipment Manufacturers (OEM) often are out of date and sometimes even irrelevant. For these reasons it is necessary and appropriate to build up knowledge about lubricating and transformer oils, and where a close dialogue and discussion with the oil suppliers form an important part.

Introduction

It is well known that correct lubrication and cooling is very important for the function and lifetime of every machine component. The lubricating oil is to perform various functions, of which the most important are:

- To lubricate the contacting surfaces of any moving components

- To dissipate heat

- To remove particulate debris

- To act as sealing and/or hydraulic medium

For each machine component it is necessary to evaluate which properties the lubricant must possess in order to be able to fulfil the above functional demands, and it must be determined how the properties of the lubricating oil are to be controlled and evaluated.

The majority of the lubricants used in a power station are extracted from crude oil. These mineral oils are characterized by large accessible quantities, they are cheap and generally they possess good lubricating properties. In order to obtain a final product fulfilling specific requirements, various additives carefully selected to match the base oil type used must be added.

However, mineral lubricating oils also have some essential faults. They are quickly degradated at operation temperatures above 100 °C, and above all they have a low self-ignition temperature which means a potential risk of fire if the lubricating oil gets in contact with hot machine components such as steam tubes or turbine rotor. In this connection it is worth remembering that still today the economical losses by turbine fires caused by outflow of mineral lubricating and hydraulic oils amounts to hundreds of millions of US $ a year world wide.

The following sections give four case stories as examples of fields, where the Joint Chemists have participated in the solution of operational problems related to lubricating, hydraulic and transformer oils: Deposits in steam turbine control circuits, lubricants in gas turbines, lubrication of gear in wind turbines and transformer diagnostics by measurement of dissolved gases in insulation oil.

Lubricating and hydraulic oils in power plants

It is worth remembering that nearly all major machine components of a power station are lubricated with oils of mineral origin. This applies to journal and thrust bearings in steam turbines, roller and ball bearings in pumps and fans, gears in coal pulverizers, air preheaters and wind turbines just to mention a few examples. Thus, knowledge of the properties of mineral oils is a necessity to be able to evaluate lubricating oils.

From crude oil are extracted the so-called base oils which are used to produce a large number of different lubricating oils, the properties of which are determined by the base oils and the additives used.

All base oils contain additives in order to get a usable lubricating oil. To reduce oxidation and thermal degradation, oxidation inhibitors are added. As can be seen below, these additives are of great importance for the properties of a turbine lubricating oil. Copper, which is a frequent metal in oil circuits, is an effective catalyst for oxidation of mineral oils, for which reason it is necessary to add so-called copper passivators. These additives are precipitated on cupreous surfaces and are thus reducing the catalytic effect of copper. Besides corrosion inhibitors, foam reducing and demulsification promoting additives as well as anti wear additives are added to the lubricating oils.

Mineral lubricating oils are not usable at operation temperatures above approx. 90-100 °C, as the lifetime of the oil drastically declines above this temperature. At the same time the risk of development of deposits in bearings, labyrinth sealings and control organs is increased. For lubrication of components, where the oil temperature exceeds 100 °C, synthetic lubricating mediums as for example PolyAlphaOlefins (PAO) or poly-ol-esters must be used. Phosphate esters, which are today mainly used as hydraulic liquids for turbine regulation, are also potential high temperature lubricants.

For characterization of the properties of lubricating and hydraulic oils a number of tests are used, of which the most important are:

- Viscosity and viscosity index
- Pour point
- Flash point
- Density
- Content of water
- Neutralisation value (Total Acid Number)
- Air release
- Water separability
- Foaming characteristics
- Oxidation stability
- Copper corrosion
- Rust preventing characteristics
- Load carrying capacity

In many cases - but far from always - the machine supplier has a specification for the lubricating oil. It is our experience that some of these supplier recommendations are out of date and/or imperfect and sometimes directly misleading. An even more problematic issue is to define the requirements which apply to used oils. Only very little useful material is available from supplier side on this subject.

For the selection of the oil systems, where we perform routine measurements and evaluations of the lubricating oils, we have used two criterions: The oil quantity in the component must exceed 200 litres or the component in question must be specifically important to the whole process, e.g. the hydraulic oil in a HP bypass station.

The main part of the oils regularly analysed by us are oils of the type: turbine oil. These oils are manufactured from specifically selected paraffinic base oils with a viscosity of 32, 46 or 68 cSt at 40°C. A good starting point for defining the requirements of an unused turbine oil is the ISO 8068 "Petroleum Lubricating Oils for Turbines - Specifications". With a view to establishing a relevant analysing programme for used oils, we have among others used

16.3

the ASTM D4378 "Standard Practice for In-Service Monitoring of Mineral Turbine Oils for Steam and Gas Turbines".

Case No. 1.   Deposits in steam turbine control circuits

During the period 1986-1994 many steam turbines in the ELSAM utility area experienced serious problems with formation of deposits in their control circuits. A sticky dark brown "glue" deposited on the surfaces of the control organs etc., which caused faults in the system and the need for very frequent cleaning of these components.

All turbines with deposits in the control circuits used a Texaco oil of the type Regal R&O 46. Table 1 shows the plants in question.

Station	Size	Manufacturer	Hydraulic regulating system	
	(MW)		Pressure (bar)	Temperatures (°C)
Fynsværket, FVO 2	195	ASEA STAL	60	50 - 70
Skærbækværket, SVS 11	105	BBC	35	50 - 60
Skærbækværket, SVS 21	285	BBC	35	50 - 60
Nordjyllandsværket, NVAB1	285	BBC	35	50 - 60

Table 1   Plants with deposits in the control circuits

Up to 1986 the turbine of Fynsværket used a hydraulic oil with insufficient oxidation stability, which resulted in the formation of black deposits in the oil circuit. The other 3 plants used a fire resistant control fluid of the type phosphate ester, which they wanted to replace by a mineral oil.

In 1986/87 Texaco introduced a new formulation of the Regal R&O 46 oil with an improved additive package. Shortly after the filling with this oil, the plants in question experienced serious operation problems in the form of malfunction of the control organs. An inspection of these components showed a thin light brown coating easily removable by organic solvents.

The first problems with deposits came in the ASEA STAL turbine at Fynsværket. The hydraulic circuit of this turbine differs from the BBC plants by a higher oil pressure (thus less clearance in the servo valve), and in the ASEA STAL turbine there is no exchange of the hydraulic oil in the control valves. The oil is more or less stationary in the valves.

The routine testing of the oils which comprised measurement of viscosity, TAN, water separability, air release and particulate could not explain why the problems arose. Not until we added measurement of inhibitor content and the oxidation stability of the oil (ASTM D 2272 "Standard Test Method for Oxidation Stability of Steam Turbine Oils by Rotating Bomb"), we found a solution.

16.4

In all turbines a quick decline of the oxidation stability of the oils could be observed. This was surprising as the oils were not exposed to high temperatures. In order to improve the oxidation stability of the new oil, a high molecular phenolic oxidation inhibitor was added, which started to precipitate after a short time. This fact resulted in a pronounced decline of the general oxidation stability of the oil, which quickly caused formation of large quantities of oil sludge in control organs, oil filters and oil tank.

Thus, the coating problems in the ASEA STAL turbine must be ascribed to precipitation of oxidation inhibitor, as the problems arose after a few months of operation with the new oil. The problems with deposits in the three BBC turbines did not arise until after a rather long time of operation and were due to the formation of considerable quantities of oil sludge, which arose when the oxidation inhibitor was precipitated.

We have discussed our problems with ABB. In Korea and in the U.S. corresponding BBC turbines are installed, which also use Texaco Regal oils, but where problems with deposits have never been seen. The reason is that the Texaco oils which are marketed in North America, in Asia and in Europe are manufactured from different base oils and thus also contain different additive packages. I.e., even if the products carry the same names and fulfil the same specifications, they can easily possess different properties.

Case No. 2   Lubricants in gas turbines

In Denmark the first CHP based on a gas turbine was commissioned in 1987. Since then a large number of gas turbines have been installed, varying in size from 3 to 60 MW$_e$. At the end of 1995 a total of 32 gas turbine plants with a total output of 450 MW$_e$ had been established.

A characteristic feature of these CHPs is that their operation profile depends on the demand for district heating. Most of the plants are dimensioned for a large specific heat production which causes start/stop of the plants up to 300 times per year.

The gas turbines used can be divided into industrial-derived and aero-derived gas turbines. The problems with lubricating oils mentioned in the following text are exclusively connected to industrial-derived gas turbines.

After a few years of operation, it became obvious that the lubricating oil used in these plants was degraded far quicker than expected. Our attention to the oil problems was further sharpened when, at the end of 1990, serious damage occurred to the bearings of one plant, and high quantities of varnish were discovered in the labyrinth sealings of another turbine.

In the light of these occurrences an R&D project examining the lubricating oils in five gas turbines was carried through within ELSAM /1/. This project demonstrated clearly that lubricating oils in small gas turbines are exposed to high thermal stresses, which result in unacceptably short lifetimes for conventional turbine lubricating oils. With a view to having the topic further examined, an R&D project was carried through in 1993/1994 in co-operation between KEMA (the Netherlands) and ELSAM. This study comprised a total of 16 gas turbines with varied sizes from 4 to 140 MW$_e$ and covering the most important turbine manufacturers, such as General Electric, ABB, Rolls Royce, KWU, Dresser Rand

and Solar. Experience was collected with 12 different types of lubricating oil, both mineral and synthetic oils.

Lubrication of journal and thrust bearings in turbines is effected through so-called hydro-dynamic lubrication. As a consequence of the rotation of the turbine shaft, an oil film is formed in the bearings. The oil film has a thickness of 25 μm or more, and thus ensures complete separation between the two surfaces. In such system the degradation of the lubricating oil is exclusively determined by the thermal stress, to which the oil is exposed. Oxidation of the hydrocarbons of the base oils is the dominating degradation process of a mineral lubricating oil. At high temperatures (>100°C) and in the presence of oxygen, unstable reaction products (peroxides) are formed in the oil. These peroxides react and form different aldehydes, ketones and organic acids, all containing oxygen. These degradation products polymerize to form "oil sludge", which causes deposits etc. in the oil circuit.

As long as the oil contains sufficient oxidation inhibitors, these will prevent the formation of peroxides and thus effectively prevent oxidation of the base oils. The degradation products called "oil sludge" primary consist of aromatic hydrocarbons and are thus to a very limited extent soluble in the paraffinic base oil. In order to avoid the disturbance of operation by deposits it is, therefore, necessary to replace the turbine oil, even after a comparatively limited degradation.

The measure used for indicating the degradation of the lubricating oil is normally the neutralisation value (TAN) of the oil, which indicates the content of "acid" components in the oil. The oxidation resistance determined by the ASTM 2272 method is a considerably better measure of the degree of degradation of the oil. This method determines the time (RBOT value) used for a complete destruction of the oil sample. The analysis is carried out by placing the sample in a "bomb", which is charged with oxygen to approx. 5 bar; a copper spiral is acting as catalyst. The bomb is placed in an oil bath of 150°C, and the time (in minutes) to reach a well-defined drop in the oxygen pressure is the RBOT value of the sample.

Turbine oils contain different types of oxidation inhibitors, of which the most important as functional groups contain phenol and/or amines. In this study we have determined the content of phenolic oxidation inhibitors on the basis of the IR spectrum of the oil. The spectrum has a well-defined band around 3650 cm⁻¹, which can be used for a quantitative determination of the inhibitor content.

Figure 1 shows the course of ageing of a conventional turbine lubricating oil, type Shell Turbo T32 and a high temperature resistant gas turbine oil, type Shell GT32 in a SOLAR MARS turbine. The oxidation stability and the inhibitor content are indicated in relative figures, the initial values of an unused oil being 100%.
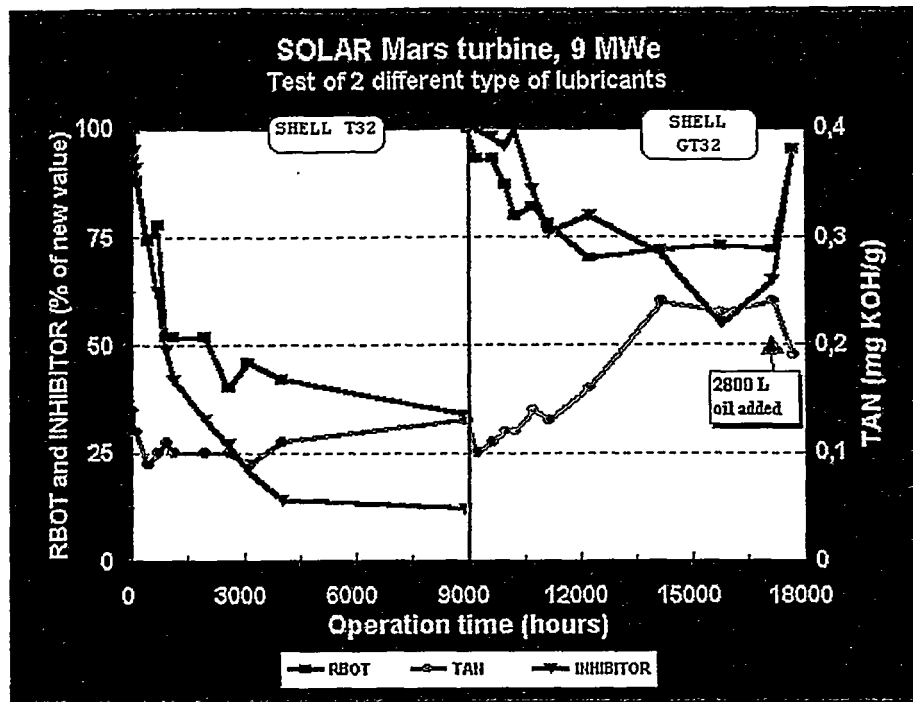
16.6

Fig. 1   Degradation of a conventional and a high temperature resistant
gas turbine oil

With the Shell Turbo T32 oil, the inhibitor content quickly declines, which again causes
a significant decline of the RBOT of the oil. It is remarkable that the neutralisation value
is constant, even after 9000 operation hours. Thus, in this case TAN is not a suitable
measure of the degree of degradation the oil.

The Shell GT32 oil is composed by specifically selected base oils added with high
temperature resistant oxidation inhibitors. It is obvious that the changes of the RBOT and
of inhibitor are much slower, corresponding to a moderate rate of degradation of this
lubricant. After approx. 8000 operation hours a large oil leak occured, which made it
necessary to add approx. 2800 litres of new oil. The effect of this addition on all three oil
parameters is obvious.

Figure 2 shows how two conventional turbine oils from Shell and Mobil degrade at
different speeds in different gas turbines. The condition of the oils is evaluated on the basis
of the three parametres TAN, RBOT and inhibitor content. Of the total number of 16 gas
turbines included in this study, we have chosen the turbines which used the conventional
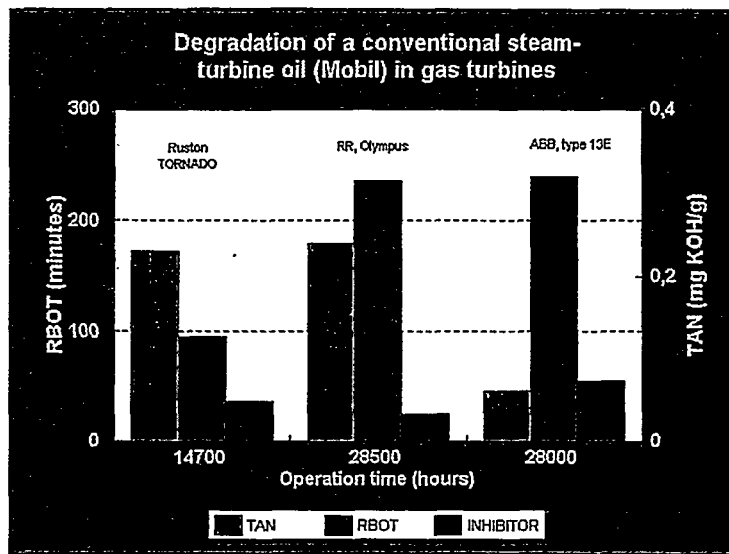turbine oils.

Fig 2a. Degradation of a conventional turbine oil, type
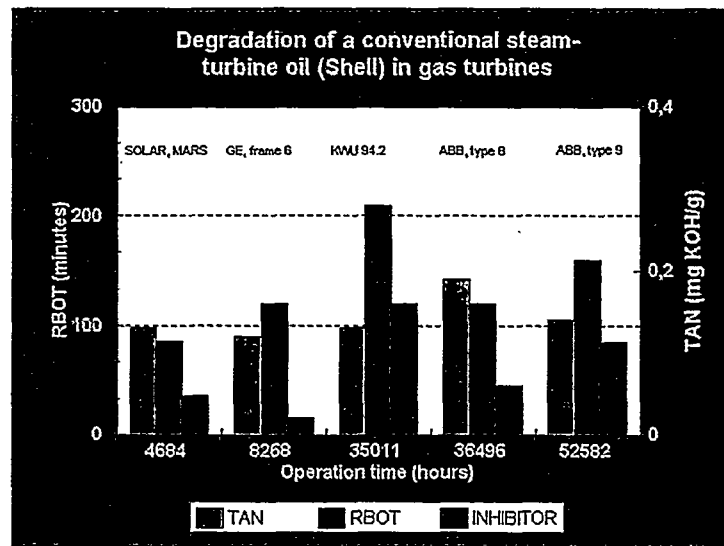Mobil in different gas turbines.

Fig 2b. Degradation of a conventional turbine oil, type
Shell in different gas turbines.

The Mobil DTE and turbine oils were used in three gas turbines, see figure 2a, of which
one (RR Olympus) is, however, an aero-derived gas turbine. The operation time of the oils
varies from approx. 15000 to 28500 hours. Correspondingly, it can be seen from figure 2b
that five gas turbines used a Shell Turbo T oil, where the operation time varied from
approx. 5000 to 52000 hours.

The variation of the TAN of the oils is limited and none of the oils has a TAN value
indicating that the oil has aged to a specifically high degree. On the contrary there is an
obvious difference between the RBOT values of the oils. It is characteristic that the oils
used in the three smallest turbines, Ruston TORNADO (6 MW$_e$) and Solar MARS(9 MWe)
as well as General Electric frame 6, had the lowest RBOT values, although these three

plants had the smallest number of operation hours. Thus the oils of these plants aged far quicker than in the larger turbines.

All small gas turbines have multi shaft rotors. Figure 3 schematically indicates how a rotor shaft can be divided. In such plant one or more journal bearings are, therefore, placed close to the warmest parts of the turbine. This will inevitably lead to a high ambient temperature around this(these) so-called "centre" bearing(s).
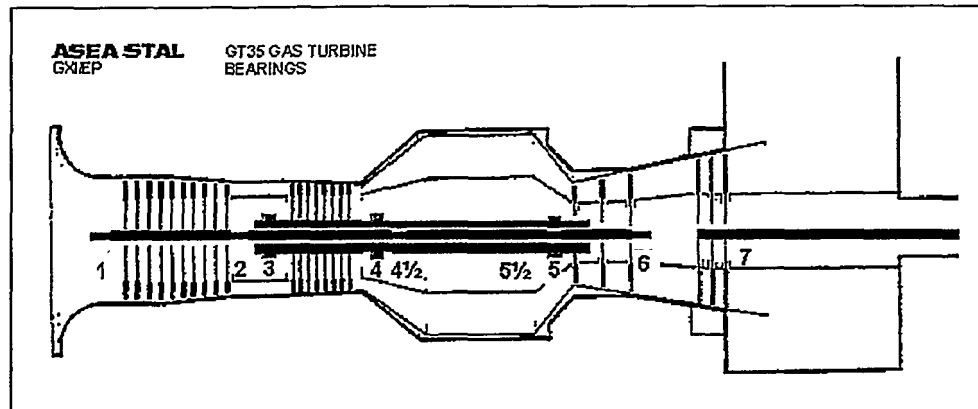

Fig 3. Multi shaft rotor with a hot "center" bearing, e.g. bearing no 5

In gas turbines hot air is used as sealing medium in the labyrinth sealings of the turbine. The sealing air is taken from the gas turbine compressor and the sealing air will thus typically have a temperature of 250 to 350 °C. Figure 4 shows how the sealing air and the oil are mixed in the bearing. The sealing air is ventilated to the open through the lubricating oil tank.
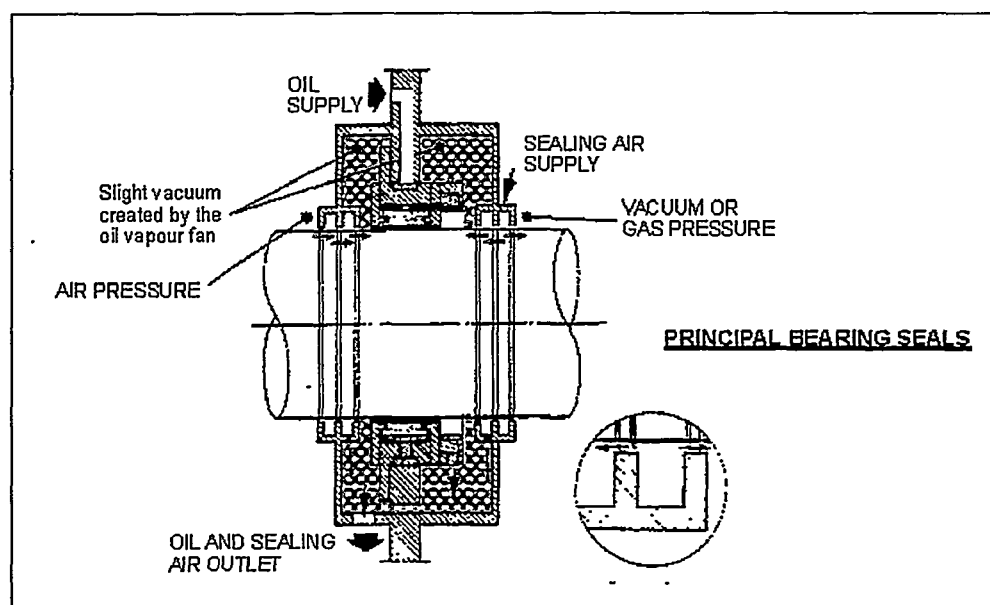

Fig 4   Mixing of sealing air and lube oil in a bearing

16.9

The intensive contact with the hot sealing air causes oxidation of the lubricating oil and loss of the oxidation inhibitors. It has been proved that several of the oxidation inhibitors used in conventional turbine lubricating oils escape together with the sealing air, which leads to a very quick degradation of the oil /1/.

The General Electric frame 6 turbine also has a hot-placed "center bearing", which causes quick ageing of conventional oil types. For this reason General Electric has indicated in their oil specification GEK 32568C: "Lubricating Oil Recommendations for Gas Turbines with Bearing Ambients Above 260 °C" that only high temperature resistant gas turbine oils should be used. It is worth noticing that the above GE specification contains a specific test to examine the thermal stability of the oxidation inhibitors.

The temperature of the lubricating oil in the warmest bearing(s) of the turbine is a good measure of the thermal stress, to which the oil is exposed in the plant. Table 2 indicates the lubricating oil temperature in oil tank, the oil temperature to the bearings and the return temperature from the warmest bearing. There is a close connection between the oil temperature in the warmest bearing and the lifetime of the oil. The highest bearing temperature was measured in GE LM2500 turbines which are aero-derived turbines, and where only synthetic lubricating oils of the type poly-ol-ester may be used. The five following plants (Dresser Rand DR990, Solar MARS and GE frame 6) are all turbines with high temperature in the center bearing and consequent short lifetime of the lubricating oil. In all these plants special high temperature resistant gas turbine oils (GT oils) are now used /2/.

Manufacturer	Size (MW$_e$)	Lubricant (first and second charge)	Oil temperatures (°C)		
			Oil tank	Supply to bearings	Return from bearings
KWU V 94.2	127	Shell Turbo T46	65	50	-
ABB type 11D	67	Teresso 46	40	47	57
RR Olympus	29	Mobil DTE Light	60	58	60
ABB type 13E	135	Mobil Turb. Oil Medium	55	47	61
ABB type 8	46	Shell Turbo T46	63	44	63
ABB type 9	30	Shell Turbo T46	40	44	68
ABB-STAL GT35	17	BP TH-HT 32	65	50	70
GE frame 9	114	Shell GT32	70	54	75
GE frame 6	37	Shell T32/Shell GT32	76	50	80
GE frame 6	37	Teresso 32/ Shell GT32	83	57	83
GE frame 6	37	Teresso 32/Teresso GT32	80	57	84
Solar MARS	9	Shell T32/Shell GT32	70	54	105
Dresser Rand DR990	4	BPTH-HT32/Shell GT32	80	65	113
Ruston TORNADO	6	Mobil DTE 68	50	50	115
GE LM 2500	22	Mobil Jet Oil II	65	70	122
GE LM 2500	22	Exxon Turbo 2380	62	62	126

Table 2   Oil temperatures in different gas turbines

16.10

During the past decade utilization of wind energy has played an increasing role in the Danish energy supply, greatly encouraged by national programmes. The ELSAM utility area has a large wind energy potential and approx. 74% of the installed wind energy capacity in Denmark is located here accounting for 463 MW by the end of 1995. The total energy production by wind turbines was 868 GWh in 1995, corresponding to 4.5% of the electricity supplied by the ELSAM utilities to the consumers.

A new agreement expanding the utility installed capacity with another 200 MW by the end of 1999 has been concluded, as wind energy has proved to be one of the most economical methods of obtaining reduction in CO_2 emissions. The target is to install 1500 MW by 2005 either by the utilities or private investors. The agreement leads to the expectation that the installed capacity in the ELSAM utility area will reach 1200 MW by 2005, /3/.

In 1986 the wind turbines typically had an output of 100 kW, which in 1995 was increased to 600-700 kW. A number of prototypes with an output of 1500 kW are being installed in 1995/96.

During the years there have been many problems with gearboxes in wind turbines. Lack of knowledge with the dynamic loads to which gears and bearings in a wind turbines are exposed resulted in underdimensioning of many gearboxes with consequent damage to the toothed wheels and bearings.

Lubrication of gears and bearings in a gearbox is done by elastohydrodynamic lubrication (EHL) and/or boundary lubrication. Figure 5 shows how a thin oil film is formed between e.g. two teeth in a gear. The contact pressure is so high that an elastic deformation of the surfaces occurs. At the same time the lubricating oil viscosity drastically increases in the boundary layer between the two surfaces, which among other things causes that the oil is retained in the boundary layer. Figure 5 b also shows the Hertzian stress profile in the contact zone. Notice, that the thickness of the oil film is of the order of 0.5 to 1 µm.
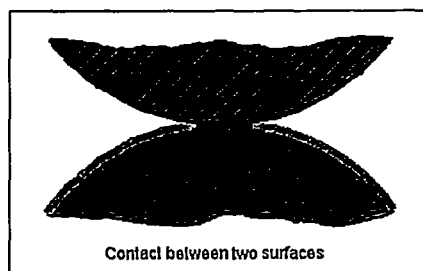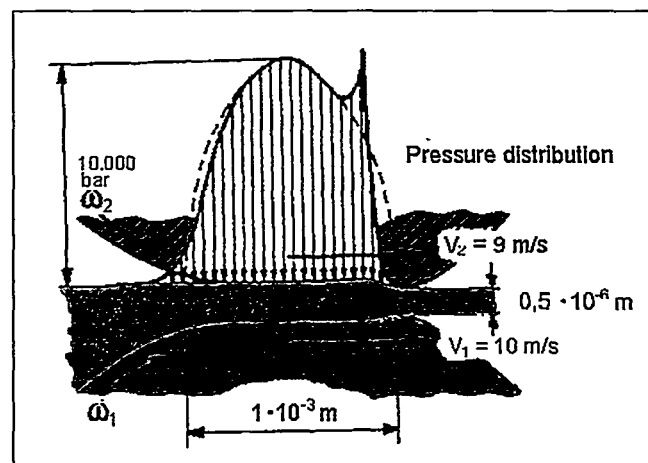

Fig 5 a. Oil film separating to surfaces

Fig 5 b. Elastohydrodynamic lubrication with elastic deformation of the surfaces.

At high load and low velocity between the contacting surfaces, the thickness of the elastohydrodynamic oil film will no longer be sufficient to keep the surfaces separated. Under these circumstances, which are named boundary lubrication, the friction and wear are determined by the surface layer, which is found on any metal surface. The lubricity of these surface layer is very dependent on the different types of antiscuff and antiwear additives which all gear oils contain.

Figure 6 shows a toothed wheel with a number of different zones where the lubrication can change from elastohydrodynamic to boundary lubrication or to a mixture of the two, called mixed film lubrication. Based on the experience gained till now with gearoils in wind turbines, these are presumably operating with mixed film lubrication, which has the consequence that the pressure between the tooth flanks is partly carried by a thin oil film and partly by metal-to-metal contact.

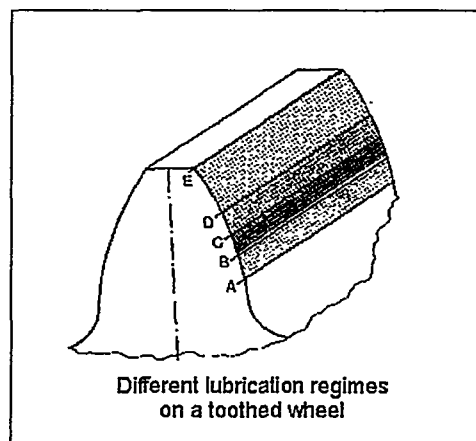Different lubrication regimes on a toothed wheel

Fig 6. Different lubrication regimes (elastohydrodynamic, mixed and boundary lubrication) on a toothed wheel.

The most frequent type of damage to toothed wheels in gears is macro- and micropitting. Pitting is a fatigue failure. It occurs when a fatigue crack is initiated at the tooth surface or at a shallow depth below the surface. Fatigue is promoted by metal-to-metal contact when the specific oil film thickness is too low. Water contamination of the lubricant can cause hydrogen embrittlement of the surface of the gear which also leads to pitting. During these years especially the phenomenon micropitting is the object of comprehensive studies, and several test methods have been developed for characterization of this type of damage. Within the frames of this paper it is not possible to go into details with the different types of damage which occurs in gears. These are closely described in /4/.

The main part of the existing wind turbines uses splash lubrication without any form of filtration or cooling of the lubricating oil. Seen from a lubrication point of view this is a very primitive form of lubrication and, therefore, it is no wonder that many cases of damage has occured in wind turbines as a consequence of insufficient lubrication. Moreover, oils with a much too low viscosity have often been used, which has resulted in pitting in many gears /5/ and /6/.

In connection with the development of large wind turbines (> 500 kW), the lifetime of gear teeth and bearings has been calculated. It turned out that the cleanliness of the lubricating oil is a decisive parameter to obtain the wanted lifetime of these components. Therefore, new gearboxes are equipped with circulating lubrication with effective filtration and cooling of the oil.

The most important contaminants in a gear oil are water and particulate. As to these two parameters the gear oil in a wind turbine must fulfil the same requirements which are today made of a turbine oil.

In order to keep a low water content in the gear oil, the breathers from the oil tank must be provided with a suitable filter and the oil should be cleaned if the water content exceeds 200 mg/kg.

The cleanliness of the oil is ensured by installing effective particle filters in the circulating oil circuit. The cleanliness of the oil is of special importance to the lifetime of the bearings. The particles causing most damage are those equal to or slightly larger in size than the lubricating film thickness. Considering that the oil film typically is 0,5 to 1 μm, rather severe requirements are made of the cleanliness of the oil.

ISO has developed a coding system (ISO 4406) to provide a simple way of using particle count data to compare various cleanliness levels. The ISO 4406 code has three range codes e.g. 17/15/11 expressing the numbers of particles greater than 2, 5 and 15 μm, respectively. Every increase in the range code by one represents a doubling of the number of particles in that size range. Gear oils in wind turbines should have a cleanliness of ISO 4406 code 16/14/12 or better, corresponding to a content of particles in 100 ml oil of:

-       maximum   64000 particles   > 2 μm
-       maximum   16000 particles   > 5 μm
-       maximum   4000 particles   > 15 μm

In order to avoid pitting, oil with a sufficiently high viscosity must be used, as this has a direct influence on the thickness of the oil film. Based on our experience, oils with a kinematic viscosity lower than 320 cSt at 40°C should not be used.

In Denmark both mineral as well as synthetic gear oils are used in wind turbines. Of the synthetic oils especially oils of the type poly-alpha-olefins are used. In gears with splash lubrication it might be an advantage to use synthetic oils with a high viscosity index, as the operation temperature of the oil often is too high. In gears with circulating lubrication, where the temperature of the oil is controlled, mineral oil can in many cases be used with advantage.

Whether a mineral or a synthetic gear oil is used, it must have good anti-scuff and anti-wear properties.

The practice used up till now and the future targets for lubrication of gears in wind turbines are summarized in table 3.

Subject	Now	Future
Run-in procedures for new gearboxes	Seldom	Compulsory
Method of lubrication	Splash lubrication	Circulating lubrication
Cooling of the oil	Seldom	Compulsory
ISO Viscosity Grade of the gear oil	150 to 320	Min. 320
Cleanliness of the oil (ISO 4406)	No requirement	Max. 16/14/12
Content of water	No requirement	Max. 200 mg/kg
Type of lubricant	Mineral/synthetic	To be evaluated

Table 3.   Comparison of gearbox lubrication now and in future.

Case No. 4   **Dissolved gases in insulation oil**

Dissolved and free gas analysis (DGA) is one of the most used diagnostic tools for detecting and evaluating faults in the electrical equipment. The principal basis functions of an insulation oil are to insulate, cool and arc-quench. Insulating oils are manufactured from special refined naphthenic base oils.

If failure occurs in an oil filled electrical equipment, the oil in the vicinity of the point where the fault is situated is heated and a number of gases are produced, which are dissolved in the insulation oil. Degradation of the insulation oil results in the formation primary of the following gases: H_2, CH_4, C_2H_6, C_2H_4 and C_2H_2, C_3H_8 while decomposition of solid cellulosic insulation (paper, pressboard and wood blocks) primarily forms CO and CO_2.

Gas content and composition depend on the type of the fault. Thus a thermal fault which will cause local heating of the insulation oil up to 300-500°C, will primarily results in formation of the hydrocarbons CH_4, C_2H_6, C_2H_4 and C_3H_8 . If an arc arises heating of the oil to 1200°C or more, C_2H_2 is formed, which is the characteristic gas for this type of fault.

The technique to measure and evaluate dissolved gases in insulation oils has been standardized and is described in details in the IEC standards 567 and 599.

Since its establishment in 1992 our gas chromatography laboratory has taken care of the measurements of insulation oils in the approx. 1200 transformers installed in the ELSAM utility area. We use a Head-space/GC for these measurements.

The primary purpose of the gas chromatography laboratory was to perform systematic analyses on all grid transformers (400 and 150 kV), all generator transformers and other important transformers in the power plants. Later it has turned out that measurements are requested also on the 60/10 kV distribution transformers.

Each year 300-400 gas chromatography measurements are performed, by which 3-5 transformers are found where the gas analysis indicates or clearly shows a fault. It is seldom possible to estimate the condition of a transformer based on a single analysis. Not until a number of measurements have been carried out is it possible to see whether there is a trend in the gas development. Interpretation of a gas chromatography analysis is further

16.14

complicated by the fact that different transformer types have different gas content dependent on the transformer design and its operation mode.

Of the examples where a gaschromatographic measurement has been used to detect faults in a transformer, two cases are mentioned below:

Example 1
60/10 kV distribution transformer

Figure 7 shows the development of the gas content in a 60/10 kV distribution transformer, type Trafo Union, 12,5 MVA. The routine measurement made in June 1995 revealed an increasing gas content of hydrogen and all hydrocarbons. Therefore, a new measurement was carried out in November 1995, which confirmed that the fault developed. Based on the gas composition and the rate of increase in the gas development, a thermal fault was concluded. The transformer was taken out of operation and was examined, and a short circuit in one of the transformer windings was found.
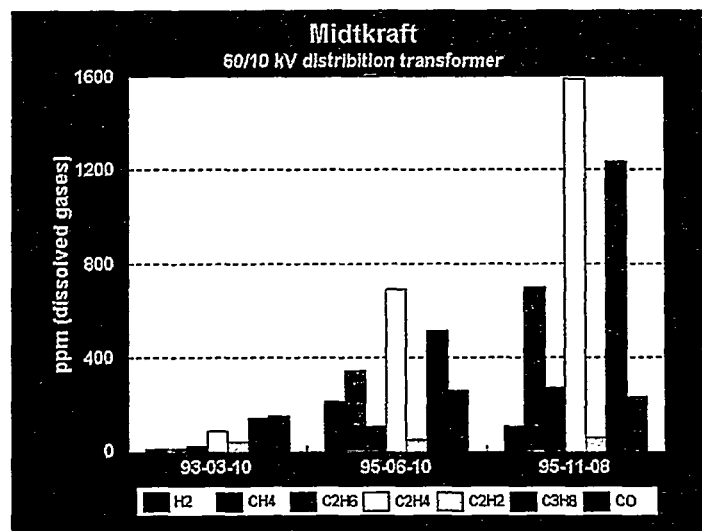
Fig 7. Development of gas content in a 60/10 kV distribution transformer with a thermal fault

Example 2
176/19 kV generator transformer

Figure 8 shows the development of the gas content of a 176/19 kV generator transformer, type Smit Nymegen, 450 MVA. Shortly after the commissioning of the plant in the middle of 1992, hydrocarbons were found in the transformer oil, primary CH_4, C_2H_4 and C_3H_8. It should be mentioned that the gas content of generator transformers normally is very low and the values which were found clearly indicated a thermal fault. During the period from 1992 to 1995 the transformer was inspected several times and two times the oil was evacuated, which removed the major part of the dissolved gases; this can also be seen from figure 8. Not until the annual overhaul in 1995 did we succeed in finding the fault. It

turned out to be a short circuit between two conductors at the outlet side from the secondary winding, which was not found until all the conductors had be deinsulated.
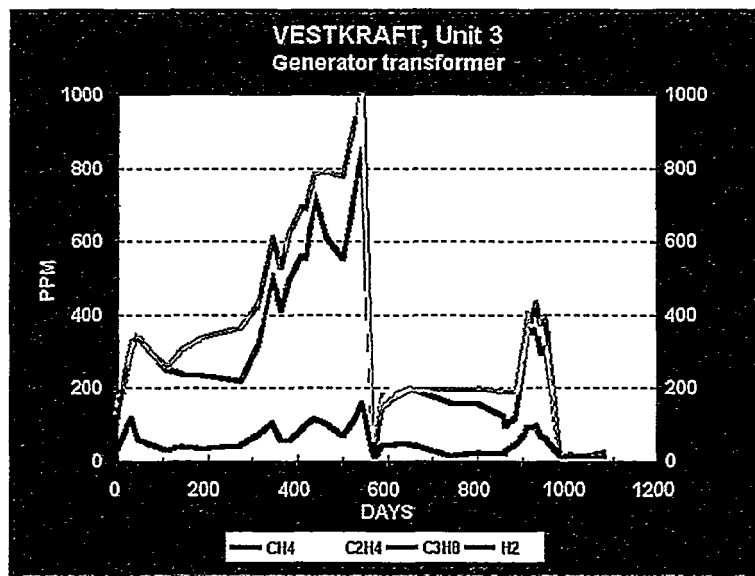

Fig 8.   Development of gas content in a 176/19 kV generator transformer with a thermal fault

Conclusion

The examination of lubricating, hydraulic and transformer oils is today an important part of the work done to improve the availability and extent the lifetime of the plants. It is our experience that a satisfactory solution to operation problems related to lubricating or transformer oils can only be obtained by actively taking part in solving the problems.

Generally there is a need to extend the knowledge of the operation staff about lubricating oils and their importance to the operation of the plants. The maintenance costs arising in many plants could be reduced and the lifetime of the components be prolonged by the correct choice of lubricating medium and by a better control with the condition of the oils. In the future market which is expected to be based on more competition these circumstances will be of a still increasing importance.

Although we have built up fundamental knowledge and experience with oils during the past 10 years, there still remain areas where we need to extend our know-how. This applies e.g. to the use of phosphat esters as lubricating oil in gas and steam turbines, gear oils for wind turbines as well as improving our transformer condition assessment techniques. We hereby invite our power station colleagues or other interested parties to participate in these projects.

References

/1/   Møller, H. "Lubricating Oil For Small Gas Turbines", ELSAM R&D-project, 1992

/2/   Zeijseink, A.G.L., Butter, L.M., Møller, H. "Lubricating Oils For Gas Turbines", Final report of a joint KEMA/ELSAM R&D-project, 1994

/3/   Saxov, J., Skovgaard, S., Friis, P., "Power Plant Operation Correlated with Wind Energy Production within the ELSAM Utility Area", Status 1995

/4/   American National Standards, Nomenclature Of Gear Tooth Failure Modes, ANSI/AGMA 110.04-1980 (reaffirmed 1989)

/5/   Muller, J. "The Lubrication of Wind Turbine Gearboxes", Lubr. Eng., **49**, 11, pp 839-843, (1993)

/6/   Friis, P., Møller, H., "Lubricants to Gearboxes in Wind Turbines", Energiministeriets og Elværkernes Vindkraftprogram, Rapport nr EEV 94-02, 1994.

VISION 2021: THE UTILITIES FUTURE

J. van Liere
KEMA
P.O. Box 9035
6800 ET ARNHEM
The Netherlands
27 June 1996

ABSTRACT

The electricity industry is gradually making the transition to a free market economy characterized by competition. With the arrival of a more market-oriented structure, the electricity companies have taken measures to reduce costs while retaining reliability and safety of the power production and distribution. Today the majority of these efforts are oriented towards optimizing the scope and the structure of the organizations and towards streamlining internal processes in order to improve productivity. These measures contribute to an improved short-term performance. However, activities must also be developed to ensure that the organization retains its viability on a longer term. For this purpose, the role and position of the utilities in the international field must be determined.

Throughout the world, the increasing competition among utilities is accompanied by the unbundling of production, transport, distribution and customer service functions. This requires precise determination of the tasks per entity. This attuning is particularly important considering the fact that the energy structure of the future could shift from central power generation to dispersed power & heat co-generation. There is a remarkable similarity between the transitions in the computer industry some years ago (from main frame to personal PC's) and in the electric utility industry today. The new structure is expected to be less centralised and more dispersed. The network will acquire a new meaning (like LAN's and WAN's) and the server will probably adopt a central position. This means that attention should be devoted to improved asset utilization, while energy storage and frequency regulation are crucial elements in this new concept.

It is expected that in the dispersed generation concept the locally deployed power plants must become smaller, more flexible, more efficient and less expensive than today's power plants. Power generation is gradually changing from a steam cycle (Rankine cycle) via the combined cycle to the gas cycle (Brayton cycle). The fuel used to power the gas turbine is expected to change in the future from high calorific to low calorific gas, generated from biomass, waste, oil residues, blast furnaces, coal, etc.

The market is on its way, and future IPPs are expected to supply "bulk power", meaning kiloWatt-hours at extremely low prices. As a result, the regular electricity companies may be forced in the direction of energy "servuction" - supplying heat and power in the form of energy services. These services may vary significantly and will pertain to power and heat as well as to advanced communication technology.

Based on the analysis, five new areas to be addressed have been identified that can be characterized as follows:

a   improved utilization of capital-intensive production resources to reduce costs

b   electrification and the supply of heat to increase sales and market share

c   sustainable developments to broaden our future resource base

d   improved efficiency based on the Brayton cycle to increase flexibility

e   development of energy services with new secondary services to stay in the market.

1. Long-term outlook

In the next thirty years, the world's energy consumption will increase by approximately seventy percent. Today some eighty percent of the world's population (~4 * 10^9 people) consume less than twenty percent of the global energy consumption. Their energetic growth will average four to five percent per year. South-East Asia will become the center of economic and energetic growth. The 25% of the world's population living there now represents 17% of the global energy consumption on an annual basis, but with an energetic growth of ten percent per year or more this will rapidly increase. Some forty percent of the global population does not have access to commercial energy. An estimated investment of six octillion US dollars is required for establishing an electricity structure to evenly electrificate the world.

For the time being, the supply of energy will continue to be based on fossil fuels. In addition, it will take about twenty more years for the price of renewables to reach a level that can compete with fossil energy. The price for oil and coals is not expected to increase in the coming ten years - a price reduction is more likely though price spikes in the price level may occur. The price of gas currently shows a slightly-increasing trend and may be forced upward by the enormous demand from the "ecological side". According to Shell estimates, the price ceiling for natural gas will stabilize in the future at the level for bio-mass gas (approximately 25 US dollars per barrel equivalent). The excess supply of fossil energy on the market is considerable. After the price of oil dropped-in 1986, all of the large oil companies reduced their operational expenses by about thirty percent. Electricity companies will have to do the same if electricity is to compete with fossil fuels. The excess market supply of energy is not expected to disappear until after the year 2010.

Between 2010 and 2050, at least ten different types of energy sources are expected to be available on the market that will acquire a market share of 5-15% each. These include fully-developed renewables. Nuclear power is expected to be accepted and to make a significant contribution in only limited parts of the world (France, Japan, Korea). Considering the uncertainty and unreliable prognoses made by planners and forecasters, it would appear to be wise to adopt a policy of diversification and flexibility. An illustrative example of these faulty prognoses is seen in the price development of oil, coal and gas as compared to the best forecasts (highest and lowest scenarios) published by the IEA (Figure 1).
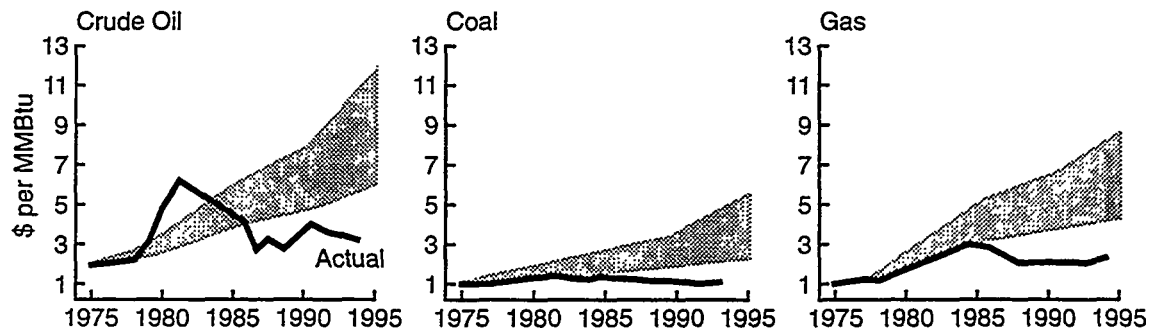
Figure 1   Price predictions and actual price developments for fossil fuels

2.   Competition, unbundling and down sizing

The increasing competition among electricity companies necessitates continued cost reductions, which can be achieved by methods that include unbundling traditionally integrated business activities into discrete entities. The separation of the production, transport, distribution and customer service functions is either taking place or about to take place throughout the world. Competition is international, affecting the price of electricity not only in certain regions, but over the entire world. The separation of the existing, integrated electricity structure into four discrete entities as described above requires precise determination of the tasks per entity. This is reflected in Table 1.

Table 1   Tasks for an unbundled energy sector

Entity	Task
Generation	Large- and small-scale electricity generation and sales
Transport + Brokerage	Non-profit network management + purchases most-economical electricity and transports it to the distribution sector and to special large-scale consumers
Distribution	(Retail) sale of electricity and heat with services representing value added, such as reliability and power quality assurance
Services	Markets services and safeguards customer satisfaction, supplies information

In the free, competitive market of the future with strongly horizontal oriented electricity companies, a generator can not take the risk of not being able to sell its products. Strong generators will therefore buy up more and more distribution companies, in time recreating a more or less vertical structure. In Great Britain, five years after privatization and a stock-market quotation, this process has already started. All of the large companies (NP, Powergen, Scottish Power) now have options on a distribution company. In the future (after the year 2020), it is expected that only a limited number of multi-national power companies will be operating in the world, in analogy to the oil companies (Shell, Exxon, etc.) and the ABBs, GEs and Westinghouses of this world.

3.   The market; the principle of servuction

In today's world, there is a direct route from the electricity generator to the final user; the future will probably be characterized by a spot market and a long-term market, each with its own price level. The "Exchange" will be the center where electricity is traded. Electricity will be traded as "futures" (virtual kWh) and as power (kWh). Companies,

chains of companies and user associations will be able to purchase electricity at the Exchange (see Figure 2).
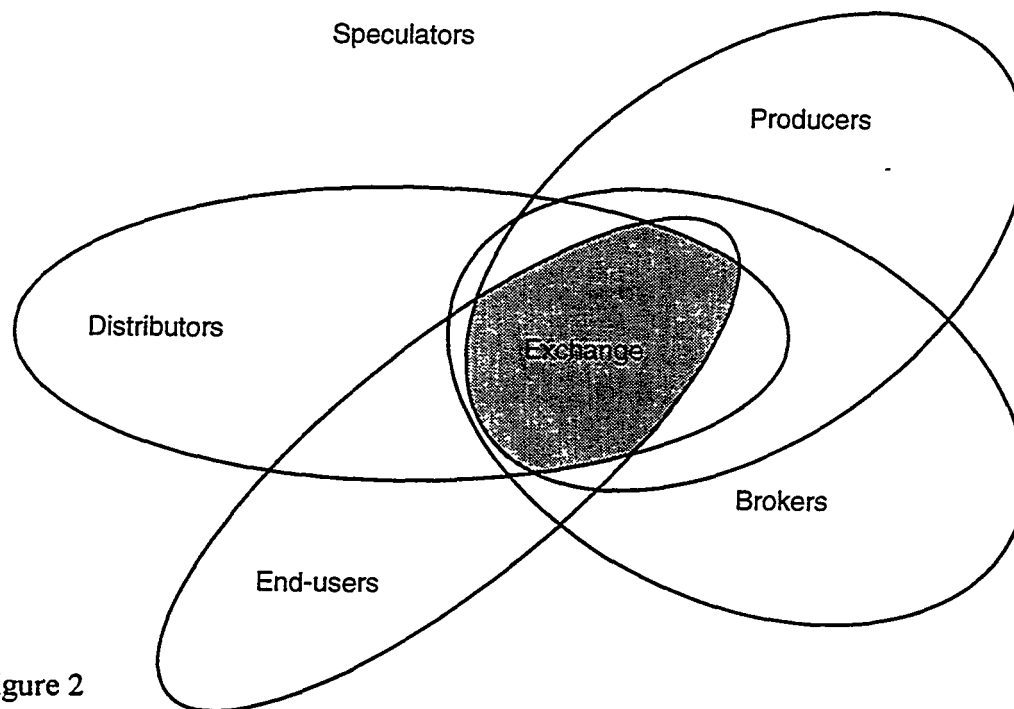

Figure 2

Two types of markets will evolve. Anonymous bulk kiloWatt-hours will be traded on the first market. The final user is invisible to the generator. The generator will also sell directly to large-scale customers. In this, it is important that packages of energy services be made available. Key in this respect is accurately feeling and estimating the customers' true needs. An energy service is a package of products that includes the primary product (the kWh) and a number of secondary products. Examples in other areas include hotels, air travel and restaurants (primary product food and drinks, secondary products service, information (the menu), accepting various methods of payment, cleanliness, waiting period, friendly personnel, etc.) (see Figure 3).
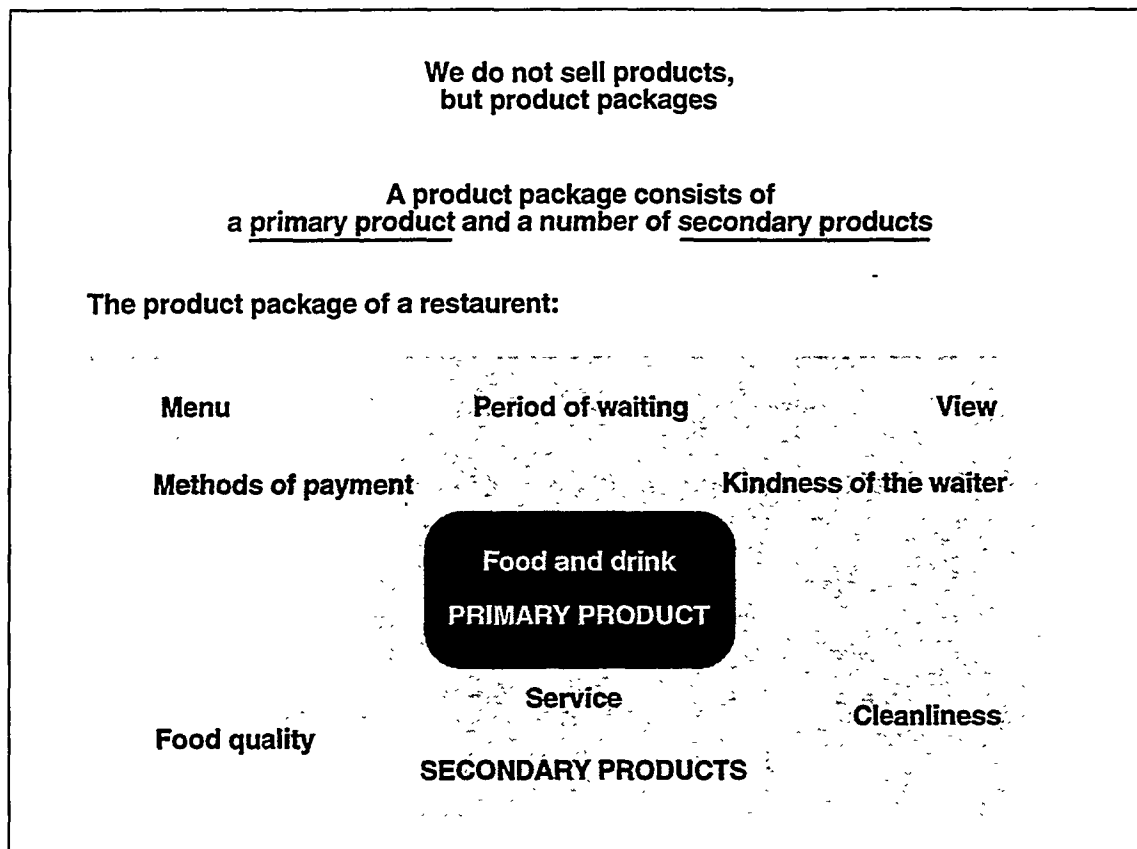
We do not sell products,
but product packages

A product package consists of
a primary product and a number of secondary products

The product package of a restaurent:

Menu   Period of waiting   View

Methods of payment   Kindness of the waiter

Food and drink

PRIMARY PRODUCT

Service   Cleanliness

Food quality

SECONDARY PRODUCTS

Figure 3   Product package with primary and secondary products

It has been learned from experience in other countries that between twenty and forty percent of captive customers will immediately leave when a monopoly position is terminated. It is also a known fact that customers often make choices based on the secondary products. Telephone companies that have been privatized travel this path, adding a variety of secondary facilities (knock-on facilities, lock facility, easy connection, etc.) to their primary product (a telephone call). Electricity companies must do the same by developing new services. In the future, R&D must therefore focus on the two markets explained above:

a   technically-oriented R&D so that reliable bulk power can be marketed at the lowest possible cost

b   developing energy services with new secondary services, such as un-interruptible power quality, green electricity, cold, heating, cooling, dry or humid air, etc. Other (related) energy products such as CO_2, gypsum, etc. are also relevant, but the same applies to these.

4.   The energy structure

In the energy structure of the past, the power plant was the central facility for feeding houses, factories and offices. With the new awareness of the advantages of (decentralized) co-generation of heat and power and the deployment of renewables such as wind energy, this situation is about to change. The new structure is expected to be less centralized and more dispersed (like in the computer industry, where a shift has been made from mainframe to stand-alone PC's). The network will acquire a new meaning, similar to a LAN or WAN in computer networks, in which the "server" will adopt a more central position. Network stability and frequency regulation will gain importance. As a result energy storage will become very important (Figure 4).
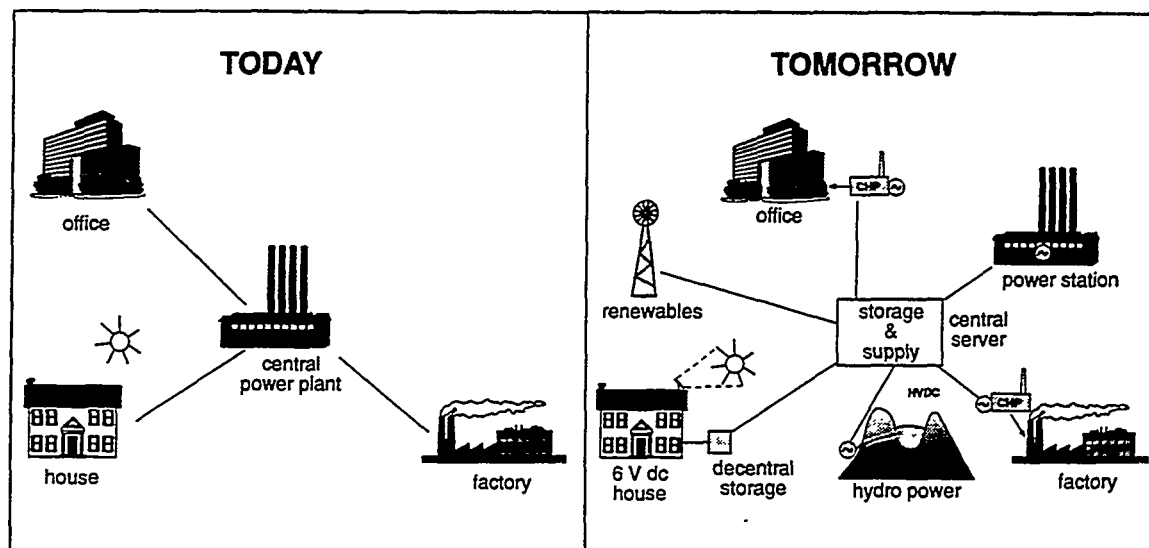

Figure 4   Transition from the "mainframe"concept to dispersed generation

17.8

In addition to a shift towards regional, dispersed generation, a continental structure through HVDC - in combination with the development in power electronics - is expected. In this respect it would appear logical to link strategically important, non-moveable sources such as hydro power and geothermal energy, bio-mass energy, CASH storage and nuclear energy (which can be viewed in the same manner). Based on this perspective, a structure will evolve as shown in Figure 5.
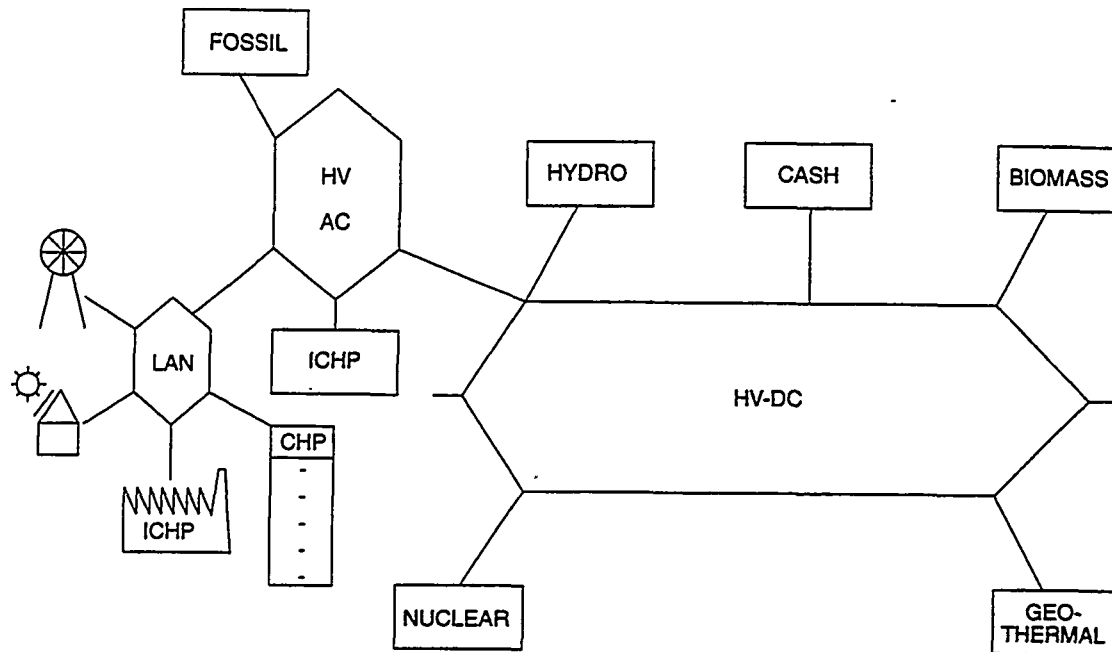

Figure 5   Continental HVDC network with regional sub-structures

The HVDC ring will also make CO_2 reduction by fossil-fuelled units possible. With HVDC, electricity can be economically transported over a distance of 1500 kilometers. According to ABB, HVDC transport over a distance of 5000 to 6000 kilometers is currently more economic than the transport of primary fuels. This means that a line with east-west orientation over three or four time zones is feasible. This will result in peak shaving and valley filling and more efficient utilization of the production units. With this line, immobile low-CO_2 production techniques can be linked, such as hydro power, geothermal generation, storage systems with compressed air in suitable underground cavities, bio-mass conversion, etc. In addition, by linking up fossil plants more efficient operation will result in lower CO_2 emissions than is the case with regional operation. Naturally this mechanism will only function properly in multi-national power companies.

It is expected that locally deployed power plants must become smaller, more flexible, more efficient and less expensive than today's power plants. But it also means that the total plant capacity required will be less than in the past despite an increase in electricity sales. It must be remembered that the nature of the fuel (in particular natural gas) makes decentralized generation possible. This means that the supply of electricity will become increasingly dependent on a single fuel. The effect of an abrupt increase in the price of gas will then turn the competitive advantage of combined power and heat generation into a competitive disadvantage. A thorough scenario analysis would appear appropriate, which should also include the possibility of alternative gaseous fuels from coals, bio-mass, waste, oil, etc.

5.   Heat and power

Both figuratively and literally, people need heat more than they do need power. In most countries in the Northern hemisphare the demand for (low-value) heat is two to five times the demand for (high-value) power. From an exergetic viewpoint, the CHP principle is an excellent way to use fuel, but the heat/power ratio in normal co-generation plants is roughly 1:1. This means that supply and demand are generally not in balance. In countries like the Netherlands, this has been "remedied" for low-temperature heat (primarily in homes) through individual boilerification with gas heating systems. Countries like Denmark have better attuned to the exergetic concept by focusing on the demand for heat and then generating basic heat for municipal heating using decentralized units based on waste/bio-mass combustion supplemented by an integrated, gas-fuelled combined cycle units for electricity and hot water and a limited number of auxiliary boilers (see Figure 6). A good or even better alternative is generating heat and power in combination with municipal heating and electrical heat pumps. An important aspect in this line of reasoning is reversing the approach. If the demand for heat (energetically speaking) is two to five times the demand for power, we should focus on heat instead of power. At the same time, we must work hard to improve the balance through the electrification of society.
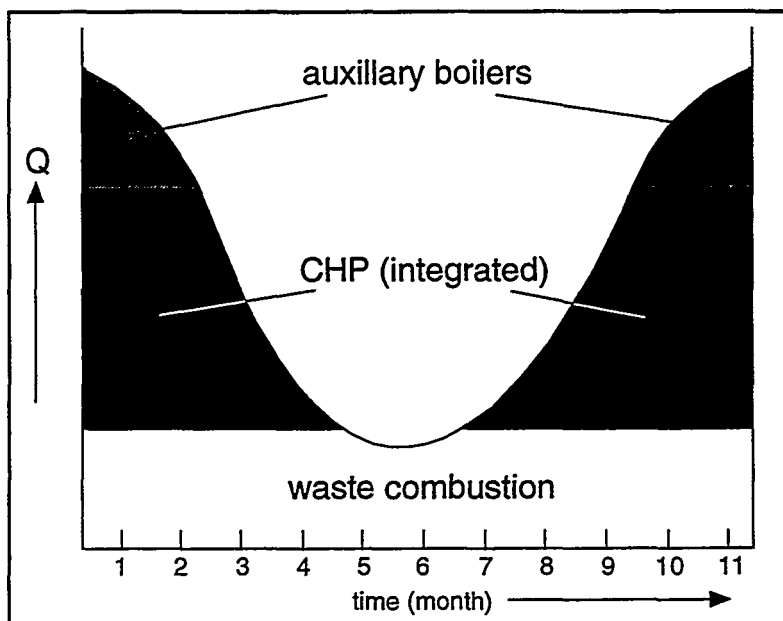
Figure 6   Danish solution to the imbalance between power and heat using small, decentralized units

6.   Reducing costs and increasing margins

Cost reductions can be achieved through reorganization, improved asset utilization, operational streamlining and by implementing new technologies and/or utilizing more efficient means of production. The poor utilization of capital-intensive resources is made vividly clear in a graph showing the utilization level as a function of time (Figure 7).
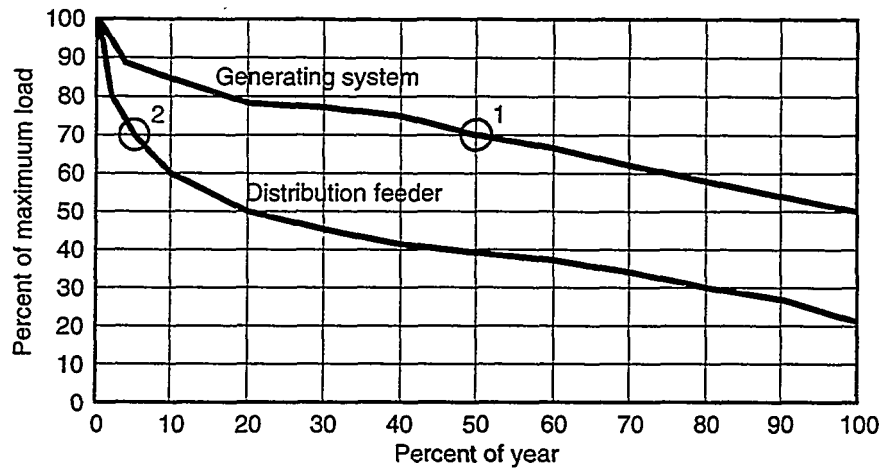
For example, data show:
1 Generation-system: 70% or greater usage ≤ 50% of the time
2 Typical feeder: 70% or greater usage ≤   5% of the time

Figure 7   Utilization level of production and transport resources

In a competitive market, a suggested similarity exists between the utilization level throughout the year and the price level of a kWh throughout the year. In countries where free market mechanisms are active (such as Australia (State of Victoria), England, etc.) and where, for example, offers for network access are made per half hour, a clearly similar relationship can be identified between the kWh price and time (Figure 8).
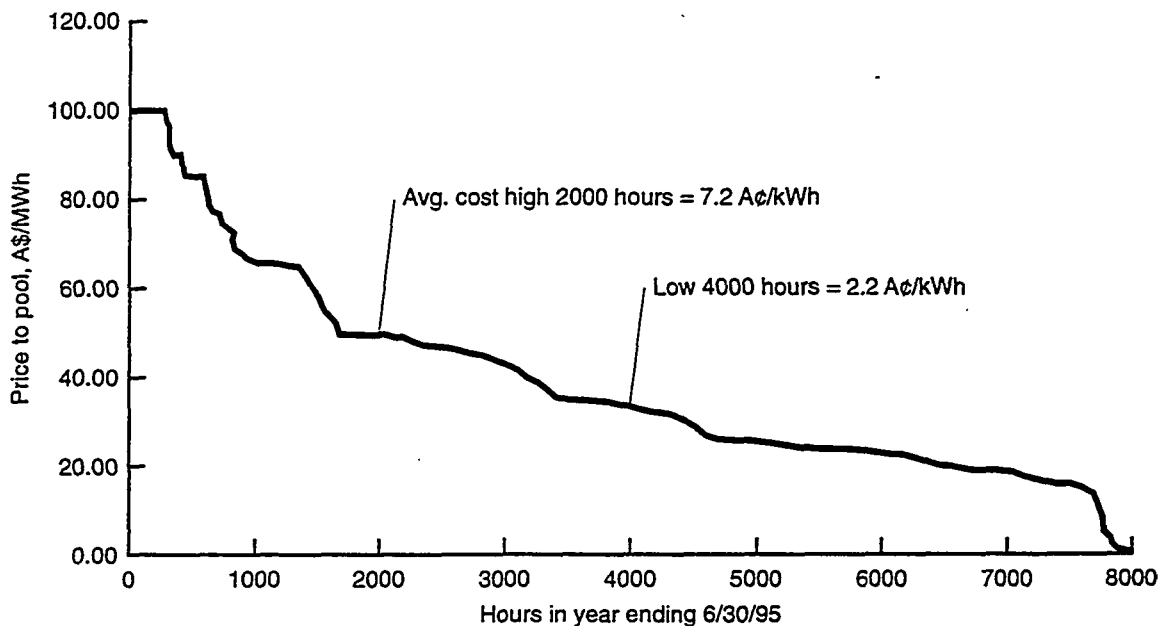

Figure 8   Price fluctuation curve for the Australian Victoria Pool (AUS$/MWh)

17.12

It has been learned that a major part of the electricity generated in low-consumption hours is made available at below-cost price. Significant profit margins are seen during a maximum of 2500 high-demand hours per year; the possible profit during 2500 to 5500 hours per year is dependent on the cost price. This means that capital expenses must be drastically reduced and the consumption pattern must be drastically improved to prepare for a competitive market.

Sales increases can be achieved through an electrification strategy, requiring either application of new electro-technologies or further implementation of electro-technologies. R&D must focus on aspects related to these main themes.

Increased sales and lower costs must create the space needed to strengthen the electricity sector and to make it a viable competitor for IPPs and foreign electricity companies hoping to gain footing in certain areas. Effective management systems must of course be applied in order to decisively translate this space into business growth.

It is to be expected that the future IPPs will want to supply bulk power - kWh - at low prices. The regular electricity companies will be forced in the direction of total energy service, meaning that they will want to sell part of their production at a high price as "uninterruptible high quality power", green electricity, etc. and part of the production as bulk power at low price. A differentiation in the energy quality is therefore imminent. In addition, throughout the world the regular electricity companies are establishing APPs (associated power producers) which will compete with the IPPs on the bulk power market.

7. Social developments

Western society is evolving from a labor-intensive to a machine-intensive and finally into an information-intensive society. In an information-oriented society, information technology and the transfer of information form the key process. The role played by an electricity company during the transition from a production society to an information society is uncertain. One important trend that has been identified is that suppliers are offering an increasing amount of information about the product together with the product as a competitive edge distinguishing them from other suppliers. The transition to an information-oriented society goes hand-in-hand with the development of advanced communication technology. This pertains to matters such as optical communication,

image transmission technology and image processing technology. Because these are essentially discrete energy packages transmitted through cables, it would be logical for energy transport and distribution companies to consider this aspect as future business. Another important change is that it is estimated that in the year 2005 half of the world's population will live in suburbs. This is expected to have an extensive effect on the energy situation. Half of the world's population will live in large cities where their business is and thus where the need for energy is. What effect will these factors have on the electricity companies? A strategic analysis of these points is recommended.

8. New areas to be addressed

a Improved asset utilization

The electricity companies have created permanent excess capacity for the production, transport and distribution of electricity in order to establish reliable margins and in order meet peak demands. In a more competitive environment, electricity companies are searching for ways in which these huge capital investments can be put to better use. It is expected that the storage of energy and smaller industrial co-generation units will result in improved utilization and a healthier structure of capital investments. Unused resources in terms of both capacity and time of the total production systems and of the transport and distribution systems are sometimes considerable. Adding new storage systems would result in the possibility of improved utilization of the (existing) infrastructure. Because the storage of energy is both necessary and desirable for utilization of renewables and durable generation in the system, considerable attention must be devoted to this point in the future. Table 3 lists various applications and the importance therein of energy storage in terms of generation, transport and distribution as well as customer services.

Table 3   Applications of Storage Systems

Entity	Objective
Generation	Reduce spinning reserves, postpone new construction, frequency regulation, load levelling, implementation of renewables
Transport	Line stability, voltage regulation, improved utilization of line capacity
Distribution	Voltage stability, distribution network deferal
Services	Peak shaving, reliability and power quality

Investments in generation systems such as power plants are 10 to 20 times higher than investments in transport and distribution systems, which means that this is where the best short-term results can be achieved!

b   Increasing Sales through Electrification and the Supply of Heat

A further increase in sales must be achieved through electrification; the ratio of electrical energy with reference to the total energy consumption is for most industrialised countries between 14% and 40%. The major areas for electro-technology and electricity applications are: industry, transport, households, greenhouse horticulture and utility construction. Exploratory source to service studies shows promising perspectives for increased sales, low emissions and low costs. If based on an integral approach to the supply of energy, extensive electrification need not represent a conflict of interests with a sustainable development. Other aspects such as the controllability of electrically-powered processes and more selective application are also important (Figure 9).
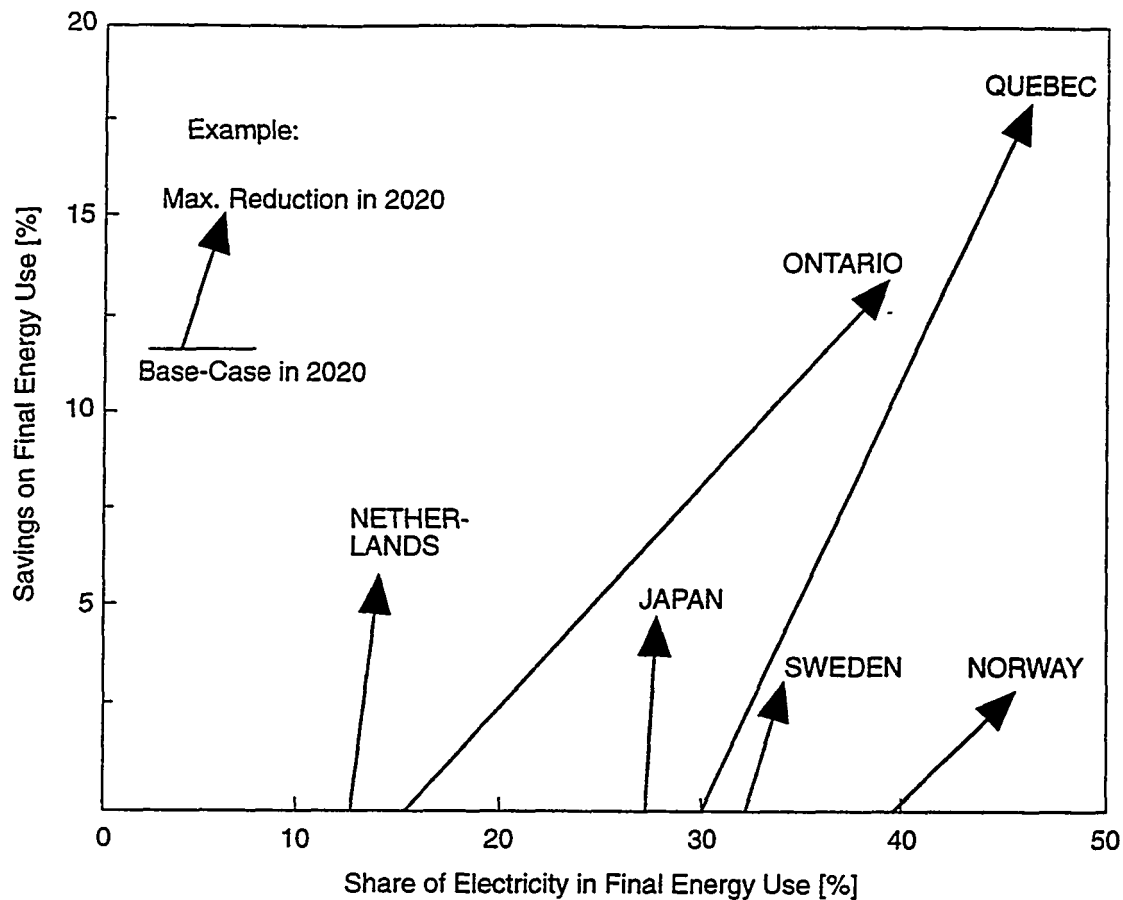
Figure 9   Electrification development

The increase in (industrial) heat/power units requires that focus be placed on the supply of heat rather than the supply of power. In order to arrive at the optimum supply of heat, industrial heat plans should be compiled. For municipal heating, a validated, thermo-dynamically energy management model should be developed in order to break through the traditional "boilerification approach" (Figure 10).
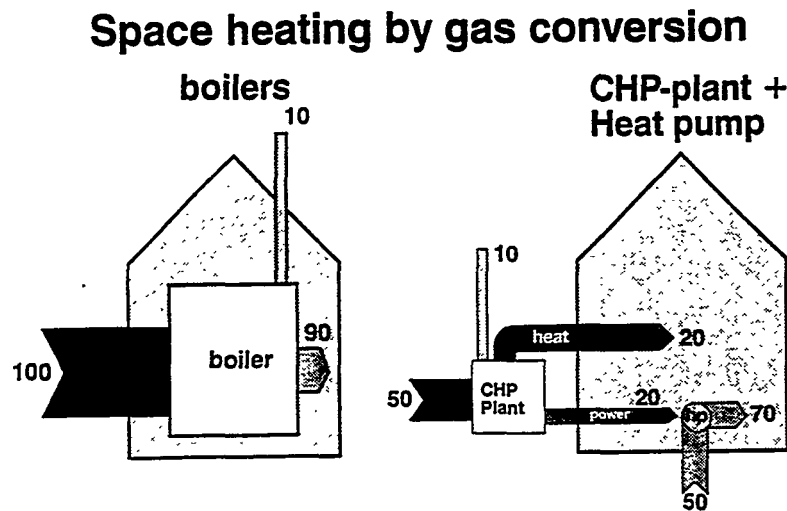
17.16

Space heating by gas conversion

Figure 10   Space heating based on natural gas. Energy savings of 50% are possible using CHP plants and heat pumps

c Sustainable Development

The stone age didn't end for lack of stones and it is highly unlikely that the fossil fuel age will end for lack of fossil fuel. The growing concern about CO_2 and the global climate may result, however, in restricted use of fossil fuels. New technologies are developed and a sustainable development is one of the cornerstones of the future policy. Sustainable means "living from interest of our resources, rather than from our resources". Of all sustainable energy types, bio-mass, hydro power, wind and photovoltaic energy appear to have the best potential for success. Each of these four requires an entirely different development focus if it is to be of significance to the power generating sector (see Table 4).

Table 4   Development Focus for Durable Energy

Type	Development Focus
Bio-mass	Co-combustion, gas-turbine technology, new generation concepts
Hydro power	HVDC lines, hydrogen technology
Photovoltaic	High yield cells, decentralized 6-12 V d.c. systems in house-holds, energy storage
Wind	Reliability, off-shore sites, energy storage

The programs for electricity conservation, such as the application of high efficiency low-energy bulbs, have a questionable side effect (rebound effect + Torremolinos effect) that essentially negates the positive effect and creates a shift in the direction of primary energy carriers. A re-evaluation of energy conversation programs should be considered in order to arrive at truly cost-effective CO_2 reductions and primary energy saving.

Source to service analyses indicate that the total efficiency of energy chains is extremely low. Many energy services (for example transportation) have a total chain efficiency of less than 5% (Figure 11). Electrification of society can improve this efficiency significantly and reduce CO_2 emissions by approx. 50%. Adding sustainable sources directly to the energy service minimizes the losses, as a result of which the total efficiency may even be higher than that of a fossil chain.
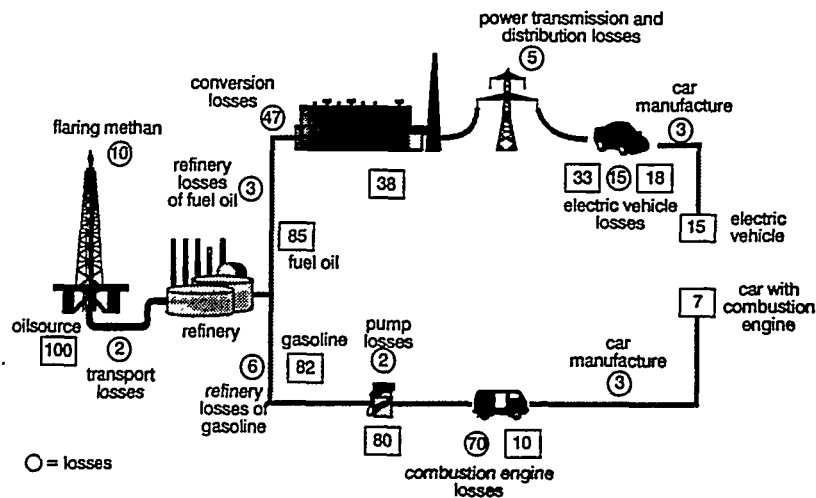
17.18

Well to Wheel

Figure 11   Well to wheel analysis for the energy service "transportation"

d   Improved Efficiency Based on the Brayton Cycle

Efficiency improvement has been consistent in the past century. Each time the limit was thought to have been reached, "new" options appeared that resulted in improvement. Changing heat into work is restricted by natural boundaries, as explained in Carnot's Law (see Figure 12). Properly developed cycles can achieve about $0.75\eta_{CARNOT}$; highly-advanced versions can achieve $0.8\eta_{CARNOT}$. This means that state-of-the-art Rankine steam cycles with 600 °C steam achieve about (0.75 x 0.63) * 100% = 48%; in the future with 700 °C and continued technical development this will be about (0.8 x 0.67) * 100% = 54%. State-of-the-art gas turbine cycles based on the Brayton cycle with 1430 °C gas intake can achieve about (0.75 x 0.81) * 100% = 60%; in the future with 1500 °C and continued technical development this will be about (0.8 x 0.83) * 100% = 66%. Coal-fuelled units based on both cycles will be somewhat lower (Figure 13).

Carnot' Law
The potential of technological development
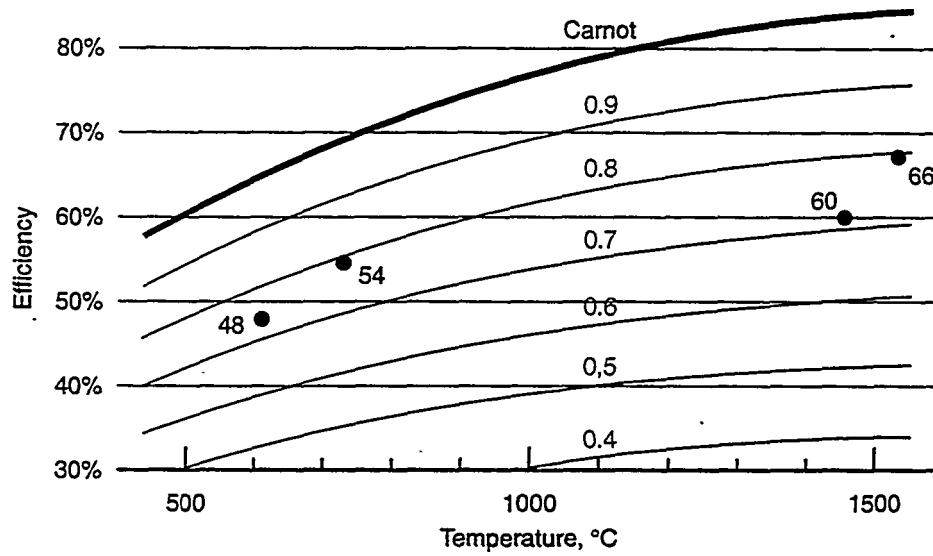

Figure 12   CARNOT yield based on the temperature

Direct water cooled air compressor in Brayton cycle
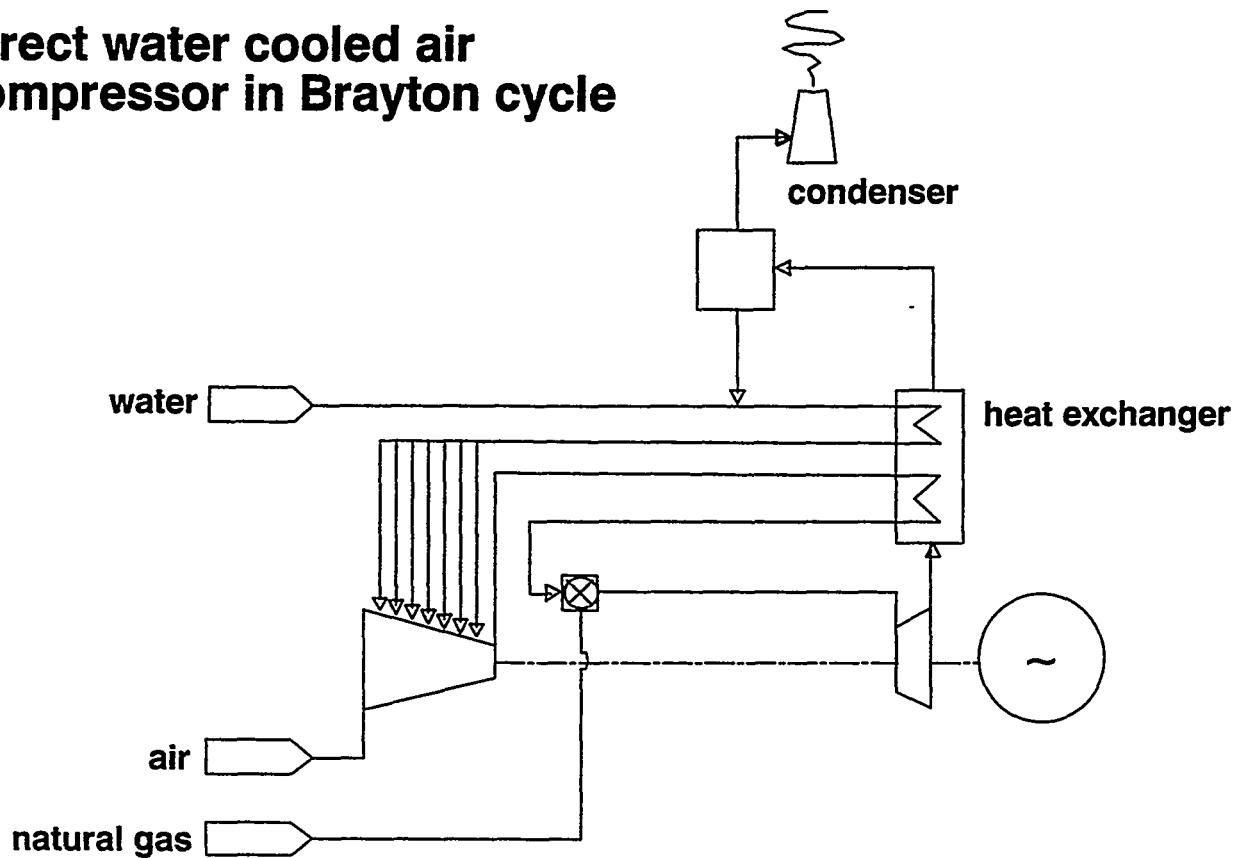

Figure 13   Brayton cycle in a new concept (TOP-HAT)

The yield of the gas cycle must be improved considerably because the exergetically-favorable field (the exergy cream) in particular shows significant room for improvement. A number of premises are currently being developed that could play an important role in this respect. These possibilities must be explored in more detail and brought into focus. In the lower exergy area, which now includes the steam cycle, a humid gas cycle is attractive in terms of the level of investment required, the yield and the flexibility. Initial calculations have rendered interesting figures. The basic idea's of a TOPHAT cycle have been worked out (Figure 13). The fuel used to power the gas turbine is expected to change in the future from high-calorific to low-calorific gas, generated (for example) from coal, bio-mass, waste, blast furnaces, oil gasification, etc. Considerable attention should be payed to the combustion of these low-calorific gasses. The combination of new developments such as the air clean-up devices, continuous GT compressor cooling, a rotating ram-jet burner for the supply of work in the high-exergetic field, a humid gas cycle, etc. must in principle result in the compact, flexible, fast responding and cheap power generating unit that fits in the new energy structure of the liberalised market.

e   Development of Energy Services with New Secondary Services

The sale of services is rarely determined by the primary product, but almost always by the package of products, in which the secondary products are determinant. It does not matter to the customer whether a gallon of high-octane gasoline with a specified octane content comes from Shell or Exxon, but the secondary aspects do matter, such as price, accessibility of the gas station, saving stamps, towels, service, etc. The same is true for a kWh: they are all the same, and the secondary aspects will be determinant in a competitive sales environment. A change must be made from "selling what we had to sell" to "servicing where we can serve". For this purpose, the market must be segmented (e.g. homes, offices, factories, schools, hospitals, greenhouses, hotels, etc.) and the product packages must be attuned to the specific needs of each market segment. Examples include:
- un-interruptible power and clean air for operating rooms in hospitals
- high-quality power for offices, computer centers, banks with numerous PCs
- conditioned heat for hotels
- bulk power for factories
- green electricity for (certain) homes
- image technology for schools.

17.21

Free additional services involving, for example, the energy consumption in chain stores, product information about CO_2 reductions with green electricity, etc. may be decisive when energy contracts are involved. A creative start should be made in finding market-oriented energy services with the relevant secondary services.

9.   References

CRIEPI, Main Research Projects in 1995, March 1995.

ELSAM, R&D committeee, private discussions

EPRI, Strategic Asset Management, Helping Electric Utilities: translation vision into value, TR-102730, February 1994.

EPRI, Power Delivery Group, RD&D Portfolio 1995 - 2000, October 1994.

ESKOM, Research Programme 1996 - 2000, Technology Group.

IEA, New Electricity 21, Paris, 22 - 24 May 1995.

IERE, A New Age for Electricity, integrating technology into business and strategy, Monte Carlo, Monaco, 25 - 28 April 1995.

Sep. Beleidsplan Onderzoek en Ontwikkeling 1996 - 1998, PO/EMT 05-011, July 1995.

Dutch Parliament, Third Energy Memorandum, session 1995 - 1996, 24 525 nos. 1 - 2.

World Energy Council, 16th Congress RoundUp, Energy for Our Common World: what will the future ask of us? Tokyo, Japan, 8 - 13 October 1995.